



School of Civil and Environmental Engineering

DEVELOPMENT OF THE CDWQ-E₂ POST-TREATMENT WATER QUALITY MODEL

A research report submitted to the Faculty of Engineering and the Built Environment,
University of the Witwatersrand, Johannesburg, in partial fulfillment of the requirements for
the degree of Master of Science in Engineering

Student: Liam Patrick Culligan (0715293H)
Supervisor: Dr Precious Biyela

Johannesburg, 2015

DECLARATION

I, Liam Patrick Culligan, declare that this research report is my own unaided work. It is being submitted to the Degree of Master of Science to the University of the Witwatersrand, Johannesburg. It has not been submitted before for any degree or examination to any other University.

A handwritten signature in black ink that reads "L. P. Culligan". The signature is written in a cursive style with a loop under the "Culligan" part.

.....
(Signature of Candidate)

16th day of September 2015

ABSTRACT

Drinking water distribution systems are considered to be the main source of drinking water contamination yet to be fully addressed. The deterioration of water quality within distribution systems is a result of a complex set of interrelated factors, currently not fully understood by water utilities, as their effect on water quality must be considered simultaneously, which creates considerable difficulty. Routine sampling and monitoring of water can play an important role in ensuring that water quality does not deteriorate within a distribution system. However, solely taking such an approach can only provide limited information, as sampling can only provide information regarding water quality at sampling locations and monitoring cannot be used to predict future water quality. The use of deterministic mathematical models is one of the best tools available to both researchers and engineers in order to gain greater insight into the numerous interrelated processes affecting water quality within distribution systems and to determine effective ways of maintaining high quality water within distribution systems. Consequently, the Expanded Comprehensive Disinfection and Water Quality Model, Version 2 (CDWQ-E₂) has been developed to utilise the latest advances in the fields of microbial growth and residual disinfectant decay modelling in order to provide greater insight into the relationship between the biological, chemical, and hydraulic factors affecting water quality. Various tools have been incorporated into the CDWQ-E₂ model to enhance its interpretative capabilities. A theoretical distribution system is used to show the fundamental soundness of the model and to exhibit its features. The results of the simulations performed demonstrate the importance of both the maintenance of an adequate disinfectant residual and low substrate concentrations in order to keep biological growth below acceptable limits. Furthermore, the simulated results testify to the potential for nitrification to occur in distribution systems utilising chloramine as a secondary disinfectant, which can establish a positive feedback loop with regard to monochloramine decay and have severe implications for drinking water quality.

TABLE OF CONTENTS

DECLARATION	2
ABSTRACT.....	3
LIST OF FIGURES.....	8
LIST OF TABLES.....	16
1 INTRODUCTION.....	17
1.1 Research Background.....	17
1.2 Research Motivation.....	18
1.3 Problem Statement.....	18
1.4 Outline of Chapters.....	19
1.4.1 Literature Review.....	19
1.4.2 Model Development.....	19
1.4.3 Batch Version Simulations.....	19
1.4.4 Distribution System Simulations.....	19
2 LITERATURE REVIEW.....	21
2.1 Microbial Growth.....	21
2.2 Impact of Microbial Growth on Water Quality.....	22
2.3 Factors Influencing Microbial Growth.....	24
2.3.1 Secondary Disinfection.....	25
2.3.2 Availability of Nutrients.....	27
2.3.3 Temperature.....	28
2.3.4 Microbial Content of Treated Water.....	28
2.3.5 Flow Velocity and Water Age.....	29
2.3.6 Pipe Material.....	30
2.4 Water Quality Modelling.....	32
3 MODEL DEVELOPMENT.....	39
3.1 Microbial Modelling.....	40

3.1.1	Biomass Growth	40
3.1.2	Aerobic Substrate Respiration	41
3.1.3	Anoxic Substrate Respiration	43
3.1.4	Endogenous Decay	45
3.1.5	Consumption of Electron Acceptor	46
3.1.6	Biofilm Modelling	47
3.2	Chlorine Reaction Submodel	51
3.2.1	Equilibrium Reactions (E_1 - E_3)	53
3.2.2	Chloramine Autocatalytic Decay Reactions (AD_1 - AD_5)	53
3.2.3	Cometabolism Reactions (B_1 - B_2)	53
3.2.4	Oxidation Reactions (OX_1 - OX_5)	54
3.2.5	Oxidation of Corrosion Products (Cr_1 - Cr_3)	55
3.2.6	Surface Catalysis (SC_1)	55
3.3	Disinfection	56
3.4	Temperature	56
3.5	pH	57
3.6	Mass Transport	59
3.6.1	Pipe Elements	60
3.6.2	Reservoir Elements	64
3.6.3	Nodes	69
3.7	Parameters and Reaction Constants Incorporated in CDWQ- E_2	73
3.8	Mass-Balance Equations	82
3.8.1	General Reactions	82
3.8.2	Specific Reaction Rates	83
3.9	CDWQ- E_2 Algorithm	106
4	BATCH VERSION SIMULATIONS	112
4.1	Introduction	112
4.2	Batch Simulations	114

4.2.1	Influence of pH on Water Quality	115
4.2.2	Influence of Temperature on Water Quality	126
4.2.3	Influence of Carbonate Buffer on Water Quality.....	134
4.2.4	Mass Closure Check	143
5	DISTRIBUTION SYSTEM SIMULATIONS.....	145
5.1	Introduction	145
5.2	Results and Discussion	150
5.2.1	Baseline Scenario	150
5.2.2	Remedial Alternatives.....	178
6	SUMMARY AND RECOMMENDATIONS FOR FUTURE RESEARCH	189
6.1	Summary	189
6.2	Future Research	190
7	REFERENCES.....	191
A.	APPENDIX A.....	204
A.1	Organic Matter and Biomass as Chemical Oxygen Demand.....	204
A.2	Moles of Carbon and Nitrogen in Biomass and Organic Matter.....	205
A.3	Cells/ml per $\mu\text{gCOD/l}$	206
A.4	Active Biomass Density	206
B.	APPENDIX B.....	207
B.1	Monoprotic Acid Derivation.....	207
B.2	Diprotic Acid Derivation	208
C.	APPENDIX C.....	210
C.1	Input Data	210
D.	APPENDIX D.....	235
D.1	Reduce Surface Catalysis by Coating Concrete Pipes	235
D.2	Use of Biofiltration to Reduce Input BOM	254
D.3	Use of a 1:1 Cl:N Ratio at the Treatment Plant to Reduce Input Ammonia	272
D.4	Booster Chloramination.....	290

D.5	Improve Primary Disinfection	308
D.6	Reduce Input BOM and Excess Ammonia.....	326
D.7	Reduce both Input BOM and Excess Ammonia, combined with Booster Chloramination.	345
D.8	Reduce both Input BOM and Excess Ammonia, as well as Surface Catalysis by Coating Concrete Pipes	365

LIST OF FIGURES

Figure 2-1: Schematic representation of the Unified Model for active biomass, EPS, SMP and inert biomass	37
Figure 3-1: Schematic Diagram Depicting Uniform Distribution of the 5 Species of Biofilm Biomass	48
Figure 3-2: Reaction Pathways incorporated in the CDWQ-CL ₂ submodel	52
Figure 3-3: Effect of Pipe Element Size on Dispersion Characteristics	60
Figure 3-4: Graph of the Exact Solution for Steady-State Advection-Dispersion with First-Order Reaction for Several Values of Dispersion Coefficient (D).....	62
Figure 3-5: Change in suspended constituent concentration for a pipe element	64
Figure 3-6: Single-Compartment Model	65
Figure 3-7: Two-Compartment Model	66
Figure 3-8: Three-Compartment Model	67
Figure 3-9: Typical Node Junction.....	70
Figure 3-10: Typical Treatment Plant Node Junction.....	71
Figure 3-11: Typical Booster Node Junction	72
Figure 3-12: CDWQ-E ₂ Algorithm.....	107
Figure 3-13: Schematic diagram of the method used to define element node and element concentrations based on imported pipe node concentrations for dissolved and suspended constituents	109
Figure 3-14: Schematic diagram of the method used to define element fixed biofilm concentrations based on imported pipe biofilm concentrations	109
Figure 4-1: Monochloramine concentration against time for varying pH values.....	115
Figure 4-2: BOM ₁ concentration against time for varying pH values	116
Figure 4-3: BOM ₂ concentration against time for varying pH values	116
Figure 4-4: Ammonia concentration against time for varying pH values	117
Figure 4-5: Nitrite concentration against time for varying pH values	117
Figure 4-6: Nitrate concentration against time for varying pH values	118
Figure 4-7: Suspended heterotroph concentration and stability factor against time for varying pH values	118
Figure 4-8: Suspended AOB concentration and stability factor against time for varying pH values..	119
Figure 4-9: Suspended NOB concentration and stability factor against time for varying pH values .	119
Figure 4-10: Relative contribution of monochloramine loss mechanisms for varying pH values	120
Figure 4-11: Relative contribution of BOM ₁ loss mechanisms for varying pH values	122
Figure 4-12: Relative contribution of BOM ₂ loss and formation mechanisms for varying pH values	123

Figure 4-13: UAP concentration against time for varying pH values	124
Figure 4-14: BAP concentration against time for varying pH values	124
Figure 4-15: EPS concentration against time for varying pH values	125
Figure 4-16: Monochloramine concentration against time for varying temperatures	126
Figure 4-17: BOM ₁ concentration against time for varying temperatures	127
Figure 4-18: BOM ₂ concentration against time for varying temperatures	127
Figure 4-19: Ammonia concentration against time for varying temperatures	128
Figure 4-20: Nitrite concentration against time for varying temperatures	128
Figure 4-21: Nitrate concentration against time for varying temperatures	129
Figure 4-22: Suspended heterotroph concentration and stability factor against time for varying temperatures	129
Figure 4-23: AOB concentration and stability factor against time for varying temperatures	130
Figure 4-24: NOB concentration and stability factor against time for varying temperatures	130
Figure 4-25: Relative contribution of monochloramine loss mechanisms for varying temperatures	131
Figure 4-26: Relative contribution of BOM ₁ loss mechanisms for varying temperatures	132
Figure 4-27: Relative contribution of BOM ₂ loss and formation mechanisms for varying temperatures	132
Figure 4-28: UAP concentration against time for varying temperatures	133
Figure 4-29: BAP concentration against time for varying temperatures	133
Figure 4-30: EPS concentration against time for varying temperatures	134
Figure 4-31: Monochloramine concentration against time for varying total carbonate concentrations	135
Figure 4-32: BOM ₁ concentration against time for varying total carbonate concentrations	135
Figure 4-33: BOM ₂ concentration against time for varying total carbonate concentrations	136
Figure 4-34: Ammonia concentration against time for varying total carbonate concentrations	136
Figure 4-35: Nitrite concentration against time for varying total carbonate concentrations	137
Figure 4-36: Nitrate concentration against time for varying total carbonate concentrations	137
Figure 4-37: Suspended heterotroph concentration and stability factor against time for varying total carbonate concentrations	138
Figure 4-38: AOB concentration and stability factor against time for varying total carbonate concentrations	138
Figure 4-39: NOB concentration and stability factor against time for varying total carbonate concentrations	139

Figure 4-40: Relative contribution of monochloramine loss mechanisms for varying carbonate concentrations	140
Figure 4-41: Relative contribution of BOM ₁ loss mechanisms for varying carbonate concentrations	140
Figure 4-42: Relative contribution of BOM ₂ loss and formation mechanisms for varying carbonate concentrations	141
Figure 4-43: UAP concentration against time for varying total carbonate concentrations	142
Figure 4-44: BAP concentration against time for varying total carbonate concentrations	142
Figure 4-45: EPS concentration against time for varying total carbonate concentrations	143
Figure 5-1: Schematic of distribution system detailing pipe numbers	146
Figure 5-2: Schematic of distribution system detailing node numbers	147
Figure 5-3: Monochloramine concentration profile for Baseline Scenario	150
Figure 5-4: Monochloramine loss mechanisms and locations for Baseline Scenario	152
Figure 5-5: BOM ₁ concentration profile for Baseline Scenario	154
Figure 5-6: BOM ₂ concentration profile for Baseline Scenario	155
Figure 5-7: Suspended heterotroph concentration profile for Baseline Scenario	156
Figure 5-8: Fixed heterotroph concentration profile for Baseline Scenario	158
Figure 5-9: Suspended heterotroph stability factor profile	159
Figure 5-10: Fixed heterotroph stability factor profile	160
Figure 5-11: Total ammonia concentration profile for Baseline Scenario	162
Figure 5-12: Suspended AOB concentration profile for Baseline Scenario	163
Figure 5-13: Fixed AOB concentration profile for Baseline Scenario	164
Figure 5-14: Suspended AOB stability factor profile	165
Figure 5-15: Fixed AOB stability factor profile	166
Figure 5-16: Nitrite concentration profile for Baseline Scenario	167
Figure 5-17: Suspended NOB concentration profile for Baseline Scenario	168
Figure 5-18: Fixed NOB concentration profile for Baseline Scenario	169
Figure 5-19: Suspended NOB stability factor profile	170
Figure 5-20: Fixed NOB stability factor profile	171
Figure 5-21: Nitrate concentration profile for Baseline Scenario	172
Figure 5-22: UAP concentration profile for Baseline Scenario	173
Figure 5-23: BAP concentration profile for Baseline Scenario	174
Figure 5-24: Suspended EPS concentration profile for Baseline Scenario	175
Figure 5-25: Fixed EPS concentration profile for Baseline Scenario	176

Figure 5-26: Dissolved oxygen concentration profile for Baseline Scenario	177
Figure 5-27: Comparison of Maximum Suspended Heterotroph Concentration for Various Simulations.....	182
Figure 5-28: Comparison of Total Ammonia Concentration for Various Simulations	182
Figure 5-29: Comparison of Maximum Nitrite Concentration for Simulations	183
Figure 5-30: Comparison of Maximum Nitrate Concentration for Various Simulations	183
Figure 5-31: Total loss of monochloramine for simulations performed due to various loss mechanisms	184
Figure 5-32: Relative loss of monochloramine for all simulations performed due to various loss mechanisms	184
Figure 5-33: Comparison of simulation results with respect to SANS 241-1:2011 limits	185
Figure D-1: Monochloramine concentration profile for Alternative 1	235
Figure D-2: Monochloramine loss mechanisms and locations for Alternative 1.....	236
Figure D-3: BOM ₁ concentration profile for Alternative 1	238
Figure D-4: BOM ₂ concentration profile for Alternative 1	239
Figure D-5: Suspended heterotroph concentration profile for Alternative 1.....	240
Figure D-6: Fixed heterotroph concentration profile for Alternative 1.....	241
Figure D-7: Total ammonia concentration profile for Alternative 1.....	242
Figure D-8: Suspended AOB concentration profile for Alternative 1	243
Figure D-9: Fixed AOB concentration profile for Alternative 1.....	244
Figure D-10: Nitrite concentration profile for Alternative 1.....	245
Figure D-11: Suspended NOB concentration profile for Alternative 1	246
Figure D-12: Fixed NOB concentration profile for Alternative 1	247
Figure D-13: Nitrate concentration profile for Alternative 1.....	248
Figure D-14: UAP concentration profile for Alternative 1	249
Figure D-15: BAP concentration profile for Alternative 1.....	250
Figure D-16: Suspended EPS concentration profile for Alternative 1.....	251
Figure D-17: Fixed EPS concentration profile for Alternative 1	252
Figure D-18: Dissolved oxygen concentration profile for Alternative 1	253
Figure D-19: Monochloramine concentration profile for Alternative 2	254
Figure D-20: Monochloramine loss mechanisms and locations for Alternative 2.....	255
Figure D-21: BOM ₁ concentration profile for Alternative 2.....	256
Figure D-22: BOM ₂ concentration profile for Alternative 2.....	257
Figure D-23: Suspended heterotroph concentration profile for Alternative 2.....	258

Figure D-24: Fixed heterotroph concentration profile for Alternative 2	259
Figure D-25: Total ammonia concentration profile for Alternative 2	260
Figure D-26: Suspended AOB concentration profile for Alternative 2	261
Figure D-27: Fixed AOB concentration profile for Alternative 2	262
Figure D-28: Nitrite concentration profile for Alternative 2	263
Figure D-29: Suspended NOB concentration profile for Alternative 2	264
Figure D-30: Fixed NOB concentration profile for Alternative 2	265
Figure D-31: Nitrate concentration profile for Alternative 2	266
Figure D-32: UAP concentration profile for Alternative 2	267
Figure D-33: BAP concentration profile for Alternative 2	268
Figure D-34: Suspended EPS concentration profile for Alternative 2	269
Figure D-35: Fixed EPS concentration profile for Alternative 2	270
Figure D-36: Dissolved oxygen concentration profile for Alternative 2	271
Figure D-37: Monochloramine concentration profile for Alternative 3	272
Figure D-38: Monochloramine loss mechanisms and locations for Alternative 3	273
Figure D-39: BOM ₁ concentration profile for Alternative 3	274
Figure D-40: BOM ₂ concentration profile for Alternative 3	275
Figure D-41: Suspended heterotroph concentration profile for Alternative 3	276
Figure D-42: Fixed heterotroph concentration profile for Alternative 3	277
Figure D-43: Total ammonia concentration profile for Alternative 3	278
Figure D-44: Suspended AOB concentration profile for Alternative 3	279
Figure D-45: Fixed AOB concentration profile for Alternative 3	280
Figure D-46: Nitrite concentration profile for Alternative 3	281
Figure D-47: Suspended NOB concentration profile for Alternative 3	282
Figure D-48: Fixed NOB concentration profile for Alternative 3	283
Figure D-49: Nitrate concentration profile for Alternative 3	284
Figure D-50: UAP concentration profile for Alternative 3	285
Figure D-51: BAP concentration profile for Alternative 3	286
Figure D-52: Suspended EPS concentration profile for Alternative 3	287
Figure D-53: Fixed EPS concentration profile for Alternative 3	288
Figure D-54: Dissolved oxygen concentration profile for Alternative 3	289
Figure D-55: Monochloramine concentration profile for Alternative 4	290
Figure D-56: Monochloramine loss mechanisms and locations for Alternative 4	291
Figure D-57: BOM ₁ concentration profile for Alternative 4	292

Figure D-58: BOM ₂ concentration profile for Alternative 4.....	293
Figure D-59: Suspended heterotroph concentration profile for Alternative 4.....	294
Figure D-60: Fixed heterotroph concentration profile for Alternative 4.....	295
Figure D-61: Total ammonia concentration profile for Alternative 4.....	296
Figure D-62: Suspended AOB concentration profile for Alternative 4.....	297
Figure D-63: Fixed AOB concentration profile for Alternative 4.....	298
Figure D-64: Nitrite concentration profile for Alternative 4.....	299
Figure D-65: Suspended NOB concentration profile for Alternative 4.....	300
Figure D-66: Fixed NOB concentration profile for Alternative 4.....	301
Figure D-67: Nitrate concentration profile for Alternative 4.....	302
Figure D-68: UAP concentration profile for Alternative 4.....	303
Figure D-69: BAP concentration profile for Alternative 4.....	304
Figure D-70: Suspended EPS concentration profile for Alternative 4.....	305
Figure D-71: Fixed EPS concentration profile for Alternative 4.....	306
Figure D-72: Dissolved oxygen concentration profile for Alternative 4.....	307
Figure D-73: Monochloramine concentration profile for Alternative 5.....	308
Figure D-74: Monochloramine loss mechanisms and locations for Alternative 5.....	309
Figure D-75: BOM ₁ concentration profile for Alternative 5.....	310
Figure D-76: BOM ₂ concentration profile for Alternative 5.....	311
Figure D-77: Suspended heterotroph concentration profile for Alternative 5.....	312
Figure D-78: Fixed heterotroph concentration profile for Alternative 5.....	313
Figure D-79: Ammonia concentration profile for Alternative 5.....	314
Figure D-80: Suspended AOB concentration profile for Alternative 5.....	315
Figure D-81: Fixed AOB concentration profile for Alternative 5.....	316
Figure D-82: Nitrite concentration profile for Alternative 5.....	317
Figure D-83: Suspended NOB concentration profile for Alternative 5.....	318
Figure D-84: Fixed NOB concentration profile for Alternative 5.....	319
Figure D-85: Nitrate concentration profile for Alternative 5.....	320
Figure D-86: UAP concentration profile for Alternative 5.....	321
Figure D-87: BAP concentration profile for Alternative 5.....	322
Figure D-88: Suspended EPS concentration profile for Alternative 5.....	323
Figure D-89: Fixed EPS concentration profile for Alternative 5.....	324
Figure D-90: Dissolved oxygen concentration profile for Alternative 5.....	325
Figure D-91: Monochloramine concentration profile for Alternative 6.....	326

Figure D-92: Monochloramine loss mechanisms and locations for Alternative 6.....	327
Figure D-93: BOM ₁ concentration profile for Alternative 6.....	329
Figure D-94: BOM ₂ concentration profile for Alternative 6.....	330
Figure D-95: Suspended heterotroph concentration profile for Alternative 6.....	331
Figure D-96: Fixed heterotroph concentration profile for Alternative 6.....	332
Figure D-97: Total ammonia concentration profile for Alternative 6.....	333
Figure D-98: Suspended AOB concentration profile for Alternative 6.....	334
Figure D-99: Fixed AOB concentration profile for Alternative 6.....	335
Figure D-100: Nitrite concentration profile for Alternative 6.....	336
Figure D-101: Suspended NOB concentration profile for Alternative 6.....	337
Figure D-102: Fixed NOB concentration profile for Alternative 6.....	338
Figure D-103: Nitrate concentration profile for Alternative 6.....	339
Figure D-104: UAP concentration profile for Alternative 6.....	340
Figure D-105: BAP concentration profile for Alternative 6.....	341
Figure D-106: Suspended EPS concentration profile for Alternative 6.....	342
Figure D-107: Fixed EPS concentration profile for Alternative 6.....	343
Figure D-108: Dissolved oxygen concentration profile for Alternative 6.....	344
Figure D-109: Monochloramine concentration profile for Alternative 7.....	345
Figure D-110: Monochloramine loss mechanisms and locations for Alternative 7.....	346
Figure D-111: BOM ₁ concentration profile for Alternative 7.....	348
Figure D-112: BOM ₂ concentration profile for Alternative 7.....	349
Figure D-113: Suspended heterotroph concentration profile for Alternative 7.....	350
Figure D-114: Suspended heterotroph concentration for final day within Pipe 487.....	351
Figure D-115: Fixed heterotroph concentration profile for Alternative 7.....	352
Figure D-116: Total ammonia concentration profile for Alternative 7.....	353
Figure D-117: Suspended AOB concentration profile for Alternative 7.....	354
Figure D-118: Fixed AOB concentration profile for Alternative 7.....	355
Figure D-119: Nitrite concentration profile for Alternative 7.....	356
Figure D-120: Suspended NOB concentration profile for Alternative 7.....	357
Figure D-121: Fixed NOB concentration profile for Alternative 7.....	358
Figure D-122: Nitrate concentration profile for Alternative 7.....	359
Figure D-123: UAP concentration profile for Alternative 7.....	360
Figure D-124: BAP concentration profile for Alternative 7.....	361
Figure D-125: Suspended EPS concentration profile for Alternative 7.....	362

Figure D-126: Fixed EPS concentration profile for Alternative 7	363
Figure D-127: Dissolved oxygen concentration profile for Alternative 7	364
Figure D-128: Monochloramine concentration profile for Alternative 8	365
Figure D-129: Monochloramine loss mechanisms and locations for Alternative 8.....	366
Figure D-130: BOM ₁ concentration profile for Alternative 8.....	368
Figure D-131: BOM ₂ concentration profile for Alternative 8.....	369
Figure D-132: Suspended heterotroph concentration profile for Alternative 8.....	370
Figure D-133: Fixed heterotroph concentration profile for Alternative 8.....	371
Figure D-134: Total ammonia concentration profile for Alternative 8.....	372
Figure D-135: Suspended AOB concentration profile for Alternative 8	373
Figure D-136: Fixed AOB concentration profile for Alternative 8.....	374
Figure D-137: Nitrite concentration profile for Alternative 8.....	375
Figure D-138: Suspended NOB concentration profile for Alternative 8	376
Figure D-139: Fixed NOB concentration profile for Alternative 8	377
Figure D-140: Nitrate concentration profile for Alternative 8.....	378
Figure D-141: UAP concentration profile for Alternative 8	379
Figure D-142: BAP concentration profile for Alternative 8.....	380
Figure D-143: Suspended EPS concentration profile for Alternative 8.....	381
Figure D-144: Fixed EPS concentration profile for Alternative 8.....	382
Figure D-145: Dissolved oxygen concentration profile for Alternative 8	383

LIST OF TABLES

Table 3-1: Reactions Constants Used in the CDWQ-Cl ₂ Reaction Submodel	75
Table 3-2: Conversion Factors.....	76
Table 3-3: Temperature Adjustment Factors.....	76
Table 3-4: Biological Parameters	78
Table 3-5: Oxygen-Related Parameters	79
Table 3-6: Biofilm Parameters	79
Table 3-7: Disinfection Parameters.....	81
Table 4-1: Initial Conditions	114
Table 4-2: Mass-balance closure errors for batch simulation	143
Table 5-1: Relevant SANS 241-1:2011 Water Quality Determinands	149
Table 5-2: Mass-balance closure errors for baseline simulation	178
Table C-1: Physical pipe data	210
Table C-2: Hydraulic flow regime (m ³ /h)	213
Table C-3: Initial node concentrations for suspended and dissolved constituents	227
Table C-4: Initial pipe biofilm concentrations.....	231
Table C-5: Treatment plant inputs for simulations performed.....	234
Table C-6: Booster chloramination inputs for Alternative 4.....	234
Table C-7: Booster chloramination inputs for Alternative 7.....	234

1 INTRODUCTION

1.1 Research Background

The provision of drinking water of acceptable quality is essential for human wellbeing. Drinking water is initially extracted from within natural water bodies or man-made reservoirs and is subsequently transported to a water treatment plant where the water is treated to meet acceptable standards. Following treatment, water is delivered to consumers via a distribution system (Jegatheesan et al, 2003).

Distribution infrastructure is typically the most important asset of a water utility and consists of pipes, pumps, valves, storage tanks, reservoirs, meters, fittings and other hydraulic components that connect treatment plants to consumers' taps. The various components are required in order for the distribution to be capable of delivering water to all of the system's customers in sufficient quantities for potable drinking water and fire protection, at the appropriate pressure, with minimum loss of water of a safe and acceptable quality, and as economically as possible (Male & Walski, 1991 in National Research Council of the National Academies, 2006).

In the past it was assumed that if water was treated to an acceptable standard, the quality of water at a consumer's tap would also be of an acceptable standard (American Water Works Association Research Foundation, 2007). Ideally, there should be no change in water quality from the time that water is distributed following treatment to the time that it reaches the point of use. However, in reality, potable water distribution systems function as continuously-fed reactors with complex physical, chemical and biological reactions taking place within drinking water distribution systems and nowadays distribution systems are considered to be the main source of drinking water contamination yet to be fully addressed (Robertson et al, 2003; Le Puil, 2004; National Research Council of the National Academies, 2006).

Reducing and eliminating contamination of water emanating from distribution systems requires addressing three components of distribution system integrity: physical integrity, which refers to the maintenance of a physical barrier between the distribution system and the external environment; hydraulic integrity, which refers to the maintenance of an acceptable flow rate and pressure, bearing in mind the requirements with respect to both potable drinking water quality and fire provision; and water quality integrity, which refers to the maintenance of finished water quality by preventing internally derived contamination (National Research Council of the National Academies, 2006).

A loss of either physical and/or hydraulic integrity can lead to the introduction of contaminants into the distribution system. Such external contamination events can introduce nutrients required for microorganism growth or decrease disinfectant concentrations within the distribution system, thereby compromising the water quality of the distribution system. However, even in the absence of external contamination, water quality can decrease due to chemical, physical and biological transformations taking place within the distribution system, as mentioned previously (Clark et al, 1993; Robertson et al, 2003; National Research Council of the National Academies, 2006; Srinivasan & Harrington, 2007).

These transformations can have severe impacts on water quality. The most critical factor that can directly influence water quality is microbial growth, particularly the development of biofilms.

1.2 Research Motivation

As discussed previously, drinking water distribution systems are considered to be the main source of drinking water contamination yet to be fully addressed. Contamination in this case refers to a decrease in water quality from the time that it is treated at a water treatment plant to the time that it reaches consumers' taps. This loss of water quality is a result of a complex set of interrelated factors. The use of deterministic mathematical models can provide researchers and engineers with significant insight into the relationship between the factors affecting water quality and hence the development of a mathematical model that incorporates the latest advances in the field of microbial growth modelling can provide greater insight into and help to address the concerns surrounding post-treatment water quality.

1.3 Problem Statement

A number of interrelated factors affect the quality of treated water in distribution systems and, as the relationship between these factors and ultimately water quality is not fully understood, drinking water utilities, sometimes, have difficulties in providing consumers with water that is of an acceptable quality.

1.4 Outline of Chapters

1.4.1 Literature Review

The literature review details the consequences of the deterioration of water quality within drinking water distribution systems, the most significant factors which cause this deterioration, the most prominent mathematical models that have been developed to assess water quality within distribution systems and the extent to which existing models are capable of accounting for the factors which cause deterioration of water quality.

1.4.2 Model Development

A detailed explanation of the model processes and the rationale for the incorporation of these processes are presented in this chapter. A detailed description of the microbial and disinfectant submodels are provided. In addition, the methods used to define mass transport throughout a distribution system are given. This includes an explanation of how the CDWQ-E₂ model defines the hydraulic system to be analysed and the means by which both the advective flow of suspended and dissolved constituents throughout a distribution system and mixing in storage tanks and/or reservoirs are modelled. All parameter values and mass-balance equations incorporated in the model are provided to demonstrate how the processes defined previously in this chapter are accounted for mathematically. Finally, an algorithm based on the ISO 5807:1985 standard is provided to describe means by which the mathematical processes are coded.

1.4.3 Batch Version Simulations

The results of several batch simulations are presented in this chapter. Various interpretive tools, incorporated as part of the model to explain the reasons for changes in water quality, are demonstrated and the results of mass-closure tests are provided to demonstrate that the model is sound with regard to the law of conservation of mass.

1.4.4 Distribution System Simulations

The results of a simulation applied to a distribution system are provided. As is the case with the batch version, various interpretive tools are used to explain the reasons for changes in water quality throughout the distribution system, in addition to the locations within the distribution system where these changes are most significant. The aforementioned tools are used to provide insight into what possible remedial actions could be utilised to improve the water quality for the simulated system

and the results of these additional simulations are given. It is demonstrated that the trends observed within the system are in accordance with those found in literature and that the model does not violate the law of conservation of mass.

2 LITERATURE REVIEW

2.1 Microbial Growth

Of particular concern with regard to water quality deterioration is the development of biofilms within distribution systems. Biofilms are defined as matrix-enclosed microbial populations, including bacteria, viruses, fungi and protozoa adherent to each other and/or to surfaces and interfaces (Costerton et al, 1995; Stoodley et al, 2002). The matrix itself is composed of extracellular polymeric substances (EPS), which have highly diverse chemical compositions and may include substituted and unsubstituted polysaccharides, substituted and unsubstituted proteins, nucleic acids and phospholipids (Wingender, Neu & Flemming, 1999 in Stoodley et al, 2002). For many years biofilms were not recognised and only planktonic growth was considered. However, since biofilm growth was first reported by Zobell and Anderson (1936) and the ubiquity of biofilms was later reported by Costerton, Geesey and Cheng (1978), increased attention has been placed on the study of biofilms (Costerton et al, 1995; Stoodley et al, 2002; Lapidou & Rittmann, 2004; Bocoş, Ciatarâş & Farkas, 2012).

It is now acknowledged that biofilms constitute a distinct growth phase of bacteria that is significantly different to the planktonic growth phase. Bacterial biofilms are considerably more efficient than mixed populations of floating, planktonic microorganisms. The biofilm matrix is capable of protecting biofilm bacteria from variations that occur in the bulk water by primitive homeostasis (Costerton et al, 1995). When compared to planktonic bacteria, biofilm bacteria and other biofilm inhabitants display superior characteristics due to specialisation and complex relationships that are established within the biofilm (Costerton, 1994 in Bocoş, Ciatarâş & Farkas, 2012). The community structure of bacteria within the biofilm results in increased chances of survival in an oligotrophic environment by offering ecological micro-niches, establishing intraspecific and interspecific cooperation relationships by communication via quorum sensing and improving individuals' resistance to disinfection agents (Bocoş, Ciatarâş & Farkas, 2012).

As a result of the abovementioned advantages, biofilms dominate in all nutrient-sufficient aquatic systems (Costerton et al, 1995) and drinking water distribution systems are no exception. Servais et al (1992, in Joret et al, 2005) compared the abundance of suspended and biofilm bacteria in 100 millimetre diameter pipes in a Parisian suburb that lacked a chlorine residual and found that biofilm bacteria numbers were between 53 to 77 times greater than the numbers of suspended bacteria. Similar findings have been made for other European distribution systems (Servais, Laurent & Randon, 1995, in Joret et al, 2005).

2.2 Impact of Microbial Growth on Water Quality

Biofilm growth in distribution systems can severely decrease water quality and affect the ability of a water authority to deliver high-quality water to consumers (Angles & Chandy, 2001). Biofilm bacteria detach from surfaces that they inhabit thereby contaminating water (National Research Council of the National Academies, 2006). The majority of drinking water-related health problems are a consequence of microbial contamination (Riley, Gerba & Elimelech, 2011 in Bocoş, Ciatarâş & Farkas, 2012) and thus it can be said that biofilms act as microbial reservoirs for further contamination (Szewzyk et al, 2000; Wingender & Flemming, 2011 in Bocoş, Ciatarâş & Farkas, 2012).

Opportunistic pathogens have been detected in biofilms and their release may be the most significant health risk associated with drinking water biofilms. Examples of opportunistic pathogenic bacteria found in distribution systems include *Legionella*, *Aeromonas spp.*, and *Mycobacterium spp.* (National Research Council of the National Academies, 2006). *Mycobacterium spp.* may be of particular concern in South Africa, where 12.2% of the population, as of 2012, was HIV positive (Shisana et al, 2014), as they are a major cause of disseminated opportunistic infections in immunocompromised patients and the second most common cause of death in HIV-positive patients (Joret et al, 2005). Therefore, water quality utilities in South Africa have an even greater responsibility to provide high quality drinking water (Venter, 2010).

Biofilms also have the potential to support the growth of microorganisms which may result in water failing to meet regulatory standards. Although coliforms present in biofilms are generally considered to pose little, if any, threat to human health, they may detach from biofilms, resulting in increased coliform detection despite the fact that the physical integrity of the system and disinfectant residual have been maintained. Even though these coliforms are generally low risk, they may indirectly pose a risk to human health by masking the presence of potentially harmful bacteria introduced during a contamination event and may also result in failure to comply with set standards for distribution system water quality in countries where these are in place (National Research Council of the National Academies, 2006).

Heterotrophs are the most common group of bacteria in distribution systems (Geldreich, 1996 in Wooschlager, 2000) and the growth of heterotrophic bacteria in biofilms is another concern in countries that are required to monitor their presence. Although heterotrophic bacteria do not typically pose a threat to the general population, they may affect the health of immunocompromised individuals (National Research Council of the National Academies, 2006) and

hence they pose a considerable threat to the large proportion of South Africa's population given the large proportion of the country's population that has acquired immune deficiency syndrome (AIDS).

Protozoa are relatively large microorganisms and typically enter distribution systems in cases where surface water is unfiltered or where uncovered finished water reservoirs exist (Geldreich, 1996 in Wooschlager, 2000). As heterotrophic bacteria form the basis of the food web in drinking water distribution systems, with protozoa forming the next trophic level (Bocoş, Ciatarâş & Farkas, 2012), biofilms may play a role in the persistence of pathogenic protozoa in distribution systems (Joret et al, 2005). Some protozoa, such as *Giardia* spp. and *Cryptosporidium* spp. may persist in drinking water, resist different disinfection procedures and accumulate in biofilms in the form of cysts and oocysts respectively (Bocoş, Ciatarâş & Farkas, 2012). A study by Helmi et al (2008 in Bocoş, Ciatarâş & Farkas, 2012) which investigated the interaction of *Giardia lamblia* and *Cryptosporidium parvum* oocysts in drinking water biofilms found that protozoa are able to attach in the biofilm matrix and survive for extended periods of time (Bocoş, Ciatarâş & Farkas, 2012). Both species of protozoa pose a significant threat to individuals diagnosed with AIDS (Metcalf & Eddy, Inc., 2004) and are therefore of particular concern in South Africa.

According to Storey and Ashbolt (2001, 2003 in Joret et al, 2005) biofilms have the potential to harbour enteric viruses. Bocoş, Ciatarâş & Farkas (2012) state that while there is no evidence that viruses are capable of multiplication within environmental biofilms, they may be able to survive for extended periods of time enclosed within the matrix, where they are afforded additional protection, until such time that they detach and find a host in the bulk water.

Nitrifying bacteria may also be present in biofilms and the presence of such organisms may result in episodes of nitrification in distribution systems with long detention times and where chloramine is used as a secondary disinfectant (Wolfe et al, 1990 in National Research Council of the National Academies, 2006). Biological nitrification occurs when bacteria oxidise reduced nitrogen compounds, such as ammonia, to nitrite and then nitrate (National Research Council of the National Academies, 2006).

The most significant problem associated with nitrification in distribution systems is the subsequent loss of the chloramine disinfectant residual. This loss occurs because a reduction of ammonia results in an increased ratio of chlorine to ammonia nitrogen (National Research Council of the National Academies, 2006). This controls the stability of monochloramine, which itself is governed by a complex set of reactions (Jafvert & Valentine, 1992 in National Research Council of the National Academies, 2006). As this molar ratio approaches 1.5, a rapid loss of monochloramine occurs, which

is attributable to the eventual oxidation of N(III) to nitrogen gas and the release of more ammonia. The ammonia that is released can then be further oxidised by nitrifying bacteria thereby establishing a positive feedback loop. Ultimately the loss of disinfectant residual removes one of the controls against microbial growth within the distribution system, resulting in the associated problems described in this section (National Research Council of the National Academies, 2006).

In addition to the loss of chloramine, other less significant health effects of nitrification may be important for certain populations. Both nitrite and nitrate can cause blue baby syndrome which results in a blockage of oxygen transport (Bouchard, Williams & Surampalli, 1992 in National Research Council of the National Academies, 2006). While blue baby syndrome generally affects infants younger than six months of age, it can impact adults of certain ethnic groups and adults suffering from a genetic deficiency of certain enzymes (Bitton, 1994 in National Research Council of the National Academies, 2006). Secondly, nitrate may be reduced to nitrite in the stomach, which reacts with amines and amides to form N-nitroso compounds which, it is argued, may be linked to different types of cancer (Bouchard, Williams & Surampalli, 1992; De Roos et al, 2003 in National Research Council of the National Academies, 2006). Finally, nitrification causes a reduction in alkalinity and pH in low alkalinity waters, which may cause corrosion of lead and copper (National Research Council of the National Academies, 2006).

Further to the negative effects bacterial growth and the persistence of non-bacterial pathogens, biofilms in distribution systems can have other negative effects on water quality. Chemical compounds produced during biofilm metabolism can result in taste, odour and aesthetic deterioration of water (Bocoş, Ciatarâş & Farkas, 2012). More specifically, actinomycetes or fungi present in biofilms may cause taste and odour problems and subsequent consumer complaints (Burman, 1965, 1973; Olson, 1982 in National Research Council of the National Academies, 2006). The two most significant taste and odour-causing compounds associated with algae are geosmin and 2-methylisoborneol (MIB) (Srinivasan & Sorial, 2011). Biofilm bacteria can contribute to the corrosion of pipe surfaces (National Research Council of the National Academies, 2006). Biofilm growth can also increase the disinfectant demand at the pipe wall which can have significant effects on water quality (National Research Council of the National Academies, 2006).

2.3 Factors Influencing Microbial Growth

Given the adverse effects of excessive microbial growth within a distribution system it is critical to understand those factors that both directly and indirectly influence microbial growth within drinking water distribution systems, particularly the formation of biofilms.

Biostability is a term that refers to the overall tendency of water to promote microbial proliferation through the presence of the nutrients necessary for microbial growth or to suppress microbial proliferation through the provision and maintenance of an adequate disinfectant residual. Therefore, biostability is viewed as a means of assessing distribution system water quality. Generally, nutrients and the disinfectant residual act as counter forces: greater nutrient concentrations require greater disinfectant concentrations in order to limit bacterial growth (Le Puil, 2004). Biostability refers specifically to microorganisms within distribution systems and does not consider the ecology of opportunistic pathogens or coliforms (Le Puil, 2004). However, the bacteria considered as part of a biostability analysis typically represent the starting point of a food-chain for the aforementioned organisms, and as such biostability is a widely used measure of water quality (Payment & Robertson, 2004).

In addition to the maintenance of residual disinfectant and the availability of nutrients, other factors indirectly influence biostability and consequently their influence on water quality will also be discussed. These additional factors are: temperature, bacterial content of treated water, water velocity and age and pipe material.

2.3.1 Secondary Disinfection

Primary disinfection is applied with the aim of removing or inactivating pathogens in order to produce water that is free of microbial pathogens. Secondary disinfection follows primary disinfection and is intended to ensure the maintenance of a disinfectant residual throughout a distribution system (Haas, 1999 in Joret et al, 2005). Both free chlorine and chloramine are used extensively as secondary disinfectants to limit microbial regrowth (Angles & Chandy, 2001). The major forms of free chlorine are hypochlorous acid (HOCl) and hypochlorite ion (OCl⁻) while chloramines mostly consist of monochloramine (NH₂Cl), some dichloramine (NHCl₂) and occasionally, some trichloramine (NCl₃) (Woolschlager, 2000).

Chloramines are considerably less reactive than chlorine (Jacangelo & Olivieri, 1985 in Joret et al, 2005). At the same concentration, monochloramine has considerably less “disinfectant power” than free chlorine. Therefore, the use of monochloramine as a secondary disinfectant rather than free chlorine is advantageous in that it allows a higher residual to be maintained with longer residence times. However, the major disadvantage with using monochloramine as a secondary disinfectant is that it requires a higher concentration-time value to disinfect microorganisms (Joret et al, 2005).

More specifically, free chlorine is more effective than chloramine when acting on suspended microorganisms (Haas & Karra, 1984 in Woolschlager, 2000). Despite being less effective at limiting

the numbers of suspended bacteria, chloramines are widely considered to be more effective than chlorine in limiting biofilm growth (Berman, Rice & Hoff, 1988; LeChevallier, Cawthon & Lee, 1988b; Mathieu et al, 1992; Chen, Griebbe & Characklis 1993; Griebbe et al, 1994; Kirmeyer et al, 1993; Pernitsky, Finch & Huck, 1995; Camper, Goodrum & Jones, 1997; Norton & LeChevallier, 1997; Momba et al, 1999 in Joret et al, 2005). Even the maintenance of a chlorine residual can have only a limited effect on biofilm growth (LeChevallier, Lowry & Lee, 1990 in Angles & Chandy, 2001) due to the limited penetration of chlorine into biofilms (LeChevallier, Cawthon & Lee, 1988b; de Beer, Srinivasan & Stewart, 1994 in Angles & Chandy, 2001). In fact, researchers have demonstrated that biofilms are between 2-100 times more resistant to chloramine disinfection than suspended cells, while biofilms are up to 3000 times more resistant to free chlorine disinfection than suspended cells.

A concern often associated with the use of chlorine is the formation of carcinogenic disinfection by-products (DBPs) due to the high reactivity of free chlorine (National Research Council of the American Academies, 2006). DBPs form from reactions of disinfectants with natural organic matter either in the bulk water or associated with pipe deposits (Rossman et al, 2001). The DBPs that form most frequently and with the highest concentrations are trihalomethanes (THMs) and haloacetic acids (HAAs) (Metcalf & Eddy, Inc., 2004), although over 600 potentially harmful DBPs have been identified (Richardson, 1998 in National Research Council of the National Academies, 2006). While many of the DBPs found in chloraminated systems are the same as those found in systems practicing chlorination, the rates of formation of most DBPs are considerably lower in chloraminated systems, especially for THMs (Kirmeyer et al, 1993 in World Health Organisation, 2004; National Research Council of the National Academies, 2006). However, some researchers have reported that the formation of other DBPs, including haloketones, chloropicrin, cyanogen chloride, haloacetic acids, haloacetonitrites, aldehydes and chlorophenols can form when using chloramine (Krasner et al, 1989; Trussell & Montgomery, 1991; Bull & Kopfler, 1991 in World Health Organisation, 2004).

There is now a growing consensus however that the levels of DBPs found in drinking water are unlikely to prove harmful to human health (Joret et al, 2005). The American Academy of Microbiology state that “there is no direct and conclusive evidence that disinfection by-products affect human health in concentrations found in drinking water... Concerns over the toxicology of DBPs should not be allowed to compromise successful disinfection of drinking water, at least without sufficient data to support such decisions” (Ford & Colwell, 1996, p 27).

2.3.2 Availability of Nutrients

All the essential elements for biological life and the growth of microorganisms are present in distribution systems (Joret et al, 2005). The ratio of carbon, nitrogen and phosphorous required for bacterial growth is approximately 100C: 10N: 1P. Since carbon is needed in the largest quantities it is most frequently the limiting nutrient (Angles & Chandy, 2001), although phosphorous has also been shown to be the limiting nutrient in Nordic regions, Japan & North America where drinking water sources are rich with humic substances and in cases where phosphorus is effectively removed during water treatment processes by conventional coagulation-sedimentation technology. (Miettinen, Vartiainen & Martikainen, 1997; Sathasivan et al, 1997; Junha, 2002 in Henning et al, 2007).

Heterotrophic bacteria are involved in the carbon cycle and these organisms are very diverse in terms of their metabolism. They can use several electron acceptors such as oxygen, nitrates, nitrites, sulphates or ferric ions. In some cases, autotrophs, such as nitrifiers, can initiate the colonisation of the inner surface of distribution systems. By converting inorganic carbon to organic carbon, autotrophs produce a nutrient source for heterotrophs. In doing so, autotrophs can act as the primary initiators of a more complex food chain and make colonisation by heterotrophs possible even under low carbon conditions. Therefore multi-nutrient monitoring is necessary in order to control bacterial growth as the limitation of carbon source alone cannot control bacterial growth in a distribution system if other nutrients such as ammonia nitrogen are present in sufficient quantities (Le Puil, 2004).

However since carbon is widely considered as the limiting nutrient, several methods for the measurement of biodegradable or assimilable organic carbon are used to evaluate biological growth in distribution systems (Le Puil, 2004). Since organic carbon is generally considered to be the limiting nutrient for bacterial growth in distribution systems, assessment of biostability in distribution systems typically relies on biodegradable organic matter (BOM) levels in finished waters (Le Puil, 2004). In general cases, where carbon is the limiting nutrient, there is a positive correlation between the concentration of biodegradable organic matter (BOM) in drinking water and bacterial growth in distribution systems (van der Kooij, 1982; Owen et al, 1995 in Angles & Chandy, 2001).

Biodegradable dissolved organic carbon (BDOC) and assimilable organic carbon (AOC) have also been used, either individually or together, to characterise the biostability of drinking water. Van der Kooij (1982 in Le Puil, 2004) demonstrated that heterotrophic bacteria in a non-chlorinated distribution system did not increase when AOC was lower than 10 µg/L, while Le Chevallier, Babcock & Lee (1987 in Le Puil, 2004) state that for systems maintaining a 3-6 mg/L chlorine residual that coliform

regrowth may be limited by AOC levels less than 50-100 µg/L. Biological stability has also been associated with BDOC and Servais et al (1993 in Le Puil, 2004) found that a BDOC concentration of 0.16 mg/L or less in the finished water, with or without residual is the threshold for biological stability (Servais et al, 1993).

Conventional treatment typically results in treated with higher levels of AOC than biologically treated water. In a pilot study, Norton and LeChevallier (2000) found that *Mycobacterium* spp. were found in three out of four samples from conventionally treated water, but none were found in samples that had been biologically treated with free chlorine used a post-disinfectant.

In addition to organic carbon and reduced nitrogen, ferrous iron, manganese, dissolved hydrogen gas, bisulphate ions, hydrogen sulphide and thiosulphate can influence biological growth (Tuovinen et al, 1980; Tuovinen & Hsu, 1982; LeChevallier, Babcock & Lee 1987; Rittman & Huck, 1989 in Wooschlager, 2000).

2.3.3 Temperature

Drinking water temperature may be the parameter that has the most significant impact on bacterial growth and hence water quality. Generally, water temperatures above 15 °C result in considerably increased growth (LeChevallier, 1990 in Henning et al, 2007). Increased temperature typically results in increased microbial growth for two reasons. Firstly, substrate utilisation rates by bacteria increase (Zhang & DiGiano, 2002) and secondly, disinfectant loss increases (Wooschlager, 2000; Vikesland, Ozekin & Valentine, 2001). More specifically, *E. coli* and other coliform bacteria exhibit exceptionally slow growth at temperatures below 20 °C (Fransolet, Villers and Masschelin, 1985 in Henning et al, 2007), while coliform bacteria are only associated with water temperatures greater than 15 °C (LeChavallier, Schulz & Lee, 1991 in Henning et al, 2007).

2.3.4 Microbial Content of Treated Water

There are two main ways in which microorganisms appear in distribution systems: either via breakthrough at a treatment plant or growth from within the distribution system. Breakthrough occurs when viable or injured bacteria pass the water treatment plant, following primary disinfection procedures, which are only intended to suppress pathogenic organisms. Injured cells have the ability to recover, while viable cells can inoculate biofilms and/or reproduce in the bulk water. Bacterial growth within the distribution system can take place either within biofilms or in the bulk water (van der Wende & Characklis, 1990 in Le Puil, 2004). Bacteria introduced into the distribution system represent the starting point of a complex trophic chain (Le Puil, 2004).

While bacterial levels in the bulk water may be affected by biofilm bacteria levels, however, as has been mentioned previously, suspended bacteria and biofilm bacteria demonstrate clear differences. For example, in a pilot study by Norton and LeChevallier (2000) more than 90% of the isolates from a chlorinated water column were gram-positive, while the biofilms contained predominantly gram-negative bacteria. The authors state that these differences could possibly be attributed to the varying attachment capabilities of gram-positive and gram-negative bacteria. Another explanation given by the authors for the population variations between suspended and biofilm bacteria is that selective pressures may be imposed on suspended bacteria by disinfection. Attachment to pipe surfaces provides adequate protection for the survival of gram-negative bacteria that are not capable of surviving as suspended cells while suspended gram-positive bacteria may be more resistant to disinfection than suspended-gram positive bacteria owing to their thicker cell walls. Once a pipe surface is colonised, protection levels and growth rates appear sufficient to maintain a substantial level of gram-negative cells in the biofilm, despite exposure to chlorinated waters which generally are predominated by gram-positive bacteria.

Based on the above, Norton and LeChevallier (2000) hypothesise that the bacteriological content of treated water has little impact on the development of a mature biofilm. Bacteria released from biologically active filters would first be exposed to chlorine disinfection, resulting in a shift of the microbial population to predominately gram-positive bacteria. Even if low levels of these organisms are released from the filters into the distribution system, they would be unlikely to colonise the distribution system due to the high levels of competition imposed by previously established organisms.

2.3.5 Flow Velocity and Water Age

Water velocity through distribution system piping is a significant factor that influences biostability in distribution systems in several ways. Firstly, shear stress within distribution system pipes increases with increasing velocity and biofilm detachment increases with increasing shear stress, resulting in higher bulk water biomass concentrations (Lu, 1991 in Lu, Biswas & Clark, 1995; Henning et al, 2007). Paul et al (2012) conducted experiments to differentiate growth adaption factors from hydrodynamic effects on biofilm physical characteristics. In line with the findings mentioned above, the researchers found that for the same substrate, shear stress largely determines average biofilm thickness, although the researchers also found that biofilm density increases with increasing shear stress. Other significant findings were made by the same researchers. Regardless of the growth conditions and the shear stress applied during growth, gradual detachment from the biofilm occurs, which led the researchers to conclude that a mature biofilm is always stratified with respect to its

cohesion. A strong basal layer, the size of which is significantly influenced by the carbon source, is always present and this basal layer is more cohesive and dense than outer layers. In fact, cohesion decreases with distance from the basal layer.

Another way in which velocity influences growth is by altering the radial diffusion rate. Increased velocity under turbulent flow conditions increases both the supply of nutrients and disinfectants to the biofilm. This may increase biofilm growth in cases where nutrient supply is predominant, or hamper biofilm growth in cases where the disinfectant predominates (Lu, Biswas & Clark, 1995).

As distribution system water ages, its quality deteriorates. The two major mechanisms by which water quality deteriorates are interactions between the pipe wall and the bulk water, and reactions within the bulk water itself. As water travels through the distribution system, it undergoes various chemical, physical and biological transformations that affect water quality, as described previously. Increased water age provides a greater opportunity for such changes to occur (American Water Works Association, 2002).

In order to maintain water quality integrity, the goal of water utilities is to ensure that excessive water ageing does not occur. However, the aim of maintaining water quality by reducing water age may be in contrast with the hydraulic requirements of the system. In addition to meeting current demands, water systems are typically designed to maintain pressures and quantities needed to meet future demands and/or to provide extra reserves for firefighting, power outages and other emergencies, which increase water age (American Water Works Association, 2002). To this end, water storage facilities form part of distribution systems and high residence times in these facilities can completely deplete the disinfectant residual, resulting in microbial proliferation downstream of such facilities (National Research Council of the National Academies, 2006; Rossman & Grayman, 1999).

Pipe sections with exceptionally low velocities and dead-ends also increase water age and have been statistically correlated with water quality deterioration, caused by the loss of disinfectant residual in such locations. The consequence of this is greater bacterial growth in low-flow and dead-end regions (Henning et al, 2007).

2.3.6 Pipe Material

The materials used for water distribution system piping have changed considerably over time. In the past, cast iron pipes were the most popular, although these have largely been phased out due to their proneness to corrosion and associated structural failures. Ductile-iron pipes have largely

replaced cast iron pipes as they are strong, durable, have high flexural strength and good resistance to external corrosion from soils. However, ductile-iron pipes are relatively heavy and may require corrosion protection in certain soils. Consequently concrete, asbestos cement, polyvinyl chloride (PVC) and high-density polyethylene pipes are now also used as they are more resistant to corrosion than iron pipes (National Research Council of the National Academies, 2006).

Despite the variety of pipe materials available, no material used in the transport of drinking water can prevent the establishment and development of biofilms. As soon as a surface comes into contact with water, adsorption of dissolved organics occurs, followed by microorganism adhesion and subsequent biofilm development (Joret et al, 2005). However, the rate and degree of microbial growth in distribution systems is influenced by the pipe material in two different ways (Henning et al, 2007). Firstly, the rate of disinfectant loss due to reactions with different pipe materials varies considerably. Secondly, different pipe materials provide varying levels of protection to biofilm bacteria from detachment caused by hydraulic shear stress. Typically the use of iron pipes results in the greatest attached bacterial density, followed by concrete pipes, followed by plastic pipes (Joret et al, 2005; Camper et al, 2003 in Clark & Haught, 2005).

The propensity of iron pipes to corrode can effect biofilm development in a number of ways. The formation of corrosion products associated with unlined iron pipes exerts a significant disinfectant demand and the formation of corrosion products also provides increased protection to microorganisms from disinfectants (Norton & LeChevallier, 2000; LeChevallier et al, 1990 in Joret et al, 2005; Sarin et al, 2004 in Clark & Haught, 2005). Norton and LeChevallier (2000) found that the rate of biofilm bacterial growth was more than one hundred times greater for a pilot system with iron pipes than for an equivalent system with chlorinated PVC pipes, which the researchers state indicates that the disinfection efficiency of free chlorine is reduced by the iron pipe surface. In addition, the corrosion of pipe surfaces results in the formation of pits which provide primary sites of attachment for biofilm bacteria due to the protection that the pits provide from shear stress thereby limiting bacterial detachment (Joret et al, 2005).

While concrete piping was previously considered to be inert, recent studies have demonstrated that concrete piping contributes to both chlorine and chloramine decay (Woolschlager & Soucie, 2003). Chemical catalysis is hypothesised to occur on concrete surfaces. Concrete is largely composed of calcium silicates and aluminates. In their pure forms, both silicates and aluminates are weak acids and can donate protons supporting acid catalysis reactions. Despite the fact that silicates and aluminates can donate protons individually, they form a much stronger proton donor when combined. When this occurs, aluminosilicate is formed which is a "superacid". When aluminosilicate

comes into contact with water, a pair of electrons can be donated from the hydroxide ion, conferring a negative charge to the aluminium atom. The proton lost from the water molecule bonds with the neighbouring oxygen atom by accepting the electron density associated with one of its lone pairs. This proton is easily donated, which increases the rate of the acid-catalysed reactions, thereby greatly increasing the rate of disinfectant decay. The donation of additional protons from the concrete is expected to cause a shift in the composition of free chlorine from a scenario where hypochlorite ion predominates to one where the more reactive hypochlorous acid predominates, resulting in a more rapid loss of the free chlorine residual. However, detailed bench studies are still required to validate this hypothesis (Woolschlager & Soucie, 2003). Additionally, Woolschlager (2000) demonstrated that chloramines are highly reactive with concrete pipes. In his study, Woolschlager found that acid-catalysis reactions accounted for up to 60 percent of the loss of monochloramine in a distribution system with concrete and concrete-lined pipes. Furthermore, like iron pipes, the roughness of concrete pipes can provide primary surfaces of attachment for biofilms by protecting them from shear stress (Chang & Rittmann, 1988 in Woolschlager, 2000).

Plastic pipes exert considerably less disinfectant demand than other pipes and for this reason, in addition to the smoother surfaces associated with plastic pipes, which provide less protection against detachment, biofilm growth is typically lower on plastic pipes (Hallam et al, 2002 in Le Puil, 2004). More specifically, some researchers have found that plastic polyethylene pipes can sustain greater biomass than PVC pipes. The release of nutrients from polyethylene pipes may explain these findings. Brocca et al (2002 in Joret et al, 2005) demonstrated that organic compounds can be released from polyethylene pipes while Rogers et al (1994 in Joret et al, 2005) found that more total organic carbon is released from polyethylene pipes than from PVC pipes. However, not all research has found that increased bacterial levels are associated with polyethylene pipes (Joret et al, 2005) and Zacheus et al, 2000; Niquette, Servais & Savoir, 2000; Hallam et al, 2001 in Joret et al, 2005 obtained slightly greater biofilm potential for PVC than for medium density polyethylene.

2.4 Water Quality Modelling

Individually, the processes described in section 2.3 can be monitored and analysed. However, the interrelated nature of the processes means that their effect on water quality must be considered simultaneously which creates considerable difficulty. Routine sampling and monitoring of water can play an important role in ensuring that water quality does not deteriorate within a distribution system. However, solely taking such an approach can only provide limited information, as sampling

can only give information regarding water quality at sampling locations and monitoring cannot be used to predict future water quality (Wu, 2006).

A mathematical model is a systematic attempt to convert conceptual understanding of a real-world system into mathematical terms (Eberl et al, 2006). The use of deterministic mathematical models is one of the best tools available to both researchers and engineers in order to gain greater insight into the numerous interrelated processes affecting water quality within distribution systems and to determine effective ways of maintaining high quality water within distribution systems (Dukan et al, 1996).

While the use of mathematical models to conduct hydraulic analyses of distribution systems dates back to the 1930s (Cross, 1936 in Henning et al, 2007), it is only recently that focus has turned to the development of water quality models, which typically require flow and velocity information as inputs (Henning et al, 2007).

The first water quality models were steady-state models that rely on first-order processes to describe reactions (Wood, 1980; Males et al, 1985; Clark & Males, 1986; Males, Grayman & Clark 1988 in National Research Council of the National Academies 2006). For steady state models, the external conditions of a distribution network do not vary over time and the nodal concentrations of the constituents that will occur if the system is allowed to reach equilibrium are determined. Steady state models can provide general information on the spatial distribution of water quality (Munavalli & Kumar, 2004). However, due to the time-variant nature of the demands placed on distribution systems, steady-state models are unlikely to be of much use, except for the smallest systems (Davidson et al, 2005).

By the mid-1980s dynamic, first-order, water quality models were in use (Grayman, Clarke & Males, 1988) in recognition of the fact that that, under normal operating conditions, network hydraulics can change over short periods of time as both the demands on the system and operating parameters change (Davidson et al, 2005). Dynamic water quality models are based on extended period simulation, quasi-steady network hydraulics and solve equations for nodal mixing and advective transport in pipes in order to compute the spatial and temporal variation of water quality parameters, thereby overcoming the limitations of earlier steady-state models (National Research Council of the National Academies, 2006).

Early dynamic models were first-order, single-species models, with the Distributed Water Quality Model (DWQM) documented by Males, Grayman & Clark (1988 in Le Puil, 2004) being the most significant. In fact, the DWQM forms the basis of the widely used EPANET hydraulic and water

quality model (Le Puil, 2004). Owing to their simplicity, such models can be promptly solved for full-scale distribution systems and the results of field studies have demonstrated that they can be adjusted to fit the propagation of disinfectant residuals and fluoride tracers in real distribution systems (Grayman, Clark, and Males, 1988; Clark, 1992; Rossman, Clark, & Grayman, 1994; Vasconcelos, et al, 1997 in Le Puil, 2004).

Despite the fact that first-order, single-species models can fit distribution system data, there are two major limitations associated with them. Firstly, unless a process can be modelled by simple, first-order reaction kinetics, it is beyond the scope of these models (Woolschlager, 2000). Secondly, unless a process can be represented as an independent species, it cannot be represented by such models. Therefore, single-species models cannot provide a complete understanding of the factors that influence distribution system water quality. Since kinetic parameters are site-specific, single species models cannot predict results for other systems or even for the same system when significant changes are made to system operation or input quality (Le Puil, 2004).

In order to overcome these limitations, complex-process, multi-species models have been developed, which more accurately describe microbial metabolism and disinfectant decay by using sets of interdependent, multi-species, mass-balance equations based on fundamental processes (Le Puil, 2004). One of the most frequently used multi-species models is the SANCHO model developed by Servais et al (1995), which has proven to be a valuable research and analysis tool (Le Puil, 2004).

The processes taken into account by the SANCHO model are: enzymatic hydrolysis of dissolved organic matter by bacteria and growth of free and fixed bacteria on hydrolysis products; bacterial mortality, which releases organic matter; reversible adsorption of bacteria and their biological attachment to inner pipe surfaces; chemical consumption of free chlorine and the impact of free chlorine on the activity of both free and fixed bacteria (Henning et al, 2007).

However, the SANCHO model is limited to the analysis of straight pipes of decreasing diameter. Despite this, the model has been applied to full-scale distribution systems by using detention times calculated by a hydraulic model to project the SANCHO water quality solution to the distribution system (Laurent et al, 1997 in Le Puil, 2004). Woolschlager (2000) refers to this solution a “projected batch” method as it is not a true network solution since it does not account for species mixing at pipe junctions or for specific pipe surface reactions in individual pipes. Thus the process descriptions for growth, attachment, detachment and inactivation of bacteria are not linked to a hydraulic model. Rather, a hydraulic model is first run to determine the residence time at each location of interest under some steady-state condition of flow and these results are then used to run the water quality

model. Consequently, the model is incapable of providing a dynamic prediction of bacterial growth caused by variations in water velocity and water quality changes entering the distribution system over time. Furthermore, the SANCHO model does not account for the effect of water velocity on bacterial detachment, chlorine demand exerted by pipe wall material, differences in attachment potential of bacteria to different pipe materials or the fact that a nutrient other than carbon, may be the growth limiting nutrient (Henning et al, 2007).

Another significant complex-process model is the PICCOBIO model, developed by Dukan et al (1996), which combines a hydraulic model (PICCOLO) with a water quality model. The PICCOBIO model was first calibrated using data obtained from a pilot system, but has since been calibrated to enable it to function for full-scale distribution networks. The model takes into account: the growth of suspended and fixed bacteria; the consumption of available nutrients in the bulk water and the biofilm; the influence of a chlorine residual on the mortality of suspended and fixed biomass, as well the natural mortality of bacteria by senescence and grazing; the deposition of suspended bacteria and the detachment of biofilm cells; the influence of temperature on bacterial activity and chlorine decay; and the chlorine decay kinetics under the influence of hydraulics and pipe materials (Henning et al, 2007). Thus, while the PICCOBIO model contains similar processes to the aforementioned SANCHO model, the models differ in that some of the processes are represented differently. The PICCOBIO model contains a complex, multi-level biofilm growth and disinfection submodel and is also capable of accounting for chlorine loss due to reactions on pipe surfaces (Woolschlager, 2000).

Unlike the SANCHO model, the PICCOBIO model has been coupled with a hydraulic network model (Dukan et al, 1996 in Henning et al, 2007). Therefore the model is capable of describing the concentration of any species as a function of time and position within a distribution system. Furthermore, unlike the SANCHO model, the detachment rate of bacteria depends on shear stress which is a function of water velocity, although the developers of the PICCOBIO model acknowledge the need for better understanding of the influence of shear stress on biofilm detachment. However, as with the SANCHO model, the PICCOBIO model is based on the assumption that carbon is the limiting nutrient (Henning et al, 2007).

The complex-process, multi-species model developed by Lu, Biswas and Clark (1995) accounts for the simultaneous transport of substrates, disinfectants, and microorganisms (Henning et al, 2007). This model is of particular interest as it contains biological processes modelling heterotrophs, nitrifiers and denitrifiers, although denitrification is yet to be established as a major process in distribution systems (Woolschlager, 2000). The model consists of a set of mass-balance equations for organic substances, ammonia, oxidised nitrogen, dissolved oxygen, alkalinity, biomass, and

disinfectants in both the bulk water and within the biofilm, under laminar and turbulent flow conditions (Henning et al, 2007). There are, however, two major limitations of the model. Firstly, the model is only capable of solving for simple, straight pipe scenarios. Secondly, the model has been validated by comparing its solutions with numerical solutions from literature and has not been calibrated with measured distribution system or pilot system data (Woolschalger, 2000; Henning et al, 2007).

Zhang, Miller & DiGiano (2004) have developed a complex-process, multi-species model by combining hydraulic network calculations, including unsteady-state flow conditions, with a description of free and attached bacterial growth, detachment, endogenous respiration and inactivation by chlorine. This model is based on the belief that processes within biofilms are currently not well-understood and therefore overly detailed descriptions relating to biofilm processes are unreasonable. Consequently, the model contains a simplification of bacterial growth, attachment, detachment and inactivation compared to the SANCHO and PICCOBIO models. Again, as is the case for both the SANCHO and PICCOBIO models, this model is based on the assumption that carbon is the limiting nutrient. (Henning et al, 2007).

Another notable multi-species model is the Comprehensive Disinfection and Water Quality Model (CDWQ) which has been developed by Woolschlager (2000). The CDWQ model has been designed for full-scale distribution systems where either chloramines or free chlorine is used as a secondary disinfectant, although the model has only been calibrated for chloramine disinfection. While previous models have used overly simplified equations to represent disinfectant reactions, this model encompasses a detailed chloramine and free chlorine chemistry subroutine which enables it accurately model chloramine and chlorine decay and hence heterotrophic and nitrifying bacterial processes (Woolschlager, 2000; Le Puil, 2004). This model incorporates mass-balance equations that are capable of predicting and analysing changes in heterotrophic counts, nitrifier counts, and chloramine decay throughout distribution systems. Essentially, the model compares the potential of treated water to support bacterial growth within a distribution system with the potential for the disinfectant residual to limit bacterial growth within the system. Therefore, a relatively straightforward equation is used to determine net microbial growth for a specific species.

$$\text{Net Biomass Growth} = \text{Substrate Utilisation} - \text{Endogenous Decay} - \text{Disinfection}$$

However, a number of inter-related factors affect both the rate of substrate utilisation for a given species of bacteria and the rate of disinfection and the essence of the CDWQ model is therefore to predict the influence of these three factors on net biomass growth.

Unlike many previous multi-species water quality models, the CDWQ model is fully linked to a hydraulic model, thereby establishing a link between microbial and chemical processes, as well as hydraulic parameters (Woolschlager, 2000).

The CDWQ forms the basis for the Expanded Comprehensive Disinfection and Water Quality Model (CDWQ-E) developed by Biyela (2010). The fundamental difference between the two models is that the CDWQ-E model makes use of recent advances in the field of microbial growth modelling that have been developed by Laspidou and Rittmann (2002a, 2002b).

The Unified Theory for extracellular polymeric substances, soluble microbial products, and active and inert biomass developed by Laspidou and Rittmann (2002a, 2002b) stipulates that cells use electrons from an electron-donor substrate in order to build active biomass, while at the same time cells produce bound EPS, a substance that is not considered in the CDWQ model, and utilisation-associated products (UAP) in proportion to substrate utilisation. Bound EPS are hydrolysed to form biomass-associated products (BAP), while active biomass undergoes endogenous decay to form residual dead cells. In order to ensure complete mass-balance of electron equivalents, an electron acceptor is consumed for respiratory energy production as part of the oxidation of the original electron-donor substrate, the oxidation of UAP and BAP as recycled electron-donor substrates and the oxidation of the biodegradable fraction of active biomass during endogenous decay. Finally, as both UAP and BAP are biodegradable, they are utilised by active biomass as recycled electron-donors substrates. Although both heterotrophic bacteria and nitrifying bacteria produce UAP and BAP, only heterotrophic bacteria are capable of utilising them as recycled electron donors (Biyela, 2010).

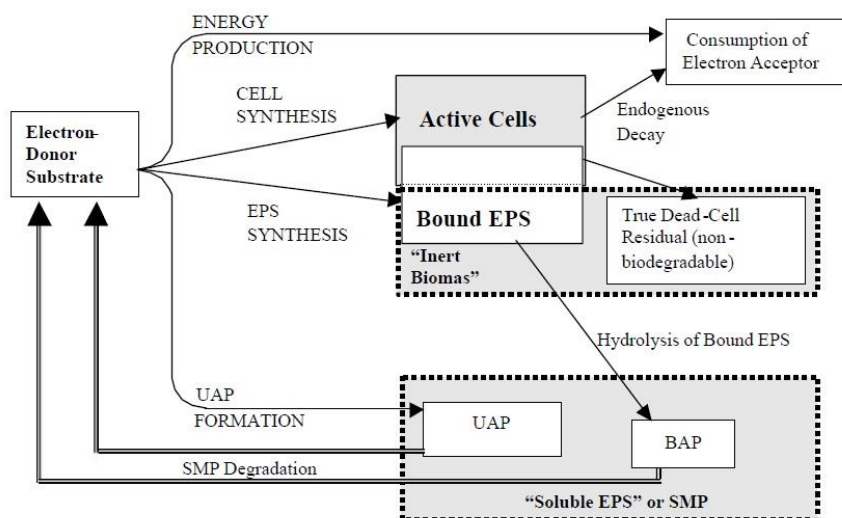


Figure 2-1: Schematic representation of the Unified Model for active biomass, EPS, SMP and inert biomass

(Laspidou & Rittmann, 2002a, p 2718)

Additionally, the CDWQ-E model utilises dual-limitation Monod kinetics such that both the availability of the electron donor and electron acceptor influence the rate of substrate utilisation and hence microbial growth. This allows for the consumption of the electron acceptor to be considered in the CDWQ-E model, which the CDWQ model was unable to account for. Furthermore, this addition allows for potential cases of denitrification to be modelled, as both the utilisation of nitrite and nitrate as electron acceptors by heterotrophic bacteria can be accounted for.

The aforementioned CDWQ-E model developed by Biyela (2010) is based on a batch reactor, modelling only the planktonic mode of bacterial growth, and is incapable of accounting for the advective flow of constituents throughout drinking water distribution systems. Hence, the aim of this project is to reconcile the CDWQ model developed by Wooschlager (2000) and the CDWQ-E model developed by Biyela (2010), in addition to incorporating various additional sources, in order to create a full-scale model, henceforth referred to as the Expanded Comprehensive Disinfection and Water Quality Model, Version 2 (CDWQ-E₂) that is able to account for complex biofilm processes, using the latest advances in the field of microbial modelling. By doing this, the model would be more applicable to drinking water distribution systems than the preceding CDWQ-E model, as the impact of a hydraulic regime on species transport, the development of biofilms and the decay of disinfectant residual due to significant pipe-wall reactions can be accounted for.

3 MODEL DEVELOPMENT

The CDWQ-E₂ model developed for this project is an amalgamation of various water quality models, particularly the CDWQ model established by Woolschlager (2000) and the CDWQ-E model developed by Biyela (2010). As a result, the model is more applicable to drinking water distribution systems than the preceding CDWQ-E model, as the impact of a hydraulic regime on species transport, the development of biofilms and the decay of disinfectant due to significant pipe-wall reactions can be accounted for. Crucially, the CDWQ-E₂ model utilises the latest advancements in microbial growth modelling as given by the Unified Theory (Laspidou & Rittmann, 2002a, 2002b) and therefore it represents an advancement on the original CDWQ model.

In order to develop the CDWQ-E₂ model, the batch version of the CDWQ-E model was first adapted and simulations with this updated batch version were performed. The mass-balance equations used in the batch version form the basis for the mass-balance equations used in the distribution system version of the model, and thus developing a batch version first was rational. Following this, the mass-balance equations in the batch version were updated to include the transport of substances throughout the distribution system and the development of biofilms within the distribution system. Both of these updates require the hydraulic system under consideration to be defined, and thus means of doing this are also incorporated in the CDWQ-E₂ model.

It is hoped that the use of the CDWQ-E₂ model will assist researchers and water utilities in answering the four key questions that, according to Tilman (2001 in Douterelo et al, 2014), need to be considering when studying microorganisms in drinking water distribution systems:

- 1) What types of microorganisms are present in the system?
- 2) How abundant are they?
- 3) How do the activities of the various species influence one another and what impact do the various species have on human health?
- 4) How does the environment within the distribution system influence the microorganisms present within the system?

From this point forward, the term “CDWQ-E₂ model” will refer specifically to the distribution system version of the model, as opposed to the batch version, unless otherwise stated. As is the case for both previous versions of the CDWQ model, all species in the CDWQ-E₂ model are represented using mass-balance equations, which are presented in section 3.8.

3.1 Microbial Modelling

Five species of biomass are incorporated into the model, namely: heterotrophs, ammonia oxidising bacteria (AOB), nitrite oxidising bacteria (NOB), extracellular polymeric substances (EPS) and inert bacteria. In the distribution system version of the model, each of the species may be either fixed to the pipe wall (as part of a biofilm) or suspended in the water, while in the batch version only suspended species are considered.

Six possible electron donor species are represented in the model. Biodegradable organic matter (BOM) is the most significant substrate for heterotrophic growth. Two types of BOM are tracked by the model: BOM₁, which represents rapidly degrading species such as ozonation products, and BOM₂, which represents slowly degraded, humic-like matter (Woolschlager, 2000). In accordance with the Unified Theory (Laspidou & Rittmann, 2002a, 2002b), utilisation associated products (UAP) and biomass associated products (BAP) are available as electron donors for heterotrophs. UAP is produced directly by all species of active biomass, while BAP is produced indirectly by the hydrolysis of EPS, which is also produced by all species of active biomass. Thus the E₂ model differs from the CDWQ model in which it was assumed that BAP is produced directly by active bacteria and EPS is not accounted for. The combination of UAP and BAP is referred to as soluble microbial products (SMP). For the nitrifying bacteria, ammonia is the electron donor for AOB and nitrite is the electron donor for NOB.

Three types of electron acceptors are used in the model. Oxygen is utilised by all species of active bacteria when respiring aerobically. However, in oxygen-limited conditions, heterotrophic bacteria, due to their classification as facultative bacteria, can continue to respire anoxically, either by utilising nitrite or nitrate as an electron acceptor.

3.1.1 Biomass Growth

In accordance with the Unified Theory, as not all substrate electrons consumed are used to produce biomass, the biomass yield (Y) must be reduced by the factor $(1 - k_{\text{eps}} - k_{\text{uap}})$. This factor accounts for the fact that a proportion of substrate electrons are diverted to produce EPS and UAP (Laspidou & Rittmann, 2002a, 2002b).

Biomass growth from either BOM, ammonia or nitrite utilisation is therefore governed by Equation 3-1:

$$\frac{dX_i}{dt} = Y_i (1 - k_{eps,i} - k_{uap,i}) \cdot UTL \cdot X_i$$

Equation 3-1

Where i = heterotrophs, AOB or NOB

Parameter	Description	Units
X_i	Active biomass concentration for a specific species	$\frac{M_x}{L^3}$
Y_i	Biomass yield for a specific species	$\frac{M_x}{M_s}$
$k_{eps,i}$	EPS formation constant for a specific species	$\frac{M_p}{M_s}$
$k_{uap,i}$	UAP formation constant for a specific species	$\frac{M_p}{M_s}$
UTL	Specific utilisation rate	$\frac{M_s}{M_x \cdot T}$

However, as the Unified Theory states, substrate electrons derived from SMP are not diverted to produce EPS and UAP. Therefore, the biomass yield for heterotrophs utilising SMP (Y_p) is not reduced by the factor above and heterotroph biomass derived from SMP utilisation is governed by Equation 3-2:

$$\frac{dX_h}{dt} = Y_p \cdot UTL_{smp} \cdot X_h$$

Equation 3-2

3.1.2 Aerobic Substrate Respiration

By incorporating electron acceptors into the model, bacterial growth can be modelled using dual-limitation Monod kinetics. This means that the concentrations of both the electron donor and the electron acceptor control the rate of substrate consumption and biomass production in a multiplicative manner (Rittman & McCarty, 2001; Biyela, 2010). Hence, the equation for the specific utilisation rate of any substrate under aerobic conditions can be represented as follows:

$$UTL = q_m \left(\frac{S}{K_S + S} \right) \left(\frac{A}{K_A + A} \right)$$

Equation 3-3

Parameter	Description	Units
UTL	Specific utilisation rate	$\frac{M_S}{M_x \cdot T}$
q_m	Maximum specific substrate utilisation rate	$\frac{M_S}{M_x \cdot T}$
S	Electron donor or substrate concentration	$\frac{M_S}{L^3}$
K_s	Half-maximum rate concentration for donor	$\frac{M_S}{L^3}$
A	Electron acceptor concentration for acceptor	$\frac{M_A}{L^3}$
K_a	Half-maximum rate concentration for acceptor	$\frac{M_A}{L^3}$

Based on Equation 3-3, the specific utilisation rates for the different substrates available under aerobic conditions are provided below.

BOM Specific Utilisation Rate Under Aerobic Conditions

$$UTL_{bom_1} = q_h \left(\frac{BOM_1}{K_{bom_1} + BOM_1} \right) \left(\frac{O_2}{K_{O_2} + O_2} \right)$$

Equation 3-4

$$UTL_{bom_2} = q_h \left(\frac{BOM_2}{K_{bom_2} + BOM_2} \right) \left(\frac{O_2}{K_{O_2} + O_2} \right)$$

Equation 3-5

$$\therefore UTL_{bom} = UTL_{bom_1} + UTL_{bom_2}$$

Equation 3-6

SMP Specific Utilisation Rate Under Aerobic Conditions

$$UTL_{uap} = q_{uap} \left(\frac{UAP}{K_{uap} + UAP} \right) \left(\frac{O_2}{K_{O_2} + O_2} \right)$$

Equation 3-7

$$UTL_{bap} = q_{bap} \left(\frac{BAP}{K_{bap} + BAP} \right) \left(\frac{O_2}{K_{O_2} + O_2} \right)$$

Equation 3-8

$$\therefore UTL_{smp} = UTL_{uap} + UTL_{bap}$$

Equation 3-9

Ammonia Specific Utilisation Rate Under Aerobic Conditions

$$UTLNH_3 = q_{NH_3} \left(\frac{NH_3}{K_{NH_3} \left(1 + \frac{NH_2Cl}{K_{NH_2Cl}} \right) + NH_3} \right) \left(\frac{O_2}{K_{O_2} + O_2} \right)$$

Equation 3-10

It is important to note that while monochloramine and chlorohydroxylamine cometabolism were not included in the CDWQ-E model, they have been included in the CDWQ-E₂ model. The rationale for this is provided in the cometabolism subsection. As cometabolism is included, competitive cometabolism kinetics (Ely et al, 1995 in Wooschlager, 2000) are included in the dual-limitation Monod equation above.

Nitrite Specific Utilisation Rate Under Aerobic Conditions

$$UTLNO_2 = q_{NO_2} \left(\frac{NO_2}{K_{NO_2} + NO_2} \right) \left(\frac{O_2}{K_{O_2} + O_2} \right)$$

Equation 3-11

3.1.3 Anoxic Substrate Respiration

For heterotrophic bacteria, the change from aerobic to anoxic respiration is governed by multiplying the specific utilisation rate by a switching factor (Biyela, 2010). Thus, when the oxygen concentration is low, the specific utilisation rate for heterotrophs effectively becomes:

$$UTL = \text{and. } q_m \left(\frac{S}{K_S + S} \right) \left(\frac{O_2}{K_{O_2} + O_2} \right) \left(\frac{K_{I,DO}}{K_{I,DO} + O_2} \right)$$

Equation 3-12

Parameter	Description	Units
and	Anoxic reduction factor	Dimensionless
O₂	Oxygen concentration	$\frac{M_A}{L^3}$
K_{O2}	Half-maximum rate concentration for oxygen	$\frac{M_A}{L^3}$
K_{I,DO}	Switching factor	$\frac{M_A}{L^3}$

Based on Equation 3-12, the specific utilisation rates for the different substrates available under anoxic conditions are provided below.

BOM Specific Utilisation Rate Under Anoxic Conditions (Nitrite Respiration)

$$and_1 bom_1 = q_h \cdot and_1 \left(\frac{BOM_1}{K_{bom_1} + BOM_1} \right) \left(\frac{NO_2}{K_{NO_2} + NO_2} \right) \left(\frac{K_{I,DO}}{K_{I,DO} + O_2} \right)$$

Equation 3-13

Parameter	Description	Units
K_{NO_2}	Half-maximum rate concentration for nitrite	$\frac{M_A}{L^3}$

$$and_1 bom_2 = q_h \cdot and_1 \left(\frac{BOM_2}{K_{bom_1} + BOM_2} \right) \left(\frac{NO_2}{K_{NO_2} + NO_2} \right) \left(\frac{K_{I,DO}}{K_{I,DO} + O_2} \right)$$

Equation 3-14

$$\therefore and_1 bom = and_1 bom_1 + and_1 bom_2$$

Equation 3-15

BOM Specific Utilisation Rate Under Anoxic Conditions (Nitrate Respiration)

$$and_2 bom_1 = q_h \cdot and_2 \left(\frac{BOM_1}{K_{bom_1} + BOM_1} \right) \left(\frac{NO_3}{K_{NO_3} + NO_3} \right) \left(\frac{K_{I,DO}}{K_{I,DO} + O_2} \right)$$

Equation 3-16

Parameter	Description	Units
K_{NO_3}	Half-maximum rate concentration for nitrate	$\frac{M_A}{L^3}$

$$and_2 bom_2 = q_h \cdot and_2 \left(\frac{BOM_2}{K_{bom_2} + BOM_2} \right) \left(\frac{NO_3}{K_{NO_3} + NO_3} \right) \left(\frac{K_{I,DO}}{K_{I,DO} + O_2} \right)$$

Equation 3-17

$$\therefore and_2 bom = and_2 bom_1 + and_2 bom_2$$

Equation 3-18

SMP Specific Utilisation Rate Under Anoxic Conditions (Nitrite Respiration)

$$and_1 uap = q_h \cdot and_1 \left(\frac{UAP}{K_{uap} + UAP} \right) \left(\frac{NO_2}{K_{NO_2} + NO_2} \right) \left(\frac{K_{I,DO}}{K_{I,DO} + O_2} \right)$$

Equation 3-19

$$and_1bap = q_h \cdot and_1 \left(\frac{BAP}{K_{bap} + BAP} \right) \left(\frac{NO_2}{K_{NO_2} + NO_2} \right) \left(\frac{K_{I,DO}}{K_{I,DO} + O_2} \right)$$

Equation 3-20

$$and_1smp = and_1uap + and_1bap$$

Equation 3-21

SMP Specific Utilisation Rate Under Anoxic Conditions (Nitrate Respiration)

$$and_2uap = q_h \cdot and_2 \left(\frac{UAP}{K_{uap} + UAP} \right) \left(\frac{NO_3}{K_{NO_3} + NO_3} \right) \left(\frac{K_{I,DO}}{K_{I,DO} + O_2} \right)$$

Equation 3-22

$$and_2bap = q_h \cdot and_2 \left(\frac{BAP}{K_{bap} + BAP} \right) \left(\frac{NO_3}{K_{NO_3} + NO_3} \right) \left(\frac{K_{I,DO}}{K_{I,DO} + O_2} \right)$$

Equation 3-23

$$and_2smp = and_2uap + and_2bap$$

Equation 3-24

3.1.4 Endogenous Decay

In order to provide energy for cell maintenance, a proportion of active biomass must be oxidised by endogenous respiration (Laspidou & Rittmann, 2002a, 2002b). The rate of biomass loss for the nitrifying species of bacteria due to endogenous respiration is given by Equation 3-25:

$$\frac{dX_i}{dt} = -b_i \cdot \left(\frac{O_2}{O_2 + K_{O_2}} \right) \cdot X_i$$

Equation 3-25

Where $i = AOB$ or NOB

Parameter	Description	Units
b_i	Endogenous decay coefficient	$\frac{1}{T}$

However, as the CDWQ-E₂ model accounts for anoxic respiration by heterotrophs using either nitrite or nitrate as an electron acceptor, the loss of heterotrophs due to endogenous respiration is defined by a different equation. The equation that is applied in the CDWQ-E₂ model is given by Equation 3-26 (de Silva & Rittmann, 2000):

$$\frac{dX_h}{dt} = -b_h \cdot \left(\frac{O_2}{O_2 + K_{O_2}} + \frac{NO_2}{K_{NO_2} + NO_2} \cdot \frac{K_{I,DO}}{K_{I,DO} + O_2} + \frac{NO_3}{K_{NO_3} + NO_3} \cdot \frac{K_{I,DO}}{K_{I,DO} + O_2} \right) \cdot X_h$$

Equation 3-26

The biodegradable fraction of active biomass lost to endogenous respiration forms carbon dioxide, while the fraction that is not biodegradable forms inert biomass (Laspidou & Rittmann, 2002a, 2002b).

3.1.5 Consumption of Electron Acceptor

For either BOM, ammonia or nitrite substrate respiration, the remaining $(1 - k_{uap,i} - k_{eps,i} - Y_i(1 - k_{uap,i} - k_{eps,i} - Y_i))$ electrons are sent to the electron acceptor to generate energy (Laspidou & Rittmann, 2002a, 2002b) such that the consumption of the electron acceptor is governed by:

$$\frac{d_A}{dt} = - (1 - k_{uap,i} - k_{eps,i} - Y_i(1 - k_{uap,i} - k_{eps,i})) UTL_{S,i} X_i$$

Equation 3-27

Where $i =$ heterotrophs, AOB or NOB

For SMP utilisation by heterotrophs, the remaining $(1 - Y_p)$ electrons are sent to the electron acceptor to generate energy (Laspidou & Rittmann, 2002a, 2002b) such that the consumption of the electron acceptor is governed by:

$$\frac{d_A}{dt} = - (1 - Y_p) \cdot UTL_{smp} X_h$$

Equation 3-28

Finally, the electron acceptor is consumed at the same rate by endogenous decay as the biodegradable fraction of active biomass (Laspidou & Rittmann, 2002a, 2002b). Hence, the consumption of the electron acceptor due to endogenous decay is given by:

$$\frac{d_A}{dt} = -f_d \cdot \left(b_i \cdot \left(\frac{A}{K_A + A} \right) \cdot X_i \right)$$

Equation 3-29

Where $i =$ heterotrophs, AOB or NOB

Parameter	Description	Units
f_d	Biodegradable fraction of biomass	Dimensionless

3.1.6 Biofilm Modelling

Many of the more complex biofilm models developed after the CDWQ model¹ for applications other than drinking water distribution systems incorporate concentration gradients within the biofilm. However, biofilms in drinking water distribution systems are typically thin (much less than 30µm) (Woolschlager, 2000) and concentration gradients within these thin biofilms are not expected to vary significantly. Consequently, concentration gradients need not be incorporated into the CDWQ-E₂ model (Rittmann & McCarty, 2001; Bakke et al, 1984) and biofilm biomass can be modelled in the same manner as suspended biomass. That is, substrate utilisation and subsequent growth is governed by dual-limitation Monod kinetics and disinfection is governed by the Chick-Watson model, which will be detailed in a subsequent section. Different parameter values are, however, used for suspended and fixed biomass.

Two processes govern the transfer of biomass from the suspended to the fixed form and vice versa, namely detachment and adsorption. Detachment is responsible for the transfer of fixed biomass to the suspended state, while adsorption is responsible for the transfer of suspended biomass to the fixed state.

Detachment

The detachment equation presented by Woolschlager and incorporated into the CDWQ-E₂ model is a function of shear stress and was originally developed by Rittmann (1982). The equation developed by Rittmann is intended only for thin biofilms, allowing Woolschlager to justify its use in the CDWQ model. However, Rittmann's equation was modified for the CDWQ model to include the protection of biofilms from shear stress by pipe roughness. In order to do this, an empirical relationship between biofilm protected thickness and the Hazen-Williams coefficient has been developed. This ensures that biomass within the protected fraction of the biofilm is not subject to detachment.

The detachment equation used in the E₂ version of the model is given by Equation 3-30:

$$r_{i,\text{det}} = k_{\text{det}} \cdot \tau^A \cdot X_{i,f} \cdot \left(\frac{X_f - X_{f(\text{pro})}}{X_f} \right)$$

Equation 3-30

¹ Examples include the Transient-State, Multiple-Species Biofilm Model for bio-filtration processes (Rittmann, Stilwell & Ohashi, 2002) and the Unified Multiple Component Cellular Automation Model (Laspidou & Rittmann, 2004).

Where i = heterotrophs, AOB, NOB, EPS or inert bacteria

Parameter	Description	Units
$r_{i,det}$	Biofilm detachment rate (for a specific species of biomass)	$\frac{M}{L^3T}$
k_{det}	Biofilm detachment rate constant	$\frac{1}{T}$
τ	Hydraulic shear stress	$\frac{M}{LT^2}$
$X_{i,f}$	Biofilm accumulation per unit volume of pipe (for a specific species of biofilm)	$\frac{M}{L^3}$
X_f	Total biofilm biomass accumulation per unit volume of pipe	$\frac{M}{L^3}$
$X_{f(pro)}$	Total biofilm biomass accumulation per unit volume of pipe that is protected from shear stress by pipe roughness	$\frac{M}{L^3}$

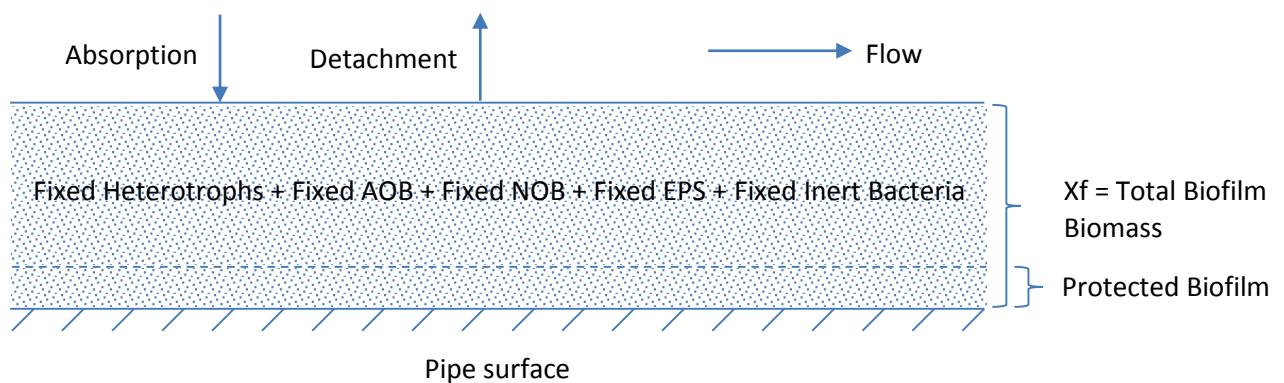


Figure 3-1: Schematic Diagram Depicting Uniform Distribution of the 5 Species of Biofilm Biomass

Figure 3-1 demonstrates how, in the CDWQ-E₂ model, the five species of biofilm biomass are assumed to be uniformly distributed throughout the biofilm, although each species comprises a different fraction of the total biofilm biomass. Therefore, the application of Equation 3-30 results in the fraction of the specific species under consideration, detached in a given time, being proportional to the fraction of both the total and exposed biofilm biomass of which the specific species comprises.

Equation 3-31 is used to calculate hydraulic shear stress for circular pipes (Chadwick & Morfett, 1993 in Wool Schlager, 2000, p 193):

$$\tau = h_f \frac{\rho \cdot g \cdot d}{4L}$$

Equation 3-31

Parameter	Description	Units
τ	Hydraulic shear stress	$\frac{N}{m^2}$
h_f	Head loss	M
ρ	Fluid density	$\frac{kg}{m^3}$
d	Pipe diameter	M
L	Pipe length	M

Head loss is calculated using Equation 3-32(Chadwick & Morfett, 1993 in Wooschlager, 2000, p 193):

$$h_f = \frac{6.78v^{1.85} \cdot L}{C^{1.85} \cdot d^{1.165}}$$

Equation 3-32

Parameter	Description	Units
v	Flow velocity	$\frac{m}{s}$
C	Hazen-Williams coefficient	Dimensionless

Equation 3-33 is used to determine the fraction of the biofilm that is protected from shear stress by pipe roughness:

$$X_{f(pro)} = L_f \cdot \rho_f \left(\frac{4}{d} \right)$$

Equation 3-33

Parameter	Description	Units
L_f	Thickness of protected biofilm	L
P_f	Assumed biofilm density of protected biofilm ²	$\frac{M}{L^3}$

Equation 3-34 is used to calculate the thickness of the protected biofilm:

$$L_f = k_{pro1} \left(\frac{1}{C} \right)^{k_{pro2}}$$

Equation 3-34

² See Appendix A.4 for derivation

Parameter	Description	Units
k_{pro1}	Protected biofilm depth coefficient	L
k_{pro2}	Protected biofilm exponent coefficient	Dimensionless

While Equations 3-30 to 3-34 are the same as those used in the CDWQ model, the definition of the total biofilm biomass accumulation per unit volume of pipe (X_f) is different in the E_2 version. Firstly, unlike in the CDWQ model, EPS is incorporated in the E_2 version. Typically, EPS forms a significant fraction of biofilm biomass in drinking water distribution systems (Laspidou & Rittmann, 2004). Therefore, in the CDWQ- E_2 model, fixed active biomass forms EPS, that is directly incorporated into the biofilm. Secondly, while the CDWQ model uses refractory organic matter (ROM), the CDWQ- E_2 version uses inert biomass. Inert biomass forms from the decay of active cells, either through endogenous respiration or disinfection. Fixed active biomass decays to form fixed inert biomass (Laspidou & Rittmann, 2004), and thus fixed inert biomass is included in the E_2 version, unlike Wooschlager's version which only considers suspended ROM.

Adsorption

Adsorption of biomass from the suspended to the fixed state is a theoretical concept (Wooschlager, 2000). The concept of adsorption is also acknowledged by Srinivasan and Harrington (2007). Using a first-order function dependent on only the suspended biomass concentration (Taylor & Jaffé, 1990 in Wooschlager 2000), Wooschlager found good fit to field data. Therefore, the same approach is taken for the E_2 version.

The rate of suspended biomass adsorption is given by Equation 3-35:

$$r_{i,ads} = k_{ads} \cdot X_{i,s} \left(\frac{4}{d} \right)$$

Equation 3-35

Parameter	Description	Units
$r_{i,ads}$	Rate of suspended biomass adsorption for a given species	$\frac{M}{L^3T}$
k_{ads}	Adsorption rate constant	$\frac{L}{T}$

Where i = heterotrophs, AOB, NOB, EPS or inert bacteria

As with detachment, there is a difference in the use of the adsorption equation in the CDWQ-E₂ model. Since both EPS and inert bacteria are included in this version, it follows that both are subject to adsorption.

3.2 Chlorine Reaction Submodel

The CDWQ-Cl₂ chlorine reaction submodel developed by Wooschlager (2000) has been incorporated in the CDWQ-E₂ model. This submodel accounts for the following reaction pathways: equilibrium reactions, chloramine autocatalytic decay, cometabolism reactions, corrosion reactions, oxidation reactions and surface catalysis. In the section that follows, each reaction pathway is briefly described and minor alterations to their incorporation in the CDWQ-E₂ are also detailed. The reaction constants incorporated in this submodel are given in Table 3-1.

As is the case with the CDWQ model, the CDWQ-E₂ model is capable of tracking both free chlorine (hypochlorous acid and hypochlorite) and combined chlorine (monochloramine, dichloramine and chlorohydroxylamine), but currently only parameters relating to combined chlorine disinfection and oxidation are available.

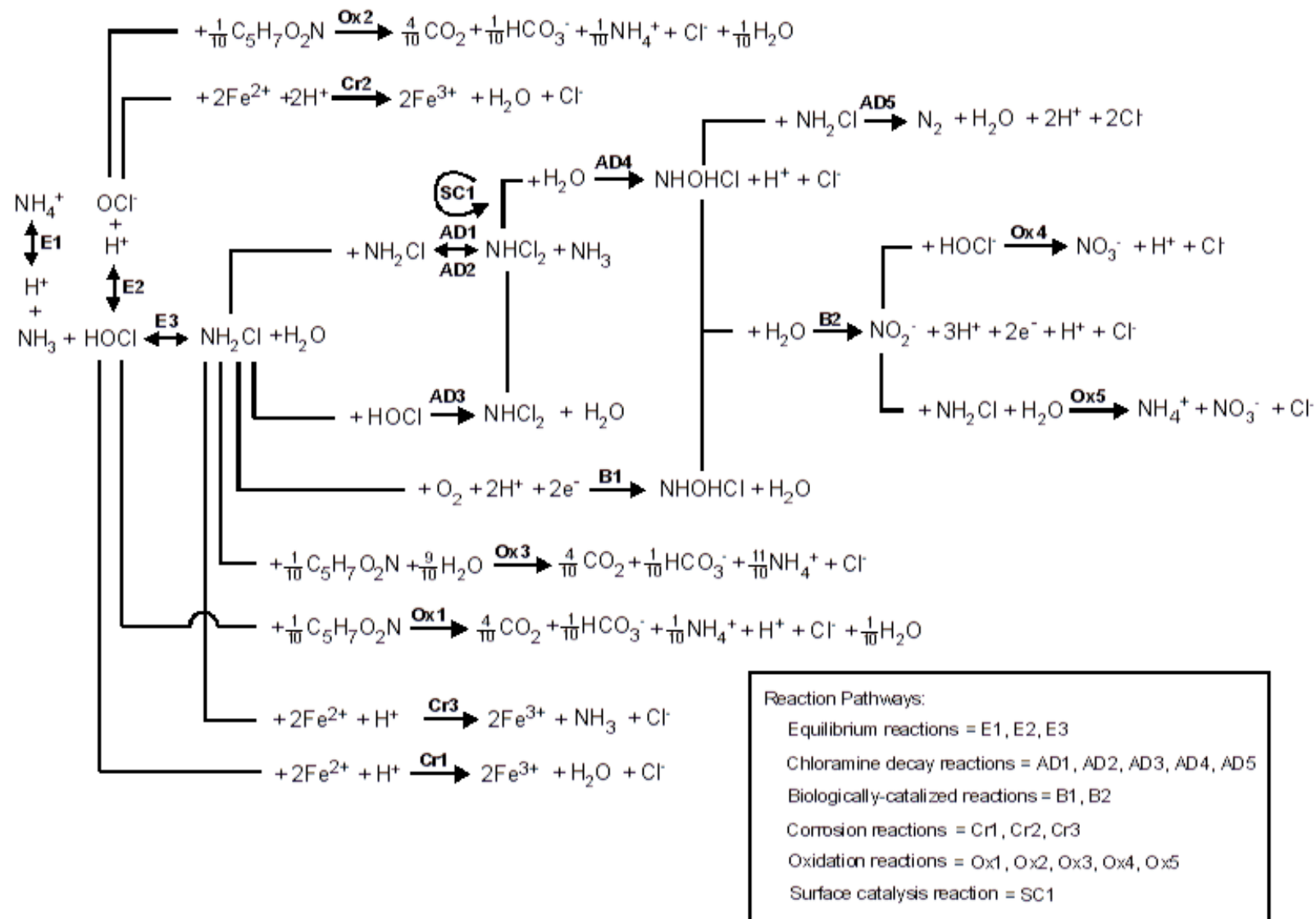


Figure 3-2: Reaction Pathways incorporated in the CDWQ-CL₂ submodel

(Woolschlager, 2000, p 152)

3.2.1 Equilibrium Reactions (E₁-E₃)

These reactions govern the balance between free chlorine and combined chlorine. As the kinetic reactions between free chlorine, ammonia and combined chlorine are very fast, a change in the concentrations of one species results in an almost instantaneous change in the other species.

3.2.2 Chloramine Autocatalytic Decay Reactions (AD₁-AD₅)

This reaction pathway accounts for the slow decay reactions that chloramine undergoes in the absence of any other reactants. Reaction AD₁ represents the acid-catalysed disproportionation reaction of monochloramine and it is this reaction that is rate-limiting with respect to autocatalytic decay. Following reaction AD₁, chloramine rapidly decays to form nitrogen gas and chloride, although the intermediate species chlorohydroxylamine (NHOHCl) will typically also be present in small quantities.

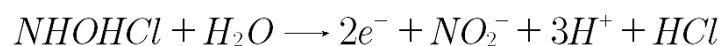
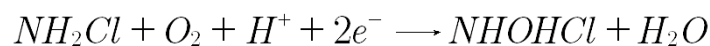
3.2.3 Cometabolism Reactions (B₁-B₂)

These reactions describe the cometabolism on monochloramine by AOB, which was originally proposed by Wooschlager (2000). Wooschlager's hypothesis with regard to cometabolism has been confirmed by Maestre, Wahman & Speitel (2013) who conducted a set of batch experiments under drinking water conditions and concluded that monochloramine cometabolism should occur in practice.

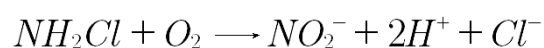
The rationale for this hypothesis is as follows:

Monochloramine has a similar chemical structure to ammonia, the substrate which supports AOB growth, and cometabolism of monochloramine is thermodynamically favourable.

Cometabolism is modelled as a two-step reaction, involving chlorohydroxylamine as a metabolic intermediate.



Hence, the overall reactions can be written as:



As in the CDWQ model, the rate of chloramine loss by cometabolism is modelled in the CDWQ-E₂ version using competitive cometabolism kinetics (Ely et al, 1995 in Wooschlager, 2000), while dual-limitation Monod kinetics are additionally incorporated. Similarly, the rate of chlorohydroxylamine loss is modelled using dual-limitation Monod kinetics, as opposed to the single-substrate limitation Monod kinetics used in the CDWQ model.

Specific Utilisation Rate for Cometabolism of Monochloramine:

$$UTLNH_2Cl = q_{NH_2Cl} \left(\frac{NH_2Cl}{K_{NH_2Cl} \left(1 + \frac{NH_3}{K_{NH_3}} \right) + NH_2Cl} \right) \left(\frac{O_2}{K_{O_2} + O_2} \right)$$

Equation 3-36

Specific Utilisation Rate for Cometabolism of Chlorohydroxylamine:

$$UTLNHOHCl = q_{NHOHCl} \left(\frac{NHOHCl}{K_{NHOHCl} + NHOHCl} \right) \left(\frac{O_2}{K_{O_2} + O_2} \right)$$

Equation 3-37

3.2.4 Oxidation Reactions (Ox₁-Ox₅)

Reactions Ox₁ to Ox₃ represent the oxidation of reduced organic matter by hypochlorous acid, hypochlorite and monochloramine respectively. The rate of oxidation is dependent on both the type of disinfectant and the type of organic matter being oxidised. The reduced organic compounds contained in the CDWQ-E₂ model that can be oxidised by free or combined chlorine are: BOM₁, BOM₂, UAP, BAP, EPS and inert bacteria³.

Reduced organic matter can be categorised depending on the rate at which it is oxidised. Organic matter that can be rapidly oxidised by chlorine consists solely of BOM₁, while the other types of reduced organic matter mentioned above are slowly oxidised by chlorine. Thus, in accordance with the CDWQ model, the E₂ version has six oxidation parameters, with a unique parameter for each combination of disinfectant (either hypochlorous acid, hypochlorite or monochloramine) and category of reduced organic matter.

Reactions Ox₄ and Ox₅ represent the oxidation of nitrite by hypochlorous acid and monochloramine respectively.

³ As opposed to the CDWQ model which contains BOM₁, BOM₂, UAP, BAP and refractory inorganic matter.

3.2.5 Oxidation of Corrosion Products (Cr₁-Cr₃)

This reaction pathway accounts for the oxidation reactions that occur between, in particular, reduced iron, released from corroded iron pipes, and free chlorine, as well as monochloramine. Iron pipes are comprised of elemental iron (Fe⁰). However, iron pipes in direct contact with drinking water typically corrode spontaneously to form ferrous iron (Fe²⁺). While chlorine is not consumed during the oxidation of elemental iron to ferrous iron, as oxygen is the preferred electron acceptor for this reaction, the chlorine species are rapidly reduced by ferrous iron.

Ideally, a submodel capable of determining the corrosion rates of iron pipes would be included in the model. However, due to the complexity of this process in drinking water distribution systems, it is currently not well characterised. As it was beyond the scope of both the original CDWQ model and the CDWQ-E₂ model to develop a submodel that is capable of accounting for the various factors that influence corrosion rate, such as pH, alkalinity, hardness, presence of dissolved oxygen, dissolved solids concentration and chloride concentration (LeChevallier et al, 1993 in Woolschlager, 2000), a first-order chlorine demand constant only for iron pipes is applied for monochloramine oxidation, while a zero-order constant is applied for free chlorine oxidation. This differs from the CDWQ model, which applies a zero-order chlorine demand constant for both species of disinfectant. Woolschlager stated that numerous researchers (Rossmann, Clark & Grayman, 1994; Vasconcelos et al, 1997; Kiene, Lu & Levi, 1998 in Woolschlager, 2000) have found that zero-order modelling of chlorine consumption at pipe surfaces provides good fit to distribution system data, and hence used a zero-order model for monochloramine oxidation. However, more recent research by Westbrook et al (2009) has found that chloramine decay rates should be modelled using first-order kinetics. The reason for the difference in approach required is that free chlorine is a stronger oxidant than chloramine and hence it reacts more readily with ferrous iron corrosion products. Therefore, the availability of corrosion products controls the rate of free chlorine decay and as a consequence, the rate of free chlorine decay due to reactions with corrosion products appears first-order with regard to free chlorine (DiGiano & Zhang, 2005). By only applying this first-order constant to demand exerted by iron pipes (as opposed to also including demand exerted by organic matter attached to pipe surfaces in such a first-order constant, as is the case with other water quality models), the model retains its predictive capabilities.

3.2.6 Surface Catalysis (SC₁)

Surface catalysis only applies when chloramines are utilised as a disinfectant and where either concrete-lined iron pipes or reinforced concrete pipes are used.

3.3 Disinfection

The CDWQ-Cl₂ submodel described previously is used to determine the concentration of the disinfectant. For all three versions of the CDWQ model, the rate of disinfection of active biomass is calculated using the Chick-Watson model, which stipulates that disinfectant concentration and contact time are the key variables that determine disinfection efficiency for a given disinfectant.

$$r_d = -k_d \cdot C^n \cdot X$$

Equation 3-38

Parameter	Description	Units
r_d	Rate of disinfection	$\frac{M}{L^3 \cdot T}$
k_d	Deactivation coefficient	$\frac{L}{M \cdot T}$
C	Concentration of disinfectant	$\frac{M}{L^3}$
n	Coefficient of dilution	Dimensionless (typically 1.0) ⁴
X	Concentration of active biomass	$\frac{M}{L^3}$

Each combination of disinfectant (hypochlorous acid, hypochlorite or monochloramine) and active biomass (either fixed or suspended heterotrophs, AOB or NOB) has a potentially unique value for the deactivation coefficient. Consequently, up to eighteen separate deactivation coefficients can be incorporated. However, as explained previously, the CDWQ model has only been calibrated for monochloramine. Therefore, only deactivation coefficients for monochloramine are available for the purposes of this project.

Active biomass lost due to disinfection can either form inert biomass or BOM₂. The fraction of active biomass that is biodegradable forms BOM₂ upon disinfection, while the fraction that is not biodegradable forms inert biomass upon disinfection.

3.4 Temperature

As described in the literature review, temperature has a significant effect on water quality. The CDWQ-E₂ model, in line with previous versions of the model, is able to account for the influence of

⁴ An n value of 1.0 is used for all three versions of the CDWQ model.

temperature on substrate utilisation rate and hence bacterial growth rates, as well as the impact of temperature on disinfectant decay, which in turn affects the rate of disinfection.

The temperature adjustment factor is based on the Arrhenius equation, which has been modified for drinking water systems (Woolschlager, 2000). The modified equation is given by Equation 3-39, with its derivation given in Appendix A.

$$\frac{k_{T1}}{k_{T2}} = \Theta^{T1-T2}$$

Equation 3-39

Parameter	Description	Units
k_{T1}	Rate of disinfection	°C
k_{T2}	Deactivation coefficient	°C
Θ	Temperature adjustment coefficient	Dimensionless

Using Equation 3-39, a baseline temperature of 20°C is set, against which the rates of substrate utilisation, disinfectant decay and oxidation of organic matter can be modified for a given temperature.

One potential limitation with this approach is that the rate of substrate utilisation will continue indefinitely with increasing temperature. In reality, above approximately 38°C the rate of substrate utilisation will begin to decrease as this temperature exceeds the denaturation temperature of proteins (Roels, 1983 in Woolschlager, 2000)). However, as temperatures in drinking water distribution systems seldom exceed 38°C (Woolschlager, 2000), the use of Equation 3-39 is satisfactory for the purposes of drinking water modelling.

3.5 pH

pH has a significant effect on water quality, as mentioned in the literature review, and consequently this effect needs to be modelled. Typically, pH fluctuations in distribution systems are small. In a study of ten drinking water systems, Wilczak et al (1996 in Woolschlager, 2000) found that pH only varied by 1.0 units between these systems, and 17 of the 20 data points assessed had pH variations of 0.5 units or less. Similarly, a study of a distribution system providing drinking water to the greater Boston area, using chloramine as a secondary disinfectant, by Xin et al (2006) found that the pH did not vary by more than 0.11 units in the system. Woolschlager, therefore, was able obtain good fit to field data using a simplified approach in which a global pH was set at the start of the simulation

period and remained constant throughout the simulation period. The CDWQ-E₂ model therefore uses the same simplified approach.

The model accounts for the influence of pH on water quality by determining the shift in speciation for the following acid-base pairs: NH_4^+ and NH_3 ; $HOCl$ and OCl^- ; carbonate species. It is able to do this with the use of ionisation fractions (Snoeyink & Jenkins, 1980 in Wooschlager, 2000, p 209). The derivations for Equations 3-40 to 3-46 are given in Appendix B.

For Monoprotic Acids:

$$[NH_4^+] = \frac{[H^+][C_{T,NH_3}]}{[H^+] + K_a}$$

Equation 3-40

$$[NH_3] = \frac{[K_a][C_{T,NH_3}]}{[H^+] + K_a}$$

Equation 3-41

$$[HOCl] = \frac{[H^+][C_{T,OCl}]}{[H^+] + K_a}$$

Equation 3-42

$$[OCl^-] = \frac{[K_a][C_{T,OCl}]}{[H^+] + K_a}$$

Equation 3-43

For Diprotic Acids:

$$[H_2CO_3] = \frac{[H^+]^2 \cdot C_{T,CO_3}}{[H^+]^2 + [H^+] \cdot K_{a1} + K_{a1} \cdot K_{a2}}$$

Equation 3-44

$$[HCO_3^-] = \frac{[H^+] \cdot K_{a1} \cdot C_{T,CO_3}}{[H^+]^2 + [H^+] \cdot K_{a1} + K_{a1} \cdot K_{a2}}$$

Equation 3-45

$$[CO_3^{2-}] = \frac{K_{a1} \cdot K_{a2} \cdot C_{T,CO_3}}{[H^+]^2 + [H^+] \cdot K_{a1} + K_{a1} \cdot K_{a2}}$$

Equation 3-46

Parameter	Description	Units
$C_{T,A}$	Total component molar concentration	$\frac{M}{L^3}$

K_a, K_{a1} and K_{a2}	Dissociation constants	Dimensionless
---	------------------------	---------------

The dissociation constants used to calculate the shift in speciation of the acid-base pairs discussed previously are temperature dependent and vary according to the van't Hoff equation:

$$K_a = C' e^{\left(\frac{-\Delta H^\circ}{R.T}\right)}$$

Equation 3-47

The values for ΔH° and C' are based on those determined by Snoeyink & Jenkins (1980 in Wooschlager, p 211).

Reaction	ΔH° at 25 °C (kJ/mol)	C'
$HOCl \xrightleftharpoons{K_a} OCl^- + H^+$	13.8	8.27E-6
$NH_4^+ \xrightleftharpoons{K_a} NH_3 + H^+$	52.2	7.03E-1
$H_2CO_3 \xrightleftharpoons{K_{a1}} HCO_3^- + H^+$	7.7	1.12E-5
$HCO_3^- \xrightleftharpoons{K_{a2}} CO_3^{2-} + H^+$	14.9	2.04E-8

The manner in which shifts of these pairs can influence water quality will be detailed using the simulations that follow later in this report.

3.6 Mass Transport

The flow distribution in a water distribution system is defined by conservation of mass and energy and it is assumed that any constituent in water does not affect either. The implication of this is that a hydraulic analysis can be performed without any consideration with regard to water quality.

However, the transport of all constituents in a distribution system are determined by the flow velocities within the distribution system and consequently (as is the case with all available water quality models), well-defined hydraulics are a pre-requisite for an accurate water quality model (Lansey & Boulos, 2005).

Like the CDWQ model, the E₂ version requires an independent hydraulic analysis to be performed and imported. Based on the time varying flow rates from the hydraulic analysis, the components required for the water quality analysis can be determined. These components are:

- Pipe elements
- Reservoir elements
- Nodes

A description of each of these components follows in subsections 3.6.1 to 3.6.3. The detailed sequence in which these components are defined and the relationships between them are given in the algorithm for the CDWQ-E₂ model in section 3.9.

3.6.1 Pipe Elements

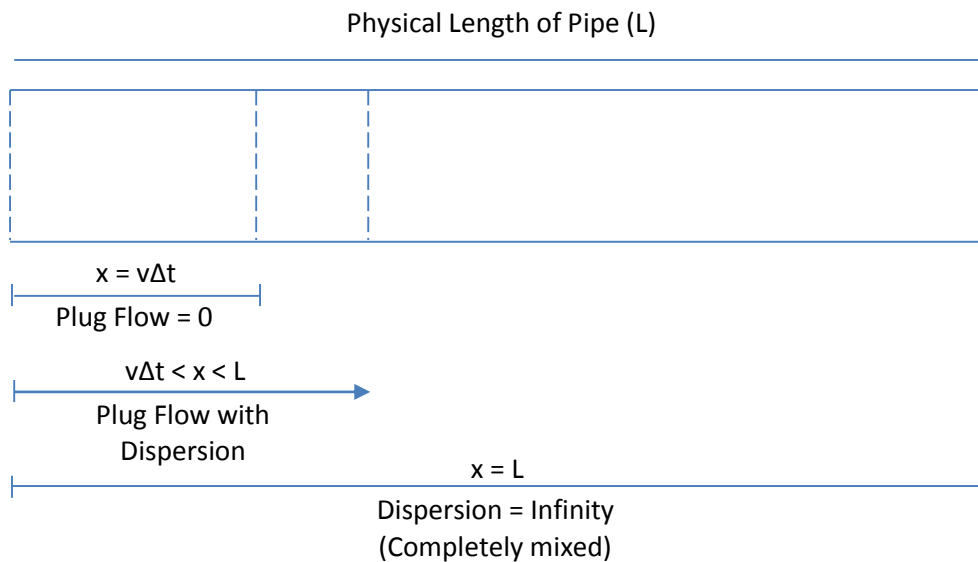


Figure 3-3: Effect of Pipe Element Size on Dispersion Characteristics

(Adapted from Wooschlager, 2000, p 217)

The incorporation of pipe elements provides a means of modelling the flow of constituents through the distribution system and the reactions that occur within each pipe without violating mass conservation. The rationale for the manner in which pipes are divided into pipe elements in the CDWQ-E₂ model follows.

Transport of a general fluid property can occur by five mechanisms: advection, molecular diffusion, turbulent diffusion, dispersion and radiation. For most water quality models, advection is the dominant mechanism of fluid transport in the pipe. Advection is defined as the movement of the constituent with the water, in the direction of flow, with the magnitude of main velocity component. Radiation need not be considered for any water quality model as it is limited to energy transport by electromagnetic waves. As water flow in distribution systems is generally turbulent with a high velocity, molecular diffusion, turbulent diffusion and dispersion are typically neglected in most water quality models (Lansey & Boulos, 2005).

The size of a pipe element is determined by the degree of dispersion assumed. If no dispersion is assumed, as is the case for most water quality models, the solution for the pipe is equivalent to a

plug-flow solution and the size of the pipe element is equal to the product of the velocity of the water in that pipe and the time step used to obtain the numerical solution ($x=v\Delta t$). If dispersion is set to infinity, the solution for the pipe is equivalent to a completely mixed solution and the length of the element is set to the length of the physical pipe $x=L$. A pipe with element lengths between these two values is equivalent to a plug flow solution with dispersion ($v\Delta t < x < L$) (Tchobanoglous & Schroeder, 1985 in Wooschlager, 2000).

Prior to the development of the CDWQ model, other water quality models, including EPANET, used a plug-flow solution. However, in order to do this, pipe element sizes need to be redefined every time the flow velocity in the pipe changes, which is a computationally intensive process (Clark et al, 1993 in Wooschlager, 2000).

Wooschlager (2000) developed a unique approach to size pipe elements which assumes that advection is the dominant mechanism of fluid transport, while neglecting the limited effect of dispersion in order to significantly reduce the computational demands required to resize pipe elements every time flow changes. This process involves defining the element size for each pipe as being equal to the product of the maximum flow velocity in the pipe for the simulation period and the time step used to obtain the numerical solution. Although such an approach would theoretically introduce a degree of dispersion, it has a negligible effect on the solution, as can be explained by analysis of the exact solution for steady-state advection-dispersion with first-order reaction, given by Equation 3-48 (Wehner & Wilhelm, 1958 in Wooschlager, 2000, p 217):

$$\frac{C_x}{C_i} = \frac{4a.e^{\left(\frac{vL}{2D}\right)}}{(1+a)^2.e^{\left(\frac{avL}{2D}\right)} - (1-a)^2.e^{\left(\frac{-avL}{2D}\right)}}$$

Equation 3-48

Where $a = \sqrt{1 + 4k\left(\frac{V}{Q}\right)\left(\frac{D}{vL}\right)}$

Parameter	Description	Units
C_x	Exit concentration leaving pipe	$\frac{M}{L^3}$
C_i	Initial concentration entering pipe	$\frac{M}{L^3}$
L	Length of pipe	L
v	Velocity	$\frac{L}{T}$

D	Dispersion coefficient	$\frac{L^2}{T}$
k	First order reaction constant	$\frac{1}{T}$
Q	Flow rate	$\frac{L^3}{T}$
V	Volume	L^3

Woolschlager (2000) plotted Equation 3-48 for several values of D in order to demonstrate that dispersion is negligible for drinking water distribution systems:

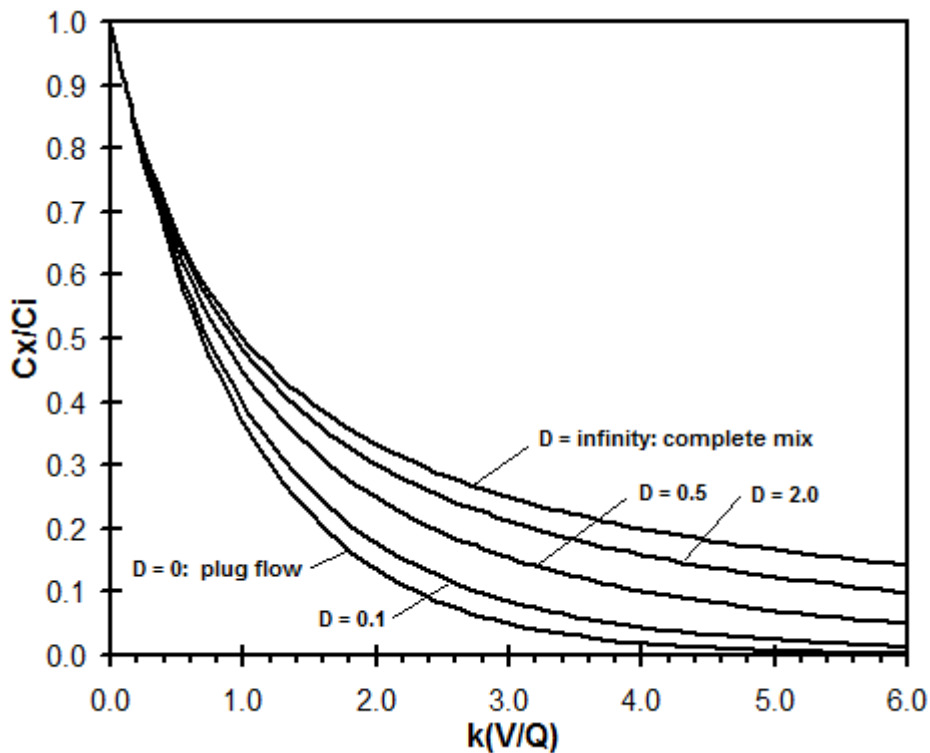


Figure 3-4: Graph of the Exact Solution for Steady-State Advection-Dispersion with First-Order Reaction for Several Values of Dispersion Coefficient (D)

(Woolschlager, 2000, p 218)

Figure 3-4 demonstrates that as the product of the reaction rate and detention time, that is $k(\frac{V}{Q})$, decreases, the plug flow and completely mixed solutions converge. Of critical importance with regard to distribution systems is the fact that $k(\frac{V}{Q})$ is always small for pipe elements defined in both the CDWQ and CDWQ-E₂ model and therefore dispersion is negligible.

In accordance with this approach, the minimum length of each pipe element ($L_{ele,min}$) is calculated as:

$$L_{ele,min}=v_{max}.\Delta t$$

The number of elements in a pipe can then be calculated. However, the number of elements within a pipe must be a whole number. Therefore, this number must be rounded down, thereby increasing the length of the pipe elements. By first determining $L_{ele,min}$, the model ensures that the element lengths are greater than the maximum water travel distance increment through the pipe. If this was not done (or if the number of elements was rounded up), the mass flowing into the element would also flow out of it within a single time step, violating mass-balance. Crucially, when rounding up $L_{ele,min}$, the effect of dispersion is still expected to be negligible based on Figure 3-4.

One important point to note is that depending on the time step used, the pipe element length calculated using this method may be greater than the physical pipe length, which cannot be permitted, as mass closure would be violated. Therefore, a constraint is introduced to the CDWQ-E₂ model that limits the size of the time step such that no pipe element length is greater than the length of the physical pipe.

Having sized pipe elements and given the assumption of advective flow, the transport of a constituent mass between discrete pipe elements is given by Equation 3-49 (Woolschlager, 2000, p 225):

$$\frac{dC}{dt} = \frac{Q}{V} C$$

Equation 3-49

Parameter	Description	Units
C	Constituent Concentration	$\frac{M}{L^3}$
Q	Flow rate in pipe element	$\frac{L^3}{T}$
V	Volume of pipe element	L^3

Within each pipe element, advective transport into the pipe element can add suspended or dissolved constituent mass while advective transport out of the pipe can reduce suspended or dissolved constituent mass. Furthermore, the chemical, biological and physical reactions included in the CDWQ-E₂ model occur within each pipe element. Therefore, the change in a suspended constituent's concentration within a pipe element is given by Equation 3-50:

$$\frac{dC}{dt} = \underbrace{\left(\frac{Q}{V} C_{node}\right)}_{\text{Advection in}} - \underbrace{\left(\frac{Q}{V} C_{pipe}\right)}_{\text{Advection out}} + \underbrace{\sum \text{reactions}}_{\text{reactions effecting constituent } C}$$

Equation 3-50

Parameter	Description	Units
C_{node}	Constituent concentration of inflow node	$\frac{M}{L^3}$
C_{pipe}	Constituent concentration of pipe element	$\frac{M}{L^3}$

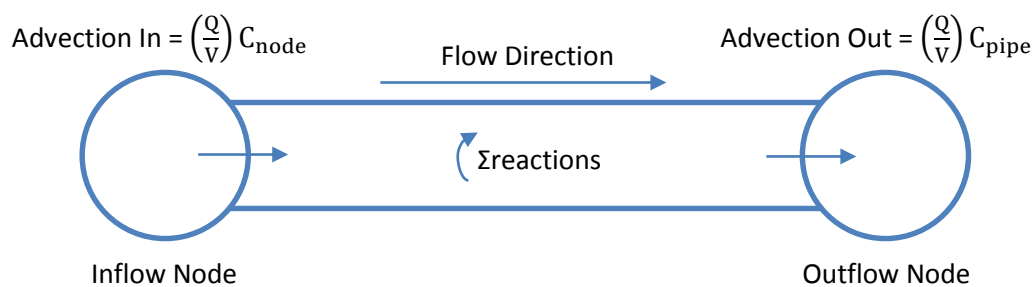


Figure 3-5: Change in suspended constituent concentration for a pipe element

3.6.2 Reservoir Elements

It is important to model water quality parameters both entering and leaving a reservoir, as well as within the reservoir itself. These factors are, in turn, influenced by the movement of water into, out of and within the reservoir (van der Walt, 2002). In order to do this, the compartmental model, developed by Clark et al (1996), is incorporated into the CDWQ-E₂ model.

The compartmental model provides an idealistic approach to mixing with distribution storage tanks and reservoirs, as opposed to computational fluid dynamics (CFD) models which attempt to model the full complexity of mixing within tanks and reservoirs (van der Walt, 2002). Given the large computational demands that would be introduced by the incorporation of a CFD model and the fact that good fit to field data has been obtained using the less computationally demanding compartmental model (Clark et al, 1996; Wooschlager, 2000), it was decided that the introduction of a CFD model was beyond the scope of the CDWQ-E₂ model.

The compartmental model divides water within a reservoir or storage tank into elements, depending on the degree of mixing that occurs. In order to ensure the accuracy of the modelled solution when compared to field data, the number of compartments to be applied should be based on which one gives the best fit to the field data for that particular system (Lemke & DeBoer, 2012).

The equations used to define transport in the compartmental model for the more common inflow/outflow reservoir are presented below. Euler's method is used in the CDWQ-E₂ model to solve the equations. The inflow concentration for the reservoir is based on the preceding pipe element's constituent concentration. Outflow from the reservoir is transferred to this same element. Reactions within reservoir elements are modelled using the same mass-balance equations used for reactions in pipe elements.

One-Compartment Model

The value of compartment A (V_A) is variable and a function of time.

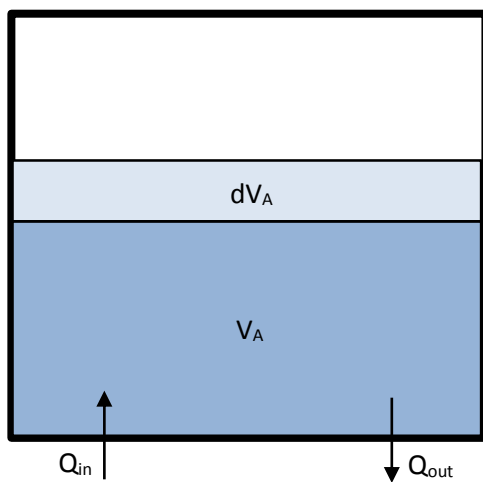


Figure 3-6: Single-Compartment Model

(Clark et al, 1996, p 817)

Inflow:

$$\frac{dC_{A,i}}{dt} = \frac{Q_{in}(C_{in,i} - C_{A,i})}{V_A}$$

Equation 3-51

Where i represents every suspended or dissolved constituent accounted for in the CDWQ-E₂ model

Outflow:

$$\frac{dC_{A,i}}{dt} = 0$$

Equation 3-52

Two-Compartment Model

V_A is fixed, while the volume of compartment B (V_B) is variable and a function of time.

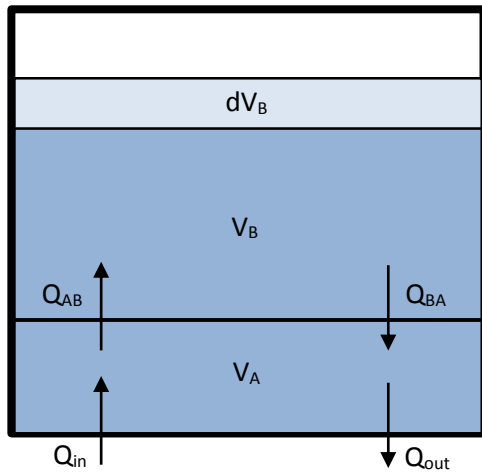


Figure 3-7: Two-Compartment Model

(Clark et al, 1996, p 817)

Inflow:

$$\frac{dC_{A,i}}{dt} = \frac{Q_{in}(C_{in,i} - C_{A,i})}{V_A}$$

Equation 3-53

$$\frac{dC_{B,i}}{dt} = \frac{Q_{in}(C_{A,i} - C_{B,i})}{V_B}$$

Equation 3-54

Outflow:

$$\frac{dC_{B,i}}{dt} = \frac{Q_{AB}(C_{B,i} - C_{B,i})}{V_B} = 0$$

Equation 3-55

$$\frac{dC_{A,i}}{dt} = \frac{Q_{out}(C_{B,i} - C_{A,i})}{V_A}$$

Equation 3-56

Three-Compartment Model

V_A and the volume of compartment C (V_C) are fixed, while V_B is variable and a function of time.

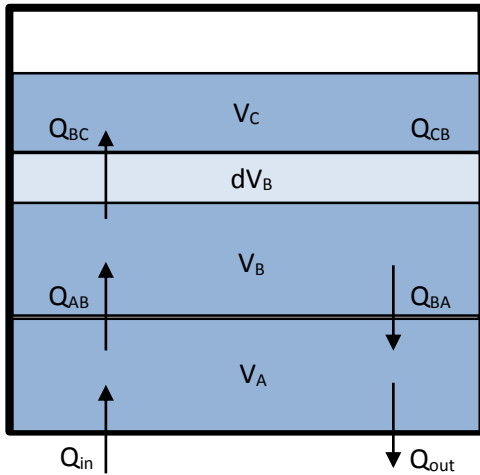


Figure 3-8: Three-Compartment Model

(Clark et al, 1996, p 817)

Inflow:

$$\frac{dC_{A,i}}{dt} = \frac{Q_{in}(C_{in,i} - C_{A,i})}{V_A}$$

Equation 3-57

$$\frac{dC_{B,i}}{dt} = \frac{Q_{in}(C_{A,i} - C_{B,i}) + Q_{BC}(C_{C,i} - C_{B,i})}{V_B}$$

Equation 3-58

$$\frac{dC_{C,i}}{dt} = \frac{Q_{BC}(C_{B,i} - C_{C,i})}{V_C}$$

Equation 3-59

Outflow:

$$\frac{dC_{C,i}}{dt} = \frac{Q_{BC}(C_{B,i} - C_{C,i})}{V_C}$$

Equation 3-60

$$\frac{dC_{B,i}}{dt} = \frac{Q_{BC}(C_{C,i} - C_{B,i})}{V_B}$$

Equation 3-61

$$\frac{dC_{A,i}}{dt} = \frac{Q_{out}(C_{B,i} - C_{A,i})}{V_A}$$

Equation 3-62

Parameter	Description	Units
$C_{A,i}$	Concentration of a given constituent in compartment A	$\frac{M}{L^3}$
$C_{B,i}$	Concentration of a given constituent in compartment B	$\frac{M}{L^3}$
$C_{C,i}$	Concentration of a given constituent in compartment C	$\frac{M}{L^3}$
V_A	Volume of compartment A	L^3
V_B	Volume of compartment B	L^3
V_C	Volume of compartment C	L^3
Q_{in}	Flow rate into reservoir	$\frac{L^3}{T}$
Q_{out}	Flow rate out of reservoir	$\frac{L^3}{T}$

Biofilm Modelling within Reservoir/Storage Tank Elements

The compartment model is intended for use with suspended or dissolved constituents. Given that biofilms within reservoir or storage tank elements are fixed to the walls and are not subject to transport into, out of or within reservoirs or tanks in the same manner as is described by the compartment model, a method of modelling biofilm concentrations within reservoirs and tanks has been developed for the CDWQ-E₂ model to be used in conjunction with the compartment model for suspended constituents.

As biofilms are attached to reservoir and storage tank walls and are not subject to transport, regardless of the flow into or out of reservoirs or storage tanks, the mass of a biofilm species must not be altered by the flow. Therefore, for flow into a reservoir or tank, the mass of biofilms within compartments of variable size cannot be altered due to this flow. Hence, the concentration of biofilms within these compartments is reduced by a factor in order to keep the total mass due to flow unchanged. Similarly, for flow out of the reservoir, the total biofilm concentration is increased by a factor in order to keep the total biofilm mass due to flow unchanged. Chemical, biological and

physical reactions can, however, affect the mass of a biofilm species within a reservoir or storage tank.

3.6.3 Nodes

A node is a theoretical concept used in water quality modelling and it is assumed that no storage is provided by a node and that water passes through nodes instantaneously. Conservation of mass is applied at nodes to account for the mixing of water with different constituent concentrations at pipe junctions. Nodes are also used to add a constituent concentration at a point or, from a hydraulic perspective, to account for water demand out of the system (Lansey & Boulos, 2005).

Typical Node-Pipe Junction

Given the assumption that nodes are infinitely small, they cannot store water and hence the mass of a constituent at a node is constant. For the same reason, no time is spent by water at a node and therefore the chemical, biological and physical reactions accounted for in the CDWQ-E₂ model do not occur at junctions. Furthermore, as the mass of a constituent at a node is constant and the sum of the flows into and out of a node must be the same due to conservation of flow, the concentration of a constituent at a node is equal to the concentration of that constituent leaving the node.

Therefore, applying conservation of a constituent mass at a typical pipe-junction node with n inflow pipes and m outflow pipes within the system under consideration, and o pipes leaving the system to account for external demands, gives (Lansey & Boulos, 2005):

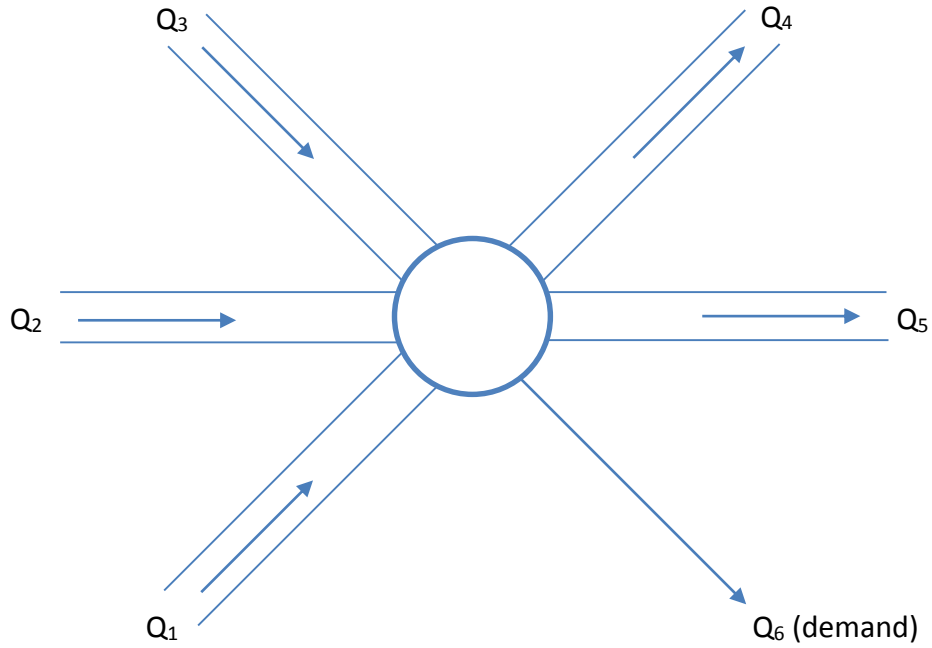


Figure 3-9: Typical Node Junction

$$\sum_{i=1}^n C_i Q_i - \sum_{j=1}^m C_{j,out} Q_j - \sum_{k=1}^o C_{k,out} Q_k = 0$$

Equation 3-63

$$\therefore C_{out} = \frac{\sum_{i=1}^n C_i Q_i}{\left(\sum_{j=1}^m Q_j + \sum_{k=1}^o Q_k\right)}$$

Equation 3-64

However, based on the continuity equation, the sum of flows at a node must be equal to zero (Chadwick, Morfett & Borthwick, 2004). Therefore, flow into a node is equal to flow out of a node and Equation 3-64 can be rewritten as Equation 3-65, which is computationally simpler, to be performed in the CDWQ-E₂ model:

$$C_{out} = \frac{\sum_{i=1}^n C_i Q_i}{\sum_{i=1}^n Q_i}$$

Equation 3-65

Treatment Plant

In the CDWQ-E₂ model, a water treatment plant is modelled as a node with various suspended and dissolved constituents injected or input over time with water. The constituent concentrations originating from the treatment plant are specified for a given time period and the flow rate from the treatment plant varies over time.

Therefore, at the treatment plant node, applying mass conservation for n outflow pipes within the system under consideration gives:

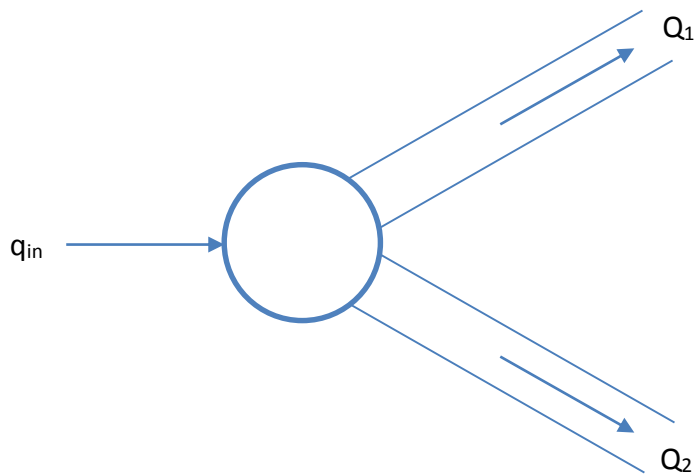


Figure 3-10: Typical Treatment Plant Node Junction

$$C_{out} = \frac{C_{in} q_{in}}{\sum_{i=1}^n Q_i}$$

Equation 3-66

However, as before, based on the continuity equation, Equation 3-66 can be rewritten as:

$$C_{out} = \frac{C_{in} q_{in}}{q_{in}}$$

Equation 3-67

Booster Disinfection

The ability to model booster chloramination or booster chlorination has been added to the CDWQ-E₂ model. The injected disinfectant is modelled as a flow-paced booster, which adds a fixed concentration of disinfectant (C_{out}^{inj}) for a given time period at the applicable node. Given this

definition, the added disinfectant mass rate at a booster node with n inflow pipes and m outflow pipes within the system under consideration, and o pipes leaving the system to account for external demands, is given by Equation 3-68 (Lansley & Boulos, 2005):

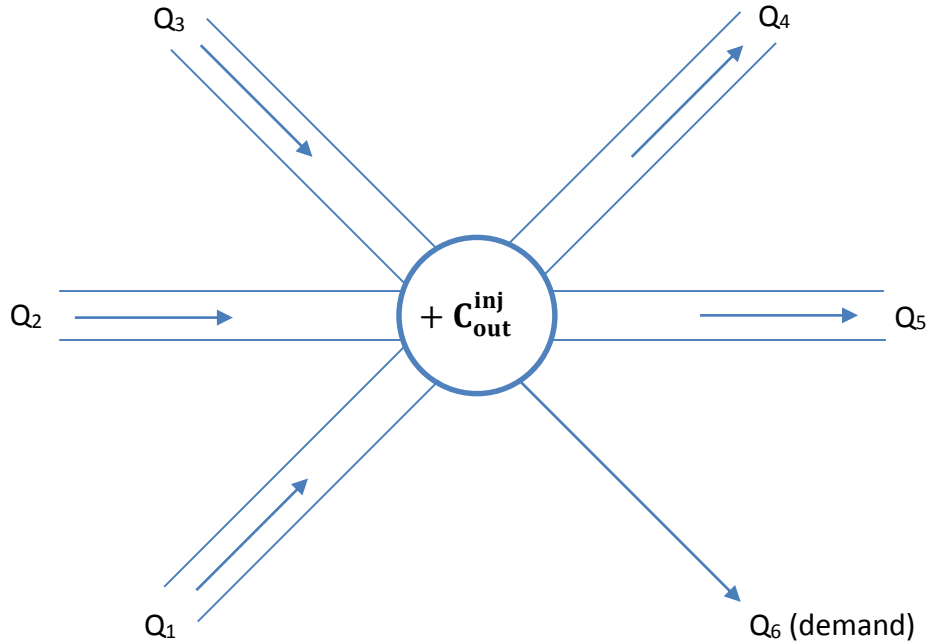


Figure 3-11: Typical Booster Node Junction

$$\frac{dm_c}{dt} = C_{out}^{inj} \left(\sum_{j=1}^m C_{j,out} Q_j + \sum_{k=1}^o C_{k,out} Q_k \right)$$

Equation 3-68

Given the assumption of no nodal storage, Equation 3-68 can be added to Equation 3-63 for nodes where booster disinfection is utilised. This gives:

$$\begin{aligned} \sum_{i=1}^n C_i Q_i - \sum_{j=1}^m C_{j,out} Q_j - \sum_{k=1}^o C_{k,out} Q_k + \frac{dm_c}{dt} &= 0 \\ \therefore \sum_{i=1}^n C_i Q_i - \sum_{j=1}^m C_{j,out} Q_j - \sum_{k=1}^o C_{k,out} Q_k + C_{out}^{inj} \left(\sum_{j=1}^m C_{j,out} Q_j + \sum_{k=1}^o C_{k,out} Q_k \right) &= 0 \\ \therefore C_{out} &= \frac{\sum_{i=1}^n C_i Q_i}{\left(\sum_{j=1}^m Q_j + \sum_{k=1}^o Q_k \right)} + C_{out}^{inj} \end{aligned}$$

Equation 3-69

3.7 Parameters and Reaction Constants Incorporated in CDWQ-E₂

Equation	Reaction	Rate expression	Reaction Constant(s)	Reference
(E ₁)	$\text{NH}_4^+ \leftrightarrow \text{NH}_3 + \text{H}^+$	Equilibrium reaction	$K_{E1} = 7.029E - 1 \times e^{\frac{-52210}{R(\text{Temp}+273.15)}}$	Snoeyink and Jenkins (1980)
(E ₂)	$\text{OCl}^- + \text{H}^+ \leftrightarrow \text{HOCl}$	Equilibrium reaction	$K_{E2} = 8.273E - 6 \times e^{\frac{-13800}{R(\text{Temp}+273.15)}}$	Snoeyink and Jenkins (1980)
(E ₃)	$\text{NH}_3 + \text{HOCl} \leftrightarrow \text{NH}_2\text{Cl} + \text{H}_2\text{O}$	Equilibrium reaction	$K_{E3} = \text{n/a}$	
(AD ₁)	$\text{NH}_2\text{Cl} + \text{NH}_2\text{Cl} \rightarrow \text{NHCl}_2 + \text{NH}_3$	$k_{AD1}[\text{NH}_2\text{Cl}]^2$	$k_{AD1} = k_{H^+}[\text{H}^+] + k_{\text{H}_2\text{CO}_3}[\text{H}_2\text{CO}_3]$ $k_{H^+} = 2.5 \times 10^7 \text{ M}^{-2}\text{h}^{-1}$ $k_{\text{H}_2\text{CO}_3} = 40000 \text{ M}^{-2}\text{h}^{-1}$	Ozegin, Valentine & Vikesland (1996); Woolschlager (2000)
(AD ₂)	$\text{NHCl}_2 + \text{NH}_3 \rightarrow \text{NH}_2\text{Cl} + \text{NH}_2\text{Cl}$	$k_{AD2}[\text{NHCl}_2][\text{NH}_3][\text{H}^+]$	$k_{AD2} = 2.16 \times 10^8 \text{ M}^{-2}\text{h}^{-1}$	Hand and Margerum (1983)
(AD ₃)	$\text{HOCl} + \text{NH}_2\text{Cl} \rightarrow \text{NHCl}_2 + \text{H}_2\text{O}$	$k_{AD3}[\text{HOCl}][\text{NH}_2\text{Cl}]$	$k_{AD3} = 1.0 \times 10^6 \text{ M}^{-1}\text{h}^{-1}$	Margerum and Gray (1978)
(AD ₄)	$\text{NHCl}_2 + \text{H}_2\text{O} \rightarrow \text{NHOHCl} + \text{HCl}$	$k_{AD4}[\text{NHCl}_2][\text{OH}^-]$	$k_{AD4} = 6.0 \times 10^5 \text{ M}^{-1}\text{h}^{-1}$	Ozegin, Valentine & Vikesland (1996); Woolschlager (2000)
(AD ₅)	$\text{NHOHCl} + \text{NH}_2\text{Cl} \rightarrow \text{N}_2 + \text{H}_2\text{O} + 2\text{HCl}$	$k_{AD5}[\text{NHOHCl}]$	$k_{AD5} = 5.0 \times 10^{-3} \text{ h}^{-1}$	Diyamandoglu (1994); Woolschlager (2000)

(B₁)	$\text{NH}_2\text{Cl} + \text{O}_2 + 2\text{H}^+ + 2\text{e}^- \rightarrow \text{NHOHCl} + \text{H}_2\text{O}$	Dual-Limitation Monod (Equation 3-36)	See Table 3-4	Wooschlager (2000)
(B₂)	$\text{NHOHCl} + \text{H}_2\text{O} \rightarrow 2\text{e}^- + \text{NO}_2^- + 3\text{H}^+ + \text{HCl}$	Dual-Limitation Monod (Equation 3-37)	See Table 3-4	Wooschlager (2000)
(O_{x1})	$\frac{1}{10}\text{C}_5\text{H}_7\text{O}_2\text{N} + \text{HOCl} \rightarrow$ $\frac{4}{10}\text{CO}_2 + \frac{1}{10}\text{HCO}_3^- + \frac{1}{10}\text{NH}_4^+ + \text{HCl} + \frac{1}{10}\text{H}_2\text{O}$	$k_{\text{ox}_1\text{x}_1}[\text{HOCl}][\text{OM}_1]^5$ $k_{\text{ox}_1\text{x}_2}[\text{HOCl}][\text{OM}_2]^6$	$k_{\text{ox}_1\text{x}_1} = \text{n/a}$ $k_{\text{ox}_1\text{x}_2} = \text{n/a}$	Qualls and Johnson (1983)
(O_{x2})	$\frac{1}{10}\text{C}_5\text{H}_7\text{O}_2\text{N} + \text{OCl}^- \rightarrow$ $\frac{4}{10}\text{CO}_2 + \frac{1}{10}\text{HCO}_3^- + \frac{1}{10}\text{NH}_4^+ + \text{Cl}^- + \frac{1}{10}\text{H}_2\text{O}$	$k_{\text{ox}_2\text{x}_1}[\text{OCl}^-][\text{OM}_1]$ $k_{\text{ox}_2\text{x}_2}[\text{OCl}^-][\text{OM}_2]$	$k_{\text{ox}_2\text{x}_1} = \text{n/a}$ $k_{\text{ox}_2\text{x}_2} = \text{n/a}$	Qualls and Johnson (1983)
(O_{x3})	$\frac{1}{10}\text{C}_5\text{H}_7\text{O}_2\text{N} + \text{NH}_2\text{Cl} + \frac{9}{10}\text{H}_2\text{O} \rightarrow$ $\frac{4}{10}\text{CO}_2 + \frac{1}{10}\text{HCO}_3^- + \frac{11}{10}\text{NH}_4^+ + \text{Cl}^-$	$k_{\text{ox}_3\text{x}_1}[\text{NH}_2\text{Cl}][\text{OM}_1]$ $k_{\text{ox}_3\text{x}_2}[\text{NH}_2\text{Cl}][\text{OM}_2]$	$K_{\text{ox}_3\text{x}_1} = 30.0 \frac{\text{l}}{\text{mole.h}}$ $K_{\text{ox}_3\text{x}_2} = 3.0 \frac{\text{l}}{\text{mole.h}}$	Qualls and Johnson (1983)
(O_{x4})	$\text{HOCl} + \text{NO}_2^- \rightarrow \text{Cl}^- + \text{HNO}_2$	$k_{\text{ox}_5}[\text{HOCl}][\text{NO}_2^-]$	$k_{\text{ox}_4} = \frac{k_{\text{ox}_{4a}} + k_{\text{ox}_{4b}}[\text{NO}_2^-]}{[\text{OH}^-]}$ $K_{\text{ox}_{4a}} = 2.3\text{E-}2 \frac{1}{\text{mole.h}}$ $K_{\text{ox}_{4b}} = 5.0 \frac{1}{\text{mole.h}}$	Johnson and Margerum (1991)

⁵ OM₁ represents rapidly degradable species of organic matter: BOM₁

⁶ OM₂ represents slowly degradable species of organic matter: BOM₂, UAP, BAP, EPS and inert bacteria

(Ox₅)	$\text{NH}_2\text{Cl} + \text{NO}_2^- + \text{H}_2\text{O} \rightarrow \text{NH}_4^+ + \text{NO}_3^- + \text{Cl}^-$	$k_{\text{ox}_5}[\text{NH}_2\text{Cl}][\text{NO}_2^-]$	$k_{\text{ox}_5} = \frac{k_{\text{ox}_{5a}}[\text{H}^+] \times (1 + k_{\text{ox}_{5b}} \cdot [\text{NO}_2^-])}{k_{\text{ox}_{5c}} \cdot \text{NH}_3 + (1 + k_{\text{ox}_{5b}} \cdot [\text{NO}_2^-])}$ $k_{\text{ox}_{5a}} = 1.36\text{E}7 \frac{1}{\text{mole.h}}$ $k_{\text{ox}_{5b}} = 2.17\text{E}2 \frac{1}{\text{mole.h}}$ $k_{\text{ox}_{5c}} = 5.5\text{E}5 \frac{1}{\text{mole.h}}$	Margerum et al (1994)
(Cr₁)	$\text{HOCl} + \text{H}^+ + 2\text{Fe}^{2+} \rightarrow 2\text{Fe}^{3+} + \text{H}_2\text{O} + \text{Cl}^-$	$k_{\text{Cr1}} \left(\frac{4}{d} \right)$	$K_{\text{Cr1}} = \text{n/a}$	Kiene et al. (1998)
(Cr₂)	$\text{OCl}^- + 2\text{H}^+ + 2\text{Fe}^{2+} \rightarrow 2\text{Fe}^{3+} + \text{H}_2\text{O} + \text{Cl}^-$	$k_{\text{Cr2}} \left(\frac{4}{d} \right)$	$K_{\text{Cr2}} = \text{n/a}$	Kiene et al. (1998)
(Cr₃)	$\text{NH}_2\text{Cl} + 2\text{H}^+ + 2\text{Fe}^{2+} \rightarrow 2\text{Fe}^{3+} + \text{NH}_4^+ + \text{Cl}^-$	$k_{\text{Cr3}} [\text{NH}_2\text{Cl}]$	$K_{\text{Cr3}} = 1.70\text{E}-2 \text{ h}^{-1}$	Westbrook et al (2009)
(SC₁)	$\text{NH}_2\text{Cl} + \text{NH}_2\text{Cl} \rightarrow \text{NHCl}_2 + \text{NH}_3$	$k_{\text{SC1}} \frac{4[\text{NH}_2\text{Cl}]^2}{d}$	$k_{\text{SC1-1}} = 1.30\text{E}6 \frac{\text{l}^2}{\text{m}^2 \cdot \text{mole.h}}$ $k_{\text{SC1-1}} = 1.30\text{E}5 \frac{\text{l}^2}{\text{m}^2 \cdot \text{mole.h}}$	Wooschlager (2000)

Table 3-1: Reactions Constants Used in the CDWQ-Cl₂ Reaction Submodel

(Adapted from Wooschlager, 2000, p 153)

Parameter	Value	Description	Units	Reference
γ_c	3.12E-08	Conversion Factor	$\frac{mole\ C}{\mu g\ COD}$	Appendix A.2
γ_N	6.24E-09	Conversion Factor	$\frac{mole\ C}{\mu g\ COD}$	Appendix A.2

Table 3-2: Conversion Factors

Parameter	Value	Description	Units	Reference
T_{bio}	1.05	Heterotroph temperature adjustment factor	-	Woolschlager (2000)
T_{bio2}	1	Nitrifier temperature adjustment factor	-	Woolschlager (2000)
T_{chem}	1.05	Chemical reaction temperature adjustment factor	-	Woolschlager (2000)

Table 3-3: Temperature Adjustment Factors

Parameter	Value	Description	Units	Reference
b_h	4.17E-03	Heterotroph endogenous decay rate	h^{-1}	Furumai & Rittmann (1992)
b_{n1}	2.08E-03	AOB endogenous decay rate	h^{-1}	Furumai & Rittmann (1992)
b_{n2}	2.08E-03	NOB endogenous decay rate	h^{-1}	Furumai & Rittmann (1992)
fd	0.8	Biodegradable fraction of biomass	-	Furumai & Rittmann (1992)
$kuap_h$	0.2	Heterotroph UAP formation rate constant	$\frac{\mu g\ COD}{\mu g\ COD_s}$	Noguera (1991)
$kuap_{n1}$	1.54E6	AOB UAP formation rate constant	$\frac{\mu g\ COD}{mole\ N}$	Noguera (1991)

kuap_{n2}	4.2E5	NOB UAP formation rate constant	$\frac{\mu g\ COD}{mole\ N}$	Noguera (1991)
keps_h	7.50E-03	Heterotroph EPS formation constant	$\frac{\mu g\ COD}{\mu g\ COD_{cell}}$	Rittmann & McCarty (2001); Laspidou & Rittmann (2002a, 2002b)
keps_{n1}	6.60E-03	AOB EPS formation constant	$\frac{\mu g\ COD}{\mu g\ COD_{cell}}$	Rittmann & McCarty (2001); Laspidou & Rittmann (2002a, 2002b)
keps_{n2}	1.80E-03	NOB EPS formation constant	$\frac{\mu g\ COD}{\mu g\ COD_{cell}}$	Rittmann & McCarty (2001); Laspidou & Rittmann (2002a, 2002b)
khyd_{EPS}	7.083E-03	EPS hydrolysis rate constant	h^{-1}	Laspidou & Rittmann (2002a, 2002b)
K_{bom1}	15000	Half-maximum BOM ₁ utilisation constant	$\frac{\mu g\ COD}{l}$	Woolschlager (2000)
K_{bom2}	120000	Half-maximum BOM ₂ utilisation constant	$\frac{\mu g\ COD}{l}$	Woolschlager (2000)
KNH₃	2.14E-06	Half-maximum ammonia utilisation constant	$\frac{mole\ N}{l}$	Woolschlager (2000)
KNO₂	5.36E-05	Half-maximum nitrite utilisation constant	$\frac{mole\ N}{l}$	Woolschlager (2000)
KNO₃	7.14E-05	Half-maximum nitrate utilisation constant	$\frac{mole\ N}{l}$	Woolschlager (2000)
KNH₂Cl	1.43E-04	Half-maximum monochloramine cometabolism constant	$\frac{mole\ N}{l}$	Woolschlager (2000)
KNHOHCl	7.14E-05	Half-maximum chlorohydroxylamine cometabolism constant	$\frac{mole\ N}{l}$	Woolschlager (2000)
K_{bap}	30000	Half-maximum BAP utilisation constant	$\frac{\mu g\ COD}{l}$	Woolschlager (2000)
K_{uap}	20000	Half-maximum UAP utilisation constant	$\frac{\mu g\ COD}{l}$	Woolschlager (2000)

q_h	4.167E-01	BOM maximum utilisation rate constant	$\frac{\mu g\ COD}{\mu g\ COD_{cell}}$	Furumai & Rittmann (1992)
q_{bap}	0.083	BAP maximum utilisation rate constant	$\frac{\mu g\ COD}{\mu g\ COD_{cell}}$	Noguera (1991)
q_{uap}	0.542	UAP maximum utilisation rate constant	$\frac{\mu g\ COD}{\mu g\ COD_{cell}}$	Noguera (1991)
q_{NH3}	4.76E-09	Ammonia maximum utilisation rate constant	$\frac{mole\ N}{\mu g\ COD_{cell}}$	Furumai & Rittmann (1992)
q_{NH2Cl}	4.76E-09	Maximum utilisation rate constant for monochloramine cometabolism	$\frac{mole\ N}{\mu g\ COD_{cell}}$	Woolschlager (2000)
q_{NHOHCl}	4.76E-09	Maximum utilisation rate constant for chlorohydroxylamine cometabolism	$\frac{mole\ N}{\mu g\ COD_{cell}}$	Woolschlager (2000)
q_{NO2}	2.08E-08	Nitrite maximum utilisation rate constant	$\frac{mole\ N}{\mu g\ COD_{cell}}$	Furumai & Rittmann (1992)
and₁	0.6	Anoxic reduction factor for nitrite respiration	-	Biyela (2010)
and₂	0.6	Anoxic reduction factor for nitrate respiration	-	Biyela (2010)
Y_h	0.6	Biomass yield for heterotrophs utilising BOM	$\frac{\mu g\ COD_{cell}}{\mu g\ COD_s}$	Biyela (2010)
Y_p	0.6	Biomass yield for heterotrophs utilising SMP	$\frac{\mu g\ COD_{cell}}{\mu g\ COD_p}$	Biyela (2010)
Y_{n1}	6.16E+06	Biomass yield for AOB	$\frac{\mu g\ COD_{cell}}{mole\ N}$	Furumai & Rittmann (1992)
Y_{n2}	1.68E+06	Biomass yield for NOB	$\frac{\mu g\ COD_{cell}}{mole\ N}$	Furumai & Rittmann (1992)

Table 3-4: Biological Parameters

Parameter	Value	Description	Units	Reference
$K_{i,DO}$	50	Trigger coefficient for denitrification	$\frac{\mu g O_2}{l}$	Bae & Rittmann (1996)
K_{O_2}	200	Half-maximum oxygen utilisation constant	$\frac{\mu g O_2}{l}$	Bae & Rittmann (1996)
k_{la}	0.042	Aeration constant	h^{-1}	Biyela (2010)

Table 3-5: Oxygen-Related Parameters

Parameter	Value	Description	Units	Reference
k_{det}	0.013	Biofilm detachment rate constant	h^{-1}	Woolschlager (2000)
k_{ads}	10	Biomass adsorption coefficient	$\frac{l}{m^2}$	Woolschlager (2000)
A	0.58	Biofilm detachment exponent	-	Woolschlager (2000)
ρ_f	4.16E+11	Assumed biofilm density	$\frac{\mu g COD}{m^3}$	Appendix A.4
k_{pro1}	1	Biofilm protection coefficient (multiplayer)	m	Woolschlager (2000)
k_{pro2}	10	Biofilm protection coefficient (exponent)	-	Woolschlager (2000)

Table 3-6: Biofilm Parameters

Parameter	Value	Description	Units	Reference
kd_1x_1	n/a	Disinfection rate constant: HOCl acting on X_{hs}	$\frac{l}{mole \cdot h}$	Wooschlager (2000)
kd_1x_2	n/a	Disinfection rate constant: HOCl acting on X_{hf}	$\frac{l}{mole \cdot h}$	Wooschlager (2000)
kd_1x_3	n/a	Disinfection rate constant: HOCl acting on X_{n1s}	$\frac{l}{mole \cdot h}$	Wooschlager (2000)
kd_1x_4	n/a	Disinfection rate constant: HOCl acting on X_{n1f}	$\frac{l}{mole \cdot h}$	Wooschlager (2000)
kd_1x_5	n/a	Disinfection rate constant: HOCl acting on X_{n2s}	$\frac{l}{mole \cdot h}$	Wooschlager (2000)
kd_1x_6	n/a	Disinfection rate constant: HOCl acting on X_{n2f}	$\frac{l}{mole \cdot h}$	Wooschlager (2000)
kd_2x_1	n/a	Disinfection rate constant: OCl^- acting on X_{hs}	$\frac{l}{mole \cdot h}$	Wooschlager (2000)
kd_2x_2	n/a	Disinfection rate constant: OCl^- acting on X_{hf}	$\frac{l}{mole \cdot h}$	Wooschlager (2000)
kd_2x_3	n/a	Disinfection rate constant: OCl^- acting on X_{n1s}	$\frac{l}{mole \cdot h}$	Wooschlager (2000)
kd_2x_4	n/a	Disinfection rate constant: OCl^- acting on X_{n1f}	$\frac{l}{mole \cdot h}$	Wooschlager (2000)
kd_2x_5	n/a	Disinfection rate constant: OCl^- acting on X_{n2s}	$\frac{l}{mole \cdot h}$	Wooschlager (2000)
kd_2x_6	n/a	Disinfection rate constant: OCl^- acting on X_{n2f}	$\frac{l}{mole \cdot h}$	Wooschlager (2000)
kd_3x_1	600	Disinfection rate constant: NH_2Cl acting on X_{hs}	$\frac{l}{mole \cdot h}$	Wooschlager (2000)

kd₃x₂	300	Disinfection rate constant: NH ₂ Cl acting on X _{hf}	$\frac{l}{mole \cdot h}$	Wooschlager (2000)
kd₃x₃	300	Disinfection rate constant: NH ₂ Cl acting on X _{n1s}	$\frac{l}{mole \cdot h}$	Wooschlager (2000)
kd₃x₄	150	Disinfection rate constant: NH ₂ Cl acting on X _{n1f}	$\frac{l}{mole \cdot h}$	Wooschlager (2000)
kd₃x₅	300	Disinfection rate constant: NH ₂ Cl acting on X _{n2s}	$\frac{l}{mole \cdot h}$	Wooschlager (2000)
kd₃x₆	150	Disinfection rate constant: NH ₂ Cl acting on X _{n2f}	$\frac{l}{mole \cdot h}$	Wooschlager (2000)

Table 3-7: Disinfection Parameters

3.8 Mass-Balance Equations

The concentrations of the various species incorporated in the model are calculated using the mass-balance equations that follow. However, it is important to note that there are several key differences between the equations that are used in the batch version and the distribution system version of the code:

- 1) The advection terms are not included in the batch version
- 2) As biofilms are not applicable for the batch version, the fixed biomass species are not included and the rates of adsorption and detachment are set to zero
- 3) Disinfectant wall-reactions are not included in the batch version

3.8.1 General Reactions

Species "C" Suspended in Pipe Element

$$C_{(t)} = C_{(t-1)} + \Delta t \left(\underbrace{\sum \frac{Q}{V} C_{(t-1)}^{in}}_{Term A} - \underbrace{\sum \frac{Q}{V} C_{(t-1)}^{out}}_{Term B} + \underbrace{\sum reactions C_{(t-1)}}_{Term C} \right)$$

Term	Explanation	Reference
A	Advection into current element from previous elements	Woolschlager (2000)
B	Advection out of current element into proceeding elements	Woolschlager (2000)
C	Reaction rate affecting specific species	Various. See 3.8.2.

Species "C" Suspended in Reservoir or Tank Element

$$C_{(t)} = C_{(t-1)} + \Delta t \left(\underbrace{Reservoir Transport C_{(t-1)}}_{Term A} + \underbrace{\sum reactions C_{(t-1)}}_{Term B} \right)$$

Term	Explanation	Reference
A	Transport or into or out of reservoir or tank element as detailed by the compartment model	Clark et al (1996)
B	Reaction rate affecting specific species	Various. See 3.8.2.

Species “C” Fixed to Pipe Wall

$$C_{(t)} = C_{(t-1)} + \Delta t \underbrace{\left(\sum \text{reactions } C_{(t-1)} \right)}_{\text{Term A}}$$

Term	Explanation	Reference
A	Reaction rate affecting specific species	Various. See 3.8.2.

Species “C” Fixed to Reservoir or Tank Wall

$$C_{(t)} = \left[C_{(t-1)} + \Delta t \underbrace{\left(\sum \text{reactions } C_{(t-1)} \right)}_{\text{Term A}} \right] \cdot \underbrace{\frac{V_{(t-1)}}{V_t}}_{\text{Term B}}$$

Term	Explanation	Reference
A	Reaction rate affecting specific species	Various. See 3.8.2.
B	Factor to account for varying reservoir volume	See page 33

3.8.2 Specific Reaction Rates

The mass-balances that follow are those used to determine the reactions influencing each constituent in the CDWQ-E₂ model regardless of whether a pipe element or reservoir/storage element is under consideration.

Suspended Heterotrophs ($\frac{ugCOD}{l}$)

$$\begin{aligned} \frac{dX_{hs}}{dt} = & \underbrace{TF_b \cdot Y_h \cdot (1 - kuap_h - keps_h) \cdot UTLbom \cdot X_{hs}}_{Term A} \\ & + \underbrace{TF_b \cdot Y_h \cdot (1 - kuap_h - keps_h) \cdot and_1 bom \cdot X_{hs}}_{Term B} \\ & + \underbrace{TF_b \cdot Y_h \cdot (1 - kuap_h - keps_h) \cdot and_2 bom \cdot X_{hs}}_{Term C} + \underbrace{TF_b \cdot Y_p \cdot UTLsmp \cdot X_{hs}}_{Term D} \\ & + \underbrace{TF_b \cdot Y_p \cdot and_1 smp \cdot X_{hs}}_{Term E} + \underbrace{TF_b \cdot Y_p \cdot and_2 smp \cdot X_{hs}}_{Term F} \\ & - b_h \cdot \left(\underbrace{\frac{O_2}{K_{O_2} + O_2} + \frac{NO_2}{K_{NO_2} + NO_2} \cdot \frac{K_{I,DO}}{K_{I,DO} + O_2} + \frac{NO_3}{K_{NO_3} + NO_3} \cdot \frac{K_{I,DO}}{K_{I,DO} + O_2}}_{Term G} \right) \cdot X_{hs} \\ & - \underbrace{(kd_1 x_1 \cdot HOCl + kd_2 x_1 \cdot OCl + kd_3 x_1 \cdot NH_2Cl) \cdot X_{hs}}_{Term H} + \underbrace{X_h \det}_{Term I} - \underbrace{X_h ads}_{Term J} \end{aligned}$$

Term	Explanation	Reference
A	Synthesis of suspended heterotrophs utilising BOM under aerobic conditions	Laspidou & Rittmann (2002a, 2002b); Biyela (2010)
B	Synthesis of suspended heterotrophs utilising BOM and respiring nitrite anoxically	Biyela (2010)
C	Synthesis of suspended heterotrophs utilising BOM and respiring nitrate anoxically	Biyela (2010)
D	Synthesis of suspended heterotrophs utilising SMP under aerobic conditions	Laspidou & Rittmann (2002a, 2002b); Biyela (2010)
E	Synthesis of suspended heterotrophs utilising SMP and respiring nitrite anoxically	Biyela (2010)
F	Synthesis of suspended heterotrophs utilising SMP and respiring nitrate anoxically	Biyela (2010)
G	Endogenous decay	de Silva & Rittmann (2000)
H	Disinfection	Wooschlager (2000)
I	Detachment of fixed heterotrophs	Wooschlager (2000)
J	Adsorption of suspended heterotrophs	Wooschlager (2000)

Fixed Heterotrophs ($\frac{ugCOD}{l}$)

$$\begin{aligned} \frac{dX_{hs}}{dt} = & \underbrace{TF_b \cdot Y_h \cdot (1 - kuap_h - keps_h) \cdot UTLbom \cdot X_{hf}}_{Term A} \\ & + \underbrace{TF_b \cdot Y_h \cdot (1 - kuap_h - keps_h) \cdot and_1 bom \cdot X_{hf}}_{Term B} \\ & + \underbrace{TF_b \cdot Y_h \cdot (1 - kuap_h - keps_h) \cdot and_2 bom \cdot X_{hf}}_{Term C} + \underbrace{TF_b \cdot Y_p \cdot UTLsmp \cdot X_{hf}}_{Term D} \\ & + \underbrace{TF_b \cdot Y_p \cdot and_1 smp \cdot X_{hf}}_{Term E} + \underbrace{TF_b \cdot Y_p \cdot and_2 smp \cdot X_{hf}}_{Term F} \\ & - b_h \cdot \left(\underbrace{\frac{O_2}{K_{O_2} + O_2} + \frac{NO_2}{K_{NO_2} + NO_2} \cdot \frac{K_{I,DO}}{K_{I,DO} + O_2} + \frac{NO_3}{K_{NO_3} + NO_3} \cdot \frac{K_{I,DO}}{K_{I,DO} + O_2}}_{Term G} \right) \cdot X_{hf} \\ & - \underbrace{(kd_1 x_2 \cdot HOCl + kd_2 x_2 \cdot OCl + kd_3 x_2 \cdot NH_2Cl) \cdot X_{hf}}_{Term H} - \underbrace{X_h \det}_{Term I} + \underbrace{X_h ads}_{Term J} \end{aligned}$$

Term	Explanation	Reference
A	Synthesis of fixed heterotrophs utilising BOM under aerobic conditions	Lapidou & Rittmann (2002a, 2002b); Biyela (2010)
B	Synthesis of fixed heterotrophs utilising BOM and respiring nitrite anoxically	Biyela (2010)
C	Synthesis of fixed heterotrophs utilising BOM and respiring nitrate anoxically	Biyela (2010)
D	Synthesis of fixed heterotrophs utilising SMP under aerobic conditions	Lapidou & Rittmann (2002a, 2002b); Biyela (2010)
E	Synthesis of fixed heterotrophs utilising SMP and respiring nitrite anoxically	Biyela (2010)
F	Synthesis of fixed heterotrophs utilising SMP and respiring nitrate anoxically	Biyela (2010)
G	Endogenous decay	de Silva & Rittmann (2000)
H	Disinfection	Woolschlager (2000)
I	Detachment of fixed heterotrophs	Woolschlager (2000)
J	Adsorption of suspended heterotrophs	Woolschlager (2000)

Suspended Ammonia Oxidising Bacteria ($\frac{\mu g COD}{l}$)

$$\frac{dX_{n1s}}{dt} = \underbrace{TF_{b2} \cdot Y_{n1} \cdot (1 - kuap_{n1} - keps_{n1}) \cdot UTLNH_3 \cdot X_{n1s}}_{Term A} - \underbrace{b_{n1} \cdot \left(\frac{O_2}{K_{O_2} + O_2} \right) \cdot X_{n1s}}_{Term B} - \underbrace{(kd_1 x_3 \cdot HOCl + kd_2 x_3 \cdot OCl + kd_3 x_3 \cdot NH_2Cl) \cdot X_{n1s}}_{Term C} + \underbrace{X_{n1} \det}_{Term D} - \underbrace{X_{n1} ads}_{Term E}$$

Term	Explanation	Reference
A	Synthesis of suspended AOB under aerobic conditions	Laspidou & Rittmann (2002a, 2002b); Biyela (2010)
B	Endogenous decay	Laspidou & Rittmann (2002a, 2002b); Rittmann, Stilwell & Ohashi (2002)
C	Disinfection	Woolschlager (2000)
D	Detachment of fixed AOB	Woolschlager (2000)
E	Adsorption of suspended AOB	Woolschlager (2000)

Fixed Ammonia Oxidising Bacteria ($\frac{\mu g COD}{l}$)

$$\frac{dX_{n1f}}{dt} = \underbrace{TF_{b2} \cdot Y_{n1} \cdot (1 - kuap_{n1} - keps_{n1}) \cdot UTLNH_3 \cdot X_{n1f}}_{Term A} - \underbrace{b_{n1} \cdot \left(\frac{O_2}{K_{O_2} + O_2} \right) \cdot X_{n1f}}_{Term B} - \underbrace{(kd_1 x_4 \cdot HOCl + kd_2 x_4 \cdot OCl + kd_3 x_4 \cdot NH_2Cl) \cdot X_{n1f}}_{Term C} - \underbrace{X_{n1} \det}_{Term D} + \underbrace{X_{n1} ads}_{Term E}$$

Term	Explanation	Reference
A	Synthesis of fixed AOB under aerobic conditions	Laspidou & Rittmann (2002a, 2002b); Biyela (2010)
B	Endogenous decay	Laspidou & Rittmann (2002a, 2002b); Rittmann, Stilwell & Ohashi (2002)
C	Disinfection	Woolschlager (2000)
D	Detachment of fixed AOB	Woolschlager (2000)
E	Adsorption of suspended AOB	Woolschlager (2000)

Suspended Nitrite Oxidising Bacteria ($\frac{ugCOD}{l}$)

$$\frac{dX_{n2s}}{dt} = \underbrace{TF_{b2} \cdot Y_{n2} \cdot (1 - kuap_{n2} - keps_{n2}) \cdot UTLNO_2 \cdot X_{n2s}}_{Term A} - \underbrace{b_{n2} \cdot \left(\frac{O_2}{K_{O_2} + O_2} \right) \cdot X_{n2s}}_{Term B} - \underbrace{(kd_1x_5 \cdot HOCl + kd_2x_5 \cdot OCl + kd_3x_5 \cdot NH_2Cl) \cdot X_{n2s}}_{Term C} + \underbrace{X_{n2} \det}_{Term D} - \underbrace{X_{n2} ads}_{Term E}$$

Term	Explanation	Reference
A	Synthesis of suspended NOB under aerobic conditions	Laspidou & Rittmann (2002a, 2002b); Biyela (2010)
B	Endogenous decay	Laspidou & Rittmann (2002a, 2002b); Rittmann, Stilwell & Ohashi (2002)
C	Disinfection	Woolschlager (2000)
D	Detachment of fixed NOB	Woolschlager (2000)
E	Adsorption of suspended NOB	Woolschlager (2000)

Fixed Nitrite Oxidising Bacteria ($\frac{ugCOD}{l}$)

$$\frac{dX_{n2f}}{dt} = \underbrace{TF_{b2} \cdot Y_{n2} \cdot (1 - kuap_{n2} - keps_{n2}) \cdot UTLNO_2 \cdot X_{n2f}}_{Term A} - \underbrace{b_{n2} \cdot \left(\frac{O_2}{K_{O_2} + O_2} \right) \cdot X_{n2f}}_{Term B} - \underbrace{(kd_1x_6 \cdot HOCl + kd_2x_6 \cdot OCl + kd_3x_6 \cdot NH_2Cl) \cdot X_{n2f}}_{Term C} - \underbrace{X_{n2} \det}_{Term D} + \underbrace{X_{n2} ads}_{Term E}$$

Term	Explanation	Reference
A	Synthesis of fixed NOB under aerobic conditions	Laspidou & Rittmann (2002a, 2002b); Biyela (2010)
B	Endogenous decay	Laspidou & Rittmann (2002a, 2002b); Rittmann, Stilwell & Ohashi (2002)
C	Disinfection	Woolschlager (2000)
D	Detachment of fixed NOB	Woolschlager (2000)
E	Adsorption of suspended NOB	Woolschlager (2000)

Suspended Inert Bacteria ($\frac{ugCOD}{l}$)

$$\begin{aligned} \frac{dX_{is}}{dt} = & \underbrace{(1 - fd) \cdot b_h \cdot \left(\frac{O_2}{K_{O_2} + O_2} + \frac{NO_2}{K_{NO_2} + NO_2} \cdot \frac{K_{I,DO}}{K_{I,DO} + O_2} + \frac{NO_3}{K_{NO_3} + NO_3} \cdot \frac{K_{I,DO}}{K_{I,DO} + O_2} \right)}_{Term A} \cdot X_{hs} \\ & + \underbrace{(1 - fd) \cdot b_{n1} \cdot \left(\frac{O_2}{K_{O_2} + O_2} \right)}_{Term B} \cdot X_{n1s} + \underbrace{(1 - fd) \cdot b_{n2} \cdot \left(\frac{O_2}{K_{O_2} + O_2} \right)}_{Term C} \cdot X_{n2s} \\ & + \underbrace{(1 - fd) \cdot (kd_1x_1 \cdot HOCl + kd_2x_1 \cdot OCl + kd_3x_1 \cdot NH_2Cl)}_{Term D} \cdot X_{hs} \\ & + \underbrace{(1 - fd) \cdot (kd_1x_3 \cdot HOCl + kd_2x_3 \cdot OCl + kd_3x_3 \cdot NH_2Cl)}_{Term E} \cdot X_{n1s} \\ & + \underbrace{(1 - fd) \cdot (kd_1x_5 \cdot HOCl + kd_2x_5 \cdot OCl + kd_3x_5 \cdot NH_2Cl)}_{Term F} \cdot X_{n2s} \\ & - \underbrace{TF_c \cdot (kox_1x_2 \cdot HOCl + kox_2x_2 \cdot OCl + kox_3x_2 \cdot NH_2Cl)}_{Term G} \cdot X_{is} + \underbrace{X_i}_{Term H} \det - \underbrace{X_i}_{Term I} ads \end{aligned}$$

Term	Explanation	Reference
A	Endogenous decay of suspended heterotrophs	de Silva & Rittmann (2000)
B	Endogenous decay of suspended AOB	Lapidou & Rittmann (2002a, 2002b); Rittmann, Stilwell & Ohashi (2002)
C	Endogenous decay of suspended NOB	Lapidou & Rittmann (2002a, 2002b); Rittmann, Stilwell & Ohashi (2002)
D	Disinfection of suspended heterotrophs	Woolschlager (2000)
E	Disinfection of suspended AOB	Woolschlager (2000)
F	Disinfection of suspended NOB	Woolschlager (2000)
G	Oxidation of suspended inert biomass by disinfectant	Woolschlager (2000)
H	Detachment of fixed inert biomass	Woolschlager (2000)
I	Adsorption of suspended inert biomass	Woolschlager (2000)

Fixed Inert Bacteria ($\frac{ugCOD}{l}$)

$$\begin{aligned} \frac{dX_{if}}{dt} = & \underbrace{(1 - fd) \cdot b_h \cdot \left(\frac{O_2}{K_{O_2} + O_2} + \frac{NO_2}{K_{NO_2} + NO_2} \cdot \frac{K_{I,DO}}{K_{I,DO} + O_2} + \frac{NO_3}{K_{NO_3} + NO_3} \cdot \frac{K_{I,DO}}{K_{I,DO} + O_2} \right)}_{Term A} \cdot X_{hf} \\ & + \underbrace{(1 - fd) \cdot b_{n1} \cdot \left(\frac{O_2}{K_{O_2} + O_2} \right)}_{Term B} \cdot X_{n1f} + \underbrace{(1 - fd) \cdot b_{n2} \cdot \left(\frac{O_2}{K_{O_2} + O_2} \right)}_{Term C} \cdot X_{n2f} \\ & + \underbrace{(1 - fd) \cdot (kd_1 x_2 \cdot HOCl + kd_2 x_2 \cdot OCl + kd_3 x_2 \cdot NH_2Cl)}_{Term D} \cdot X_{hf} \\ & + \underbrace{(1 - fd) \cdot (kd_1 x_4 \cdot HOCl + kd_2 x_4 \cdot OCl + kd_3 x_4 \cdot NH_2Cl)}_{Term E} \cdot X_{n1f} \\ & + \underbrace{(1 - fd) \cdot (kd_1 x_6 \cdot HOCl + kd_2 x_6 \cdot OCl + kd_3 x_6 \cdot NH_2Cl)}_{Term F} \cdot X_{n2f} \\ & - \underbrace{TF_c \cdot (kox_1 x_2 \cdot HOCl + kox_2 x_2 \cdot OCl + kox_3 x_2 \cdot NH_2Cl)}_{Term G} \cdot X_{if} - \underbrace{X_i}_{Term H} \det + \underbrace{X_i}_{Term I} ads \end{aligned}$$

Term	Explanation	Reference
A	Endogenous decay of fixed heterotrophs	de Silva & Rittmann (2000)
B	Endogenous decay of fixed AOB	Lapidou & Rittmann (2002a, 2002b); Rittmann, Stilwell & Ohashi (2002)
C	Endogenous decay of fixed NOB	Lapidou & Rittmann (2002a, 2002b); Rittmann, Stilwell & Ohashi (2002)
D	Disinfection of fixed heterotrophs	Woolschlager (2000)
E	Disinfection of fixed AOB	Woolschlager (2000)
F	Disinfection of fixed NOB	Woolschlager (2000)
G	Oxidation of fixed inert biomass by disinfectant	Woolschlager (2000)
H	Detachment of fixed inert biomass	Woolschlager (2000)
I	Adsorption of suspended inert biomass	Woolschlager (2000)

Suspended EPS ($\frac{ugCOD}{l}$)

$$\begin{aligned} \frac{dEPS_s}{dt} = & \underbrace{TF_b \cdot keps_h \cdot UTLbom \cdot X_{hs}}_{Term A} + \underbrace{TF_{b2} \cdot \left(\frac{keps_{n1}}{\gamma_n}\right) \cdot UTLNH_3 \cdot X_{n1s}}_{Term B} \\ & + \underbrace{TF_{b2} \cdot \left(\frac{keps_{n2}}{\gamma_n}\right) \cdot UTLNO_2 \cdot X_{n2s}}_{Term C} + \underbrace{TF_b \cdot keps_h \cdot and_1 bom \cdot X_{hs}}_{Term D} \\ & + \underbrace{TF_b \cdot keps_h \cdot and_2 bom \cdot X_{hs}}_{Term E} - \underbrace{k_{hyd} EPS \cdot EPS_s}_{Term F} \\ & - \underbrace{TF_c \cdot kox_3 x_2 \cdot NH_2Cl \cdot EPS_s}_{Term G} - \underbrace{TF_c \cdot kox_1 x_2 \cdot HOCl \cdot EPS_s}_{Term H} \\ & - \underbrace{TF_c \cdot kox_2 x_2 \cdot OCl \cdot EPS_s}_{Term I} + \underbrace{EPS \det}_{Term J} - \underbrace{EPS ads}_{Term K} \end{aligned}$$

Term		
A	Synthesis of suspended EPS by suspended heterotrophs utilising BOM under aerobic conditions	Laspidou & Rittmann (2002a, 2002b); Biyela (2010)
B	Synthesis of suspended EPS by suspended AOB respiring aerobically	Laspidou & Rittmann (2002a, 2002b); Biyela (2010)
C	Synthesis of suspended EPS by suspended NOB respiring aerobically	Laspidou & Rittmann (2002a, 2002b); Biyela (2010)
D	Synthesis of suspended EPS by suspended heterotrophs utilising BOM and respiring nitrite anoxically	Biyela (2010)
E	Synthesis of suspended EPS by suspended heterotrophs utilising BOM and respiring nitrate anoxically	Biyela (2010)
F	Hydrolysis of suspended EPS	Laspidou & Rittmann (2002a, 2002b); Biyela (2010)
G	Oxidation of suspended EPS by NH ₂ Cl	Woolschlager (2000); Biyela (2010)
H	Oxidation of suspended EPS by HOCl	Woolschlager (2000); Biyela (2010)
I	Oxidation of suspended EPS by OCl ⁻	Woolschlager (2000); Biyela (2010)
J	Detachment of fixed EPS	Woolschlager (2000)
K	Adsorption of suspended EPS	Woolschlager (2000)

Fixed EPS ($\frac{ugCOD}{l}$)

$$\begin{aligned} \frac{dEPS_f}{dt} = & \underbrace{TF_b.keps_h.UTLbom.X_{hf}}_{Term A} + \underbrace{TF_{b2}.\left(\frac{keps_{n1}}{\gamma_n}\right).UTLNH_3.X_{n1f}}_{Term B} \\ & + \underbrace{TF_{b2}.\left(\frac{keps_{n2}}{\gamma_n}\right).UTLNO_2.X_{n2f}}_{Term C} + \underbrace{TF_b.keps_h.and_1bom.X_{hf}}_{Term D} \\ & + \underbrace{TF_b.keps_h.and_2bom.X_{hf}}_{Term E} - \underbrace{khydEPS.EPS_f}_{Term F} \\ & - \underbrace{TF_c.kox_3x_2.NH_2Cl.EPS_f}_{Term G} - \underbrace{TF_c.kox_1x_2.HOCl.EPS_f}_{Term H} \\ & - \underbrace{TF_c.kox_2x_2.OCl.EPS_f}_{Term I} - \underbrace{EPS_{det}}_{Term J} + \underbrace{EPS_{ads}}_{Term K} \end{aligned}$$

Term	Explanation	Reference
A	Synthesis of fixed EPS by fixed heterotrophs utilising BOM under aerobic conditions	Laspidou & Rittmann (2002a, 2002b); Biyela (2010)
B	Synthesis of fixed EPS by fixed AOB respiring aerobically	Laspidou & Rittmann (2002a, 2002b); Biyela (2010)
C	Synthesis of fixed EPS by fixed NOB respiring aerobically	Laspidou & Rittmann (2002a, 2002b); Biyela (2010)
D	Synthesis of fixed EPS by fixed heterotrophs utilising BOM and respiring nitrite anoxically	Biyela (2010)
E	Synthesis of fixed EPS by fixed heterotrophs utilising BOM and respiring nitrate anoxically	Biyela (2010)
F	Hydrolysis of fixed EPS	Laspidou & Rittmann (2002a, 2002b); Biyela (2010)
G	Oxidation of fixed EPS by NH ₂ Cl	Woolschlager (2000); Biyela (2010)
H	Oxidation of fixed EPS by HOCl	Woolschlager (2000); Biyela (2010)
I	Oxidation of fixed EPS by OCl ⁻	Woolschlager (2000); Biyela (2010)
J	Detachment of fixed EPS	Woolschlager (2000)
K	Adsorption of suspended EPS	Woolschlager (2000)

$$BOM_1 \left(\frac{ugCOD}{l} \right)$$

$$\frac{dBOM_1}{dt} = - \underbrace{TF_b \cdot UTLbom_1 \cdot X_h}_{Term A} - \underbrace{TF_b \cdot and_1 bom_1 \cdot X_h}_{Term B} - \underbrace{TF_b \cdot and_2 bom_1 \cdot X_h}_{Term C} - \underbrace{TF_c \cdot (kox_1 x_1 \cdot HOCl + kox_2 x_1 \cdot OCl + kox_3 x_1 \cdot NH_2Cl) \cdot BOM_1}_{Term D}$$

Term	Explanation	Reference
A	BOM ₁ utilisation by heterotrophs respiring aerobically	Laspidou & Rittmann (2002a, 2002b); Biyela (2010)
B	BOM ₁ utilisation by heterotrophs respiring nitrite anoxically	Biyela (2010)
C	BOM ₁ utilisation by heterotrophs respiring nitrate anoxically	Biyela (2010)
D	Oxidation of BOM ₁ by disinfectant	Woolschlager (2000)

$$BOM_2 \left(\frac{ugCOD}{l} \right)$$

$$\begin{aligned} \frac{dBOM_2}{dt} = & - \underbrace{TF_b \cdot UTLbom_2 \cdot X_h}_{Term A} - \underbrace{TF_b \cdot and_1 bom_2 \cdot X_h}_{Term B} - \underbrace{TF_b \cdot and_2 bom_2 \cdot X_h}_{Term C} \\ & + \underbrace{fd \cdot (kd_1 x_1 \cdot HOCl + kd_2 x_1 \cdot OCl + kd_3 x_1 \cdot NH_2Cl) \cdot X_{hs}}_{Term D} \\ & + \underbrace{fd \cdot (kd_1 x_3 \cdot HOCl + kd_2 x_3 \cdot OCl + kd_3 x_3 \cdot NH_2Cl) \cdot X_{n1s}}_{Term E} \\ & + \underbrace{fd \cdot (kd_1 x_5 \cdot HOCl + kd_2 x_5 \cdot OCl + kd_3 x_5 \cdot NH_2Cl) \cdot X_{n2s}}_{Term F} \\ & + \underbrace{fd \cdot (kd_1 x_2 \cdot HOCl + kd_2 x_2 \cdot OCl + kd_3 x_2 \cdot NH_2Cl) \cdot X_{hf}}_{Term G} \\ & + \underbrace{fd \cdot (kd_1 x_4 \cdot HOCl + kd_2 x_4 \cdot OCl + kd_3 x_4 \cdot NH_2Cl) \cdot X_{n1f}}_{Term H} \\ & + \underbrace{fd \cdot (kd_1 x_6 \cdot HOCl + kd_2 x_6 \cdot OCl + kd_3 x_6 \cdot NH_2Cl) \cdot X_{n2f}}_{Term I} \\ & - \underbrace{TF_c \cdot (kox_1 x_2 \cdot HOCl + kox_2 x_2 \cdot OCl + kox_3 x_2 \cdot NH_2Cl) \cdot BOM_2}_{Term J} \end{aligned}$$

Term	Explanation	Reference
A	BOM ₂ utilisation by heterotrophs respiring aerobically	Laspidou & Rittmann (2002a, 2002b); Biyela (2010)
B	BOM ₂ utilisation by heterotrophs respiring nitrite anoxically	Biyela (2010)

C	BOM ₂ utilisation by heterotrophs respiring nitrate anoxically	Biyela (2010)
D	Formation of BOM ₂ due to disinfection of suspended heterotrophs	Woolschlager (2000)
E	Formation of BOM ₂ due to disinfection of suspended AOB	Woolschlager (2000)
F	Formation of BOM ₂ due to disinfection of suspended NOB	Woolschlager (2000)
G	Formation of BOM ₂ due to disinfection of fixed heterotrophs	Woolschlager (2000)
H	Formation of BOM ₂ due to disinfection of fixed AOB	Woolschlager (2000)
I	Formation of BOM ₂ due to disinfection of fixed NOB	Woolschlager (2000)
J	Oxidation of BOM ₂ by disinfectant	Woolschlager (2000)

$$UAP \left(\frac{ugCOD}{l} \right)$$

$$\begin{aligned} \frac{dUAP}{dt} = & \underbrace{TF_b \cdot kuap_h \cdot UTLbom \cdot X_h}_{Term A} + \underbrace{TF_{b2} \cdot \left(\frac{kuap_{n1}}{\gamma_n} \right) \cdot UTLNH_3 \cdot X_{n1}}_{Term B} \\ & + \underbrace{TF_{b2} \cdot \left(\frac{kuap_{n2}}{\gamma_n} \right) \cdot UTLNO_2 \cdot X_{n2}}_{Term C} - \underbrace{TF_b \cdot UTLuap \cdot X_h}_{Term D} + \underbrace{TF_b \cdot kuap_h \cdot and_1 bom \cdot X_h}_{Term E} \\ & + \underbrace{TF_b \cdot kuap_h \cdot and_2 bom \cdot X_h}_{Term F} - \underbrace{TF_b \cdot and_1 uap \cdot X_h}_{Term G} - \underbrace{TF_b \cdot and_2 uap \cdot X_h}_{Term H} \\ & - \underbrace{TF_c \cdot (kox_1 x_2 \cdot HOCl + kox_2 x_2 \cdot OCl + kox_3 x_2 \cdot NH_2Cl) \cdot UAP}_{Term I} \end{aligned}$$

Term	Explanation	Reference
A	Synthesis of UAP by heterotrophs utilising BOM under aerobic conditions	Laspidou & Rittmann (2002a, 2002b); Biyela (2010)
B	Synthesis of UAP by AOB respiring aerobically	Laspidou & Rittmann (2002a, 2002b); Biyela (2010)
C	Synthesis of UAP by NOB respiring aerobically	Laspidou & Rittmann (2002a, 2002b); Biyela (2010)
D	Utilisation of UAP by heterotrophs under aerobic conditions	Laspidou & Rittmann (2002a, 2002b); Biyela (2010)
E	Synthesis of UAP by heterotrophs utilising BOM and respiring nitrite anoxically	Biyela (2010)

F	Synthesis of UAP by heterotrophs utilising BOM and respiring nitrate anoxically	Biyela (2010)
G	Utilisation of UAP by heterotrophs respiring nitrite anoxically	Biyela (2010)
H	Utilisation of UAP by heterotrophs respiring nitrate anoxically	Biyela (2010)
I	Oxidation of UAP by disinfectant	Woolschlager (2000)

BAP ($\frac{\mu gCOD}{l}$)

$$\frac{dBAP}{dt} = \underbrace{k_{hyd}EPS.EPS}_{Term A} - \underbrace{TF_b.UTL_{bap}.X_h}_{Term B} - \underbrace{TF_b.and_1_{bap}.X_h}_{Term C} - \underbrace{TF_b.and_2_{bap}.X_h}_{Term D} - \underbrace{TF_c.(kox_1x_2.HOCl + kox_2x_2.OCl + kox_3x_2.NH_2Cl).BAP}_{Term E}$$

Term	Explanation	Reference
A	Hydrolysis of EPS	Lapidou & Rittmann (2002a, 2002b); Biyela (2010)
B	BAP utilisation by heterotrophic bacteria respiring aerobically	Lapidou & Rittmann (2002a, 2002b); Biyela (2010)
C	BAP utilisation by heterotrophic bacteria respiring nitrite anoxically	Biyela (2010)
D	BAP utilisation by heterotrophic bacteria respiring nitrate anoxically	Biyela (2010)
E	Oxidation of BAP by disinfectant	Woolschlager (2000)

Monochloramine ($\frac{\text{mole}}{\text{l}}$)

$$\begin{aligned} \frac{d\text{NH}_2\text{Cl}}{dt} = & - \underbrace{2 \times TF_c \cdot k_{AD3} \cdot \left(\text{NH}_2\text{Cl} \cdot \frac{k_{Cl_e}}{\text{NH}_3} \right) \cdot \text{NH}_2\text{Cl}}_{\text{Term A}} - \underbrace{2 \times TF_c \cdot k_{AD1} \cdot \text{NH}_2\text{Cl} \cdot \text{NH}_2\text{Cl}}_{\text{Term B}} \\ & + \underbrace{2 \times TF_c \cdot k_{AD2} \cdot \text{NH}_2\text{Cl} \cdot \text{NH}_3 \cdot H}_{\text{Term C}} - \underbrace{TF_c \cdot k_{AD5} \cdot \text{NHOHCl}}_{\text{Term D}} \\ & - \underbrace{TF_c \cdot k_{ox5} \cdot \text{NH}_2\text{Cl} \cdot \text{NO}_2}_{\text{Term E}} - \underbrace{TF_{b2} \cdot \text{UNH}_2\text{Cl} \cdot X_{n1}}_{\text{Term F}} \\ & - \underbrace{TF_c \cdot k_{cr3} \cdot \text{NH}_2\text{Cl}}_{\text{Term G}} \\ & - \underbrace{TF_{c2} \cdot k_{SC1} \cdot \text{NH}_2\text{Cl} \cdot \text{NH}_2\text{Cl} \cdot \left(\frac{4}{\text{diameter} \left(\frac{l}{m^3} \right) \cdot 1000} \right)}_{\text{Term H}} \\ & - \underbrace{2 \times TF_c \cdot \gamma_c \cdot \left(k_{ox3x1} \cdot \text{BOM}_1 + k_{ox3x2} \cdot \text{BOM}_2 + k_{ox3x2} \cdot \text{BAP} \right.}_{\text{Term I}} \\ & \quad \left. + k_{ox3x2} \cdot \text{UAP} + k_{ox3x2} X_i + k_{ox3x2} \cdot \text{EPS} \right) \cdot \text{NH}_2\text{Cl} \end{aligned}$$

Term	Explanation	Reference
A	Autocatalytic reaction AD ₁	Woolschlager (2000)
B	Autocatalytic reaction AD ₂	Woolschlager (2000)
C	Autocatalytic reaction AD ₃	Woolschlager (2000)
D	Autocatalytic reaction AD ₅	Woolschlager (2000)
E	Oxidation of nitrite by NH ₂ Cl	Woolschlager (2000)
F	NH ₂ Cl cometabolism	Woolschlager (2000); Maestre, Wahman & Speitel (2013)
G	Corrosion reaction for iron pipe with NH ₂ Cl	Westbrook et al (2009)
H	NH ₂ Cl surface catalysis	Woolschlager (2000)
I	Oxidation of organic matter by NH ₂ Cl	Woolschlager (2000)

Dichloramine ($\frac{\text{mole}}{\text{l}}$)

$$\begin{aligned} \frac{dNHCl_2}{dt} = & \underbrace{TF_c \cdot k_{AD1} \cdot NH_2Cl \cdot NH_2Cl}_{\text{Term A}} - \underbrace{TF_c \cdot k_{AD2} \cdot NHCl_2 \cdot NH_3 \cdot H}_{\text{Term B}} \\ & + \underbrace{TF_c \cdot k_{AD3} \cdot \left(NH_2Cl \cdot \frac{k_{Cle}}{NH_3} \right) \cdot NH_2Cl}_{\text{Term C}} - \underbrace{TF_c \cdot k_{AD4} \cdot NHCl_2 \cdot OH}_{\text{Term D}} \\ & + \underbrace{TF_c \cdot k_{SC1} \cdot NH_2Cl \cdot NH_2Cl \cdot \left(\frac{4}{\text{diameter} \left(\frac{\text{l}}{\text{m}^3} \right) \cdot 1000} \right)}_{\text{Term E}} \end{aligned}$$

Term	Explanation	Reference
A	Autocatalytic reaction AD ₁	Woolschlager (2000)
B	Autocatalytic reaction AD ₂	Woolschlager (2000)
C	Autocatalytic reaction AD ₃	Woolschlager (2000)
D	Autocatalytic reaction AD ₄	Woolschlager (2000)
E	NH ₂ Cl surface catalysis	Woolschlager (2000)

Chlorohydroxylamine ($\frac{\text{mole}}{\text{l}}$)

$$\begin{aligned} \frac{dNHOHCl}{dt} = & \underbrace{TF_{b2} \cdot UNH_2Cl \cdot X_{n1}}_{\text{Term A}} - \underbrace{TF_{b2} \cdot UTLNHOHCl \cdot X_{n1}}_{\text{Term B}} \\ & + \underbrace{TF_c \cdot k_{AD4} \cdot NHCl_2 \cdot OH}_{\text{Term C}} - \underbrace{TF_c \cdot k_{AD5} \cdot NHOHCl}_{\text{Term D}} \end{aligned}$$

Term	Explanation	Reference
A	NH ₂ Cl cometabolism	Woolschlager (2000); Maestre, Wahman & Speitel (2013)
B	NHOHCl cometabolism	Woolschlager (2000); Maestre, Wahman & Speitel (2013)
C	Autocatalytic reaction AD ₄	Woolschlager (2000)
D	Autocatalytic reaction AD ₅	Woolschlager (2000)

Free Chlorine ($\frac{\text{mole}}{\text{l}}$)

$$\begin{aligned} \frac{dC_{\text{tOCl}}}{dt} = & -2 \times TF_c \cdot \gamma_c \cdot \underbrace{\left(kox_1x_1 \cdot BOM_1 + kox_1x_2 \cdot BOM_2 + kox_1x_2 \cdot BAP \right)}_{\text{Term A}} \cdot HOCl \\ & + kox_1x_2 \cdot EPS + kox_1x_2 \cdot UAP + kox_1x_2 \cdot X_i \\ & - 2 \times TF_c \cdot \gamma_c \cdot \underbrace{\left(kox_2x_1 \cdot BOM_1 + kox_2x_2 \cdot BOM_2 + kox_2x_2 \cdot BAP \right)}_{\text{Term B}} \cdot OCl \\ & + kox_2x_2 \cdot EPS + kox_2x_2 \cdot UAP + kox_2x_2 \cdot X_i \\ & - \underbrace{TF_c \cdot kox_4 \cdot HOCl \cdot NO_2}_{\text{Term C}} \\ & - \underbrace{TF_c \cdot k_{cr1} \cdot \left(\frac{4}{\text{diameter} \left(\frac{l}{m^3} \right) \cdot 1000} \right)}_{\text{Term D}} - \underbrace{TF_c \cdot k_{cr2} \cdot \left(\frac{4}{\text{diameter} \left(\frac{l}{m^3} \right) \cdot 1000} \right)}_{\text{Term E}} \end{aligned}$$

Term	Explanation	Reference
A	Oxidation of organic matter by HOCl	Wooschlager (2000)
B	Oxidation of organic matter by OCl ⁻	Wooschlager (2000)
C	Oxidation of nitrite by HOCl	Wooschlager (2000)
D	Corrosion reaction for iron pipe with HOCl	Wooschlager (2000)
E	Corrosion reaction for iron pipe with OCl ⁻	Wooschlager (2000)

Total Ammonia ($\frac{\text{mole}}{l}$)

$$\begin{aligned}
 \frac{dCtNH_3}{dt} = & - \underbrace{TF_{b2}.UTLNH_3.X_{n1}}_{\text{Term A}} - \underbrace{TF_{b2}.\gamma_n.Y_{n1}.(1 - kuap_{n1} - keps_{n1}).UTLNH_3.X_{n1}}_{\text{Term B}} \\
 & - \underbrace{TF_{b2}.\gamma_n.Y_{n2}.(1 - kuap_{n2} - keps_{n2}).UTLNO_2.X_{n2}}_{\text{Term C}} \\
 & - \underbrace{TF_{b2}.\gamma_n.\left(\frac{kuap_{n1}}{\gamma_n}\right).UTLNH_3.X_{n1}}_{\text{Term D}} - \underbrace{TF_{b2}.\gamma_n.\left(\frac{kuap_{n2}}{\gamma_n}\right).UTLNO_2.X_{n2}}_{\text{Term E}} \\
 & - \underbrace{TF_{b2}.\gamma_n.\left(\frac{keps_{n1}}{\gamma_n}\right).UTLNH_3.X_{n1}}_{\text{Term F}} - \underbrace{TF_{b2}.\gamma_n.\left(\frac{keps_{n2}}{\gamma_n}\right).UTLNO_2.X_{n2}}_{\text{Term G}} \\
 & + \underbrace{TF_c.k_{SCl}.NH_2Cl.NH_2Cl.\left(\frac{4}{\text{diameter}\left(\frac{l}{m^3}\right).1000}\right)}_{\text{Term H}} \\
 & + \gamma_n.f.d.\left[\underbrace{b_h.\left(\frac{O_2}{K_{O_2} + O_2} + \frac{NO_2}{K_{NO_2} + NO_2} \cdot \frac{K_{I,DO}}{K_{I,DO} + O_2} + \frac{NO_3}{K_{NO_3} + NO_3} \cdot \frac{K_{I,DO}}{K_{I,DO} + O_2}\right).X_h}_{\text{Term I}} \right. \\
 & \quad \left. + b_{n1}.\left(\frac{O_2}{K_{O_2} + O_2}\right).X_{n1} + b_{n2}.\left(\frac{O_2}{K_{O_2} + O_2}\right).X_{n2} \right] \\
 & + \underbrace{TF_c.k_{AD1}.NH_2Cl.NH_2Cl}_{\text{Term J}} - \underbrace{TF_c.k_{AD2}.NHCl_2.NH_3.H}_{\text{Term K}} \\
 & + \underbrace{TF_c.k_{ox5}.NH_2Cl.NO_2}_{\text{Term L}} + \underbrace{TF_c.k_{AD3}.\left(NH_2Cl.\frac{k_{Cle}}{NH_3}\right).NH_2Cl}_{\text{Term M}} \\
 & + 11 \times \underbrace{TF_c.\gamma_n.\left(kox_3x_1.BOM_1 + kox_3x_2.BOM_2 + kox_3x_2.EPS\right).NH_2Cl}_{\text{Term N}} \\
 & + \underbrace{TF_c.k_{cr3}.NH_2Cl}_{\text{Term O}} + \underbrace{TF_b.\gamma_n.(1 - Y_p).UTLsmp.X_h}_{\text{Term P}} \\
 & + \underbrace{TF_b.\gamma_n.(1 - Y_p).and_1smp.X_h}_{\text{Term Q}} + \underbrace{TF_b.\gamma_n.(1 - Y_p).and_2smp.X_h}_{\text{Term R}} \\
 & + \underbrace{TF_b.\gamma_n.(1 - Y_h).(1 - kuap_h - keps_h) - (kuap_h + keps_h).UTLbom.X_h}_{\text{Term S}} \\
 & + \underbrace{TF_b.\gamma_n.(1 - Y_h).(1 - kuap_h - keps_h) - (kuap_h + keps_h).and_1bom.X_h}_{\text{Term T}} \\
 & + \underbrace{TF_b.\gamma_n.(1 - Y_h).(1 - kuap_h - keps_h) - (kuap_h + keps_h).and_2bom.X_h}_{\text{Term U}}
 \end{aligned}$$

Term	Explanation	Reference
A	NH ₃ utilisation by AOB respiring aerobically	Laspidou & Rittmann (2002a, 2002b); de Silva & Rittmann (2000); Rittmann, Stilwell & Ohashi (2002)
B	NH ₃ incorporation by AOB respiring aerobically	Laspidou & Rittmann (2002a, 2002b); de Silva & Rittmann (2000); Rittmann, Stilwell & Ohashi (2002)
C	NH ₃ incorporation by NOB respiring aerobically	Laspidou & Rittmann (2002a, 2002b); de Silva & Rittmann (2000); Rittmann, Stilwell & Ohashi (2002)
D	NH ₃ incorporation by AOB during UAP synthesis	Laspidou & Rittmann (2002a, 2002b); de Silva & Rittmann (2000); Rittmann, Stilwell & Ohashi (2002)
E	NH ₃ incorporation by NOB during UAP synthesis	Laspidou & Rittmann (2002a, 2002b); de Silva & Rittmann (2000); Rittmann, Stilwell & Ohashi (2002)
F	NH ₃ incorporation by AOB during EPS synthesis	Laspidou & Rittmann (2002a, 2002b); de Silva & Rittmann (2000); Rittmann, Stilwell & Ohashi (2002)
G	NH ₃ incorporation by NOB during EPS synthesis	Laspidou & Rittmann (2002a, 2002b); de Silva & Rittmann (2000); Rittmann, Stilwell & Ohashi (2002)
H	NH ₂ Cl surface catalysis	Woolschlager (2000)
I	Endogenous decay of active biomass	de Silva & Rittmann (2000)
J	Autocatalytic reaction AD ₁	Woolschlager (2000)
K	Autocatalytic reaction AD ₂	Woolschlager (2000)
L	Oxidation of nitrite by NH ₂ Cl	Woolschlager (2000)
M	Autocatalytic reaction AD ₃	Woolschlager (2000)
N	Oxidation of organic matter by NH ₂ Cl	Woolschlager (2000)
O	Corrosion reaction for iron pipe with NH ₂ Cl	Westbrook et al (2009)
P	NH ₃ incorporation by heterotrophs utilising SMP under aerobic conditions	Laspidou & Rittmann (2002a, 2002b); de Silva & Rittmann (2000); Rittmann, Stilwell & Ohashi (2002)
Q	NH ₃ incorporation by heterotrophs utilising SMP and respiring nitrite anoxically	Laspidou & Rittmann (2002a, 2002b); de Silva & Rittmann (2000); Rittmann, Stilwell & Ohashi (2002)
R	NH ₃ incorporation by heterotrophs utilising SMP and respiring nitrate anoxically	Laspidou & Rittmann (2002a, 2002b); de Silva & Rittmann (2000); Rittmann, Stilwell & Ohashi (2002)

S	NH ₃ incorporation by heterotrophs utilising BOM under aerobic conditions and synthesis of UAP and EPS under same conditions	Laspidou & Rittmann (2002a, 2002b); de Silva & Rittmann (2000); Rittmann, Stilwell & Ohashi (2002)
T	NH ₃ incorporation by heterotrophs utilising BOM and respiring nitrite anoxically and synthesis of UAP and EPS under same conditions	Laspidou & Rittmann (2002a, 2002b); de Silva & Rittmann (2000); Rittmann, Stilwell & Ohashi (2002)
U	NH ₃ incorporation by heterotrophs utilising BOM and respiring nitrate anoxically and synthesis of UAP and EPS under same conditions	Laspidou & Rittmann (2002a, 2002b); de Silva & Rittmann (2000); Rittmann, Stilwell & Ohashi (2002)

Nitrite ($\frac{mole}{l}$)

$$\begin{aligned}
\frac{dNO_2}{dt} = & - \underbrace{TF_{b2} \cdot UTLNO_2 \cdot X_{n2}}_{Term A} - \underbrace{TF_b \cdot \gamma_n \cdot (1 - kuap_h - keps_h - Y_h \cdot (1 - kuap_h - keps_h)) \cdot and_1 \cdot bom \cdot X_h}_{Term B} \\
& - \underbrace{TF_b \cdot \gamma_n \cdot (1 - Y_p) \cdot and_1 \cdot smp \cdot X_h}_{Term C} + \underbrace{TF_b \cdot \gamma_n \cdot (1 - kuap_h - keps_h - Y_h \cdot (1 - kuap_h - keps_h)) \cdot and_2 \cdot bom \cdot X_h}_{Term D} \\
& + \underbrace{TF_b \cdot \gamma_n \cdot (1 - Y_p) \cdot and_2 \cdot smp \cdot X_h}_{Term E} \\
& - \underbrace{\gamma_n \cdot fd \cdot b_h \cdot \left(\frac{NO_2}{K_{NO_2} + NO_2} \cdot \frac{K_{L,DO}}{K_{L,DO} + O_2} \right) \cdot X_h}_{Term F} + \underbrace{\gamma_n \cdot fd \cdot b_h \cdot \left(\frac{NO_3}{K_{NO_3} + NO_3} \cdot \frac{K_{L,DO}}{K_{L,DO} + O_2} \right) \cdot X_h}_{Term G} \\
& + \underbrace{TF_{b2} \cdot UTLNH_3 \cdot X_{n1}}_{Term H} + \underbrace{TF_{b2} \cdot UTLNHOHCl \cdot X_{n1}}_{Term I} - \underbrace{TF_c \cdot kox_5 \cdot NH_2Cl \cdot NO_2}_{Term J}
\end{aligned}$$

Term	Explanation	Reference
A	NO ₂ utilisation by NOB respiring aerobically	Laspidou & Rittmann (2002a, 2002b); Biyela (2010)
B	Consumption of nitrite as electron acceptor by heterotrophs respiring BOM anoxically	Laspidou & Rittmann (2002a, 2002b)
C	Consumption of nitrite as electron acceptor by heterotrophs respiring SMP anoxically	Laspidou & Rittmann (2002a, 2002b)
D	Consumption of nitrate as electron acceptor by heterotrophs respiring BOM anoxically	Laspidou & Rittmann (2002a, 2002b)
E	Consumption of nitrate as electron acceptor by heterotrophs respiring SMP anoxically	Laspidou & Rittmann (2002a, 2002b)
F	Endogenous decay with nitrite respiration	de Silva & Rittmann (2000)
G	Endogenous decay with nitrate respiration	de Silva & Rittmann (2000)
H	NH ₃ utilisation by AOB respiring aerobically	Woolschlager (2000); Biyela (2010)
I	NHOHCl cometabolism	Woolschlager (2000); Maestre, Wahman & Speitel (2013)
J	Oxidation of nitrite by NH ₂ Cl	Woolschlager (2000)

Nitrate ($\frac{\text{mole}}{\text{l}}$)

$$\begin{aligned} \frac{dNO_3}{dt} = & \underbrace{TF_{b2} \cdot UTLNO_2 \cdot X_{n2}}_{\text{Term A}} - \underbrace{TF_b \cdot \gamma_n \cdot (1 - kuap_h - keps_h - Y_h \cdot (1 - kuap_h - keps_h)) \cdot and_2 \cdot bom \cdot X_h}_{\text{Term B}} \\ & - \underbrace{TF_b \cdot \gamma_n \cdot (1 - Y_p) \cdot and_2 \cdot smp \cdot X_h}_{\text{Term C}} - \underbrace{\gamma_n \cdot fd \cdot b_h \cdot \left(\frac{NO_3}{K_{NO3} + NO_3} \cdot \frac{K_{I,DO}}{K_{I,DO} + O_2} \right) \cdot X_h}_{\text{Term D}} \\ & + \underbrace{TF_c \cdot kox_5 \cdot NH_2Cl \cdot NO_2}_{\text{Term E}} \end{aligned}$$

Term	Explanation	Reference
A	NO ₂ utilisation by NOB respiring aerobically	Lapidou & Rittmann (2002a, 2002b); Biyela (2010)
B	Consumption of nitrate as electron acceptor by heterotrophs respiring BOM anoxically	Lapidou & Rittmann (2002a, 2002b)
C	Consumption of nitrate as electron acceptor by heterotrophs respiring SMP anoxically	Lapidou & Rittmann (2002a, 2002b)
D	Endogenous respiration with nitrate	de Silva & Rittmann (2000)
E	Oxidation of nitrite by NH ₂ Cl	Woolschlager (2000)

Nitrogen Gas ($\frac{\text{mole}}{\text{l}}$)

$$\begin{aligned} \frac{dN_2}{dt} = & \underbrace{TF_b \cdot \frac{1}{2} \cdot \gamma_n \cdot (1 - kuap_h - keps_h - Y_h \cdot (1 - kuap_h - keps_h)) \cdot and_1 \cdot bom \cdot X_h}_{\text{Term A}} \\ & + \underbrace{TF_b \cdot \frac{1}{2} \cdot \gamma_n \cdot (1 - Y_p) \cdot and_1 \cdot smp \cdot X_h}_{\text{Term B}} \\ & + \underbrace{\gamma_n \cdot \frac{1}{2} \cdot fd \cdot b_h \cdot \left(\frac{NO_2}{K_{NO2} + NO_2} \cdot \frac{K_{I,DO}}{K_{I,DO} + O_2} \right) \cdot X_h}_{\text{Term C}} + \underbrace{TF_c \cdot k_{AD_5} \cdot NHOHCl}_{\text{Term D}} \end{aligned}$$

Term	Explanation	Reference
A	Consumption of nitrite as electron acceptor by heterotrophs respiring BOM anoxically	Lapidou & Rittmann (2002a, 2002b); Matějů et al (1992)
B	Consumption of nitrite as electron acceptor by heterotrophs respiring SMP anoxically	Lapidou & Rittmann (2002a, 2002b); Matějů et al (1992)
C	Endogenous respiration with nitrite	de Silva & Rittmann (2000)
D	Autocatalytic reaction AD ₅	Woolschlager (2000)

Chloride ($\frac{\text{mole}}{\text{l}}$)

$$\begin{aligned}
 \frac{dCl}{dt} = & \underbrace{TF_c.k_{AD4}.NHCl_2.OH}_{\text{Term A}} + \underbrace{2 \times TF_c.k_{AD5}.NHOHCl}_{\text{Term B}} + \underbrace{TF_{b2}.UTLNHOHCl.X_{n1}}_{\text{Term C}} \\
 & + \underbrace{TF_c.k_{ox4}.HOCl.NO_2}_{\text{Term D}} + \underbrace{TF_c.k_{ox5}.NH_2Cl.NO_2}_{\text{Term E}} \\
 & + 2 \times TF_c.\gamma_C \cdot \underbrace{\left(k_{ox1x1}.BOM_1 + k_{ox1x2}.BOM_2 + k_{ox1x2}.BAP \right.}_{\text{Term F}} \\
 & \quad \left. + k_{ox1x2}.UAP + k_{ox1x2}.X_i + k_{ox1x2}.EPS \right) .HOCl \\
 & + 2 \times TF_c.\gamma_C \cdot \underbrace{\left(k_{ox2x1}.BOM_1 + k_{ox2x2}.BOM_2 + k_{ox2x2}.BAP \right.}_{\text{Term G}} \\
 & \quad \left. + k_{ox2x2}.UAP + k_{ox2x2}.X_i + k_{ox2x2}.EPS \right) .OCl \\
 & + 2 \times TF_c.\gamma_C \cdot \underbrace{\left(k_{ox3x1}.BOM_1 + k_{ox3x2}.BOM_2 + k_{ox3x2}.BAP \right.}_{\text{Term H}} \\
 & \quad \left. + k_{ox3x2}.UAP + k_{ox3x2}.X_i + k_{ox3x2}.EPS \right) .NH_2Cl \\
 & + \underbrace{TF_c.k_{cr1} \cdot \left(\frac{4}{\text{diameter} \left(\frac{l}{m^3} \right) \cdot 1000} \right)}_{\text{Term I}} + \underbrace{TF_c.k_{cr2} \cdot \left(\frac{4}{\text{diameter} \left(\frac{l}{m^3} \right) \cdot 1000} \right)}_{\text{Term J}} \\
 & + \underbrace{TF_c.k_{cr3}.NH_2Cl}_{\text{Term K}}
 \end{aligned}$$

Term	Explanation	Reference
A	Autocatalytic reaction AD ₄	Woolschlager (2000)
B	Autocatalytic reaction AD ₅	Woolschlager (2000)
C	NHOHCl cometabolism	Woolschlager (2000); Maestre, Wahman & Speitel (2013)
D	Oxidation of nitrite by HOCl	Woolschlager (2000)
E	Oxidation of nitrite by NH ₂ Cl	Woolschlager (2000)
F	Oxidation of organic matter by HOCl	Woolschlager (2000)
G	Oxidation of organic matter by OCl ⁻	Woolschlager (2000)
H	Oxidation of organic matter by NH ₂ Cl	Woolschlager (2000)
I	Corrosion reaction for iron pipe with HOCl	Woolschlager (2000)
J	Corrosion reaction for iron pipe with OCl ⁻	Woolschlager (2000)
K	Corrosion reaction for iron pipe with NH ₂ Cl	Westbrook et al (2009)

Carbon Dioxide ($\frac{ugCOD}{l}$)

$$\begin{aligned}
 \frac{dCO_2}{dt} = & \underbrace{TF_b \cdot (1 - Y_h \cdot (1 - kuap_h - keps_h) - (kuap_h + keps_h)) \cdot UTL_{bom} \cdot X_h}_{Term A} \\
 & + \underbrace{TF_b \cdot (1 - Y_h \cdot (1 - kuap_h - keps_h) - (kuap_h + keps_h)) \cdot and_1_{bom} \cdot X_h}_{Term B} \\
 & + \underbrace{TF_b \cdot (1 - Y_h \cdot (1 - kuap_h - keps_h) - (kuap_h + keps_h)) \cdot and_2_{bom} \cdot X_h}_{Term C} \\
 & + \underbrace{TF_b \cdot (1 - Y_p) \cdot UTL_{smp} \cdot X_h}_{Term D} + \underbrace{TF_b \cdot (1 - Y_p) \cdot and_1_{smp} \cdot X_h}_{Term E} \\
 & + \underbrace{TF_b \cdot (1 - Y_p) \cdot and_2_{smp} \cdot X_h}_{Term F} \\
 & - \underbrace{TF_{b2} \cdot \left(Y_{n1} \cdot (1 - kuap_{n1} - keps_{n1}) + \left(\frac{kuap_{n1}}{\gamma_n} + \frac{keps_{n1}}{\gamma_n} \right) \right) \cdot UTL_{NH_3} \cdot X_{n1}}_{Term G} \\
 & - \underbrace{TF_{b2} \cdot \left(Y_{n2} \cdot (1 - kuap_{n2} - keps_{n2}) + \left(\frac{kuap_{n2}}{\gamma_n} + \frac{keps_{n2}}{\gamma_n} \right) \right) \cdot UTL_{NO_2} \cdot X_{n2}}_{Term H} \\
 & + fd \cdot \left(b_h \cdot \left(\frac{O_2}{K_{O_2} + O_2} + \frac{NO_2}{K_{NO_2} + NO_2} \cdot \frac{K_{I,DO}}{K_{I,DO} + O_2} + \frac{NO_3}{K_{NO_3} + NO_3} \cdot \frac{K_{I,DO}}{K_{I,DO} + O_2} \right) \cdot X_h \right. \\
 & \left. + b_{n1} \cdot \left(\frac{O_2}{K_{O_2} + O_2} \right) \cdot X_{n1} + b_{n2} \cdot \left(\frac{O_2}{K_{O_2} + O_2} \right) \cdot X_{n2} \right)_{Term I} \\
 & + \underbrace{TF_c \cdot \left(kox_3x_1 \cdot BOM_1 + kox_3x_2 \cdot BOM_2 + kox_3x_2 \cdot BAP \right) \cdot NH_2Cl}_{Term J} \\
 & + \underbrace{TF_c \cdot \left(kox_1x_1 \cdot BOM_1 + kox_1x_2 \cdot BOM_2 + kox_1x_2 \cdot BAP \right) \cdot HOCl}_{Term K} \\
 & + \underbrace{TF_c \cdot \left(kox_2x_1 \cdot BOM_1 + kox_2x_2 \cdot BOM_2 + kox_2x_2 \cdot BAP \right) \cdot OCl}_{Term L}
 \end{aligned}$$

Term	Explanation	Reference
A	BOM utilisation by heterotrophs respiring aerobically and UAP and EPS formation by heterotrophs respiring aerobically	Lapidou & Rittmann (2002a, 2002b)
B	BOM utilisation by heterotrophs respiring nitrite anoxically and UAP and EPS formation by heterotrophs respiring nitrite anoxically	Lapidou & Rittmann (2002a, 2002b)
C	BOM utilisation by heterotrophs respiring nitrate anoxically and UAP and EPS formation by heterotrophs respiring nitrate anoxically	Lapidou & Rittmann (2002a, 2002b)

D	SMP utilisation by heterotrophs respiring aerobically	Laspidou & Rittmann (2002a, 2002b)
E	SMP utilisation by heterotrophs respiring nitrite anoxically	Laspidou & Rittmann (2002a, 2002b)
F	SMP utilisation by heterotrophs respiring nitrate anoxically	Laspidou & Rittmann (2002a, 2002b)
G	Carbon dioxide assimilation by AOB respiring aerobically and UAP and EPS formation by AOB respiring aerobically	Laspidou & Rittmann (2002a, 2002b)
H	Carbon dioxide assimilation by NOB respiring aerobically and UAP and EPS formation by NOB respiring aerobically	Laspidou & Rittmann (2002a, 2002b)
I	Endogenous decay of active biomass	de Silva & Rittmann (2000)
J	Oxidation of organic matter by NH ₂ Cl	Wooschlagler (2000)
K	Oxidation of organic matter by HOCl	Wooschlagler (2000)
L	Oxidation of organic matter by OCl ⁻	Wooschlagler (2000)

Oxygen ($\frac{ug}{l}$)

$$\begin{aligned}
\frac{dO_2}{dt} = & - \underbrace{TF_b \cdot (1 - kuap_h - keps_h - Y_h \cdot (1 - kuap_h - keps_h)) \cdot UTLbom \cdot X_h}_{Term A} \\
& - \underbrace{TF_b \cdot (1 - Y_p) \cdot UTLSmp \cdot X_h}_{Term B} \\
& - \underbrace{TF_{b2} \cdot (1 - kuap_{n1} - keps_{n1} - Y_{n1} \cdot (1 - kuap_{n1} - keps_{n1})) \cdot UTLNH_3 \cdot X_{n1}}_{Term C} \\
& - \underbrace{TF_{b2} \cdot (1 - kuap_{n2} - keps_{n2} - Y_{n2} \cdot (1 - kuap_{n2} - keps_{n2})) \cdot UTLNO_2 \cdot X_{n2}}_{Term D} \\
& - \underbrace{fd \cdot \left(b_h \cdot \left(\frac{O_2}{K_{O_2} + O_2} \right) \cdot X_h + b_{n1} \cdot \left(\frac{O_2}{K_{O_2} + O_2} \right) \cdot X_{n1} + b_{n2} \cdot \left(\frac{O_2}{K_{O_2} + O_2} \right) \cdot X_{n2} \right)}_{Term E} \\
& + \underbrace{kla \cdot (O_{2s} - O_2)}_{Term F}
\end{aligned}$$

Term	Explanation	Reference
------	-------------	-----------

A	BOM utilisation by heterotrophs respiring aerobically and UAP and EPS formation by heterotrophs respiring aerobically	Laspidou & Rittmann (2002a, 2002b)
B	SMP utilisation by heterotrophs respiring aerobically	Laspidou & Rittmann (2002a, 2002b)
C	NH ₃ utilisation by AOB respiring aerobically and UAP and EPS formation by AOB respiring aerobically	Laspidou & Rittmann (2002a, 2002b)
D	NO ₂ utilisation by NOB respiring aerobically and UAP and EPS formation by NOB respiring aerobically	Laspidou & Rittmann (2002a, 2002b)
E	Endogenous decay of active biomass	Laspidou & Rittmann (2002a, 2002b); Rittmann, Stilwell & Ohashi (2002); de Silva & Rittmann (2000)
F	Aeration	Laspidou & Rittmann (2002a, 2002b); Biyela (2010)

3.9 CDWQ-E₂ Algorithm

The algorithm set out on the following page is written according to the ISO 5807:1985 standard. It presents the steps in which the procedures detailed previously in this chapter are performed in the CDWQ-E₂ model in order to execute the required water quality analysis. All differential equations are solved using Euler's method and the code is written in Matlab R2011a. In addition, numerous differences between the coding of the CDWQ and CDWQ-E₂ model are highlighted.

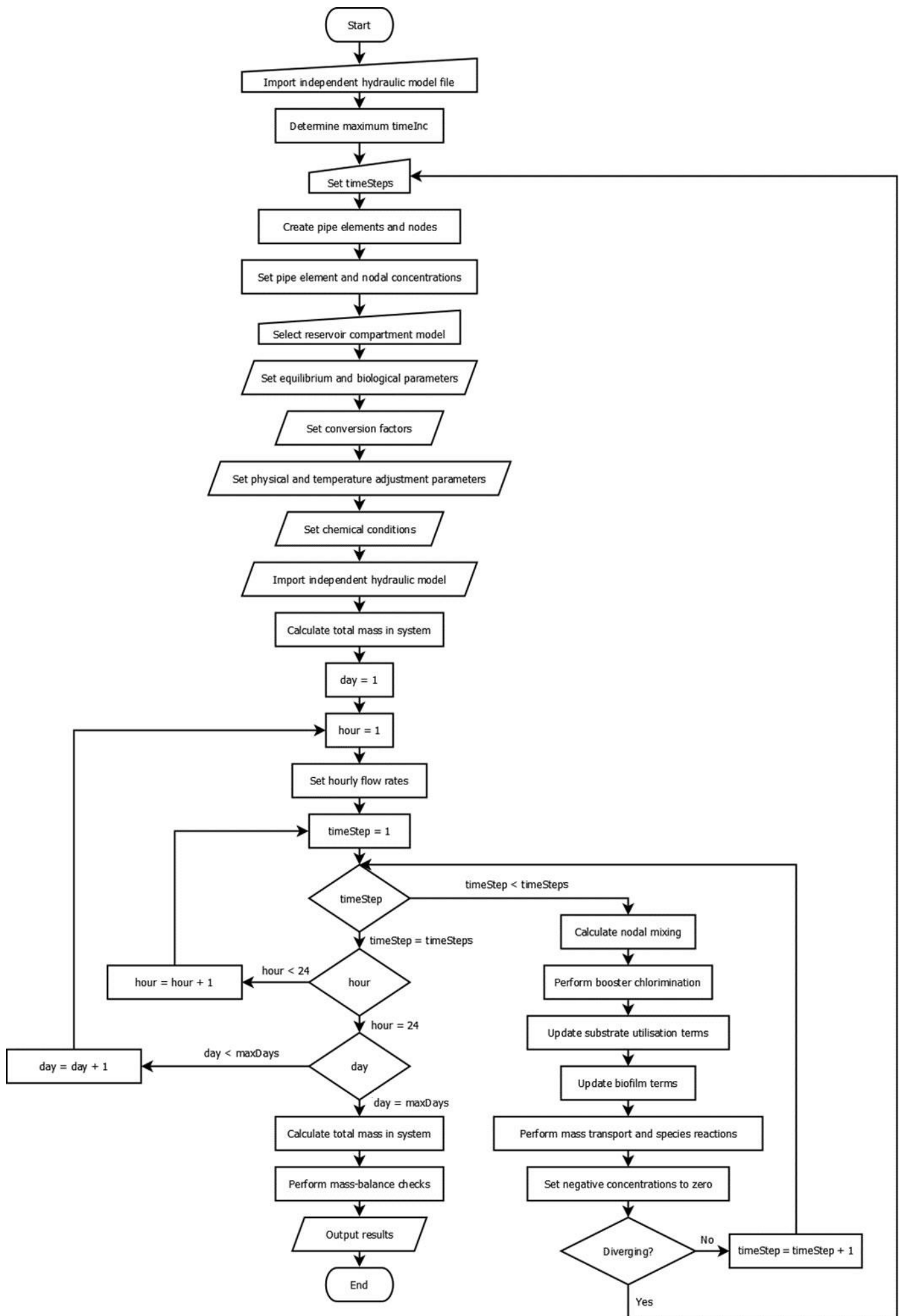


Figure 3-12: CDWQ-E₂ Algorithm

1. Import independent hydraulic model file:

- In CDWQ-E₂, the hydraulic model is incorporated into a single Microsoft Excel file with separate sheets containing pipe properties, dynamic flow rates, initial suspended and dissolved constituent concentrations, initial biofilm concentrations, treatment plant inputs and booster chloramination/chlorination data. This is in keeping with the secondary aim of the E₂ version of the model specifically regarding coding, which is to make the model more user-friendly. In the CDWQ model, each input was contained in a separate text file, which was cumbersome and required an intricate understanding of the working of the code and knowledge of handling text files in order to edit any input data.
- Based on the imported pipe properties and hydraulic data, the CDWQ-E₂ model automatically determines the maximum time step that will ensure mass closure with respect to the requirement of pipe element sizing⁷. The user is prompted to either use this recommended time step or enter a custom time step. The user may wish to utilise a larger time step in order to reduce the computational time to obtain a first approximation of the water quality solution and by doing so, mass closure errors will be introduced within certain pipe elements.
- Based on the selected time step, the CDWQ-E₂ model automatically divides each pipe into elements, sizes them accordingly and creates nodes to link each element. This differs from the CDWQ model, in which this process had to be performed manually.
- If one or more reservoirs are present in the hydraulic model, the user is prompted to select whether these reservoirs are analysed using the one-, two- or three-compartment model⁸.
- Suspended and dissolved constituents are imported from the Excel file, in which they are initially defined at the pipe nodes. Linear interpolation is used to redistribute these known pipe node concentrations to the new element nodes, and element concentrations are computed as the average of each element's start and end node concentrations, as shown in Figure 3-13:

⁷ See section 3.6.1 for detailed explanation

⁸ See section 3.6.2 for detailed explanation

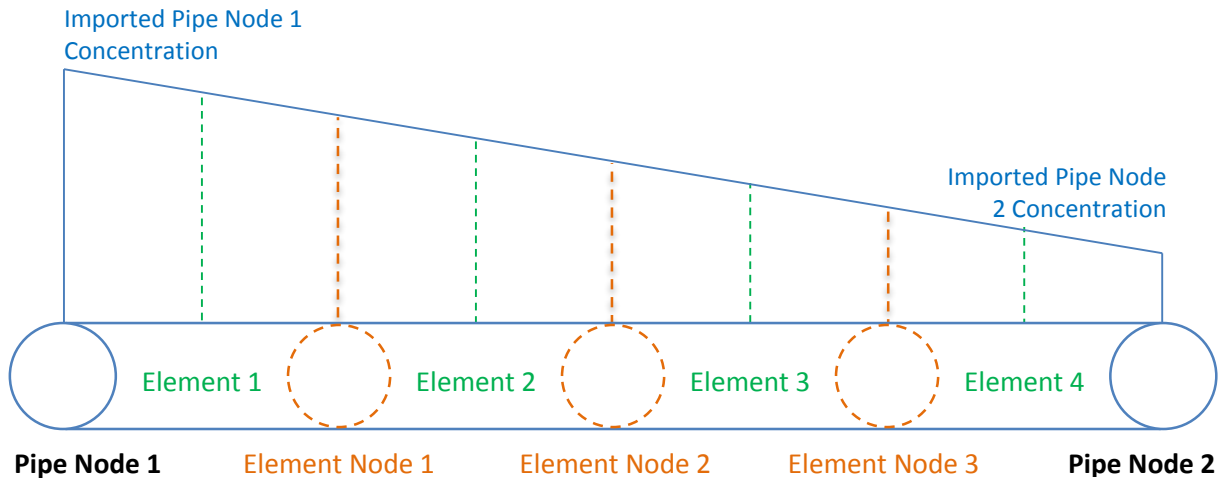


Figure 3-13: Schematic diagram of the method used to define element node and element concentrations based on imported pipe node concentrations for dissolved and suspended constituents

- Fixed biofilms are imported from the Excel file and are initially defined for each pipe. As discussed previously, a node is a theoretical concept used to determine mixing of water and has no storage volume, and therefore fixed biofilm concentrations are equal to zero at the nodes. Element fixed biofilm concentrations are set to match those of the pipes to which they belong, as shown in Figure 3-14:

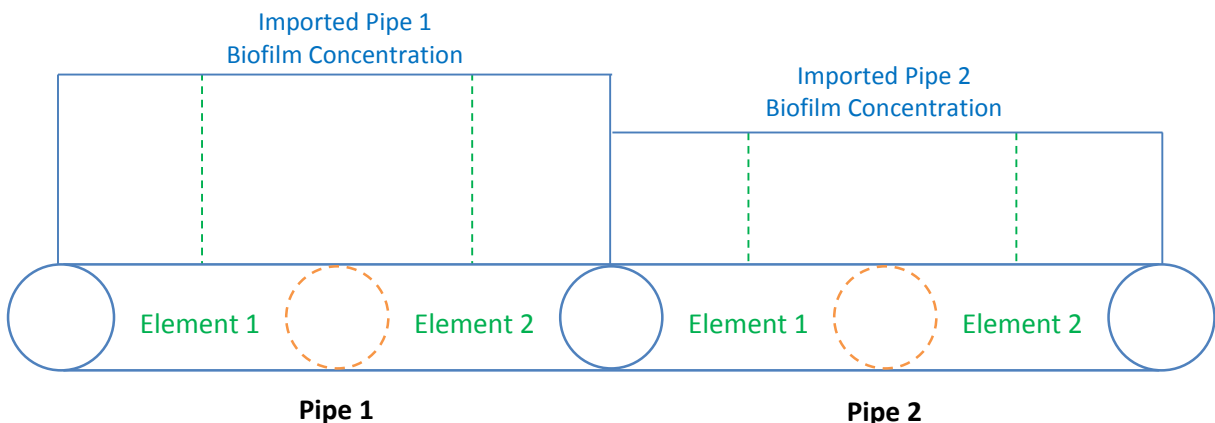


Figure 3-14: Schematic diagram of the method used to define element fixed biofilm concentrations based on imported pipe biofilm concentrations

- Coordinates defining the layout of the distribution system are imported from the Excel file.
2. Define the global parameters and reaction constants incorporated into the CDWQ-E₂ model, which do not vary for the simulation period⁹.
 3. Define the global conditions, namely pH, carbonate concentration and temperature, based on the treatment plant input.

⁹ See Table 3-1 to Table 3-7 for parameters incorporated and values used.

4. Determine the ammonia and ammonium fraction of the total ammonia for each element based on the global pH using equilibrium reaction E_1^{10} .
5. Determine the hypochlorous acid and hypochlorite ion fraction of the free chlorine for each element based on the global pH using equilibrium reaction E_2^{11} .
6. Calculate flexible kinetic constants k_{AD1} , k_{OX4} and k_{OX5} for each element¹².
7. Calculate substrate utilisation rates for each element¹³.
8. Define start and end nodes for each element based on flow directions, such that the flow in each element is always from the start node to the end node. Whereas this process had to be manually performed for every change in flow direction in the CDWQ model, it has been automated in the E_2 version.
9. Add treatment plant suspended and dissolved constituents at the treatment plant node.
10. Using Euler's method, update concentrations of each of the 24 species in every element using mass-balance equations, including chemical, physical and biological reactions as well as mass transport from element nodes for the suspended and dissolved constituents.
11. Update concentrations of each of the 24 species in each reservoir according to the selected compartment model.
12. Set any negative concentrations for any species to zero.
13. Based on the updated element concentrations, perform nodal mixing to determine nodal concentrations for suspended and dissolved constituents for mass transport.
14. If solution is diverging, terminate simulation and notify user.
15. Repeat steps 8 to 14 for the required number of time steps.
16. Output results for final day of simulation in multiple user-friendly formats in order to maximise interpretive and predictive potential:
 - In the CDWQ model, results for all modelled species are saved to text files for each hour of the final day of the simulation, making interpretation difficult and cumbersome. In

¹⁰ See Table 3-1 for equilibrium reaction E_1

¹¹ See Table 3-1 for equilibrium reaction E_2

¹² See Table 3-1 for equations used to calculate these flexible kinetic constants

¹³ See section 3.1.2 and 3.1.3 for substrate utilisation formulae

the E₂ version, both element and nodal concentrations for every species are output to matrices, which allow for easier handling and manipulation of the data.

- More significantly, concentration profiles for any species can be plotted for any user-specified time period based on the aforementioned matrices and the imported distribution system coordinates. This presents the results in a visual format, making the assessment of results and trends within the distribution system considerably easier and more effective.

17. End simulation.

4 BATCH VERSION SIMULATIONS

4.1 Introduction

One of the most significant benefits of the CDWQ-E₂ model is that it is capable of not only predicting water quality changes, but unlike many other water quality models, it is also capable of interpreting the reasons for such changes. This enables water utilities to better understand the reasons for the water quality changes that occur throughout their distribution systems.

One particular concern for water utilities is biostability, which refers to the overall tendency of water to promote or suppress microbial proliferation. This can be demonstrated mathematically by an equation, known as the stability factor equation, which was originally developed by Wooschlager (2000). The stability factor equations have been updated for the CDWQ-E₂ model to account for the diversion of electrons from the substrate to produce bound extracellular polymeric substances and utilisation products, in accordance with the Unified Theory developed by Laspidou and Rittmann (2002a, 2002b), as well as the availability of an electron acceptor and anoxic respiration by heterotrophs.

$$\begin{aligned}
 \text{Stability Factor } X_{hs} = & TF_b \cdot Y_h \cdot (1 - kuap_h - keps_h) \cdot UTLbom + TF_b \cdot Y_p \cdot UTLsmp \\
 & + TF_b \cdot Y_h \cdot (1 - kuap_h - keps_h) \cdot and_1bom \\
 & + TF_b \cdot Y_h \cdot (1 - kuap_h - keps_h) \cdot and_2bom \\
 & + TF_b \cdot Y_p \cdot and_1smp + TF_b \cdot Y_p \cdot and_2smp \\
 & - b_h \cdot \left(\frac{O_2}{K_{O_2} + O_2} + \frac{NO_2}{K_{NO_2} + NO_2} \cdot \frac{K_{I,DO}}{K_{I,DO} + O_2} + \frac{NO_3}{K_{NO_3} + NO_3} \cdot \frac{K_{I,DO}}{K_{I,DO} + O_2} \right) \\
 & - (kd_1x_1 \cdot HOCl + kd_2x_1 \cdot OCl + kd_3x_1 \cdot NH_2Cl)
 \end{aligned}$$

Equation 4-1: Suspended Heterotroph Stability Factor

$$\begin{aligned}
 \text{Stability Factor } X_{hf} = & TF_b \cdot Y_h \cdot (1 - kuap_h - keps_h) \cdot UTLbom + TF_b \cdot Y_p \cdot UTLsmp \\
 & + TF_b \cdot Y_h \cdot (1 - kuap_h - keps_h) \cdot and_1bom \\
 & + TF_b \cdot Y_h \cdot (1 - kuap_h - keps_h) \cdot and_2bom \\
 & + TF_b \cdot Y_p \cdot and_1smp + TF_b \cdot Y_p \cdot and_2smp \\
 & - b_h \cdot \left(\frac{O_2}{K_{O_2} + O_2} + \frac{NO_2}{K_{NO_2} + NO_2} \cdot \frac{K_{I,DO}}{K_{I,DO} + O_2} + \frac{NO_3}{K_{NO_3} + NO_3} \cdot \frac{K_{I,DO}}{K_{I,DO} + O_2} \right) \\
 & - (kd_1x_2 \cdot HOCl + kd_2x_2 \cdot OCl + kd_3x_2 \cdot NH_2Cl)
 \end{aligned}$$

Equation 4-2: Fixed Heterotroph Stability Factor

$$\begin{aligned}
 \text{Stability Factor } X_{n1s} = & TF_{b2} \cdot Y_{n1} \cdot (1 - kuap_{n1} - keps_{n1}) \cdot UTLNH_3 - b_{n1} \left(\frac{O_2}{K_{O_2} + O_2} \right) \\
 & - (kd_1x_3 \cdot HOCl + kd_2x_3 \cdot OCl + kd_3x_3 \cdot NH_2Cl)
 \end{aligned}$$

Equation 4-3: Suspended AOB Stability Factor

$$\text{Stability Factor } X_{n1f} = TF_{b2} \cdot Y_{n1} \cdot (1 - kuap_{n1} - keps_{n1}) \cdot UTLNH_3 - b_{n1} \left(\frac{O_2}{K_{O_2} + O_2} \right) - (kd_1x_4.HOCl + kd_2x_4.OCl + kd_3x_4.NH_2Cl)$$

Equation 4-4: Fixed AOB Stability Factor

$$\text{Stability Factor } X_{n2s} = TF_{b2} \cdot Y_{n2} \cdot (1 - kuap_{n2} - keps_{n2}) \cdot UTLNO_2 - b_{n2} \left(\frac{O_2}{K_{O_2} + O_2} \right) - (kd_1x_5.HOCl + kd_2x_5.OCl + kd_3x_5.NH_2Cl)$$

Equation 4-5: Suspended NOB Stability Factor

$$\text{Stability Factor } X_{n2f} = TF_{b2} \cdot Y_{n2} \cdot (1 - kuap_{n2} - keps_{n2}) \cdot UTLNO_2 - b_{n2} \left(\frac{O_2}{K_{O_2} + O_2} \right) - (kd_1x_6.HOCl + kd_2x_6.OCl + kd_3x_6.NH_2Cl)$$

Equation 4-6: Fixed NOB Stability Factor

The stability factor equations mathematically demonstrate the competing effects of net synthesis and death or inactivation of cells caused by disinfection on biostability. Net synthesis (which includes endogenous decay) is fuelled by the oxidation of the electron donor, which varies depending on the type of bacteria. Heterotrophic bacteria utilise BOM as a substrate, while AOB and NOB, by definition, utilise ammonia and nitrite respectively as their substrates.

When the stability factor is greater than 0, the balance can be said to be in favour of the substrate, and net growth will occur. Similarly, when the stability factor is less than 0, net death will occur. Thus, an analysis of the stability factor enables one to determine the extent to which reducing the concentration of a substrate, increasing the concentration of a disinfectant, or both of these options in combination, will be successful in improving the biostability of water.

An issue of particular concern with regard to biostability is the proliferation of nitrifying bacteria, that is AOB and NOB, which can result in instances of nitrification in drinking water distribution systems. Biologically driven nitrification is a two-step biochemical process, in which ammonia is first oxidised to nitrite by AOB, and following this, nitrite is oxidised to nitrate by NOB (American Water Works Association & Economic and Environmental Engineering Services, Inc., 2002; Liu et al, 2005).

Ammonia is typically present in drinking water through naturally-occurring processes, but the use of chloramine as a secondary disinfectant can significantly increase the ammonia concentration of drinking water (American Water Works Association & Economic and Environmental Engineering Services, Inc., 2002). The release of ammonia from chloramines is detailed in the CDWQ-Cl₂ submodel. As chloramines decay and release ammonia, the concentration of AOB will increase and hence the rate of monochloramine cometabolism will also increase. Furthermore, as the rate of ammonia utilisation increases, more nitrite is formed, which increases the rate of monochloramine

oxidation (Reaction Ox₅ in the CDWQ-Cl₂ submodel), which itself releases more ammonia. Thus, nitrification in drinking water distribution systems utilising chloramine as a secondary disinfectant establishes a positive feedback loop with regard to monochloramine decay, which may pose significant challenges to drinking water utilities. Nitrification can have such significant consequences with regard to water quality that Le Puil (2004, p 59) terms it a “death spiral”.

In the section that follows, a batch version of the model is simulated for 30 days with the initial conditions provided in Table 4-1, which are representative of typical distribution system conditions. Although this simulation period is significantly greater than is typical for distribution systems, it is used to represent a potential worst case scenario (American Water Works Association, 2005; Biyela, 2010). The influence of pH, temperature and carbonate concentration on water quality is demonstrated by varying each of these parameters in turn.¹⁴ As can be seen from the results, the stability factor for each of the three suspended active biomass species compliments the net growth rate for a given time. That is, when the stability factor is greater than 0, net growth occurs and when the stability factor is less than 0, net death occurs.

4.2 Batch Simulations

Table 4-1: Initial Conditions

Parameter	Value
BOM ₁	$0.337 \frac{mg}{l} \text{ as } C$
BOM ₂	$1.54 \frac{mg}{l} \text{ as } C$
Total Ammonia	$0.319 \frac{mg}{l} \text{ as } N$
Nitrite	$0.032 \frac{mg}{l} \text{ as } N$
Nitrate	$0.532 \frac{mg}{l} \text{ as } N$
Heterotrophs	$962 \frac{cells}{ml}$
Ammonia Oxidising Bacteria	$96 \frac{cells}{ml}$
Nitrite Oxidising Bacteria	$96 \frac{cells}{ml}$
Monochloramine	$3.12 \frac{mg}{l} \text{ as } Cl_2$
Oxygen	$8.38 \frac{mg}{l}$
pH	7.0; 7.5; 8.0

¹⁴ The batch version of the code and simulation outputs are provided on an accompanying CD.

Temperature	15.0; 20.0; 25.0 °C
Carbonate Buffer	1.0; 3.0; 5.0 millimoles (mM)

4.2.1 Influence of pH on Water Quality

The batch model can be used to assess the impact of pH on water quality. The graphs that follow present the results of three simulations in which the pH varied between 7.0 and 8.0 with a fixed temperature of 20°C and a carbonate concentration of 3.0 mM.

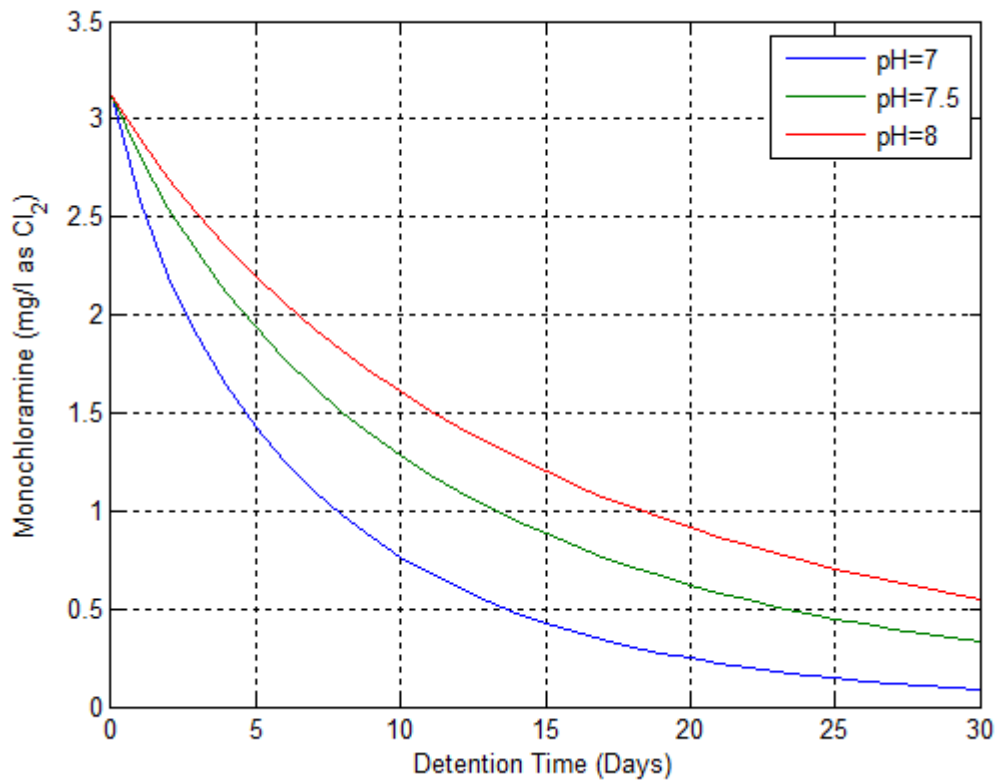


Figure 4-1: Monochloramine concentration against time for varying pH values

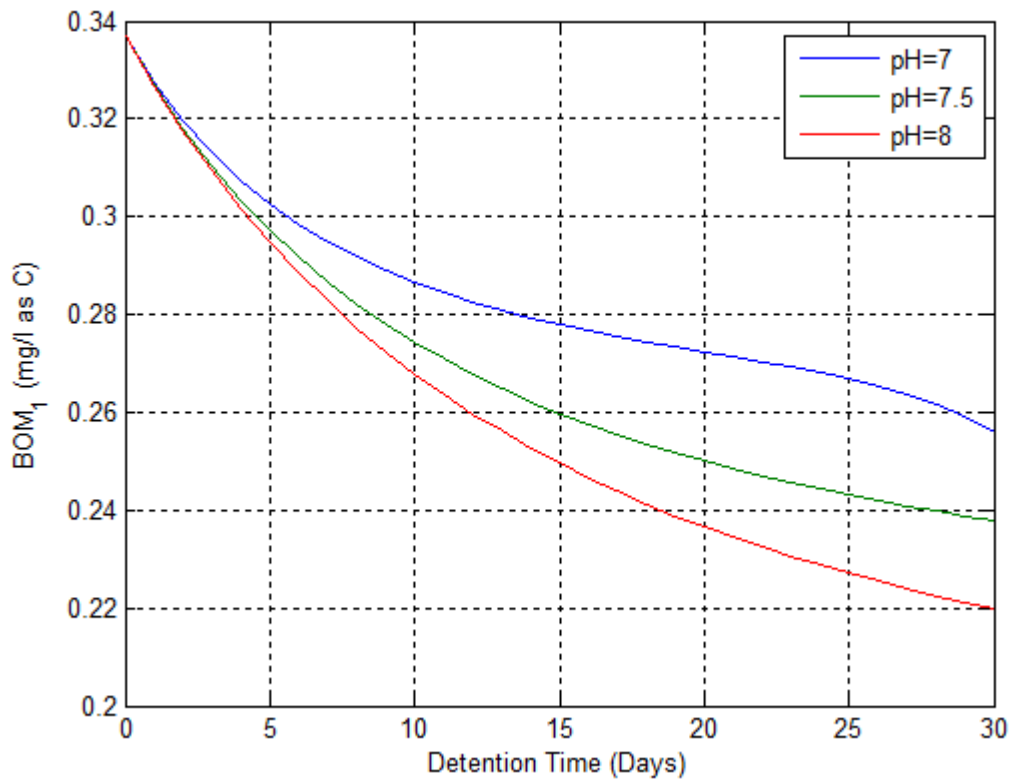


Figure 4-2: BOM₁ concentration against time for varying pH values

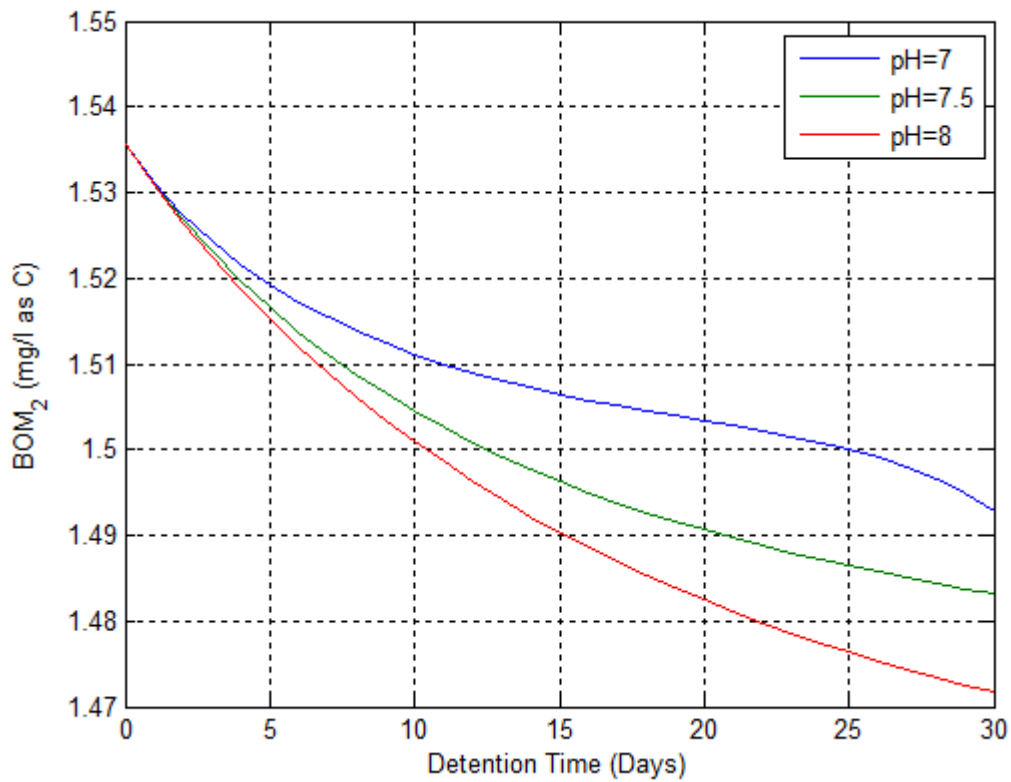


Figure 4-3: BOM₂ concentration against time for varying pH values

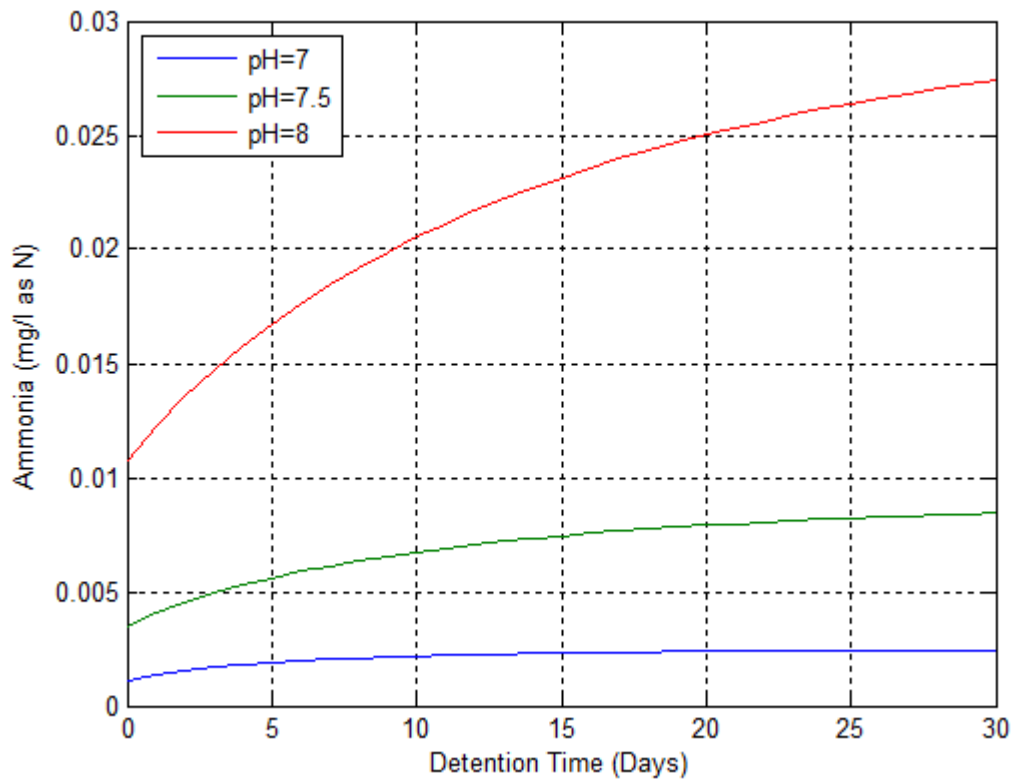


Figure 4-4: Ammonia concentration against time for varying pH values

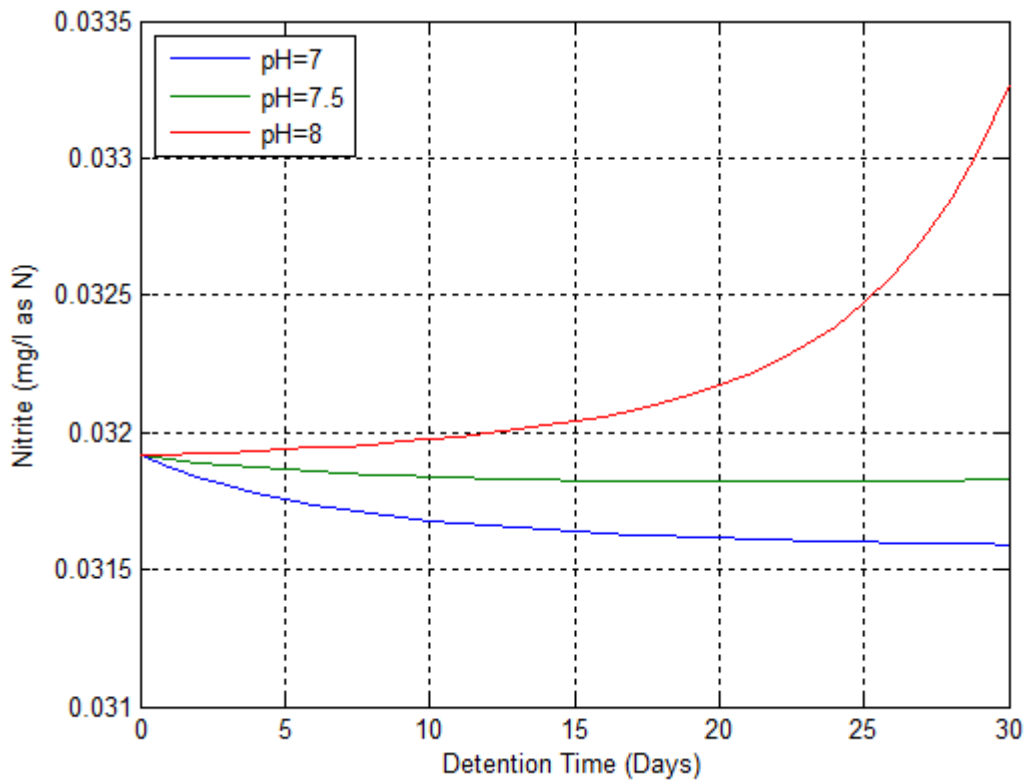


Figure 4-5: Nitrite concentration against time for varying pH values

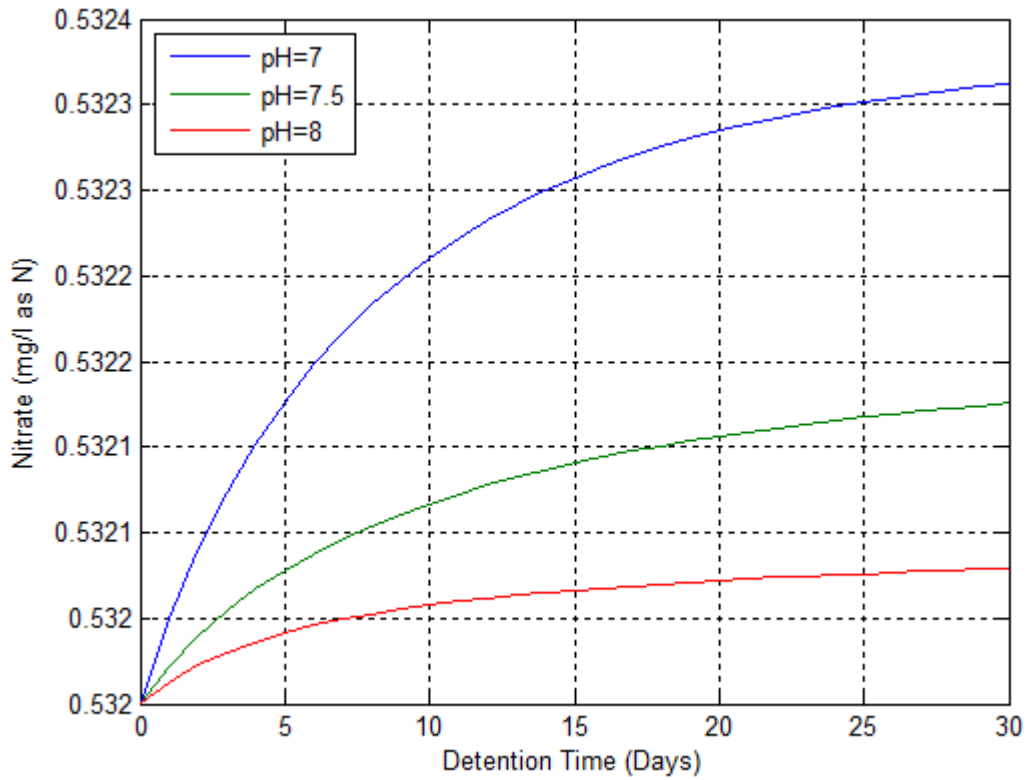


Figure 4-6: Nitrate concentration against time for varying pH values

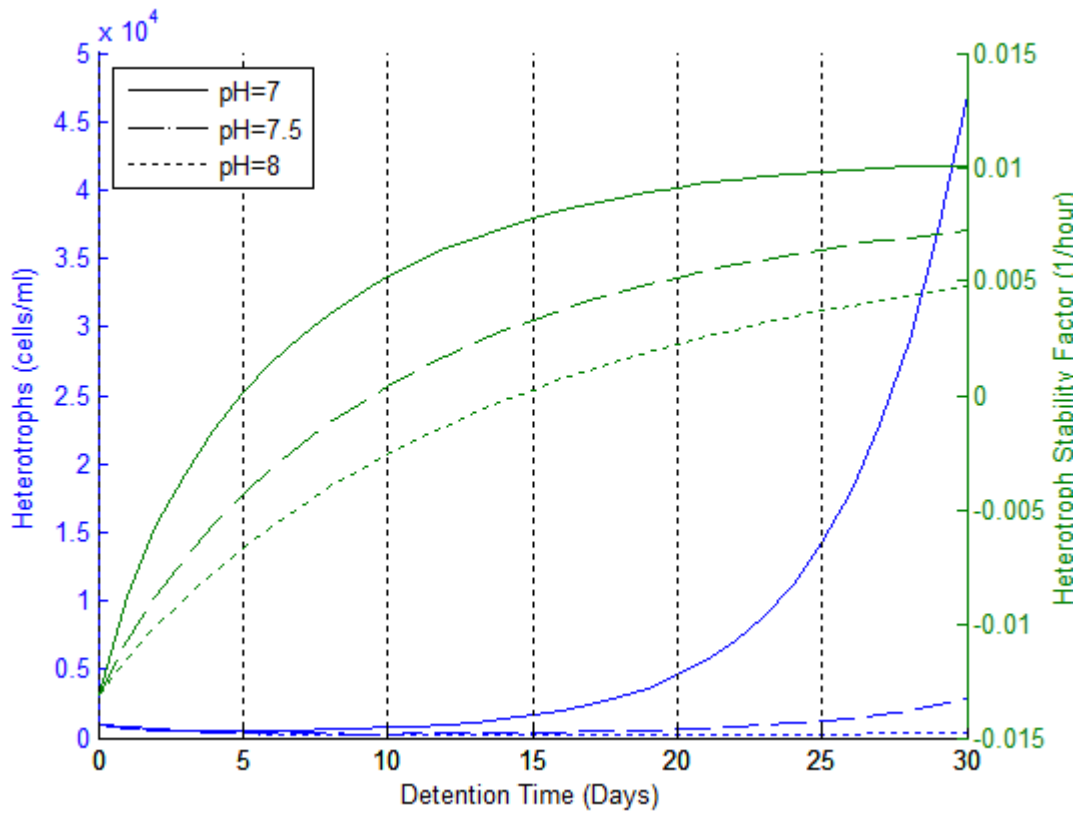


Figure 4-7: Suspended heterotroph concentration and stability factor against time for varying pH values

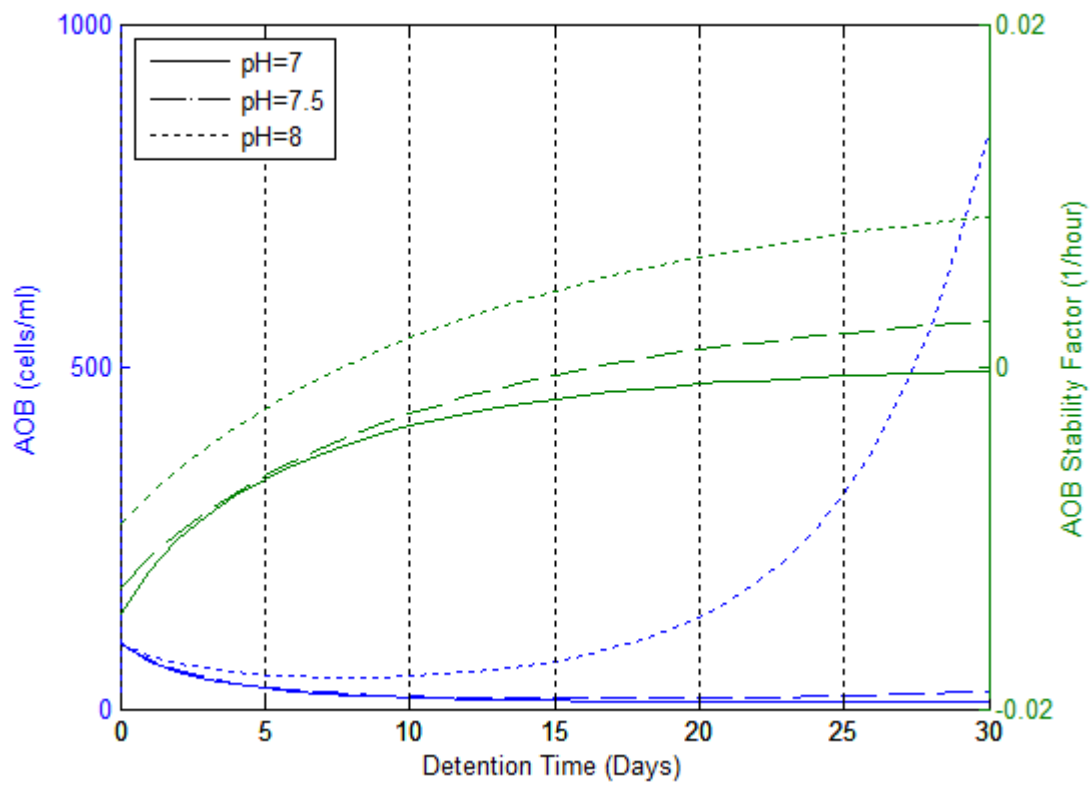


Figure 4-8: Suspended AOB concentration and stability factor against time for varying pH values

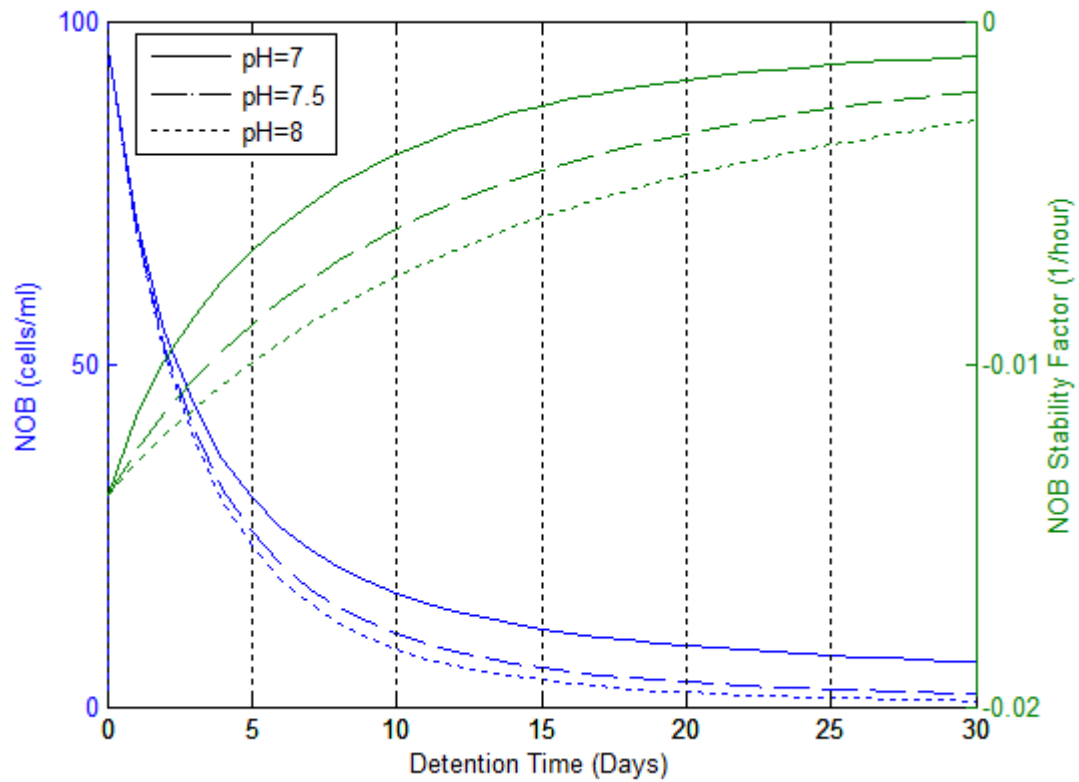


Figure 4-9: Suspended NOB concentration and stability factor against time for varying pH values

It is apparent that as the pH increases between 7.0 and 8.0, the rate of monochloramine decay decreases. These findings are in accordance with those made by various researchers who found that the rate of chloramine autocatalytic decay decreases with increasing pH (Vikesland, Ozekin & Valentine, 2001; Zaklikowski, 2006; Arevalo, 2007). The reason for the increased stability of monochloramine at increasing pH is that the rate of dichloramine formation due to autocatalytic decay reaction AD₁ decreases with increasing pH, and it is this reaction that is rate-limiting with regard to the autocatalytic decay of monochloramine (Vikesland et al, 2001). This is demonstrated using Figure 4-10, the creation of which has been incorporated as part of the CDWQ-E₂ model in order to enhance its interpretive capabilities. Furthermore, based on Figure 4-10, it is apparent that the loss of monochloramine due to the oxidation of organic matter increases with increasing pH. The reason for this is that the loss of monochloramine due to organic matter oxidation is a function of both monochloramine and organic matter concentration. Thus, for this scenario, as less monochloramine is lost at pH 8.0 due to autocatalytic decay reactions, the loss of monochloramine due to organic matter oxidation is greater.

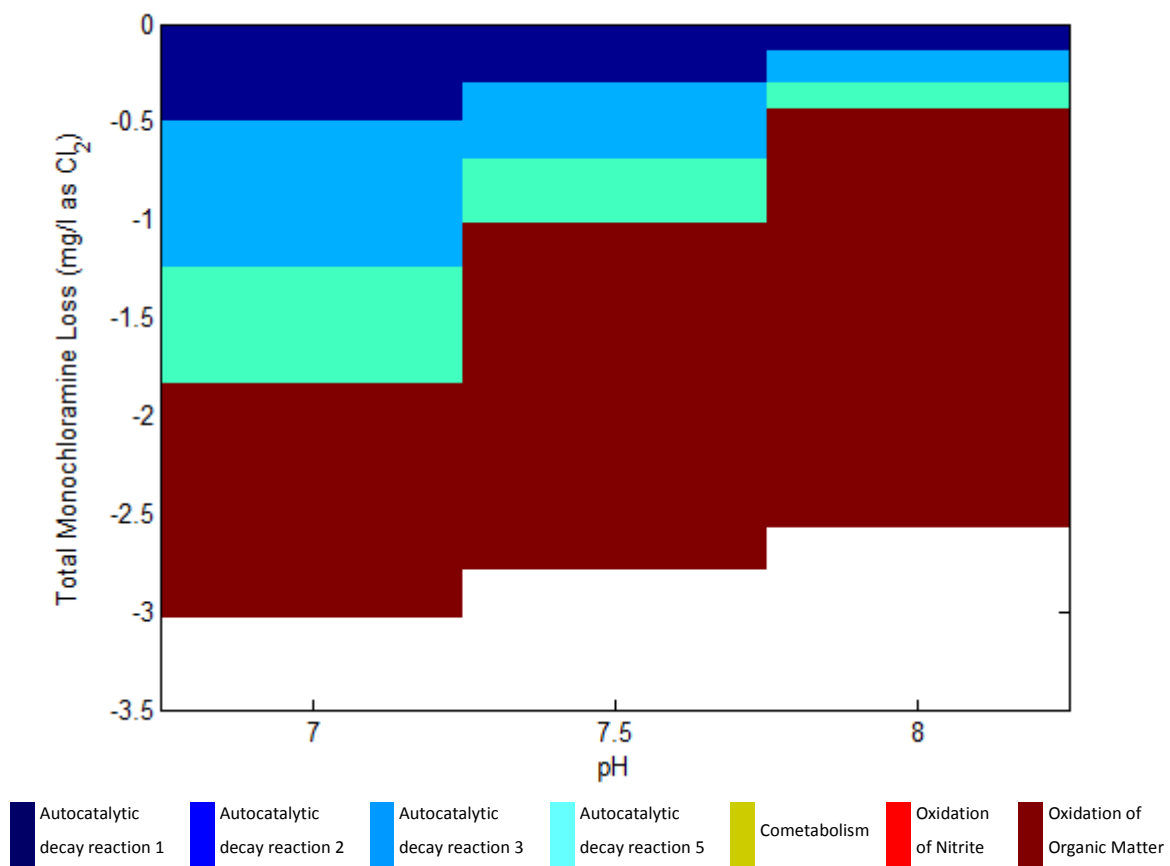
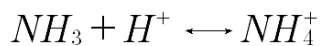


Figure 4-10: Relative contribution of monochloramine loss mechanisms for varying pH values

As one would expect, as a consequence of the increased stability of monochloramine with increasing pH, heterotroph and NOB concentrations decrease as the pH increases. However, the concentration of AOB increases with increasing pH, which may appear counterintuitive.

The reasons for this result can be explained by analysing the stability factor for AOB at the various pH values. As can be seen in Figure 4-8, the AOB stability factor for the simulation performed is always greater for the higher pH value assessed. Thus, as pH increases, the rate of net synthesis must be increasing at a greater rate than the rate of disinfection. Given that the rate of disinfection increases with increasing pH, analysis of the AOB stability factor leads to the conclusion that with increasing pH, the rate of net synthesis increases at a greater rate than disinfection for this simulation. This, in turn, must mean that the substrate concentration, ammonia in this case, is increasing as the pH increases. The shift in the balance of total ammonia towards ammonia, which is the biologically-available form for AOB (as opposed to ammonium), is governed by the equilibrium reaction below:



As both the AOB concentration and the ammonia concentration are greatest at pH 8, in accordance with Monod kinetics, the utilisation of ammonia is greatest at this pH and consequently the production of nitrite from ammonia utilisation (the first step of nitrification) is also greatest at this pH. In fact, for these simulations, the first step of the nitrification process is not significant for the two lower pH values, as evidenced by the stable nitrite concentrations for these simulations. However, even for a pH value of 8, the concentration of nitrate remains relatively constant over the simulation period, which indicates that the rate of nitrite utilisation by NOB, which produces nitrate (the second step of nitrification), is not significant. Analysis of the NOB stability factor, demonstrated in Figure 4-9, provides an explanation for this result: the concentration of monochloramine at all pH values over the entire simulation period results in the rate of disinfection outpacing the rate of net synthesis of NOB resulting from nitrite utilisation. The result of this batch simulation is in accordance with findings made by Wolfe et al (1990), who state that in distribution systems it is typically only the first step of nitrification that takes place.

The rate of BOM loss increases with increasing pH. Again, this may seem counterintuitive given that BOM is the substrate for heterotrophic bacteria. However, as is demonstrated using Figure 4-11 and Figure 4-12, BOM oxidation by monochloramine increases with increasing pH. Thus, for this simulation, the reduced consumption of BOM by heterotrophs at a higher pH is less significant with

regard to BOM loss than the increased rate of oxidation of BOM at the higher pH, and hence BOM concentration is greatest at the lowest pH, despite the increased concentration of heterotrophs.

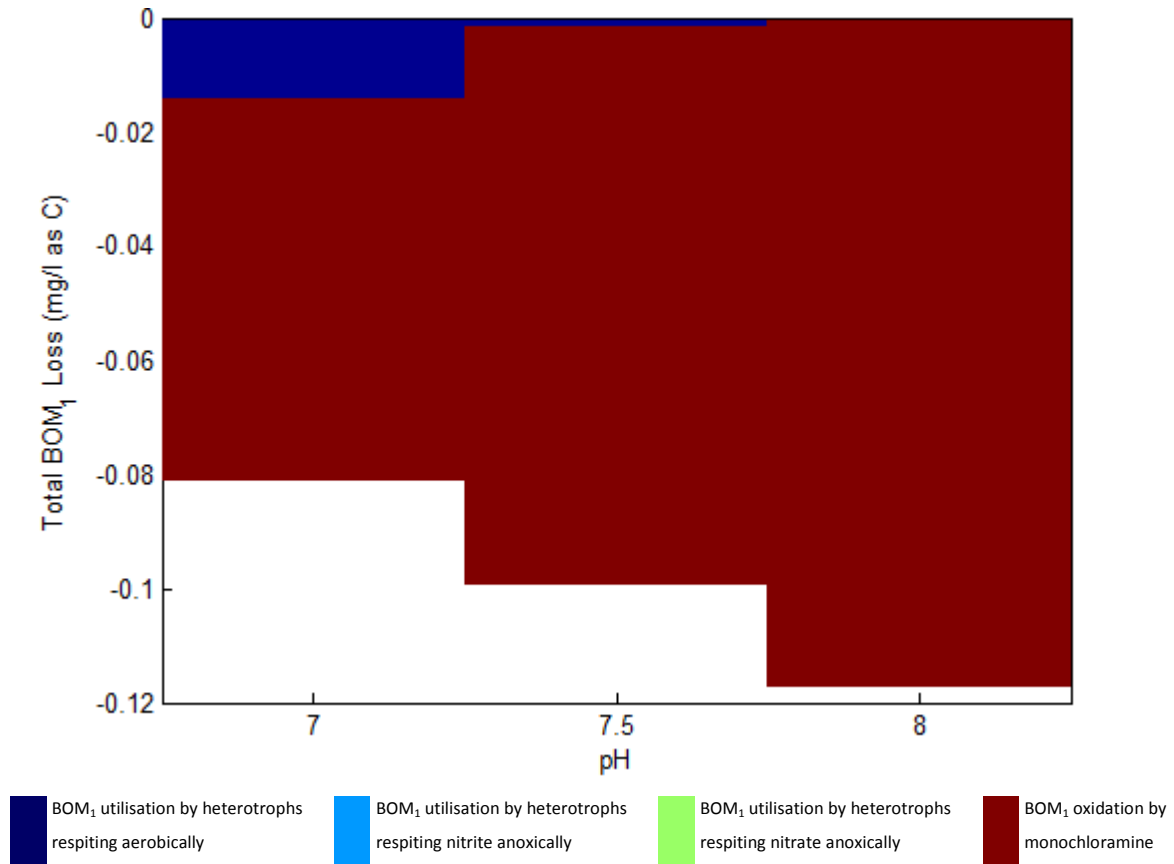


Figure 4-11: Relative contribution of BOM₁ loss mechanisms for varying pH values

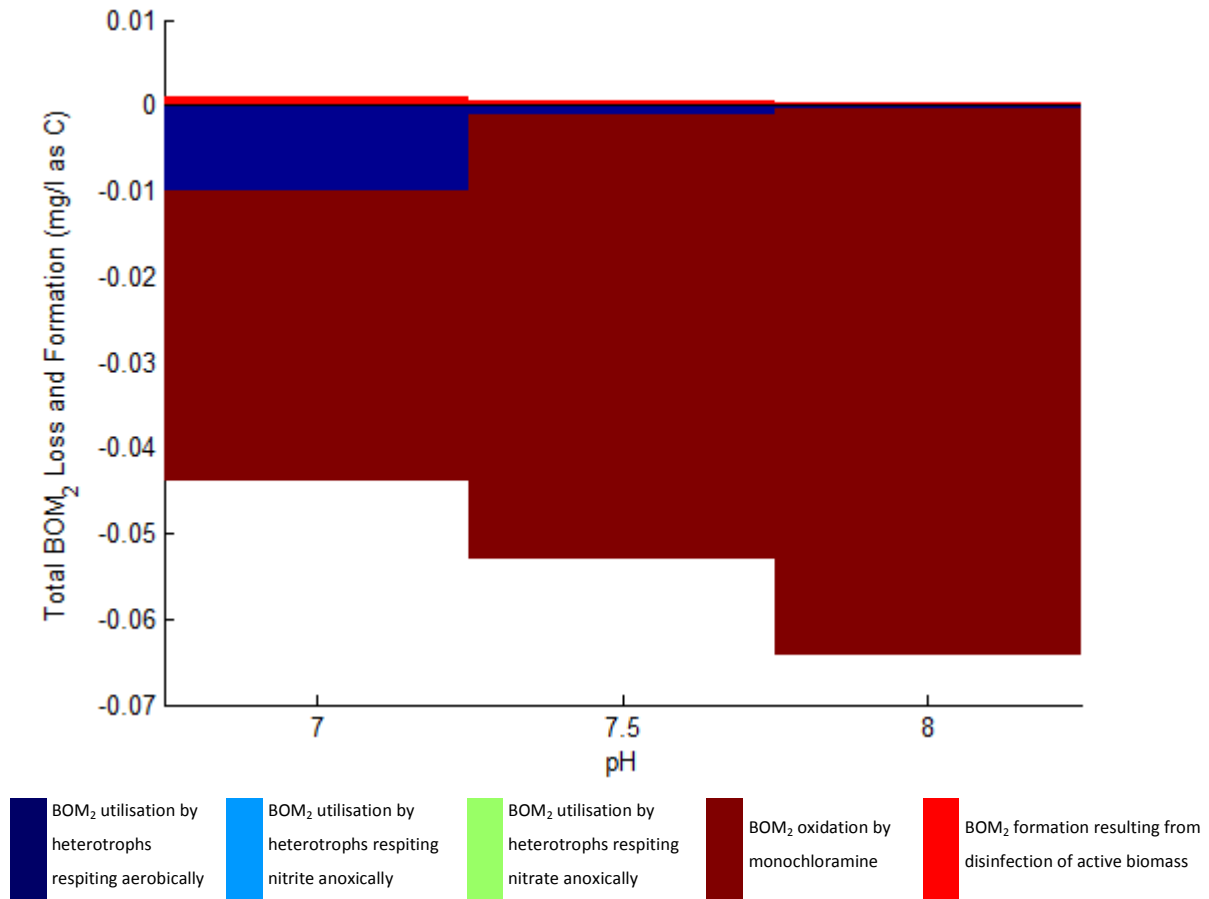


Figure 4-12: Relative contribution of BOM₂ loss and formation mechanisms for varying pH values

Based on an analysis of the heterotrophic stability factor, it is apparent that given the initial monochloramine concentration, the concentration of BOM is not sufficient to allow for net heterotrophic growth at the start of the simulation period. However, despite the fact that the concentration of both BOM₁ and BOM₂ decrease from the onset of the simulation, the decrease in the monochloramine concentration is a more significant factor with regard to the heterotrophic stability factor and hence the stability factor for heterotrophs increases over time. For this simulation, the heterotrophic stability factor increases more rapidly with reducing pH for two interrelated reasons: the BOM concentration is greater at this pH for the majority of the simulation period, while the monochloramine concentration is lower throughout the simulation period, as explained previously.

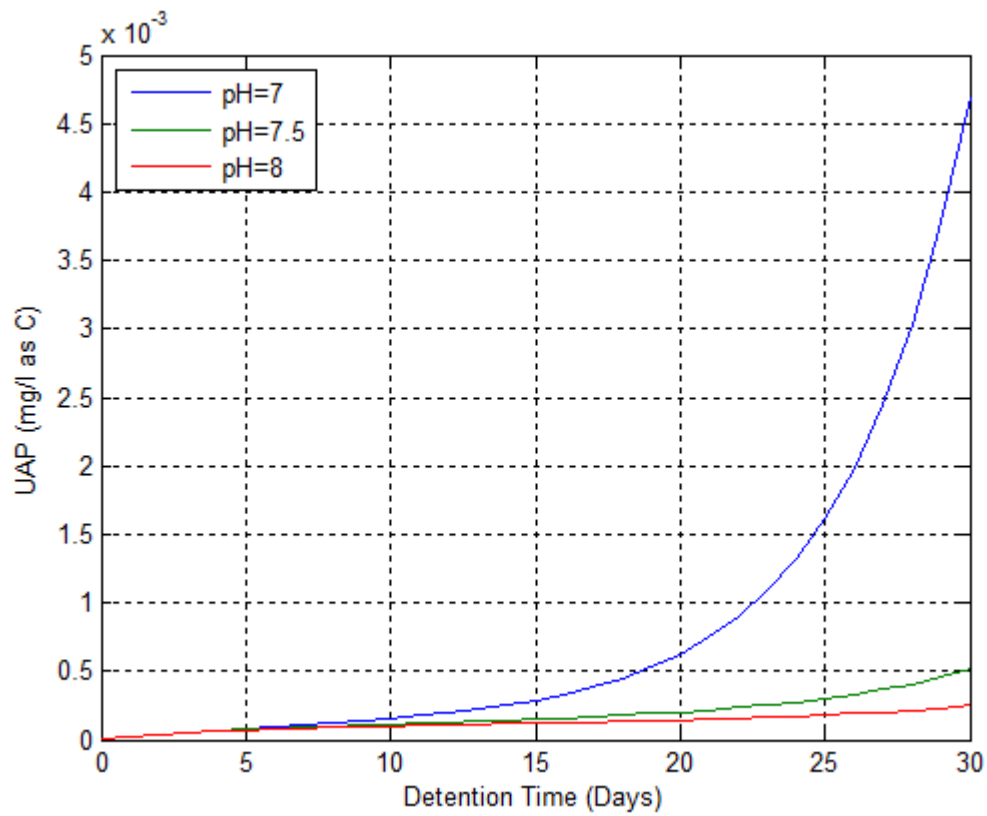


Figure 4-13: UAP concentration against time for varying pH values

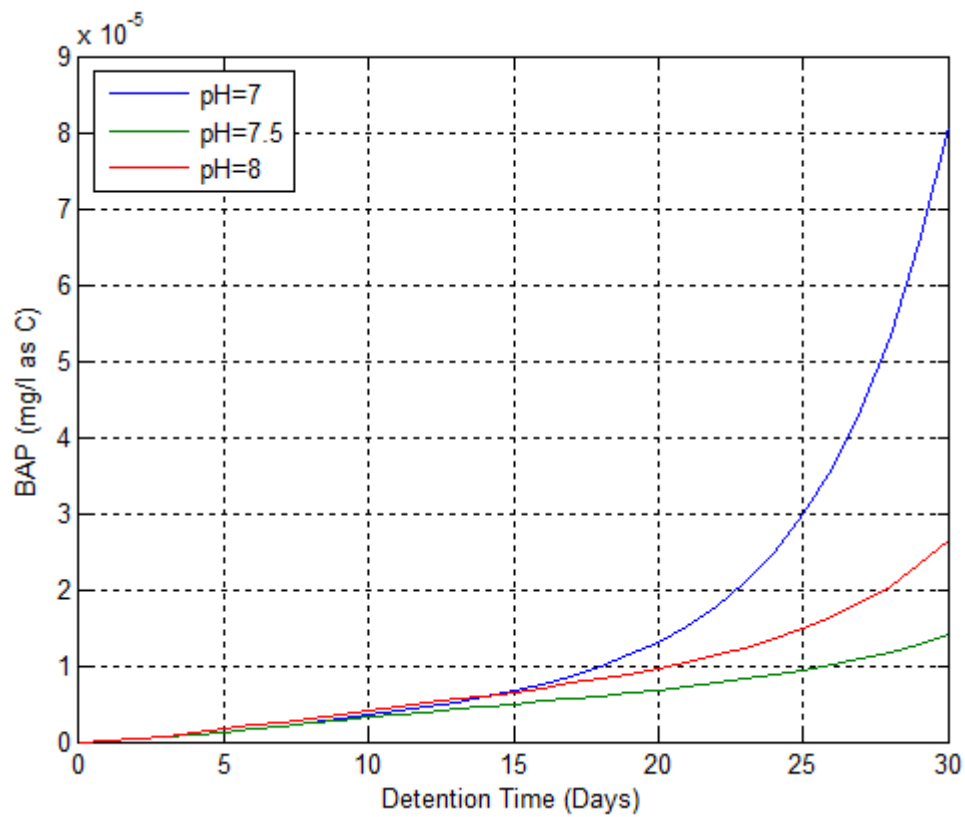


Figure 4-14: BAP concentration against time for varying pH values

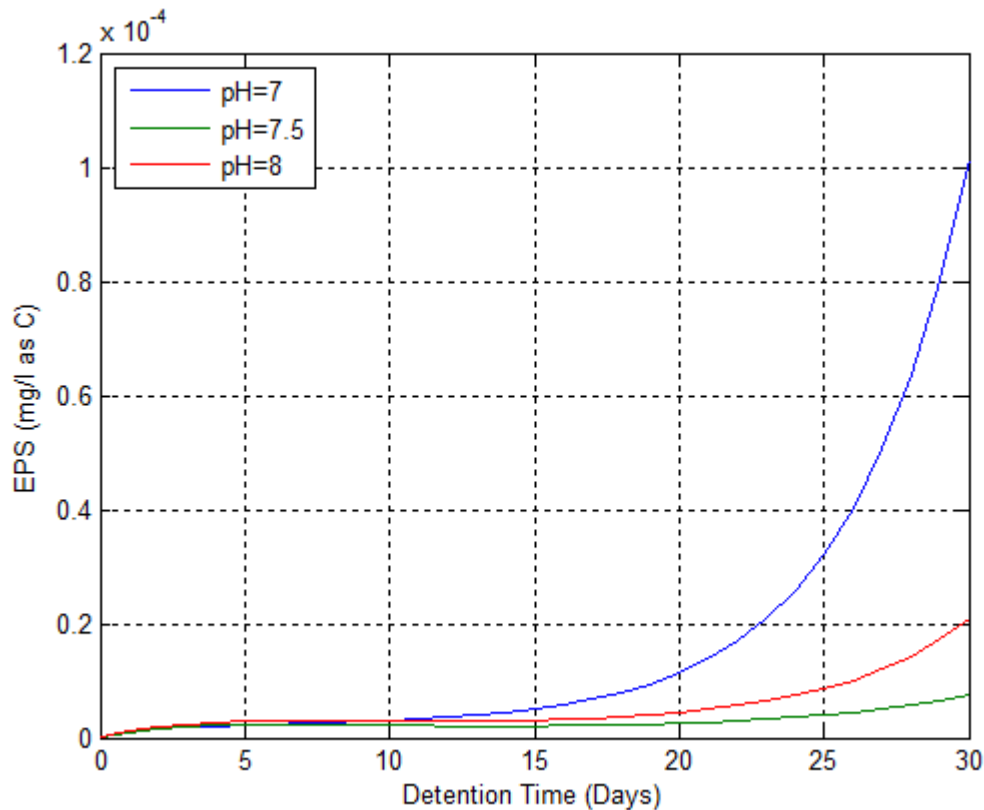


Figure 4-15: EPS concentration against time for varying pH values

The production of both SMP and EPS track the synthesis of active biomass. For this simulation it is interesting to note that marginally more EPS, and hence more BAP as it is produced from the hydrolysis of EPS, forms at a pH of 8.0 than at pH of 7.5. This is because:

- 1) Heterotroph concentration is only slightly greater at a pH of 7.5 and therefore EPS formed by heterotrophs is only slightly greater.
- 2) AOB concentration is slightly greater at a pH of 8.0 for the reasons explained previously, and therefore slightly more EPS is formed by AOB at this pH.
- 3) The concentration of NOB is much less than the concentration of AOB and heterotrophs and the NOB EPS formation rate constant ($k_{eps_{n2}}$) has the smallest value of all species of active biomass. Therefore, the concentration of EPS formed by NOB for this simulation is negligible.
- 4) The heterotroph EPS formation rate constant (k_{eps_n}) has a similar value to the AOB EPS formation rate constant ($k_{eps_{n1}}$) and this factor, in conjunction with the 3 previous points, results in EPS, and hence BAP, being slightly greater at a pH of 8.0 as opposed to 7.5 for this simulation.

The same does not, however, hold true for the UAP concentration, which increases with decreasing pH. This is because the heterotroph UAP formation rate constant (k_{uap_n}) is much greater than for

either species of nitrifying bacteria, and hence the concentration of UAP is largely determined by the heterotroph concentration, which increases with decreasing pH.

As the concentration of SMP is much lower than the concentration of BOM for this simulation, the utilisation of SMP by heterotrophs in this simulation has only a limited effect on heterotrophic growth. This effect is confirmed by an analysis of the stability factor. Neglecting the utilisation of SMP by heterotrophs has little effect on the stability factor.

4.2.2 Influence of Temperature on Water Quality

The simulated results that follow demonstrate the influence of temperature on water quality. For the three simulations, the temperature was varied between 15 and 25°C with a fixed pH of 7.5 and a carbonate concentration of 3.0 mM.

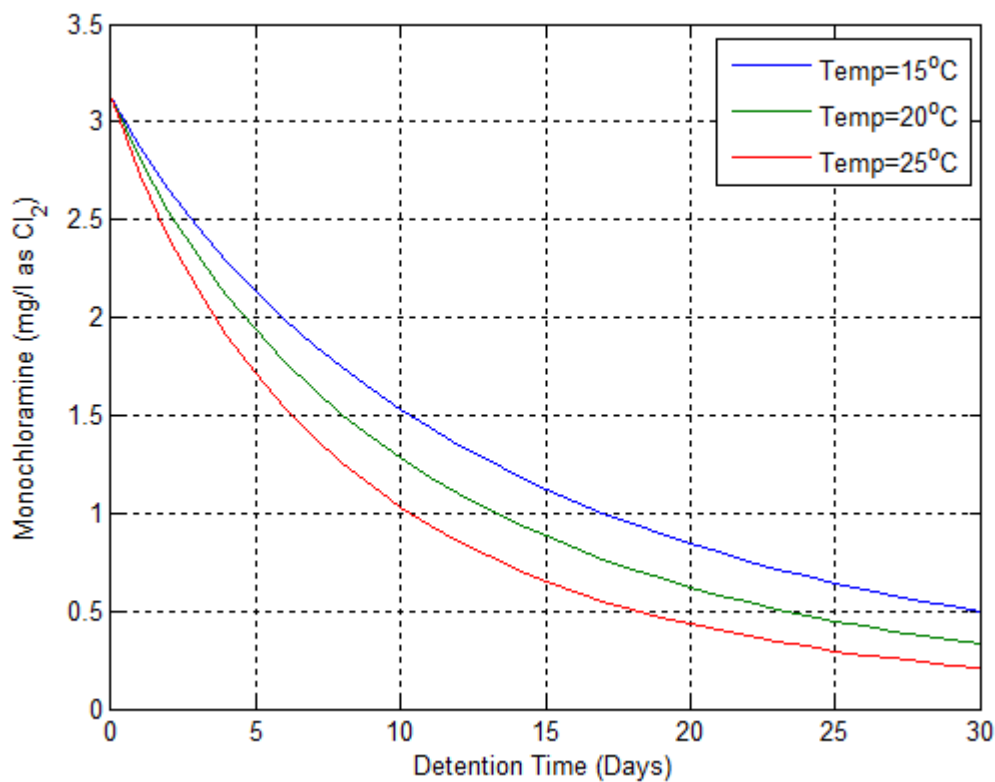


Figure 4-16: Monochloramine concentration against time for varying temperatures

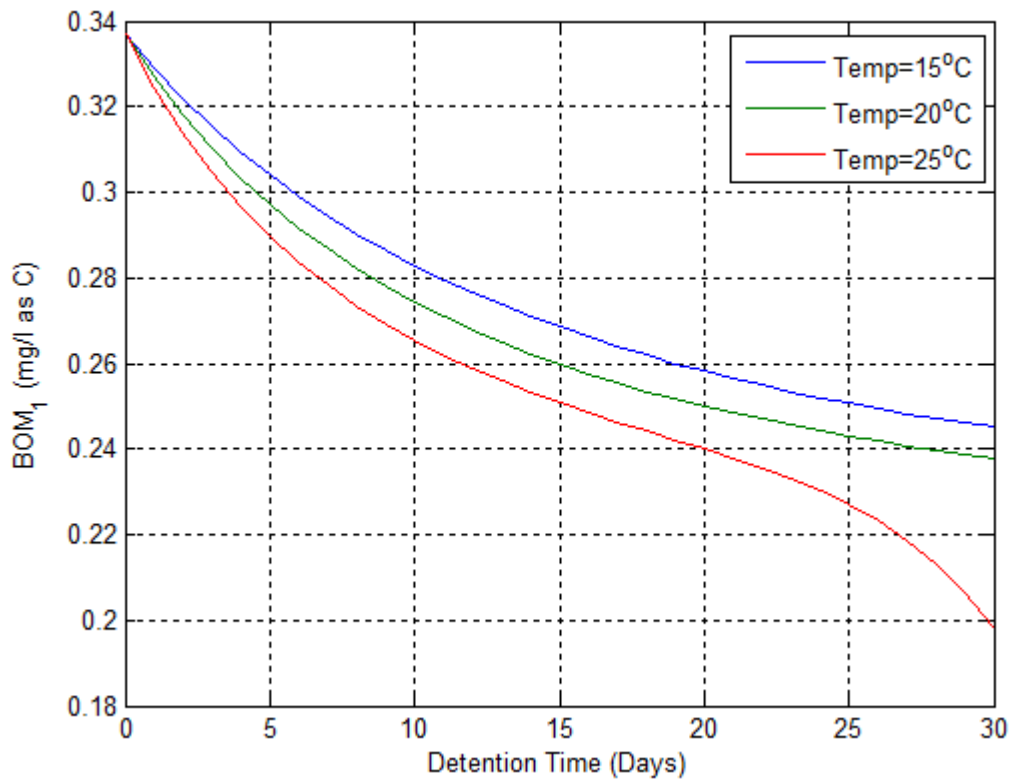


Figure 4-17: BOM₁ concentration against time for varying temperatures

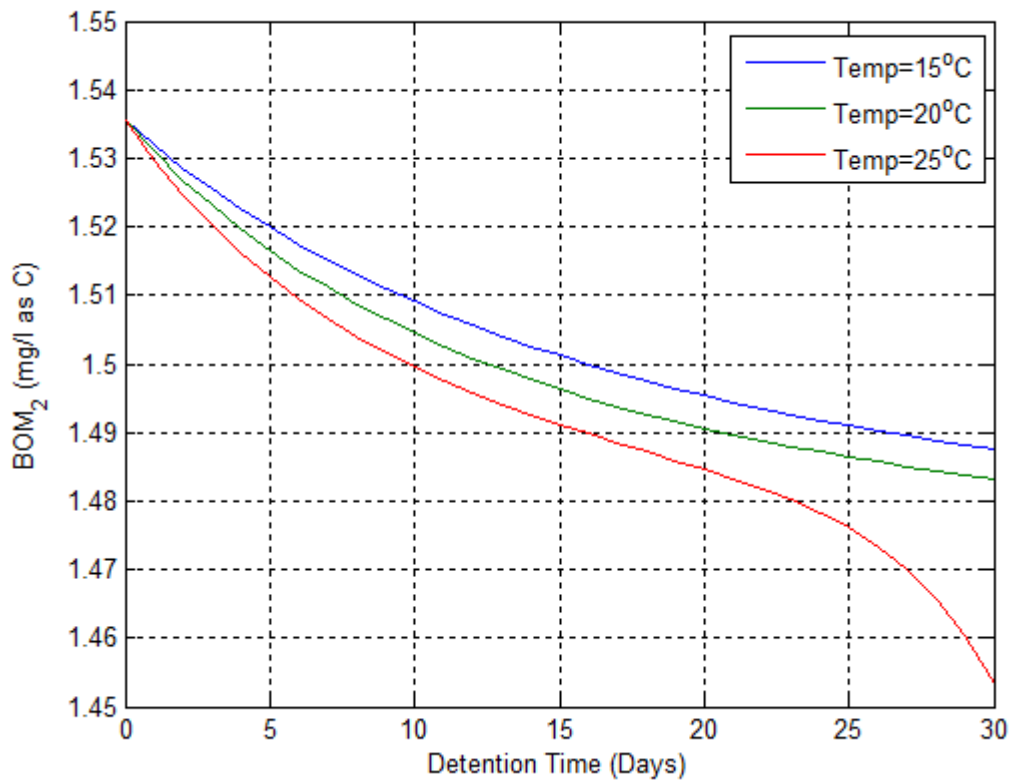


Figure 4-18: BOM₂ concentration against time for varying temperatures

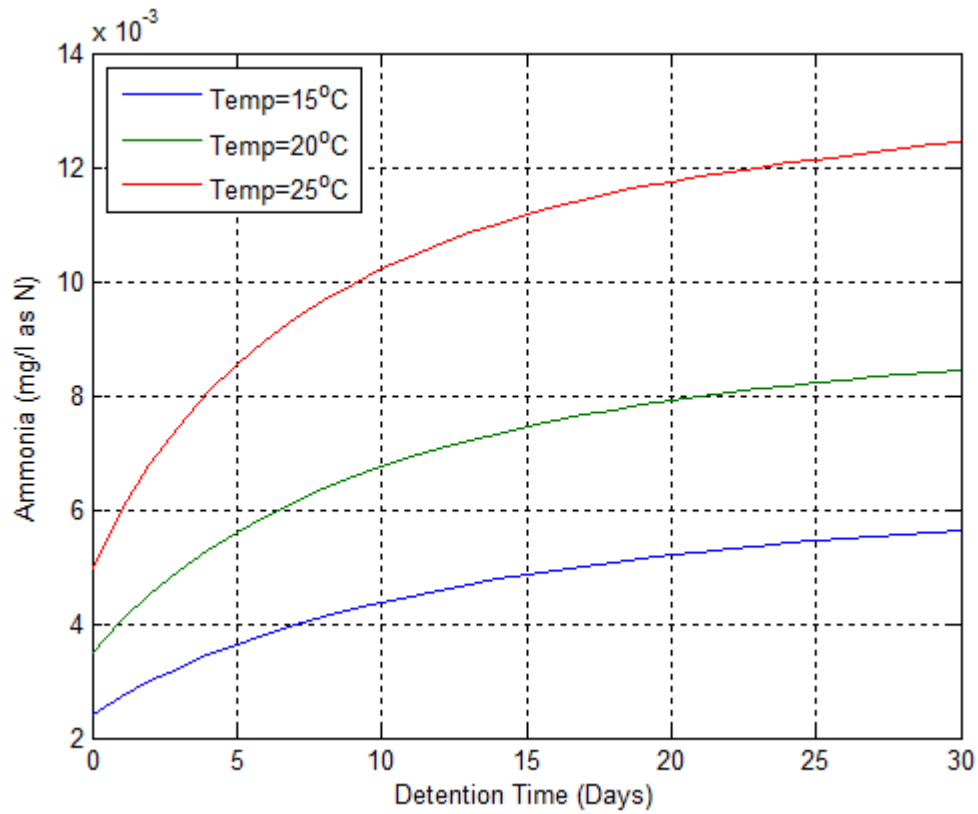


Figure 4-19: Ammonia concentration against time for varying temperatures

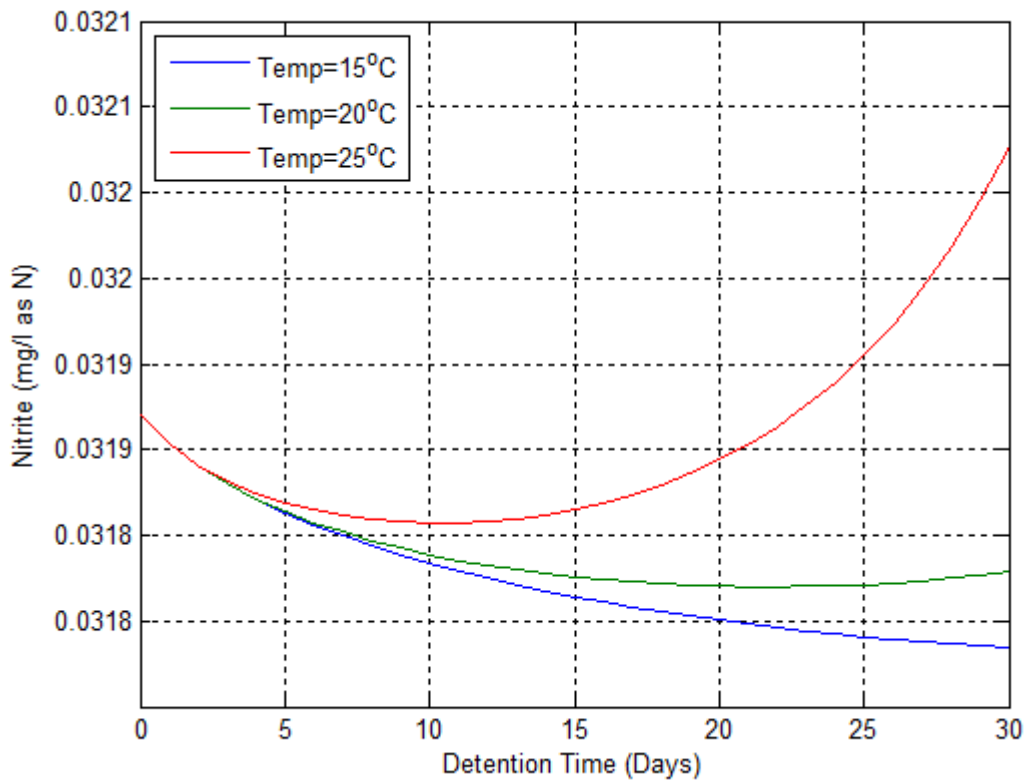


Figure 4-20: Nitrite concentration against time for varying temperatures

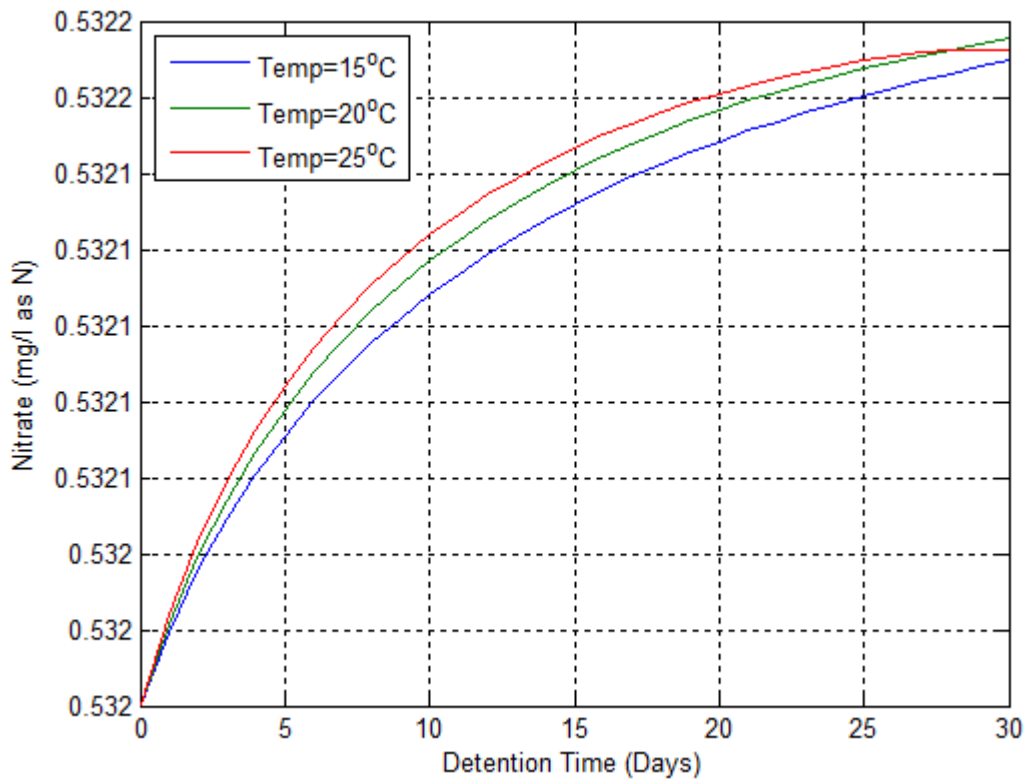


Figure 4-21: Nitrate concentration against time for varying temperatures

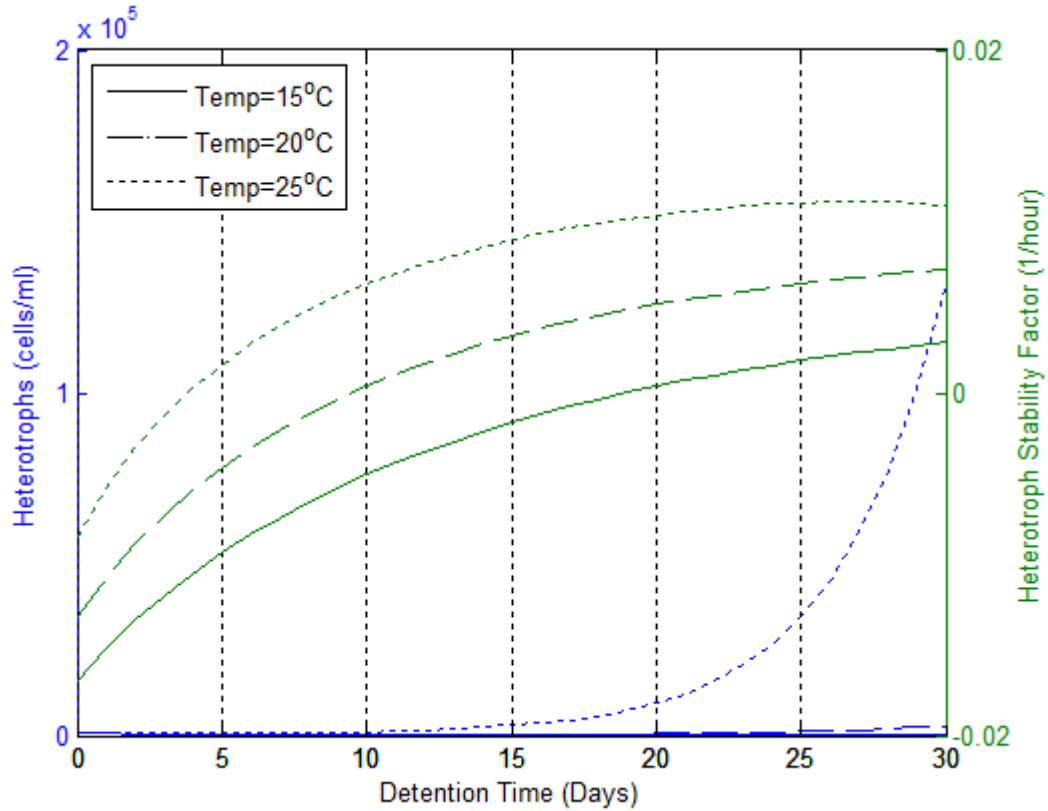


Figure 4-22: Suspended heterotroph concentration and stability factor against time for varying temperatures

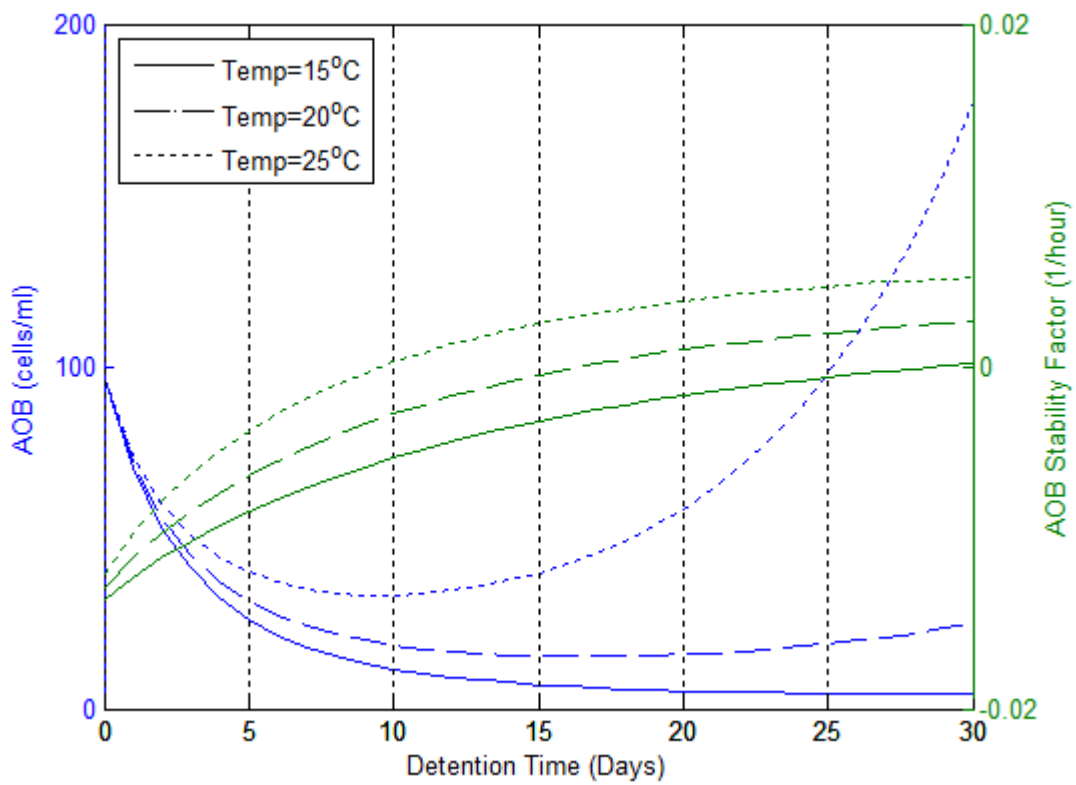


Figure 4-23: AOB concentration and stability factor against time for varying temperatures

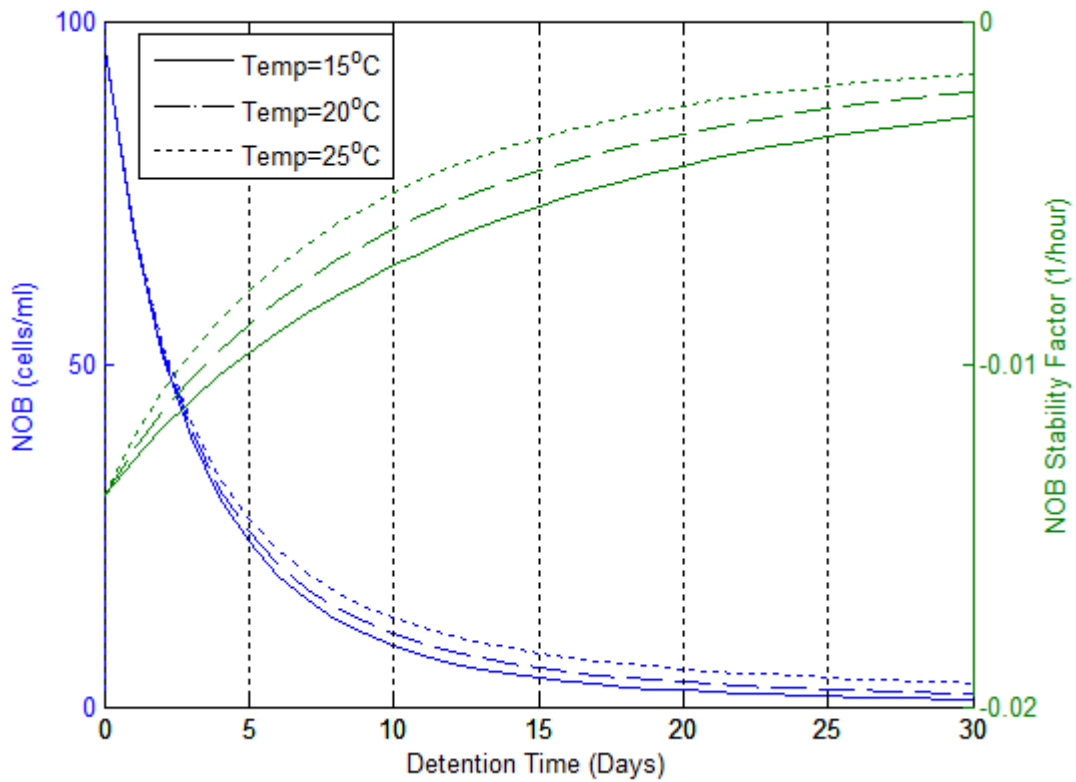


Figure 4-24: NOB concentration and stability factor against time for varying temperatures

As temperature increases, the stability factor for all species of bacteria increases, and hence net microbial growth increases. There are two reasons for this. Firstly, increasing temperature results in an increased rate of monochloramine decay, a finding also made by Vikesland, Ozekin & Valentine (2001), which increases the stability factor for all species of bacteria.

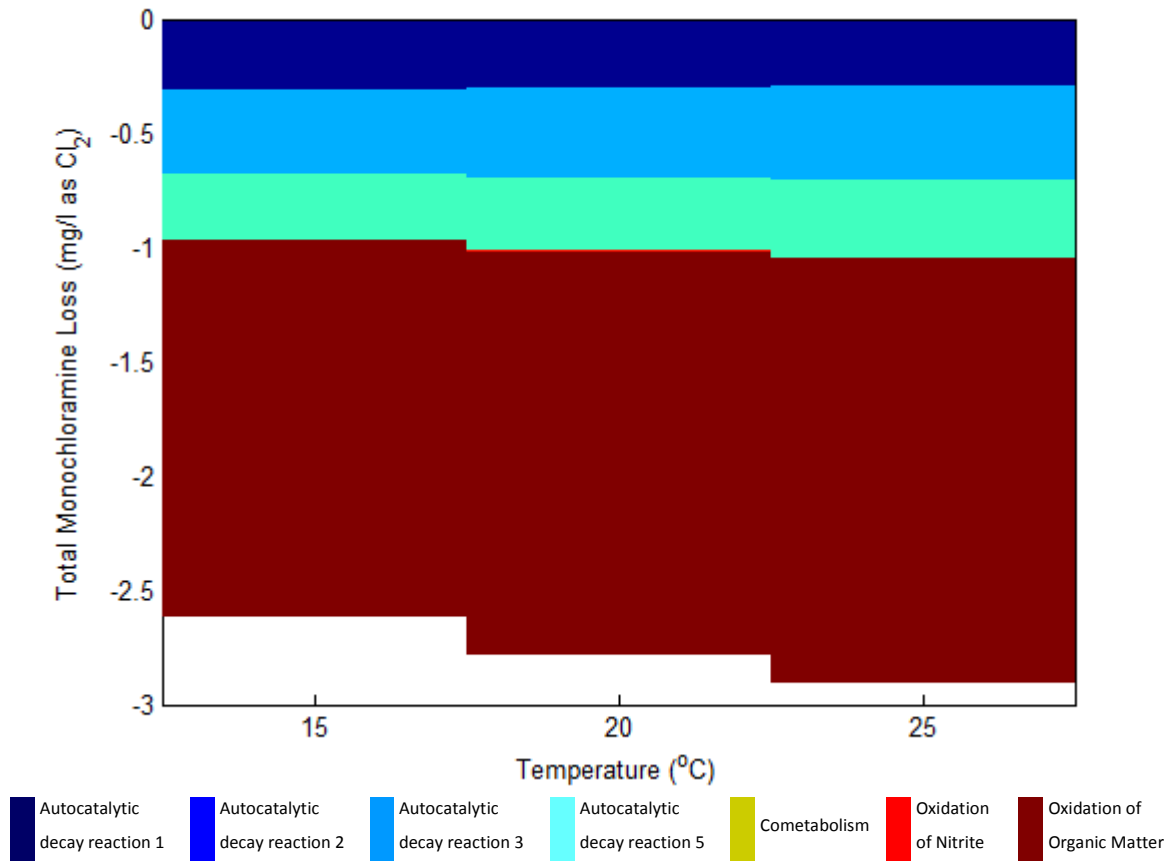


Figure 4-25: Relative contribution of monochloramine loss mechanisms for varying temperatures

Secondly, increased temperature also results in an increased substrate utilisation rate for heterotrophic bacteria, as shown in Figure 4-26 and Figure 4-27, a finding also made by Zhang & DiGiano (2002), thereby increasing the stability factor for heterotrophs. However, increasing temperature does not have a direct influence the substrate utilisation rates for nitrifying bacteria, as has been demonstrated by Wooschlager (2000). This is, however, not always the case, and if one were to deduce that the substrate utilisation rates for the specific nitrifying bacteria in a study area are directly influenced by temperature, the temperature adjustment factor for the nitrifying species can be altered accordingly. Indirectly, however, increasing temperature increases the stability factor for both nitrifying species. The increased decay of monochloramine at higher temperatures results in the production of more ammonia, which increases the utilisation rate of ammonia by AOB. The utilisation of ammonia in turn produces more nitrite, which increases the rate of nitrite utilisation by NOB.

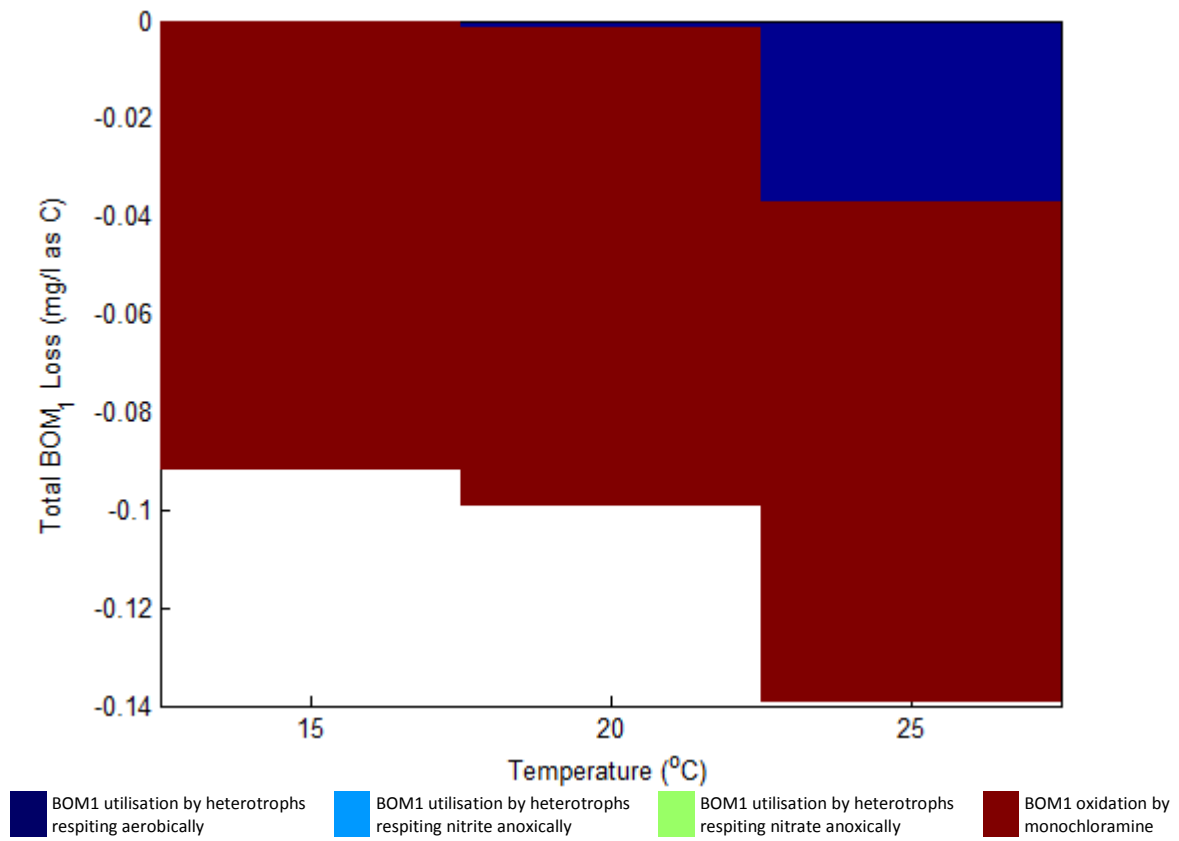


Figure 4-26: Relative contribution of BOM₁ loss mechanisms for varying temperatures

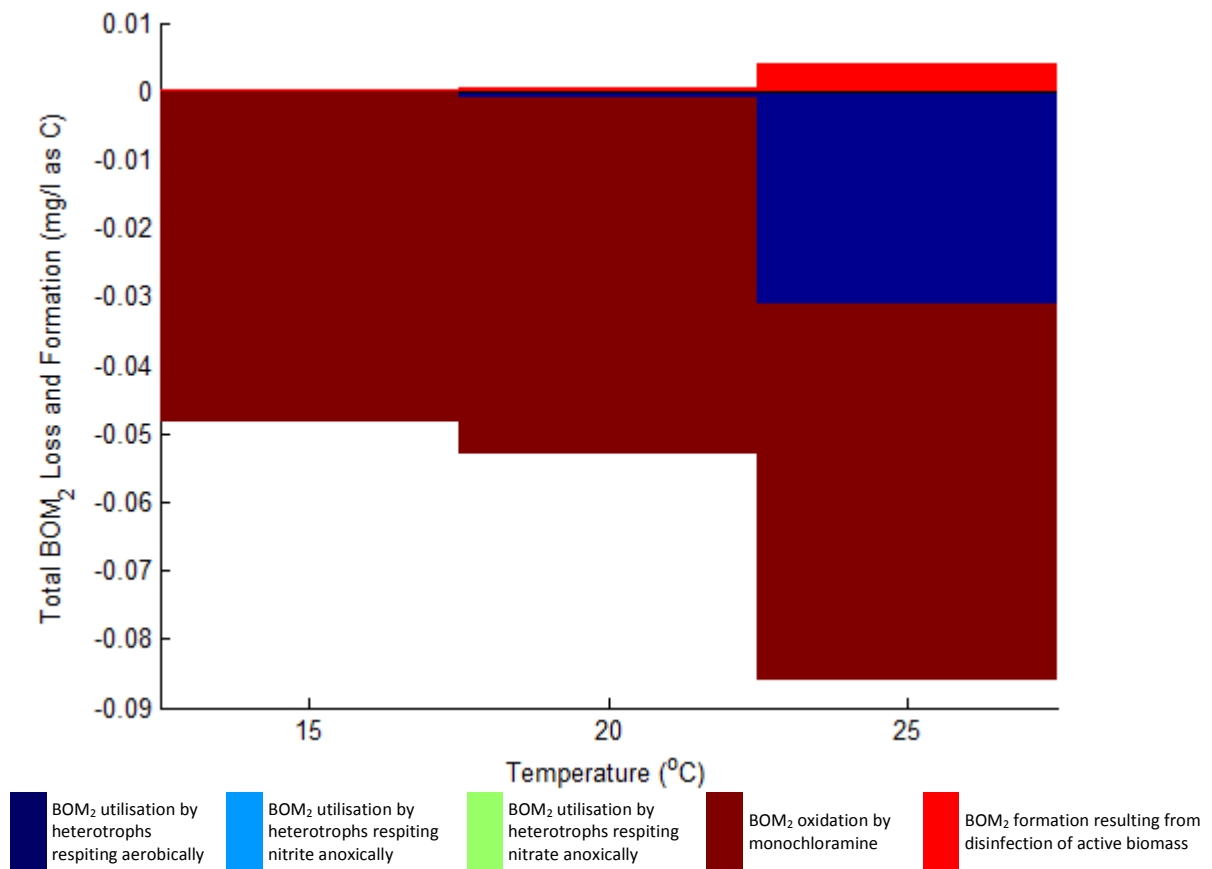


Figure 4-27: Relative contribution of BOM₂ loss and formation mechanisms for varying temperatures

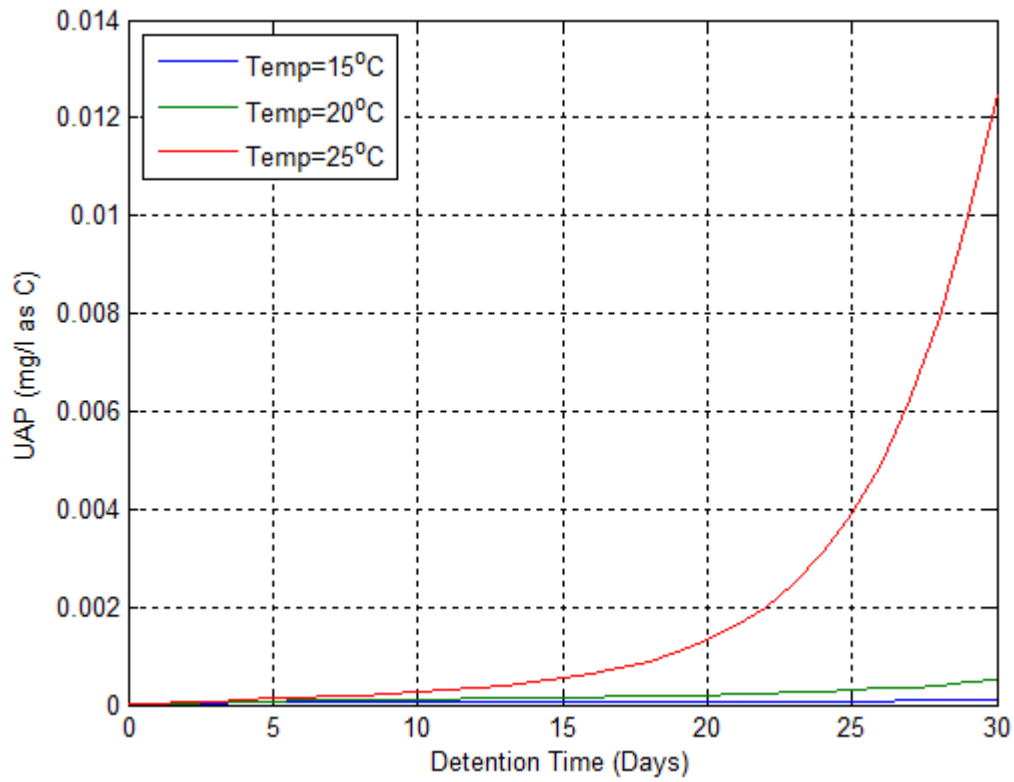


Figure 4-28: UAP concentration against time for varying temperatures

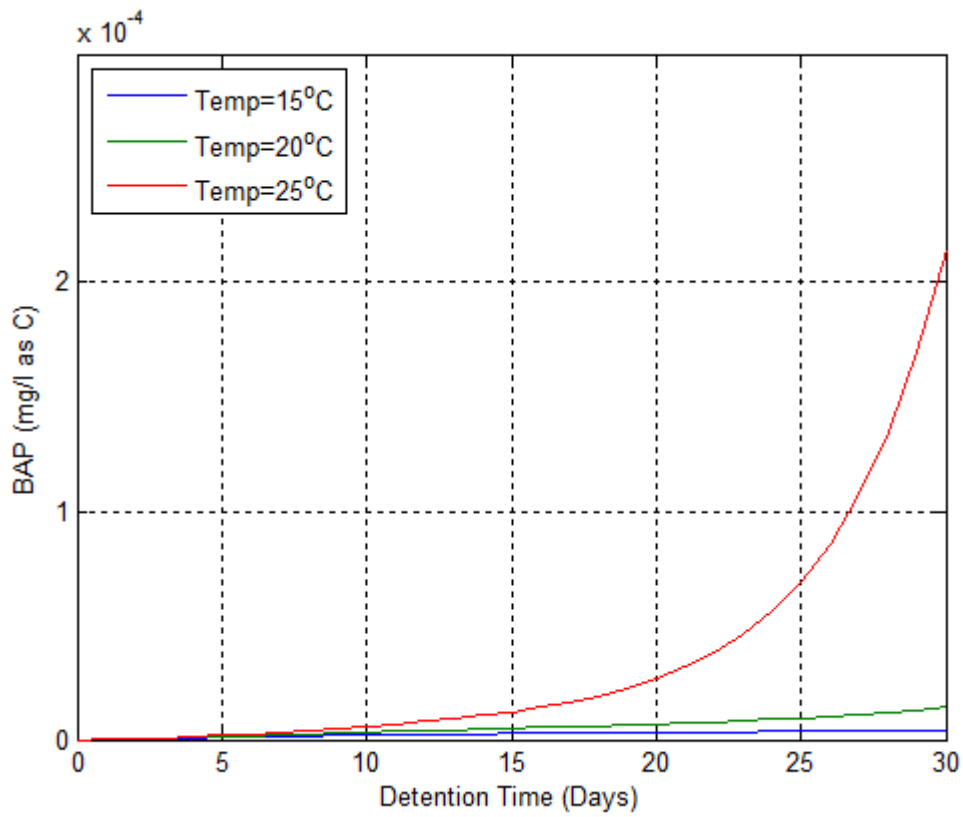


Figure 4-29: BAP concentration against time for varying temperatures

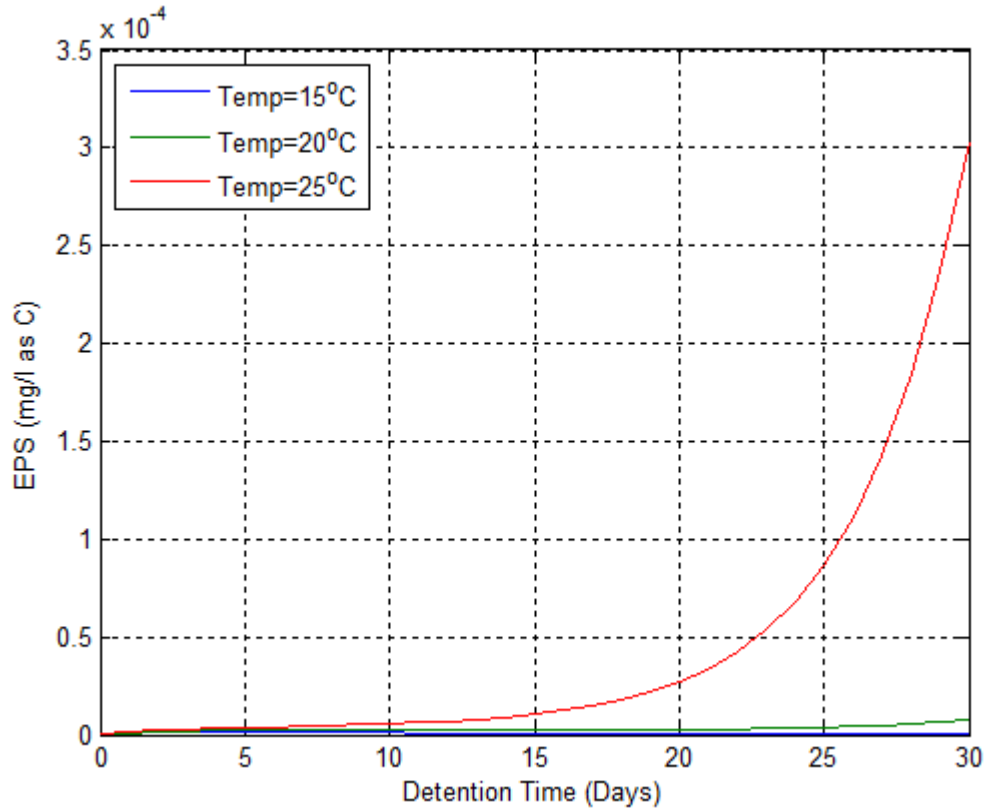


Figure 4-30: EPS concentration against time for varying temperatures

As the formation of all species of active biomass increases with increasing temperature, the production of SMP and EPS also increases with increasing temperature.

4.2.3 Influence of Carbonate Buffer on Water Quality

The simulated results that follow demonstrate the influence of carbonate concentration on monochloramine, and hence water quality. For the three simulations the concentration of the carbonate buffer was increased from 1.0mM to 5.0mM with a fixed pH of 7.5 and a temperature of 20°C.

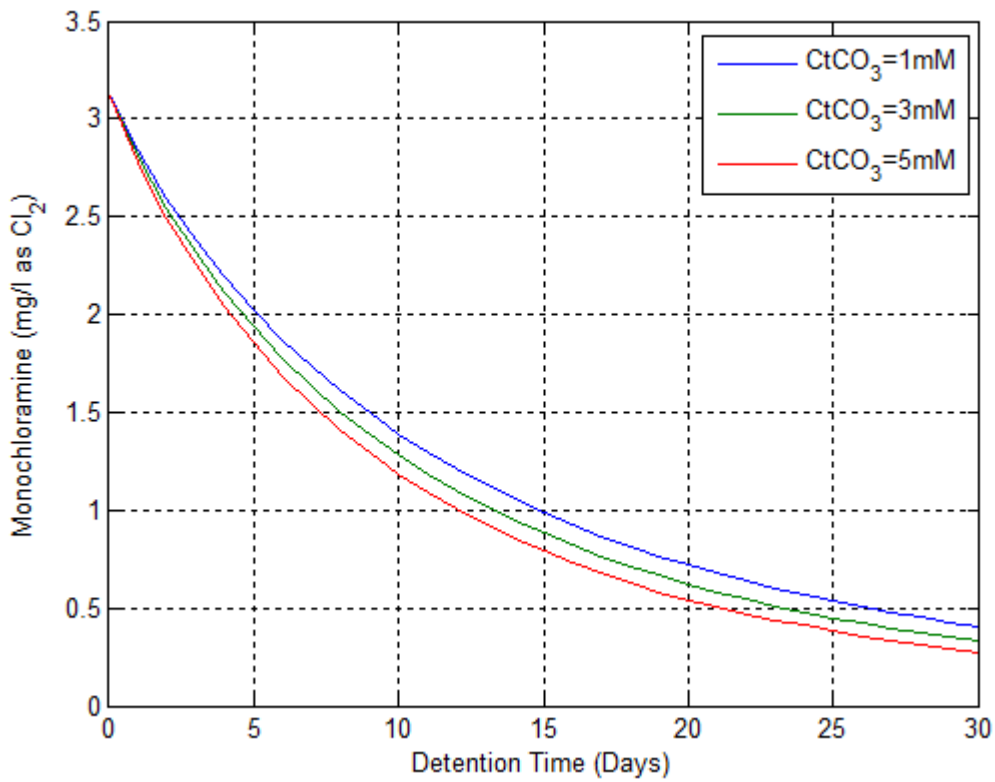


Figure 4-31: Monochloramine concentration against time for varying total carbonate concentrations

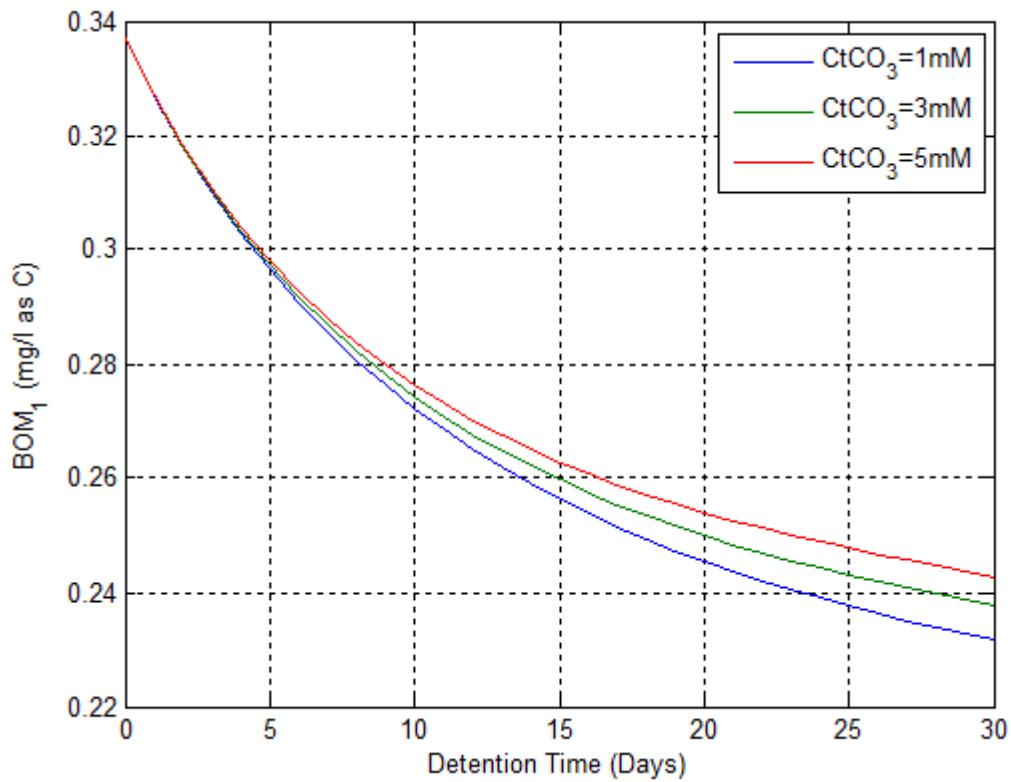


Figure 4-32: BOM₁ concentration against time for varying total carbonate concentrations

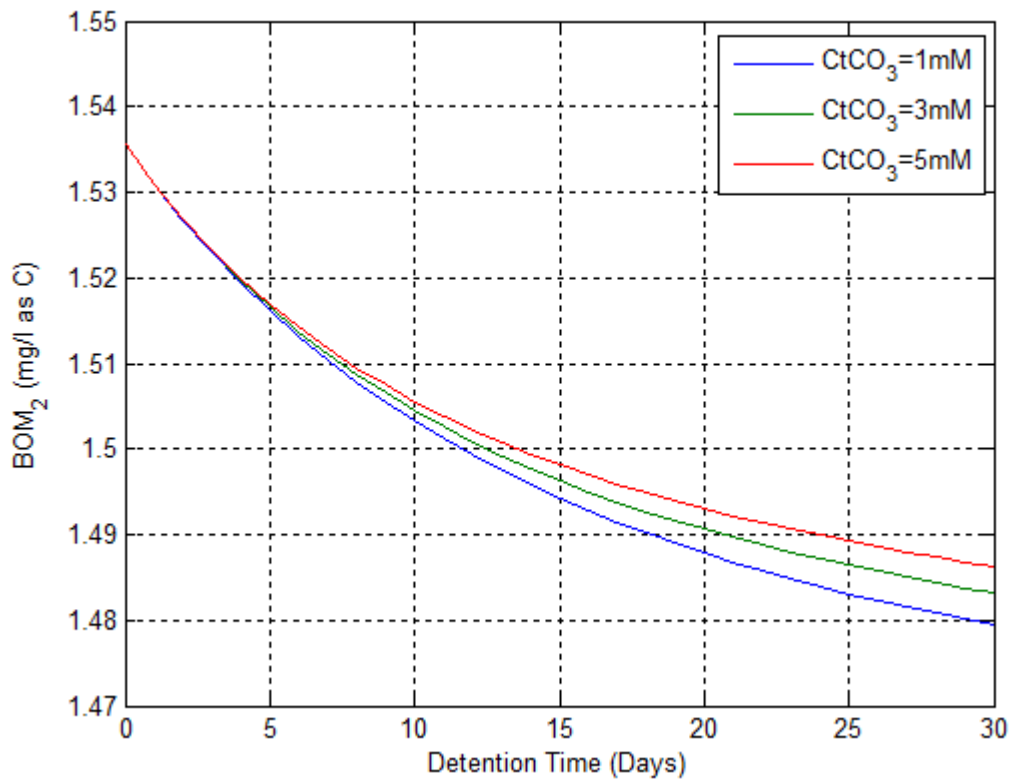


Figure 4-33: BOM₂ concentration against time for varying total carbonate concentrations

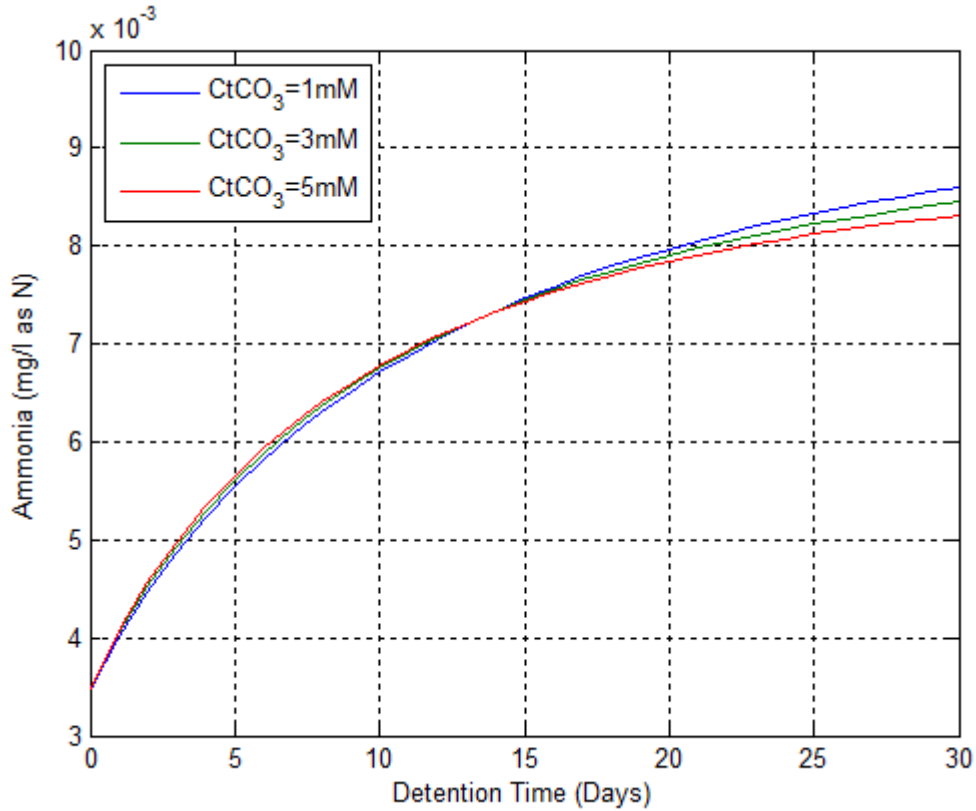


Figure 4-34: Ammonia concentration against time for varying total carbonate concentrations

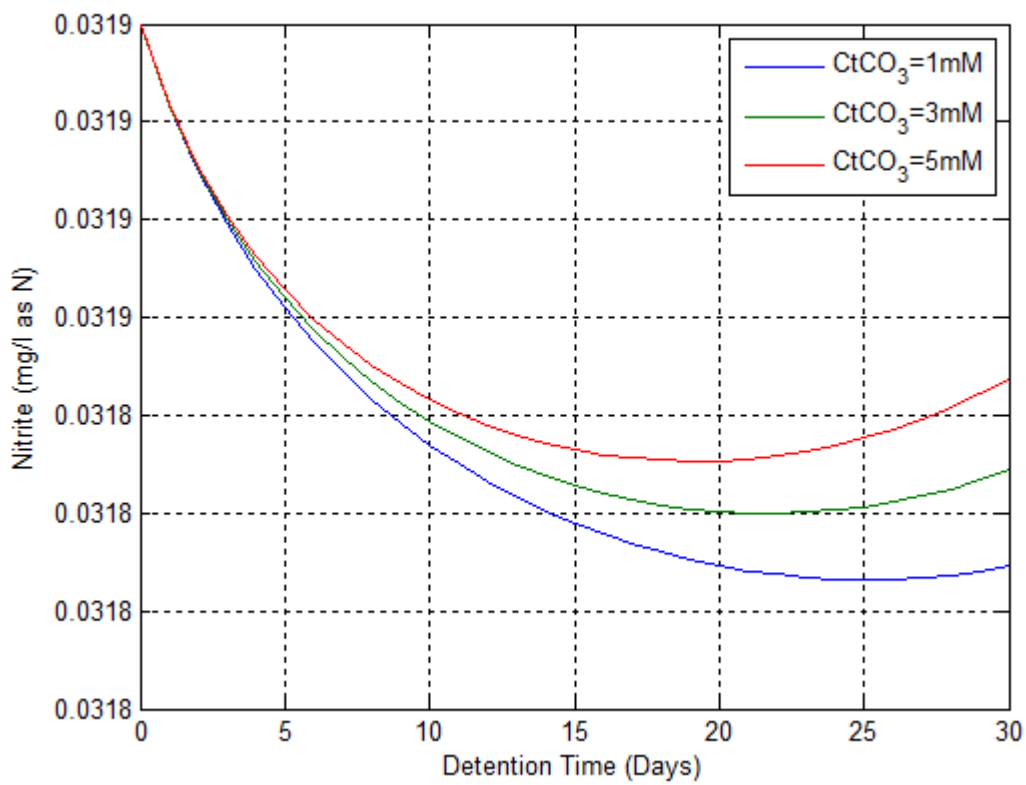


Figure 4-35: Nitrite concentration against time for varying total carbonate concentrations

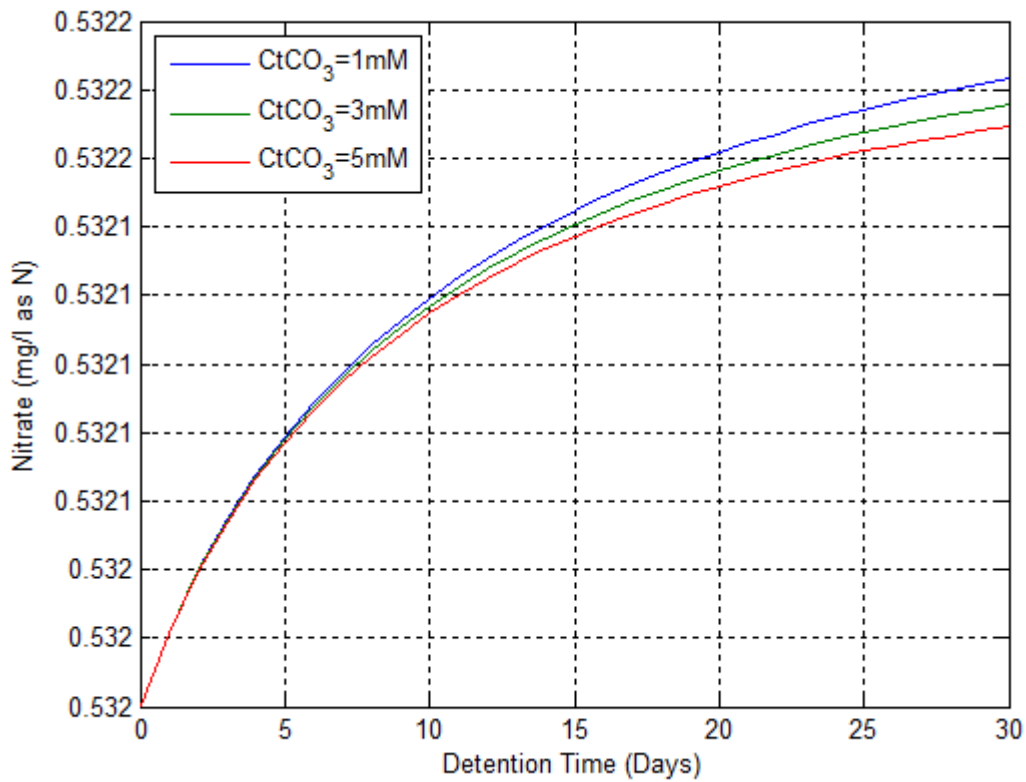


Figure 4-36: Nitrate concentration against time for varying total carbonate concentrations

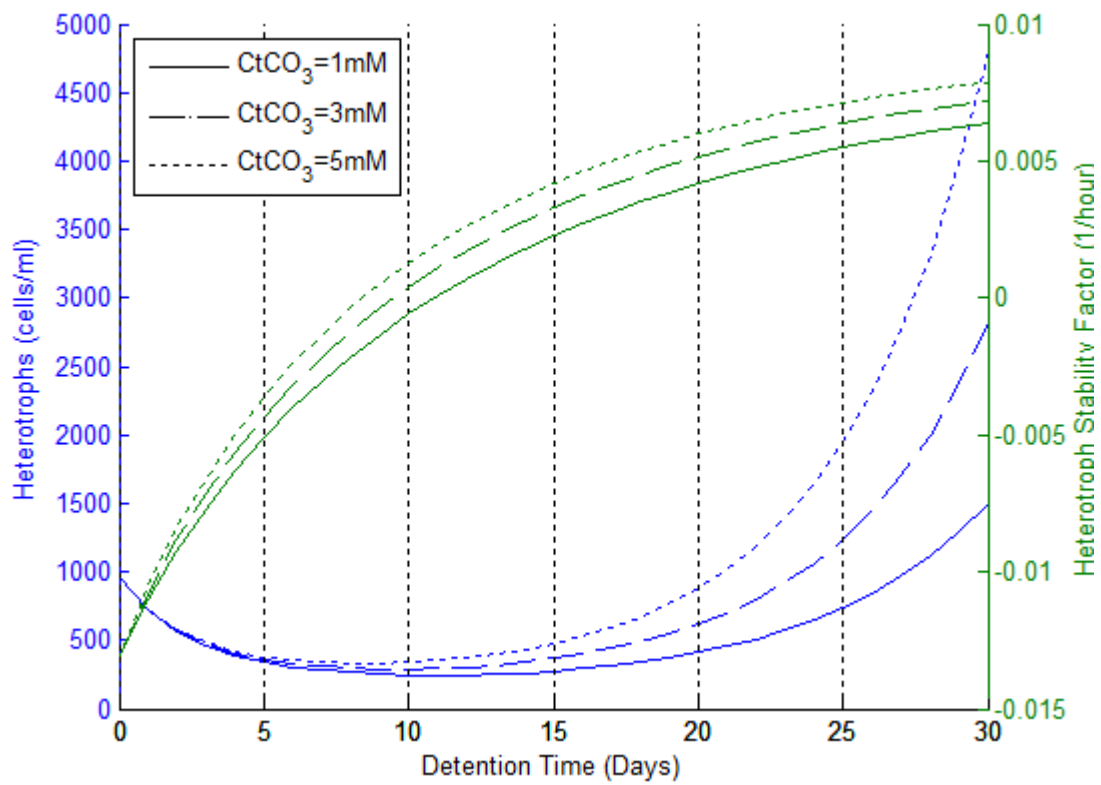


Figure 4-37: Suspended heterotroph concentration and stability factor against time for varying total carbonate concentrations

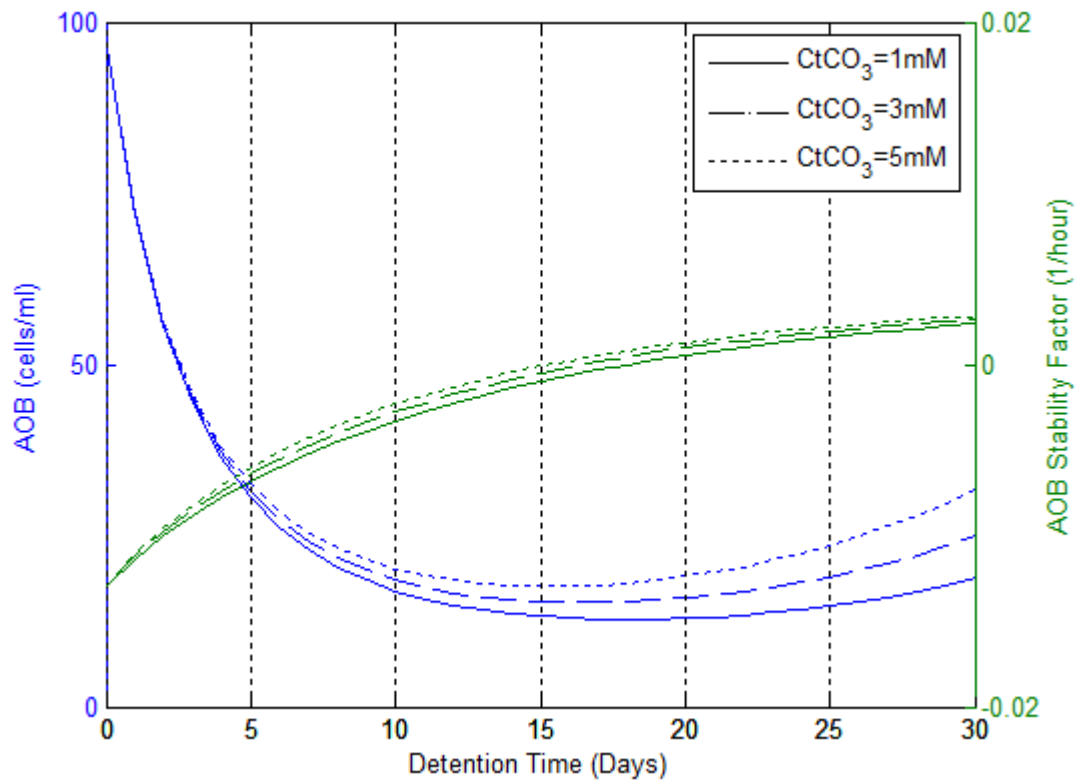


Figure 4-38: AOB concentration and stability factor against time for varying total carbonate concentrations

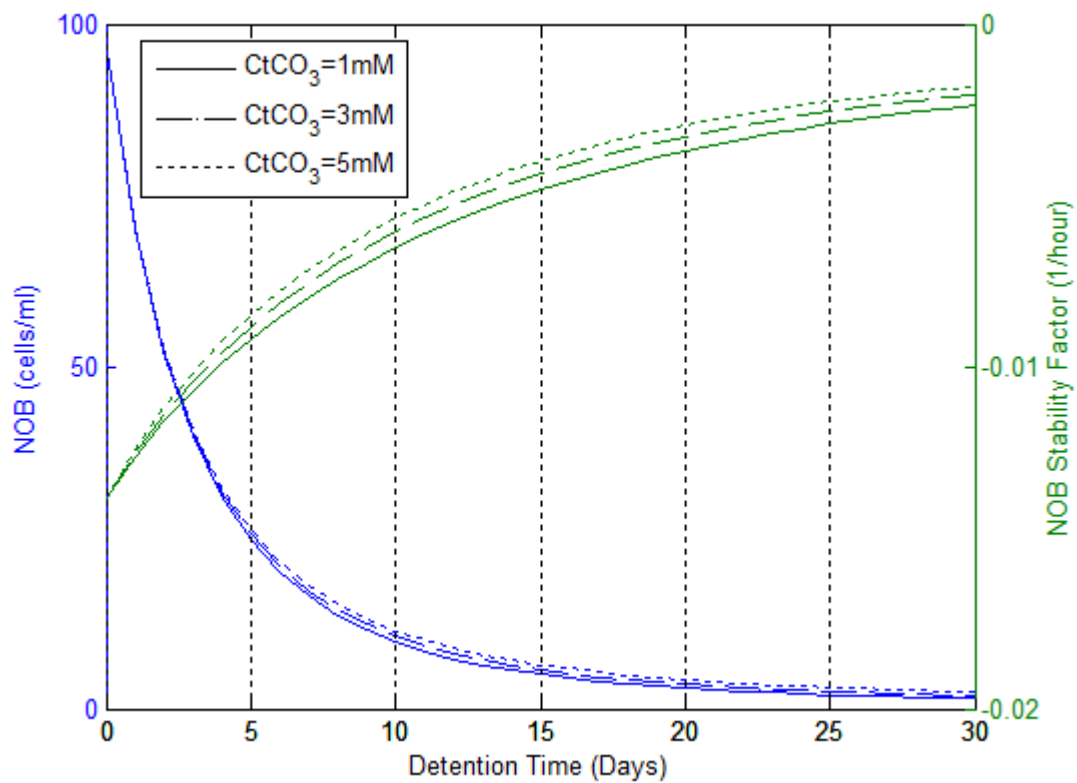


Figure 4-39: NOB concentration and stability factor against time for varying total carbonate concentrations

In accordance with research undertaken by Valentine and Jafvert (1988) and Vikesland, Ozekin and Valentine (2001), increasing the carbonate concentration increases the rate of monochloramine autocatalytic decomposition, as demonstrated in Figure 4-31, and hence the rate of microbial growth. This is because carbonate species have the potential to accelerate monochloramine decay by catalysing monochloramine disproportionation, as show in Figure 4-40. Therefore, for a given pH, an increase in carbonate concentration accelerates the rate of monochloramine loss (Vikesland, Ozekin & Valentine 2001).

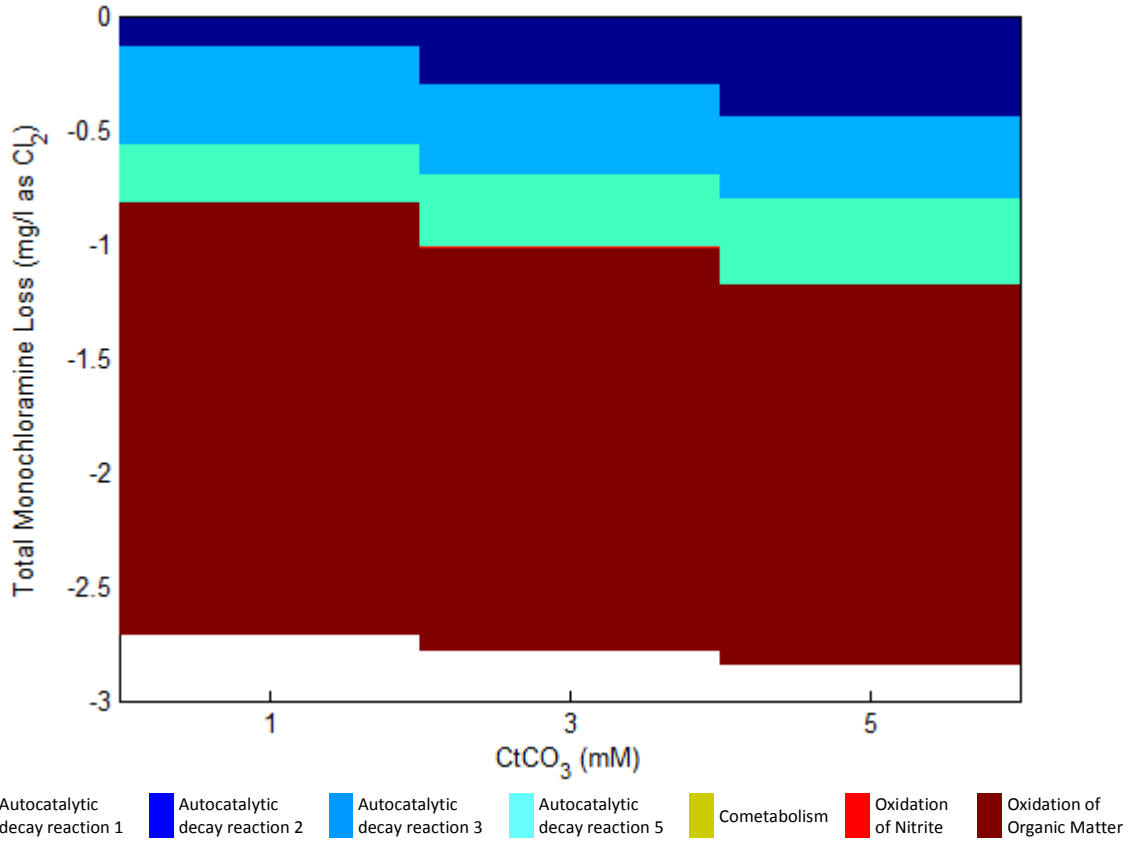


Figure 4-40: Relative contribution of monochloramine loss mechanisms for varying carbonate concentrations

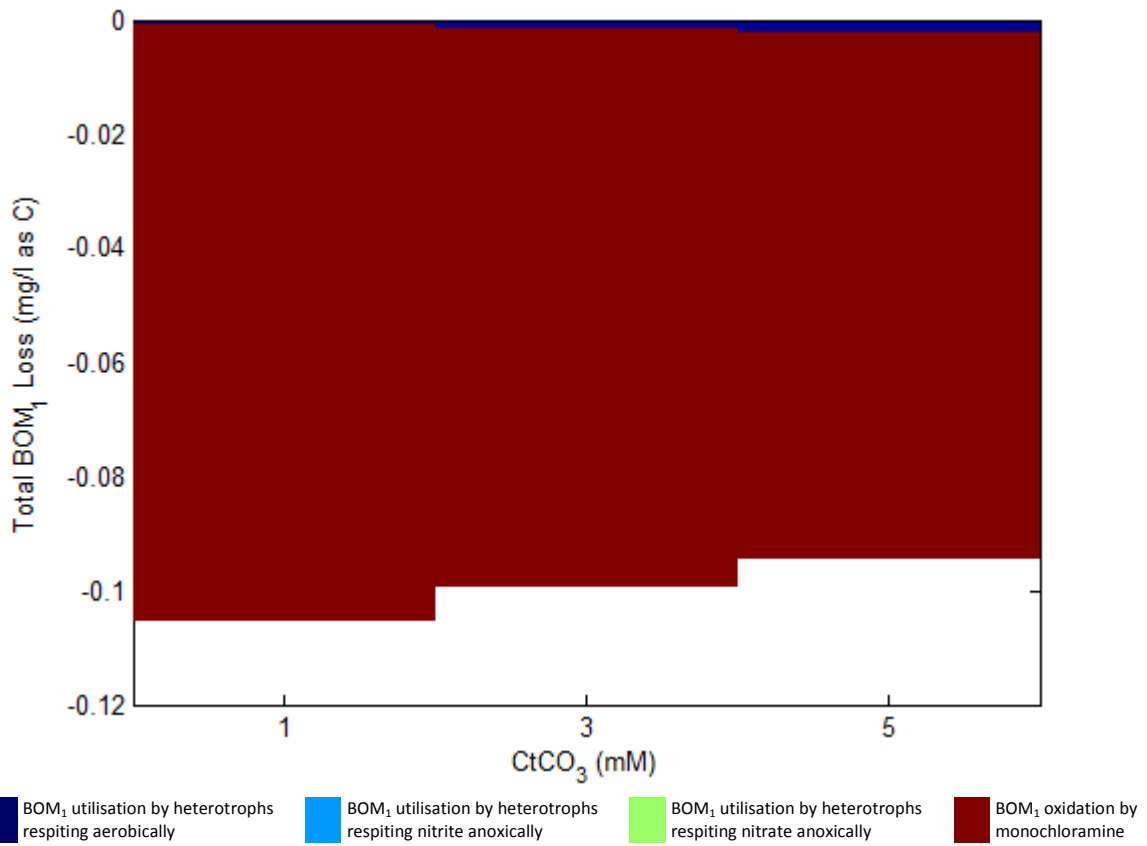


Figure 4-41: Relative contribution of BOM₁ loss mechanisms for varying carbonate concentrations

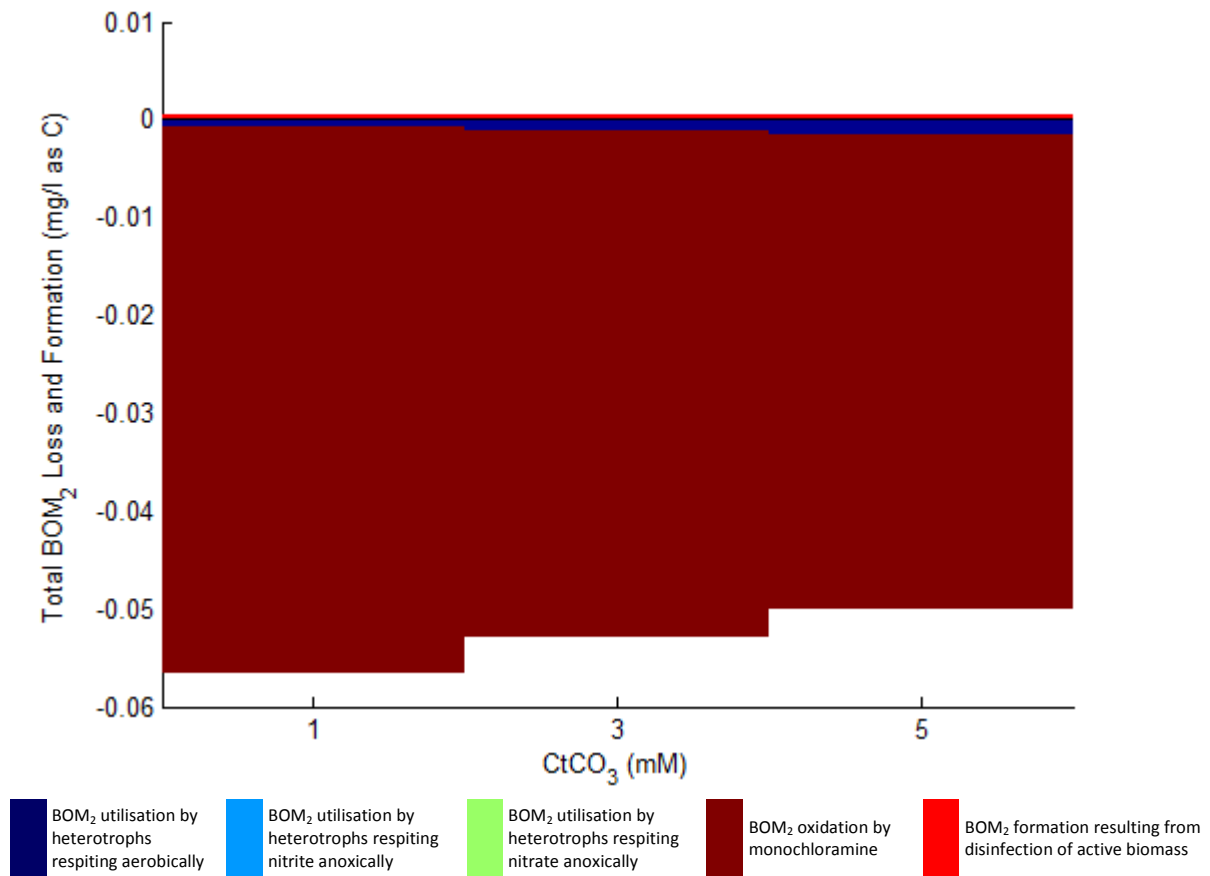


Figure 4-42: Relative contribution of BOM₂ loss and formation mechanisms for varying carbonate concentrations

Figure 4-41 and Figure 4-42 demonstrate that as heterotrophic growth is low for all three simulations, the loss of BOM due to its utilisation by heterotrophs is negligible and the loss of BOM can be almost entirely attributed to oxidation by monochloramine.

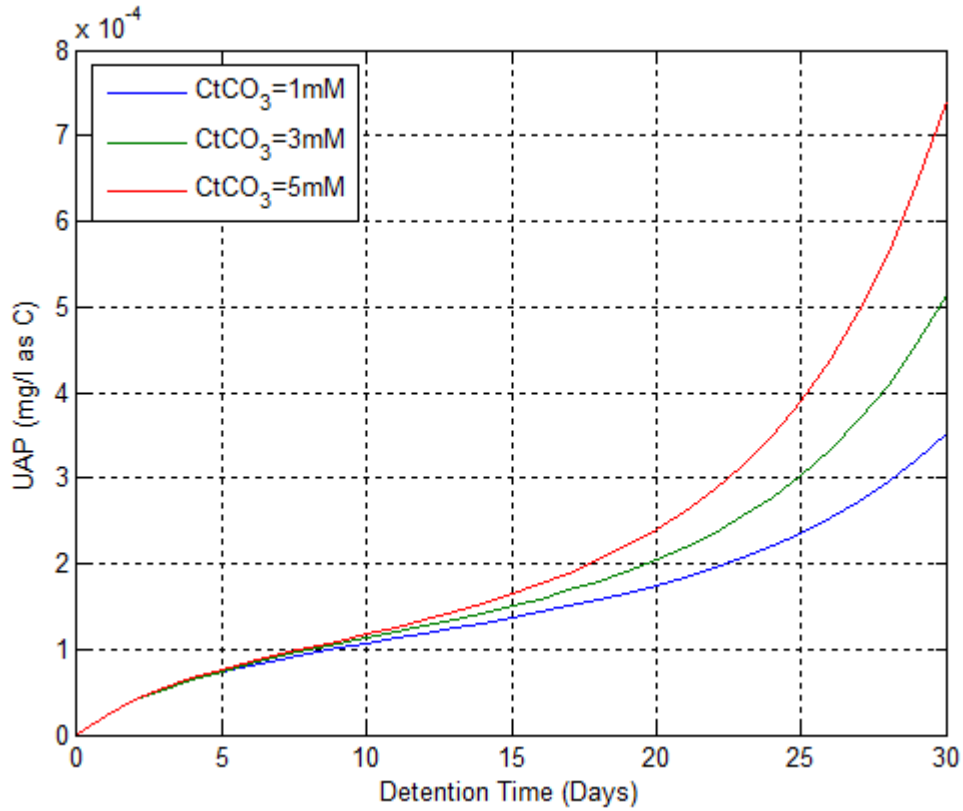


Figure 4-43: UAP concentration against time for varying total carbonate concentrations

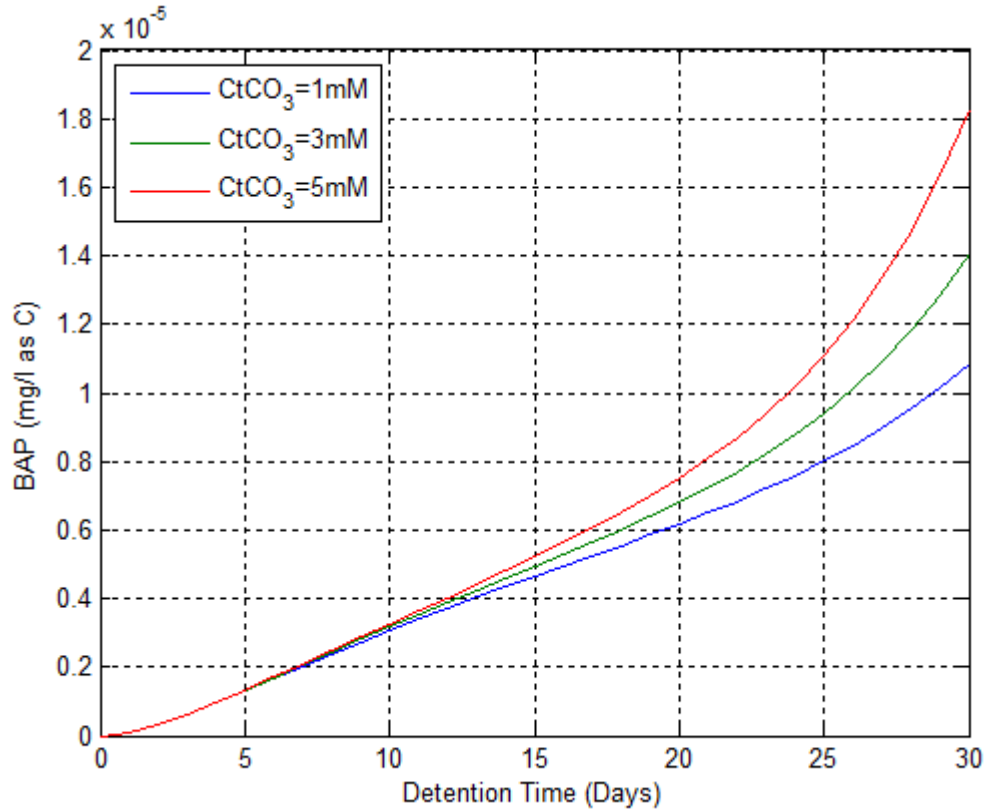


Figure 4-44: BAP concentration against time for varying total carbonate concentrations

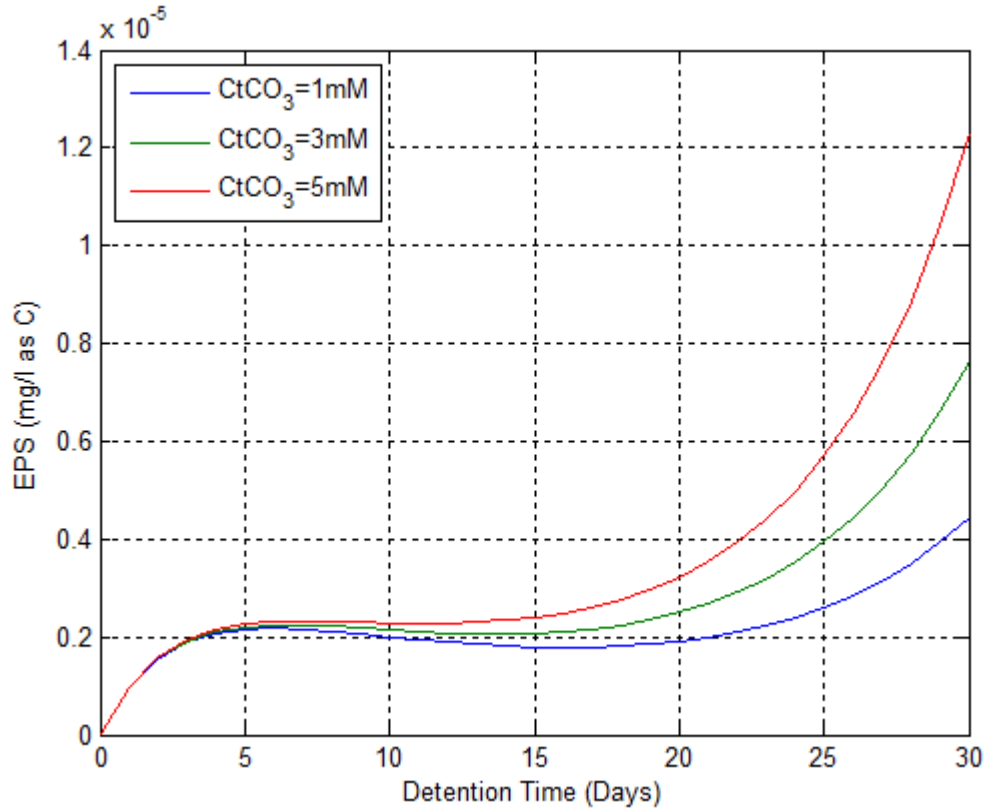


Figure 4-45: EPS concentration against time for varying total carbonate concentrations

As the concentrations of each of the three species of active biomass increase with increasing carbonate concentration, the concentrations of SMP and EPS also increase with increasing carbonate concentration.

4.2.4 Mass Closure Check

It is essential that the model does not violate the law of conservation of mass either as a result of numerical errors being introduced by too large a time step, incorrect equations, unit conversions or coding errors. For the simulations performed in section 4.2, a time step of three minutes was utilised and the following results were obtained for a pH of 7.5, a temperature of 20°C and a carbonate concentration of 0.3mM.

Chemical Element	Total Change Over 30 Days (%)
Cl	4×10^{-13}
N	1×10^{-13}
C	9×10^{-14}

Table 4-2: Mass-balance closure errors for batch simulation

The results in Table 4-2 demonstrate that the model is sound with regard to mass closure. The mass closure errors were similar and negligible for all simulations performed. A smaller time step is not required, as the solution does not diverge from that obtained using a considerably smaller time step. Given that the solution of the batch version is near-instantaneous using a three minute time step, there is no need to utilise a larger time step.

5 DISTRIBUTION SYSTEM SIMULATIONS

5.1 Introduction

As it was beyond the scope of this project to perform the range of water quality tests required to utilise the CDWQ-E₂ model to analyse a new distribution system, information provided by Wooschlager (2000) has been used to demonstrate the features of the E₂ version. The hydraulic data used to perform the simulations that follow were the same as that used by Wooschlager (2000) in his CDWQ simulations. However, the microbiological and chemical data used as inputs in the CDWQ model are not detailed in Wooschlager's work. Therefore, to ensure that the input concentrations used in the simulations that follow were realistic, they were formulated based on the experimental results of the CDWQ model detailed by Wooschlager. Consequently, no attempt can or has been made to compare the results of the CDWQ-E₂ model with the CDWQ model.

The simulated distribution system assessed consists of:

- 1 treatment plant
- 98 pipes with a total length of 62 kilometres
- 74 pipe junctions
- 1 reservoir

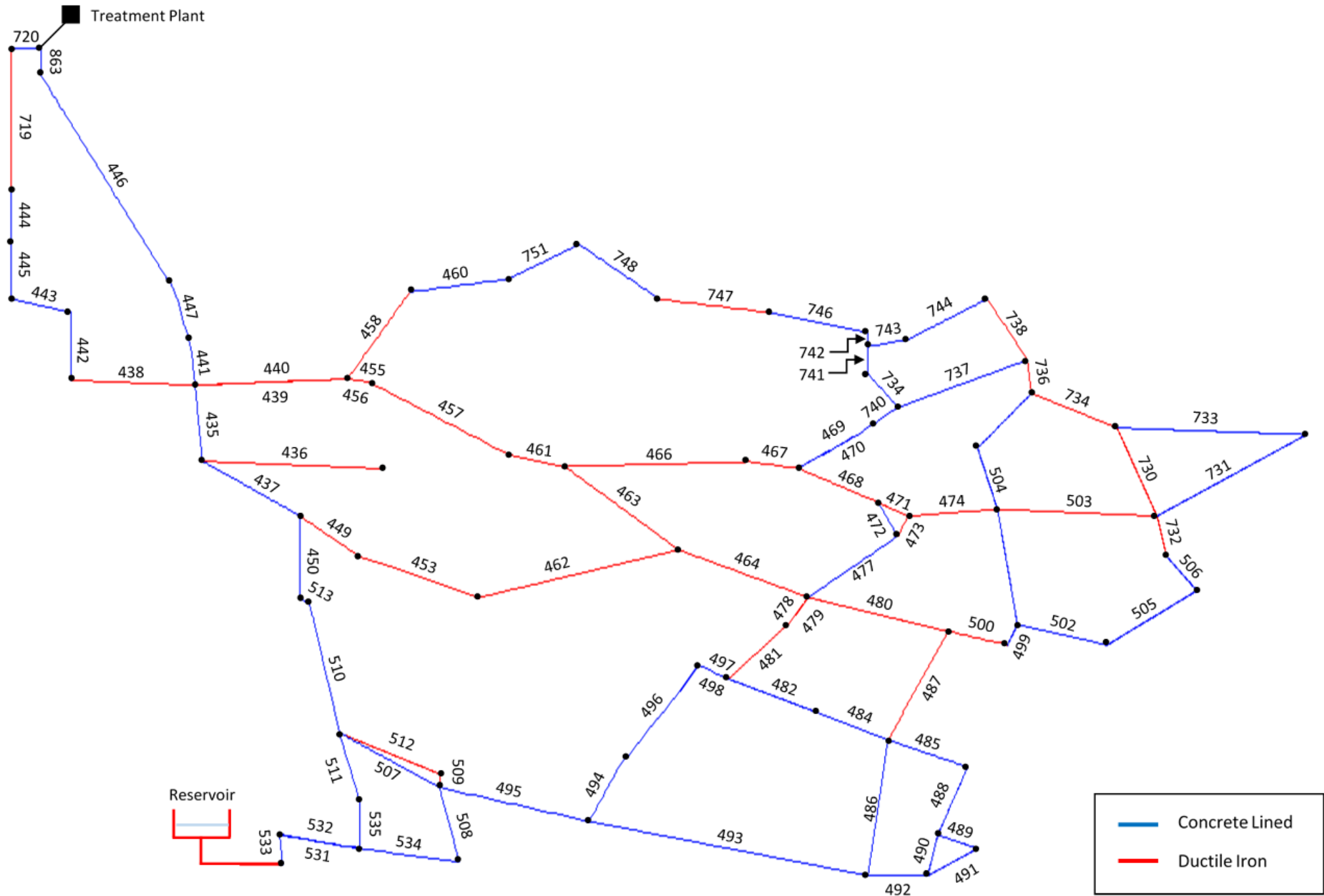


Figure 5-1: Schematic of distribution system detailing pipe numbers

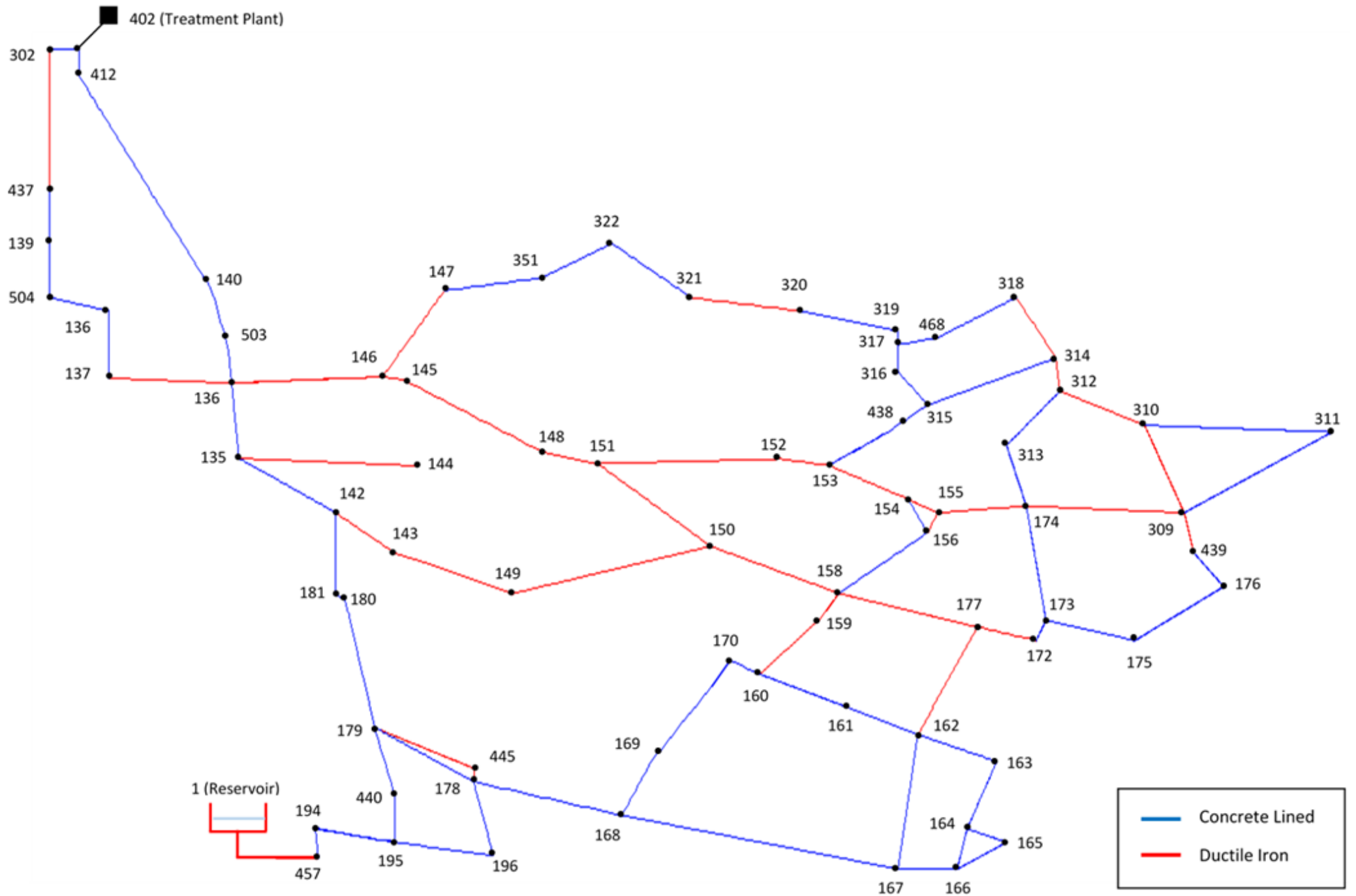


Figure 5-2: Schematic of distribution system detailing node numbers

The hydraulic model imported is a dynamic model with flow varying cyclically every hour over a 24-hour period. Therefore, in order to obtain the water quality solution, the simulations were run for the number of days required for the constituent concentrations to become stable and cyclical in line with the hydraulic pattern (Helbling & VanBriesen, 2009). As no field data was available with regards to reservoir mixing, a one-compartment model was used to model mixing within the reservoir.

The water quality of the distribution system is assessed and interpreted using the CDWQ-E₂ model. The initial conditions¹⁵ for the system are indicative of a system facing severe problems with regard to water quality. Throughout the system, the heterotrophic plate count is significantly greater than the threshold of 1000 CFU/ml stipulated by SANS 241-1:2011. Although the input heterotrophic concentrations are large, they are not unrealistic, as they are based on Wooschlager's (2000) monitoring results, and other researchers have reported similar values (Allen et al, 2004 in Francisque et al, 2009; Rizet et al, 1982; Maul et al, 1985; Prevost et al, 1991, 1998 in van der Kooij, 2003). Similarly, while there is no limit for biofilm bacteria concentrations in South Africa, the initial values are realistic as they are based on Wooschlager's (2000) monitoring results and are in accordance with the findings of various researchers (Donlan & Pipes, 1988; Levi et al, 1992; Mathieu et al, 1992; Pedersen, 1990 in Le Puil, 2004) that the counts of biofilm bacteria in distribution systems can range from 10⁶ to 10⁸ cells/ml. A significant number of pipes used in the simulations that follow have input biofilm concentrations with similar values to this upper limit and therefore it can be said that the initial input conditions represent a case with severe biofilm growth.

The simulation results are compared in Table 5-1 to the relevant parameter limits defined in SANS 241-1: 2011, which specifies the quality of acceptable drinking water in terms of microbial, physical, chemical and aesthetic determinands. Despite the fact that it is not a requirement to monitor all 25 different microbial and chemical species that are accounted for in the E₂ model, all of these parameters do have either a direct or indirect effect on the water quality determinands given in Table 5-1.

Determinand	Standard Limit
Heterotrophic Plate Count	$\leq 1000 \frac{CFU}{ml}$
Monochloramine	$\leq 3.0 \frac{mg}{l}$
Ammonia	$\leq 1.5 \frac{mg}{l}$ as N

¹⁵ Refer to Appendix C for initial node and pipe concentrations.

Nitrite	$\leq 0.9 \frac{mg}{l}$ as N
Nitrate	$\leq 11.0 \frac{mg}{l}$ as N

Table 5-1: Relevant SANS 241-1:2011 Water Quality Determinands

While specific compliance guidelines for the abovementioned determinands are provided in SANS 241-2: 2011, these guidelines are provided for monitoring purposes. For the modelled results, a target of 100% compliance with SANS 241-1:2011 limits for every determinand throughout the distribution system is used.

In order to convert the suspended heterotrophic bacteria concentration from $\frac{\mu g COD}{l}$ to colony forming units per millilitre (CFU/ml), a ratio of 4.3 respireable cells to CFU/ml is applied. This selected ratio is based on the experimental results of Wooschlager (2000) and while the ratio varies for different distribution systems, it is used for the simulations that follow, given the absence of available experimental data. The factor used to first convert $\frac{\mu g COD}{l}$ to respireable cells per millilitre is given in Appendix A.3.

SANS 241-1: 2011 does not specifically set limits for nitrifying bacteria. However, limits are set on both the concentration of nitrite and nitrate, which are products of nitrifier growth, and hence modelling the growth of nitrifying bacteria is essential. Furthermore, no limit is set in South Africa with regard to biofilm growth. Despite this, modelling biofilm growth is crucial, as biofilm bacteria greatly influence the concentrations of the aforementioned determinands. In particular, the detachment of heterotrophic biofilm bacteria contributes significantly to the concentration of suspended heterotrophs.

The interpretive capabilities of the model are demonstrated by using the results of the initial simulation to test various alternatives to improve the water quality of the distribution system. The results of these alternatives are presented and their effectiveness assessed.¹⁶

¹⁶ The distribution system version of the code and simulation outputs are provided on an accompanying CD.

5.2 Results and Discussion

5.2.1 Baseline Scenario

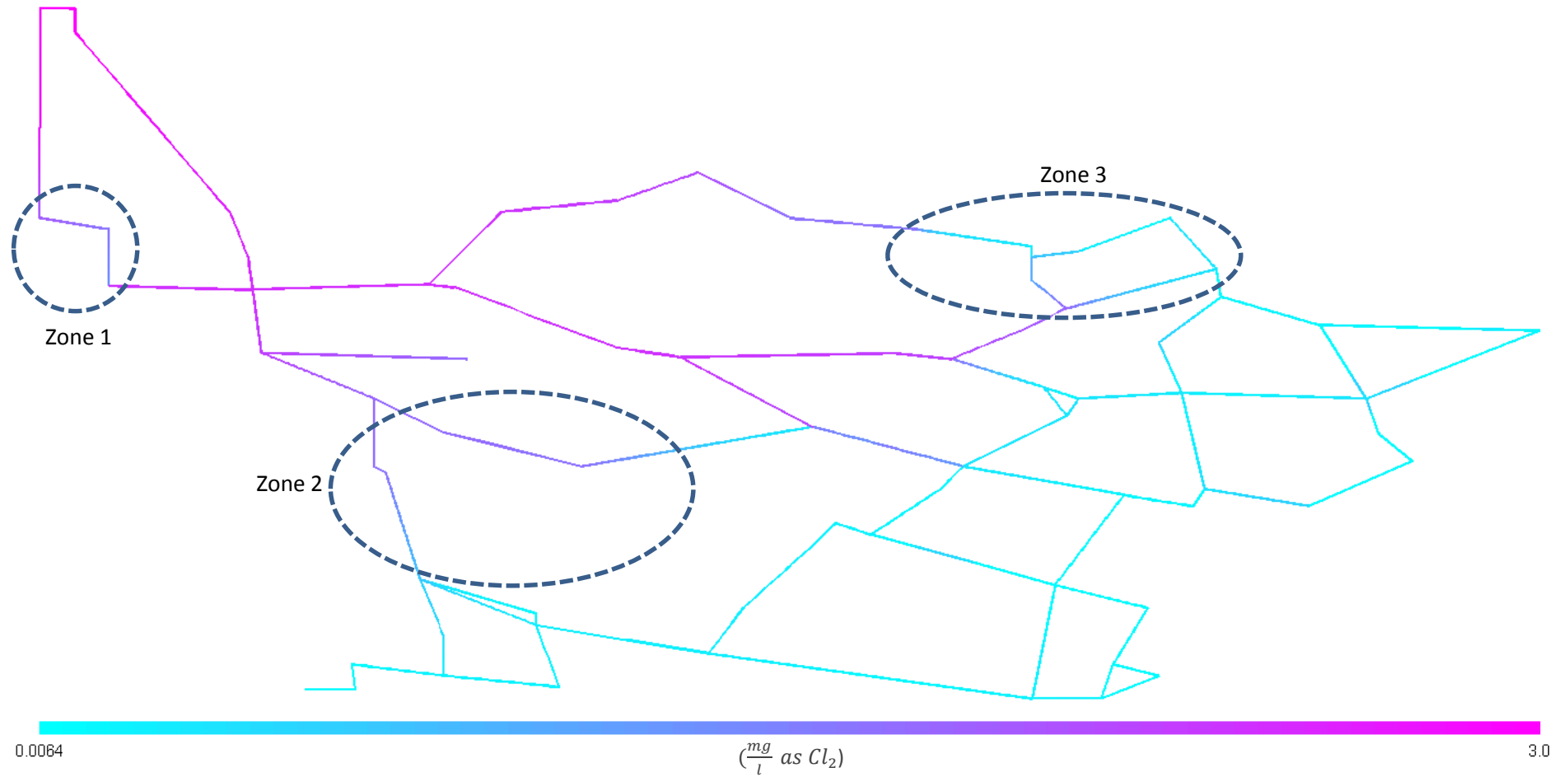


Figure 5-3: Monochloramine concentration profile for Baseline Scenario

Significant loss of monochloramine occurs in highlighted zones 1, 2 and 3. The reasons for the losses in those zones can be determined utilising Figure 5-4. The loss of monochloramine in zone 1 is primarily due to surface catalysis and the oxidation of the high concentration of organic matter originating from the treatment plant. The loss of monochloramine due to surface catalysis in zone 1 is particularly large due to the relatively small diameter of the concrete pipes in this zone. The loss of monochloramine in zone 2 is attributable to a combination of surface catalysis, cometabolism and the oxidation of organic matter. The loss of monochloramine in zone 3 is largely a result of the cometabolism of monochloramine due to the AOB concentration being greatest in this zone.

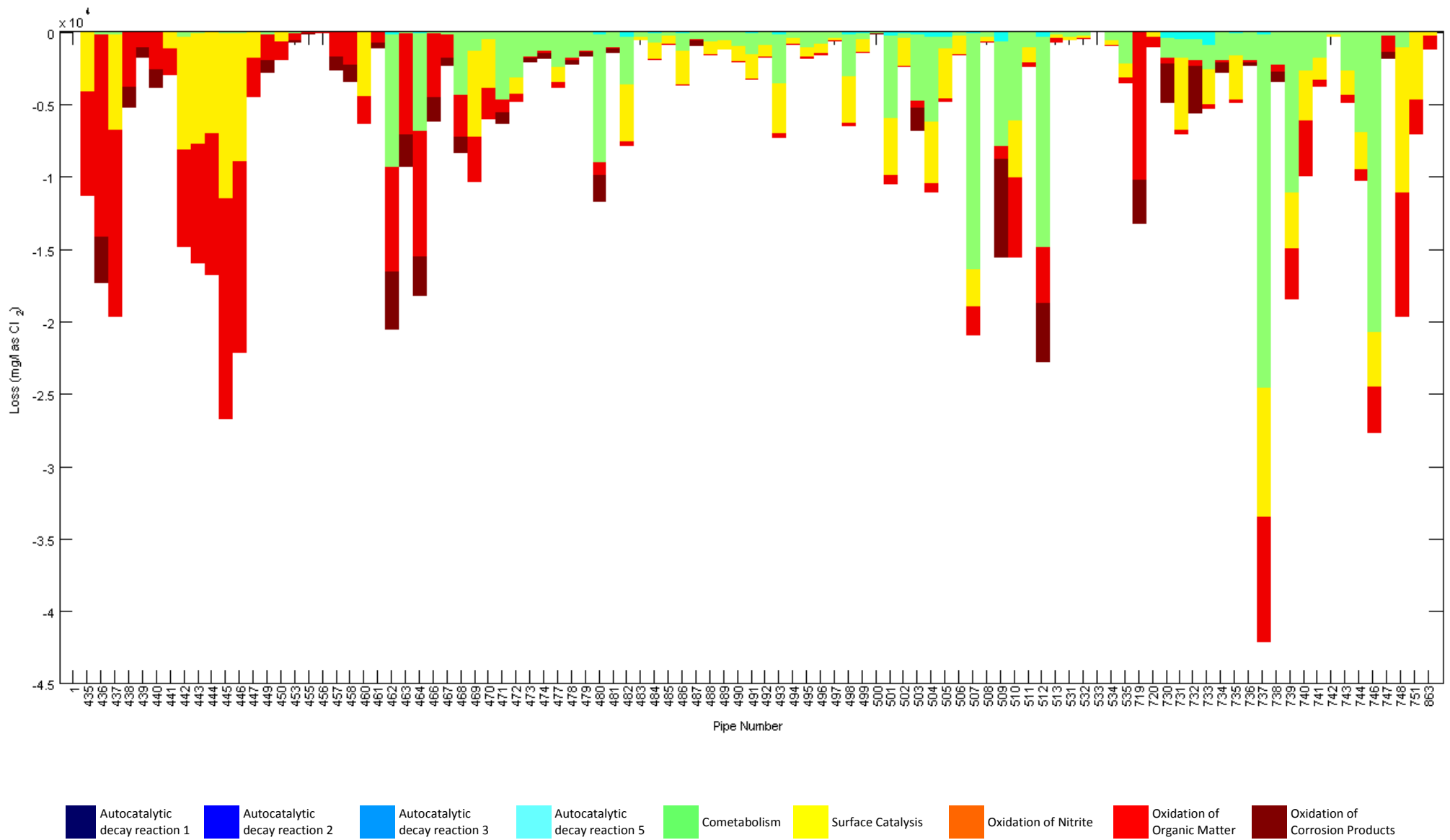


Figure 5-4: Monochloramine loss mechanisms and locations for Baseline Scenario

The capability to assess the locations where disinfectant loss is greatest and the mechanisms responsible for disinfectant loss has been added to the CDWQ-E₂ model. Surface catalysis, cometabolism and the oxidation of the organic matter are the most significant monochloramine loss mechanisms for this simulation. Total loss of monochloramine is greater in those regions with higher monochloramine concentrations as monochloramine loss due to these loss mechanisms is a function of its concentration. In general, bulk water autocatalytic decay reactions have little impact on the overall monochloramine decay for this simulation.

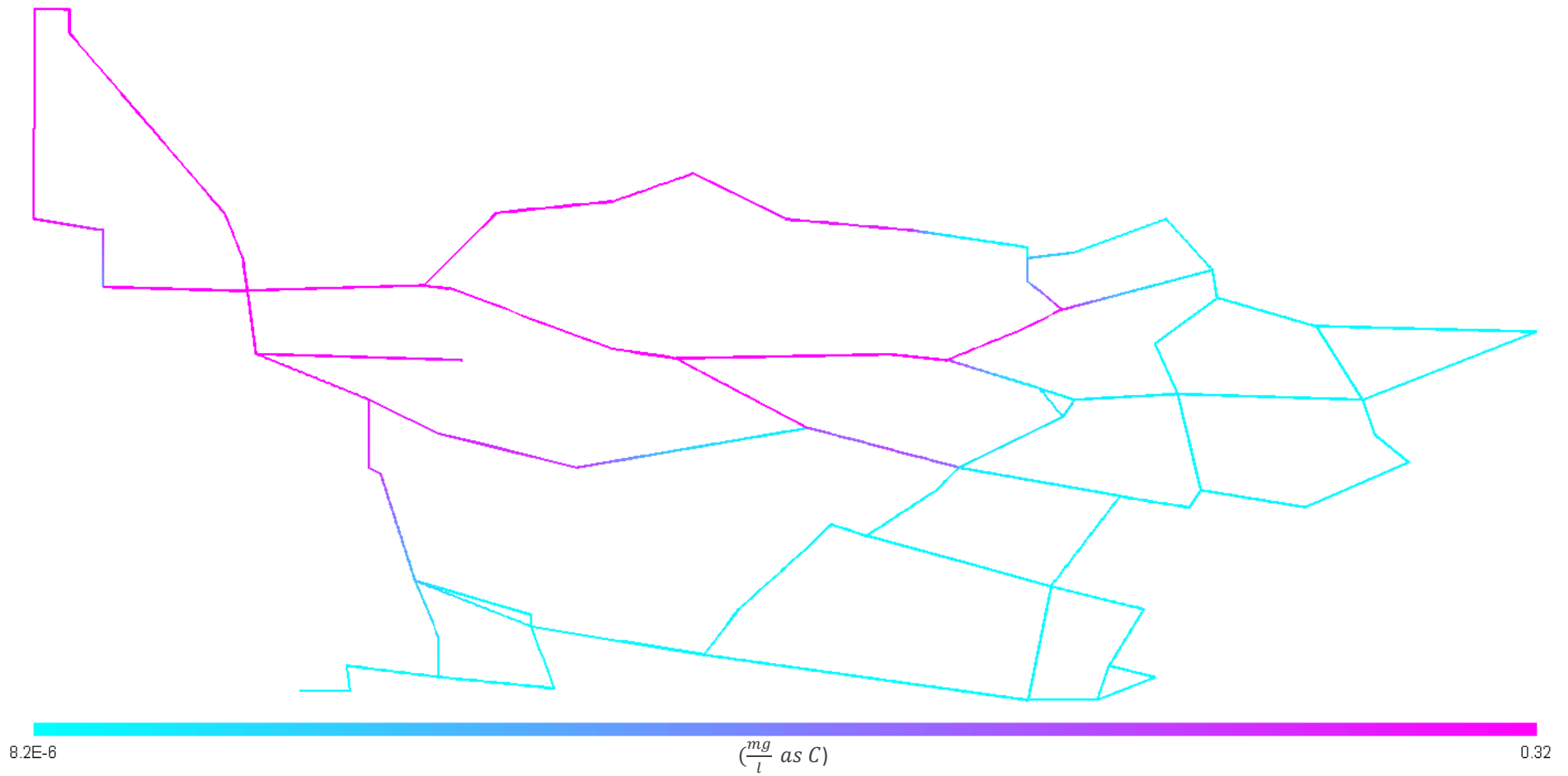


Figure 5-5: BOM₁ concentration profile for Baseline Scenario

BOM₁ concentration is relatively stable for a certain distance from the treatment plant until a sudden drop in its concentration occurs. This is due to consumption by heterotrophic bacteria, specifically fixed heterotrophs which can grow rapidly in these areas due to the reduced concentration of disinfectant. BOM₁ is almost entirely consumed in these regions by heterotrophs and hence the concentration of BOM₁ in the furthest reaches of the distribution system approaches $0 \frac{mg}{l}$ as C.

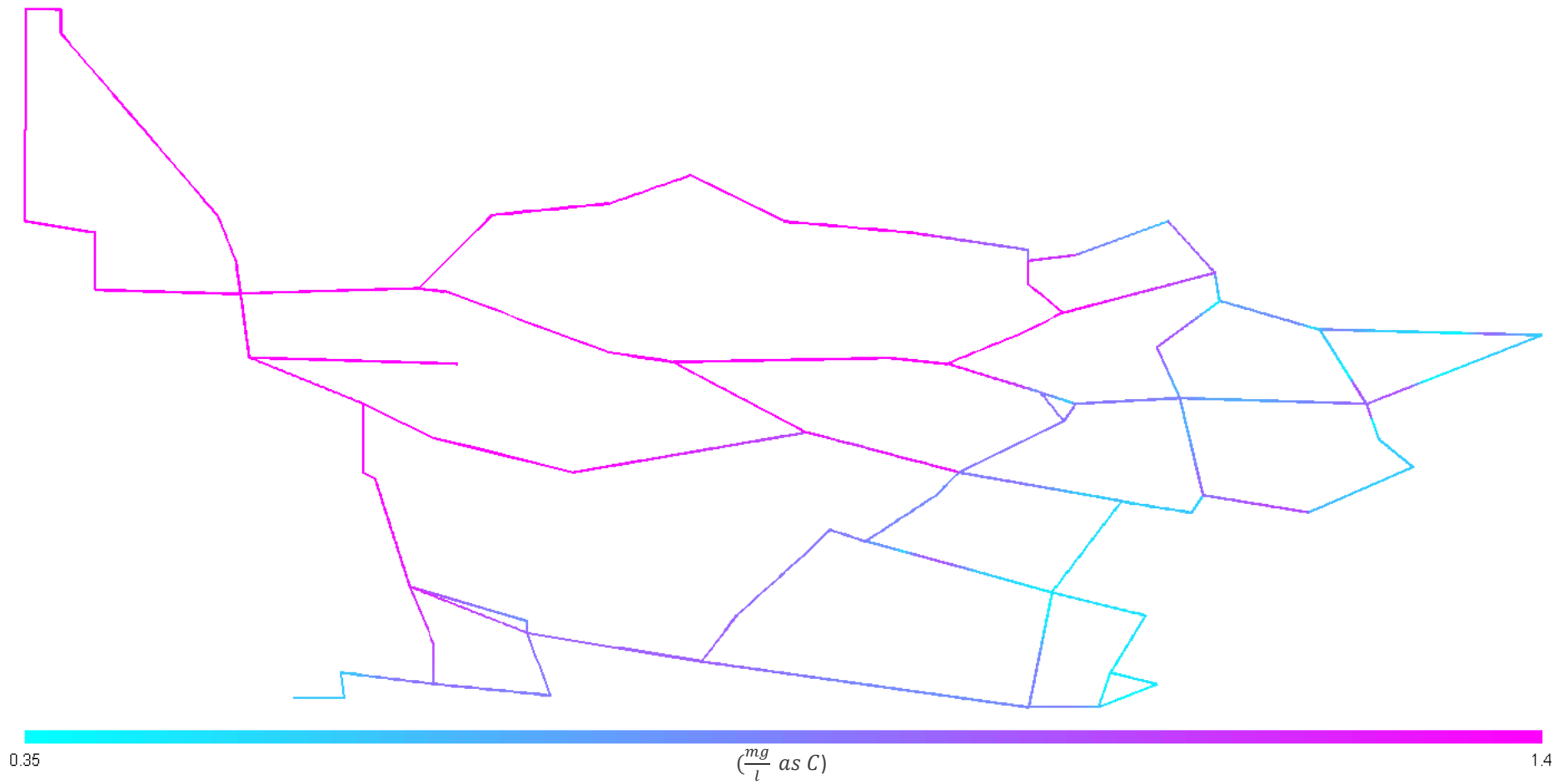


Figure 5-6: BOM₂ concentration profile for Baseline Scenario

The BOM₂ concentration profile is similar to that of BOM₁, although its decrease is less significant due to the lower rate of BOM₂ utilisation by heterotrophs and hence a relatively significant concentration of BOM₂ is present, even in the furthest reaches of the distribution system.

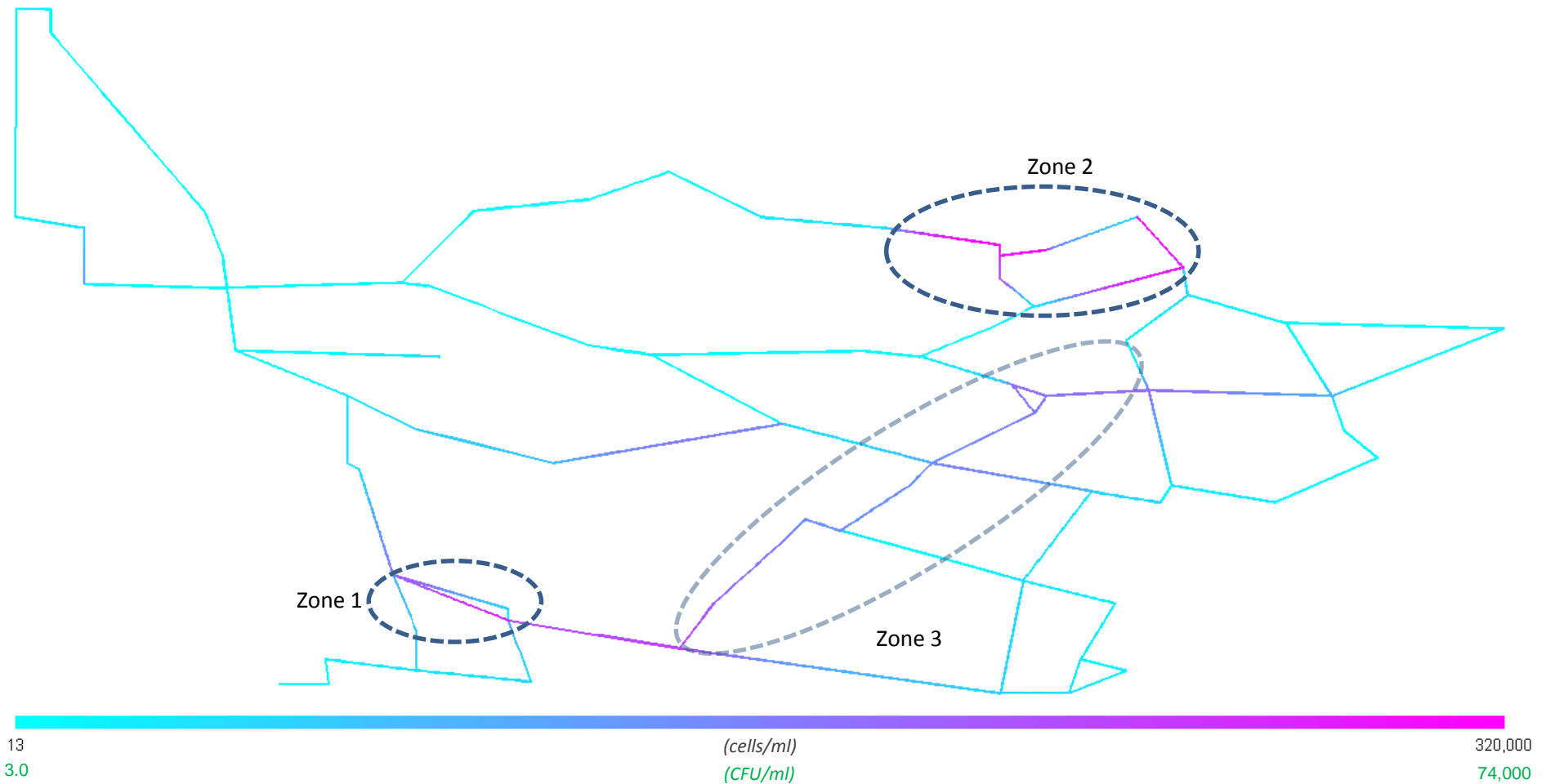


Figure 5-7: Suspended heterotroph concentration profile for Baseline Scenario

The concentration of suspended heterotrophs is greatest in zones 1 and 2 where the stability factor is greatest due to the lower disinfectant residual in these locations, combined with high BOM, particularly BOM₁ concentrations. Heterotrophic growth significantly exceeds the limit of $1000 \frac{CFU}{ml}$ or approximately $4300 \frac{cells}{ml}$ in zones 1 and 2. In zone 3, the heterotrophic concentration also greatly exceeds the maximum limit, although the heterotrophic concentration is lower than in the aforementioned zones. The stability factor analyses for suspended and fixed heterotrophs that follow can be used to explain the reasons for the presence of excessive heterotrophic growth in each

of these zones. Heterotrophic growth in the furthest reaches of the system is minimal, primarily due to the low BOM₁ concentrations, as well as the low BOM₂ concentrations in these regions, despite the disinfectant residual approaching 0 $\frac{mg}{l}$ as Cl₂.

Despite the low concentration of suspended heterotrophs in the furthest sections from the treatment plant due to the limited availability of substrates, such a scenario is still concerning. This is because the occurrence of any intrusion event in this region, which may, for example, be caused by a pipe cracking, could result in a significant contamination event given the absence of disinfectant residual in this region.

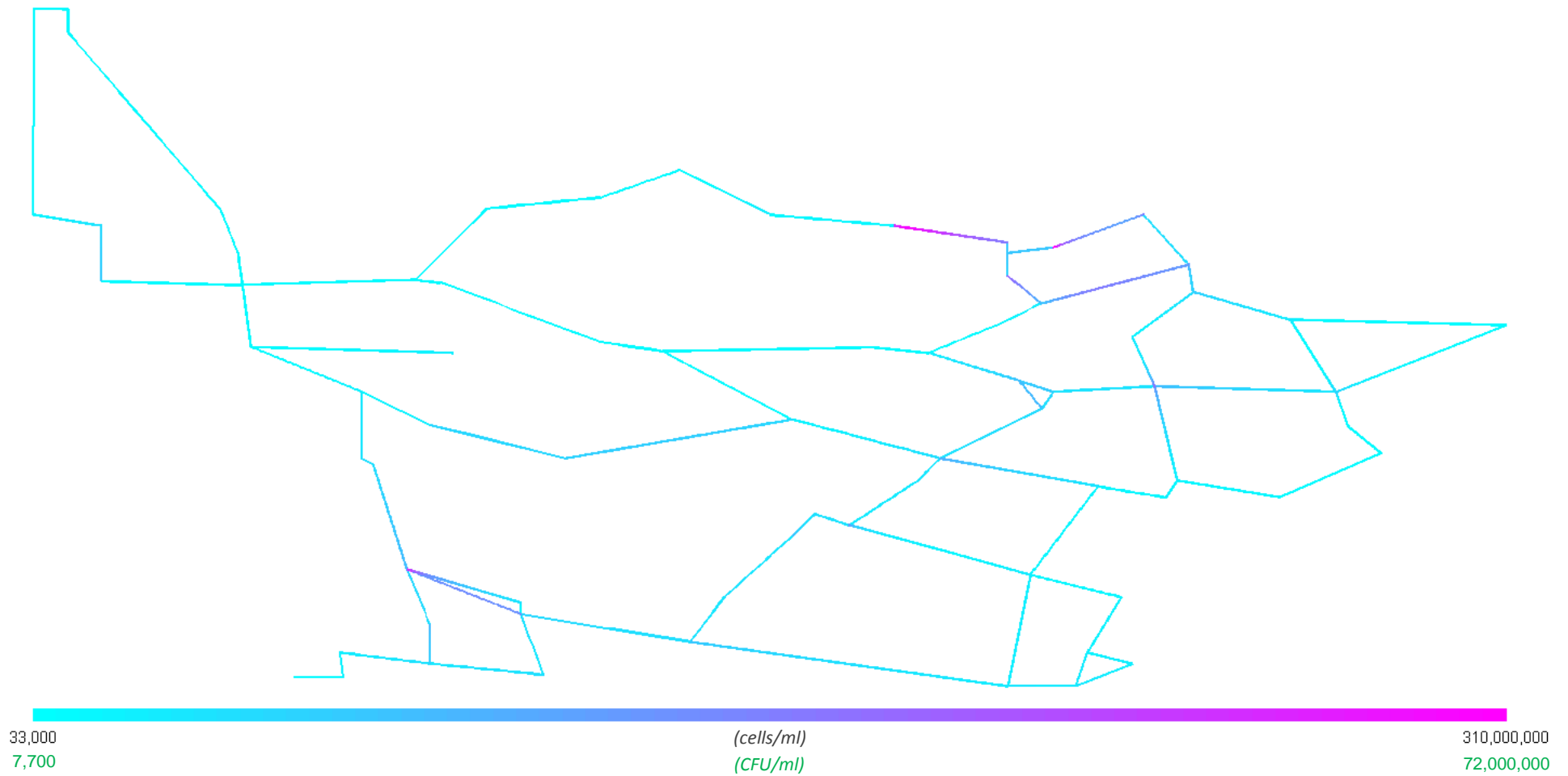


Figure 5-8: Fixed heterotroph concentration profile for Baseline Scenario

The concentration profile for fixed heterotrophs is similar to that of suspended heterotrophs, although the fixed concentrations are much greater.

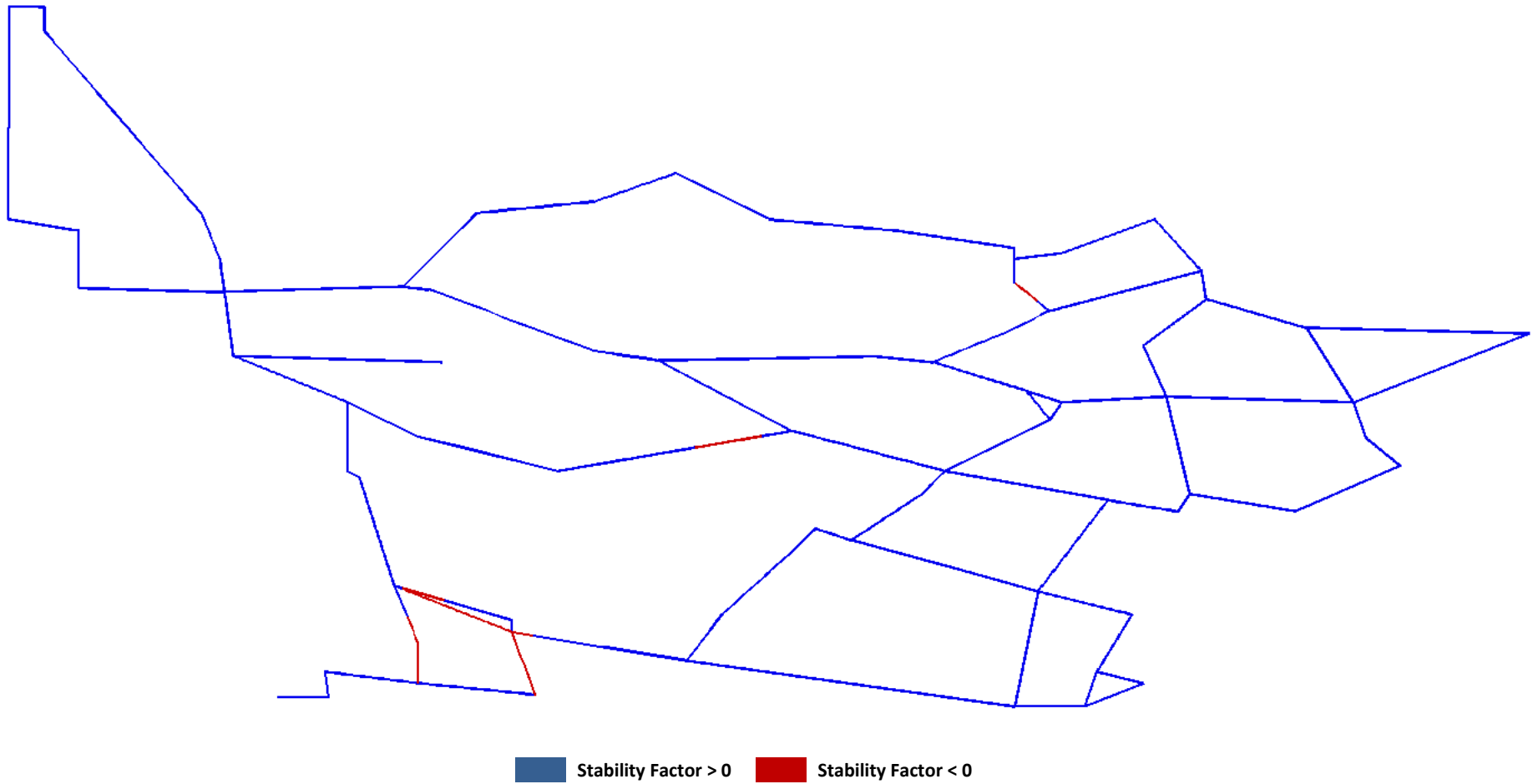


Figure 5-9: Suspended heterotroph stability factor profile

The stability factor analysis demonstrates that throughout most of the system, suspended heterotrophs are not capable of net growth. Only in relatively small areas of the system are suspended heterotrophs capable of net growth.

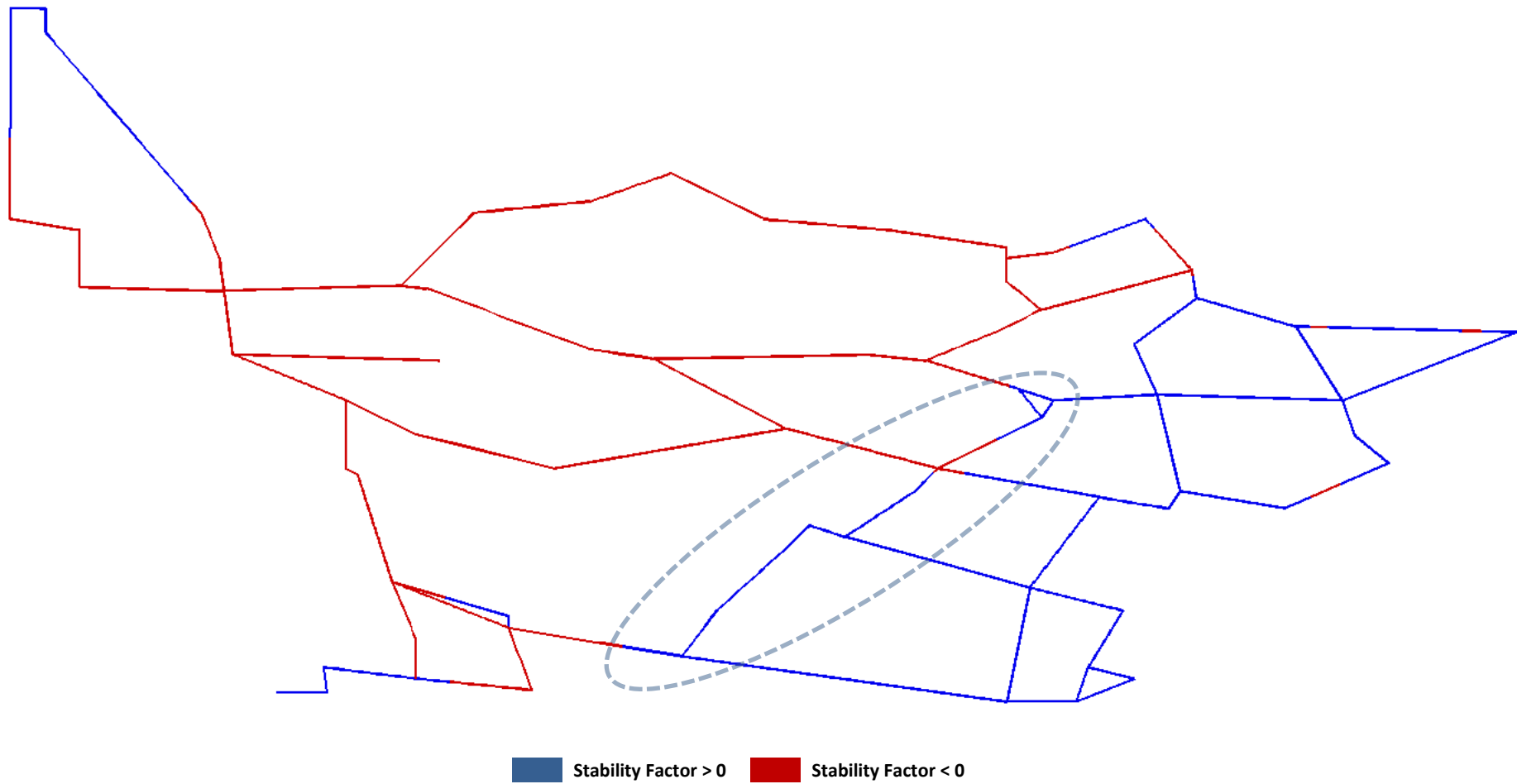


Figure 5-10: Fixed heterotroph stability factor profile

The stability factor analysis shows that there is net growth of fixed heterotrophs throughout a significant portion of the system. This is due to the reduced efficiency of disinfectant when acting on fixed as opposed to suspended bacteria. The stability analyses for both fixed and suspended heterotrophs also demonstrates that the detachment of fixed bacteria is significant reason for the large concentrations of suspended bacteria in certain regions of the system, rather than excessive net growth of suspended heterotrophs. It is also important to note that the stability factor analysis reveals that fixed heterotrophs are not capable of growth in regions where the BOM_1 concentration approaches zero, despite the fact that the monochloramine concentration also approaches zero in the same region. This emphasises the point that BOM_1 has

a greater influence on heterotrophic growth rate than BOM_2 , a finding which is in accordance with that made by Wooschlagler (2000) and Escobar and Randall (2001). Finally, given that the stability factors for both fixed and suspended heterotrophs in the highlighted zone are negative, the presence of excessive suspended heterotrophic concentrations in the same zone must be a result of heterotrophic growth in other regions, which is subsequently advected to the highlighted zone.

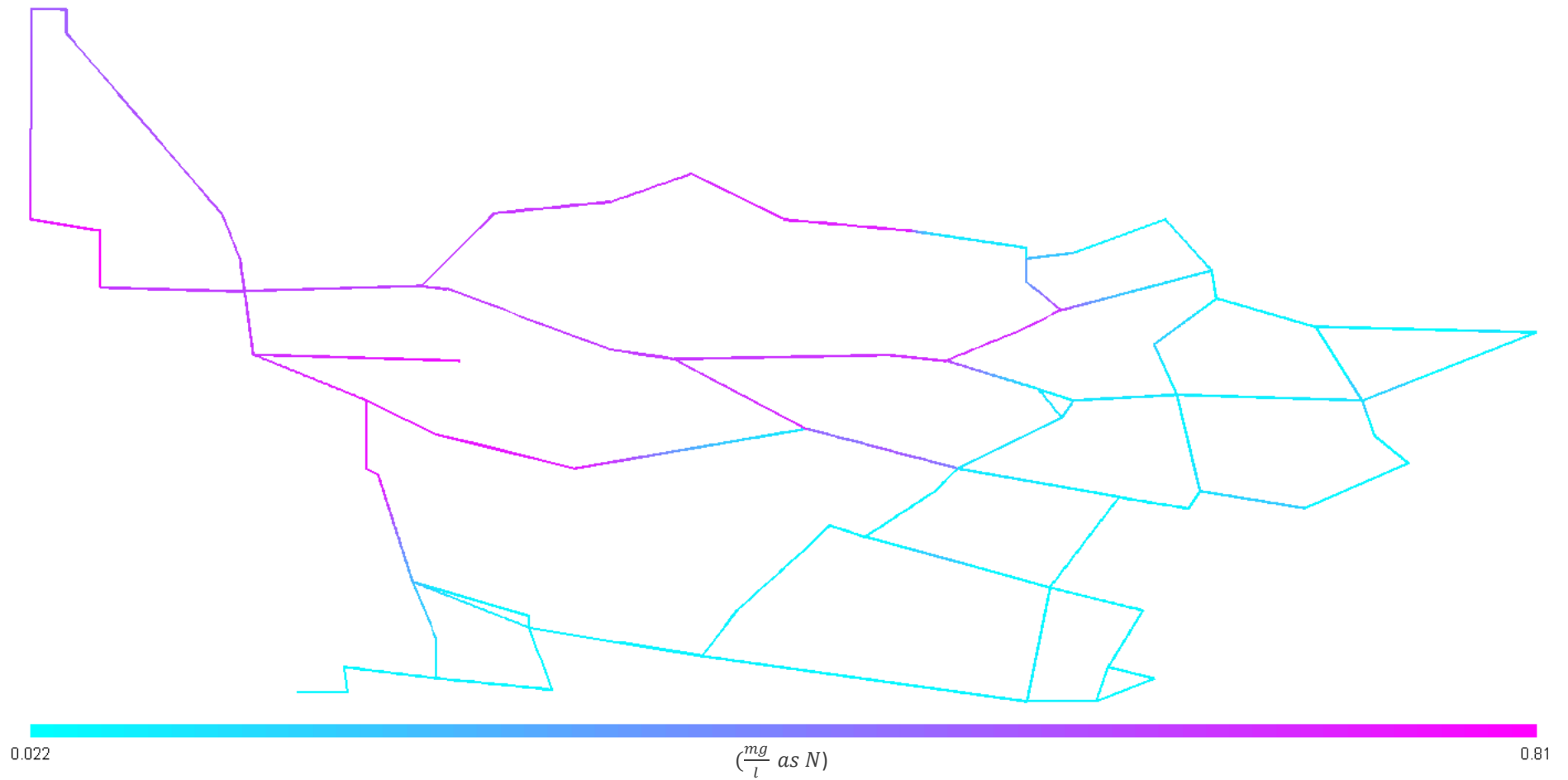


Figure 5-11: Total ammonia concentration profile for Baseline Scenario

The ammonia concentration increases in certain pipes due to the loss of monochloramine in these regions, which produces ammonia. However, the ammonia concentration never exceeds the maximum limit of $1.5 \frac{mg}{l}$ as N. The sudden drop in ammonia shortly after is evidence of ammonia consumption by AOB.

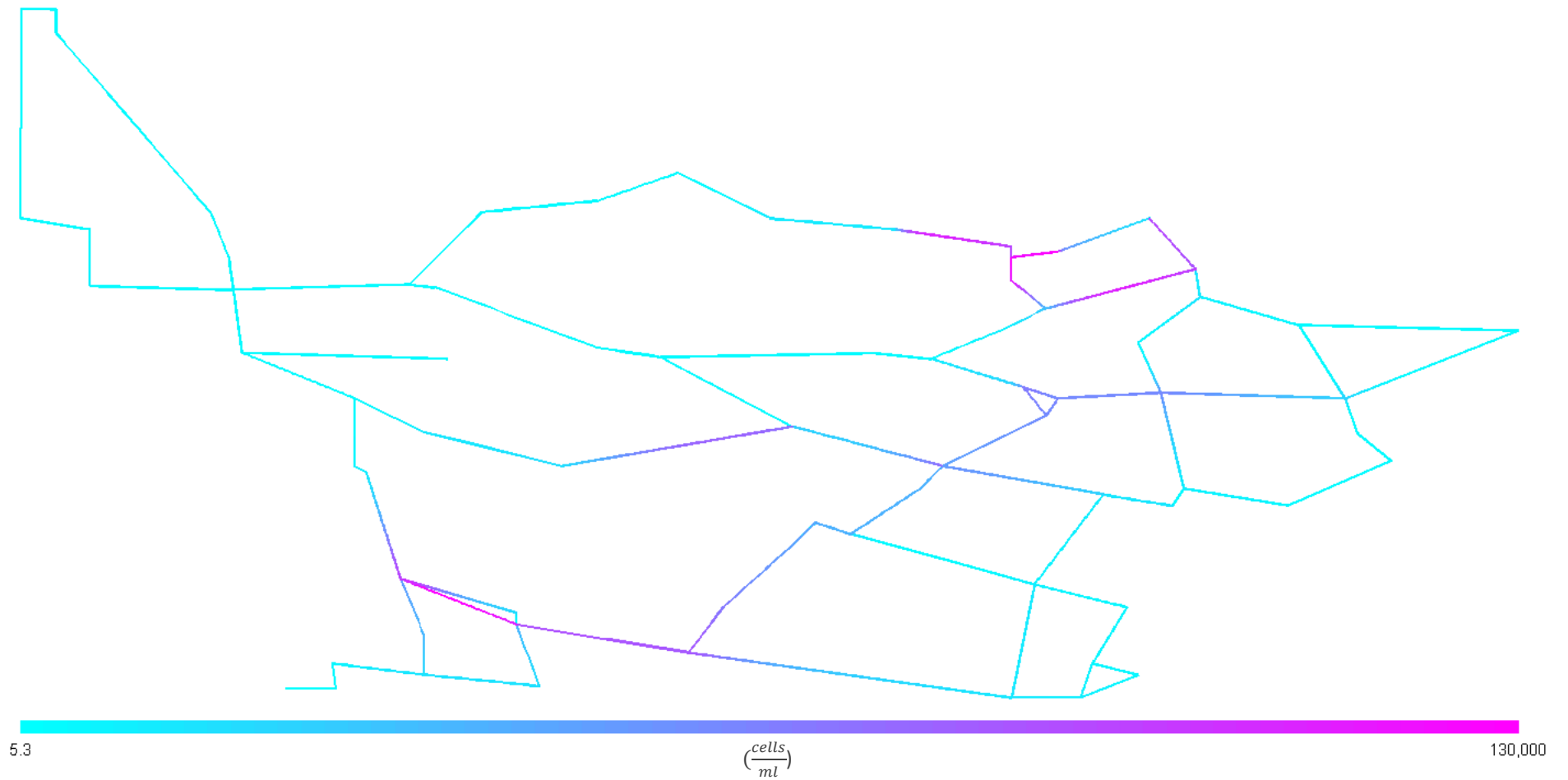


Figure 5-12: Suspended AOB concentration profile for Baseline Scenario

The suspended AOB concentrations are greatest in regions where the stability factor is greatest due to the loss of disinfectant residual, combined with the associated increase in ammonia in these regions. Despite the low disinfectant residual in the furthest reaches of the system, the suspended AOB concentration is low due to the low concentration of ammonia.

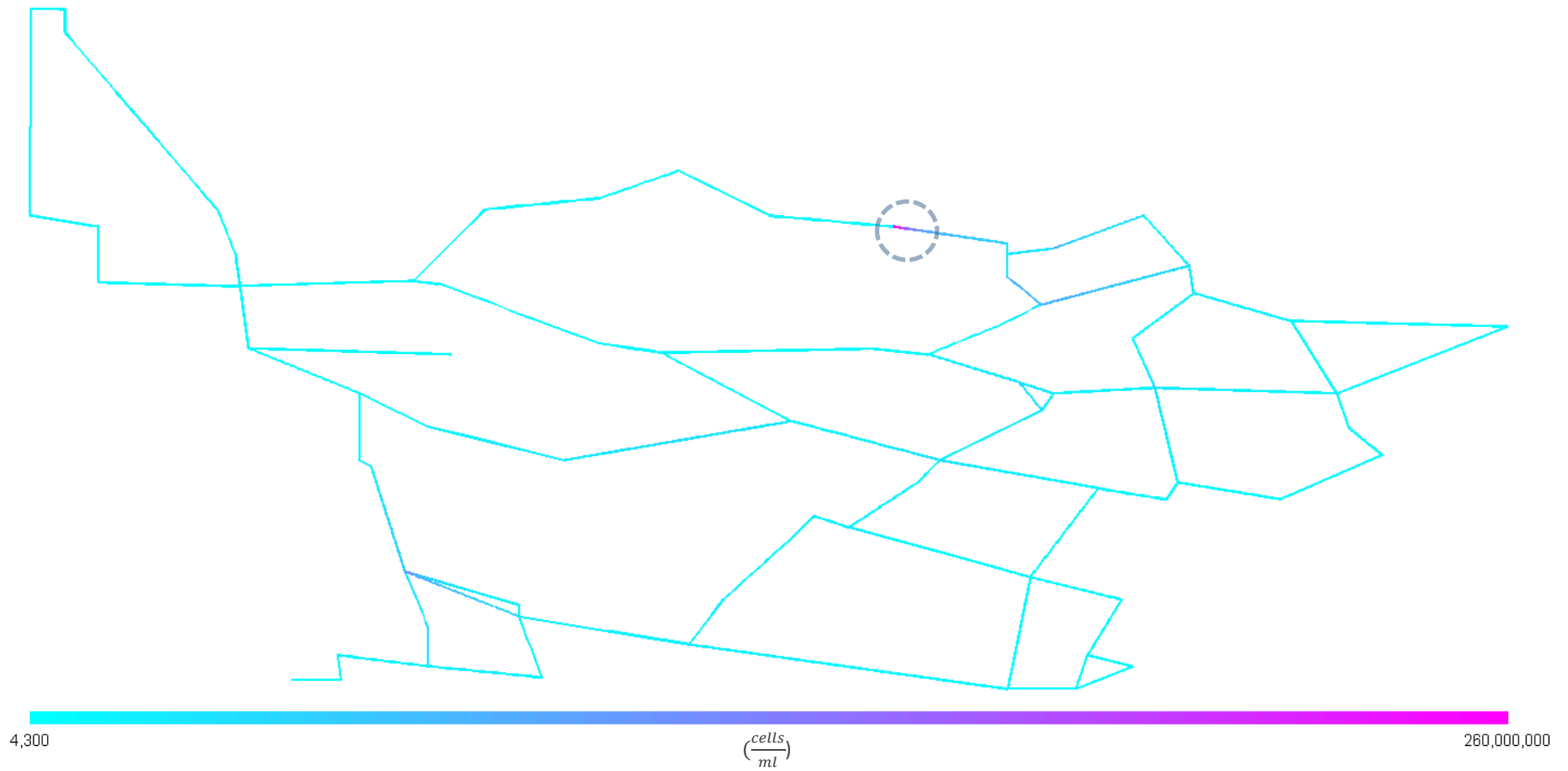


Figure 5-13: Fixed AOB concentration profile for Baseline Scenario

The concentration profile for fixed AOB is similar to that of suspended AOB, although the fixed concentrations are much greater. Fixed AOB growth is greatest in the highlighted zone, which explains why significant loss of monochloramine due to cometabolism occurs in the same region.

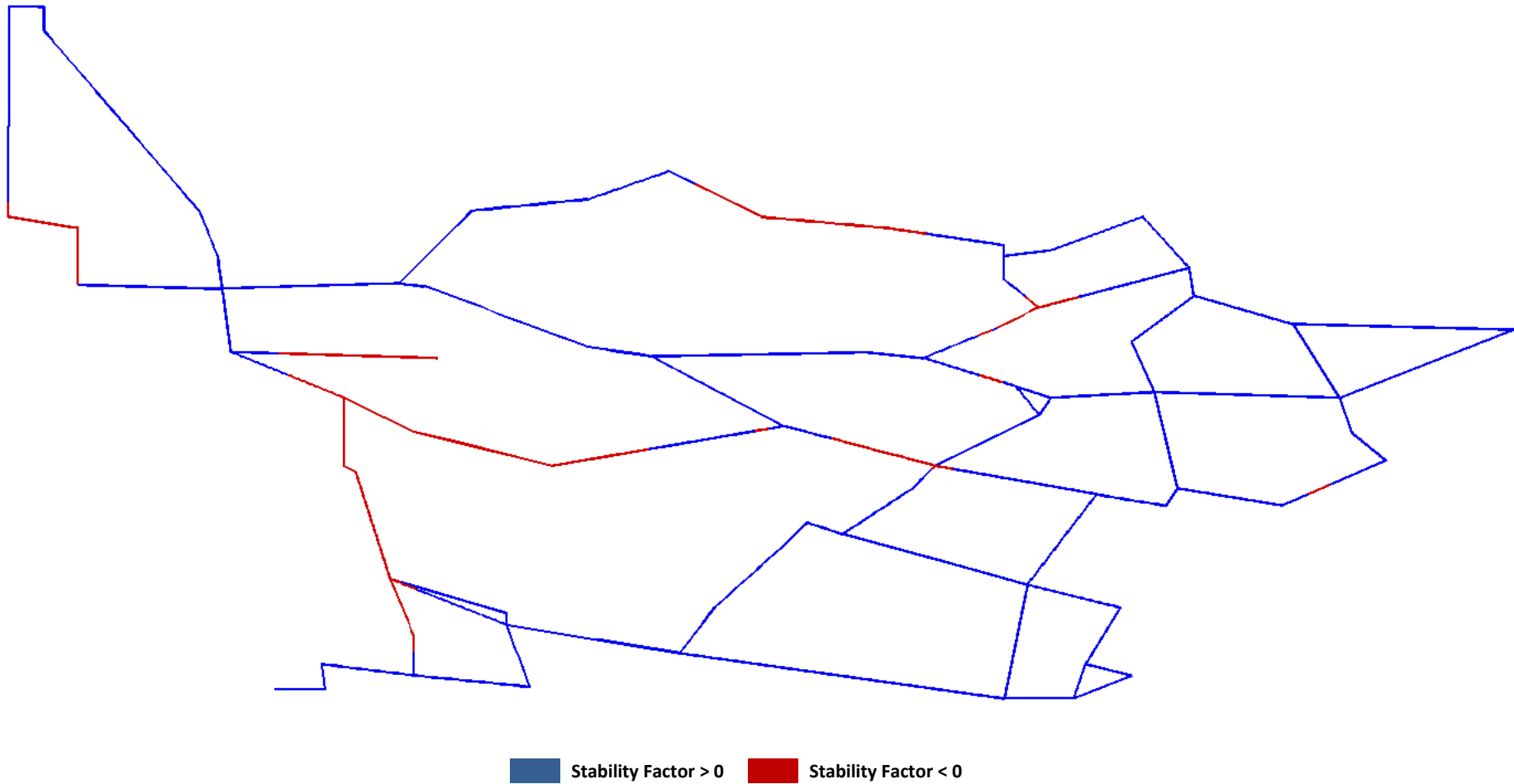


Figure 5-14: Suspended AOB stability factor profile

The stability factor analysis demonstrates that suspended AOB are capable of net growth in areas the system where the disinfectant residual has depleted sufficiently, which in turn, produces the ammonia substrate required for AOB growth. Suspended AOB are not capable of growth in the furthest reaches of the system due to the low concentration of ammonia, despite the limited concentration of disinfectant in these regions.

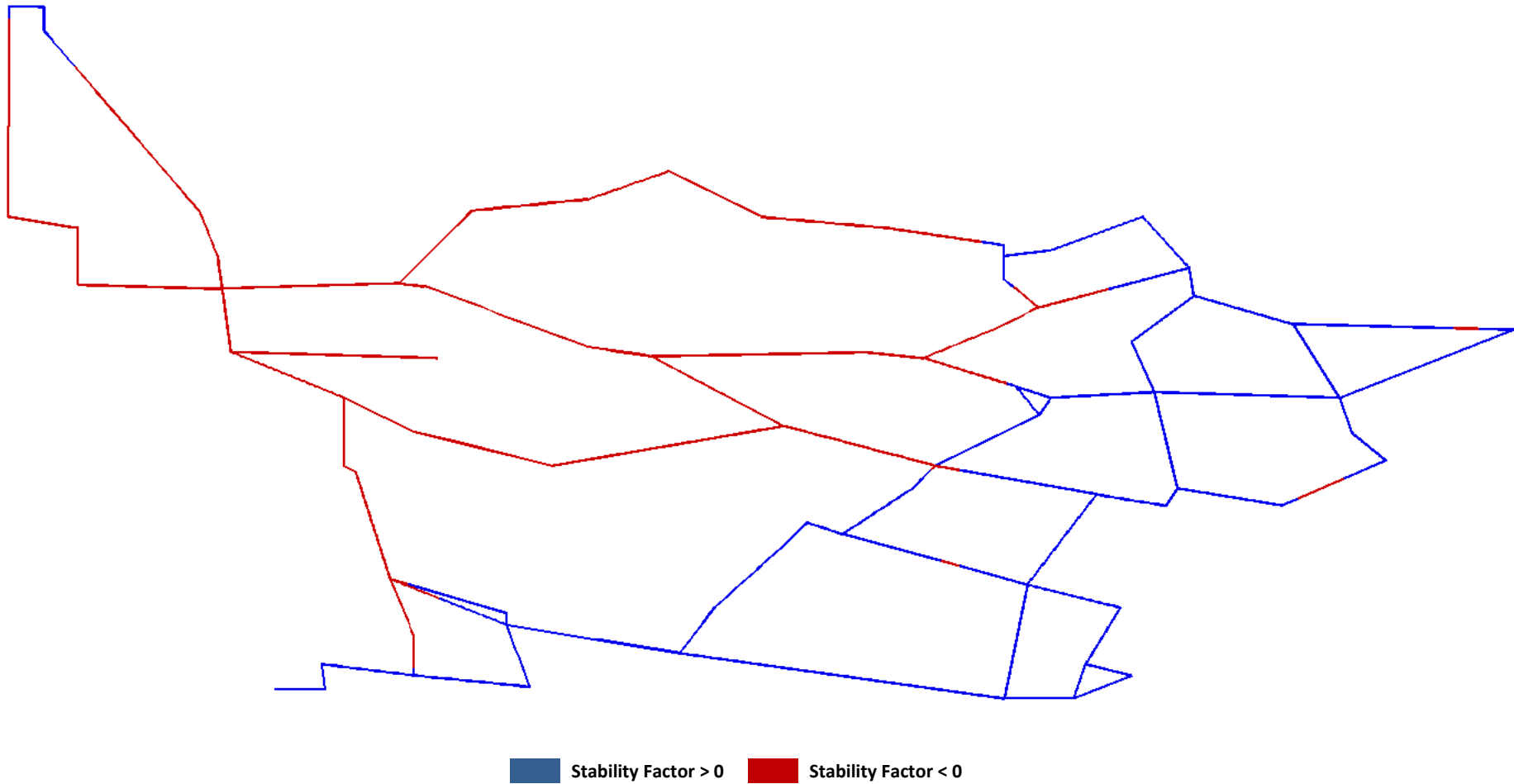


Figure 5-15: Fixed AOB stability factor profile

The stability factor analysis shows that fixed AOB are capable of net growth throughout a significant portion of the system. As is the case with heterotrophs, the stability factor analyses for AOB demonstrate that the detachment of fixed bacteria is the more significant reason for the high concentrations of suspended AOB than the net growth of suspended AOB themselves.

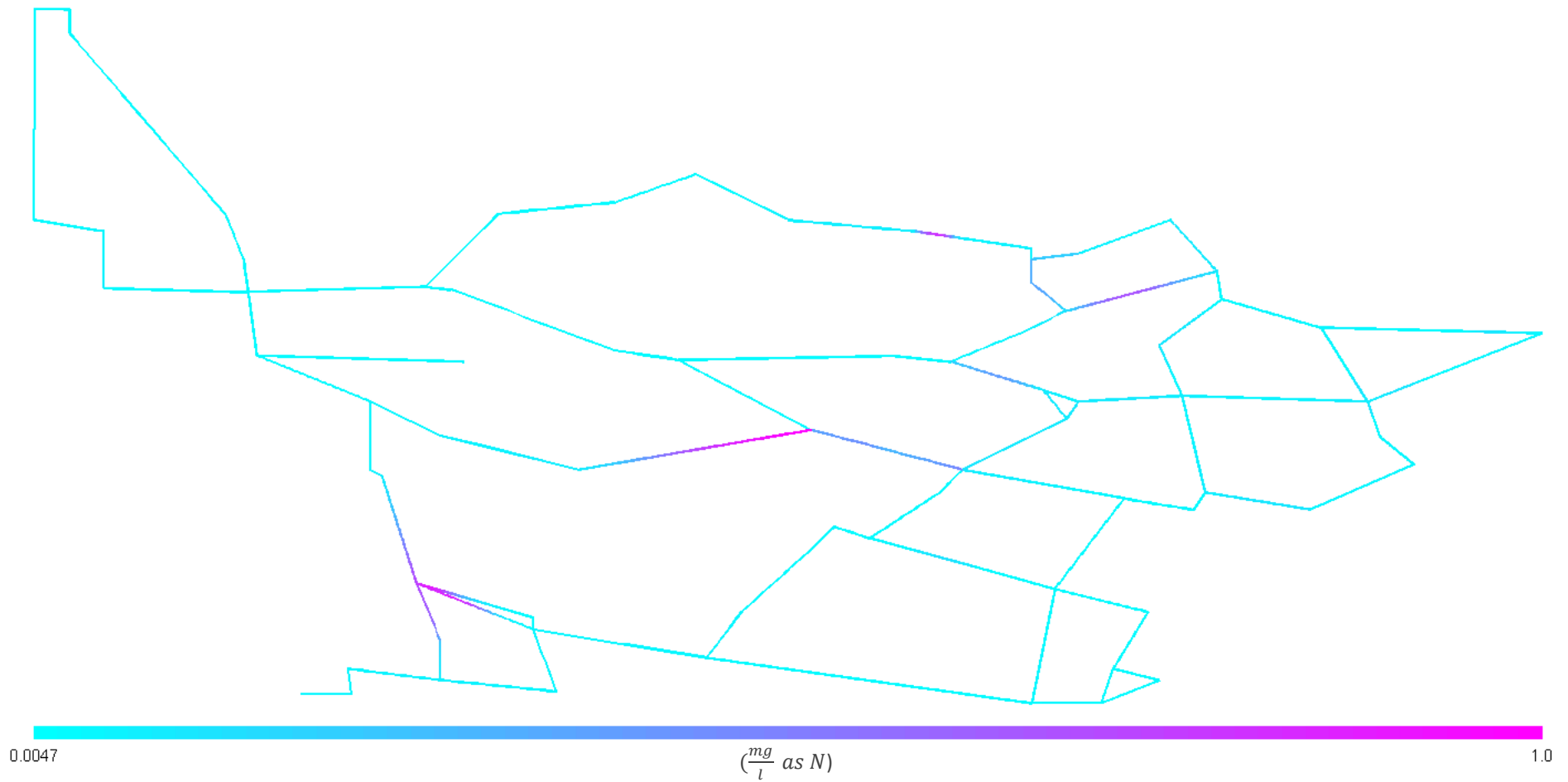


Figure 5-16: Nitrite concentration profile for Baseline Scenario

The utilisation of ammonia by AOB in certain pipe sections produces nitrite, which combined with the decrease in ammonia, is evidence of nitrification in these zones (Pintar & Slawson, 2003; Wolfe et al, 1990; Cuncliffe, 1991 in Sathasivan et al, 2008; Odell et al, 1996 in Le Pui, 2004). In these zones where nitrification occurs, the concentration of nitrite is greater than the maximum limit of $0.9 \frac{mg}{l}$ as N.

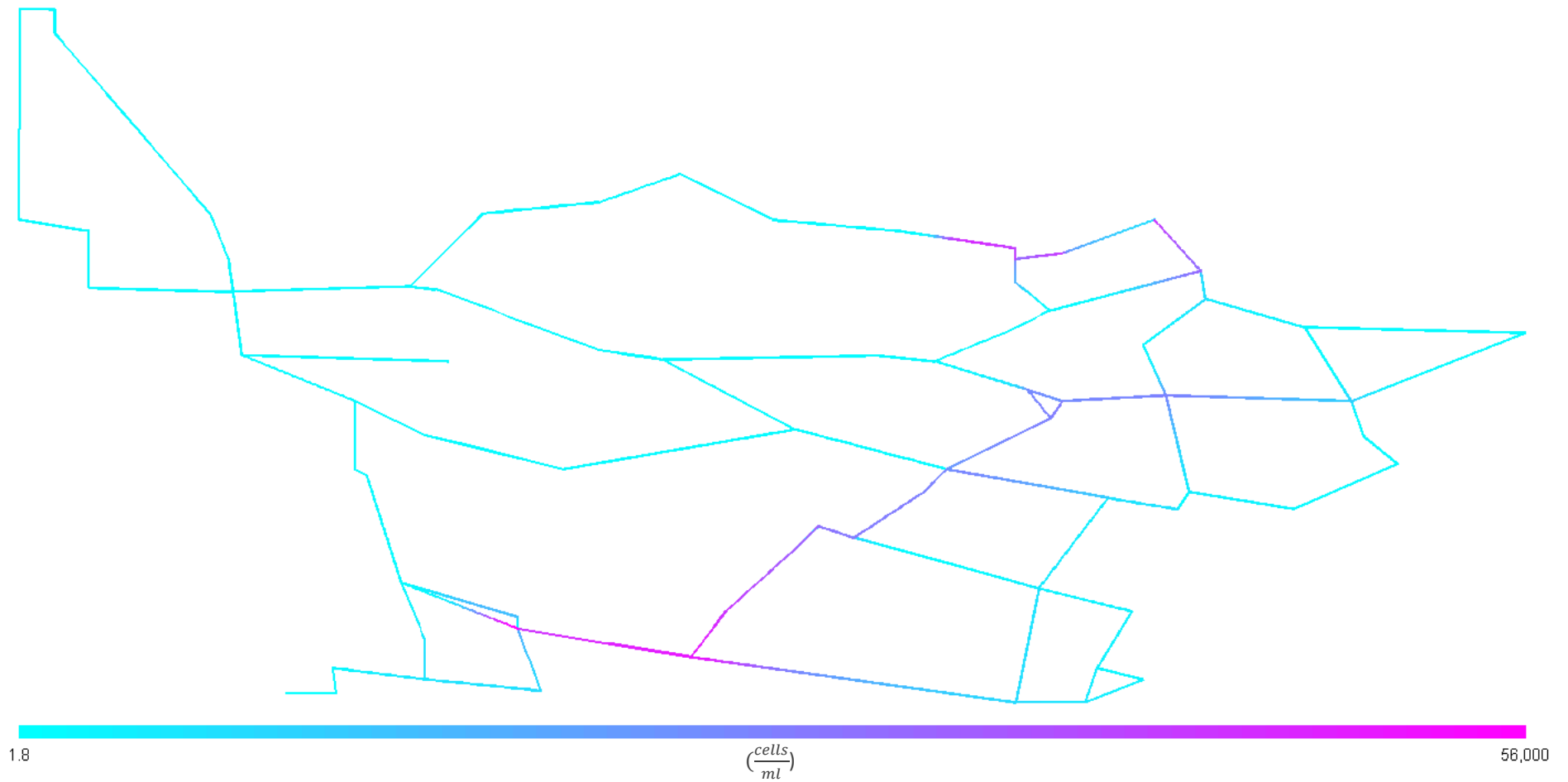


Figure 5-17: Suspended NOB concentration profile for Baseline Scenario

Suspended NOB mirrors the growth of AOB. Suspended NOB growth is greatest in those regions where the stability factor is greatest due to the decrease in disinfectant residual that has occurred and the production of nitrite by AOB utilising ammonia.

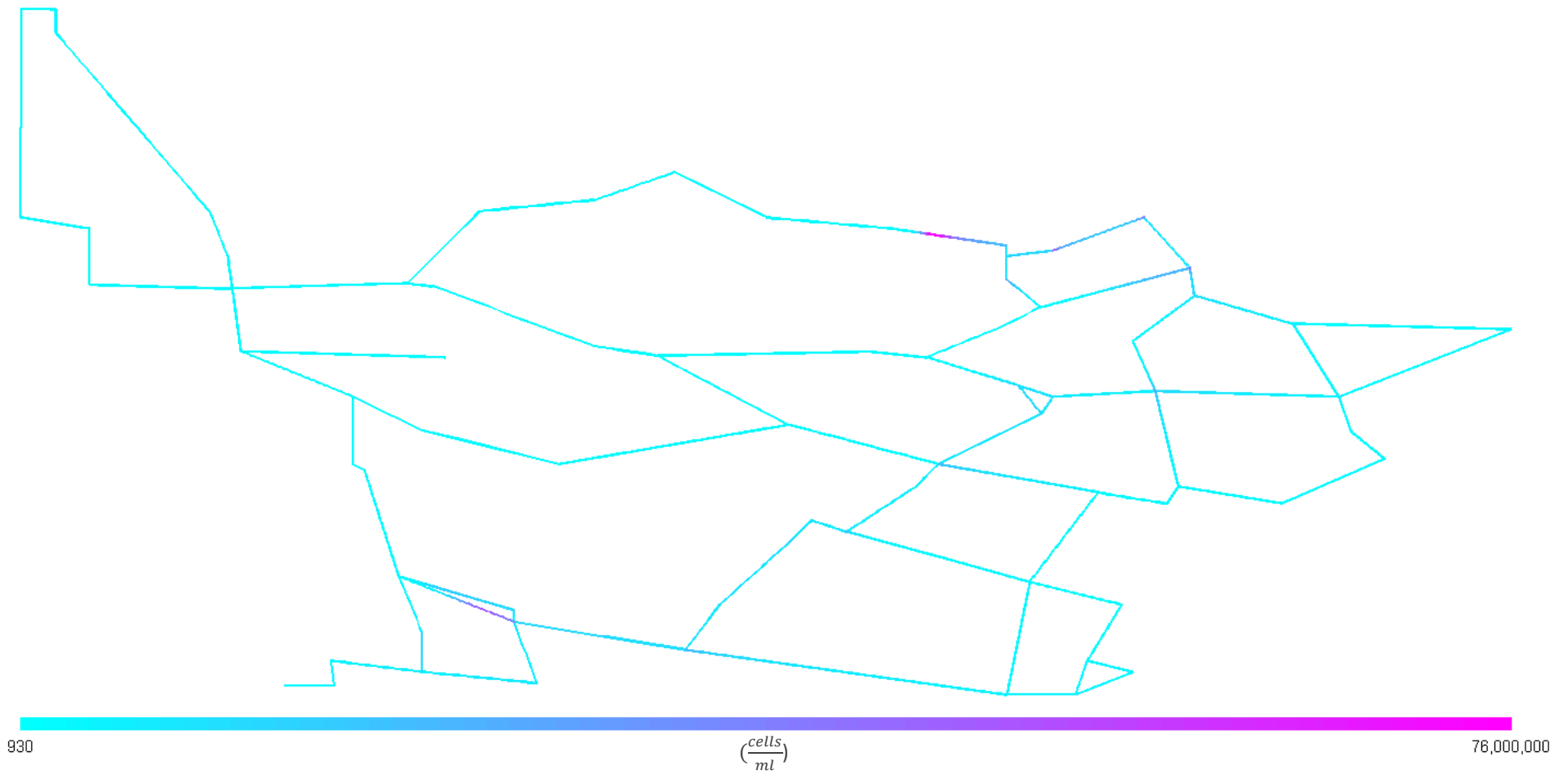


Figure 5-18: Fixed NOB concentration profile for Baseline Scenario

The concentration profile for fixed NOB is similar to that of suspended NOB, although the fixed concentrations are much greater.

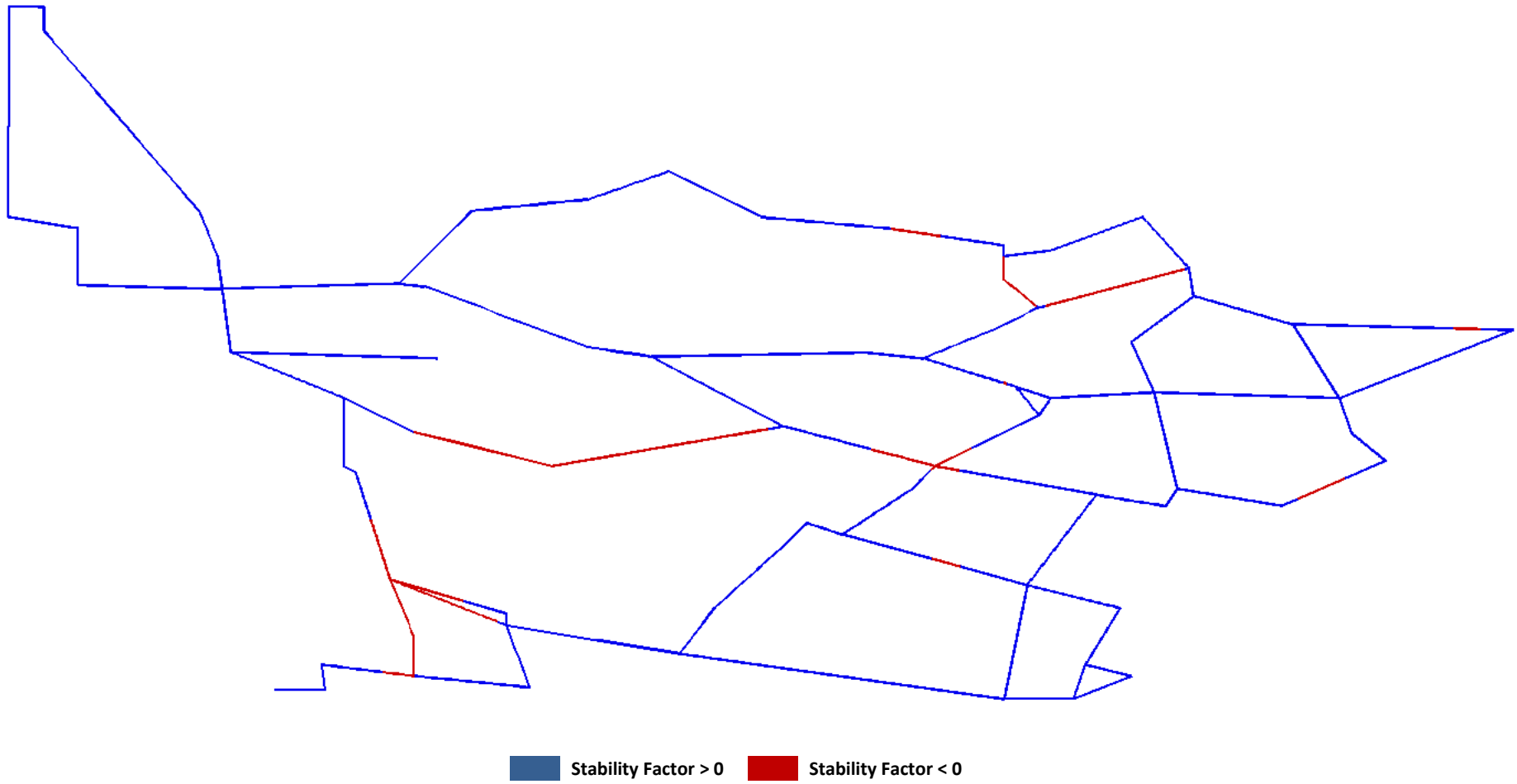


Figure 5-19: Suspended NOB stability factor profile

The stability factor is positive in the regions where nitrite concentration has increased as a consequence of nitrification. Elsewhere in the system, nitrite concentration approaches zero and hence the stability factor is negative.

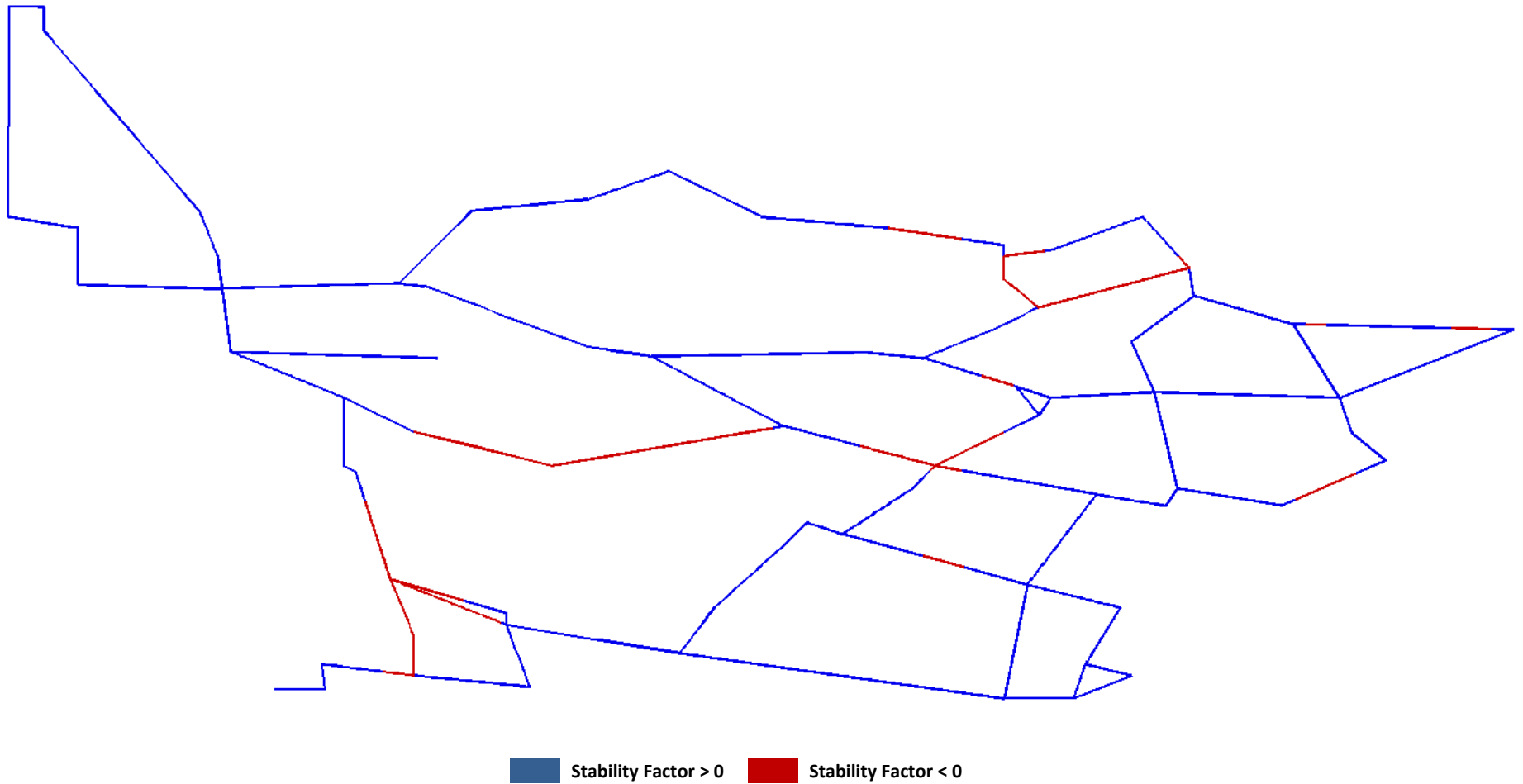


Figure 5-20: Fixed NOB stability factor profile

The stability factor profile for fixed NOB is similar to suspended NOB.

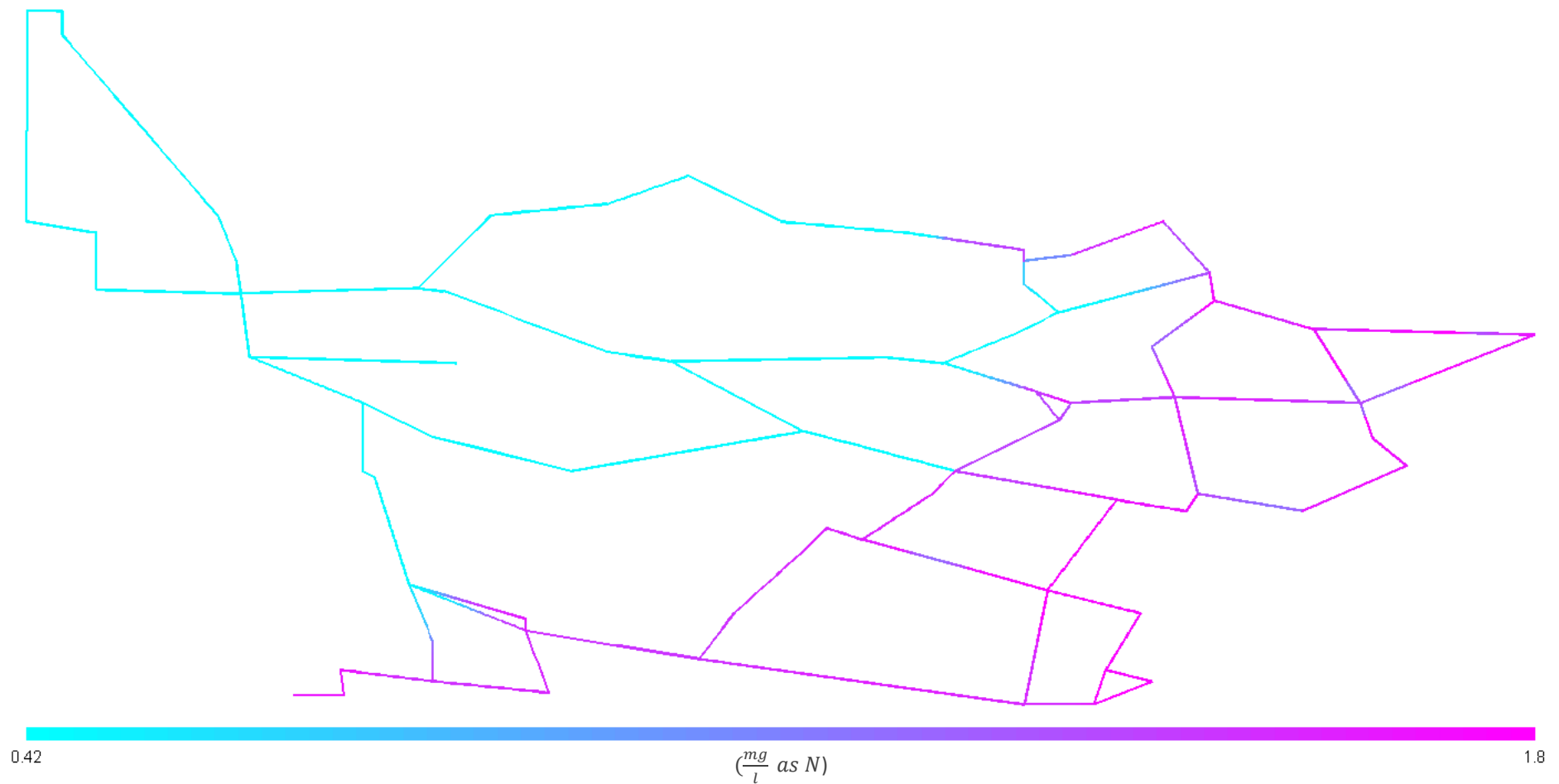


Figure 5-21: Nitrate concentration profile for Baseline Scenario

Nitrate is produced in regions where nitrification is significant and is subsequently advected to the furthest reaches of the system. Nitrate can only be consumed by heterotrophic bacteria respiring anoxically and given that the oxygen concentration never approaches zero for this simulation, the nitrate concentration does not decrease in the furthest reaches of the system. Furthermore, the nitrate concentration is well below the maximum limit of $11 \frac{mg}{l}$ as N. The relatively low increase in concentration of nitrate in the system indicates that the second step of nitrification is not significant for this system, a finding which is in accordance with those made by Wolfe et al (1990).

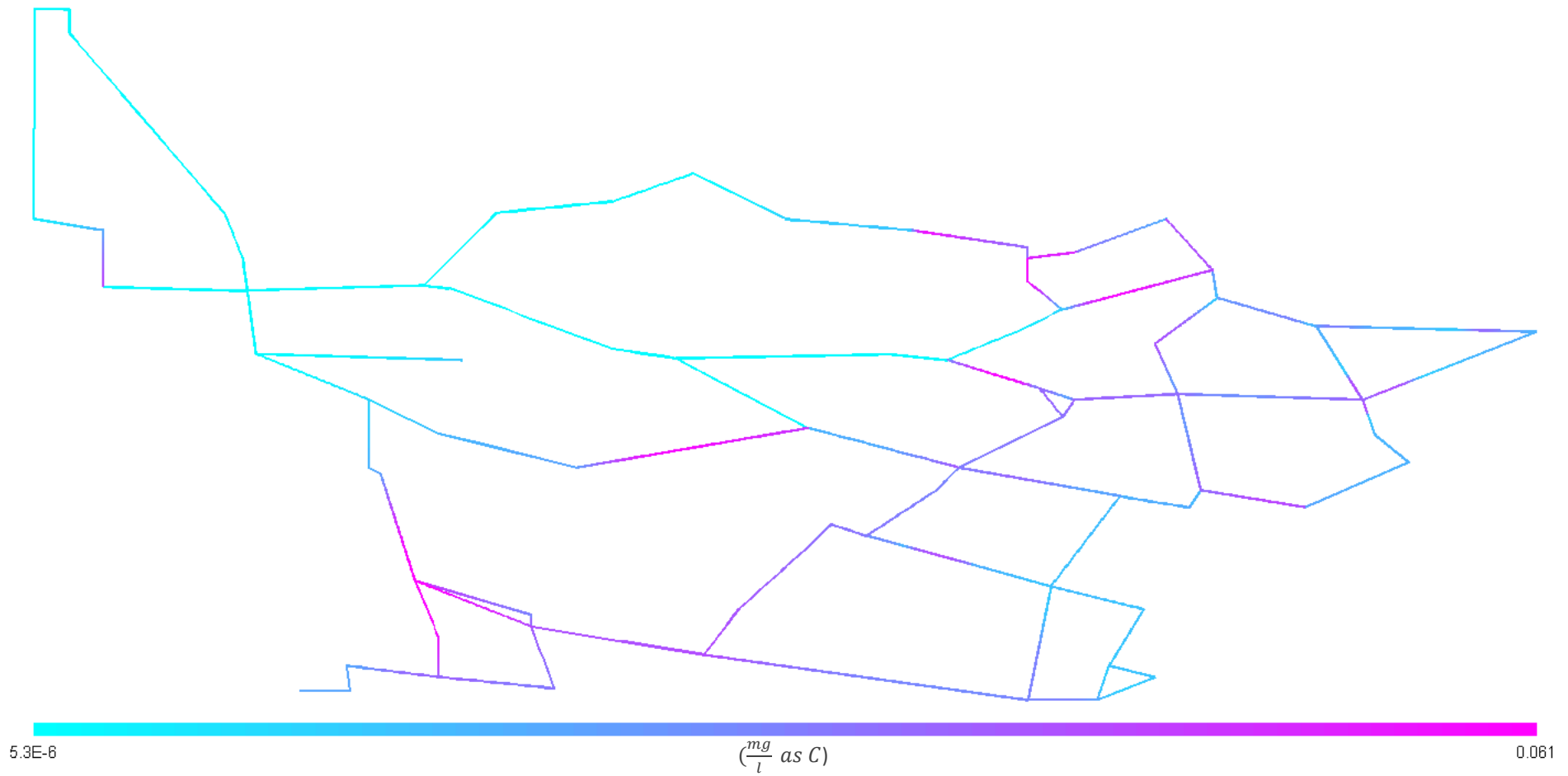


Figure 5-22: UAP concentration profile for Baseline Scenario

UAP production occurs in those zones where microbial growth is greatest and UAP is advected from these regions to the furthest reaches of the system due to the flow pattern. As UAP is advected from the regions where it is mostly produced, its concentration decreases and approaches $0 \frac{mg}{l}$ as C in the furthest reaches of the system due to the rapid utilisation kinetics of UAP by heterotrophs.

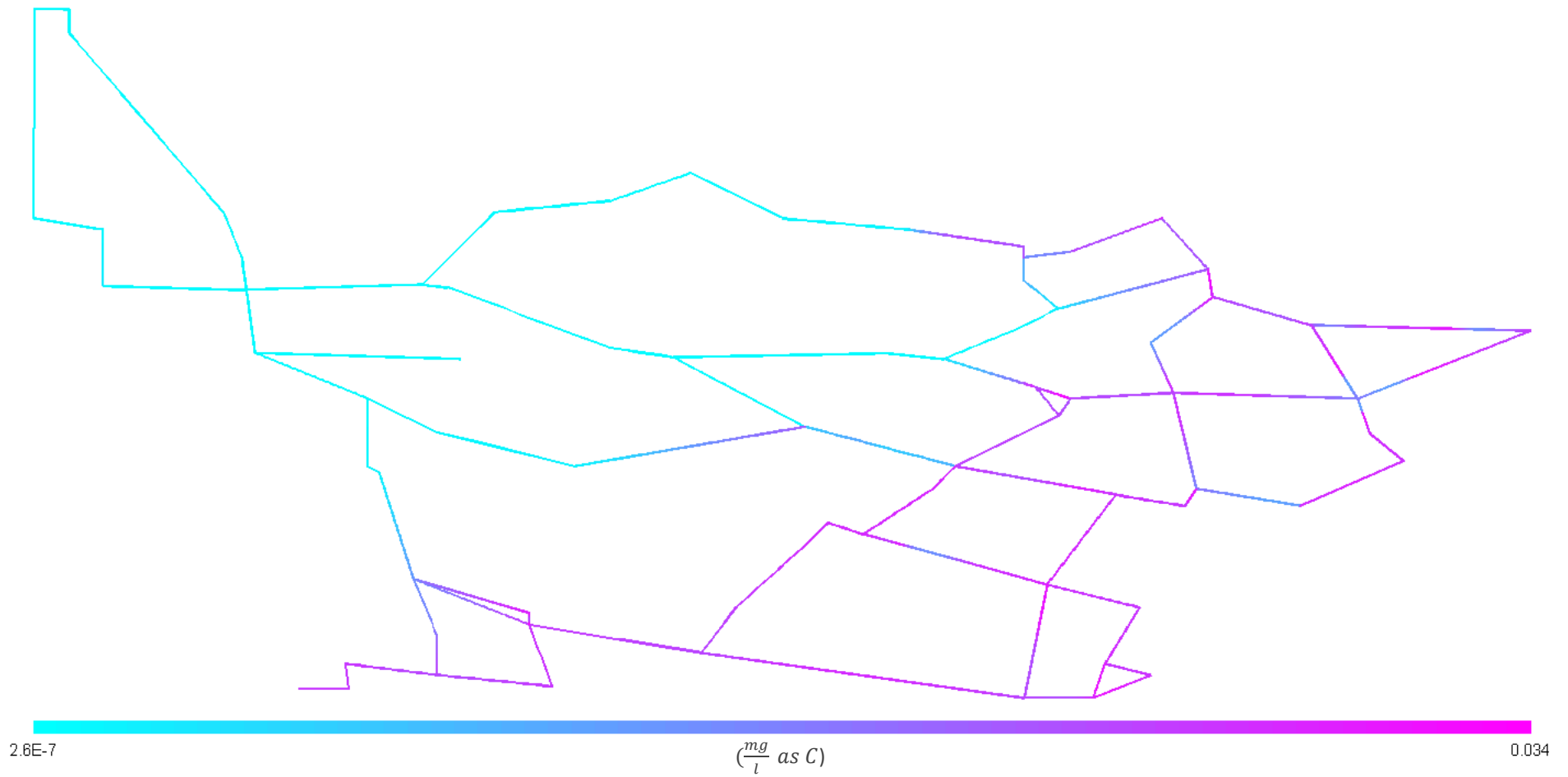


Figure 5-23: BAP concentration profile for Baseline Scenario

BAP is produced from the hydrolyses of both fixed and suspended EPS, a product of microbial growth and hence the concentration profile of BAP is similar to that of UAP, although BAP is present in greater concentrations in the furthest reaches of the system due to the lower rate of BAP utilisation by heterotrophs.

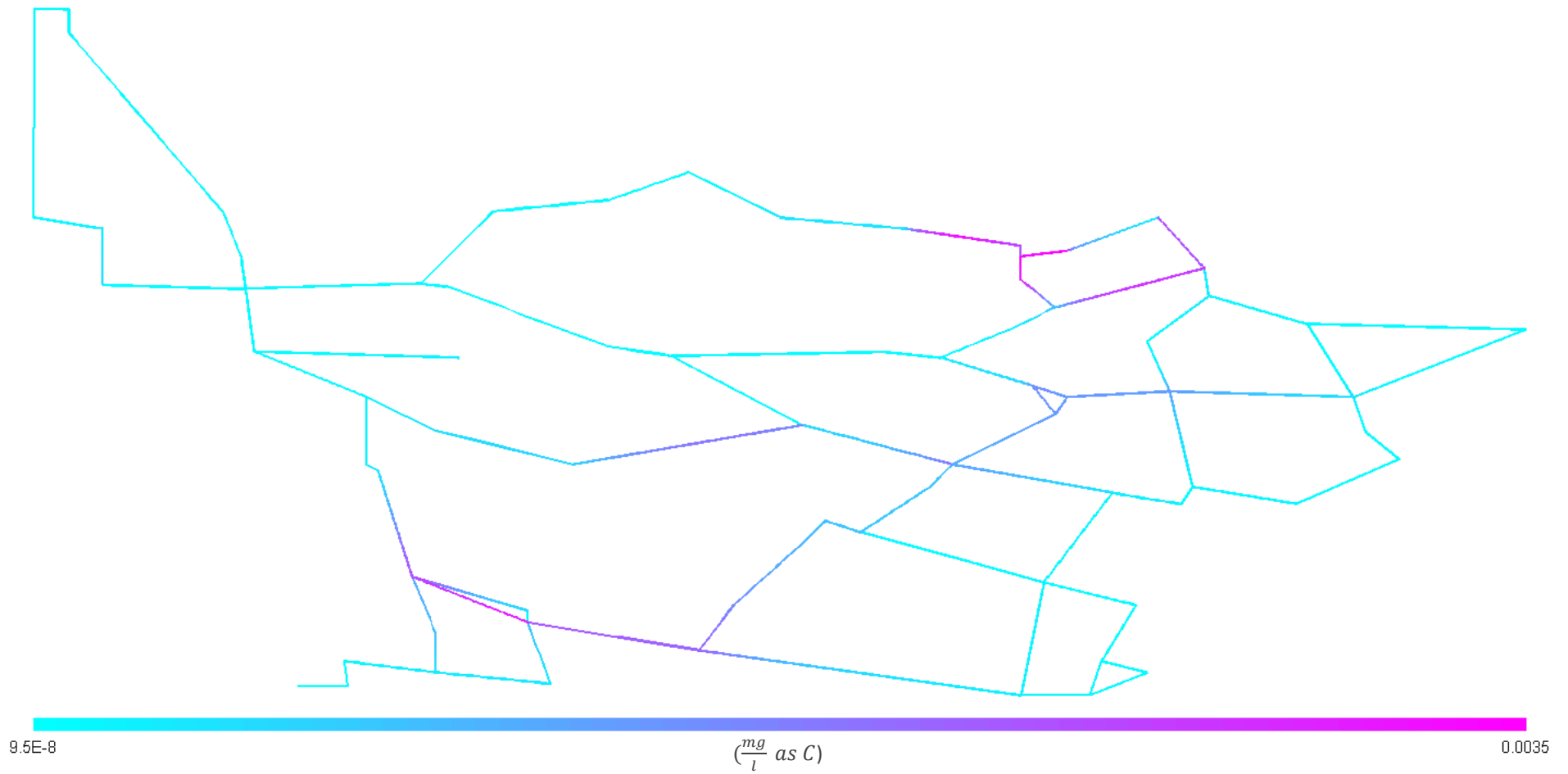


Figure 5-24: Suspended EPS concentration profile for Baseline Scenario

Suspended EPS production occurs in those zones where microbial growth is greatest. EPS is hydrolysed to form BAP and thus the concentration of suspended EPS approaches zero in the furthest reaches of the system.

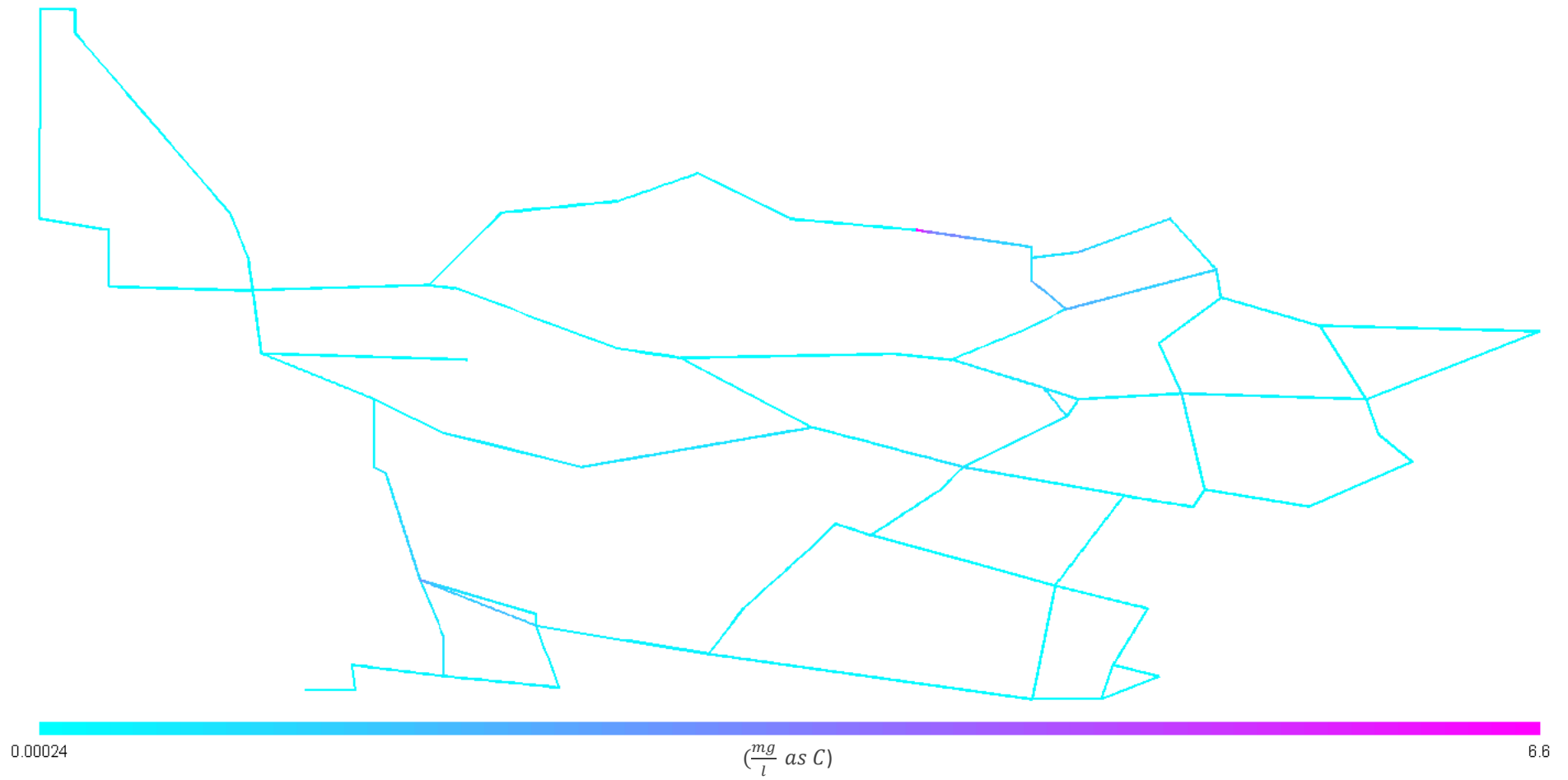


Figure 5-25: Fixed EPS concentration profile for Baseline Scenario

The fixed EPS concentration profile is similar to the suspended EPS profile, although the concentration of fixed EPS is significantly greater.

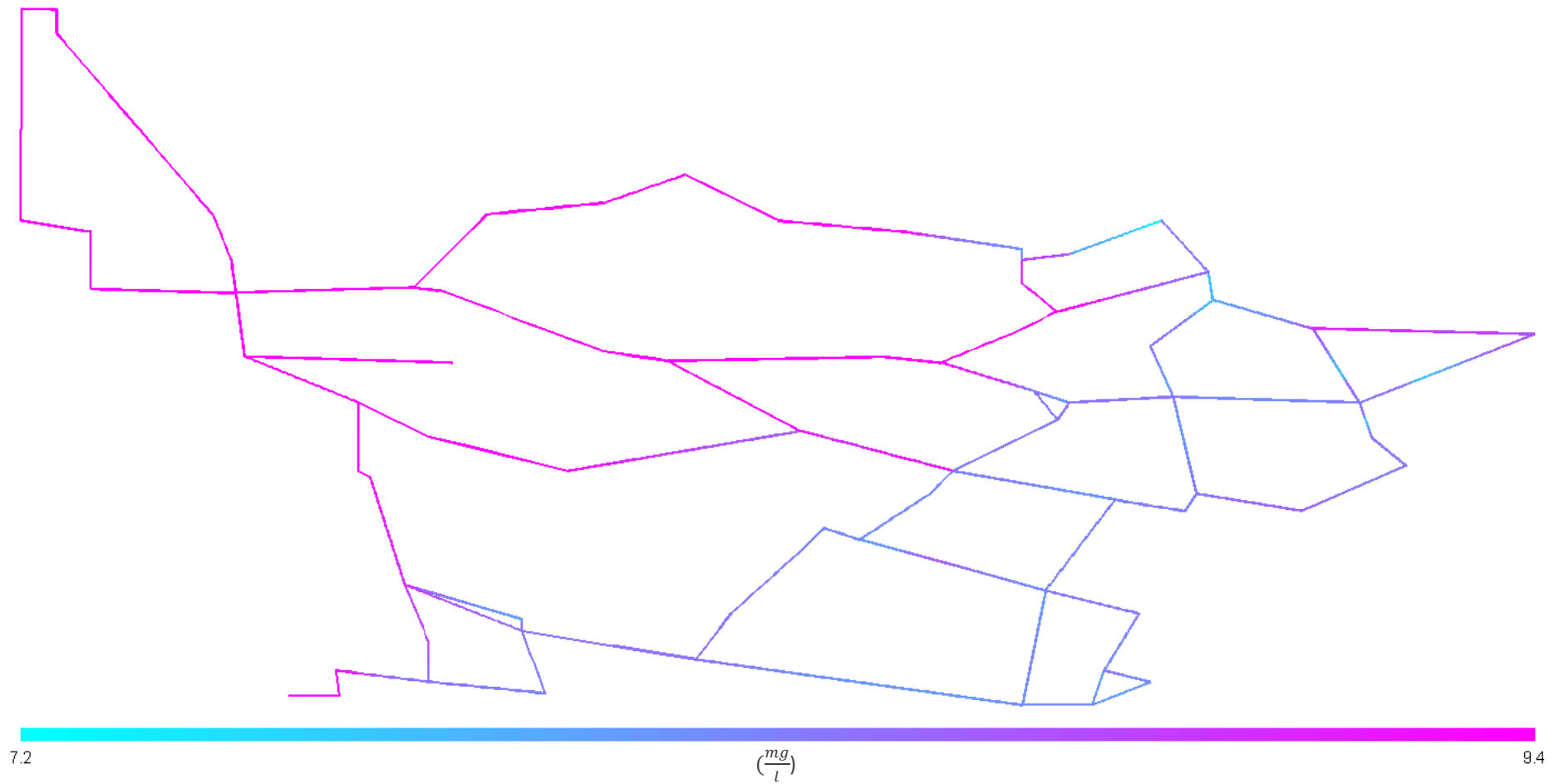


Figure 5-26: Dissolved oxygen concentration profile for Baseline Scenario

The oxygen concentration profile reflects the profile for that of active biomass. Where the active biomass concentration is greatest, oxygen is consumed more rapidly as an electron acceptor. As the oxygen concentration does not approach zero anywhere in the distribution system for this simulation, denitrification is not significant (Matějů et al, 1992; Biyela, 2010).

According to Sathasiven et al (2008), often it is difficult to determine whether nitrification is the primary cause of disinfectant decay or whether the growth of nitrifying bacteria is a consequence of disinfectant decay due to other mechanisms. However, such an analysis can be performed using the CDWQ-E₂ model. Loss of disinfectant due to nitrification refers to the loss of the disinfectant due to the oxidation of nitrite by the disinfectant. Therefore, for this simulation, as evidenced by Figure 5-4, it is clear that nitrification is not a significant mechanism resulting in the loss of monochloramine. However, as is demonstrated in the same figure, cometabolism of monochloramine by AOB is a significant loss mechanism for this scenario. Therefore, while nitrification itself is not a significant loss mechanism, the presence of AOB in significant concentrations is responsible for considerable monochloramine decay. Thus, for this simulation it can be concluded that the loss of monochloramine is most significantly due to surface catalysis and means other than nitrification produce ammonia, both of which increase the AOB stability factor, resulting in the growth of AOB and subsequent nitrification.

Mass Closure Check

Chemical Element	Total Change Over 60 Days (%)
Cl	-7×10^{-4}
N	-4×10^{-4}
C	-7×10^{-4}

Table 5-2: Mass-balance closure errors for baseline simulation

Table 5-2 demonstrates that the CDWQ-E₂ model is sound with regard to mass closure over the 60 day simulation period. The mass closure errors are similar for all alternatives tested in the section that follows. For all simulations, a time step of 1.2 minutes is used. This is the minimum time step deemed acceptable such that mass closure is not violated with regard to the requirement of pipe element sizing. Based on the sound mass closure results, there is no need to utilise a smaller time step, which would further increase the already large computational demands.

5.2.2 Remedial Alternatives

A significant benefit of understanding both the locations where disinfectant loss is greatest and the mechanisms responsible for this disinfectant loss, is that solutions specific to the problem can be devised and tested, with the aim of improving water quality. In addition to and in combination with this, stability factor analyses can be used to assess whether the substrate concentrations, combined with the disinfectant residual, are sufficiently low to ensure the biostability of drinking water.

Based on this simulation, it is clear that three major mechanisms are responsible for the considerable loss of disinfectant residual that occurs in the system: surface catalysis, cometabolism and the oxidation of organic matter. The stability factor analyses also show that microbial growth is significant for all three species of bacteria, particularly the biofilm bacteria, which suggests that in addition to reducing the loss of disinfectant residual, means of reducing the substrate available for the bacteria may improve biostability. This, in turn, would limit the growth of suspended heterotrophs and the production of nitrite (primarily caused by the excessive growth of AOB), both of which exceed the SANS 241-1:2011 limits in the baseline scenario.

Therefore, in the section that follows, the effectiveness of various remedial alternatives aimed at improving the biostability of the system will be tested in order to ensure that the water quality parameters within the system never exceed the relevant SANS determinand limits. The following alternatives are tested:

1. Reduce Surface Catalysis by Coating Concrete Pipes

In reality it may not be possible to replace concrete pipes with other, less reactive pipes throughout the distribution system. However, concrete pipes could be coated with surface binding agents such as polymer additives or a carbonate coating. This solution was suggested by Wooschlager (2000), who noted that it is only a theoretical strategy, although he estimated that it could reduce the rate of surface catalysis, i.e. the surface catalysis constants, by half. Given the problem with regard to surface catalysis for the simulation performed for this research, and based on the findings demonstrated in Figure 5-4, the impact of the same approach would be expected to improve the water quality of the system.

2. Use of Biofiltration at the Treatment Plant to Reduce Input BOM

The treatment plant inputs used in the baseline case are based on a treatment plant utilising rapid sand filters that are continually disinfected with free chlorine to prevent the accumulation of bacteria. The BOM substrate available for heterotrophic bacteria can be significantly reduced by converting these filters to biofilters. This, in turn, would be expected to limit the production of organic matter and hence the loss of disinfectant due to the oxidation of organic matter. The BOM inputs utilised for this case are based on the results given by Wooschlager (2000) which were determined using the CDWQ-Biofilter model (Wooschlager & Rittmann, 1995a, 1995b).

3. Use of a 1:1 Cl:N Ratio at the Treatment Plant to Reduce Input Ammonia

The baseline scenario assumes a Cl:N ratio of approximately 0.5, which results in excess ammonia entering the system at the treatment plant. The use of a 1:1 Cl:N ratio at the treatment plant to form chloramine reduces the excess ammonia input to zero (Woolschlager, 2000). This alternative would reduce the AOB stability factors for the system and thus the AOB concentration, thereby improving water quality for three reasons: firstly, it would reduce the formation of nitrite in the system; secondly, less organic matter would be produced, which would reduce the loss of disinfectant due to the oxidation of organic matter; finally, the loss of monochloramine due to cometabolism would be reduced.

4. Application of Booster Chloramination at Appropriate Sites

Booster chloramination can be used to ensure the maintenance of a disinfectant residual throughout a system (Carrico & Singer, 2009). The results of the baseline scenario can be used to determine the locations where significant disinfectant residual is lost, which are potential sites where booster chloramination may prove effective. Based on the baseline scenario, the effectiveness of installing booster chloramination at nodes 179 and 320 is tested in this alternative. An input concentration of $2.0 \frac{mg}{l}$ as Cl_2 is applied at node 179, and a concentration of $1.2 \frac{mg}{l}$ as Cl_2 is applied at node 320 to ensure that the maximum concentration of monochloramine in the system does not exceed the SANS 241-1:2011 limit of $3.0 \frac{mg}{l}$ as Cl_2 .

5. Improve Primary Disinfection

The concentration of suspended heterotrophs entering the distribution system following primary disinfection at the treatment plant is relatively large for the baseline scenario. If primary disinfection is improved, it would be possible to produce water at the treatment plant with a heterotrophic plate count of approximately $10 \frac{CFU}{ml}$ (Payment & Robertson, 2004). This can be converted to a value of either $0.018 \frac{ug\ COD}{l}$ or $43 \frac{cells}{ml}$ based on the assumptions given previously.

6. Reduce both Input BOM and Excess Ammonia

This Alternative is a combination of Alternatives 2 and 3. The rationale for this approach is that limiting the input BOM should limit heterotrophic growth and that limiting the ammonia input from the treatment plant should limit the excessive growth of AOB, which is responsible for excessive loss

of monochloramine due to cometabolism and the excessive production of nitrite in the baseline scenario. In addition, the total biomass in the system should be reduced, thereby reducing the loss of disinfectant to the oxidation of organic matter.

7. Reduce both Input BOM and Excess Ammonia, combined with Booster Chloramination

This Alternative tests the effectiveness of a booster chloramination input of $2.5 \frac{mg}{l}$ as Cl_2 at node 161 in order to reduce the heterotrophic growth that occurs in the furthest reaches of the distribution system for the previous alternative.

8. Reduce both Input BOM and Excess Ammonia, as well as Surface Catalysis by Coating Concrete Pipes

This Alternative compares the effectiveness of coating concrete pipes in order to reduce surface catalysis, in conjunction with reducing both input BOM and excess ammonia from the treatment plant.

Comparison of Alternatives

The effect of these alternatives on the water quality of the system is presented in this section, as well as an explanation for the effectiveness of the various alternatives. The maximum concentrations during any time period of the final day for each of the alternatives tested are compared against both the baseline case and the SANS 241-1:2011 limits relevant to the model. The full set of results for each alternative tested is presented in Appendix D.

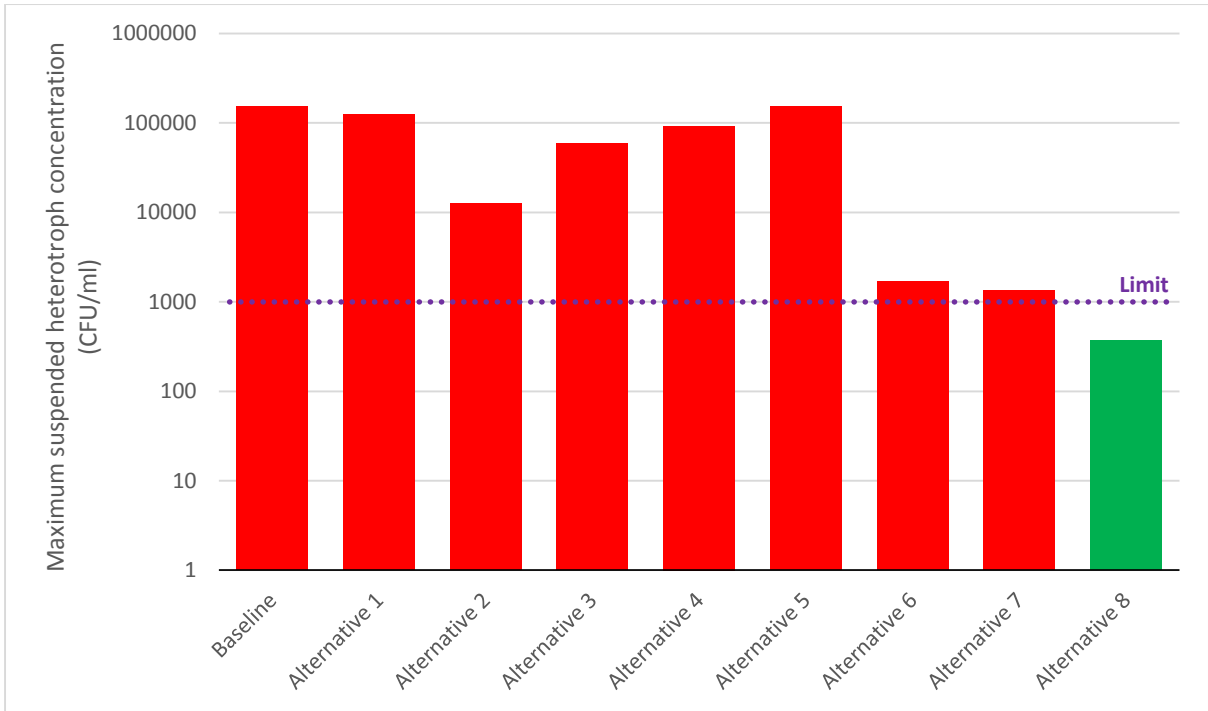


Figure 5-27: Comparison of Maximum Suspended Heterotroph Concentration for Various Simulations

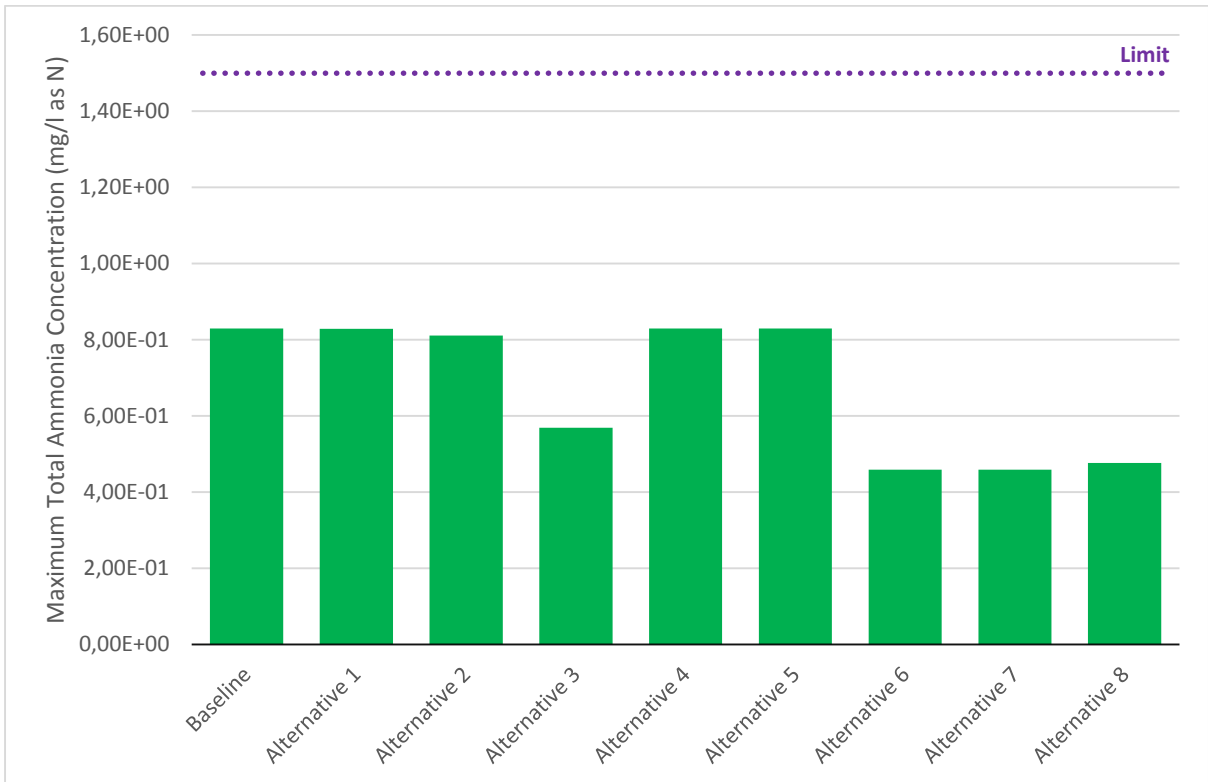


Figure 5-28: Comparison of Total Ammonia Concentration for Various Simulations

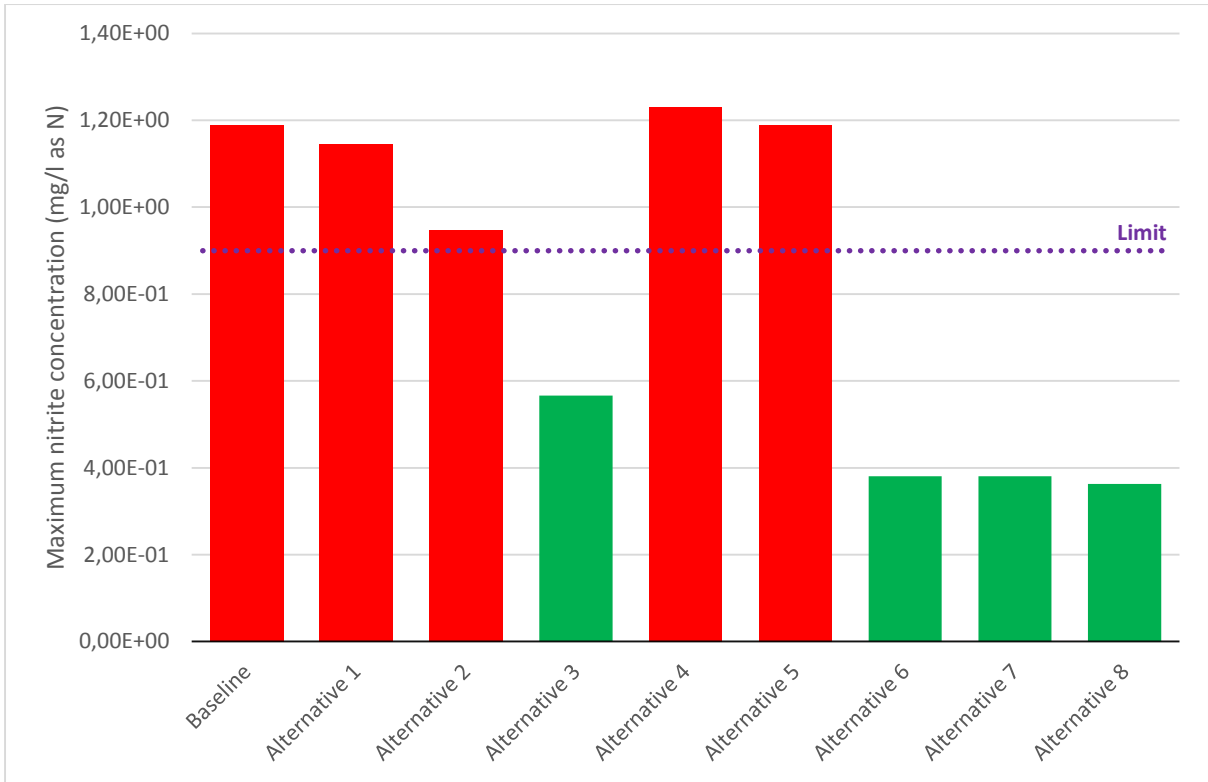


Figure 5-29: Comparison of Maximum Nitrite Concentration for Simulations

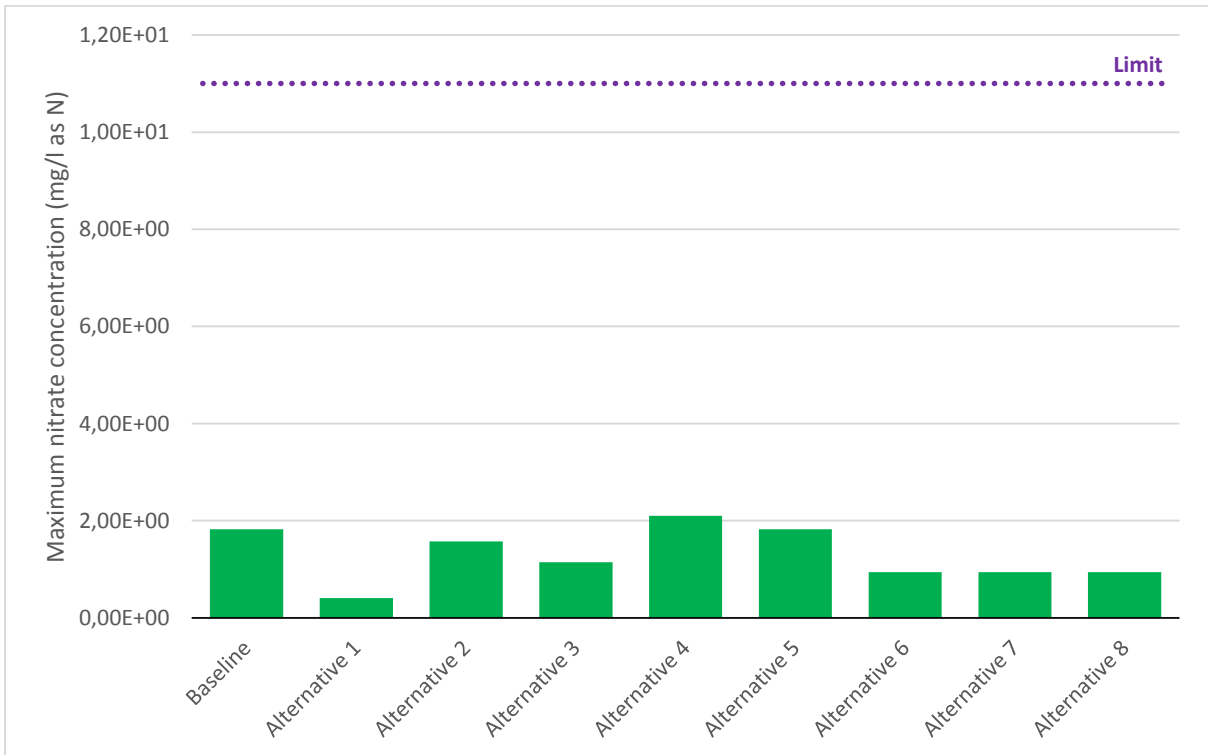
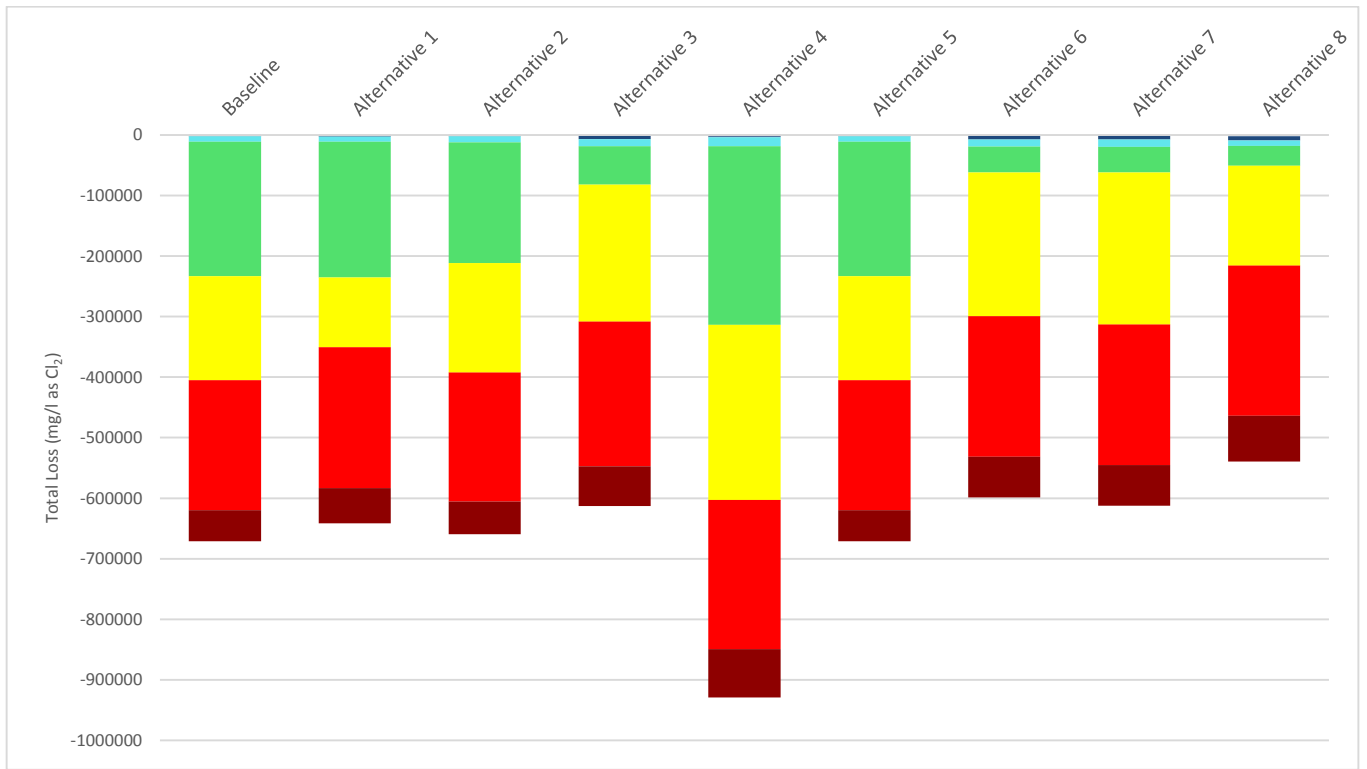
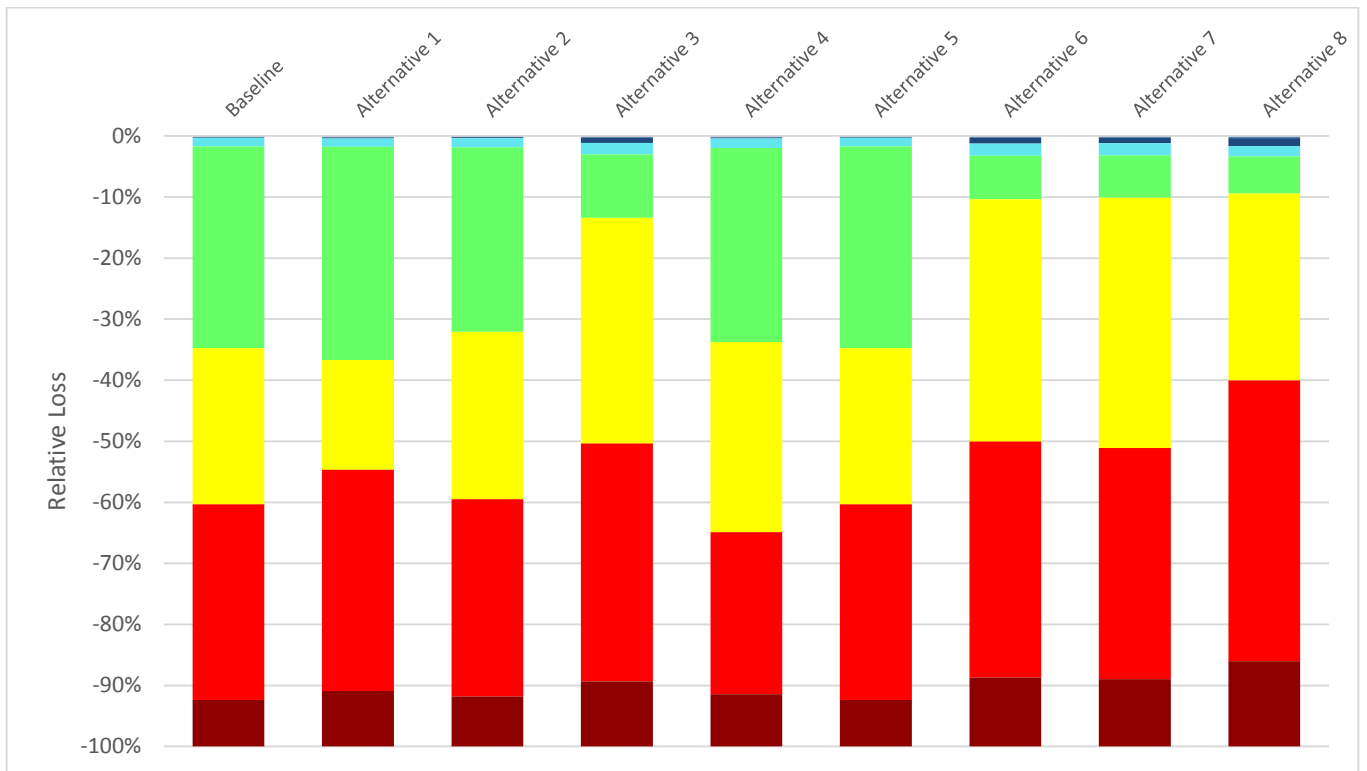


Figure 5-30: Comparison of Maximum Nitrate Concentration for Various Simulations



Autocatalytic decay reaction 1, Autocatalytic decay reaction 2, Autocatalytic decay reaction 3, Autocatalytic decay reaction 5, Cometabolism, Surface Catalysis, Oxidation of Nitrite, Oxidation of Organic Matter, Oxidation of Corrosion Products

Figure 5-31: Total loss of monochloramine for simulations performed due to various loss mechanisms



Autocatalytic decay reaction 1, Autocatalytic decay reaction 2, Autocatalytic decay reaction 3, Autocatalytic decay reaction 5, Cometabolism, Surface Catalysis, Oxidation of Nitrite, Oxidation of Organic Matter, Oxidation of Corrosion Products

Figure 5-32: Relative loss of monochloramine for all simulations performed due to various loss mechanisms

	Suspended Heterotrophs	Monochloramine	Ammonia	Nitrite	Nitrate
Baseline	Red	Green	Green	Red	Green
Alternative 1	Red	Green	Green	Red	Green
Alternative 2	Red	Green	Green	Red	Green
Alternative 3	Red	Green	Green	Green	Green
Alternative 4	Red	Green	Green	Red	Green
Alternative 5	Red	Green	Green	Red	Green
Alternative 6	Red	Green	Green	Green	Green
Alternative 7	Red	Green	Green	Green	Green
Alternative 8	Green	Green	Green	Green	Green

■ Within Acceptable Limits ■ Above Acceptable Limits

Figure 5-33: Comparison of simulation results with respect to SANS 241-1:2011 limits

The concentration of ammonia and nitrate within the system never exceeds the relevant limits. However, the concentration of suspended heterotrophs and nitrite is problematic for numerous simulations. The alternatives that aim to reduce the total ammonia input at the treatment plant (Alternatives 3, 6, 7 and 8) are all successful in reducing the maximum nitrite concentration to within acceptable limits. By reducing the ammonia concentration, less substrate is available for both the suspended and fixed AOB within the system, and hence the utilisation of ammonia and subsequent formation of nitrite decreases. In addition, the concentration of AOB also decreases, and consequently the loss of monochloramine due to cometabolism decreases. This result contributes to decreased microbial growth for all three modelled species, namely heterotrophs, AOB and NOB. However, the contribution of reducing the loss of monochloramine due to cometabolism alone is not significant enough to reduce the maximum heterotrophic concentration within the system below acceptable limits.

Any alternative that does not include reducing the excess ammonia input at the treatment plant is incapable of reducing the maximum nitrite concentration below acceptable limits. These are Alternatives 1, 2, 4 and 5. Alternative 1 aims to reduce the loss of monochloramine due to surface catalysis in order to reduce both the concentration of suspended heterotrophs and indirectly reduce the formation of nitrite in the system. However, this alternative applied in isolation is not effective, as despite the fact that the loss of monochloramine due to surface catalysis is reduced, the total loss of monochloramine is similar to the baseline case. This is because the loss of monochloramine due to cometabolism, the oxidation of organic matter and the oxidation of corrosion products are

functions of monochloramine concentration. Consequently, the effectiveness of reducing the rate of catalysis on the total loss of monochloramine is limited in this scenario, as the three aforementioned loss mechanisms, particularly the loss of monochloramine due to the oxidation of organic matter, become more significant.

Alternative 2 aims to reduce the BOM substrate input at the treatment plant, which is required for heterotrophic growth. Despite significantly reducing the maximum heterotroph concentrations in the system, the maximum values still greatly exceed the stipulated limit. This is because Alternative 2 has little effect on the loss of residual disinfectant in the furthest reaches of the system. It is particularly interesting to note that the loss of monochloramine due to the oxidation of organic matter is largely unchanged in Alternative 2, despite significantly reducing the substrate available for heterotrophic growth. Consequently, excessive heterotrophic growth can occur, even in the presence of limited substrate. In addition, as this approach has a limited effect on the disinfectant residual and hence total ammonia concentrations, it is not successful in decreasing the maximum nitrite concentration below acceptable limits.

The application of booster chloramination at nodes 179 and 320 in Alternative 4 has a limited effect on the relevant determinands. The booster chloramine applied at node 179 results in the maintenance of a significant disinfectant residual in the pipe sections near this node, and hence the biostability of the system in this region improves. However, the booster chloramine applied at node 320 rapidly depletes, resulting in this booster site having a limited effect on biostability in this region. The flow from node 320 is always into pipe 746, which is a concrete pipe. For the baseline case, cometabolism is a significant loss mechanism in this pipe. The application of booster disinfection considerably reduces the AOB concentration in this pipe and hence the loss of monochloramine due to cometabolism in this pipe. However, this is offset by the increase in the loss of monochloramine that occurs due to surface catalysis in this pipe, as the loss of monochloramine due to surface catalysis is a function of the monochloramine concentration squared.

Alternative 5 refers to improving the effectiveness of primary disinfection in order to reduce the input of suspended heterotrophs at the treatment plant. The effectiveness of this approach is negligible. It has no effect on the concentration of the BOM substrate or the concentration of the disinfectant residual throughout the system. Most significantly, the maximum suspended heterotroph concentrations in the system are very similar to the baseline scenario. This suggests that the detachment of biofilm bacteria is a more significant reason for the high suspended heterotroph concentrations for the simulations performed, as opposed to the high concentration of suspended heterotrophs introduced at the treatment plant for the baseline scenario. These findings

are in agreement with those made by Dukan et al (1996) who found that the detachment of bacterial biomass is primarily responsible for the occurrence of suspended biomass.

Alternative 6 is a combination of Alternatives 2 and 3 and thus this alternative refers to reducing both the ammonia and BOM input at the treatment plant. Combining these approaches significantly increases the disinfectant residual throughout the system by reducing monochloramine loss caused by cometabolism, and directly decreases the substrate available for heterotroph and AOB growth, and indirectly reduces the substrate available for NOB growth. This significantly improves the biostability of the system, and consequently the maximum nitrite concentration (which is formed due to AOB growth) is well below the stipulated limit, and the maximum heterotroph concentration is only slightly greater than the maximum allowable limit in a few pipes in the furthest reaches of the system.

In Alternative 7, in order to reduce the excessive heterotrophic growth that occurs in a small number of pipes in Alternative 6, booster chloramination is applied at node 161 in addition to the measures introduced in Alternative 6. This node is adjacent to the pipes with excessive heterotrophic concentrations and the predominant direction of flow is from this node towards the aforementioned pipes. Alternative 7 is unsuccessful in reducing the maximum concentration of suspended heterotrophs below acceptable limits. The reason for this is that monochloramine loss due to surface catalysis becomes significant in pipes 482 and 484, which are the pipes adjacent to the booster site. The loss of monochloramine is so great in these two pipes that little monochloramine input at the booster site is able to permeate the system. Surface catalysis in these two pipes is significant for two reasons: firstly, loss due to surface catalysis is a function of the square of the monochloramine concentration, and hence the effectiveness of booster chloramination is limited for concrete pipes; secondly, the flow rates in these pipes are low, resulting in increased detention times, thereby compounding the problem.

Given the problem with regard to booster chloramination described above, Alternative 8 tests the effectiveness of reducing the rate of surface catalysis, in addition to the measures introduced as part of Alternative 6. Surface catalysis is the most significant monochloramine loss mechanism for Alternative 6, and this approach significantly reduces the rate of monochloramine loss due to catalysis compared to Alternative 6. In addition, the loss of monochloramine due to cometabolism is significantly reduced compared to the baseline case due to the reduced ammonia substrate available for AOB. The loss of monochloramine due to the oxidation of organic matter increases slightly, as disinfectant loss due to this mechanism is a function of monochloramine concentration, but this does not offset the reduced loss of disinfectant due to the two aforementioned mechanisms.

Consequently, the total loss of monochloramine in the system is reduced. Therefore, the disinfectant residual in the furthest reaches of the system, where heterotrophic growth is greatest, is significantly increased, and hence the maximum suspended heterotrophic concentration in the system is reduced to within acceptable limits. Furthermore, the maintenance of an adequate disinfectant residual in the furthest reaches of the system is beneficial as it would provide some protection from potential microbial growth that could occur in the occurrence of a contamination event.

6 SUMMARY AND RECOMMENDATIONS FOR FUTURE RESEARCH

6.1 Summary

The CDWQ-E₂ model represents a significant development in the field of water quality modelling. Many of the manual processes required in order to run the original CDWQ model have been automated, including pipe element sizing, element node creation, initial pipe element concentration calculations and flow direction determination. Furthermore, the model utilises the latest advancements in microbial growth modelling, as given by the Unified Theory of Laspidou and Rittmann (2002a, 2002b), and incorporated in the preceding CDWQ-E model (Biyela, 2010). Crucially, the CDWQ-E₂ model advances the preceding version by accounting for the transport of dissolved and suspended constituents throughout a distribution system. Consequently the CDWQ-E₂ model is capable of modelling:

- The advective transport of suspended and dissolved constituents throughout a distribution system.
- The transport of suspended and dissolved constituents both into and out of reservoirs and/or storage tanks.
- The growth of biofilm bacteria on pipe and reservoir walls and the transfer of bacteria between the suspended and the fixed state.
- The dual requirement of both electron donor and electron acceptor for both substrate utilisation and microbial growth.
- The diversion of electrons from the substrate to produce bound extracellular polymeric substances and utilisation products, in accordance with the Unified Theory developed by Laspidou and Rittmann (2002a, 2002b).
- The loss of residual disinfectant(s) due to both bulk-water and wall-loss reactions.
- The effect of residual disinfectant(s) on the net growth of a given bacteria.
- The potential for denitrification within a drinking water distribution system.

Various tools have also been incorporated as part of the CDWQ-E₂ model. These tools improve the interpretive capabilities of the model. Most significantly, the E₂ version is capable of assessing both the locations where disinfectant loss is significant and the specific mechanisms responsible for disinfectant loss. Another significant improvement is that concentration profiles for each of the 24 modelled species can be plotted, further enhancing the interpretive capabilities of the model. Furthermore, the stability factor equations developed by Wooschlager (2000) have been updated to

account for the diversion of electrons from the substrate to produce bound extracellular polymeric substances and utilisation products, in accordance with the Unified Theory developed by Laspidou and Rittmann (2002a, 2002b), as well as the availability of an electron acceptor and anoxic respiration by heterotrophs.

6.2 Future Research

Ultimately, as part of a separate project, the CDWQ-E₂ model is intended to be applied to a section of Johannesburg Water's distribution network. This will require an extensive monitoring programme and set of experiments to be designed and implemented. While it is beyond the scope of this project to design the required experiments and monitoring programme, a brief overview of the requirements to apply the model to a section of Johannesburg Water's distribution network is provided below.

The biodegradable organic parameters utilised for this project are based on available literature. However, these parameters are location specific and consequently biodegradable dissolved organic carbon (BDOC) tests should be used to obtain specific values for the system to be assessed. Following this, batch tests can be used in order to calibrate the model for use with free chlorine, as free chlorine is used as a secondary disinfectant by Rand Water, the utility that supplies Johannesburg Water with potable water. Batch tests can be used to determine the oxidation constants for free chlorine with reduced organic matter and the disinfection constants for free chlorine acting on both suspended and fixed species of heterotrophs and nitrifying bacteria. The constants accounting for the wall-decay of free chlorine, which will be dependent on the pipe materials of the distribution system to be assessed, can be determined by fitting the modelled results to the real distribution system data.

In addition, a detailed water monitoring programme for the section of the distribution system to be assessed must be designed and implemented over an extended period of time. A sufficient number of monitoring sites must be selected to accurately represent the water quality characteristics of the system and crucially biofilm sampling sites must be provided. As part of this monitoring programme, all of the species tracked by the E₂ model must be monitored. The sampling frequency for each species must be selected based on the variability of each species.

Finally, it is imperative that the area to be studied is characterised by well-defined hydraulics as the water quality solution is dependent on the accuracy of the hydraulic model.

7 REFERENCES

- American Water Works Association. (2002). *Effects of Water Age on Distribution System Water Quality*. Washington D.C.: U.S. Environmental Protection Agency.
- American Water Works Association. (2005). *Computer Modeling of Water Distribution Systems: AWWA Manual M-32*. Denver, Colorado: American Water Works Association.
- American Water Works Association. (2005). *Computer Modeling of Water Distribution Systems: AWWA Manual M-32*. Denver, Colorado: American Water Works Association.
- American Water Works Association Research Foundation. (2007). *Advancing the Science of Water: AwwaRF and Distribution System Water Quality*. USA: American Water Works Association.
- American Water Works Association; Economic and Environmental Engineering Services, Inc. . (2002). *Nitrification*. Washington D.C.: Environmental Protection Agency.
- Angles, M., & Chandy, J. (2001). Determination of Nutrients Limiting Biofilm Formation and the Subsequent Impact on Disinfectant Decay. *Water Research*, 35(11), 2677–2682.
- Arevalo, J. M. (2007). *Modeling Free Chlorine & Chloramine Decay in a Pilot Distribution System*. Orlando, Florida: Ph.D. Thesis, University of Central Florida.
- Bae, W., & Rittmann, B. E. (1996). A structured Model of Dual-Limitation Kinetics. *Biotechnology and Bioengineering*, 49(6), 683-689.
- Bakke, R., Trulear, M. G., Robinson, J. A., & Characklis, W. G. (1984). Activity of *Pseudomonas aeruginosa* in biofilms: steady state. *Biotechnol. Bioeng.*, 26(12), 1418-1424.
- Baribeau, H., Pozos, N., Boulos, L., Crozes, G., Gagnon, G., Rutledge, S., . . . Warn, E. (2005). *Impact of Distribution System Water Quality on Disinfection Efficacy*. Denver, Colorado: AwwaRF.
- Berman, D., Rice, E., & Hoff, J. (1988). Inactivation of Particle-Associated Coliforms by Chlorine and Monochloramine. *Appl. Environ. Microbiol.*, 54(2), 507-512.
- Bitton, G. (1994). Role of Microorganisms in Biogeochemical Cycles. In G. Bitton, *Wastewater Microbiology* (pp. 51-73). New York: John Wiley.
- Biyela, P. T. (2010). *Water Quality Decay and Pathogen Survival in Drinking Water Distribution Systems*. Phoenix, Arizona: Ph.D. Thesis, University of Arizona.
- Bocoş, A., Ciatarâş, D., & Farkas, B. (2012). Biofilms Impact on Drinking Water Quality. In K. Voudouris, *Ecological Water Quality – Water Treatment and Reuse* (pp. 141-160). 2012: InTech.
- Bouchard, D., Williams, M., & Surampalli, R. (1992). Nitrate Contamination of Groundwater: Sources and Potential Health Impacts. *J. Amer. Water Works Assoc.*, 84(9), 84-90.
- Brocca, D., Arvin, E., & Mosbaek, H. (2002). Identification of organic compounds migrating from polyethylene pipelines into drinking water. *Water Res.*, 36(15), 3675-3680.

- Bull, R. J., & Kopfler, F. C. (1991). Chloramine by-product profiles. In R. J. Bull, F. C. Kopfler, & J. Richard, *Health effects of disinfectants and disinfection by-products* (p. 36). Denver, Colorado: AWWA Research Foundation.
- Burlingame, G., Choi, J., Fadel, M., Gammie, L., Rahman, J., & Paran, J. (1994). Stiff New Mains ... Before Customers Complain. *Opflow*, 20(10), 3.
- Burman, N. (1965). Taste and Odor due to Stagnation and Local Warming in Long Lengths of Piping. *Symposium on consumer complaints*. 14, pp. 125-131. Proceeding of the Society for Water Treatment and Examination.
- Burman, N. (1973). The Occurrence and Significance of Actinomycetes in Water Supply. In G. Sykes, & F. Skinner, *Actinomycetales; Characteristics and Practical Importance* (pp. 219-230). London and New York: Academic Press.
- Camper, A., Brastrup, K., Sandvig, K., Clement, J., Spencer, C., & Capuzzi, A. (2003). Effect of Distribution System Materials on Bacterial Growth. *J. Am. Water Works Assoc*, 95(7), 107-121.
- Camper, A., Goodrum, L., & Jones, W. (1997). Comparison of Chlorine and Monochloramine for the Control of Biofilm in Model Distribution System Biofilms. *The AWWA Water Quality Technology Conference*. Denver, Colorado: AWWA.
- Can, Z. S. (2014). Acid-Base Speciation as a Function of pH. *ENV209: Environmental Engineering Process Chemistry*. Istanbul: Marmara Üniversitesi Bilişim Merkezi.
- Carrico, B., & Singer, P. (2009). Impact of Booster Chlorination on Chlorine Decay and THM Production: Simulated Analysis. *Journal of Environmental Engineering*, 135(10), 928–935.
- Chadwick, A., & Morfett, J. (1993). *Hydraulics in civil and environmental engineering* (1st ed.). London: E & FN Spon.
- Chadwick, A., Morfett, J., & Borthwick, M. (2004). *Hydraulics in Civil and Environmental Engineering* (4th ed.). Abingdon, Oxfordshire: Spon Press.
- Chambless, J., Hunt, S., & Stewart, P. (2006). A three-dimensional computer model of four hypothetical mechanisms protecting biofilms from antimicrobials. *Applied Environmental Microbiology*, 72(3), 2005-2013.
- Chang, H., & Rittmann, B. (1988). Comparative Study of Biofilm Shear Loss on Different Adsorptive Media. *Biotechnol. Bioeng.*, 60(3), 499-506.
- Chen, C., Griebel, T., & Characklis, W. (1993). Biocide Action of Monochloramine on Biofilm Systems of *Pseudomonas aeruginosa*. *Biofouling*, 7(1), 1-17.
- Chen, X., & Stewart, P. (1996). Chlorine Penetration into Artificial Biofilm is Limited by a Reaction-Diffusion Interaction. *Environ. Sci. Technol.*, 30(6), 2078-2083.
- Clark, M. (1992). Water quality modeling in distribution systems. *Journal of Environmental Science & Health*, 25(2), 1329-1366.

- Clark, R. M., Grayman, W. M., Males, R. M., & Hess, A. (1993). Modeling contaminant propagation in drinking-water distribution systems. *Journal of Environmental Engineering*, 119(2), 349-364.
- Clark, R., & Haught, R. (2005). Characterizing Pipe Wall Demand: Implications for Water Quality Modeling. *Journal of Water Resources Planning & Management*, 131(3), 208-217.
- Clark, R., & Males, R. (1986). Developing and Applying the Water Supply Simulation Model. *J. Amer. Water Works Assoc.*, 78(8), 61-65.
- Costerton, J. (1994). Structure of biofilms. In H. Flemming, G. Geesey, & Z. Lewandowski, *Biofouling and Biocorrosion in Industrial Water Systems*. United States of America: Lewis Publishers.
- Costerton, J., Caldwell, D., Korber, D., Lappin-Scott, H., & Lewandowski, Z. (1995). Microbial Biofilms. *Annual Review of Microbiology*, 49(1), 711-745.
- Costerton, J., Geesey, G., & Cheng, K. (1978). How Bacteria Stick. *Sci. Amer.*, 238(1), 86-95.
- Cross, H. (1936). Analysis of flow in network of conduits or conductors. *Engineering Experiment Station. Bulletin; no. 286*. Urbana: University of Illinois.
- Cuncliffe, D. A. (1991). Bacterial nitrification in chloraminated water supplies. *Appl. Environ. Microbiol.*, 57(11), 3399-3402.
- Davidson, J., Bouchart, F., Cavill, S., & Jowitt, P. (2005). Real-Time Connectivity Modeling of Water Distribution Networks to Predict Contamination Spread. *J. Comput. Civ. Eng.*, 19(4), 377-386.
- de Beer, D., Srinivasan, R., & Stewart, P. (1994). Direct Measurement of Chlorine Penetration into Biofilms During Disinfection. *Appl. Environ. Microbiol.*, 60(12), 4339-4344.
- De Roos, A., Ward, M., Lynch, C., & Cantor, K. (2003). Nitrate in Public Water Supplies and the Risk of Colon and Rectum Cancers. *Epidemiology*, 14(6), 640-649.
- de Silva, D. G., & Rittmann, B. E. (2000). Nonsteady-State Modeling of Multispecies Activated-Sludge Processes. *Water Environment Research*, 72(5), 554-565.
- DiGiano, F. A., & Zhang, W. (2005). Pipe section reactor to evaluate chlorine-wall reaction. *Journal AWWA*, 97(1), 74-85.
- Diyamandoglu, V. (Water Sci. Technol.). Nitrate and chloride formation in chloramination. 1994, 30(9), 101-110.
- Dodge, D., Francis, A., Gillow, J., Halada, G., & Clayton, C. (2002). Association of Uranium with Iron Oxides Typically Formed on Corroding Steel Surfaces. *Environ. Sci. Technol.*, 36(16), 3504-3511.
- Doutero, I., Boxall, J. B., Deines, P., Sekar, R., Fish, K. E., & Biggs, C. A. (2014). Methodological approaches for studying the microbial ecology of drinking water distribution systems. *Water Research*, 65, 134-156.

- Dukan, S., Levi, Y., Piriou, P., Guyon, F., & Villon, P. (1996). Dynamic Modelling of Bacterial Growth in Drinking Water Networks. *Wat. Res.*, 30(9), 1991-2002.
- Eberl, H., Morgenroth, E., Noguera, D., Picioreanu, C., Rittmann, B., van Loosdrecht, M., & Wanner, O. (2006). *Mathematical Modeling of Biofilms*. London: IWA Publishing.
- Ely, R. L., Guenther, K. J., Hyman, M. R., & Arp, D. J. (1995). A cometabolic kinetics model incorporating enzyme inhibition, inactivation, and recovery: Model development, analysis and testing. *Biotechnol Bioeng*, 54, 218-231.
- Escobar, I. C., & Randall, A. A. (2001). Assimilable Organic Carbon (AOC) and Biodegradable Dissolved Organic Carbon (BDOC): Complimentary Measurements. *Wat. Res.*, 35(18), 4444-4454.
- Fransolet, G., Villers, G., & Masschelin, W. (1985). Influence of Temperature on Bacterial Development in Waters. *Ozone Sci.Eng.*, 7(3), 205-227.
- Furumai, H., & Rittmann, B. (1992). Advanced modeling of mixed populations of heterotrophs and nitrifiers considering the formation and exchange of soluble microbial products. *Water Sci. Technol.*, 26(3/4), 493-502.
- Geldreich, E. (1996). *Microbial Quality of Water Supply in Distribution Systems*. New York: Lewis Publishers.
- Grayman, W., Clark, R., & Males, R. (1988). Modeling Distribution System Water Quality: A Dynamic Approach. *American Water Works Association*, 114(3), 67-77.
- Griebe, T., Chen, C., Srinivasan, R., & Stewart, P. (1994). Analysis of Biofilm Disinfection by Monochloramine and Free Chlorine. In G. Geesey, Z. Lewandowski, & H. Flemming, *Biofouling and Biocorrosion in Industrial Systems* (pp. 151-161). Boca Raton, Florida: CRC Press.
- Haas, C. (1999). Disinfection. In R. Letterman, *Water Quality and Treatment: A Handbook of Community Water Supplies*. 5th ed (pp. 14.1-14.60). New York: McGraw-Hill.
- Haas, C., & Karra, S. (1984). Kinetics of Microbial Inactivation by Chlorine – I: Review of Results in Demand-Free Systems. *Water Res.*, 18(11), 1443-1449.
- Hallam, N. B., West, J. R., Forster, C. F., Powell, J. C., & Spence, I. (2002). The decay of chlorine associated with the pipe wall in water distribution systems. *Water Research*, 36(14), 3479-3488.
- Hallam, N., West, J., Forster, C., & Simms, J. (2001). The Potential for Biofilm Growth in Water Distribution Systems. *Water Research*, 35(17), 4063-4071.
- Hand, V. C., & Margerum, D. W. (1983). Kinetics and mechanisms of the decomposition of dichloramine in aqueous solution. *Inorg. Chem*, 22, 1449-1456.
- Helbling, D. E., & VanBriesen, J. M. (2009). Modeling Residual Chlorine Response to a Microbial Contamination Event in Drinking Water Distribution Systems. *Journal of Environmental Engineering*, 135(10), 918-927.

- Helmi, K., Skraber, S., Gantzer, C., Williame, R., Hofmann, L., & Cauchie, H. (2008). Interactions of *Cryptosporidium parvum*, *Giardia lamblia*, vaccinal poliovirus type 1 and bacteriophages ϕ X174 and MS2 with a drinking water biofilm and a wastewater biofilm. *Appl. Environ. Microb.*, 74(7), 2079-2088.
- Henning, L., Junha, T., Korth, A., & Rubulis, J. (2007). *Methodology of Modeling Bacterial Growth in Drinking Water Systems*. Techneau.
- ISO 5807:1985. Information processing - Documentation, symbols and conventions for data, program and system flowcharts, program network charts and system resources charts. (1985). Geneva: International Standards Organisation.
- Jacangelo, J., & Olivieri, V. (1985). Aspect of the Mode of Action of Monochloramine. In W. Davis, S. Katz, M. Roberts, & V. Jacobs, *Water, Chlorination, Chemistry, Environmental Impact and Health Effects* (pp. 575-586). Chelsea, Michigan: Lewis Publishers.
- Jafvert, C., & Valentine, R. (1992). Reaction Scheme for the Chlorination of Ammoniacal Water. *Environ. Sci. Technol.*, 26(3), 577-586.
- Jegatheesean, V., Kastl, G., Fisher, I., Chandy, J., & Angles, M. (2003). Water Quality Modelling for Drinking Water Distribution Systems. *International Congress on Modelling and Simulation* (pp. 332-337). Townsville, QLD, Australia: Modelling and Simulation Society of Australia and New Zealand.
- Johnson, D. W., & Margerum, D. W. (1991). Non-metal redox kinetics: A re-examination of the mechanism of the reaction between hypochlorite and nitrite ions. *Inorg. Chem.*, 30, 4845-4851.
- Joret, J., Laurent, P., Prévost, M., & Servais, P. (2005). *Biodegradable Organic Matter in Drinking Water Treatment and Distribution*. United States of America: American Water Works Association.
- Junha, T. (2002). Aspects of drinking water supply in areas of humic water. *Academic Dissertation*. Lulea University of Technology.
- Kaplan, L. A., Bott, T. L., & Reasoner, D. J. (1993). Evaluation and Simplification of the Assimilable Organic Carbon Nutrient Bioassay for Bacterial Growth in Drinking Water. *American Society for Microbiology*, 59(5), 1532-1539.
- Khiari, D., Barrett, S., Chinn, R., Bruchet, A., Piriou, P., Matia, L., . . . Leutweiler, P. (2002). *Distribution Generated Taste-and-Odour Phenomena*. Denver, Colorado: AwwaRF.
- Kiene, L., Lu, W., & Levi, Y. (1998). Relative importance of the phenomena responsible for chlorine decay in drinking water distribution systems. *Water Sci. Technol.*, 38(6), 219-227.
- Kirmeyer, G., Foust, G., Pierson, G., Simmler, J., & Le Chevallier, M. (1993). *Optimising Chloramine Treatment*. Denver, Colorado: Awwa Research Foundation and AWWA.

- Krasner, S. W., McGuire, M. J., Jacangelo, J. G., Patania, N. L., Reagan, K. M., & Aieta, E. M. (1989). The occurrence of disinfection by-products in US drinking water. *Journal-American Water Works Association*, 81(8), 41-53.
- Lansey, K., & Boulos, P. (2005). *Comprehensive Handbook on Water Quality Analysis for Distribution Systems*. Broomfield, Colorado: MWH Soft.
- Laspidou, C., & Rittmann, B. (2002a). A unified theory for extracellular polymeric substances, soluble microbial products, and active and inert biomass. *Water Research*, 36(11), 2711–2720.
- Laspidou, C., & Rittmann, B. (2002b). Non-steady state modeling of extracellular polymeric substances, soluble microbial products, and active and inert biomass. *Water Research*, 36(8), 1983-1992.
- Laspidou, C., & Rittmann, B. (2004). Evaluating trends in biofilm density using the UMCCA model. *Water Research*, 38(14), 3362–3372.
- Le Puil, M. (2004). *Biostability in Drinking Water Distribution Systems: Study at Pilot-Scale*. Orlando, Florida: Ph.D. dissertation, University of Central Florida.
- LeChevallier, M. (1990). Coliform Regrowth in Drinking Water: A review. *Journal of the AWWA*, 82(11), 74-86.
- LeChevallier, M. W., Lowry, C. O., Lee, R. G., & Gibbon, D. L. (1993). Examining the relationship between iron corrosion and the disinfection of biofilm bacteria. *Journal of American Water Works Association*, 85(7), 111-123.
- LeChevallier, M., Babcock, T., & Lee, R. (1987). Examination and characterization of distribution system biofilms. *Appl. Environ. Microbiol.*, 53(12), 2714-2724.
- LeChevallier, M., Cawthon, C., & Lee, R. (1988a). Factors Promoting the Survival of Bacteria in Chlorinated Water Supplies. *Appl. Environ. Microbiol.*, 54(3), 649-654.
- LeChevallier, M., Cawthon, C., & Lee, R. (1988b). Inactivation of Biofilm Bacteria. *Applied Environmental Microbiology*, 54(10), 2714-2724.
- LeChevallier, M., Lowry, C., & Lee, R. (1990). Disinfecting biofilms in a model distribution system. *J. Am. Water Works Assoc.*, 82(7), 87-99.
- LeChevallier, M., Schulz, W., & Lee, R. (1991). Bacterial Nutrients in Drinking Water. *Applied Environmental Microbiology*, 57(3), 857-862.
- Lemke, A., & DeBoer, D. E. (2012). *Effect of storage tank mixing on water quality*. Brookings: Water & Environmental Engineering Research Centre South Dakota State University.
- Liu, S., Taylor, J. S., Randall, A. A., & Dietz, J. D. (2005). Nitrification modeling in chloraminated distribution systems. *Journal (American Water Works Association)*, 97(10), 98-108.

- Lowther, E., & Moser, R. (1984). Detecting and Eliminating Coliform Regrowth. *In Proceedings of the AWWA, Water Quality Technical Conference* (pp. 413-414). Denver, Colorado: American Water Works Association.
- Lu, C. (1991). *Theoretical Study of Particle, Chemical and Microbial Transport in Drinking Water Distribution Systems*. Cincinnati: Ph.D. Thesis, University of Cincinnati.
- Lu, C., Biswas, P., & Clark, R. (1995). Simultaneous Transport of Substrates, Disinfectants and Microorganisms in Water Pipes. *Wat. Res.*, 29(3), 881-894.
- Lytle, D., Sorg, A., & Frietch, C. (2004). The Accumulation of Arsenic in Water Distribution Systems. *Environ. Sci. Technol.*, 38(20), 5365-5372.
- Lytle, D., Sorg, T., & Frietch, C. (2002). The Significance of Arsenic-Bound Solids in Drinking Water Distribution Systems. *AWWA Water Quality Conference*. Seattle, WA: American Water Works Association.
- Maestre, W. R., Wahman, D. G., & Speitel, G. E. (2013). Monochloramine Cometabolism by *Nitrosomonas europaea* under Drinking Water Conditions. *Water Research*, 47, 4701-4709.
- Male, J., & Walski, T. (1991). *Water Distribution Systems: A Troubleshooting Manual*. Chelsea, Michigan: Lewis Publishers, Inc.
- Males, R., Clark, R., Wehrman, P., & Gates, W. (1985). Algorithm for Mixing Problems in Water Systems. *Journal of the Hydraulics Division*, 111(2), 206-211.
- Males, R., Grayman, W., & Clark, R. (1988). Modeling Water Quality in Distribution Systems. *Journal of Water Resources Planning and Management*, 114(2), 197-209.
- Margerum, D. W., Schurter, L. M., Hobson, J., & Moore, E. E. (1994). Water chlorination chemistry: Nonmetal redox kinetics of chloramine and nitrite ion. *Environ. Sci. Technol.*, 28(2), 331-337.
- Matějů, V., Čížinská, S., Krejčí, J., & Janoch, T. (1992). Biological Water Denitrification - A Review. *Enzyme Microb. Technol.*, 14(3), 170-183.
- Mathieu, L., Paquin, J., Block, J., Randon, G., Maillard, J., & Reasoner, D. (1992). Parameters Governing Bacterial Growth in Water Distribution Systems. *Revue des Sciences de l'Eau*, 5(1), 91-112.
- McNeil, L. (2000). *Water Quality Factors Influencing Iron and Lead Corrosion in Drinking Water*. Blacksburg, Virginia: Ph.D. dissertation, Virginia Polytechnic Institute and State University.
- Metcalf & Eddy, Inc. (2004). *Wastewater Engineering: Treatment and Reuse* (4th ed.). New York: McGraw-Hill.
- Miettinen, I., Vartiainen, T., & Martikainen, P. (1997). Phosphorus and bacterial growth in drinking water. *Appl. Environ. Microbiol.*, 63(8), 3242-3245.

- Momba, M., Cloete, T., Venter, S., & Kfir, R. (1999). Examination of the Behaviour of *Escherichia coli* in Biofilms Established in Laboratory-Scale Units Receiving Chlorinated and Chloraminated Water. *Water Research*, 33(13), 2937-2940.
- Morgan, S. L., & Walla, M. D. (n.d.). *Computation and Display of Acid-Base Species Distribution*. Columbia: University of South Carolina, Department of Chemistry.
- Munavalli, G., & Kumar, M. (2004). Modified Lagrangian method for modeling water quality in distribution systems. *Water Research*, 38(13), 2973–2988.
- National Research Council of the National Academies. (2006). *Drinking Water Distribution Systems: Assessing and Reducing Risks*. Washington, D.C.: The National Academies Press.
- Niquette, P., Servais, P., & Savoie, R. (2000). Impacts of Pipe Materials on Densities of Fixed Bacterial Biomass in a Drinking Water Distribution System. *Water Research*, 34(6), 1952-1956.
- Noguera, D. R. (1991). *Soluble microbial products (SMP) modeling in biological processes*. MS Thesis, University of Illinois, Urbana.
- Norton, C., & Le Chevallier, M. (1997). Chloramination: Its Effect on Distribution System Water Quality. *Jour. AWWA*, 89(7), 66-77.
- Norton, C., & LeChevallier, M. (2000). A Pilot Study of Bacteriological Population Changes through Potable Water Treatment and Distribution. *Applied and Environmental Microbiology*, 66(1), 268–276.
- Odell, L. H., Kirmeyer, G. J., Wilczak, A., Jacangelo, J. G., Marcinko, J. P., & Wolfe, R. L. (1996). Controlling Nitrification in Chloraminated Systems. *J. AWWA*, 88(7), 86-98.
- Olson, B. (1982). *Assessment and Implications of Bacterial Regrowth in Water Distribution Systems*. EPA-600/S2-82-072. Washington, DC: EPA.
- Opeim, D., Grochowski, J., & Smith, D. (1988). Isolation of coliforms from water main tubercles. *Abstracts Ann.Mtg.Amer.Soc.Microbiol.*
- Owen, M., Amy, G., Chowdhury, G., Paode, R., McCoy, G., & Viscosil, K. (1995). NOM characterization and treatability. *J. Am. Water Works Assoc.*, 87(1), 46–63.
- Ozekin, K., Valentine, R. L., & Vikesland, P. J. (1996). Modeling the decomposition of disinfection residuals of chloramine. In R. A. Milner, & L. A. G, *Water disinfection & natural organic matter* (pp. 115-125). Washington D.C.: American Chemical Society.
- Paul, E., Ochoa, J., Pechaud, Y., Liu, Y., & Line´, A. (2012). Effect of shear stress and growth conditions on detachment and physical properties of biofilms. *Water Research*, 46(17), 5499-5508.
- Payment, P., & Robertson, W. (2004). The microbiology of piped distribution systems and public health. In World Health Organisation, & R. Ainsworth (Ed.), *Safe Piped Water: Managing Microbial Water Quality in Piped Distribution Systems* (pp. 1-18). London: IWA Publishing.

- Pernitsky, D., Finch, G., & Huck, P. (1995). Disinfection Kinetics of Heterotrophic Plate Count Bacteria in Biologically Treated Potable Water. *Water Research*, 29(5), 1235-1241.
- Pintar, K. D., & Slawson, R. M. (2003). Effect of temperature and disinfection strategies on ammonia-oxidizing bacteria in a bench-scale drinking water distribution system. *Water Research*, 37(8), 1805-1817.
- Power, K., & Nagy, L. (1989). *Bacterial Regrowth in Water Supplies*. Melbourne: Report No. 4 Urban Water Research Association of Australia.
- Qualls, R. G., & Johnson, J. D. (1983). Kinetics of the short-term consumption chlorine by fulvic acid. *Environ. Sci. Technol.*, 17(11), 692-698.
- Richardson, S. (1998). Drinking Water Disinfection By-Products. In R. Meyers, *Encyclopedia of Environmental Analysis and Remediation* (pp. 1398-1421). New York: John Wiley & Sons.
- Riley, M., Gerba, C., & Elimelech, M. (2001). Biological approaches for addressing the grand challenge of providing access to clean drinking water. *J Biol Eng*, 5(2), 1754-1611.
- Rittmann, B. (1982). The effect of shear stress on biofilm loss rate. *Biotech Bioeng*, 24(2), 501-506.
- Rittmann, B. E., Stilwell, D., & Ohashi, A. (2002). The transient-state, multiple-species biofilm model for biofiltration processes. *Water Research*, 36(9), 2342-2356.
- Rittmann, B., & Huck, P. (1989). Biological treatment of public water supplies. *CRC Critical Reviews in Environmental Control*, 19(2), 119-184.
- Rittmann, B., & McCarty, P. (2001). *Environmental Biotechnology: Principles and Applications*. Boston: McGraw-Hill.
- Robertson, W., Stanfield, G., Howard, G., & Bartram, J. (2003). Monitoring the quality of drinking water during storage and distribution. In W. H. Organization, & T. O.-o. Development, *Assessing microbial safety of drinking water: improving approaches and methods* (pp. 179-204). London: IWA Publishing.
- Roels, J. A. (1983). *Energetics and kinetics in biotechnology*. Amsterdam: Eisenier Biomedical Press.
- Rogers, J., Dowsett, A. B., Dennis, P. J., Lee, J. V., & Keevil, C. W. (1994). Influence of plumbing materials on biofilm formation and growth of *Legionella pneumophila* in potable water systems. *Appl. Environ. Microbiol.*, 60(6), 1842-1851.
- Rossmann, A., Brown, R., Singer, P., & Nuckols, J. (2001). DBP Formation Kinetics in a Simulated Distribution System. *Water Research*, 35(14), 3483-3489.
- Rossmann, L. A., & Grayman, W. M. (1999). Scale model studies of mixing in drinking water storage tanks. *Journal of the Environmental Engineering Division of the ASCE*, 125(8), 755-761.
- Rossmann, L. A., Clark, R. M., & Grayman, W. M. (1994). Modeling chlorine residuals in drinking-water distribution systems. *J. of Env. Eng.*, 120(4), 803-819.

- SANS 241-1:2011 (South African National Standard. Drinking Water). (2011). Part 1: Microbiological, physical, aesthetic and chemical determinands. Edition 1. Pretoria: SABS Standards Division.
- SANS 241-2:2011 (South African National Standard. Drinking Water). (2011). Part 2: Application of SANS 241-1. Edition 1. Pretoria: SABS Standards Division.
- Sarin, P., Snoeyink, V., Lytle, D., & Kriven, W. (2004). Iron corrosion scales: Models for scale growth, iron release, and colored water formation. *Journal of Environmental Engineering*, 130(4), 364–373.
- Sathasivan, A., Fisher, I., & Tam, T. (2008). Onset of severe nitrification in mildly nitrifying chloraminated bulk waters and its relation to biostability. *Water Research*, 42(14), 3623-3632.
- Sathasivan, A., Ohgaki, S., Yamamoto, K., & Kamiko, N. (1997). Role of inorganic phosphorus in controlling regrowth in water distribution system. *Wat.Sci.Tech.*, 33(1), 37-44.
- Servais, P., Billen, G., Laurent, P., Lévi, Y., & Randon, G. (1992). Studies of BDOC & Bacterial Dynamics in the Drinking Water Distribution System of the Northern Parisian Suburb. *Revue des Sciences de l'Eau*, 5(Special Issue), 69-89.
- Servais, P., Billen, G., Laurent, P., Lévi, Y., & Randon, G. (1993). Bacterial regrowth in distribution systems. *Proceedings AWWAWQTC Conference*. Miami, Florida.
- Servais, P., Laurent, P., & Randon, G. (1995). Comparison of the bacterial dynamics in various French distribution systems. *Aqua, Journal of Water Supply Research and Technology*, 44(1), 10-17.
- Servais, P., Laurent, P., Billen, G., & Gatel, D. (1995). Development of a model of BDOC and bacterial biomass fluctuations in distribution systems. *Revue des Sciences de l'Eau*, 8(4), 427-462.
- Shisana, O., Rehle, T., Simbayi, L. C., Zuma, K., Jooste, S., Zungu, N., & et al. (2014). *South African National HIV Prevalence, Incidence and Behaviour Survey 2012*. Cape Town: HSRC Press.
- Snoeyink, V. L., & Jenkins, D. (1980). *Water Chemistry*. New York: John Wiley & Sons.
- Srinivasan, R., & Sorial, G. (2011). Treatment of taste and odor causing compounds 2-methyl isoborneol and geosmin in drinking water: A critical review. *Journal of Environmental Sciences*, 23(1), 1-13.
- Srinivasan, S., & Harrington, G. W. (2007). Biostability analysis for drinking water distribution systems. *Water Research*, 41(10), 2127-2138.
- Stewart, P., & Raquepas, J. (1995). Implications of Reaction-Diffusion Theory for the Disinfection of Microbial Biofilms by Reactive Antimicrobial Agents. *Chem. Eng. Sci.*, 50(19), 3099-3104.
- Stoodley, P., Sauer, K., Davies, D., & Costerton, J. (2002). Biofilms as Complex Differentiated Communities. *Annu. Rev. Microbiol.*, 56(1), 187-209.
- Storey, M., & Ashbolt, N. (2001). Persistence of Two Model Enteric Viruses (B40-8 and MS-2 bacteriophages) in Water Distribution Pipe Biofilms. *Water Sci. Technol.*, 43(12), 133-138.

- Storey, M., & Ashbolt, N. (2003). A Risk Model for Enteric Virus Accumulation and Release from Recycled Water Distribution Pipe Biofilms. *Water Sci. Technol. Water Supply*, 3(3), 73-80.
- Szewzyk, R., Szewzyk, U., Manz, W., & Schleifer, K. (2000). Microbiological safety of drinking water. *Annual Review of Microbiology*, 54(1), 81-127.
- Taylor, S., & Jaffé, P. (1996). Substrate and biomass transport in a porous medium. *Water Research*, 26(9), 2181-2194.
- Tchobanoglous, G., & Schroeder, E. D. (1985). *Water Quality*. Reading, Massachusetts: Addison-Wesley Publishing Company.
- Tilman, D. (2001). Functional Diversity. In S. A. Levin, *Encyclopedia of Biodiversity* (pp. 109-120). San Diego, California: Academic Press.
- Trussell, R. R., & Montgomery, J. M. (23-27 June 1991). Control strategy 1: Alternative oxidants and disinfectants. *Proceedings of the Annual American Water Works Association Conference* (p. 43). Philadelphia: AWWA.
- Tuovinen, O., & Hsu, J. (1982). Aerobic and anaerobic microorganisms in tubercles of the Columbus, Ohio, water distribution system. *Appl. Environ. Microbiol.*, 44(3), 761-764.
- Tuovinen, O., Button, K., Vuorinen, A., Carlson, L., Mair, D., & Yut, L. (1980). Bacterial, chemical, and mineralogical characteristics of tubercles in distribution pipelines. *J. Am. Water Works Assoc.*, 72(11), 626-635.
- Valentine, R. L., & Jafvert, C. T. (1988). General acid catalysis of monochloramine disproportionation. *Environ. Sci. Tech.*, 22(6), 691-696.
- Valentine, R., & Stearns, S. (1994). Radon Release from Water Distribution System Deposits. *Environ. Sci. Technol.*, 28(3), 534-537.
- van der Kooij, D. (1992). Assimilable organic carbon as an indicator of bacterial regrowth. *J. Am. Water Works Assoc.*, 84(2), 57-65.
- van der Walt, J. J. (2002). *The modelling of water treatment process tanks*. Johannesburg: A Thesis submitted at Faculty of Engineering for degree Doctor in Civil Engineering, Rand Afrikaans University.
- van der Wende, E., & Characklis, W. (1990). Biofilms in Potable Water Distribution Systems. In G. McFeters, *Drinking Water Microbiology*. New York: Springer-Verlag.
- Vasconcelos, J. J., Rossman, L. A., Grayman, W. M., Boules, P. F., & Clark, R. M. (1997). Kinetics of chlorine decay. *Journal of the American Water Works Association*, 84(7), 54-65.
- Venter, L. (2010). *Presence of potentially pathogenic heterotrophic plate count (HPC) bacteria occurring in a drinking water distribution system in the North-West Province, South-Africa*. Potchefstroom: MSc Thesis, North-West University.

- Vikesland, P. J., Ozekin, K., & Valentine, R. L. (2001). Monochloramine decay in model and distribution system waters. *Wat. Res.*, 35(7), 1766-1776.
- Wehner, J. F., & Wilhelm, R. F. (1958). Boundary conditions of flow reactor. *Chemical Eng. Sci.*, 6(1), 89-92.
- Westbrook, A., DiGiano, F. A., & Pontius, N. L. (2009). Rate of chloramine decay at pipe surfaces. *Journal American Water Works Association*, 101(7), 58-70.
- Wilczak, A., Jacangelo, J., Marcinko, J., Odell, L., Kirmeyer, G., & Wolf, R. (1996). Occurrence of nitrification in chloraminated distribution systems. *Journal of the American Water Works Association*, 88(7), 74-85.
- Wingender, J., & Flemming, H. (2011). Biofilms in drinking water and their role as reservoir for pathogens. *Int J Hyg Environ Heal*, 214(6), 190-197.
- Wingender, J., Neu, T., & Flemming, H. (1999). What are Bacterial Extracellular Polymeric Substances? In J. Wingender, T. Neu, & H. Flemming, *Microbial Extracellular Polymeric Substances* (pp. 93–112). Berlin: Springer.
- Wolfe, R. L., Lieu, N. L., Izaguirre, G., & Means, E. G. (1990). Ammonia oxidizing bacteria in a chloraminated distribution system: seasonal occurrence, distribution, and disinfection resistance. *Appl. Environ. Microbiol.*, 56(2), 451-462.
- Wolfe, R., Lieu, G., Izaguirre, G., & Means, E. (1990). Ammonia Oxidizing Bacteria in Chloraminated Distribution System: Seasonal Occurrence, Distribution and Disinfection Resistance. *Appl. Environ. Microbiol.*, 451-462.
- Wood, J. (1980). Slurry Flow in Pipe Networks. *Journal of Hydraulics*, 106(1), 55-70.
- Woolschlager, J. (2000). *A Comprehensive Disinfection and Water Quality Model*. Evanston, Illinois: Ph.D. Dissertation, Northwestern University.
- Woolschlager, J., & Rittmann, B. (1995a). Evaluating what is measured by BDOC and AOC tests. *Revue des Sciences de L'eau*, 8(3), 371-385.
- Woolschlager, J., & Rittmann, B. (1995b). Determining the actual amount of biodegradable organic matter in drinking water supplies. *Annual Meeting of the American Water Works Association*. Denver, Colorado: AWWA.
- Woolschlager, J., & Soucie, W. (2003). Chlorine Reactivity with Concrete Pipe Surfaces. *World Water & Environmental Resources Congress*, 10(40685), 1-8.
- World Health Organisation. (2004). *Monochloramine in Drinking Water: Background Document for Development of WHO Guidelines for Drinking Water Quality*. Geneva: World Health Organisation.
- Wu, Z. (2006). Optimal Calibration Method for Water Distribution Water Quality Model. *Journal of Environmental Science and Health*, 41(7), 1-16.

- Xin, C. H., Irvine, W. W., & Sung, W. (June 11-15 2006). Greater Boston Drinking Water Quality - Comparison of Full Scale and Pilot Study I: Monochloramine and pH change. *125th AWWA Annual Conference & Exposition* (pp. 1-19). San Antonio, Texas: AWWA.
- Xu, P., Chen, X., & Stewart, P. (1996). Transport Limitation of Chlorine Disinfection of *Pseudomonas Aeruginosa* Entrapped in Alginate Beads. *Biotechnol. Bioeng.*, 49(1), 93-100.
- Zacheus, O., Iivanainen, T., Nissinen, M., Lehtola, & Martikainen, P. (2000). Bacterial Biofilm Formation of Polyvinyl Chloride, Polyethylene & Stainless Steel Exposed to Ozonated Water. *Water Research*, 34(1), 63-70.
- Zaklikowski, A. E. (2006). *The Effect of Chlorine and Chloramines on the Viability and Activity of Nitrifying Bacteria*. Blacksburg, Virginia: MSc Thesis, Virginia Polytechnic Institute and State University.
- Zhang, W., & DiGiano, F. A. (2002). Comparison of bacterial regrowth in distribution systems using free chlorine and chloramine: a statistical study of causative factors. *Water Research*, 36(6), 1469-1482.
- Zhang, W., Miller, C., & DiGiano, F. (2004). Bacterial Regrowth Model for Water Distribution Systems Incorporating Alternating Split-Operator Solution Technique. *J. of Env. Eng.*, 130(9), 932-941.
- Zobell, C., & Anderson, D. (1936). Observations on the Multiplication of Bacteria in Different Volumes of Stored Seawater and the Influence of Oxygen Tension and Solid Surface. *Biol. Bull.*, 71(2), 324-342.

A. APPENDIX A

A.1 Organic Matter and Biomass as Chemical Oxygen Demand

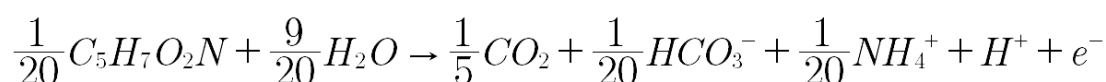
In accordance with both the CDWQ model (Woolschlager, 2000) and subsequent CDWQ-E model (Biyela, 2010), all organic matter and biomass incorporated in the CDWQ-E₂ model is converted to chemical oxygen demand (COD), which is the theoretical mass of oxygen used in an oxidation-reduction reaction in which all electrons contained in carbon are removed and transferred to oxygen. Such an approach is required in order to maintain consistent units and track the oxidation state of carbon in the model.

There are two assumptions on which all three versions of the CDWQ model rely:

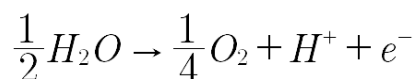
- 1) All organic matter is assumed to have the same chemical formula as biomass, that is C₅H₇O₂N (Hoover & Porges, 1952 in Woolschlager, 2000).
- 2) All organic matter is assumed to have an oxidation state of zero.

Given the assumptions above, the necessary conversions to COD can be derived from the reactions that follow.

Reaction for bacterial cell synthesis with ammonia as nitrogen source:



Reaction for oxygen as an electron acceptor:



Given the aforementioned assumptions and the half-reactions above, the conversions that follow can be derived:

$$\begin{aligned} \left(\frac{\frac{1}{4} \text{ mole } O_2}{1 e^- \text{ eq}}\right) \left(\frac{32 \text{ g } O_2}{\text{mole } O_2}\right) &= \frac{8 \text{ g } O_2}{1 e^- \text{ eq}} \\ \&\& \left(\frac{\frac{1}{20} \text{ mole } C_5H_7O_2N}{1 e^- \text{ eq}}\right) \left(\frac{60 \text{ g } C}{\text{mole } C_5H_7O_2N}\right) &= \frac{30 \text{ g } C}{e^- \text{ eq}} \\ \therefore \left(\frac{8 \text{ g } O_2}{1 e^- \text{ eq}}\right) \left(\frac{1 e^- \text{ eq}}{3.0 \text{ g } C}\right) &= \frac{2.67 \text{ g } O_2}{\text{g } C} = \underline{\underline{\frac{2.67 \mu\text{g } COD}{\mu\text{g } C}}} \end{aligned}$$

Kaplan et al (1993 in Wooschlagler, 2000) measured *P. fluorescens* cells as having a carbon content of $1.56E-7 \frac{\mu\text{g } COD}{\text{cell}}$. Therefore, in order to perform the cell-to-COD conversion:

$$\begin{aligned} \left(\frac{8 \text{ g } O_2}{1 e^- \text{ eq}}\right) \left(\frac{(4-0) e^- \text{ eq}}{\text{mole } C}\right) &= \frac{32 \text{ g } O_2}{\text{mole } C} \\ \therefore \left(\frac{32 \text{ g } O_2}{\mu\text{mole } C}\right) \left(\frac{1.56E-7 \mu\text{g } C}{\text{cell}}\right) \left(\frac{\mu\text{mole } C}{12 \mu\text{g } C}\right) &= \underline{\underline{4.16E-7 \frac{\mu\text{g } COD}{\text{cell}}}} \end{aligned}$$

A.2 Moles of Carbon and Nitrogen in Biomass and Organic Matter

The CDWQ-E₂ model tracks BOM, biomass and carbon dioxide as $\frac{\mu\text{g } COD}{l}$ and nitrogen species (total ammonia, nitrite, nitrate and nitrogen gas) as $\frac{\text{mole } N}{l}$. The incorporation of carbon and nitrogen in biomass and the release of carbon and nitrogen from organic matter and biomass requires the following conversions:

$$\begin{aligned} \gamma_c &= 3.12E-8 \frac{\text{mole } C}{\mu\text{g } COD} \\ \gamma_N &= 6.24E-9 \frac{\text{mole } N}{\mu\text{g } COD} \end{aligned}$$

Given the assumption that all carbon in COD is at an oxidation state of zero, the derivation of these terms is as follows:

$$\begin{aligned} \gamma_c &= \left(\frac{\mu\text{g } C}{2.67 \mu\text{g } COD}\right) \left(\frac{\text{mole } C}{12E6 \mu\text{g } C}\right) = \underline{\underline{3.12E-8 \frac{\text{mole } C}{\mu\text{g } COD}}} \\ \gamma_N &= \left(\frac{3.12E-8 \text{ mole } C}{\mu\text{g } COD}\right) \left(\frac{\frac{1}{5} \text{ mole } N}{\text{mole } C}\right) = \underline{\underline{6.24E-9 \frac{\text{mole } N}{\mu\text{g } COD}}} \end{aligned}$$

A.3 Cells/ml per $\mu\text{gCOD/l}$

In order to convert biomass from $\frac{\mu\text{gCOD}}{l}$ to $\frac{\text{cells}}{ml}$, if required, a conversion of $2404 \frac{\text{cells/ml}}{\mu\text{gCOD/l}}$ is applied.

The derivation is provided below:

$$\left(\frac{\text{cell}}{4.16E-7 \mu\text{g COD}}\right) \left(\frac{l}{1000 \text{ ml}}\right) = \frac{2404 \frac{\text{cells}}{\text{ml}}}{\frac{\mu\text{g COD}}{l}}$$

A.4 Active Biomass Density

The assumed biofilm density proposed by Wooschlager (2000) is based on the assumption that the average cell diameter in the biofilm is $1 \mu\text{m}$. The derivation is presented below:

$$\rho_f = \left(\frac{4.16E-7 \mu\text{g COD}}{\text{cell}}\right) \left(\frac{1.0E18 \text{ cells}}{m^3}\right) = \underline{4.16E11 \frac{\mu\text{g COD}}{m^3}}$$

B. APPENDIX B

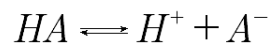
B.1 Monoprotic Acid Derivation

The materials balance for a monoprotic acid is given by Equation B-1:

$$C_{T,A} = [A^-] + [HA]$$

Equation B-1

Thus, for a monoprotic acid (HA) with a dissociation constant, K_a :



$$K_a = \frac{[H^+][A^-]}{[HA]}$$

Equation B-2

Rearranging the K_a expression:

$$\frac{[A^-]}{[HA]} = \frac{K_a}{[H^+]}$$

Equation B-3

By adding a value of 1.0 to each side of Equation B-3:

$$\frac{[HA]}{[HA]} + \frac{[A^-]}{[HA]} = \frac{K_a}{[H^+]}$$

Equation B-4

Substituting Equation B-1 into Equation B-3:

$$[HA] = \frac{[H^+].C_{T,A}}{[H^+] + K_a}$$

Equation B-5

Equation B-6 can be rewritten by taking its reciprocal and adding 1.0 to each side:

$$\frac{[HA]}{[A^-]} + \frac{[A^-]}{[A^-]} = \frac{[H^+]}{K_a} + \frac{K_a}{K_a}$$

Equation B-6

Again, substituting Equation B-1 into Equation B-6:

$$[A^-] = \frac{[K_a] \cdot C_{T,A}}{[H^+] + K_a}$$

Equation B-7

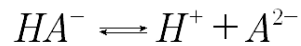
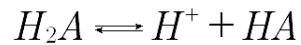
(Can, 2014)

B.2 Diprotic Acid Derivation

The materials balance for a diprotic acid is given by Equation B-8:

$$C_{T,A} = [A^{2-}] + [HA^-] + [H_2A]$$

Equation B-8



The dissociation constants for the chemical reactions above are K_{a1} and K_{a2} respectively.

The dissociation constants can be written as:

$$K_{a1} = \frac{[H^+][HA^-]}{[H_2A]}$$

Equation B-9

$$K_{a2} = \frac{[H^+][A^{2-}]}{[HA^-]}$$

Equation B-10

Substituting Equation B-9 and Equation B-10 into Equation B-8:

$$C_{T,A} = \frac{[H^+][HA^-]}{K_{a1}} + [HA^-] + \frac{[HA^-] \cdot K_{a2}}{H^+}$$

Equation B-11

Rearranging Equation B-11:

$$C_{T,A} = [HA^-] \left(\frac{[H^+]}{K_{a1}} + 1 + \frac{K_{a2}}{H^+} \right)$$

Equation B-12

Therefore:

$$[HA^-] = \frac{[H^+] \cdot K_{a1} \cdot C_{T,A}}{[H^+]^2 + [H^+] \cdot K_{a1} + K_{a1} \cdot K_{a2}}$$

Equation B-13

Similarly:

$$[H_2A] = \frac{[H^+]^2 \cdot C_{T,A}}{[H^+]^2 + [H^+] \cdot K_{a1} + K_{a1} \cdot K_{a2}}$$

Equation B-14

$$[A^{2-}] = \frac{K_{a1} \cdot K_{a2} \cdot C_{T,A}}{[H^+]^2 + [H^+] \cdot K_{a1} + K_{a1} \cdot K_{a2}}$$

Equation B-15

(Morgan & Walla, n.d.)

C. APPENDIX C

C.1 Input Data

Table C-1: Physical pipe data

Pipe	Initial Node	Final Node	Diameter (m)	Length (m)	C-Factor	Material
1 (Reservoir)	457	1000	71.3232	8.5	100	D.I.
435	135	136	0.7620	731.5	125	C.L.
436	135	144	0.2032	975.4	75	D.I.
437	135	142	0.7620	1371.6	125	C.L.
438	136	137	0.4064	914.4	80	D.I.
439	136	146	0.4064	975.4	80	D.I.
440	136	146	0.2032	975.4	75	D.I.
441	136	503	0.9144	365.8	125	C.L.
442	137	138	0.4064	609.6	125	C.L.
443	138	504	0.4064	518.2	125	C.L.
444	139	437	0.4064	304.8	125	C.L.
445	139	504	0.4064	579.1	125	C.L.
446	140	412	0.9144	2194.6	125	C.L.
447	140	503	0.9144	548.6	125	C.L.
449	142	143	0.3048	426.7	65	D.I.
450	142	181	0.7620	182.9	125	C.L.
453	143	149	0.3048	50.8	65	D.I.
455	145	146	0.3048	50.8	75	D.I.
456	145	146	0.4064	50.8	80	D.I.
457	145	148	0.4064	914.4	80	D.I.
458	146	147	0.3048	1005.8	75	D.I.
460	147	351	0.3048	609.6	120	C.L.
461	148	151	0.4064	426.7	80	D.I.
462	149	150	0.3048	1280.2	65	D.I.
463	150	151	0.3048	1127.7	65	D.I.
464	150	158	0.3048	853.5	65	D.I.
466	151	152	0.4064	1005.8	80	D.I.
467	152	153	0.4064	335.3	80	D.I.
468	153	154	0.4064	792.5	80	D.I.
469	153	438	0.2032	335.3	120	C.L.

470	153	438	0.3048	335.3	120	C.L.
471	154	155	0.4064	426.7	80	D.I.
472	154	156	0.4064	335.3	125	C.L.
473	155	156	0.3048	243.8	75	D.I.
474	155	174	0.4064	487.7	80	D.I.
477	156	158	0.4064	731.5	125	C.L.
478	158	159	0.3048	426.7	75	D.I.
479	158	159	0.4064	426.7	80	D.I.
480	158	177	0.2032	975.4	75	D.I.
481	159	160	0.5080	487.7	80	D.I.
482	160	161	0.3048	609.6	120	C.L.
483	160	171	0.5080	243.8	125	C.L.
484	161	162	0.2032	487.7	120	C.L.
485	162	163	0.2032	609.6	120	C.L.
486	162	167	0.2032	1158.2	120	C.L.
487	162	177	0.2032	975.3	75	D.I.
488	163	164	0.3048	670.5	120	C.L.
489	164	165	0.3048	182.9	120	C.L.
490	164	166	0.3048	365.8	120	C.L.
491	165	166	0.3048	487.7	120	C.L.
492	166	167	0.4064	365.8	125	C.L.
493	167	168	0.4064	1767.9	125	C.L.
494	168	169	0.5080	518.2	125	C.L.
495	168	178	0.6096	731.5	125	C.L.
496	169	170	0.5080	792.5	125	C.L.
497	170	171	0.5080	243.8	125	C.L.
498	170	171	0.3048	944.9	120	C.L.
499	172	173	0.4064	365.8	125	C.L.
500	172	177	0.2032	335.3	75	D.I.
501	173	174	0.4064	975.4	125	C.L.
502	173	175	0.2032	670.6	120	C.L.
503	174	309	0.4064	1036.3	80	D.I.
504	174	313	0.4064	487.6	125	C.L.
505	175	176	0.3048	853.4	120	C.L.
506	176	439	0.3048	243.8	120	C.L.

507	178	179	0.7620	914.4	125	C.L.
508	178	196	0.5080	548.6	125	C.L.
509	178	445	0.4064	1036.3	80	D.I.
510	179	180	0.7620	1280.2	125	C.L.
511	179	440	0.3048	487.7	120	C.L.
512	179	445	0.3048	792.4	75	D.I.
513	180	181	0.7620	61.0	125	C.L.
531	194	195	0.6096	487.7	125	C.L.
532	194	195	0.4064	304.8	125	C.L.
533	194	457	0.6096	152.4	125	C.L.
534	195	196	0.6096	609.6	125	C.L.
535	195	440	0.4064	457.2	125	C.L.
719	302	437	0.3048	1218.0	75	D.I.
720	302	406	1.2192	304.8	125	C.L.
730	309	310	0.3048	914.4	75	D.I.
731	309	311	0.3048	1219.1	120	C.L.
732	309	439	0.4572	487.7	80	D.I.
733	310	311	0.4064	1262.2	125	C.L.
734	310	312	0.3048	518.2	75	D.I.
735	312	313	0.2032	731.5	120	C.L.
736	312	314	0.3048	304.8	75	D.I.
737	314	315	0.4064	1188.7	125	C.L.
738	314	318	0.3048	640.1	75	D.I.
739	315	316	0.3048	365.8	120	C.L.
740	315	438	0.4064	426.7	125	C.L.
741	316	317	0.2032	274.3	120	C.L.
742	317	319	0.2032	121.9	120	C.L.
743	317	468	0.2032	365.8	120	C.L.
744	318	468	0.2032	426.7	120	C.L.
746	319	320	0.3048	731.5	120	C.L.
747	320	321	0.2032	548.6	75	D.I.
748	321	322	0.3048	853.4	120	C.L.
751	322	351	0.3048	548.6	120	C.L.
863	406	412	1.2192	61.0	125	C.L.

C.L. = Concrete Lined; D.I. = Ductile Iron

Table C-2: Hydraulic flow regime (m³/h)

Pipe	In Hour 1	Out Hour 1	In Hour 2	Out Hour 2	In Hour 3	Out Hour 3	In Hour 4	Out Hour 4	In Hour 5	Out Hour 5	In Hour 6	Out Hour 6	In Hour 7	Out Hour 7	In Hour 8	Out Hour 8
1	400	0	450	0	500	0	450	0	150	0	10.97	0	0	-213.99	0	-66.4
435	-562.594	-562.594	-570.64	-570.64	-593.831	-593.831	-583.419	-583.419	-550.761	-550.761	-496.174	-496.174	-444.585	-444.585	-582.157	-582.157
436	10.097	10.097	9.62373	9.62373	8.8349	8.8349	9.30819	9.30819	9.93926	9.93926	11.2014	11.2014	15.9344	15.9344	17.66979	17.66979
437	491.441	491.441	504.851	504.851	530.252	530.252	515.264	515.264	468.249	468.249	392.049	392.049	314.743	314.743	440.1671	440.1671
438	147.669	147.669	146.091	146.091	148.616	148.616	149.247	149.247	152.717	152.717	160.448	160.448	168.021	168.021	207.7778	207.7778
439	360.969	360.969	360.495	360.495	344.403	344.403	344.719	344.719	345.034	345.034	338.25	338.25	337.619	337.619	423.0198	423.0198
440	54.7448	54.7448	54.587	54.587	52.2205	52.2205	52.2205	52.2205	52.2205	52.2205	51.274	51.274	51.1162	51.1162	64.0365	64.0365
441	-1140.65	-1140.65	-1145.54	-1145.54	-1152.48	-1152.48	-1143.96	-1143.96	-1118.09	-1118.09	-1068.08	-1068.08	-1028	-1028	-1310.72	-1310.72
442	-68.1549	-68.1549	-68.4704	-68.4704	-69.5748	-69.5748	-68.9437	-68.9437	-67.2083	-67.2083	-64.8418	-64.8418	-62.9486	-62.9486	-70.8369	-70.8369
443	-72.4146	-72.4146	-72.4146	-72.4146	-73.519	-73.519	-73.2034	-73.2034	-72.2568	-72.2568	-71.1525	-71.1525	-70.6792	-70.6792	-79.1985	-79.1985
444	-76.6743	-76.6743	-76.5165	-76.5165	-77.4631	-77.4631	-77.3053	-77.3053	-77.3053	-77.3053	-77.6209	-77.6209	-78.4097	-78.4097	-87.5601	-87.5601
445	72.4146	72.4146	72.4146	72.4146	73.519	73.519	73.2034	73.2034	72.2568	72.2568	71.1525	71.1525	70.6792	70.6792	79.19853	79.19853
446	-1144.91	-1144.91	-1149.64	-1149.64	-1156.42	-1156.42	-1148.06	-1148.06	-1123.14	-1123.14	-1074.54	-1074.54	-1035.58	-1035.58	-1319.08	-1319.08
447	1140.65	1140.65	1145.54	1145.54	1152.48	1152.48	1143.96	1143.96	1118.09	1118.09	1068.08	1068.08	1028	1028	1310.72	1310.72
449	-10.5703	-10.5703	-17.3543	-17.3543	-25.2426	-25.2426	-20.5096	-20.5096	-4.57521	-4.57521	22.4028	22.4028	48.9075	48.9075	49.22299	49.22299
450	482.606	482.606	508.638	508.638	544.293	544.293	521.259	521.259	446.478	446.478	323.105	323.105	200.047	200.047	327.5222	327.5222
453	-18.3009	-18.3009	-22.5605	-22.5605	-30.1333	-30.1333	-26.8202	-26.8202	-15.9344	-15.9344	4.10192	4.10192	26.1892	26.1892	22.08724	22.08724
455	-91.662	-91.662	-91.8198	-91.8198	-97.4994	-97.4994	-96.395	-96.395	-92.4509	-92.4509	-83.9315	-83.9315	-79.5141	-79.5141	-100.4711	-100.4711
456	-208.251	-208.251	-208.724	-208.724	-221.661	-221.661	-219.137	-219.137	-210.144	-210.144	-190.739	-190.739	-180.8	-180.8	-228.3865	-228.3865
457	291.078	291.078	293.287	293.287	312.219	312.219	307.801	307.801	291.867	291.867	259.841	259.841	241.066	241.066	314.7432	314.7432
458	115.642	115.642	114.538	114.538	77.3053	77.3053	81.2495	81.2495	94.6596	94.6596	114.854	114.854	128.422	128.422	158.1987	158.1987

APPENDIX C

460	114.696	114.696	112.014	112.014	117.536	117.536	118.64	118.64	121.638	121.638	120.375	120.375	120.06	120.06	151.4554	151.4554
461	291.078	291.078	293.287	293.287	312.219	312.219	307.801	307.801	291.867	291.867	259.841	259.841	241.066	241.066	314.7432	314.7432
462	-18.3009	-18.3009	-22.5605	-22.5605	-30.1333	-30.1333	-26.8202	-26.8202	-15.9344	-15.9344	4.10192	4.10192	26.1892	26.1892	22.08724	22.08724
463	-78.883	-78.883	-81.8806	-81.8806	-91.662	-91.662	-88.349	-88.349	-77.4631	-77.4631	-59.1623	-59.1623	-42.2813	-42.2813	-62.4753	-62.4753
464	40.8614	40.8614	43.0701	43.0701	46.2254	46.2254	44.3322	44.3322	38.1794	38.1794	30.7644	30.7644	25.8736	25.8736	35.18182	35.18182
466	189.792	189.792	193.263	193.263	203.676	203.676	200.047	200.047	186.637	186.637	160.132	160.132	143.883	143.883	188.0571	188.0571
467	177.171	177.171	183.324	183.324	194.525	194.525	189.319	189.319	170.703	170.703	135.679	135.679	110.278	110.278	148.3	148.3
468	95.764	95.764	104.914	104.914	130.315	130.315	122.269	122.269	92.7664	92.7664	35.3396	35.3396	-20.1889	-20.1889	5.995108	5.995108
469	18.7742	18.7742	18.4586	18.4586	14.83	14.83	15.2994	15.2994	17.1965	17.1965	21.4562	21.4562	27.2935	27.2935	29.66001	29.66001
470	54.2715	54.2715	53.3249	53.3249	43.2279	43.2279	44.4786	44.4786	50.0118	50.0118	62.4753	62.4753	79.1985	79.1985	86.14024	86.14024
471	31.7028	31.7028	30.9221	30.9221	29.3445	29.3445	31.0799	31.0799	31.5451	31.5451	44.0167	44.0167	53.9421	53.9421	63.1064	63.1064
472	63.5797	63.5797	73.9923	73.9923	100.97	100.97	91.031	91.031	60.5821	60.5821	-8.67713	-8.67713	-74.1310	-74.1310	-57.1113	-57.1113
473	5.2049	5.2049	13.5679	13.5679	25.8736	25.8736	21.1406	21.1406	-0.4732	-0.4732	-26.5047	-26.5047	-40.7036	-40.7036	-42.5968	-42.5968
474	26.4979	26.4979	17.512	17.512	3.47085	3.47085	9.93926	9.93926	32.0183	32.0183	70.5214	70.5214	94.9751	94.9751	105.7032	105.7032
477	59.6355	59.6355	79.3563	79.3563	119.271	119.271	103.652	103.652	49.5385	49.5385	-51.4317	-51.4317	-135.048	-135.048	-124.32	-124.32
478	24.4537	24.4537	32.6576	32.6576	46.6987	46.6987	40.5459	40.5459	19.0897	19.0897	-18.1431	-18.1431	-48.9075	-48.9075	-45.1211	-45.1211
479	55.3759	55.3759	74.15	74.15	106.177	106.177	92.2931	92.2931	43.2279	43.2279	-41.0192	-41.0192	-111.067	-111.067	-102.39	-102.39
480	1.14065	1.14065	-0.6309	-0.6309	-0.9464	-0.9464	-2.05096	-2.05096	2.05096	2.05096	5.9936	5.9936	8.3616	8.3616	8.992662	8.992662
481	70.0481	70.0481	98.7615	98.7615	145.145	145.145	124.162	124.162	50.4851	50.4851	-75.4121	-75.4121	-181.273	-181.273	-172.123	-172.123
482	8.99266	8.99266	10.7281	10.7281	13.8834	13.8834	12.779	12.779	8.04607	8.04607	5.99511	5.99511	-0.21614	-0.21614	3.15532	3.15532
483	58.2157	58.2157	85.6669	85.6669	129.21	129.21	109.016	109.016	39.126	39.126	-86.1402	-86.1402	-187.11	-187.11	-182.22	-182.22
484	6.15287	6.15287	8.3616	8.3616	11.6747	11.6747	10.2548	10.2548	4.73298	4.73298	1.46407	1.46407	-6.31064	-6.31064	-3.94415	-3.94415
485	4.41745	4.41745	7.8883	7.8883	12.6213	12.6213	10.4126	10.4126	1.89319	1.89319	-9.30819	-9.30819	-20.6673	-20.6673	-20.0363	-20.0363

APPENDIX C

486	2.99755	2.99755	5.83734	5.83734	9.46596	9.46596	7.73053	7.73053	0.81249	0.81249	-8.3616	-8.3616	-17.512	-17.512	-17.1965	-17.1965
487	-7.57277	-7.57277	-10.2522	-10.2522	-11.0408	-11.0408	-13.2523	-13.2523	-5.52181	-5.52181	8.8326	8.8326	18.3009	18.3009	17.51203	17.51203
488	0.81249	0.81249	4.89075	4.89075	9.93926	9.93926	7.25724	7.25724	-2.36649	-2.36649	-15.1455	-15.1455	-28.3979	-28.3979	-28.8712	-28.8712
489	0.7273	0.7273	2.20872	2.20872	4.41745	4.41745	3.31309	3.31309	-0.54272	-0.54272	-5.83734	-5.83734	-11.2014	-11.2014	-11.3592	-11.3592
490	-0.63264	-0.63264	2.05096	2.05096	4.89075	4.89075	3.31309	3.31309	-2.68202	-2.68202	-10.5703	-10.5703	-18.7742	-18.7742	-19.4052	-19.4052
491	-0.70837	-0.70837	1.07912	1.07912	3.31309	3.31309	2.05096	2.05096	-2.20872	-2.20872	-8.20383	-8.20383	-14.3567	-14.3567	-14.9878	-14.9878
492	-2.83979	-2.83979	1.89319	1.89319	7.09947	7.09947	4.10192	4.10192	-6.62617	-6.62617	-21.1406	-21.1406	-36.1284	-36.1284	-38.0216	-38.0216
493	-1.13907	-1.13907	6.46841	6.46841	15.4611	15.4611	10.5703	10.5703	-7.57277	-7.57277	-31.8687	-31.8687	-56.7958	-56.7958	-58.8467	-58.8467
494	-47.0143	-47.0143	-76.5165	-76.5165	-120.375	-120.375	-99.2348	-99.2348	-25.7159	-25.7159	104.599	104.599	211.406	211.406	210.3021	210.3021
495	45.2788	45.2788	82.3539	82.3539	135.363	135.363	109.174	109.174	17.3543	17.3543	-137.572	-137.572	-269.78	-269.78	-270.884	-270.884
496	-52.6938	-52.6938	-81.0917	-81.0917	-124.793	-124.793	-104.126	-104.126	-32.4998	-32.4998	95.4484	95.4484	199.258	199.258	196.2609	196.2609
497	-47.0143	-47.0143	-72.4146	-72.4146	-111.383	-111.383	-92.9242	-92.9242	-29.0289	-29.0289	85.0359	85.0359	177.802	177.802	175.1203	175.1203
498	-5.67958	-5.67958	-8.67713	-8.67713	-13.4101	-13.4101	-11.2014	-11.2014	-3.47085	-3.47085	10.2548	10.2548	21.4562	21.4562	21.14064	21.14064
499	-16.2499	-16.2499	-19.2475	-19.2475	-25.8736	-25.8736	-23.9804	-23.9804	-15.1455	-15.1455	-1.73543	-1.73543	5.20628	5.20628	1.893192	1.893192
500	6.46841	6.46841	10.8831	10.8831	11.9871	11.9871	15.4611	15.4611	3.47085	3.47085	-14.8262	-14.8262	-26.5047	-26.5047	-26.5047	-26.5047
501	-26.0314	-26.0314	-25.8736	-25.8736	-29.5022	-29.5022	-29.8178	-29.8178	-27.9246	-27.9246	-25.8736	-25.8736	-28.0823	-28.0823	-35.1818	-35.1818
502	-0.12243	-0.12243	-1.56504	-1.56504	-3.94415	-3.94415	-2.83979	-2.83979	1.10278	1.10278	7.73053	7.73053	11.9902	11.9902	12.46351	12.46351
503	3.47085	3.47085	-2.20872	-2.20872	-12.6213	-12.6213	-8.67713	-8.67713	5.67958	5.67958	26.978	26.978	40.5459	40.5459	42.12352	42.12352
504	-8.04607	-8.04607	-10.097	-10.097	-17.0387	-17.0387	-15.1455	-15.1455	-8.3616	-8.3616	8.20383	8.20383	13.2523	13.2523	12.93681	12.93681
505	-9.93926	-9.93926	-9.62373	-9.62373	-11.6747	-11.6747	-11.5169	-11.5169	-10.5703	-10.5703	-8.51936	-8.51936	-9.30819	-9.30819	-12.148	-12.148
506	-9.93926	-9.93926	-9.62373	-9.62373	-11.6747	-11.6747	-11.5169	-11.5169	-10.5703	-10.5703	-8.51936	-8.51936	-9.30819	-9.30819	-12.148	-12.148
507	-327.049	-327.049	-340.932	-340.932	-356.867	-356.867	-344.088	-344.088	-303.7	-303.7	-236.649	-236.649	-168.81	-168.81	-240.278	-240.278
508	385.58	385.58	437.643	437.643	507.375	507.375	467.461	467.461	332.571	332.571	106.019	106.019	-98.7615	-98.7615	-25.8736	-25.8736

APPENDIX C

509	-15.9344	-15.9344	-16.7232	-16.7232	-17.512	-17.512	-16.881	-16.881	-14.83	-14.83	-11.5169	-11.5169	-8.20383	-8.20383	-11.6747	-11.6747
510	-476.611	-476.611	-503.747	-503.747	-539.717	-539.717	-516.053	-516.053	-439.536	-439.536	-313.323	-313.323	-187.268	-187.268	-312.692	-312.692
511	118.798	118.798	133.786	133.786	153.822	153.822	142.305	142.305	103.337	103.337	40.7036	40.7036	-21.6139	-21.6139	23.6649	23.6649
512	15.9344	15.9344	16.7232	16.7232	17.512	17.512	16.881	16.881	14.83	14.83	11.5169	11.5169	8.20383	8.20383	11.67468	11.67468
513	-476.611	-476.611	-503.747	-503.747	-539.717	-539.717	-516.053	-516.053	-439.536	-439.536	-313.323	-313.323	-187.268	-187.268	-312.692	-312.692
531	-349.452	-349.452	-397.255	-397.255	-460.361	-460.361	-423.759	-423.759	-300.544	-300.544	-95.9217	-95.9217	93.3975	93.3975	11.83245	11.83245
532	-149.089	-149.089	-169.441	-169.441	-196.419	-196.419	-180.8	-180.8	-128.264	-128.264	-40.8614	-40.8614	39.9148	39.9148	5.048512	5.048512
533	557.703	557.703	636.901	636.901	738.345	738.345	678.709	678.709	476.296	476.296	125.424	125.424	-207.936	-207.936	-64.5263	-64.5263
534	-385.58	-385.58	-437.643	-437.643	-507.375	-507.375	-467.461	-467.461	-332.571	-332.571	-106.019	-106.019	98.7615	98.7615	25.87362	25.87362
535	-118.798	-118.798	-133.786	-133.786	-153.822	-153.822	-142.305	-142.305	-103.337	-103.337	-40.7036	-40.7036	21.6139	21.6139	-23.6649	-23.6649
719	76.6743	76.6743	76.5165	76.5165	77.4631	77.4631	77.3053	77.3053	77.3053	77.3053	77.6209	77.6209	78.4097	78.4097	87.56013	87.56013
720	-963.95	-963.95	-927.506	-927.506	-860.929	-860.929	-880.334	-880.334	-966.475	-966.475	-1101.84	-1101.84	-1202.65	-1202.65	-4222.61	-4222.61
730	-5.04851	-5.04851	-7.09947	-7.09947	-12.4635	-12.4635	-11.0436	-11.0436	-5.04851	-5.04851	3.94415	3.94415	8.20383	8.20383	6.468406	6.468406
731	-6.31064	-6.31064	-8.67713	-8.67713	-15.3033	-15.3033	-13.4101	-13.4101	-6.15287	-6.15287	4.89075	4.89075	10.097	10.097	8.046066	8.046066
732	9.93926	9.93926	9.62373	9.62373	11.6747	11.6747	11.5169	11.5169	10.5703	10.5703	8.51936	8.51936	9.30819	9.30819	12.14798	12.14798
733	6.31064	6.31064	8.67713	8.67713	15.3033	15.3033	13.4101	13.4101	6.15287	6.15287	-4.89075	-4.89075	-10.097	-10.097	-8.04607	-8.04607
734	-16.2499	-16.2499	-19.563	-19.563	-31.3954	-31.3954	-28.5556	-28.5556	-17.3543	-17.3543	-0.55376	-0.55376	5.20628	5.20628	-0.87876	-0.87876
735	8.04607	8.04607	10.097	10.097	17.0387	17.0387	15.1455	15.1455	8.3616	8.3616	-8.20383	-8.20383	-13.2523	-13.2523	-12.9368	-12.9368
736	-29.1867	-29.1867	-33.6042	-33.6042	-51.905	-51.905	-47.9609	-47.9609	-32.0265	-32.0265	-1.73543	-1.73543	5.36404	5.36404	-3.31309	-3.31309
737	-70.6792	-70.6792	-74.3078	-74.3078	-78.4097	-78.4097	-76.6743	-76.6743	-68.786	-68.786	-53.3249	-53.3249	-54.4293	-54.4293	-64.053	-64.053
738	41.4925	41.4925	40.7036	40.7036	26.5047	26.5047	28.7134	28.7134	36.7595	36.7595	51.5895	51.5895	59.7933	59.7933	60.73991	60.73991
739	-2.52426	-2.52426	-6.31064	-6.31064	-23.8227	-23.8227	-20.6673	-20.6673	-7.8883	-7.8883	21.1406	21.1406	39.126	39.126	36.44395	36.44395
740	-73.0457	-73.0457	-71.7835	-71.7835	-58.0579	-58.0579	-59.7780	-59.7780	-67.2083	-67.2083	-83.9315	-83.9315	-106.492	-106.492	-115.8	-115.8

APPENDIX C

741	-2.52426	-2.52426	-6.31064	-6.31064	-23.8227	-23.8227	-20.6673	-20.6673	-7.8883	-7.8883	21.1406	21.1406	39.126	39.126	36.44395	36.44395
742	-47.9609	-47.9609	-50.1696	-50.1696	-65.9462	-65.9462	-63.5797	-63.5797	-53.7982	-53.7982	-32.8153	-32.8153	-15.9344	-15.9344	-28.8712	-28.8712
743	35.6551	35.6551	36.1284	36.1284	35.0241	35.0241	34.5508	34.5508	33.6042	33.6042	35.0241	35.0241	29.0289	29.0289	34.39299	34.39299
744	-11.3592	-11.3592	-12.148	-12.148	-14.83	-14.83	-13.7256	-13.7256	-10.5703	-10.5703	-6.9417	-6.9417	0.85036	0.85036	-1.89319	-1.89319
746	-47.9609	-47.9609	-50.1696	-50.1696	-65.9462	-65.9462	-63.5797	-63.5797	-53.7982	-53.7982	-32.8153	-32.8153	-15.9344	-15.9344	-28.8712	-28.8712
747	-47.9609	-47.9609	-50.1696	-50.1696	-65.9462	-65.9462	-63.5797	-63.5797	-53.7982	-53.7982	-32.8153	-32.8153	-15.9344	-15.9344	-28.8712	-28.8712
748	-64.5263	-64.5263	-64.9996	-64.9996	-75.2544	-75.2544	-74.3078	-74.3078	-69.8903	-69.8903	-57.5846	-57.5846	-47.6453	-47.6453	-65.1574	-65.1574
751	-106.177	-106.177	-105.388	-105.388	-111.383	-111.383	-111.541	-111.541	-110.909	-110.909	-104.126	-104.126	-97.6572	-97.6572	-124.951	-124.951
863	1144.91	1144.91	1149.64	1149.64	1156.42	1156.42	1148.06	1148.06	1123.14	1123.14	1074.54	1074.54	1035.58	1035.58	1319.082	1319.082

Pipe	In Hour 9	Out Hour 9	In Hour 10	Out Hour 10	In Hour 11	Out Hour 11	In Hour 12	Out Hour 12	In Hour 13	Out Hour 13	In Hour 14	Out Hour 14	In Hour 15	Out Hour 15	In Hour 16	Out Hour 16
1	0	-3.73	34.58	0	101.64	0	0	-153.75	0	-130.86	0	-150.34	0	-165.77	0	-224.7
435	-593.2	-593.2	-575.0571	-575.0571	-582.945	-582.945	-446.162	-446.162	-445.689	-445.689	-435.592	-435.592	-430.543	-430.543	-422.497	-422.497
436	17.0387	17.0387	15.61883	15.61883	14.5145	14.5145	14.9878	14.9878	14.3567	14.3567	14.1989	14.1989	14.1989	14.1989	15.3033	15.3033
437	456.733	456.733	447.5821	447.5821	458.468	458.468	321.685	321.685	321.527	321.527	309.695	309.695	303.384	303.384	291.236	291.236
438	204.623	204.623	202.0982	202.0982	200.994	200.994	165.97	165.97	166.759	166.759	168.494	168.494	169.283	169.283	170.23	170.23
439	429.124	429.124	406.4586	406.4586	411.296	411.296	332.728	332.728	329.415	329.415	323.263	323.263	320.896	320.896	322.316	322.316
440	64.9996	64.9996	61.5129	61.5129	62.3176	62.3176	50.4851	50.4851	49.8541	49.8541	48.9075	48.9075	48.5919	48.5919	48.7497	48.7497
441	-1319.55	-1319.55	-1278.536	-1278.536	-1283.43	-1283.43	-1020.9	-1020.9	-1017.59	-1017.59	-1002.76	-1002.76	-996.292	-996.292	-991.244	-991.244
442	-71.3102	-71.3102	-69.10151	-69.10151	-69.417	-69.417	-62.6331	-62.6331	-62.4753	-62.4753	-62.1598	-62.1598	-62.002	-62.002	-61.6865	-61.6865
443	-79.1985	-79.1985	-76.67428	-76.67428	-76.832	-76.832	-70.0481	-70.0481	-70.0481	-70.0481	-69.8903	-69.8903	-69.7326	-69.7326	-69.7326	-69.7326
444	-87.2446	-87.2446	-84.24704	-84.24704	-84.4048	-84.4048	-77.4631	-77.4631	-77.6209	-77.6209	-77.6209	-77.6209	-77.6209	-77.6209	-77.7786	-77.7786

445	79.1985	79.1985	76.67428	76.67428	76.832	76.832	70.0481	70.0481	70.0481	70.0481	69.8903	69.8903	69.7326	69.7326	69.7326	69.7326
446	-1327.6	-1327.6	-1286.108	-1286.108	-1290.84	-1290.84	-1028.32	-1028.32	-1025.16	-1025.16	-1010.49	-1010.49	-1004.18	-1004.18	-999.29	-999.29
447	1319.55	1319.55	1278.536	1278.536	1283.43	1283.43	1020.9	1020.9	1017.59	1017.59	1002.76	1002.76	996.292	996.292	991.244	991.244
449	45.5944	45.5944	39.75703	39.75703	34.0775	34.0775	44.3322	44.3322	41.4925	41.4925	41.4925	41.4925	42.1235	42.1235	46.8565	46.8565
450	351.66	351.66	351.6604	351.6604	370.119	370.119	218.033	218.033	221.661	221.661	207.305	207.305	198.943	198.943	178.276	178.276
453	19.2475	19.2475	15.7766	15.7766	10.7281	10.7281	22.7183	22.7183	20.6673	20.6673	20.9829	20.9829	21.6139	21.6139	25.5581	25.5581
455	-104.599	-104.599	-97.9475	-97.9475	-100.497	-100.497	-78.4097	-78.4097	-77.6209	-77.6209	-75.8854	-75.8854	-75.0966	-75.0966	-75.2544	-75.2544
456	-237.753	-237.753	-222.5507	-222.5507	-228.445	-228.445	-178.433	-178.433	-176.225	-176.225	-172.28	-172.28	-170.703	-170.703	-171.018	-171.018
457	320.738	320.738	307.4859	307.4859	310.01	310.01	238.7	238.7	236.333	236.333	230.812	230.812	228.603	228.603	228.13	228.13
458	151.771	151.771	147.4733	147.4733	144.671	144.671	126.371	126.371	125.424	125.424	124.004	124.004	123.689	123.689	124.793	124.793
460	155.557	155.557	146.0913	146.0913	144.514	144.514	116.905	116.905	113.749	113.749	110.909	110.909	110.278	110.278	113.118	113.118
461	320.738	320.738	307.4859	307.4859	310.01	310.01	238.7	238.7	236.333	236.333	230.812	230.812	228.603	228.603	228.13	228.13
462	19.2475	19.2475	15.7766	15.7766	10.7281	10.7281	22.7183	22.7183	20.6673	20.6673	20.9829	20.9829	21.6139	21.6139	25.5581	25.5581
463	-65.1574	-65.1574	-63.89523	-63.89523	-67.3661	-67.3661	-44.1745	-44.1745	-44.9633	-44.9633	-43.3857	-43.3857	-42.4391	-42.4391	-39.126	-39.126
464	36.6017	36.6017	36.12841	36.12841	36.4439	36.4439	26.6625	26.6625	26.8202	26.8202	26.0314	26.0314	25.7159	25.7159	24.4537	24.4537
466	192.317	192.317	186.0061	186.0061	188.688	188.688	143.409	143.409	142.62	142.62	139.15	139.15	137.572	137.572	136.468	136.468
467	153.033	153.033	150.0355	150.0355	155.557	155.557	112.487	112.487	113.118	113.118	110.121	110.121	108.227	108.227	103.968	103.968
468	9.3058	9.3058	17.98532	17.98532	30.4488	30.4488	-11.2014	-11.2014	-8.6749	-8.6749	-8.67713	-8.67713	-11.0436	-11.0436	-21.1406	-21.1406
469	29.0289	29.0289	27.76682	27.76682	26.3469	26.3469	26.5047	26.5047	25.7159	25.7159	25.5581	25.5581	25.5581	25.5581	26.5047	26.5047
470	84.0893	84.0893	80.46066	80.46066	76.5165	76.5165	76.832	76.832	74.7811	74.7811	74.15	74.15	74.15	74.15	76.9898	76.9898
471	62.1438	62.1438	58.8316	58.8316	56.1503	56.1503	52.3783	52.3783	50.7876	50.7876	50.3274	50.3274	50.1696	50.1696	51.905	51.905
472	-52.8380	-52.8380	-40.86139	-40.86139	-25.4003	-25.4003	-63.5797	-63.5797	-59.4625	-59.4625	-59.0045	-59.0045	-61.2132	-61.2132	-73.0457	-73.0457
473	-41.0192	-41.0192	-38.4850	-38.4850	-35.1728	-35.1728	-38.0216	-38.0216	-36.4439	-36.4439	-36.1284	-36.1284	-36.6017	-36.6017	-39.5993	-39.5993

474	103.337	103.337	97.3166	97.3166	91.3231	91.3231	90.3999	90.3999	87.4024	87.4024	86.4558	86.4558	86.7713	86.7713	91.5043	91.5043
477	-113.592	-113.592	-100.6547	-100.6547	-80.934	-80.934	-121.795	-121.795	-113.749	-113.749	-114.38	-114.38	-116.905	-116.905	-132.681	-132.681
478	-40.8614	-40.8614	-35.49735	-35.49735	-28.5556	-28.5556	-43.7012	-43.7012	-40.7036	-40.7036	-41.0192	-41.0192	-41.9658	-41.9658	-47.8031	-47.8031
479	-92.9242	-92.9242	-80.77619	-80.77619	-64.9996	-64.9996	-99.3926	-99.3926	-92.4509	-92.4509	-93.0819	-93.0819	-95.1329	-95.1329	-108.701	-108.701
480	8.8326	8.8326	8.203832	8.203832	7.57277	7.57277	7.8883	7.8883	7.57277	7.57277	7.57277	7.57277	7.57277	7.57277	8.04607	8.04607
481	-157.608	-157.608	-138.0453	-138.0453	-114.38	-114.38	-163.288	-163.288	-152.56	-152.56	-153.191	-153.191	-156.188	-156.188	-176.54	-176.54
482	3.94415	3.94415	4.259682	4.259682	5.83734	5.83734	0.53798	0.53798	0.97026	0.97026	0.72572	0.72572	0.46068	0.46068	-0.63106	-0.63106
483	-168.336	-168.336	-148.4578	-148.4578	-126.213	-126.213	-169.441	-169.441	-159.028	-159.028	-159.344	-159.344	-162.183	-162.183	-181.589	-181.589
484	-2.83979	-2.83979	-1.893192	-1.893192	-0.03739	-0.03739	-5.20628	-5.20628	-4.57521	-4.57521	-4.73298	-4.73298	-4.89075	-4.89075	-6.31064	-6.31064
485	-18.4586	-18.4586	-16.2499	-16.2499	-13.7256	-13.7256	-18.7742	-18.7742	-17.512	-17.512	-17.6698	-17.6698	-17.9853	-17.9853	-20.0363	-20.0363
486	-16.0921	-16.0921	-14.19894	-14.19894	-12.148	-12.148	-15.9344	-15.9344	-14.9878	-14.9878	-14.9878	-14.9878	-15.1455	-15.1455	-17.0387	-17.0387
487	16.7189	16.7189	14.51447	14.51447	12.3057	12.3057	16.5654	16.5654	15.4611	15.4611	15.6188	15.6188	15.7766	15.7766	17.8276	17.8276
488	-27.1358	-27.1358	-24.1382	-24.1382	-21.1406	-21.1406	-26.0314	-26.0314	-24.6115	-24.6115	-24.4537	-24.4537	-24.7693	-24.7693	-27.2935	-27.2935
489	-10.5703	-10.5703	-9.46596	-9.46596	-8.20383	-8.20383	-10.2548	-10.2548	-9.62373	-9.62373	-9.62373	-9.62373	-9.78149	-9.78149	-10.7281	-10.7281
490	-18.3009	-18.3009	-16.40766	-16.40766	-14.5145	-14.5145	-17.1965	-17.1965	-16.2499	-16.2499	-16.2499	-16.2499	-16.4077	-16.4077	-17.9853	-17.9853
491	-14.0412	-14.0412	-12.62128	-12.62128	-11.2014	-11.2014	-13.0946	-13.0946	-12.4635	-12.4635	-12.4635	-12.4635	-12.6213	-12.6213	-13.7256	-13.7256
492	-35.8129	-35.8129	-32.18426	-32.18426	-28.8712	-28.8712	-33.2886	-33.2886	-31.711	-31.711	-31.5532	-31.5532	-31.8687	-31.8687	-34.7085	-34.7085
493	-55.3759	-55.3759	-49.38076	-49.38076	-44.0167	-44.0167	-52.2205	-52.2205	-49.3808	-49.3808	-49.223	-49.223	-49.8541	-49.8541	-54.587	-54.587
494	195.63	195.63	173.3848	173.3848	149.878	149.878	192.317	192.317	181.115	181.115	181.273	181.273	183.955	183.955	204.623	204.623
495	-252.741	-252.741	-224.3433	-224.3433	-195.472	-195.472	-246.115	-246.115	-232.074	-232.074	-231.916	-231.916	-235.229	-235.229	-260.629	-260.629
496	182.062	182.062	160.9213	160.9213	138.045	138.045	180.958	180.958	170.072	170.072	170.387	170.387	173.069	173.069	193.106	193.106
497	162.499	162.499	143.5671	143.5671	123.215	123.215	161.395	161.395	151.771	151.771	151.929	151.929	154.453	154.453	172.28	172.28
498	19.563	19.563	17.35426	17.35426	14.83	14.83	19.4052	19.4052	18.3009	18.3009	18.3009	18.3009	18.6164	18.6164	20.8251	20.8251

499	1.09805	1.09805	0.945018	0.945018	-0.87402	-0.87402	4.25968	4.25968	3.78638	3.78638	3.94415	3.94415	4.25968	4.25968	5.67958	5.67958
500	-25.5515	-25.5515	-22.7183	-22.7183	-19.8785	-19.8785	-24.4537	-24.4537	-23.0338	-23.0338	-23.0338	-23.0338	-23.3494	-23.3494	-25.8736	-25.8736
501	-34.8663	-34.8663	-32.18426	-32.18426	-31.8687	-31.8687	-27.1358	-27.1358	-26.5047	-26.5047	-26.0314	-26.0314	-25.8736	-25.8736	-26.0314	-26.0314
502	11.9902	11.9902	11.35915	11.35915	10.2548	10.2548	11.3592	11.3592	10.8859	10.8859	10.8859	10.8859	10.8859	10.8859	11.6747	11.6747
503	40.7036	40.7036	38.65267	38.65267	35.0241	35.0241	38.4949	38.4949	37.075	37.075	36.9172	36.9172	37.075	37.075	39.5993	39.5993
504	12.4635	12.4635	11.99022	11.99022	10.7281	10.7281	12.779	12.779	12.3057	12.3057	12.3057	12.3057	12.4635	12.4635	13.2523	13.2523
505	-11.9902	-11.9902	-10.41256	-10.41256	-10.5703	-10.5703	-8.67713	-8.67713	-8.51936	-8.51936	-8.3616	-8.3616	-8.20383	-8.20383	-8.3616	-8.3616
506	-11.9902	-11.9902	-10.41256	-10.41256	-10.5703	-10.5703	-8.67713	-8.67713	-8.51936	-8.51936	-8.3616	-8.3616	-8.20383	-8.20383	-8.3616	-8.3616
507	-260.787	-260.787	-262.0493	-262.0493	-273.882	-273.882	-174.489	-174.489	-169.441	-169.441	-165.181	-165.181	-161.71	-161.71	-153.664	-153.664
508	14.0412	14.0412	44.33225	44.33225	85.8247	85.8247	-68.6282	-68.6282	-59.7933	-59.7933	-64.053	-64.053	-70.9947	-70.9947	-105.23	-105.23
509	-12.779	-12.779	-12.77905	-12.77905	-13.4101	-13.4101	-8.51936	-8.51936	-8.3616	-8.3616	-8.04607	-8.04607	-7.8883	-7.8883	-7.57277	-7.57277
510	-337.304	-337.304	-338.5658	-338.5658	-357.656	-357.656	-206.042	-206.042	-209.987	-209.987	-195.788	-195.788	-187.584	-187.584	-166.128	-166.128
511	27.7668	27.7668	30.92214	30.92214	39.126	39.126	-7.25724	-7.25724	3.15532	3.15532	-6.15287	-6.15287	-10.8859	-10.8859	-25.2426	-25.2426
512	12.779	12.779	12.77905	12.77905	13.4101	13.4101	8.51936	8.51936	8.3616	8.3616	8.04607	8.04607	7.8883	7.8883	7.57277	7.57277
513	-337.304	-337.304	-338.5658	-338.5658	-357.656	-357.656	-206.042	-206.042	-209.987	-209.987	-195.788	-195.788	-187.584	-187.584	-166.128	-166.128
531	-19.2475	-19.2475	-43.70118	-43.70118	-78.883	-78.883	61.6865	61.6865	47.8031	47.8031	57.2691	57.2691	65.4729	65.4729	99.8659	99.8659
532	-8.20383	-8.20383	-18.61639	-18.61639	-33.6042	-33.6042	26.3469	26.3469	20.3518	20.3518	24.4537	24.4537	27.9246	27.9246	42.5968	42.5968
533	-3.62862	-3.62862	33.60416	33.60416	98.7615	98.7615	-149.404	-149.404	-127.159	-127.159	-146.091	-146.091	-161.079	-161.079	-218.348	-218.348
534	-14.0412	-14.0412	-44.33225	-44.33225	-85.8247	-85.8247	68.6282	68.6282	59.7933	59.7933	64.053	64.053	70.9947	70.9947	105.23	105.23
535	-27.7668	-27.7668	-30.92214	-30.92214	-39.126	-39.126	7.25724	7.25724	-3.15532	-3.15532	6.15287	6.15287	10.8859	10.8859	25.2426	25.2426
719	87.2446	87.2446	84.24704	84.24704	84.4048	84.4048	77.4631	77.4631	77.6209	77.6209	77.6209	77.6209	77.6209	77.6209	77.7786	77.7786
720	-4167.55	-4167.55	-4280.349	-4280.349	-4235.39	-4235.39	-1208.96	-1208.96	-1214.32	-1214.32	-1240.83	-1240.83	-1254.4	-1254.4	-1270.81	-1270.81
730	6.15287	6.15287	6.468406	6.468406	5.20628	5.20628	8.04607	8.04607	7.73053	7.73053	7.73053	7.73053	7.8883	7.8883	8.3616	8.3616

731	7.415	7.415	7.8883	7.8883	6.31064	6.31064	9.78149	9.78149	9.46596	9.46596	9.46596	9.46596	9.62373	9.62373	10.2548	10.2548
732	11.9902	11.9902	10.41256	10.41256	10.5703	10.5703	8.67713	8.67713	8.51936	8.51936	8.3616	8.3616	8.20383	8.20383	8.3616	8.3616
733	-7.415	-7.415	-7.8883	-7.8883	-6.31064	-6.31064	-9.78149	-9.78149	-9.46596	-9.46596	-9.46596	-9.46596	-9.62373	-9.62373	-10.2548	-10.2548
734	-1.73543	-1.73543	0.345508	0.345508	-1.42778	-1.42778	5.67958	5.67958	5.83734	5.83734	5.99511	5.99511	5.99511	5.99511	5.99511	5.99511
735	-12.4635	-12.4635	-11.99022	-11.99022	-10.7281	-10.7281	-12.779	-12.779	-12.3057	-12.3057	-12.3057	-12.3057	-12.4635	-12.4635	-13.2523	-13.2523
736	-4.41745	-4.41745	-1.542951	-1.542951	-3.62862	-3.62862	6.46841	6.46841	6.78394	6.78394	7.09947	7.09947	7.09947	7.09947	6.62617	6.62617
737	-64.2108	-64.2108	-61.37097	-61.37097	-61.5287	-61.5287	-53.6404	-53.6404	-52.5361	-52.5361	-51.5895	-51.5895	-51.274	-51.274	-51.7472	-51.7472
738	59.7933	59.7933	59.79331	59.79331	57.9001	57.9001	60.1088	60.1088	59.32	59.32	58.689	58.689	58.3734	58.3734	58.3734	58.3734
739	33.6042	33.6042	32.81533	32.81533	28.5556	28.5556	37.5483	37.5483	36.4439	36.4439	36.6017	36.6017	37.075	37.075	39.126	39.126
740	-113.118	-113.118	-108.2275	-108.2275	-102.863	-102.863	-103.179	-103.179	-100.497	-100.497	-99.5503	-99.5503	-99.7081	-99.7081	-103.494	-103.494
741	33.6042	33.6042	32.81533	32.81533	28.5556	28.5556	37.5483	37.5483	36.4439	36.4439	36.6017	36.6017	37.075	37.075	39.126	39.126
742	-32.6576	-32.6576	-30.76437	-30.76437	-34.393	-34.393	-17.1965	-17.1965	-17.3543	-17.3543	-15.9344	-15.9344	-14.9878	-14.9878	-12.9368	-12.9368
743	35.6551	35.6551	35.81288	35.81288	37.075	37.075	30.7644	30.7644	30.9221	30.9221	30.1333	30.1333	29.1867	29.1867	26.978	26.978
744	-3.47085	-3.47085	-4.101916	-4.101916	-5.67958	-5.67958	-0.67839	-0.67839	-1.15642	-1.15642	-0.7273	-0.7273	-0.26189	-0.26189	1.52875	1.52875
746	-32.6576	-32.6576	-30.76437	-30.76437	-34.393	-34.393	-17.1965	-17.1965	-17.3543	-17.3543	-15.9344	-15.9344	-14.9878	-14.9878	-12.9368	-12.9368
747	-32.6576	-32.6576	-30.76437	-30.76437	-34.393	-34.393	-17.1965	-17.1965	-17.3543	-17.3543	-15.9344	-15.9344	-14.9878	-14.9878	-12.9368	-12.9368
748	-68.6282	-68.6282	-64.68406	-64.68406	-66.2617	-66.2617	-47.4876	-47.4876	-46.3832	-46.3832	-44.6478	-44.6478	-43.8589	-43.8589	-43.7012	-43.7012
751	-129.368	-129.368	-122.1109	-122.1109	-122.426	-122.426	-96.2373	-96.2373	-94.1863	-94.1863	-91.5043	-91.5043	-90.5577	-90.5577	-91.5043	-91.5043
863	1327.6	1327.6	1286.108	1286.108	1290.84	1290.84	1028.32	1028.32	1025.16	1025.16	1010.49	1010.49	1004.18	1004.18	999.29	999.29

Pipe	In Hour 17	Out Hour 17	In Hour 18	Out Hour 18	In Hour 19	Out Hour 19	In Hour 20	Out Hour 20	In Hour 21	Out Hour 21	In Hour 22	Out Hour 22	In Hour 23	Out Hour 23	In Hour 24	Out Hour 24
1	2.11	0	0	-150.83	0	-325.53	0	-380.89	0	-238.83	0	-298.25	38.8	0	365.77	0
435	-583.892	-583.892	-568.904	-568.904	-546.186	-546.186	-540.191	-540.191	-561.489	-561.489	-430.2279	-430.2279	-480.3975	-480.3975	-528.8316	-528.8316
436	16.40766	16.40766	19.2475	19.2475	21.7717	21.7717	22.7183	22.7183	20.6673	20.6673	17.66979	17.66979	12.46351	12.46351	9.781492	9.781492
437	444.7424	444.7424	417.764	417.764	380.374	380.374	369.1724	369.1724	404.039	404.039	296.2845	296.2845	375.1675	375.1675	446.7933	446.7933
438	206.6735	206.6735	209.829	209.829	217.244	217.244	219.768	219.768	213.457	213.457	168.9674	168.9674	160.9213	160.9213	152.2442	152.2442
439	420.1807	420.1807	431.648	431.648	432.91	432.91	429.1711	429.1711	434.172	434.172	332.9585	332.9585	333.9049	333.9049	345.4188	345.4188
440	63.7211	63.7211	65.3151	65.3151	65.6307	65.6307	64.9829	64.9829	65.7884	65.7884	50.3144	50.3144	50.6299	50.6299	52.3649	52.3649
441	-1311.51	-1311.51	-1306.3	-1306.3	-1295.26	-1295.26	-1295.42	-1295.42	-1306.46	-1306.46	-1015.066	-1015.066	-1053.404	-1053.404	-1102.469	-1102.469
442	-70.5214	-70.5214	-69.7326	-69.7326	-69.417	-69.417	-69.417	-69.417	-69.8903	-69.8903	-62.47534	-62.47534	-64.52629	-64.52629	-66.57725	-66.57725
443	-78.7252	-78.7252	-78.5675	-78.5675	-79.1985	-79.1985	-79.3563	-79.3563	-79.0408	-79.0408	-70.36364	-70.36364	-70.83693	-70.83693	-71.468	-71.468
444	-87.0868	-87.0868	-87.5601	-87.5601	-88.8223	-88.8223	-89.2956	-89.2956	-88.1912	-88.1912	-78.09417	-78.09417	-77.14757	-77.14757	-76.51651	-76.51651
445	78.72523	78.72523	78.5675	78.5675	79.1985	79.1985	79.3563	79.3563	79.0408	79.0408	70.36364	70.36364	70.83693	70.83693	71.468	71.468
446	-1319.87	-1319.87	-1315.14	-1315.14	-1305.04	-1305.04	-1305.36	-1305.36	-1315.61	-1315.61	-1022.797	-1022.797	-1059.714	-1059.714	-1107.36	-1107.36
447	1311.509	1311.509	1306.3	1306.3	1295.26	1295.26	1295.417	1295.417	1306.46	1306.46	1015.066	1015.066	1053.404	1053.404	1102.469	1102.469
449	43.85895	43.85895	56.9535	56.9535	68.786	68.786	72.73013	72.73013	63.4219	63.4219	56.1647	56.1647	30.6066	30.6066	3.470852	3.470852
450	342.6678	342.6678	295.811	295.811	233.178	233.178	213.4574	213.4574	268.675	268.675	170.8606	170.8606	297.0734	297.0734	410.5071	410.5071
453	19.08969	19.08969	29.1867	29.1867	38.8104	38.8104	41.96576	41.96576	34.2352	34.2352	32.0265	32.0265	11.83245	11.83245	-9.623726	-9.623726
455	-99.6825	-99.6825	-102.232	-102.232	-102.075	-102.075	-100.7866	-100.7866	-103.021	-103.021	-78.7050	-78.7050	-80.5977	-80.5977	-85.8027	-85.8027
456	-226.8093	-226.8093	-232.232	-232.232	-232.074	-232.074	-229.0174	-229.0174	-233.967	-233.967	-179.0184	-179.0184	-182.9616	-182.9616	-195.1064	-195.1064
457	311.5879	311.5879	310.957	310.957	308.433	308.433	308.4325	308.4325	312.061	312.061	240.7509	240.7509	251.9523	251.9523	274.0395	274.0395
458	157.4100	157.4100	162.499	162.499	164.234	164.234	164.3500	164.3500	162.972	162.972	125.5495	125.5495	120.9755	120.9755	116.8746	116.8746
460	145.618	145.618	151.771	151.771	156.504	156.504	159.6592	159.6592	156.346	156.346	126.5283	126.5283	119.5866	119.5866	115.6425	115.6425

461	311.5879	311.5879	310.957	310.957	308.433	308.433	308.4325	308.4325	312.061	312.061	240.7509	240.7509	251.9523	251.9523	274.0395	274.0395
462	19.08969	19.08969	29.1867	29.1867	38.8104	38.8104	41.96576	41.96576	34.2352	34.2352	32.0265	32.0265	11.83245	11.83245	-9.623726	-9.623726
463	-62.7909	-62.7909	-56.638	-56.638	-48.4342	-48.4342	-45.5944	-45.5944	-53.4827	-53.4827	-37.39054	-37.39054	-53.16714	-53.16714	-69.10151	-69.10151
464	36.44395	36.44395	34.0775	34.0775	30.2911	30.2911	28.71341	28.71341	32.6576	32.6576	23.50713	23.50713	30.6066	30.6066	34.07746	34.07746
466	187.8993	187.8993	184.271	184.271	180.484	180.484	179.8532	179.8532	183.64	183.64	142.6205	142.6205	154.4529	154.4529	174.3314	174.3314
467	149.7199	149.7199	139.938	139.938	129.21	129.21	126.5283	126.5283	136.31	136.31	104.9144	104.9144	127.3172	127.3172	156.3461	156.3461
468	9.623726	9.623726	-17.5075	-17.5075	-37.8638	-37.8638	-46.2136	-46.2136	-25.8736	-25.8736	-31.71097	-31.71097	16.40766	16.40766	66.41949	66.41949
469	29.34448	29.34448	32.1843	32.1843	34.0775	34.0775	34.70852	34.70852	33.4464	33.4464	28.55565	28.55565	23.82267	23.82267	20.03628	20.03628
470	85.35141	85.35141	93.3975	93.3975	99.077	99.077	100.8125	100.8125	97.1839	97.1839	82.82715	82.82715	69.10151	69.10151	58.05789	58.05789
471	61.52874	61.52874	65.1406	65.1406	69.7326	69.7326	70.5033	70.5033	67.6642	67.6642	56.6235	56.6235	48.90746	48.90746	32.4998	32.4998
472	-51.905	-51.905	-82.6482	-82.6482	-107.754	-107.754	-116.7169	-116.7169	-94.1863	-94.1863	-88.82226	-88.82226	-32.4998	-32.4998	33.91969	33.91969
473	-40.8614	-40.8614	-47.9609	-47.9609	-55.2181	-55.2181	-57.7424	-57.7424	-51.7340	-51.7340	-45.4249	-45.4249	-31.39543	-31.39543	-15.61883	-15.61883
474	102.3901	102.3901	113.749	113.749	124.951	124.951	128.8948	128.8948	119.3982	119.3982	102.0484	102.0484	80.30289	80.30289	48.11863	48.11863
477	-115.485	-115.485	-154.611	-154.611	-191.37	-191.37	-203.045	-203.045	-173.543	-173.543	-157.1349	-157.1349	-81.09172	-81.09172	5.679576	5.679576
478	-40.7036	-40.7036	-55.6914	-55.6914	-70.0481	-70.0481	-74.7811	-74.7811	-63.1064	-63.1064	-57.58459	-57.58459	-28.08235	-28.08235	2.997554	2.997554
479	-92.6086	-92.6086	-126.371	-126.371	-159.186	-159.186	-169.914	-169.914	-143.409	-143.409	-130.9458	-130.9458	-63.73746	-63.73746	6.941704	6.941704
480	8.834896	8.834896	9.93926	9.93926	11.0436	11.0436	11.3562	11.3562	10.5703	10.5703	8.992662	8.992662	6.783938	6.783938	4.259682	4.259682
481	-156.031	-156.031	-207.936	-207.936	-257.632	-257.632	-274.04	-274.04	-233.967	-233.967	-211.5642	-211.5642	-109.0163	-109.0163	-2.682022	-2.682022
482	3.313086	3.313086	0.80303	0.80303	-1.73543	-1.73543	-2.36649	-2.36649	-0.32026	-0.32026	-1.57766	-1.57766	3.470852	3.470852	8.67713	8.67713
483	-165.812	-165.812	-215.982	-215.982	-264.1	-264.1	-279.877	-279.877	-241.54	-241.54	-216.455	-216.455	-117.3779	-117.3779	-14.98777	-14.98777
484	-3.15532	-3.15532	-6.46841	-6.46841	-9.78149	-9.78149	-10.7281	-10.7281	-8.04607	-8.04607	-8.203832	-8.203832	-1.339433	-1.339433	5.206278	5.206278
485	-18.3009	-18.3009	-23.8227	-23.8227	-29.1867	-29.1867	-30.9221	-30.9221	-26.6625	-26.6625	-23.98043	-23.98043	-12.93681	-12.93681	-2.839788	-2.839788
486	-15.7766	-15.7766	-20.3518	-20.3518	-24.6115	-24.6115	-26.0314	-26.0314	-22.5605	-22.5605	-20.19405	-20.19405	-11.20139	-11.20139	-3.313086	-3.313086

487	16.2499	16.2499	20.9829	20.9829	25.7159	25.7159	27.2865	27.2865	23.3494	23.3494	21.14064	21.14064	11.67468	11.67468	3.15532	3.15532
488	-26.5047	-26.5047	-33.1309	-33.1309	-39.4415	-39.4415	-41.4925	-41.4925	-36.6017	-36.6017	-32.18426	-32.18426	-19.08969	-19.08969	-7.415002	-7.415002
489	-10.2548	-10.2548	-13.0946	-13.0946	-15.6188	-15.6188	-16.4077	-16.4077	-14.3567	-14.3567	-12.77905	-12.77905	-7.415002	-7.415002	-2.682022	-2.682022
490	-17.8276	-17.8276	-22.0872	-22.0872	-25.8736	-25.8736	-27.2935	-27.2935	-24.1382	-24.1382	-21.14064	-21.14064	-12.93681	-12.93681	-5.679576	-5.679576
491	-13.7256	-13.7256	-16.881	-16.881	-19.7208	-19.7208	-20.6673	-20.6673	-18.4586	-18.4586	-16.09213	-16.09213	-9.939258	-9.939258	-4.575214	-4.575214
492	-34.7085	-34.7085	-42.5968	-42.5968	-49.8541	-49.8541	-52.2205	-52.2205	-46.6987	-46.6987	-40.54586	-40.54586	-25.40033	-25.40033	-12.14798	-12.14798
493	-53.7982	-53.7982	-66.735	-66.735	-78.5675	-78.5675	-82.6694	-82.6694	-73.2034	-73.2034	-64.053	-64.053	-39.12597	-39.12597	-17.19649	-17.19649
494	191.6857	191.6857	245.484	245.484	296.6	296.6	313.481	313.481	272.935	272.935	242.6441	242.6441	137.0987	137.0987	29.50224	29.50224
495	-247.219	-247.219	-314.112	-314.112	-377.219	-377.219	-398.201	-398.201	-348.19	-348.19	-308.4325	-308.4325	-177.4868	-177.4868	-47.64533	-47.64533
496	178.7489	178.7489	230.812	230.812	280.35	280.35	296.7578	296.7578	257.159	257.159	229.5495	229.5495	129.8081	129.8081	22.24501	22.24501
497	159.5014	159.5014	205.885	205.885	250.059	250.059	264.7313	264.7313	229.55	229.55	204.7803	204.7803	115.7705	115.7705	19.87852	19.87852
498	19.24745	19.24745	24.7693	24.7693	30.1333	30.1333	31.86873	31.86873	27.6091	27.6091	24.76926	24.76926	14.0376	14.0376	2.36649	2.36649
499	2.208724	2.208724	5.04851	5.04851	8.20383	8.20383	9.150428	9.150428	6.46841	6.46841	7.09947	7.09947	1.271594	1.271594	-5.206278	-5.206278
500	-24.927	-24.927	-30.9221	-30.9221	-36.7595	-36.7595	-38.6427	-38.6427	-33.9197	-33.9197	-30.13331	-30.13331	-18.45862	-18.45862	-7.415002	-7.415002
501	-32.6576	-32.6576	-34.7085	-34.7085	-36.1284	-36.1284	-36.6017	-36.6017	-36.1284	-36.1284	-29.02894	-29.02894	-25.55809	-25.55809	-22.40277	-22.40277
502	12.14798	12.14798	14.0412	14.0412	15.7766	15.7766	16.40766	16.40766	14.9878	14.9878	13.25234	13.25234	9.623726	9.623726	4.417448	4.417448
503	41.80799	41.80799	47.0143	47.0143	52.6938	52.6938	54.42927	54.42927	50.0118	50.0118	44.17448	44.17448	33.28863	33.28863	15.46107	15.46107
504	13.09458	13.09458	14.6722	14.6722	16.4077	16.4077	17.03873	17.03873	15.6188	15.6188	14.35671	14.35671	10.88585	10.88585	3.15532	3.15532
505	-10.5703	-10.5703	-11.8325	-11.8325	-12.6213	-12.6213	-13.0946	-13.0946	-12.6213	-12.6213	-9.781492	-9.781492	-7.572768	-7.572768	-8.203832	-8.203832
506	-10.5703	-10.5703	-11.8325	-11.8325	-12.6213	-12.6213	-13.0946	-13.0946	-12.6213	-12.6213	-9.781492	-9.781492	-7.572768	-7.572768	-8.203832	-8.203832
507	-255.265	-255.265	-228.445	-228.445	-206.2	-206.2	-195.788	-195.788	-224.501	-224.501	-155.2417	-155.2417	-221.819	-221.819	-289.0273	-289.0273
508	14.04117	14.04117	-81.8806	-81.8806	-168.967	-168.967	-201.152	-201.152	-120.533	-120.533	-151.9287	-151.9287	50.48512	50.48512	251.7945	251.7945
509	-12.4635	-12.4635	-11.2014	-11.2014	-10.097	-10.097	-9.62373	-9.62373	-11.0436	-11.0436	-7.572768	-7.572768	-10.88585	-10.88585	-14.19894	-14.19894

510	-329.1	-329.1	-280.35	-280.35	-215.982	-215.982	-195.788	-195.788	-252.11	-252.11	-157.1349	-157.1349	-286.8186	-286.8186	-402.7766	-402.7766
511	27.13575	27.13575	1.89319	1.89319	-43.0701	-43.0701	-53.7982	-53.7982	-24.6115	-24.6115	-40.3881	-40.3881	28.24011	28.24011	80.77619	80.77619
512	12.46351	12.46351	11.2014	11.2014	10.097	10.097	9.623726	9.623726	11.0436	11.0436	7.572768	7.572768	10.88585	10.88585	14.19894	14.19894
513	-329.1	-329.1	-280.35	-280.35	-215.982	-215.982	-195.788	-195.788	-252.11	-252.11	-157.1349	-157.1349	-286.8186	-286.8186	-402.7766	-402.7766
531	-19.4052	-19.4052	66.8928	66.8928	160.606	160.606	191.2124	191.2124	113.276	113.276	144.5137	144.5137	-47.8031	-47.8031	-227.8141	-227.8141
532	-8.20383	-8.20383	28.5556	28.5556	68.4704	68.4704	81.56502	81.56502	48.2764	48.2764	61.68651	61.68651	-20.35181	-20.35181	-97.18386	-97.18386
533	2.050958	2.050958	-146.565	-146.565	-316.321	-316.321	-370.119	-370.119	-232.074	-232.074	-289.8161	-289.8161	37.70607	37.70607	355.4468	355.4468
534	-14.0412	-14.0412	81.8806	81.8806	168.967	168.967	201.1517	201.1517	120.533	120.533	151.9287	151.9287	-50.48512	-50.48512	-251.7945	-251.7945
535	-27.1358	-27.1358	-1.89319	-1.89319	43.0701	43.0701	53.79821	53.79821	24.6115	24.6115	40.3881	40.3881	-28.24011	-28.24011	-80.77619	-80.77619
719	87.08683	87.08683	87.5601	87.5601	88.8223	88.8223	89.29556	89.29556	88.1912	88.1912	78.09417	78.09417	77.14757	77.14757	76.51651	76.51651
720	-4247.06	-4247.06	-4323.89	-4323.89	-4448.53	-4448.53	-4493.96	-4493.96	-4402.14	-4402.14	-1262.601	-1262.601	-1171.886	-1171.886	-1051.037	-1051.037
730	7.415002	7.415002	8.04607	8.04607	8.99266	8.99266	9.308194	9.308194	8.51936	8.51936	8.834896	8.834896	6.783938	6.783938	0.165654	0.165654
731	8.992662	8.992662	9.93926	9.93926	11.0436	11.0436	11.35915	11.35915	10.5703	10.5703	10.88585	10.88585	8.361598	8.361598	0.20194	0.20194
732	10.57032	10.57032	11.8325	11.8325	12.6213	12.6213	13.09458	13.09458	12.6213	12.6213	9.781492	9.781492	7.572768	7.572768	8.203832	8.203832
733	-8.99266	-8.99266	-9.93926	-9.93926	-11.0436	-11.0436	-11.3592	-11.3592	-10.5703	-10.5703	-10.88585	-10.88585	-8.361598	-8.361598	-0.20194	-0.20194
734	1.572927	1.572927	0.74781	0.74781	0.22561	0.22561	-0.05837	-0.05837	0.72415	0.72415	5.048512	5.048512	4.575214	4.575214	-6.626172	-6.626172
735	-13.0946	-13.0946	-14.6722	-14.6722	-16.4077	-16.4077	-17.0387	-17.0387	-15.6188	-15.6188	-14.35671	-14.35671	-10.88585	-10.88585	-3.15532	-3.15532
736	-0.12069	-0.12069	-1.73543	-1.73543	-3.15532	-3.15532	-3.78638	-3.78638	-2.05096	-2.05096	4.890746	4.890746	5.048512	5.048512	-9.7790	-9.7790
737	-62.002	-62.002	-65.1574	-65.1574	-65.7884	-65.7884	-65.3151	-65.3151	-66.735	-66.735	-55.37587	-55.37587	-52.37831	-52.37831	-57.7275	-57.7275
738	61.84427	61.84427	63.4219	63.4219	62.6331	62.6331	61.52874	61.52874	64.6841	64.6841	60.26661	60.26661	57.42682	57.42682	47.9485	47.9485
739	37.86384	37.86384	43.2279	43.2279	47.4876	47.4876	49.38076	49.38076	45.5944	45.5944	41.33469	41.33469	29.81777	29.81777	12.14798	12.14798
740	-114.696	-114.696	-125.582	-125.582	-133.155	-133.155	-135.521	-135.521	-130.63	-130.63	-111.3828	-111.3828	-92.76641	-92.76641	-77.9364	-77.9364
741	37.86384	37.86384	43.2279	43.2279	47.4876	47.4876	49.38076	49.38076	45.5944	45.5944	41.33469	41.33469	29.81777	29.81777	12.14798	12.14798

APPENDIX C

742	-25.4003	-25.4003	-21.4562	-21.4562	-16.7232	-16.7232	-12.779	-12.779	-20.5096	-20.5096	-15.14554	-15.14554	-25.71586	-25.71586	-38.65267	-38.65267
743	33.60416	33.60416	30.1333	30.1333	24.4537	24.4537	20.66735	20.66735	29.3445	29.3445	27.13575	27.13575	34.55075	34.55075	36.91724	36.91724
744	-1.89319	-1.89319	1.89319	1.89319	6.15287	6.15287	8.519364	8.519364	3.31309	3.31309	2.524256	2.524256	-4.890746	-4.890746	-9.781492	-9.781492
746	-25.4003	-25.4003	-21.4562	-21.4562	-16.7232	-16.7232	-12.779	-12.779	-20.5096	-20.5096	-15.14554	-15.14554	-25.71586	-25.71586	-38.65267	-38.65267
747	-25.4003	-25.4003	-21.4562	-21.4562	-16.7232	-16.7232	-12.779	-12.779	-20.5096	-20.5096	-15.14554	-15.14554	-25.71586	-25.71586	-38.65267	-38.65267
748	-61.371	-61.371	-60.8977	-60.8977	-59.6355	-59.6355	-58.5312	-58.5312	-61.8443	-61.8443	-49.38076	-49.38076	-53.16714	-53.16714	-59.47778	-59.47778
751	-120.218	-120.218	-122.111	-122.111	-122.426	-122.426	-124.162	-124.162	-124.793	-124.793	-101.2858	-101.2858	-101.4435	-101.4435	-103.6523	-103.6523
863	1319.87	1319.87	1315.14	1315.14	1305.04	1305.04	1305.356	1305.356	1315.61	1315.61	1022.797	1022.797	1059.714	1059.714	1107.36	1107.36

Table C-3: Initial node concentrations for suspended and dissolved constituents

Node	CtOCI (M/l)	NH2Cl (M/l)	NHCl2 (M/l)	NHOHCl (M/l)	Cl (M/l)	BOM1 (ug/l)	BOM2 (ug/l)	Xis (ug/l)	Xhs (ug/l)	CtNH3 (M/l)	NO2 (M/l)	NO3 (M/l)	N2 (M/l)	Xn1s (ug/l)	Xn2s (ug/l)	CO2 (ug/l)	UAP (ug/l)	BAP (ug/l)	O2 (ug/l)	EPSs (ug/l)	Det. Time (h)
135	0	2.95E-05	8.36E-06	4.99E-06	5.28E-06	857.9	3866.66	3866.64	0.42	5.15E-05	1.03E-06	3.03E-05	1E-08	0.41	0.4	2.8	0.01	0.01	9200	0.008	2.15
136	0	3.44E-05	7.69E-06	3.21E-06	3.43E-06	858.21	3866.79	3866.77	0.42	4.94E-05	1.03E-06	3.03E-05	1E-08	0.41	0.4	2.23	0.01	0.01	9300	0.008	1.6
137	0	3.59E-05	5.44E-06	4.64E-06	5.04E-06	852.14	3865.19	3866.98	0.62	4.89E-05	1.02E-06	3.03E-05	2E-08	0.4	0.39	7.03	1.64	0.82	9350	0.011	2.79
138	0	4.22E-05	3.17E-06	2.21E-06	2.71E-06	856.44	3866.05	3866.02	0.41	4.51E-05	0.000001	3.03E-05	1E-08	0.39	0.38	5.51	0.03	0.02	9350	0.007	3.33
139	0	4.22E-05	1.37E-06	4.23E-07	6.65E-07	857.94	3866.68	3866.66	0.41	4.19E-05	1.03E-06	3.03E-05	0	0.4	0.4	2.74	0.01	0.01	9400	0.007	1.56
140	0	3.89E-05	6.79E-06	1.9E-06	2.05E-06	858.49	3866.91	3866.89	0.42	4.75E-05	1.04E-06	3.02E-05	0	0.41	0.41	1.7	0	0.01	9400	0.008	1.14
142	0	2.19E-05	7.82E-06	9.22E-06	9.7E-06	850.76	3864.16	3866.97	1.72	5.47E-05	1.02E-06	3.03E-05	5E-08	0.4	0.39	7.79	2.09	1.05	8900	0.031	3.46
143	0	2.16E-05	5.53E-06	1.16E-05	1.23E-05	755.47	3827.18	3875.15	19.96	5.54E-05	1.04E-06	3.03E-05	8E-08	0.47	0.39	67.74	31.75	16.91	8400	0.357	4.43
144	0	2.92E-05	3.82E-06	9.51E-06	1.02E-05	766.9	3839.06	3875.89	9.64	5.22E-05	1.01E-06	3.03E-05	7E-08	0.4	0.39	60.39	28.2	14.75	9200	0.173	4.2
145	0	3.44E-05	6.69E-06	4.21E-06	4.46E-06	853.22	3865.57	3867.24	0.57	4.95E-05	1.03E-06	3.03E-05	1E-08	0.41	0.4	5.49	1.52	0.76	9200	0.01	1.95
146	0	3.44E-05	6.78E-06	4.12E-06	4.37E-06	853.63	3865.67	3867.20	0.56	4.95E-05	1.03E-06	3.03E-05	1E-08	0.41	0.4	5.22	1.39	0.7	9200	0.01	1.92
147	0	3.44E-05	5.6E-06	5.27E-06	5.6E-06	845.87	3863.77	3867.95	0.83	4.95E-05	1.03E-06	3.03E-05	2E-08	0.4	0.4	10.25	3.75	1.87	8900	0.015	2.4
148	0	3.44E-05	5.8E-06	5.08E-06	5.39E-06	848.8	3864.48	3867.64	0.71	4.95E-05	1.03E-06	3.03E-05	2E-08	0.4	0.4	8.42	2.84	1.42	9100	0.013	2.31
149	0	2.13E-05	4.89E-06	1.24E-05	1.31E-05	676.85	3792.17	3883.17	25.68	5.59E-05	1.15E-06	3.03E-05	1E-07	0.55	0.38	121.24	55.8	31.98	7800	0.46	4.81
150	0	3.3E-05	3.01E-06	8.29E-06	9.21E-06	770.16	3831.37	3877.60	9.86	5.03E-05	1.35E-06	3.03E-05	1E-07	0.83	0.38	66.45	26.42	18.48	7400	0.176	4.88
151	0	3.44E-05	5.41E-06	5.44E-06	5.78E-06	846.75	3863.97	3867.82	0.77	4.95E-05	1.02E-06	3.03E-05	2E-08	0.4	0.4	9.78	3.46	1.72	9000	0.014	2.48
152	0	3.45E-05	4.16E-06	6.6E-06	7.05E-06	838.64	3861.98	3868.56	1.02	4.95E-05	1.02E-06	3.03E-05	3E-08	0.4	0.39	15.17	5.89	2.95	8800	0.018	3.14
153	0	3.45E-05	3.75E-06	6.98E-06	7.49E-06	835.35	3861.16	3868.87	1.12	4.96E-05	1.02E-06	3.03E-05	4E-08	0.4	0.39	17.37	6.88	3.45	8500	0.02	3.41
154	0	3.07E-05	4.47E-07	7.43E-06	1.75E-05	577.54	3617.72	3914.45	36.28	4.41E-05	5.99E-06	3.67E-05	7.9E-07	9.59	0.96	249.86	81.97	123.38	7000	0.649	40.54
155	0	2.29E-05	4.59E-07	9.45E-06	2.33E-05	466.1	3507.02	3935.96	60.01	4.37E-05	8.6E-06	3.95E-05	1.07E-06	15.13	1.3	348.24	115.11	178.26	6700	1.074	52.03
156	0	1.64E-05	1.04E-06	1.27E-05	2.54E-05	436.48	3514.56	3940.72	74.08	4.66E-05	8.32E-06	3.96E-05	8.9E-07	16.64	1.67	359.27	125.38	182.82	6800	1.326	41.33

APPENDIX C

158	0	1.78E-05	1.32E-06	1.36E-05	2.23E-05	463.52	3614.09	3932.24	70.22	4.93E-05	7.08E-06	3.63E-05	5.1E-07	14.3	1.4	302.81	120.35	141.49	7000	1.257	21.91
159	0	1.26E-05	1.6E-06	1.52E-05	2.51E-05	363.9	3562.5	3946.83	87.16	5.05E-05	8.18E-06	3.73E-05	5.4E-07	16.36	1.58	369.79	151.73	169.43	7100	1.56	23.06
160	0	1.21E-05	1.98E-06	1.55E-05	2.44E-05	359.54	3560.76	3943.32	81.9	5.24E-05	6.58E-06	3.69E-05	4.9E-07	12.46	1.5	376.44	152.11	162.47	7300	1.466	21.19
161	0	7.95E-06	3.26E-07	1.21E-05	3.61E-05	187.89	3302.15	3997.26	66.93	3.69E-05	1.69E-05	4.98E-05	1.26E-06	21.3	2.51	503.95	209.56	308.77	7000	1.198	50
162	0	8.22E-07	1.21E-08	3.35E-06	5.23E-05	36.65	2566.9	4061.34	151.22	1.55E-05	1.38E-05	8.78E-05	2.35E-06	59.98	11	871.98	232.97	634.62	6500	2.707	121.13
163	0	8.94E-07	1.21E-08	3.67E-06	5.21E-05	33.69	2562.54	4076.22	158.25	1.74E-05	9.73E-06	9E-05	2.43E-06	60.79	12.22	893.92	231.44	624.92	6500	2.833	124.4
164	0	5.32E-07	1.21E-08	2.33E-06	5.36E-05	25.95	2436.51	4074.37	161.13	1.23E-05	9.47E-06	9.63E-05	2.65E-06	63.48	12.36	964.1	226.74	697.35	6700	2.884	140.86
165	0	5.8E-07	1.21E-08	2.56E-06	5.35E-05	27.06	2464.88	4075.25	161.47	1.34E-05	7.77E-06	9.65E-05	2.72E-06	62.69	12.77	946.93	228.21	680.63	6700	2.89	145.13
166	0	1.78E-06	1.69E-07	4.34E-06	5.02E-05	71.69	2643.33	4038.41	149.46	1.62E-05	1.73E-05	8.09E-05	2.46E-06	60.67	9.75	838.63	223.35	609.65	6800	2.675	127.73
167	0	6.89E-06	1.02E-06	1.16E-05	3.61E-05	207.93	3370.47	3989.24	127.2	3.3E-05	1.81E-05	5.33E-05	8.5E-07	45.81	7.24	416.29	214.67	309.98	7100	2.277	38.81
168	0	1.08E-05	3.44E-06	1.64E-05	2.16E-05	399.22	3598.56	3920.33	73.04	5.75E-05	4.85E-06	3.27E-05	2.6E-07	6.88	0.78	333.36	139.64	119.4	7800	1.307	10.43
169	0	1.13E-05	3.03E-06	1.66E-05	2.17E-05	389.31	3604.91	3924.79	73.2	5.73E-05	4.86E-06	3.27E-05	2.6E-07	7.08	0.77	342.29	142.6	121.94	7700	1.31	10.67
170	0	1.24E-05	2.5E-06	1.67E-05	2.17E-05	384.26	3623.1	3931.07	74.23	5.67E-05	0.000005	3.26E-05	2.8E-07	7.5	0.76	347.11	144.31	123.81	7500	1.329	11.16
171	0	1.18E-05	2.14E-06	1.56E-05	2.42E-05	355.98	3559.95	3942.20	81.28	5.28E-05	6.49E-06	3.67E-05	4.5E-07	12.1	1.49	376.37	153.38	160.87	7500	1.455	19.51
172	0	6.86E-06	4.83E-08	8.44E-06	4.11E-05	164.56	3093.44	4010.03	122.33	2.99E-05	1.53E-05	6.24E-05	1.56E-06	46.44	7.83	574.74	212.29	394.27	6500	2.19	70
173	0	2.41E-05	1.53E-06	1.28E-05	1.62E-05	544.85	3805.19	3919.62	24.76	4.68E-05	9.23E-06	3.13E-05	2.8E-07	8.56	0.77	169.96	103.71	82.73	6500	0.443	12.31
174	0	2.01E-05	3.38E-07	9.84E-06	2.59E-05	437.78	3458.22	3942.26	64.33	4.29E-05	1.01E-05	4.08E-05	1.28E-06	17.71	1.33	376.85	123.55	199.2	6500	1.152	60.94
175	0	7.89E-06	3.5E-07	1.17E-05	3.61E-05	237.38	3347.66	3971.96	92.23	4.04E-05	1.96E-05	4.33E-05	1.23E-06	24.52	2.15	446.45	195.1	266.75	6600	1.651	37.63
176	0	3.6E-06	2.42E-08	9.11E-06	4.34E-05	109.79	3151.05	3993.80	121.9	3.32E-05	2.59E-05	5.07E-05	1.3E-06	33.03	2.99	534.56	235.98	357.26	6600	2.182	34.32
177	0	6.15E-06	4.83E-08	7.7E-06	4.26E-05	145.06	3013.44	4018.08	127.66	2.81E-05	1.48E-05	6.57E-05	1.74E-06	48.38	8.02	624.95	214.75	427.46	5500	2.285	81.2
178	0	1.16E-05	3.67E-06	1.62E-05	2.07E-05	425.78	3601.77	3912.15	72.85	5.77E-05	3.94E-06	3.25E-05	2.5E-07	5.43	0.8	313.77	131.18	109.69	7900	1.304	9.58
179	0	1.55E-05	5.31E-06	1.48E-05	1.57E-05	646.1	3770.99	3883.75	36.47	5.86E-05	1.02E-06	3.03E-05	1.4E-07	0.42	0.38	142.55	65.06	37.19	8000	0.653	5.74
180	0	2.1E-05	7.38E-06	1.01E-05	1.07E-05	813.47	3849.87	3870.03	7.73	5.53E-05	1.02E-06	3.03E-05	6E-08	0.4	0.39	30.8	13.75	7.05	8700	0.138	3.77

181	0	2.1E-05	7.59E-06	9.89E-06	1.04E-05	824.13	3853.99	3869.15	6.04	5.52E-05	1.02E-06	3.03E-05	5E-08	0.4	0.39	24.19	10.42	5.32	8800	0.108	3.69
194	0	1.73E-05	9.43E-07	1.28E-05	2.47E-05	423.88	3530.8	3968.18	68.11	4.97E-05	5.57E-06	3.88E-05	1.3E-06	5.78	0.6	397.89	127.72	171.98	7200	1.219	66.3
195	0	1.78E-05	1.47E-06	1.5E-05	2.04E-05	472.45	3664.39	3920.72	65.66	5.45E-05	3.8E-06	0.000033	5.1E-07	4.44	0.59	288.83	116.67	103.74	7300	1.175	20.36
196	0	1.39E-05	2.49E-06	1.61E-05	2.09E-05	419.33	3618.41	3920.27	73.57	5.65E-05	3.94E-06	3.29E-05	3.2E-07	5.51	0.77	324.13	132.76	114.34	7600	1.317	12.45
302	0	4.21E-05	6.77E-07	2.42E-08	3.63E-08	859.32	3867.27	3867.26	0.42	4.08E-05	1.05E-06	3.02E-05	0	0.42	0.42	0.14	0	0	9440	0.008	0.08
309	0	2.82E-05	3.14E-07	0.000012	1.56E-05	546.32	3793.92	3918.20	34.63	4.62E-05	8.24E-06	3.13E-05	3.3E-07	11.49	0.82	180.7	101.45	81.39	6300	0.62	13.74
310	0	5.79E-06	3.63E-08	8.89E-06	4.17E-05	131.46	3065.6	4021.82	91.38	3.37E-05	2.25E-05	5.14E-05	2.05E-06	27.08	2.71	686.56	210.5	392.14	6200	1.636	68.46
311	0	5.39E-06	1.09E-07	1.07E-05	4.01E-05	168.88	3270.48	4006.22	89.38	3.4E-05	2.18E-05	4.98E-05	1.96E-06	30.35	2.62	540.56	213.59	338.83	6000	1.6	72.47
312	0	7.14E-06	1.09E-07	7.63E-06	4.13E-05	141.96	3034.77	4011.42	89.28	2.87E-05	2.37E-05	5.67E-05	9.5E-07	24.02	2.77	614.67	213.24	412.36	6800	1.598	28.3
313	0	1.22E-05	6.89E-07	1.23E-05	3.09E-05	214.11	3437.18	4002.49	43.66	3.36E-05	2.22E-05	4.46E-05	5.5E-07	13.18	1.7	443.41	205.12	288.44	6800	0.782	18.86
314	0	2.85E-05	2.45E-06	1.08E-05	1.2E-05	791.06	3848.53	3872.69	5.09	5.24E-05	9.9E-07	3.03E-05	1.4E-07	0.38	0.36	47.41	20.11	10.35	6900	0.091	7.17
315	0	3.2E-05	3.47E-06	8.44E-06	9.11E-06	834.9	3860.8	3868.61	1.13	5.06E-05	1.01E-06	3.03E-05	6E-08	0.4	0.38	18.28	6.87	3.45	7800	0.02	4.33
316	0	2.89E-05	3.2E-06	1.02E-05	1.1E-05	812.64	3853.84	3870.65	3.08	5.2E-05	0.000001	3.03E-05	1E-07	0.39	0.38	32.51	13.72	6.97	7800	0.055	5.37
317	0	2.69E-05	3.05E-06	1.12E-05	1.22E-05	792.48	3847.15	3872.55	5.69	5.3E-05	0.000001	3.03E-05	1.2E-07	0.4	0.37	45.59	19.9	10.29	7800	0.102	6.16
318	0	3.15E-05	2.09E-06	9.47E-06	1.11E-05	728.03	3824.83	3883.98	9.3	5.08E-05	1.96E-06	3.03E-05	1.2E-07	0.78	0.35	95.15	39.18	27.5	7000	0.166	8.24
319	0	2.63E-05	2.9E-06	1.16E-05	1.27E-05	776.27	3841.61	3874.14	7.87	5.33E-05	1.01E-06	3.03E-05	1.3E-07	0.4	0.37	55.84	24.94	12.99	8000	0.141	6.39
320	0	3.02E-05	3.65E-06	9.16E-06	9.86E-06	830.38	3859.07	3868.97	2.47	5.14E-05	1.01E-06	3.03E-05	7E-08	0.4	0.38	21.07	8.28	4.17	8300	0.044	4.49
321	0	3.08E-05	4.44E-06	8.16E-06	8.74E-06	844.8	3863.33	3867.61	0.95	5.11E-05	1.01E-06	3.03E-05	5E-08	0.4	0.39	11.96	3.83	1.92	8500	0.017	3.91
322	0	3.29E-05	5.09E-06	6.48E-06	6.9E-06	845.59	3863.65	3867.80	0.83	5.02E-05	1.02E-06	3.03E-05	3E-08	0.4	0.39	10.85	3.73	1.86	8700	0.015	3
351	0	3.37E-05	5.34E-06	5.87E-06	6.25E-06	845.71	3863.71	3867.88	0.83	4.98E-05	1.02E-06	3.03E-05	2E-08	0.4	0.39	10.56	3.75	1.87	8800	0.015	2.69
412	0	4.24E-05	4.83E-08	0	1.21E-08	859.35	3867.28	3867.27	0.42	4.03E-05	1.05E-06	3.02E-05	0	0.42	0.42	0.1	0	0	9440	0.008	0.05
437	0	4.29E-05	4.59E-07	2.42E-07	4.11E-07	858.35	3866.86	3866.84	0.41	4.09E-05	1.03E-06	3.03E-05	0	0.41	0.41	1.96	0.01	0.01	9400	0.007	1.1
438	0	3.34E-05	3.75E-06	7.5E-06	8.07E-06	835.19	3861.06	3868.78	1.12	5E-05	1.01E-06	3.03E-05	5E-08	0.4	0.39	17.72	6.87	3.45	8200	0.02	3.75

APPENDIX C

439	0	3.49E-06	1.21E-08	8.63E-06	4.38E-05	95.96	3120.33	4005.70	126.38	3.16E-05	2.59E-05	5.28E-05	1.33E-06	35.23	3.35	569.32	238.51	380.04	6500	2.262	36.63
440	0	1.47E-05	3.87E-06	1.63E-05	1.75E-05	631.85	3763.59	3884.99	37.36	5.9E-05	1.03E-06	3.03E-05	1.8E-07	0.44	0.37	153.4	69.25	40.09	7500	0.669	6.94
445	0	6.5E-06	1.23E-06	1.2E-05	3.51E-05	100.03	3300.71	4049.48	117.51	2.65E-05	1.87E-05	6.1E-05	2.3E-07	38.64	7.85	528.86	247.49	391.58	8100	2.103	10.39
457	0	1.51E-05	7.25E-07	1.15E-05	2.9E-05	376.66	3405.23	4006.44	71.13	4.63E-05	7.04E-06	4.37E-05	1.95E-06	7.11	0.65	494.16	138.85	231.51	7100	1.273	104.13
468	0	2.65E-05	3.06E-06	1.13E-05	1.24E-05	791.57	3847.37	3872.65	5.68	5.32E-05	0.000001	3.03E-05	1.3E-07	0.4	0.37	46.49	20.11	10.41	7200	0.102	6.54
503	0	3.61E-05	7.41E-06	2.67E-06	2.86E-06	858.32	3866.84	3866.82	0.42	4.87E-05	1.03E-06	3.03E-05	1E-08	0.41	0.41	2.03	0.01	0.01	9350	0.008	1.41
504	0	4.23E-05	2.61E-06	1.22E-06	1.6E-06	857.13	3866.33	3866.30	0.41	4.37E-05	1.01E-06	3.03E-05	0	0.4	0.39	4.26	0.01	0.01	9350	0.007	2.5
1000	0	2.14E-06	1.21E-08	5.23E-06	5.17E-05	111.11	2731.85	-1.52	84.87	2.91E-05	1.48E-05	7.01E-05	5.32E-06	13.71	0.89	1015.91	202.49	550.53	6900	1.519	301.35

Table C-4: Initial pipe biofilm concentrations

Pipe	Xhf (ug/l)	Xn1f (ug/l)	Xn2f (ug/l)	EPSf (ug/l)	Xif (ug/l)
1	0.00	32.55	16.68	1.16	4.92
435	2559.97	0.12	0.00	60.42	256.01
436	3000.00	1.00	0.00	70.82	300.10
437	5246.01	20.97	0.00	124.30	526.70
438	3000.00	2.00	0.00	70.85	300.20
439	3200.00	3.00	0.00	75.59	320.30
440	3200.00	3.00	0.00	75.59	320.30
441	860.17	0.09	0.00	20.30	86.03
442	2718.83	1.12	0.00	64.19	271.99
443	2439.89	0.33	0.00	57.59	244.02
444	952.86	0.05	0.00	22.49	95.29
445	1675.17	0.26	0.00	39.54	167.54
446	587.18	0.00	0.00	13.86	58.72
447	801.45	0.05	0.00	18.92	80.15
449	5800.00	28.00	0.00	137.54	582.80
450	5500.00	25.00	0.00	130.39	552.50
453	6000.00	30.00	0.00	142.31	603.00
455	15965.88	259.60	0.00	382.92	1622.55
456	16503.31	254.67	0.00	395.49	1675.80
457	7998.51	137.58	0.00	192.01	813.61
458	8078.60	155.60	0.00	194.33	823.42
460	2120.53	201.30	0.00	54.80	232.18
461	4376.30	385.22	0.01	112.37	476.15
462	16484.17	59.40	6.27	390.58	1654.98
463	2858.64	86.41	0.00	69.50	294.51
464	8963.20	690.93	292.43	234.74	994.66
466	2932.90	387.91	0.03	78.37	332.08
467	2682.04	2284.89	0.41	117.23	496.73
468	4416.91	558.46	98.94	119.75	507.43
469	2555.95	1948.61	2.21	106.36	450.68
470	1613.30	1707.20	0.99	78.39	332.15
471	8910.55	430.73	160.76	224.25	950.21
472	1901.60	273.31	44.82	52.39	221.97

473	10875.90	1473.12	544.17	304.28	1289.32
474	7454.50	316.64	141.52	186.74	791.27
477	1745.10	169.29	48.26	46.32	196.27
478	14744.64	1665.48	544.30	400.12	1695.44
479	15354.47	2329.17	743.15	434.87	1842.68
480	6233.53	23.16	8.48	147.86	626.52
481	18375.81	2223.80	711.44	502.94	2131.11
482	3500.90	9.47	3.48	82.93	351.39
483	1699.57	388.44	127.35	52.28	221.54
484	2283.83	30.67	11.85	54.90	232.64
485	2726.36	80.45	28.41	66.91	283.52
486	5904.93	100.88	37.28	142.62	604.31
487	2988.78	32.38	12.57	71.60	303.37
488	3399.64	52.76	20.44	81.96	347.28
489	3484.51	77.05	28.39	84.72	358.99
490	4687.79	103.28	41.29	114.04	483.24
491	4553.10	59.74	23.78	109.42	463.66
492	3298.08	94.61	35.10	80.90	342.78
493	3467.07	53.75	27.77	83.75	354.86
494	1779.75	212.78	109.43	49.61	210.20
495	1254.50	87.80	68.79	33.30	141.11
496	1786.78	118.99	47.52	46.10	195.33
497	1833.60	408.13	143.37	56.29	238.51
498	5685.26	53.98	18.52	135.88	575.78
499	1742.96	4.63	2.60	41.30	175.02
500	2969.05	173.50	65.07	75.70	320.76
501	2421.52	16.34	7.21	57.70	244.51
502	2783.35	38.61	9.25	66.82	283.12
503	4779.63	23.88	8.25	113.56	481.18
504	3561.72	26.53	8.14	84.87	359.64
505	996.24	2.49	0.99	23.59	99.97
506	1227.86	9.96	4.02	29.31	124.18
507	10184.22	1021.20	37.41	265.33	1124.28
508	1626.36	470.72	99.16	51.83	219.62
509	1702.94	6.65	1.96	40.39	171.16

510	6271.69	161.98	0.00	151.83	643.37
511	5457.27	1175.20	201.63	161.28	683.41
512	27101.06	16.36	4.81	640.08	2712.22
513	8604.96	1604.14	0.01	240.93	1020.91
531	798.93	122.01	20.29	22.21	94.12
532	1410.37	402.60	80.19	44.68	189.32
533	363.76	113.67	32.40	12.03	50.98
534	995.03	157.71	31.13	27.94	118.39
535	3578.42	677.91	126.44	103.43	438.28
719	1115.96	0.02	0.00	26.34	111.60
720	199.98	0.01	0.00	4.72	20.00
730	1828.46	7.83	2.25	43.39	183.85
731	1603.65	3.22	0.79	37.94	160.77
732	2118.89	2.30	0.93	50.08	212.21
733	579.53	2.48	0.61	13.75	58.26
734	3628.27	179.01	73.12	91.58	388.04
735	5039.91	105.85	32.53	122.21	517.83
736	10245.61	1604.84	75.00	281.44	1192.54
737	1860.14	122.45	0.26	46.80	198.28
738	23729.25	1538.77	75.00	598.10	2534.30
739	3066.10	1166.10	54.67	101.17	428.69
740	843.27	482.71	0.38	31.30	132.64
741	3276.09	3435.24	190.49	162.88	690.18
742	5730.13	3009.48	200.00	210.97	893.96
743	4076.06	1768.79	311.38	145.29	615.62
744	12321.94	678.73	216.82	311.93	1321.75
746	15953.99	3000.00	177.95	730.45	3095.12
747	6303.71	623.64	20.45	167.69	710.53
748	2224.10	139.79	0.00	55.79	236.39
751	2145.83	249.33	0.00	56.53	239.52
863	137.97	0.01	0.00	3.26	13.80

Table C-5: Treatment plant inputs for simulations performed

Scenario	CtOCl (M/l)	NH ₂ Cl (M/l)	NHCl ₂ (M/l)	NHOHCl (M/l)	Cl (M/l)	BOM ₁ (ug/l)	BOM ₂ (ug/l)	X _{is} (ug/l)	X _{hs} (ug/l)	CtNH ₃ (M/l)	NO ₂ (M/l)	NO ₃ (M/l)	N ₂ (M/l)	X _{n1s} (ug/l)	X _{n2s} (ug/l)	CO ₂ (ug/l)	UAP (ug/l)	BAP (ug/l)	O ₂ (ug/l)	EPSs (ug/l)	Temp °C	pH
Baseline	0	4.24E-05	0	0	0	859.4	3867.3	3867.3	0.42	3.65E-05	1.05E-06	3.02E-05	0	0.04	0.04	0	0	0	9440	0.009	18	8
Alternative 1	0	4.24E-05	0	0	0	859.4	3867.3	3867.3	0.42	3.65E-05	1.05E-06	3.02E-05	0	0.04	0.04	0	0	0	9440	0.009	18	8
Alternative 2	0	4.24E-05	0	0	0	172.4	3093.6	3867.3	0.42	3.65E-05	1.05E-06	3.02E-05	0	0.04	0.04	0	0	0	9440	0.009	18	8
Alternative 3	0	4.24E-05	0	0	0	859.4	3867.3	3867.3	0.42	0.00E+00	1.05E-06	3.02E-05	0	0.04	0.04	0	0	0	9440	0.009	18	8
Alternative 4	0	4.24E-05	0	0	0	859.4	3867.3	3867.3	0.42	3.65E-05	1.05E-06	3.02E-05	0	0.04	0.04	0	0	0	9440	0.009	18	8
Alternative 5	0	4.24E-05	0	0	0	859.4	3867.3	3867.3	0.018	3.65E-05	1.05E-06	3.02E-05	0	0.04	0.04	0	0	0	9440	0.002	18	8
Alternative 6	0	4.24E-05	0	0	0	172.4	3093.6	3867.3	0.42	0.00E+00	1.05E-06	3.02E-05	0	0.04	0.04	0	0	0	9440	0.009	18	8
Alternative 7	0	4.24E-05	0	0	0	172.4	3093.6	3867.3	0.42	0.00E+00	1.05E-06	3.02E-05	0	0.04	0.04	0	0	0	9440	0.009	18	8
Alternative 8	0	4.24E-05	0	0	0	172.4	3093.6	3867.3	0.42	0.00E+00	1.05E-06	3.02E-05	0	0.04	0.04	0	0	0	9440	0.009	18	8

Table C-6: Booster chloramination inputs for Alternative 4

Node	NH ₂ Cl (M/l)
179	2.82E-05
320	1.69E-05

Table C-7: Booster chloramination inputs for Alternative 7

Node	NH ₂ Cl (M/l)
161	3.53E-05

D. APPENDIX D

D.1 Reduce Surface Catalysis by Coating Concrete Pipes

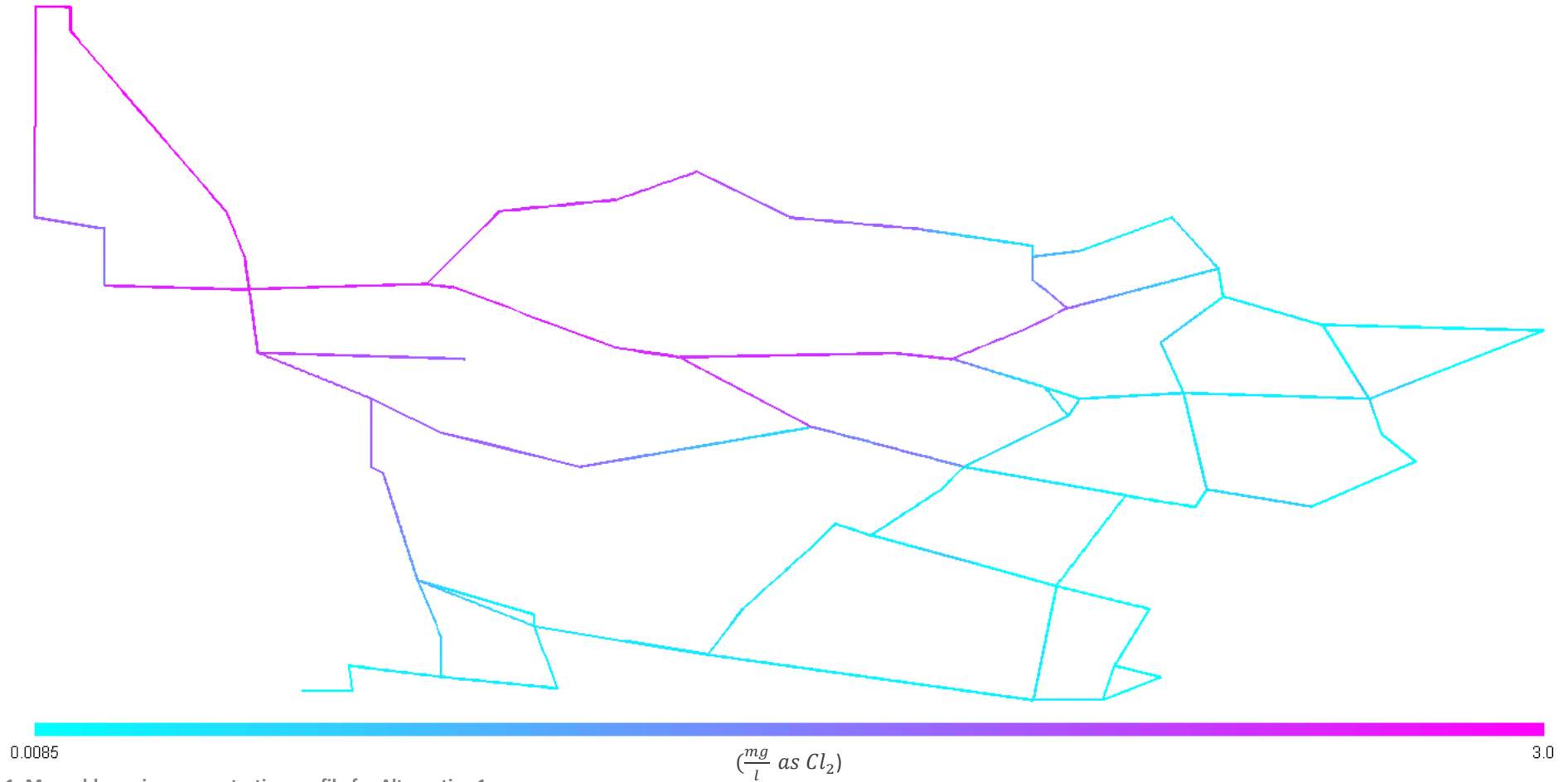


Figure D-1: Monochloramine concentration profile for Alternative 1

The monochloramine concentration profile is similar to the baseline scenario. The minimum disinfectant residual concentration is only slightly increased using this alternative.

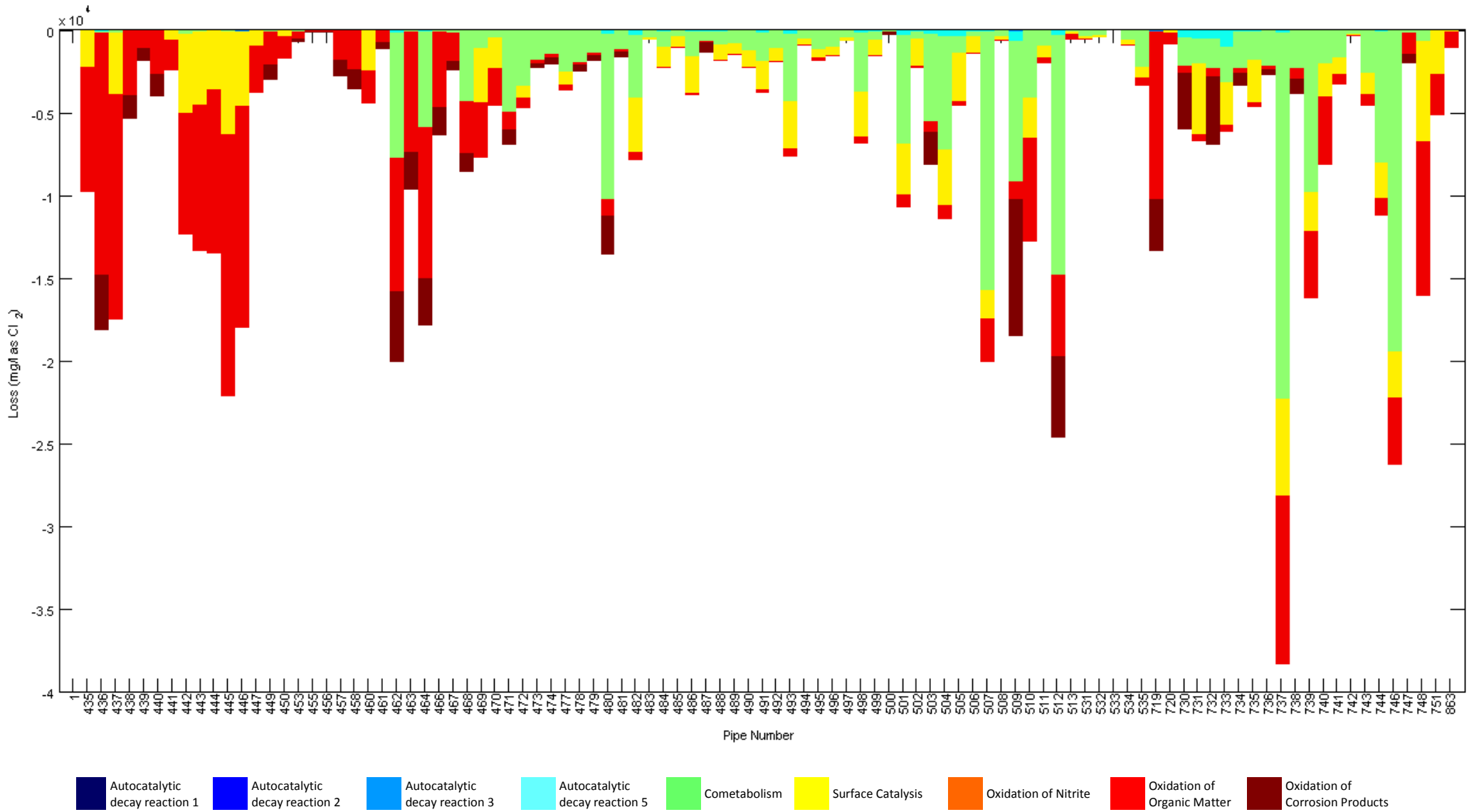


Figure D-2: Monochloramine loss mechanisms and locations for Alternative 1

The loss of monochloramine due to surface catalysis has been significantly reduced. However, the total loss of monochloramine is similar to the baseline case. This is because the loss of monochloramine due to cometabolism, the oxidation of organic matter and the oxidation of corrosion products is a function of monochloramine

concentration. Consequently, the effectiveness of reducing the rate of catalysis on the total loss of monochloramine is limited in this scenario, as the three aforementioned loss mechanisms, particularly the loss of monochloramine due to the oxidation of organic matter, becomes more significant.

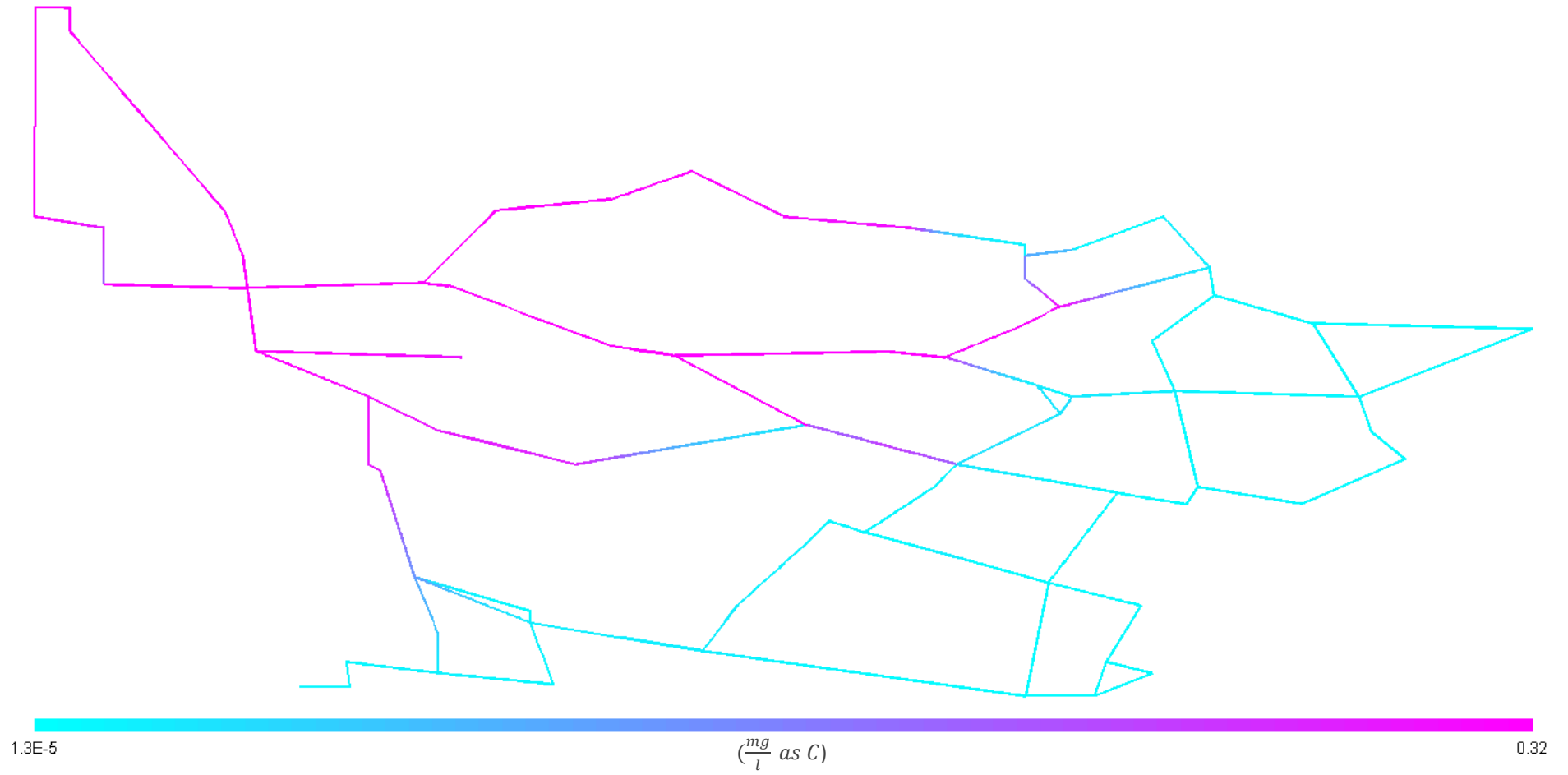


Figure D-3: BOM₁ concentration profile for Alternative 1

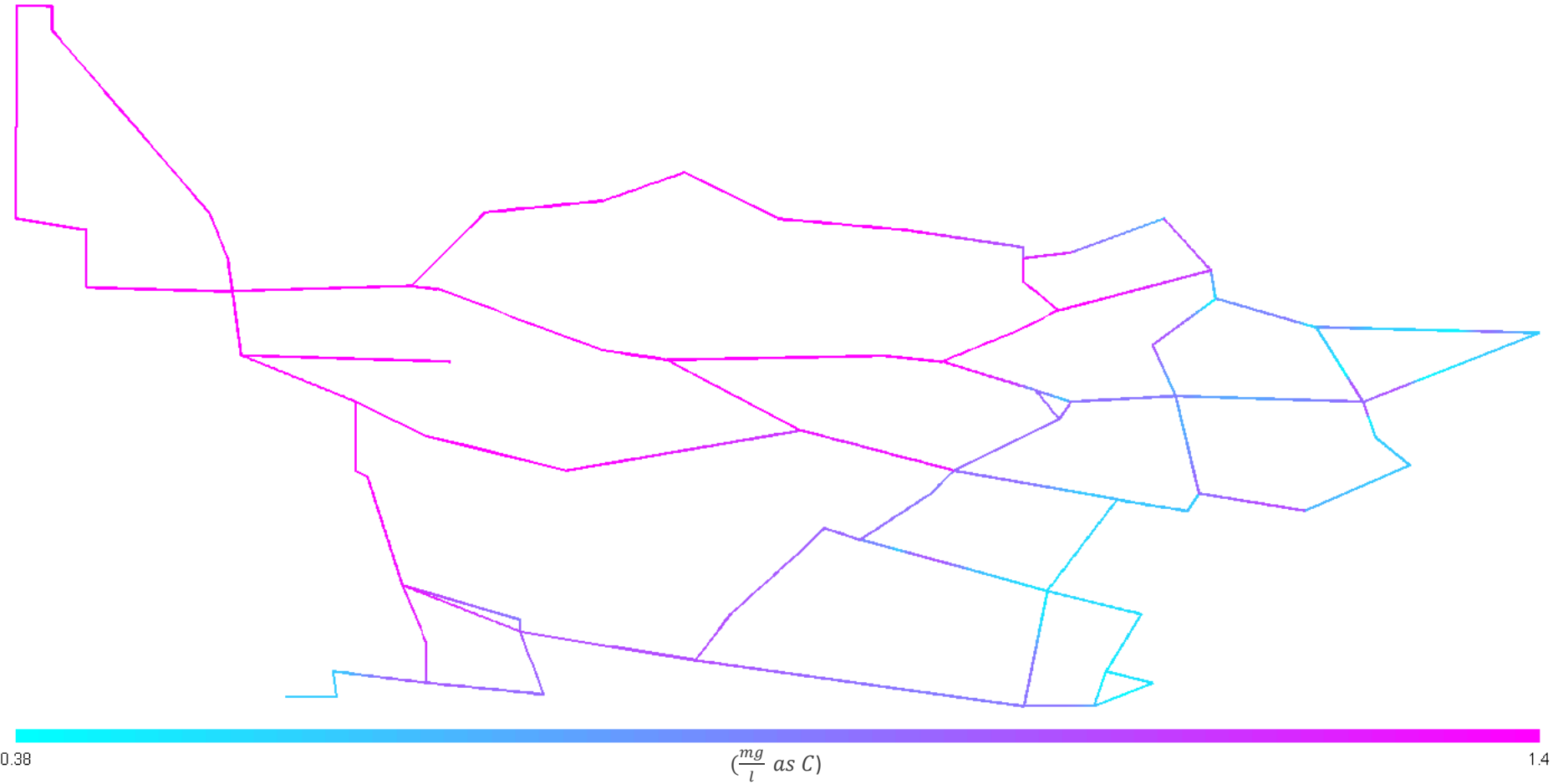


Figure D-4: BOM₂ concentration profile for Alternative 1

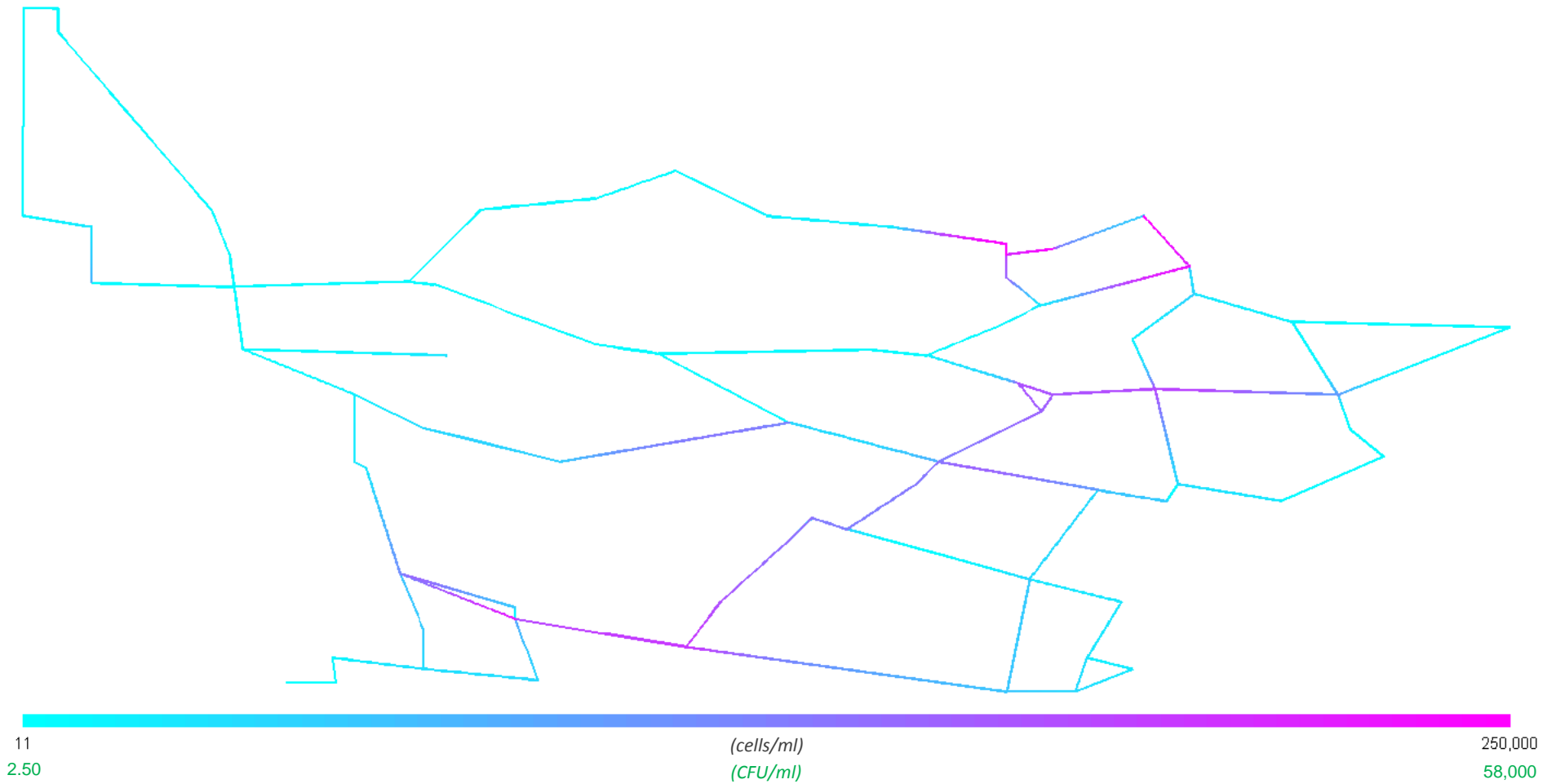


Figure D-5: Suspended heterotroph concentration profile for Alternative 1

The maximum suspended heterotroph concentration still significantly exceeds the limit of $4300 \frac{\text{cells}}{\text{ml}}$. This is because this alternative does not reduce input BOM and has only a limited effect on increase the concentration of residual disinfectant.

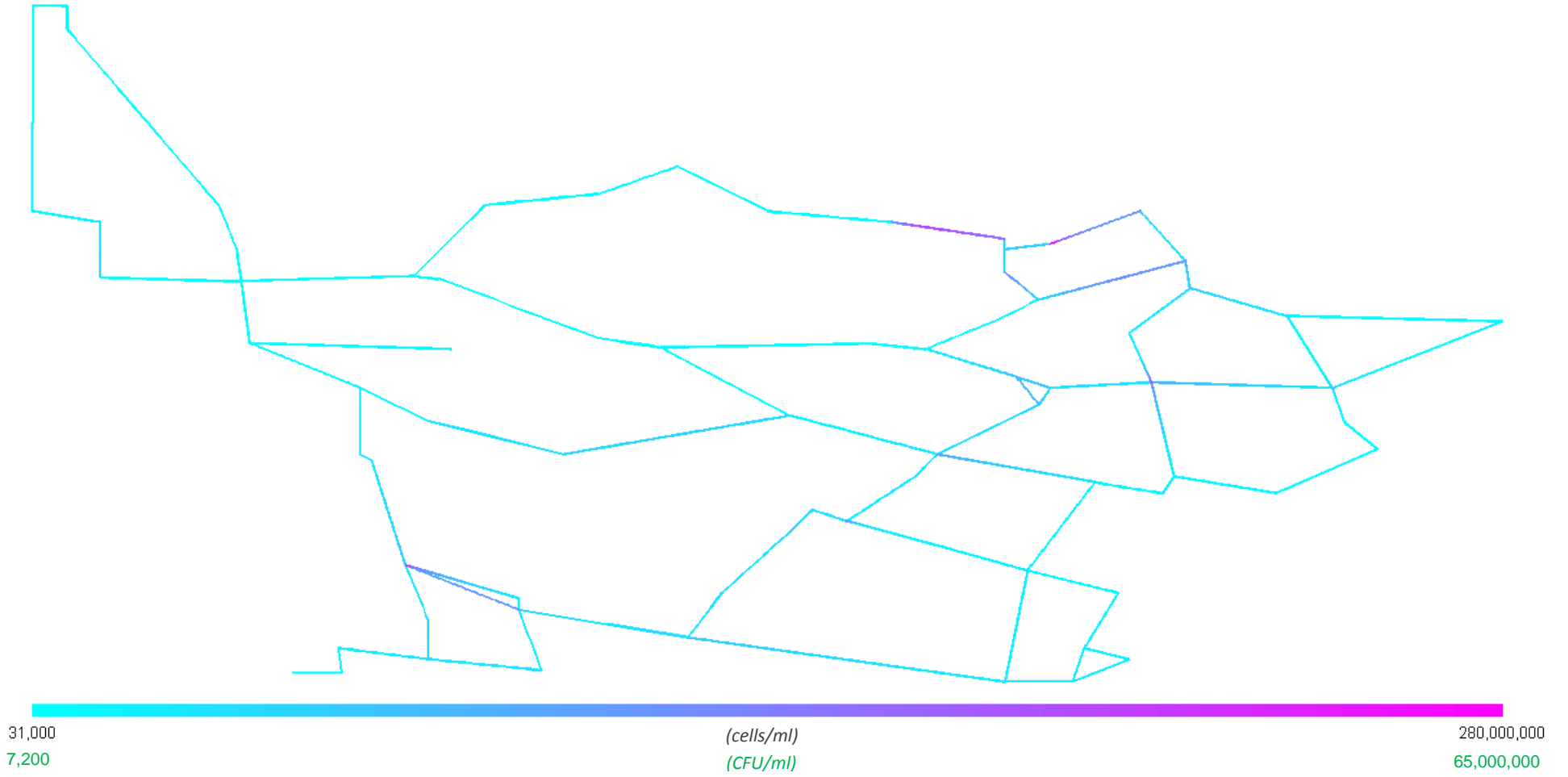


Figure D-6: Fixed heterotroph concentration profile for Alternative 1

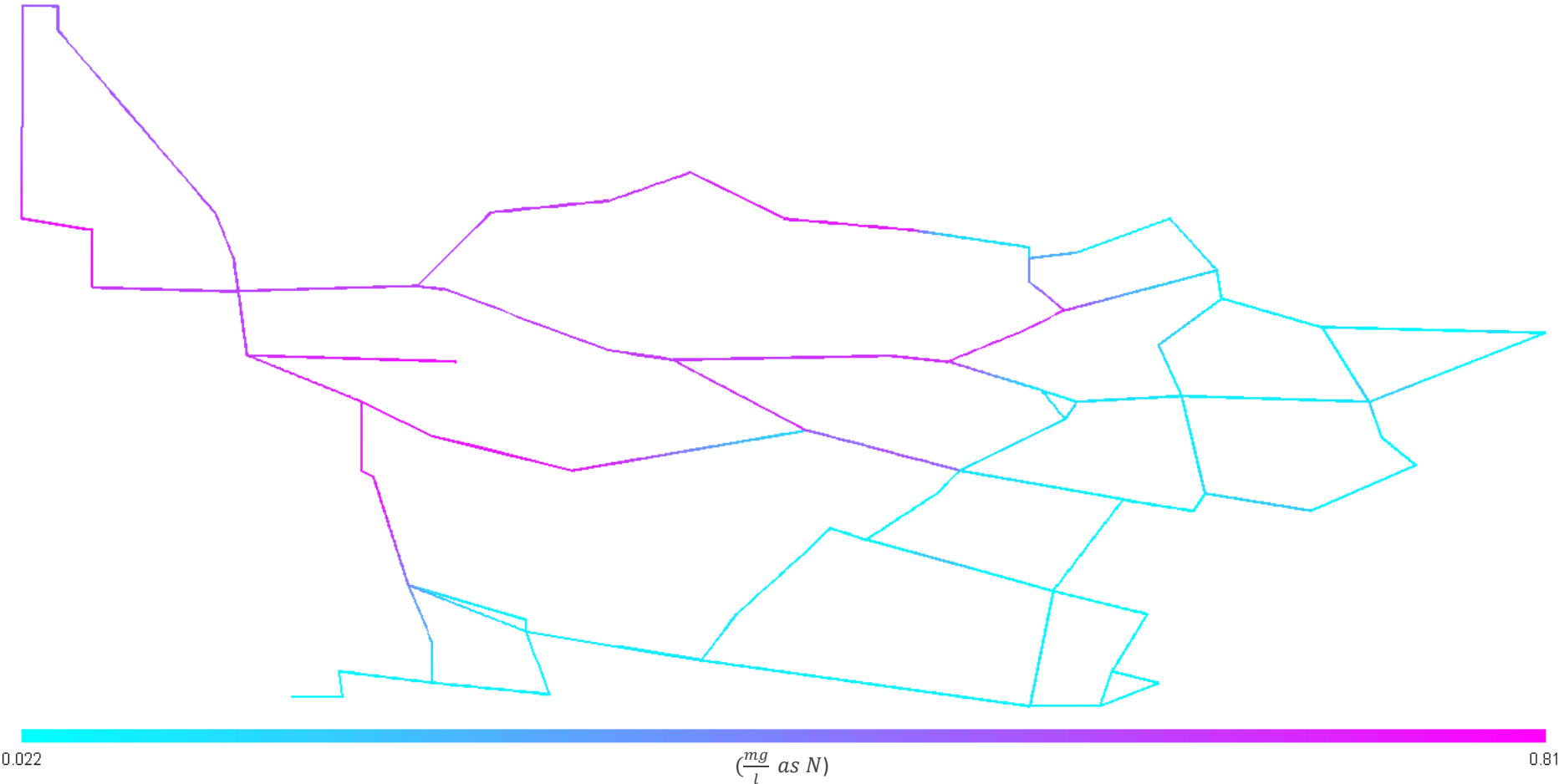


Figure D-7: Total ammonia concentration profile for Alternative 1

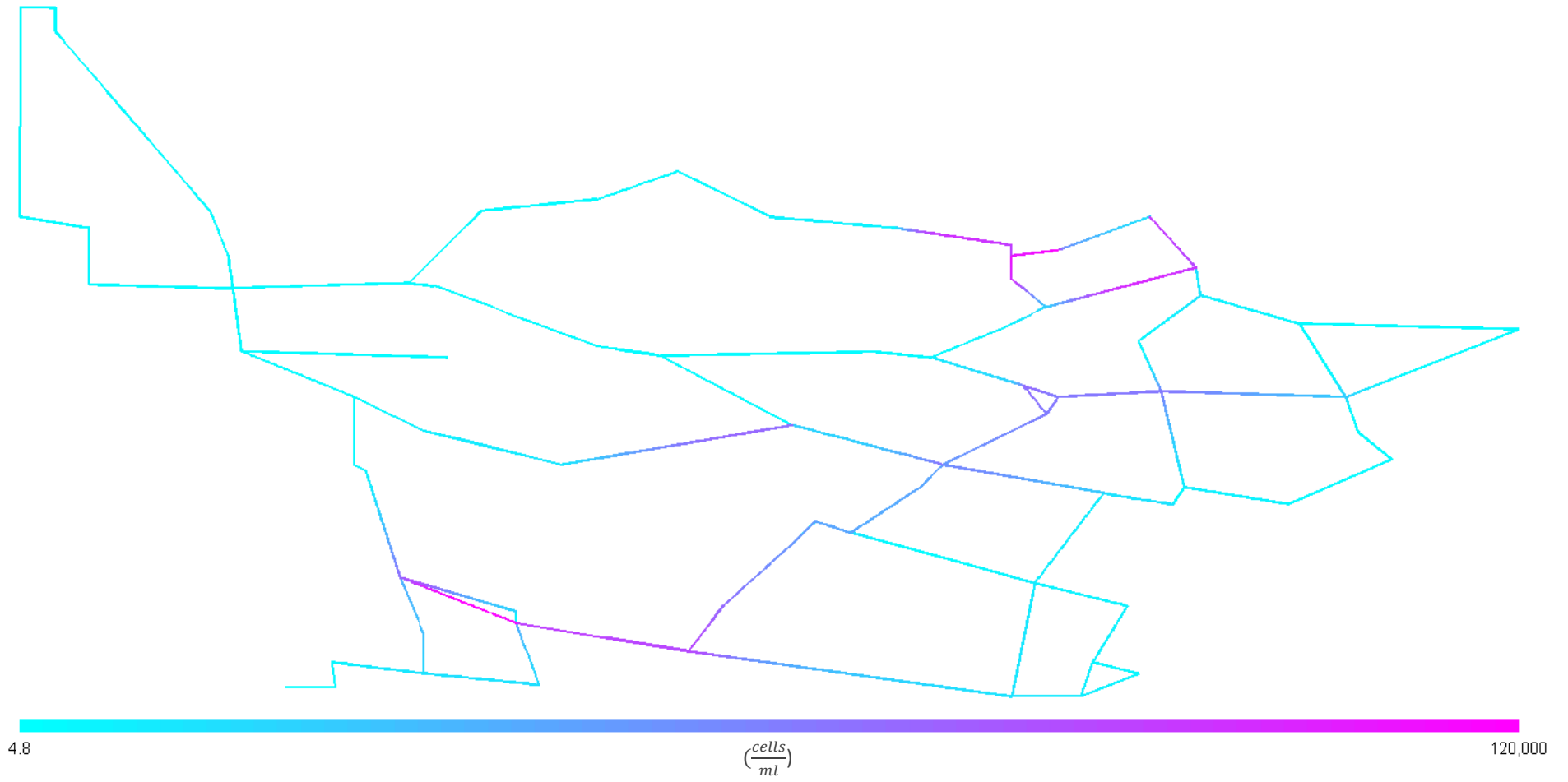


Figure D-8: Suspended AOB concentration profile for Alternative 1

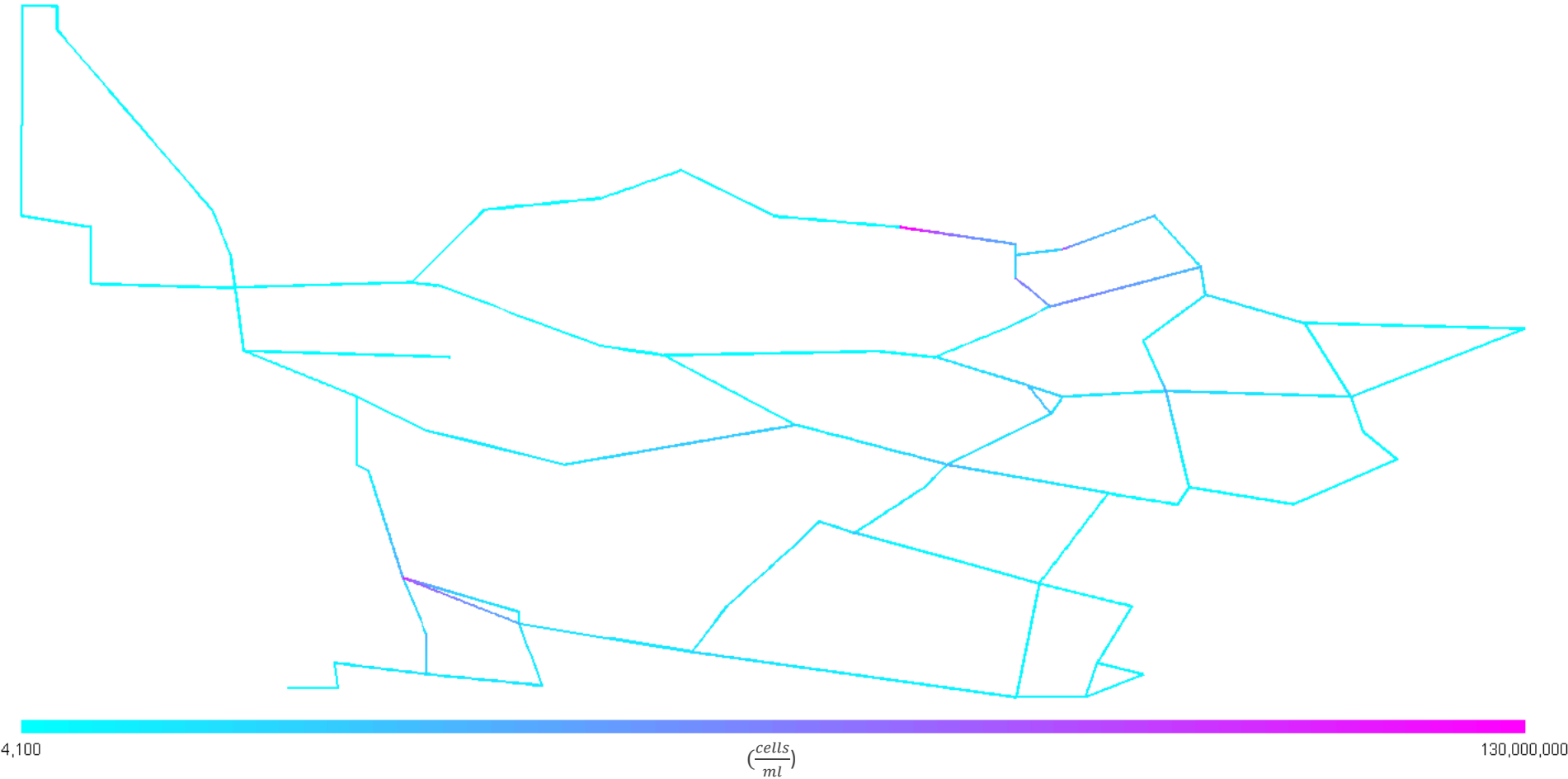


Figure D-9: Fixed AOB concentration profile for Alternative 1

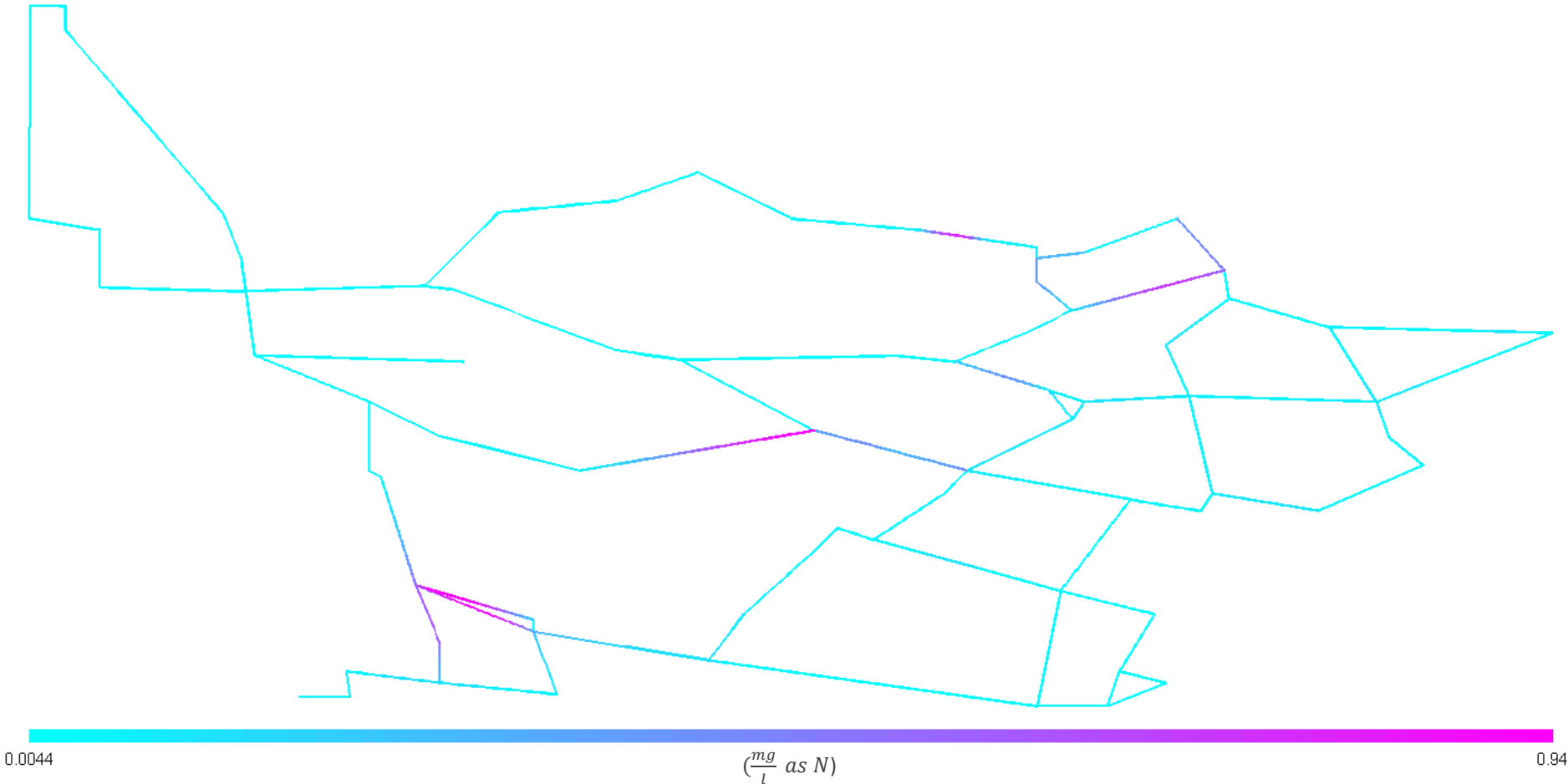


Figure D-10: Nitrite concentration profile for Alternative 1

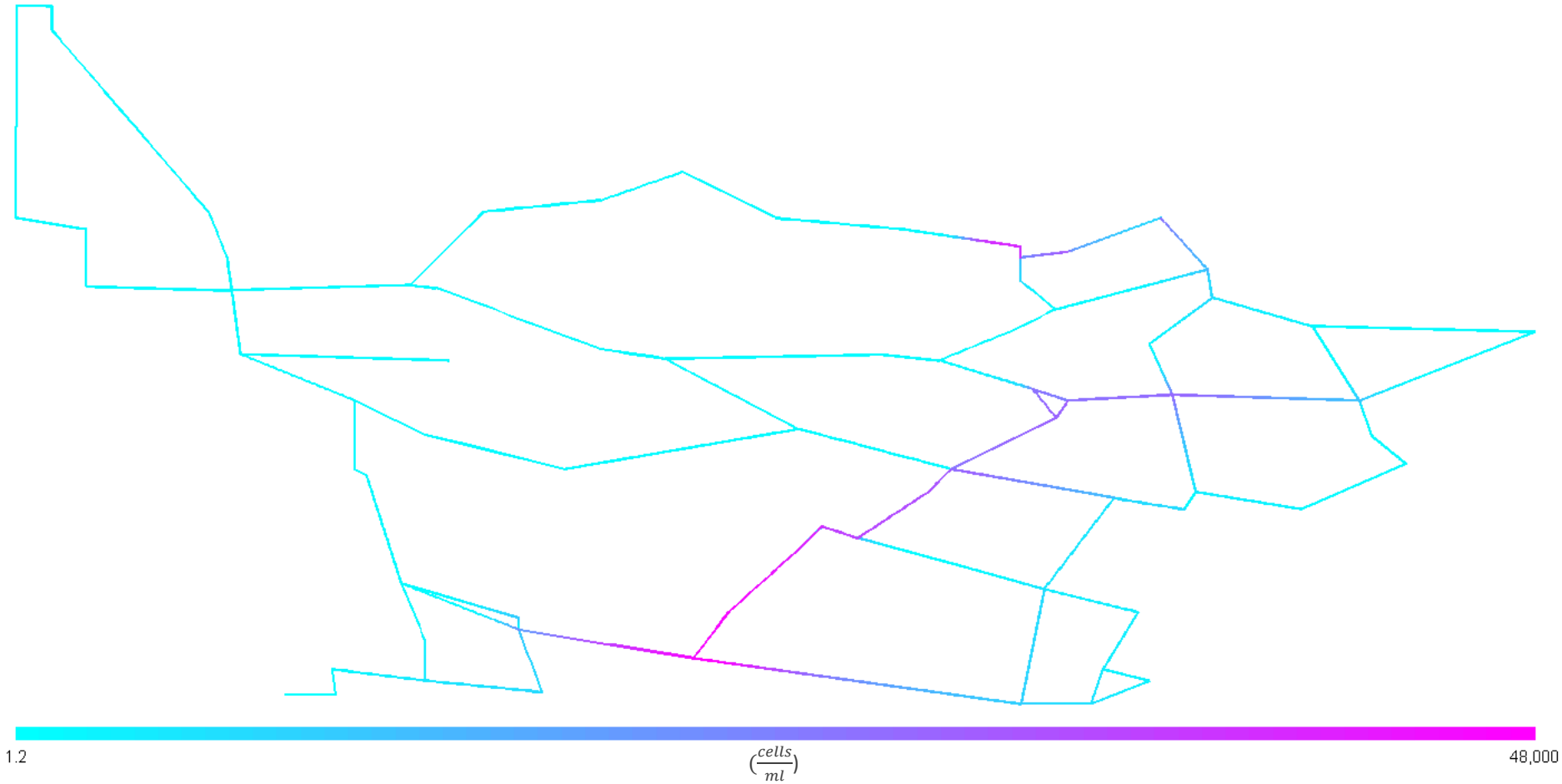


Figure D-11: Suspended NOB concentration profile for Alternative 1

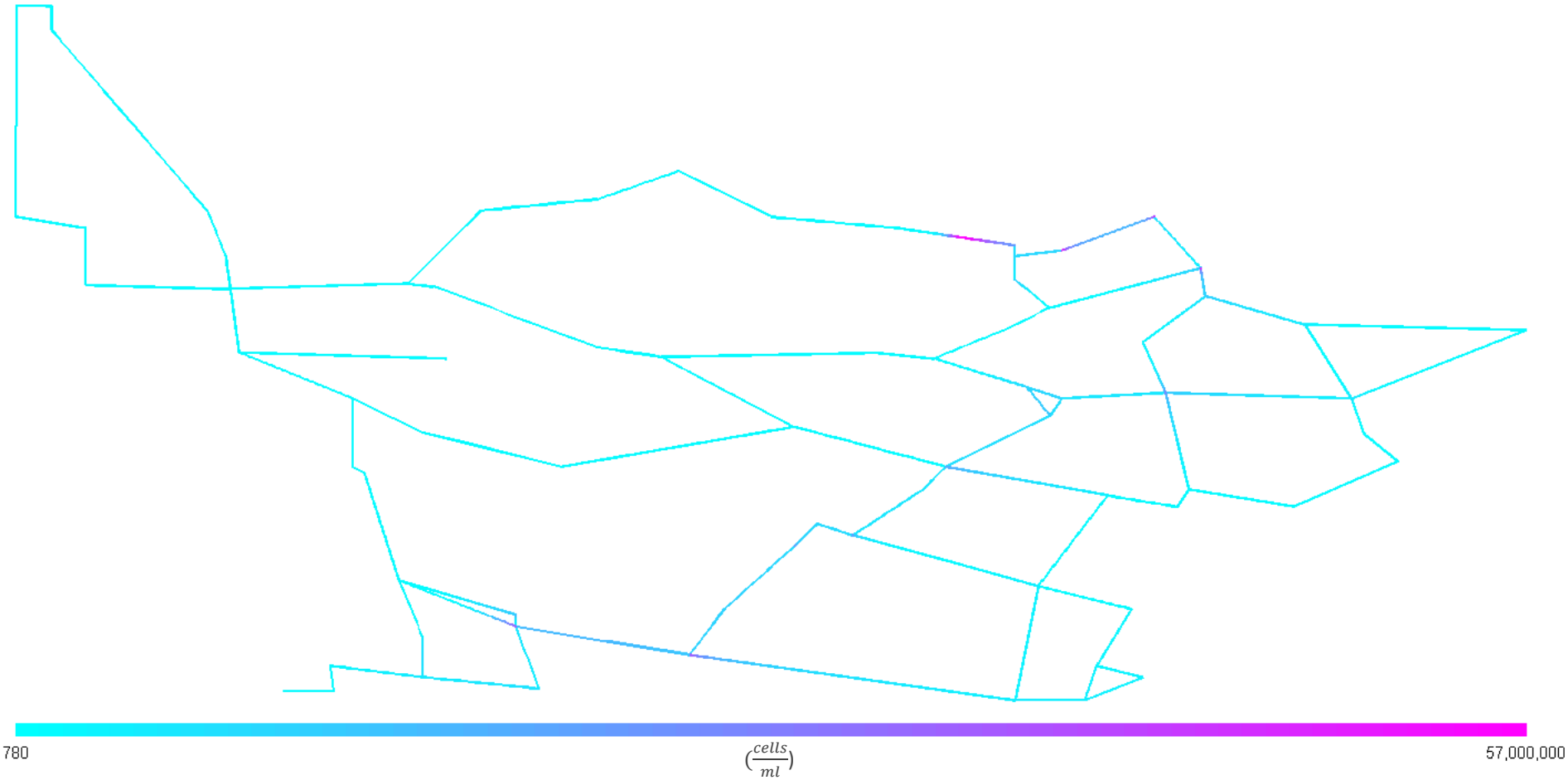


Figure D-12: Fixed NOB concentration profile for Alternative 1

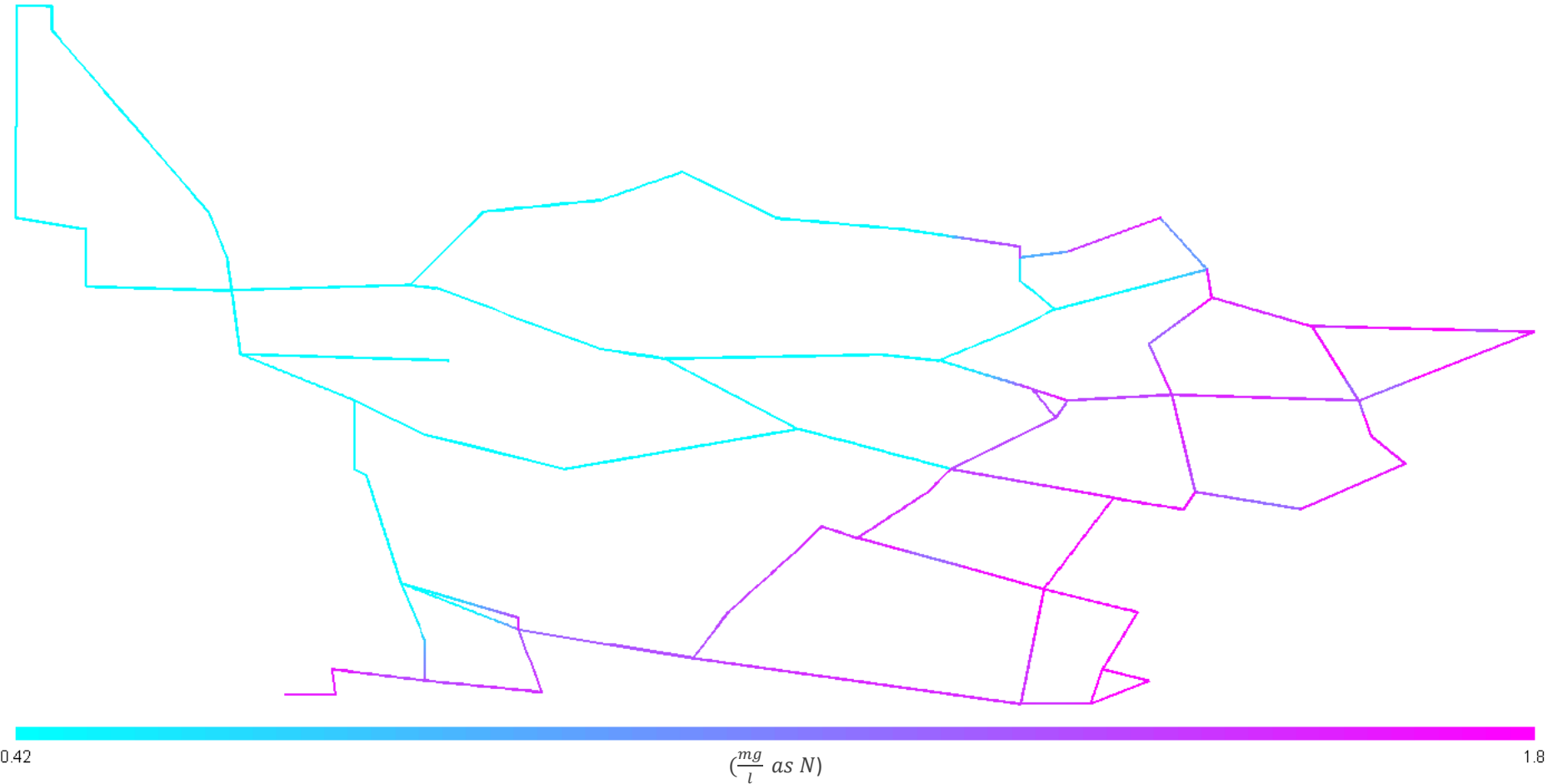


Figure D-13: Nitrate concentration profile for Alternative 1

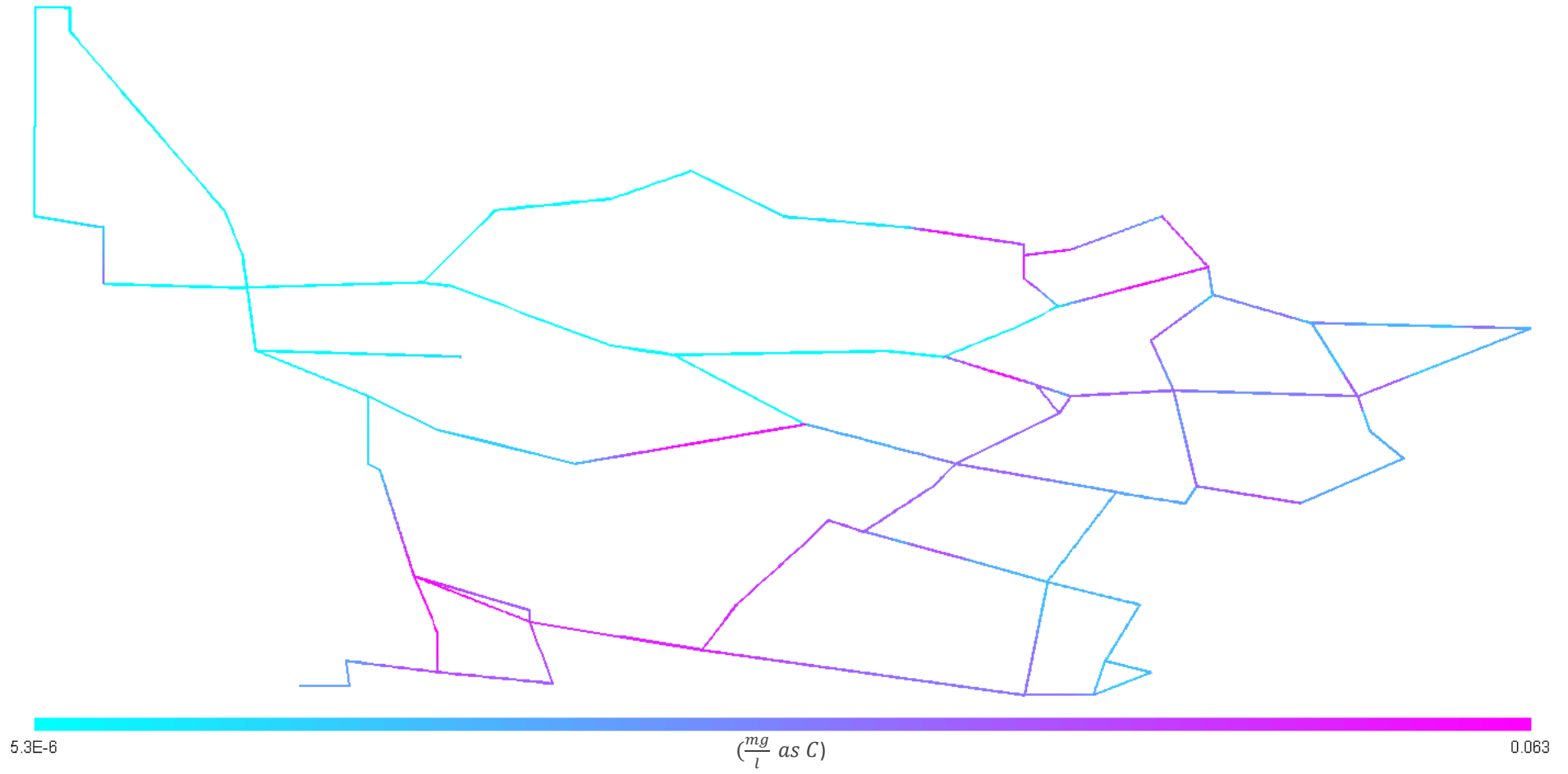


Figure D-14: UAP concentration profile for Alternative 1

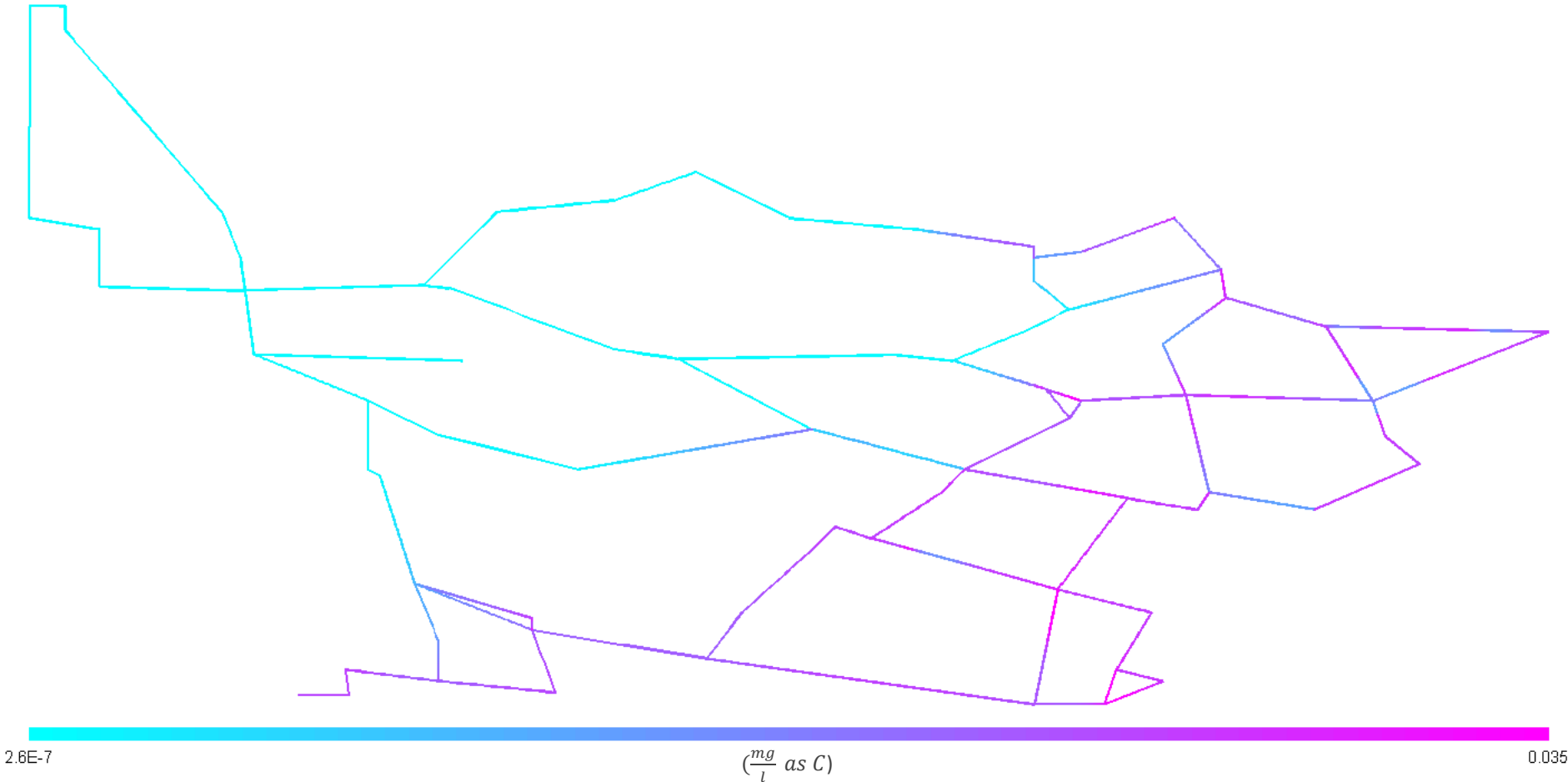


Figure D-15: BAP concentration profile for Alternative 1

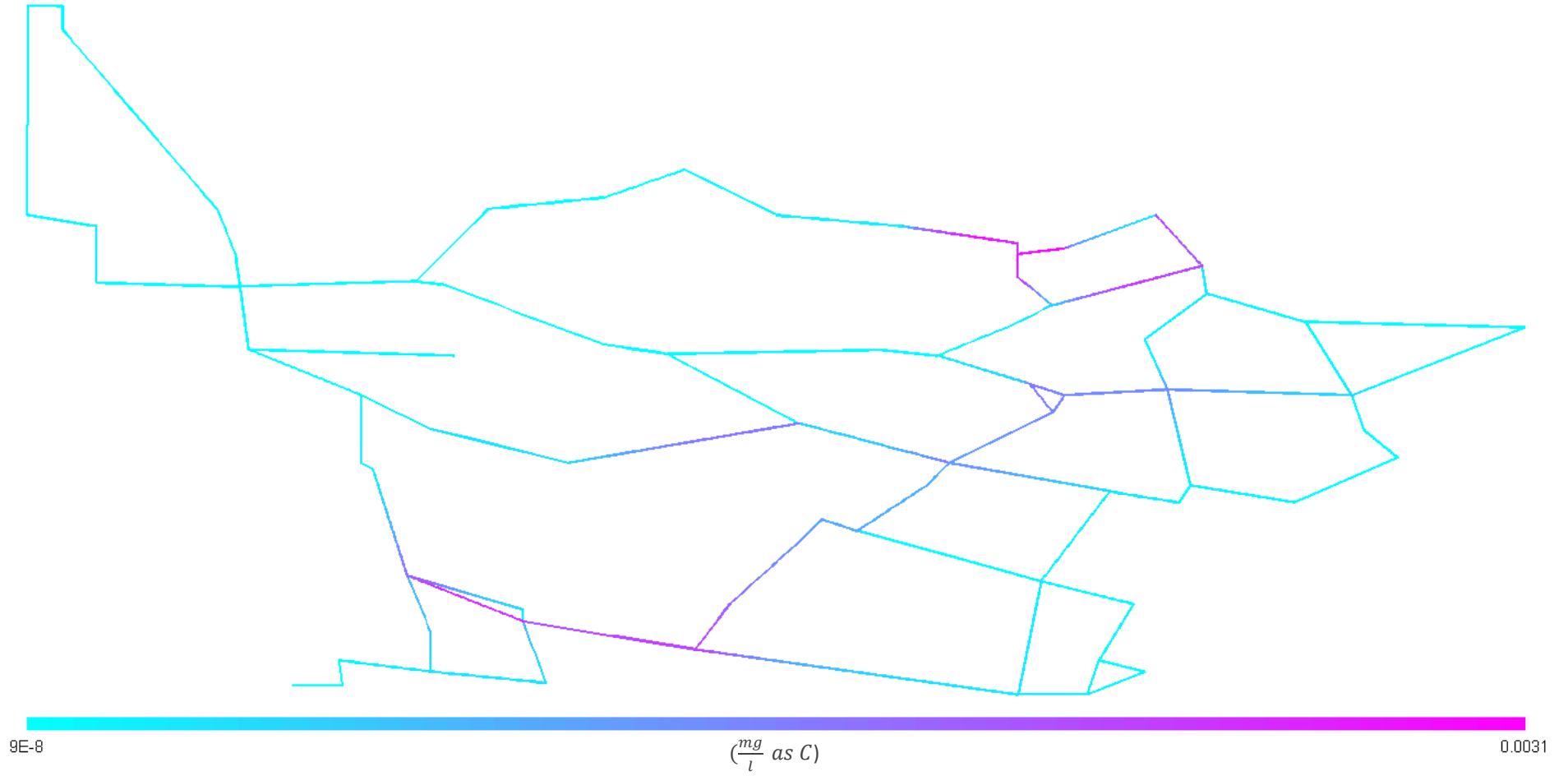


Figure D-16: Suspended EPS concentration profile for Alternative 1

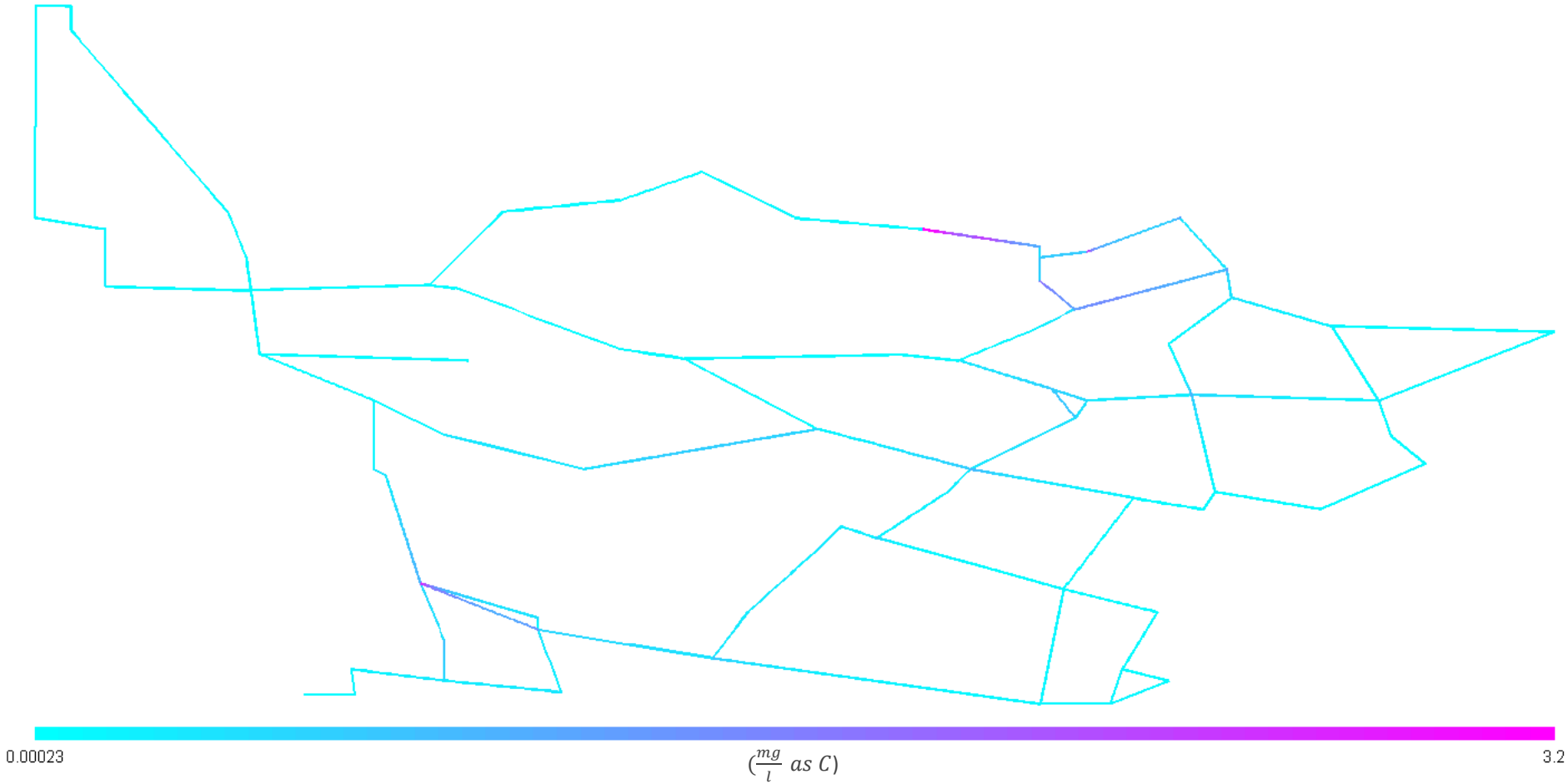


Figure D-17: Fixed EPS concentration profile for Alternative 1

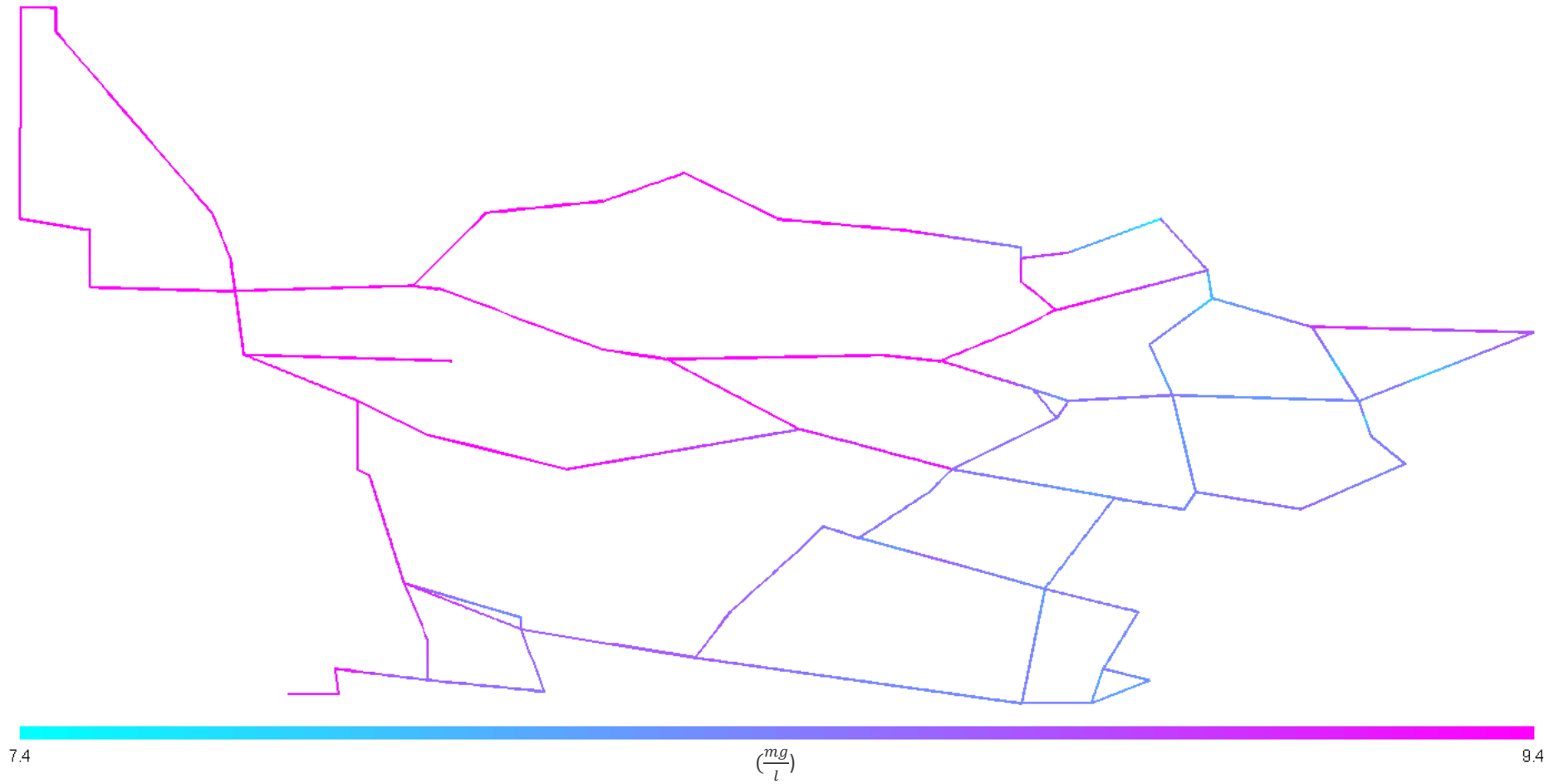


Figure D-18: Dissolved oxygen concentration profile for Alternative 1

D.2 Use of Biofiltration to Reduce Input BOM

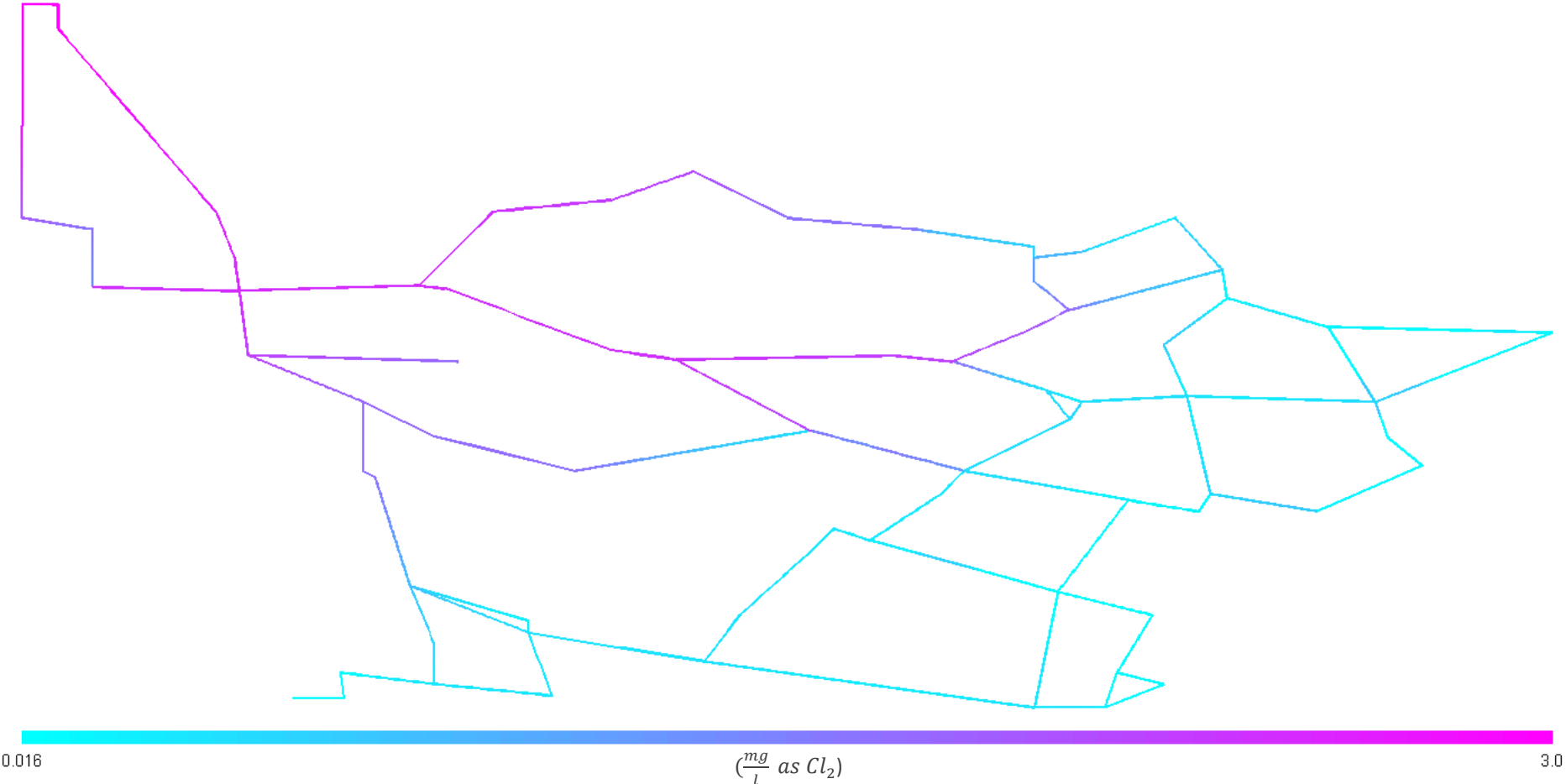


Figure D-19: Monochloramine concentration profile for Alternative 2

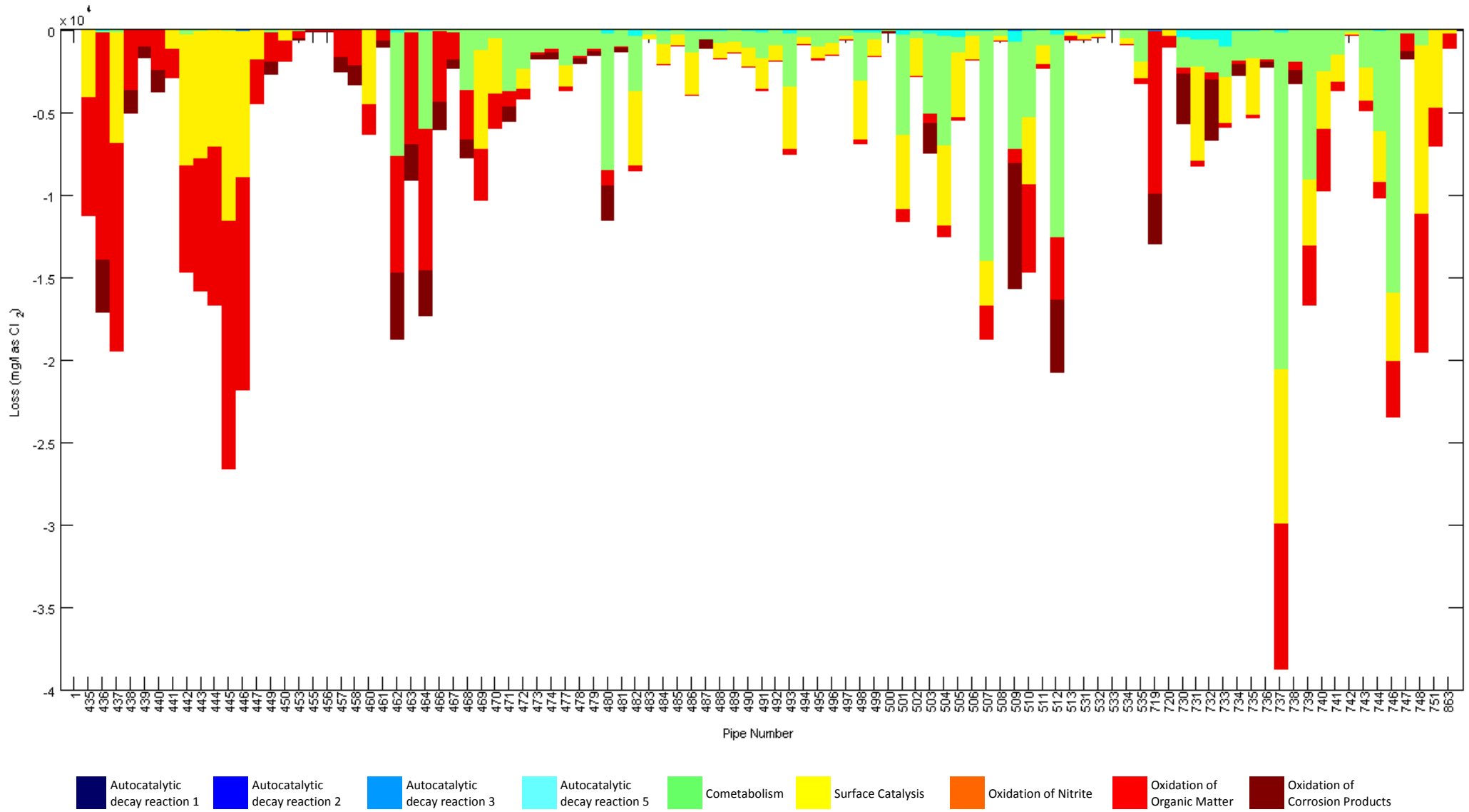


Figure D-20: Monochloramine loss mechanisms and locations for Alternative 2

Reducing the input BOM has a limited effect on the loss of monochloramine compared to the baseline scenario. It is particularly interesting to note that the loss of monochloramine due to the oxidation of organic matter has changed little, despite the concentrations of both suspended and fixed heterotrophs decreasing significantly.

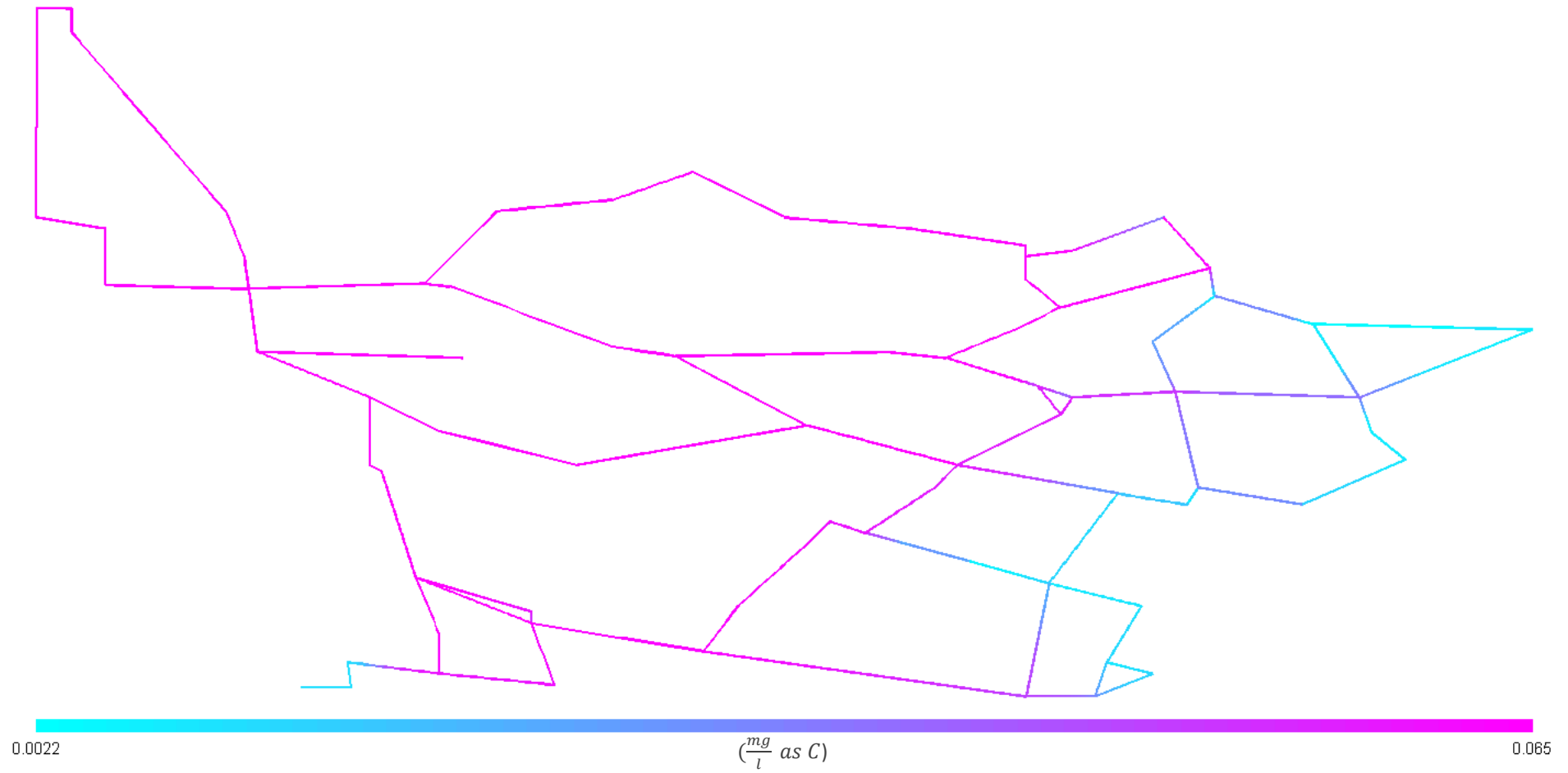


Figure D-21: BOM₁ concentration profile for Alternative 2

Reducing the BOM₁ input at the treatment plant significantly reduces its concentration throughout the system.

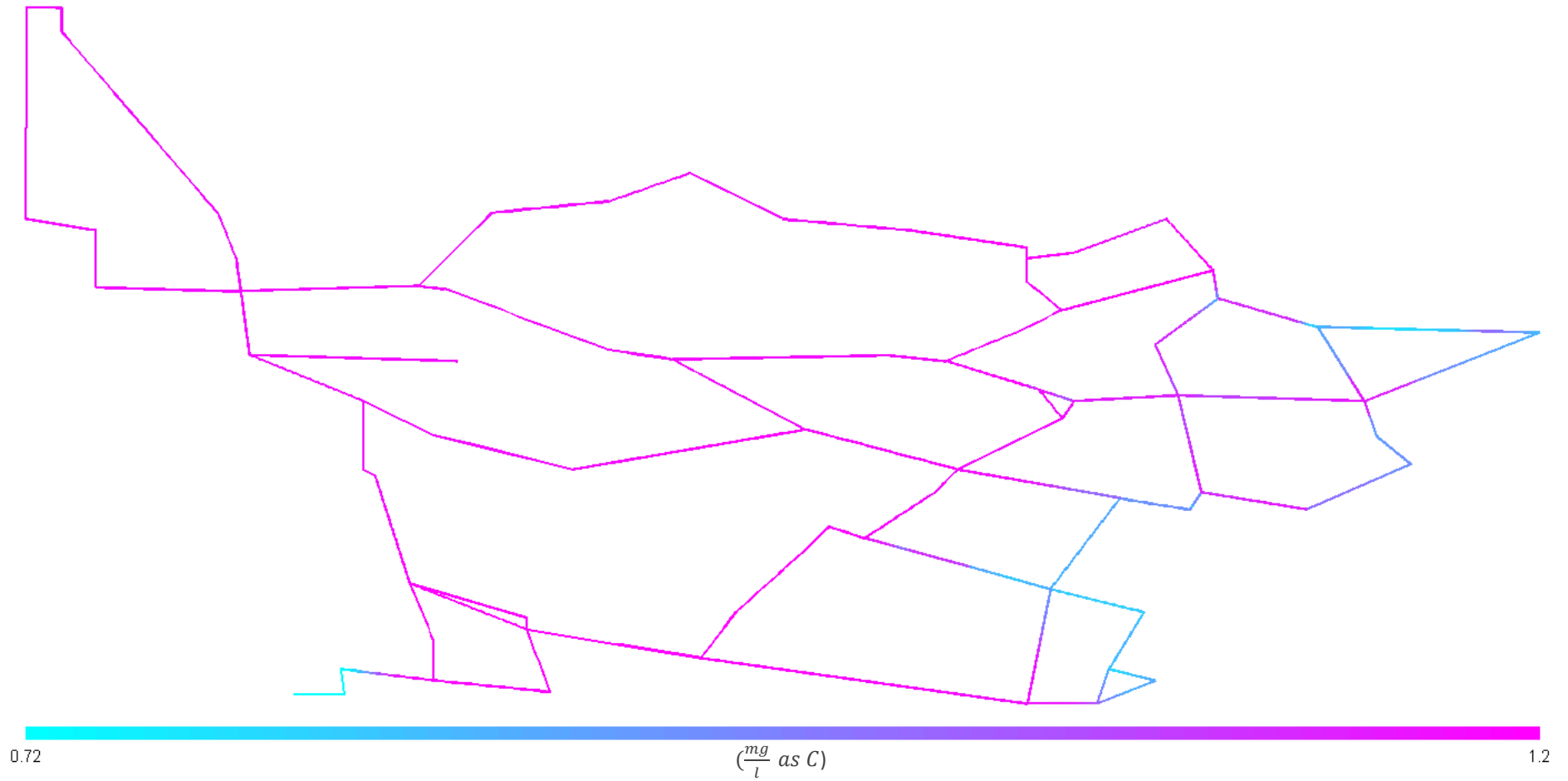


Figure D-22: BOM₂ concentration profile for Alternative 2

Reducing the BOM₂ input at the treatment plant significantly reduces its concentration throughout the system.

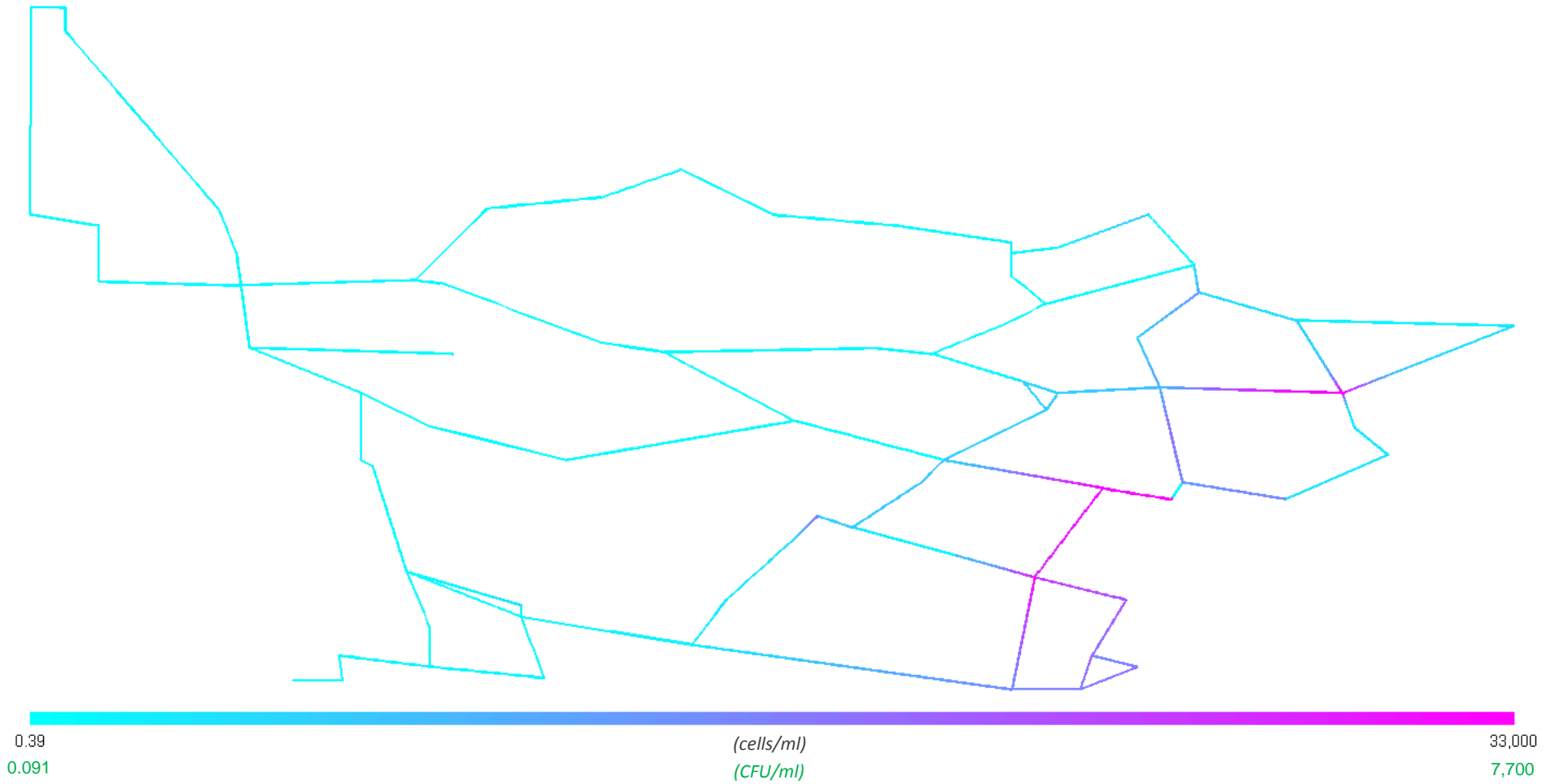


Figure D-23: Suspended heterotroph concentration profile for Alternative 2

The suspended heterotroph concentrations are significantly reduced due to the reduced availability of substrate, although they still exceed the maximum permissible limit of $4300 \frac{\text{cells}}{\text{ml}}$.

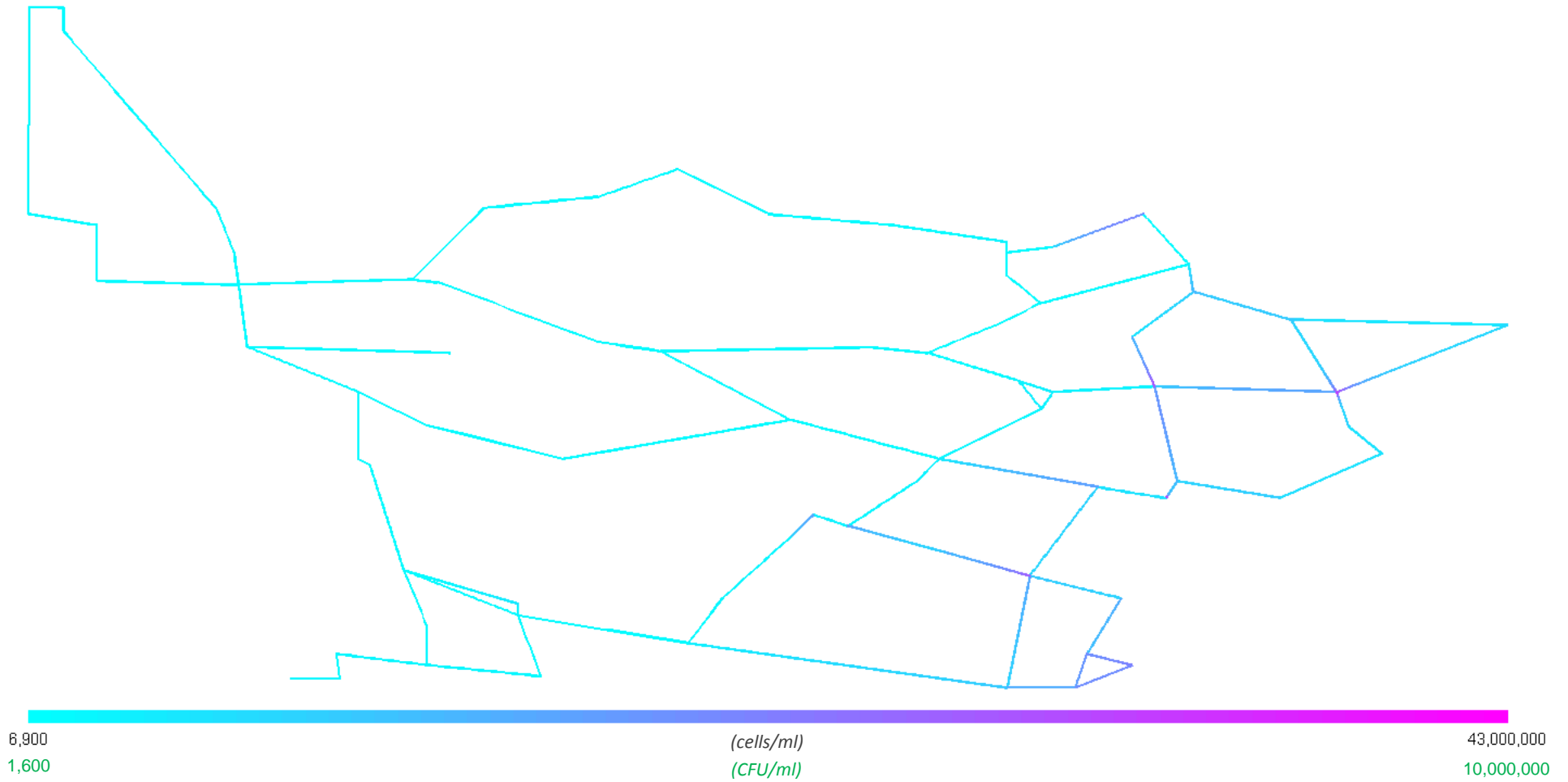


Figure D-24: Fixed heterotroph concentration profile for Alternative 2

The fixed heterotroph concentrations are significantly reduced due to reduced availability of substrate, which is a significant reason for the reduced concentration of suspended heterotrophs.

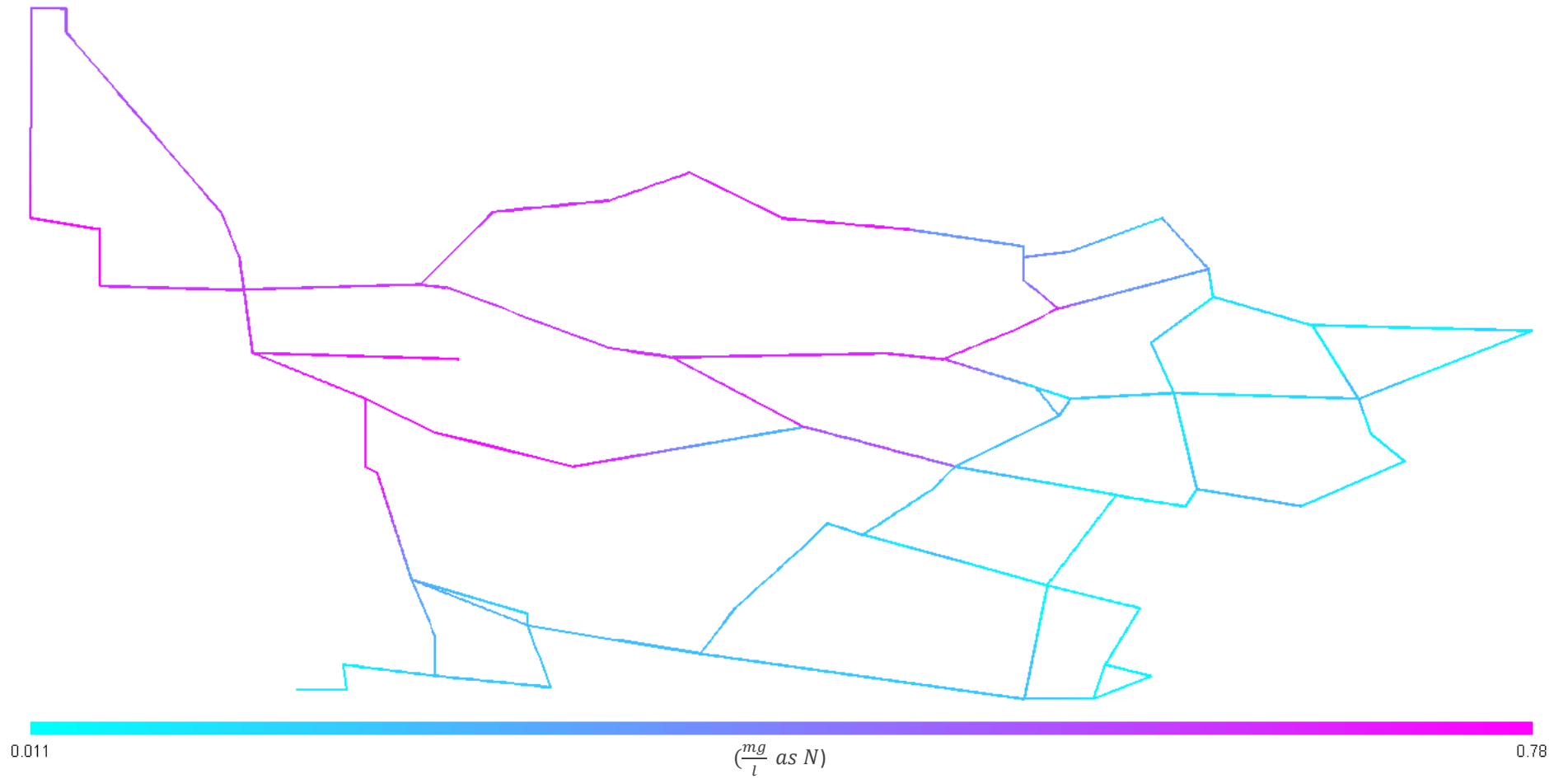


Figure D-25: Total ammonia concentration profile for Alternative 2

The ammonia concentrations are only slightly reduced.

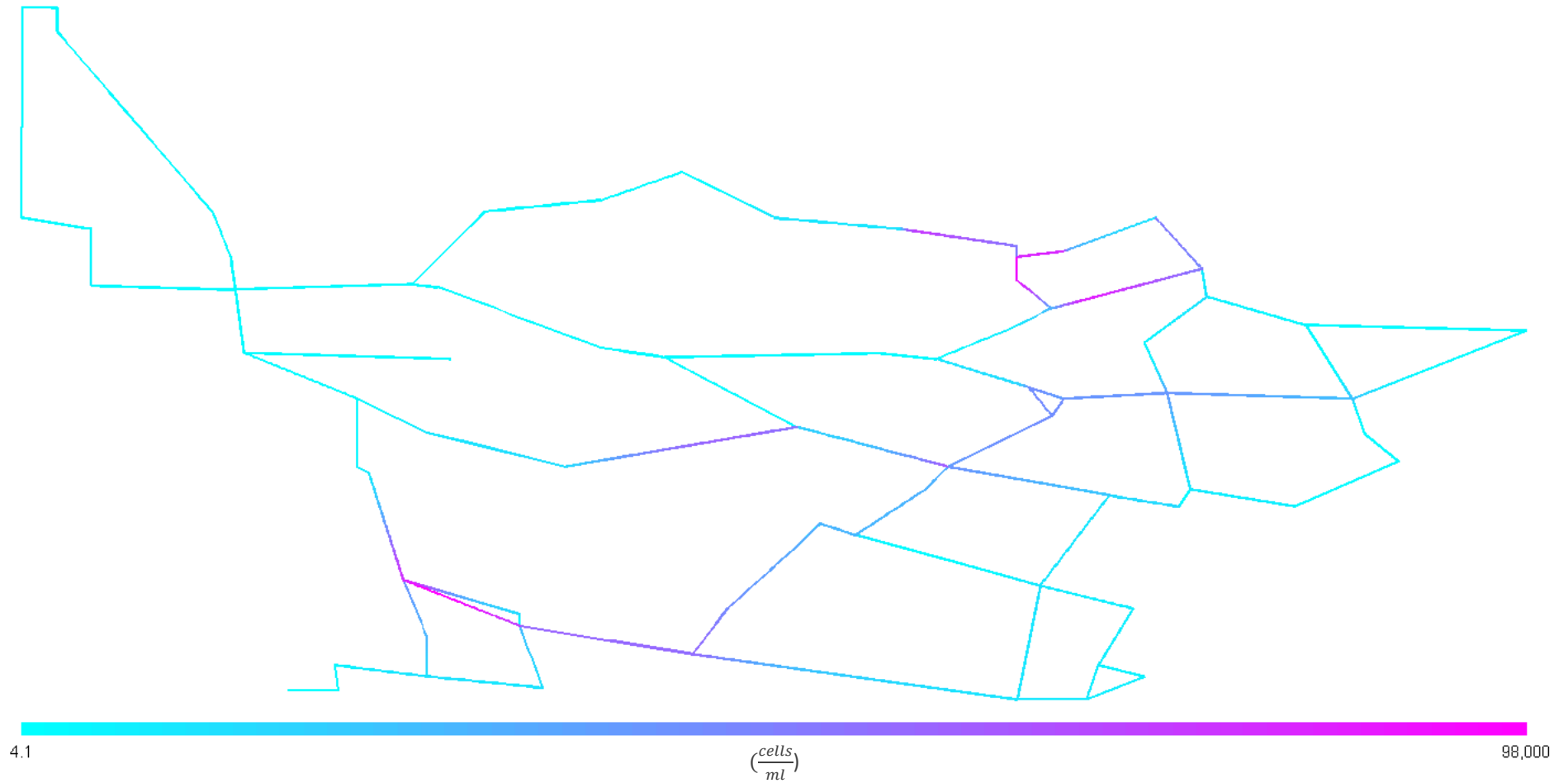


Figure D-26: Suspended AOB concentration profile for Alternative 2

Despite the fact that the monochloramine concentration has only increased slightly and the ammonia concentration has only decreased slightly for this alternative, the concentrations of both suspended and fixed AOB have decreased significantly. This demonstrates the sensitivity of the AOB stability factors to disinfectant and substrate.

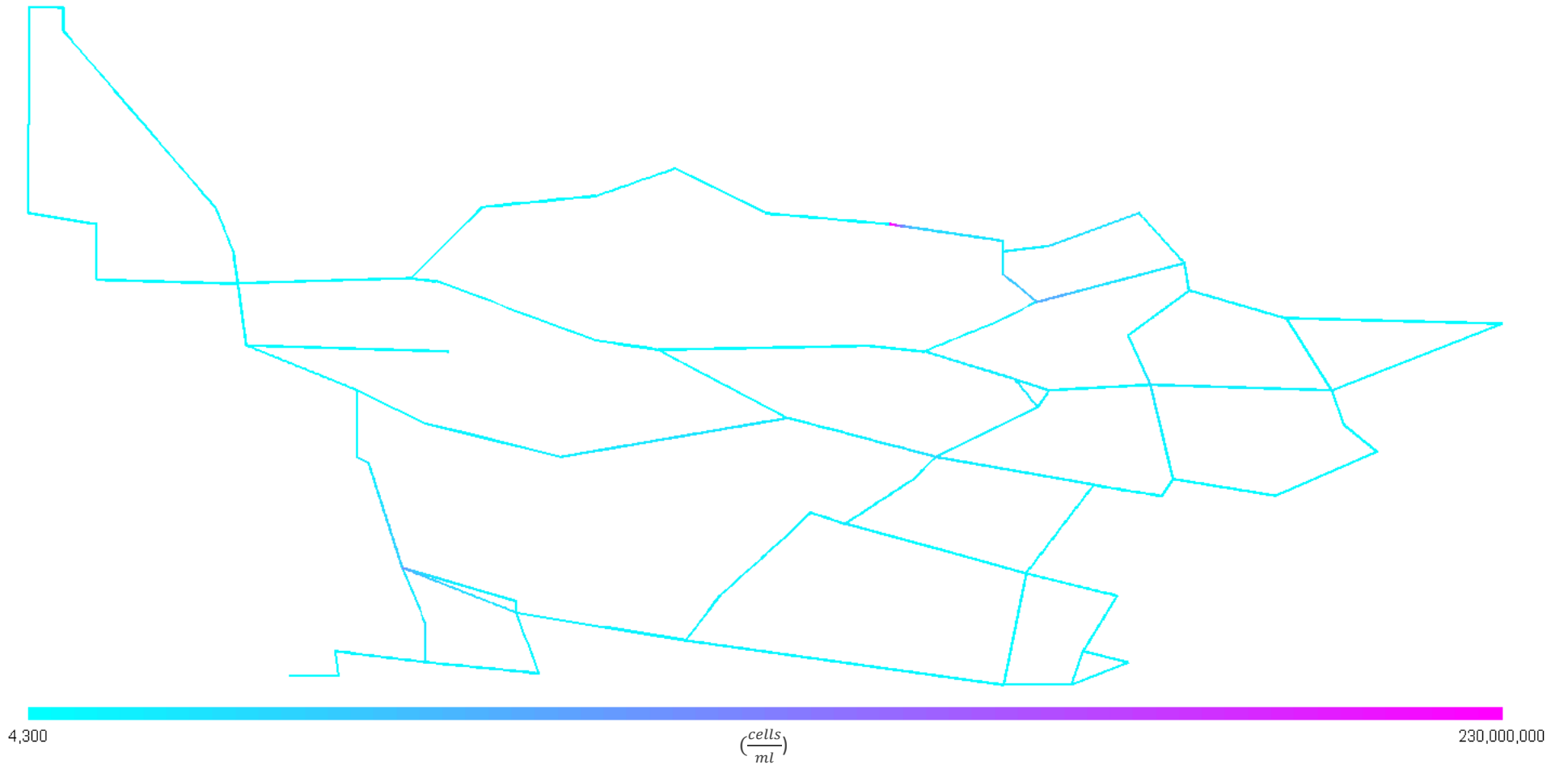


Figure D-27: Fixed AOB concentration profile for Alternative 2

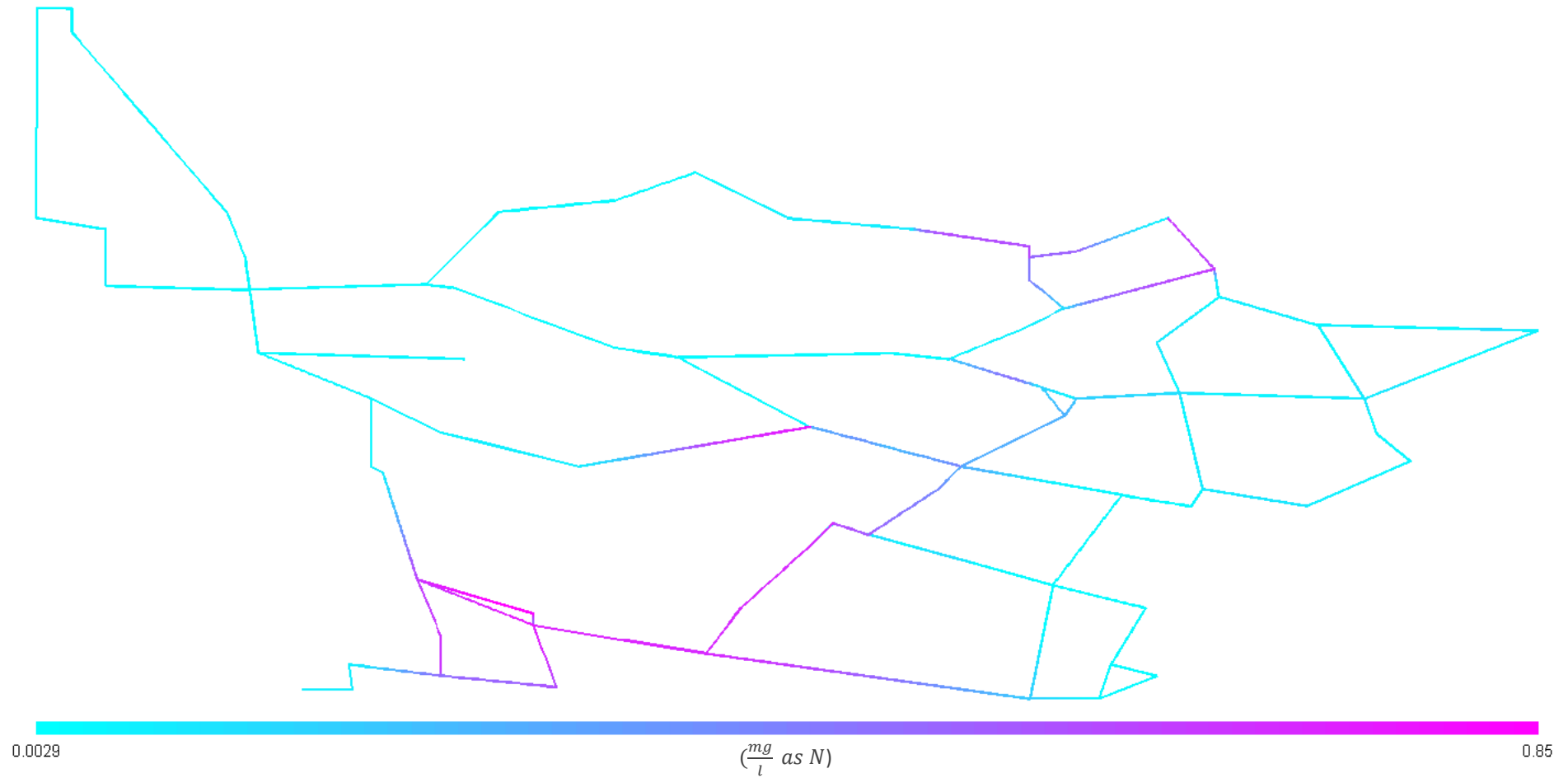


Figure D-28: Nitrite concentration profile for Alternative 2

The nitrite concentrations are significantly lower than the baseline scenario and are now within acceptable limits. This is due to the reduced utilisation of ammonia by AOB.

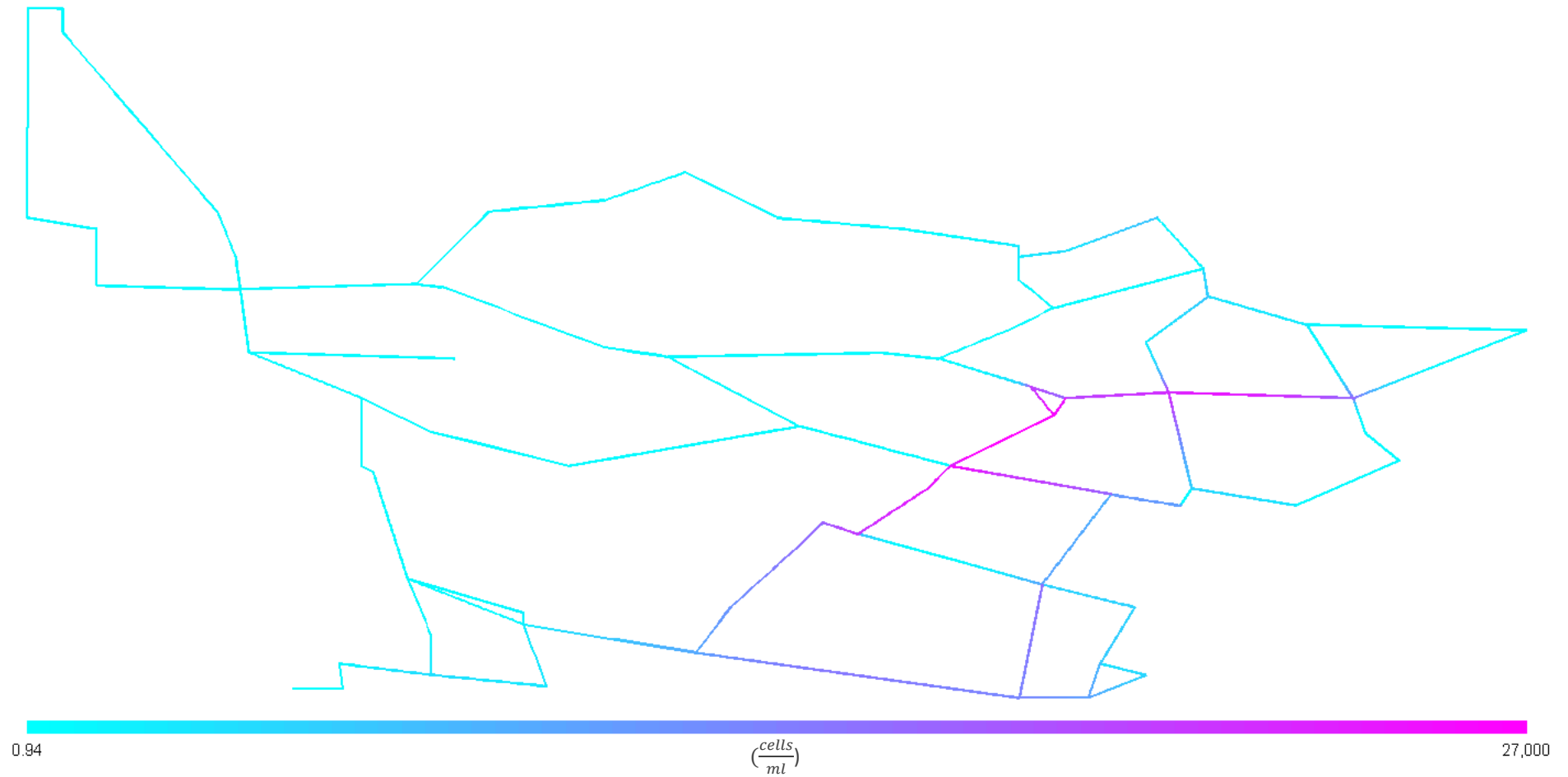


Figure D-29: Suspended NOB concentration profile for Alternative 2

The reduction of nitrite in the system results in significantly lower concentrations of both suspended and fixed NOB.

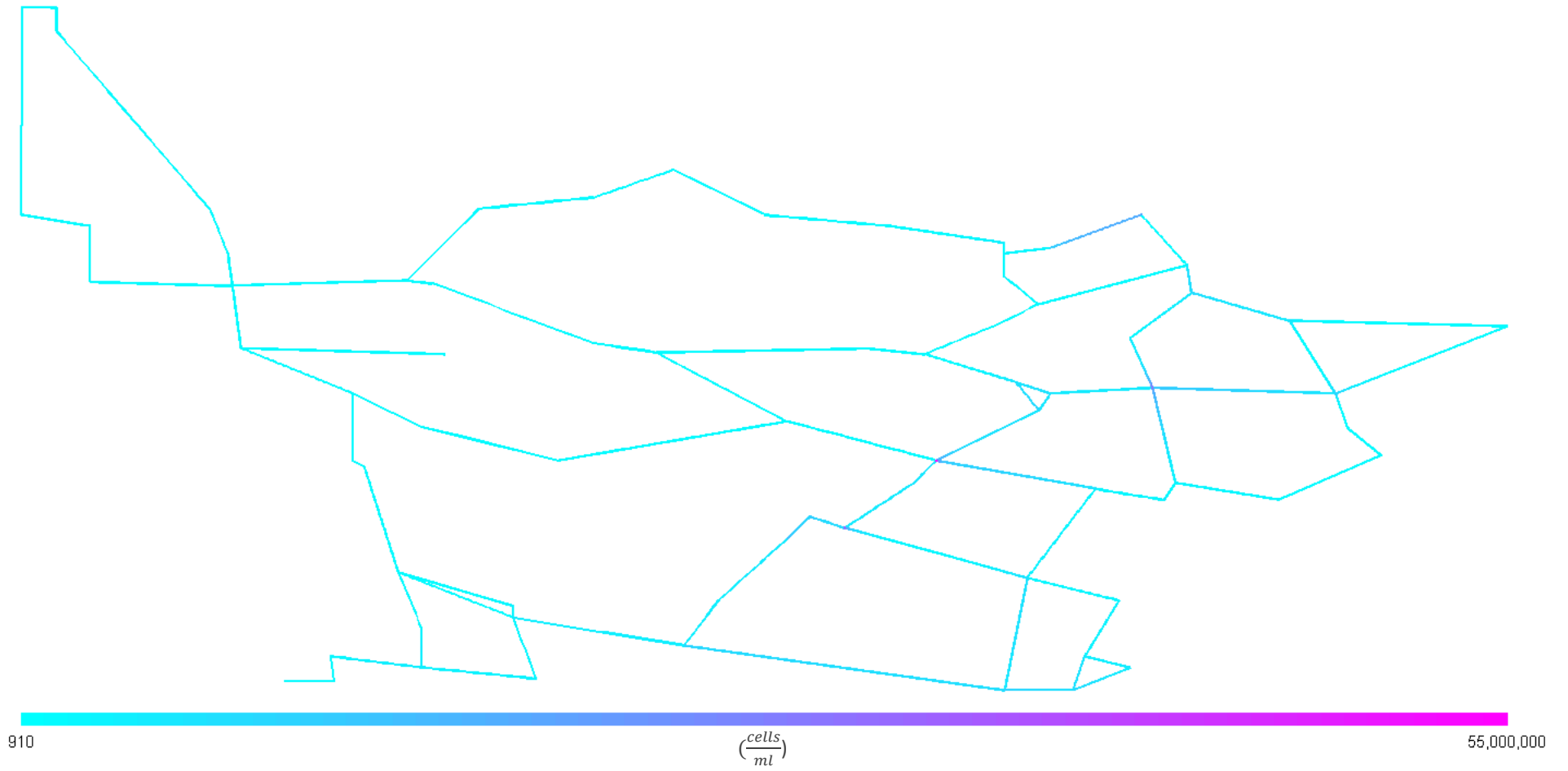


Figure D-30: Fixed NOB concentration profile for Alternative 2

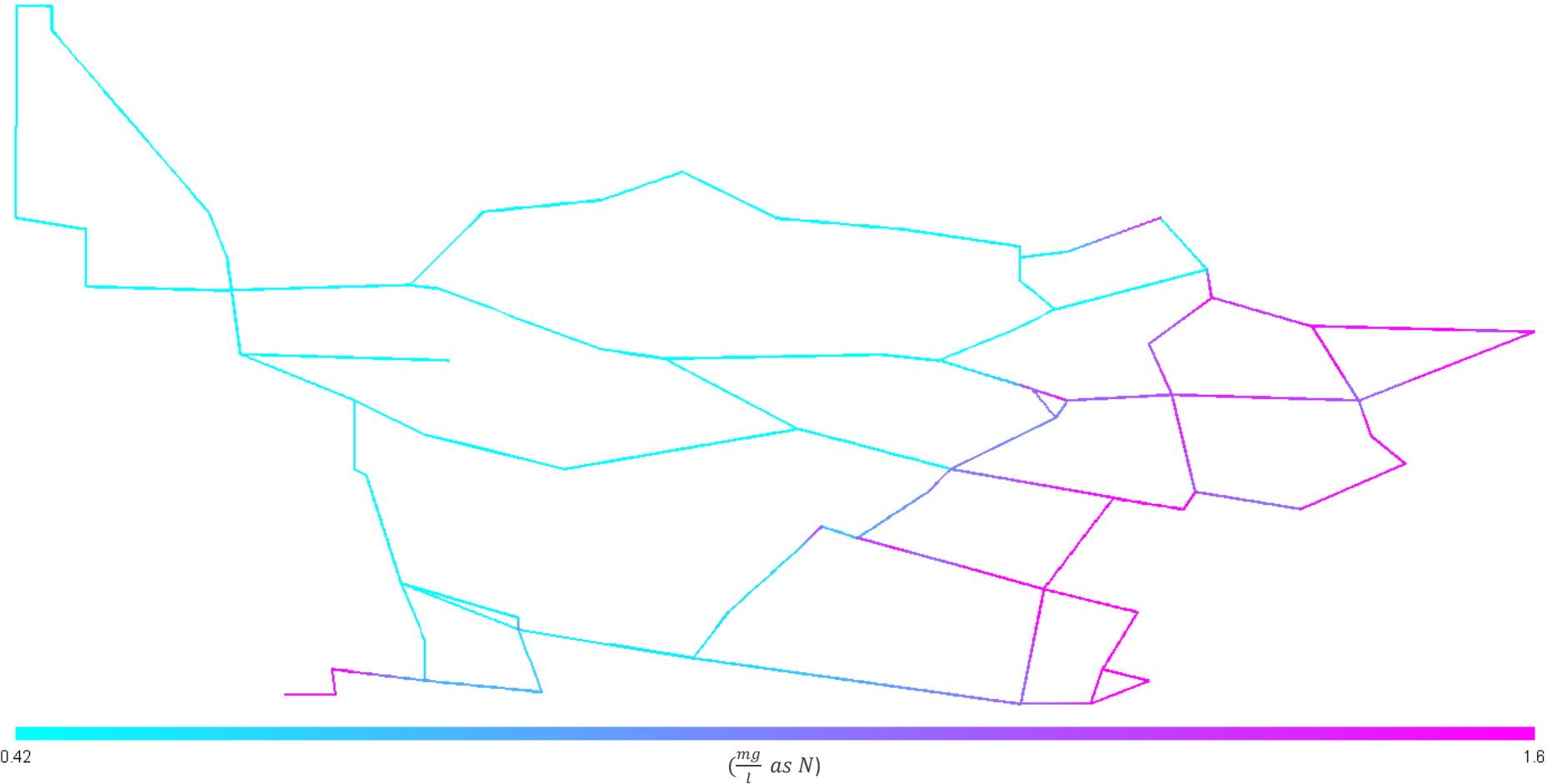


Figure D-31: Nitrate concentration profile for Alternative 2

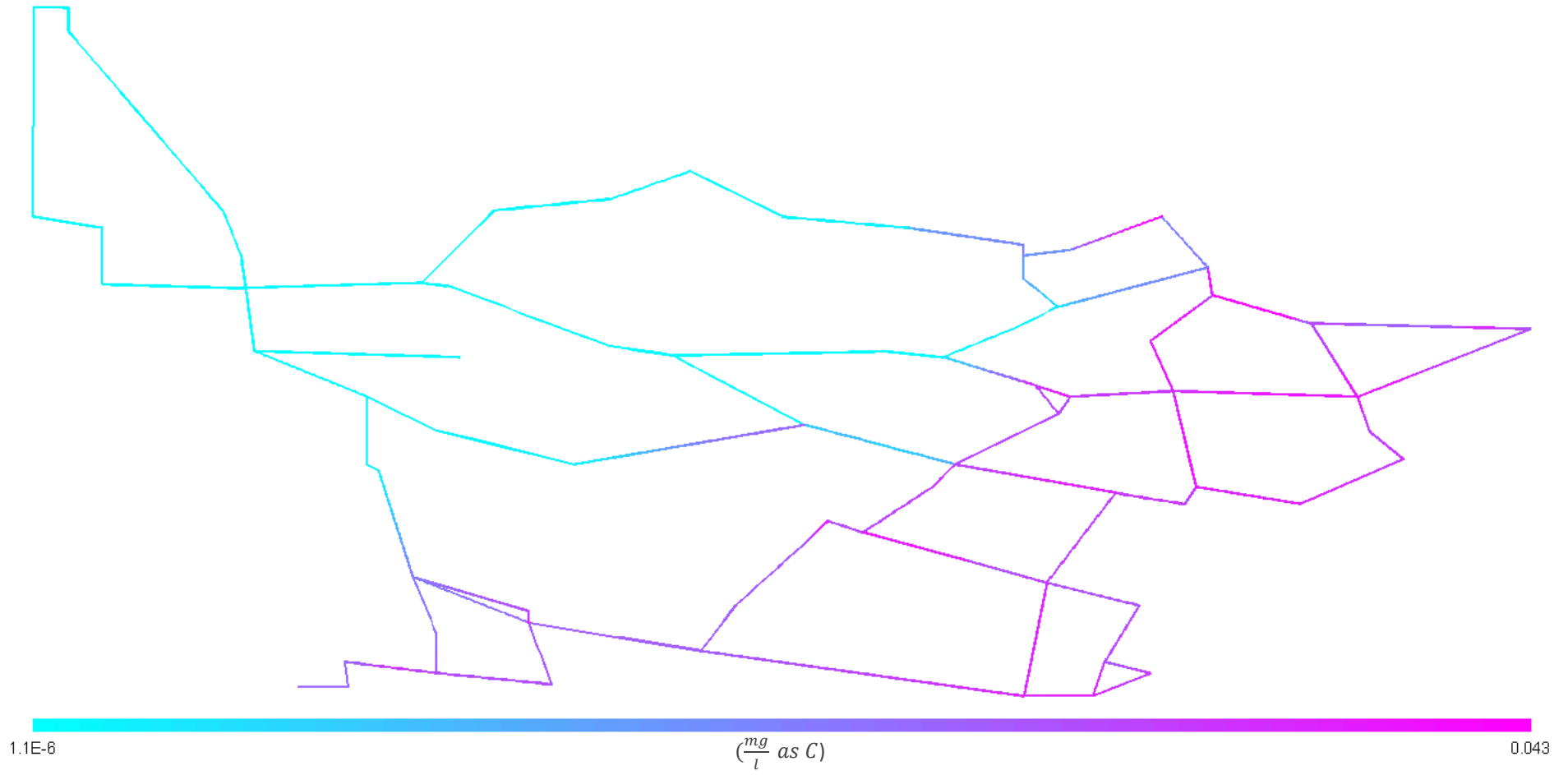


Figure D-32: UAP concentration profile for Alternative 2

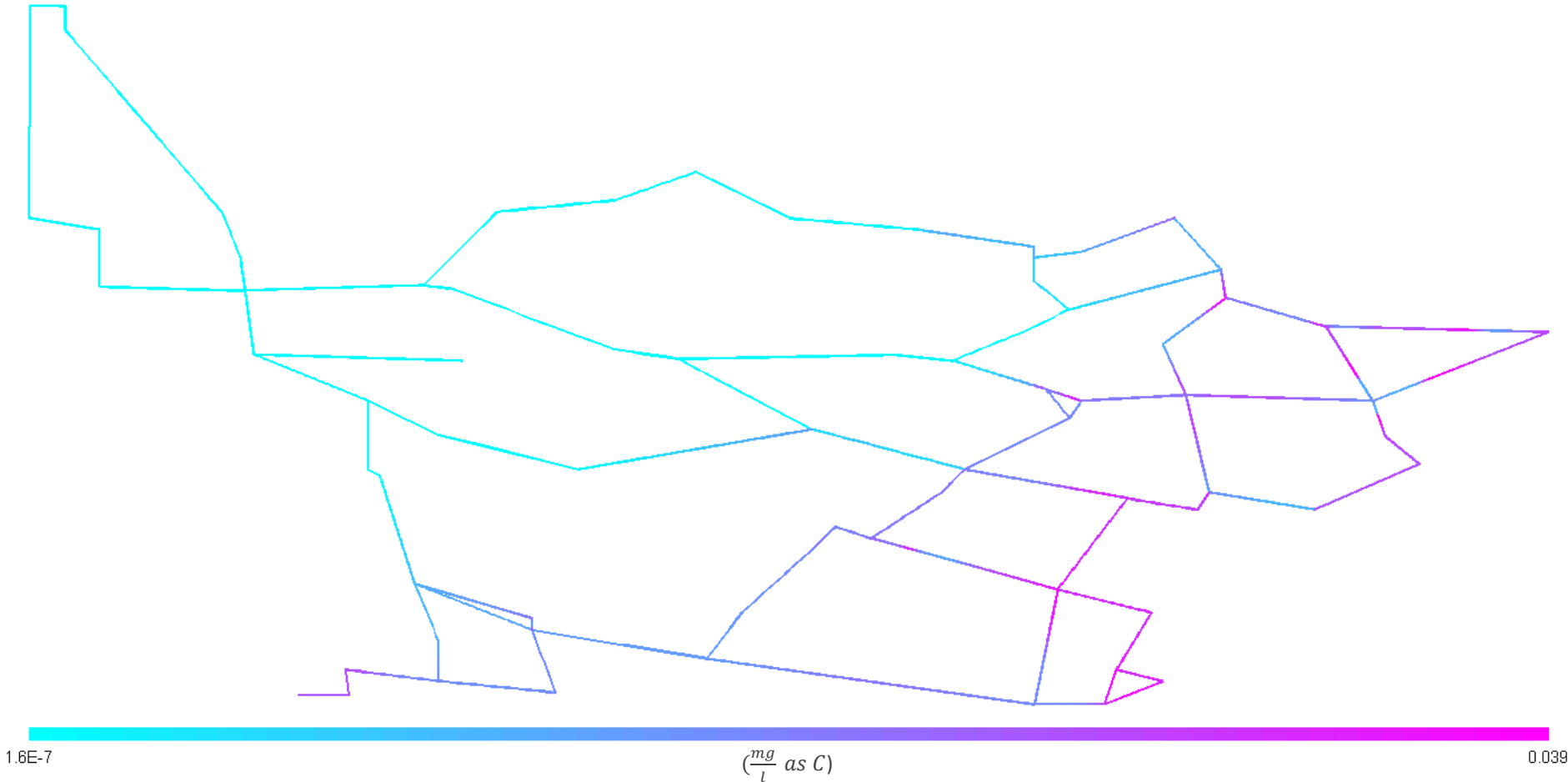


Figure D-33: BAP concentration profile for Alternative 2

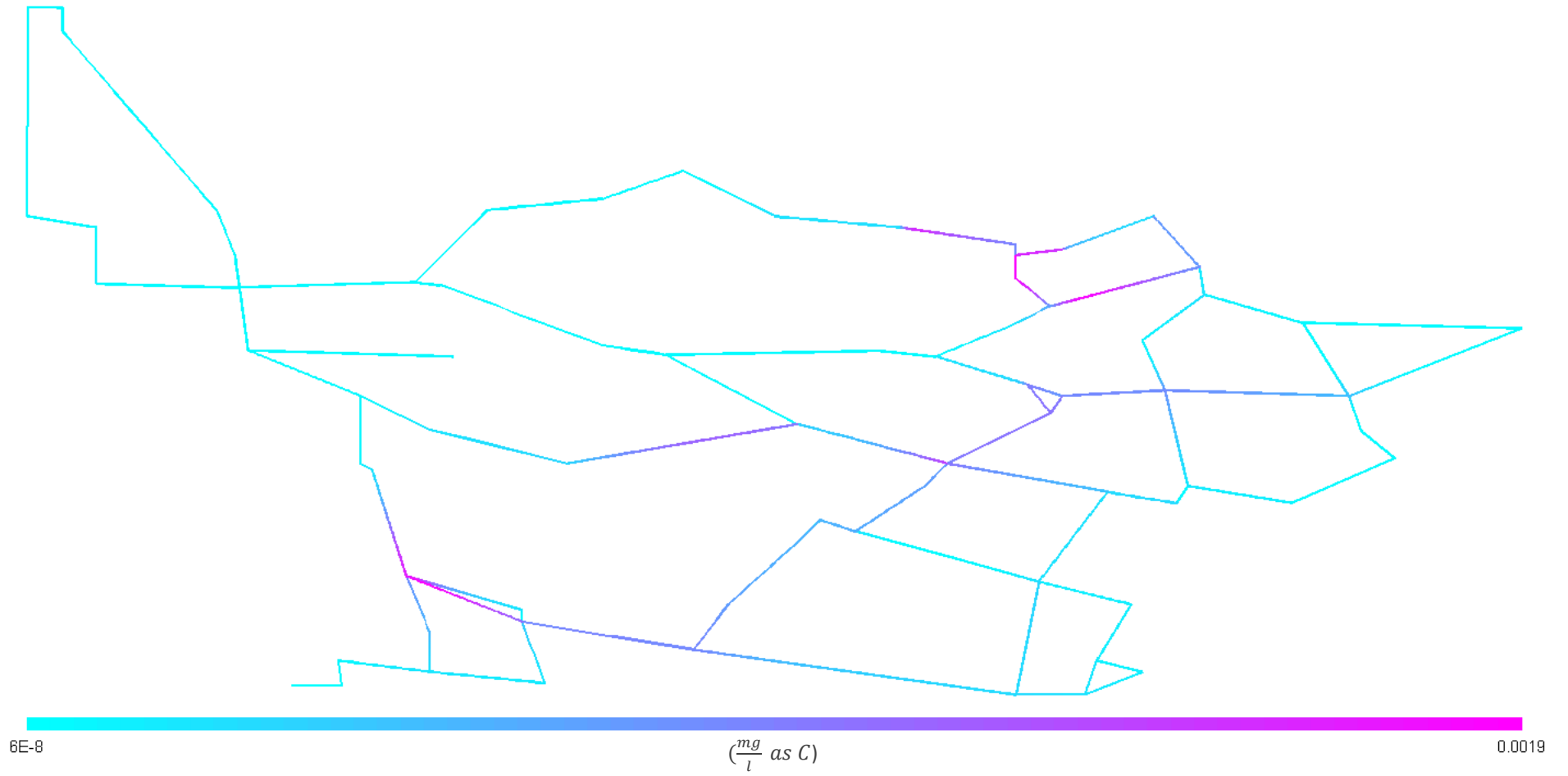


Figure D-34: Suspended EPS concentration profile for Alternative 2

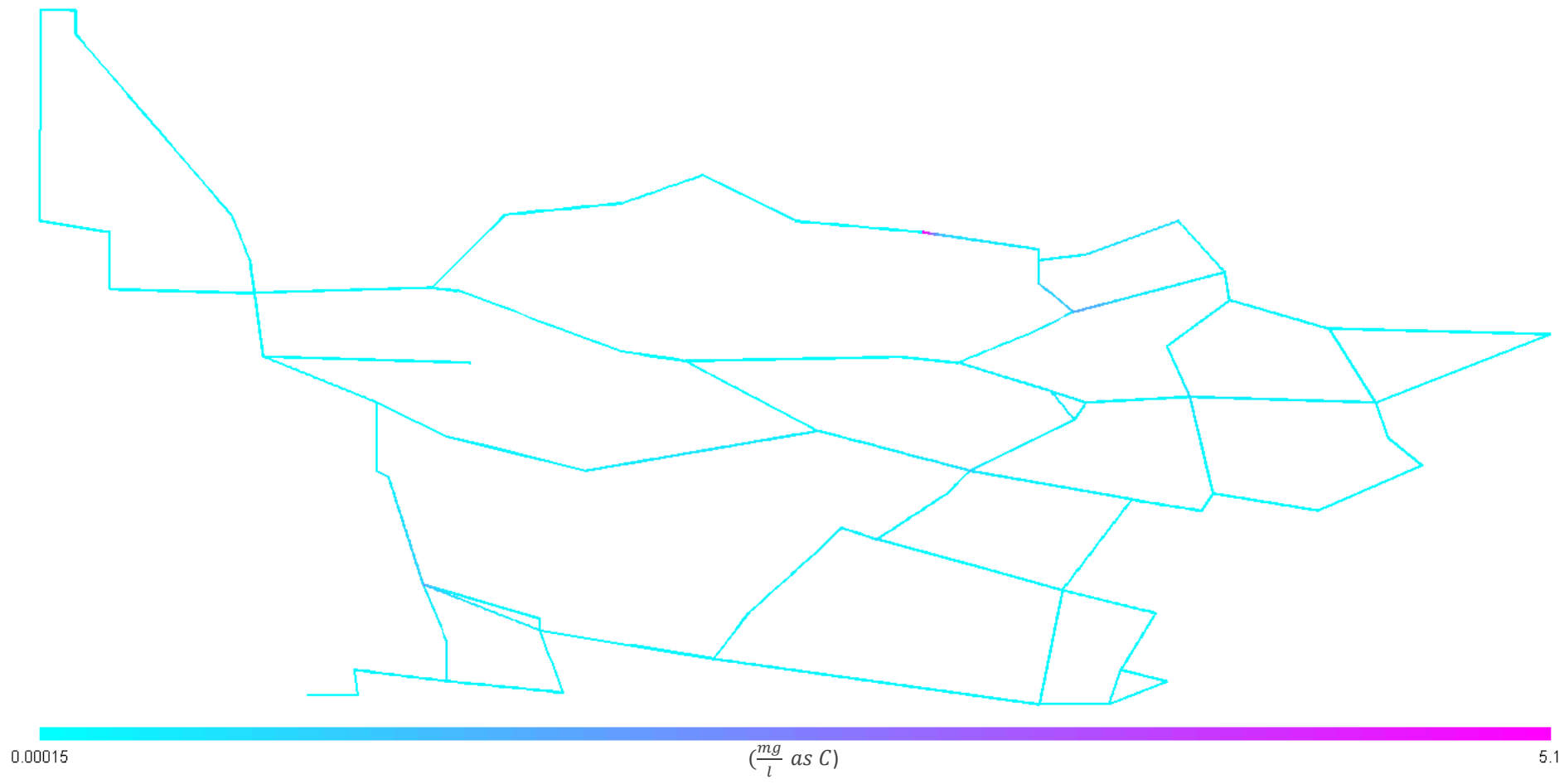


Figure D-35: Fixed EPS concentration profile for Alternative 2

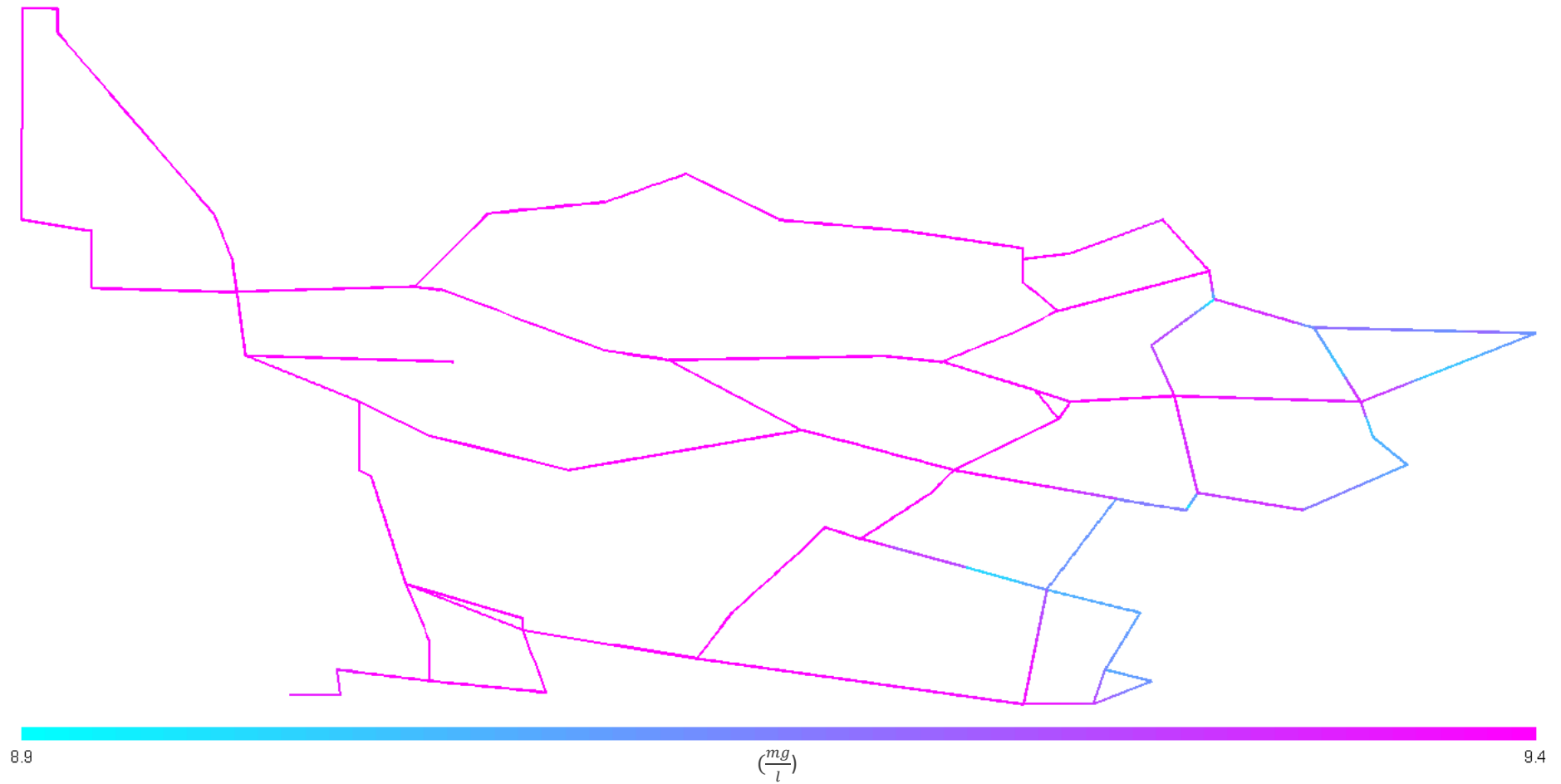


Figure D-36: Dissolved oxygen concentration profile for Alternative 2

The greater oxygen concentrations are a result of reduced active biomass concentrations for this alternative.

D.3 Use of a 1:1 Cl:N Ratio at the Treatment Plant to Reduce Input Ammonia

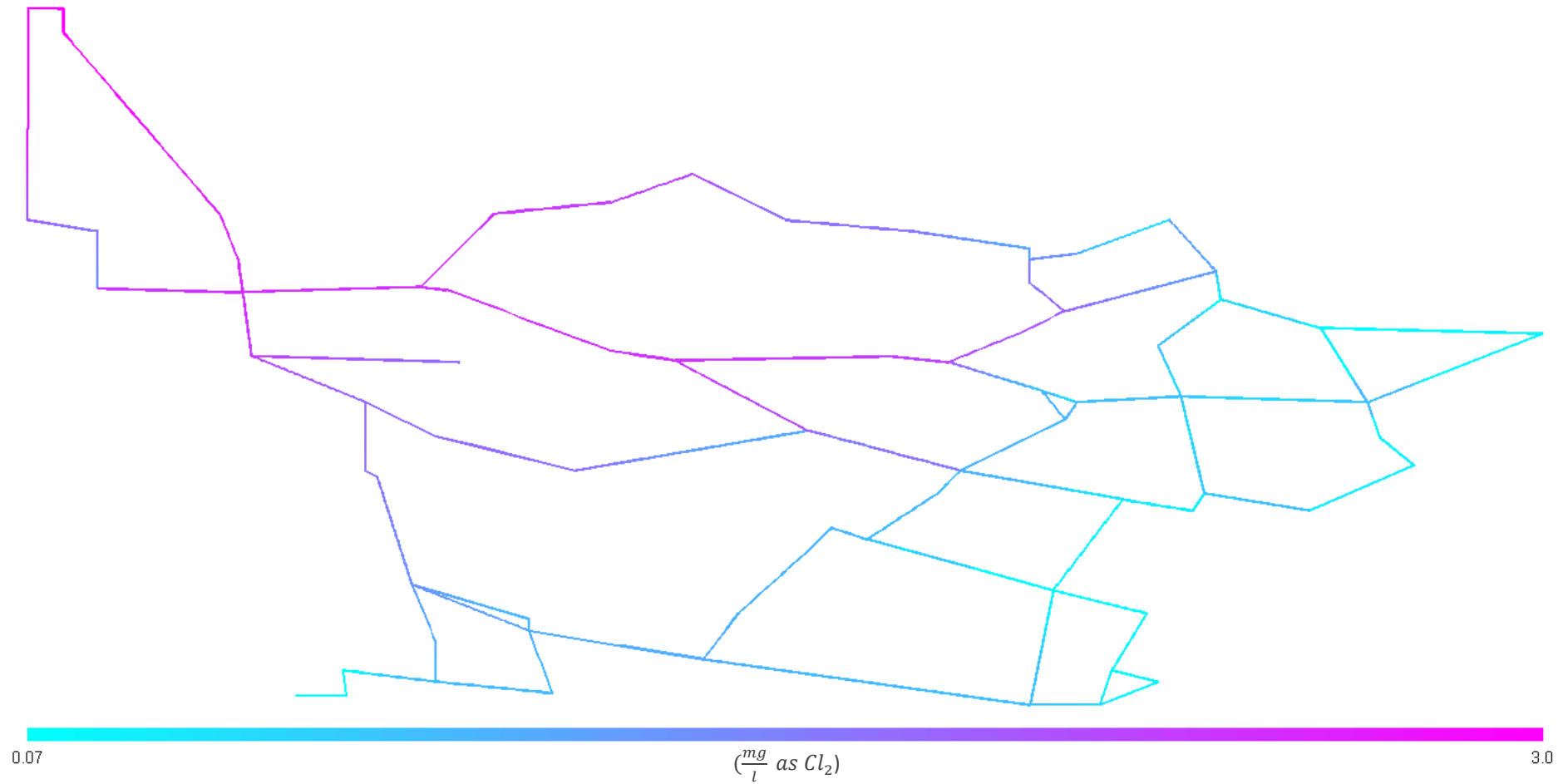


Figure D-37: Monochloramine concentration profile for Alternative 3

The monochloramine residual is increased throughout the system.

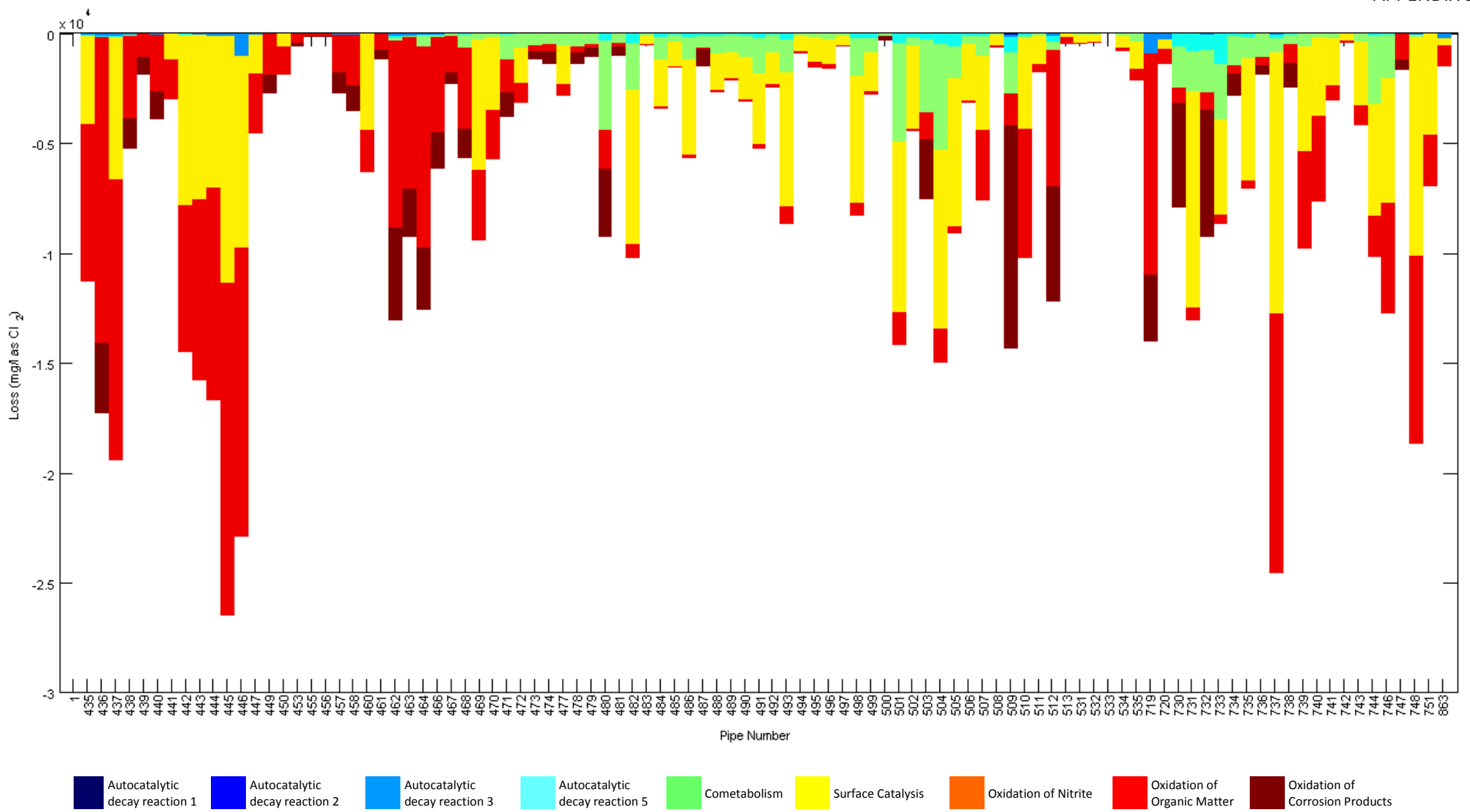


Figure D-38: Monochloramine loss mechanisms and locations for Alternative 3

The total loss of monochloramine is significantly reduced as cometabolism is no longer a major loss mechanism. For this alternative, the reduction in disinfectant loss due to reduced cometabolism is not offset by an increase in the other loss mechanisms and consequently the disinfectant residual throughout the system increases.

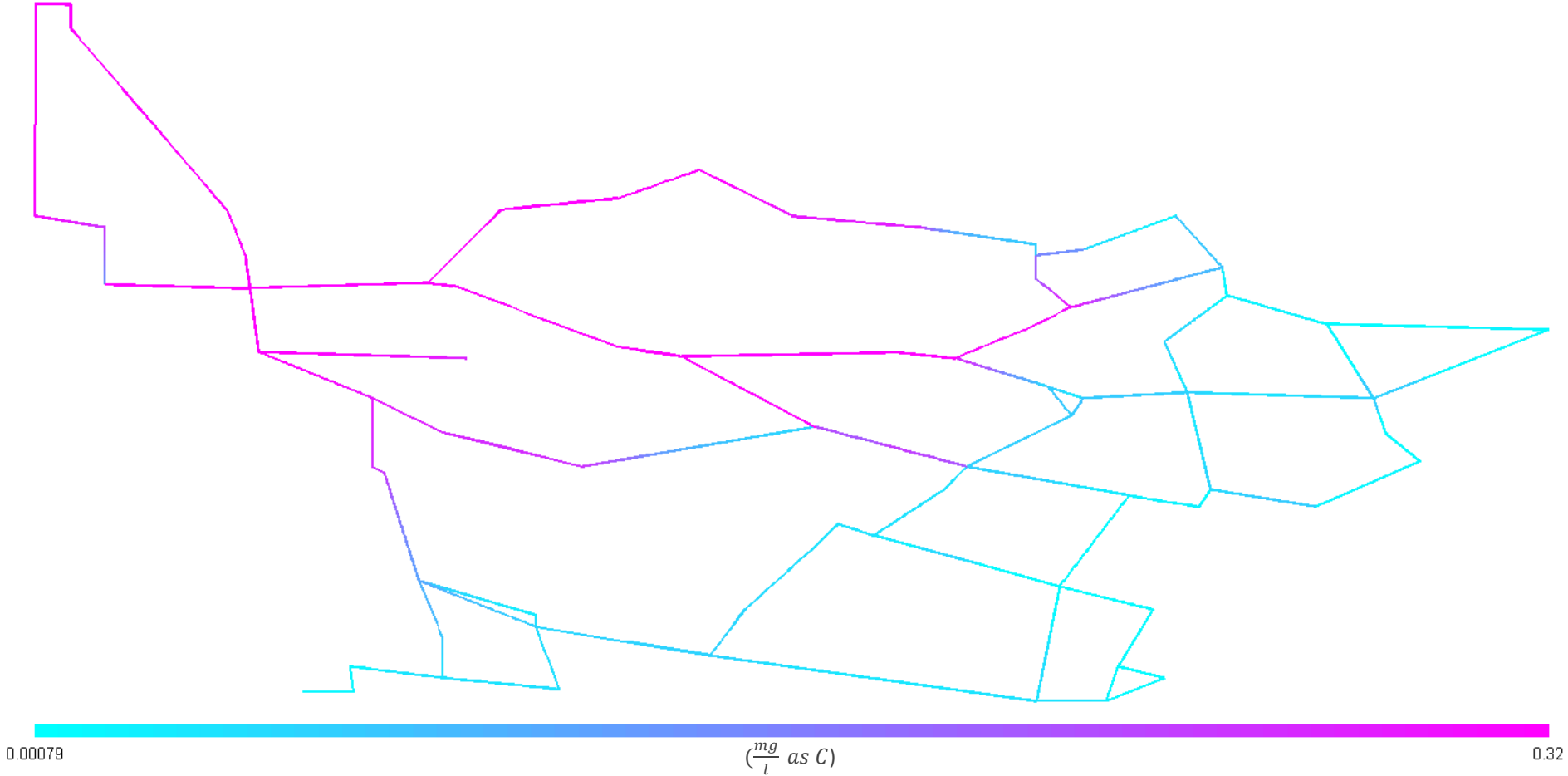


Figure D-39: BOM₁ concentration profile for Alternative 3

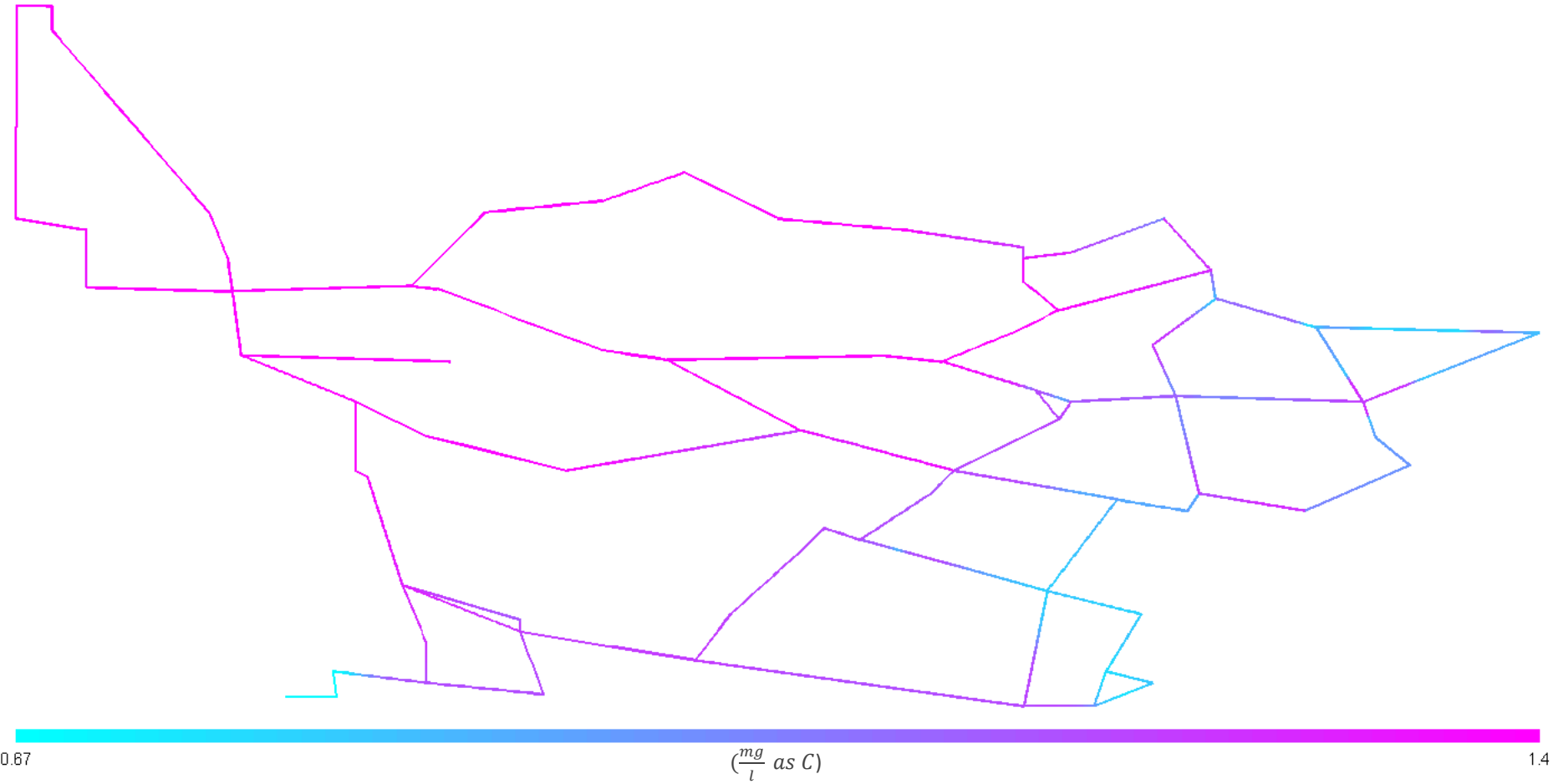


Figure D-40: BOM₂ concentration profile for Alternative 3

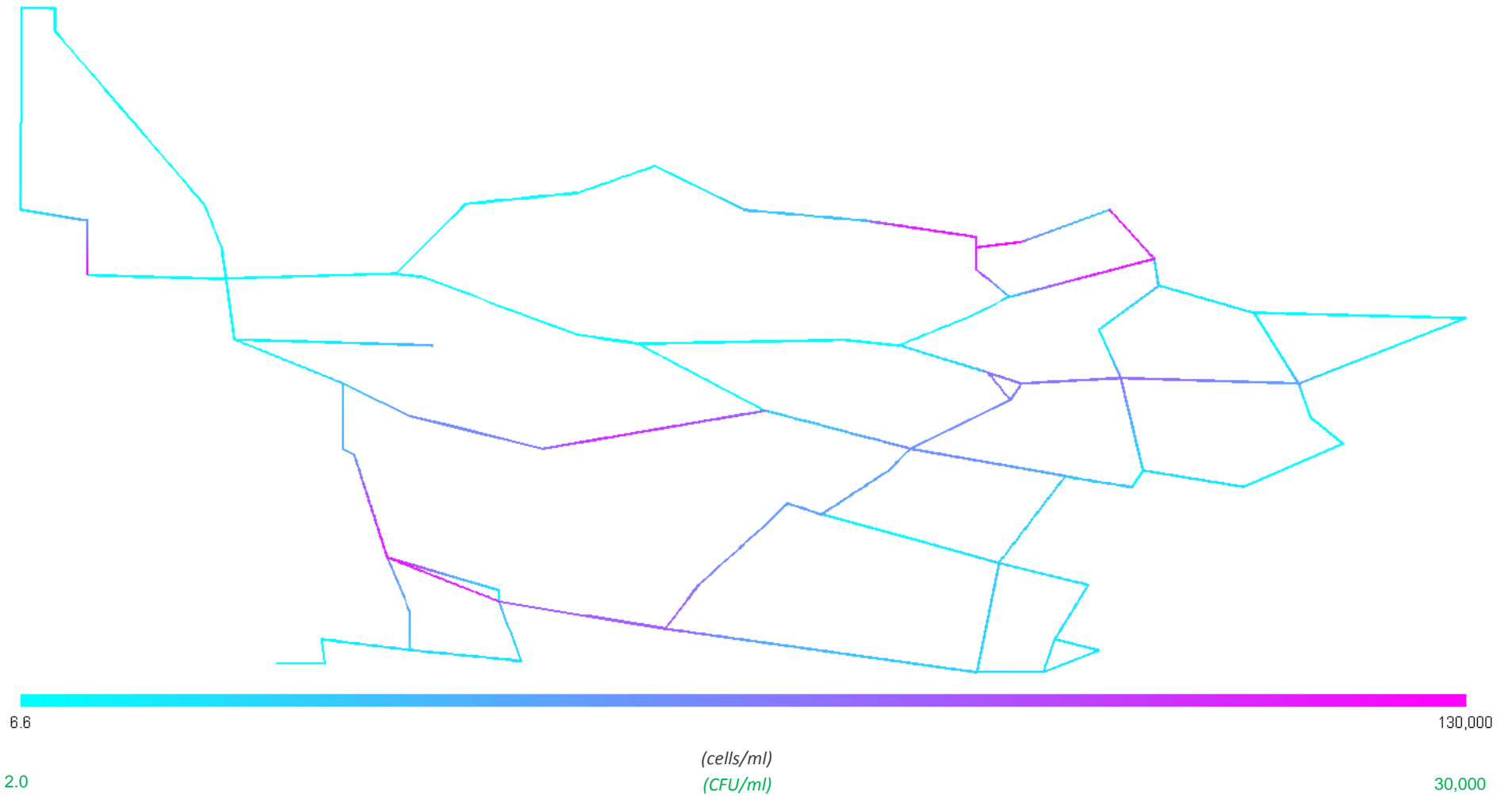


Figure D-41: Suspended heterotroph concentration profile for Alternative 3

The concentration of both suspended and fixed heterotrophs is primarily reduced to due to the increased concentration of disinfectant residual. The decreased concentration of active biomass, results in decreased SMP concentrations, which also contributes, in part, to the lower heterotroph concentrations.

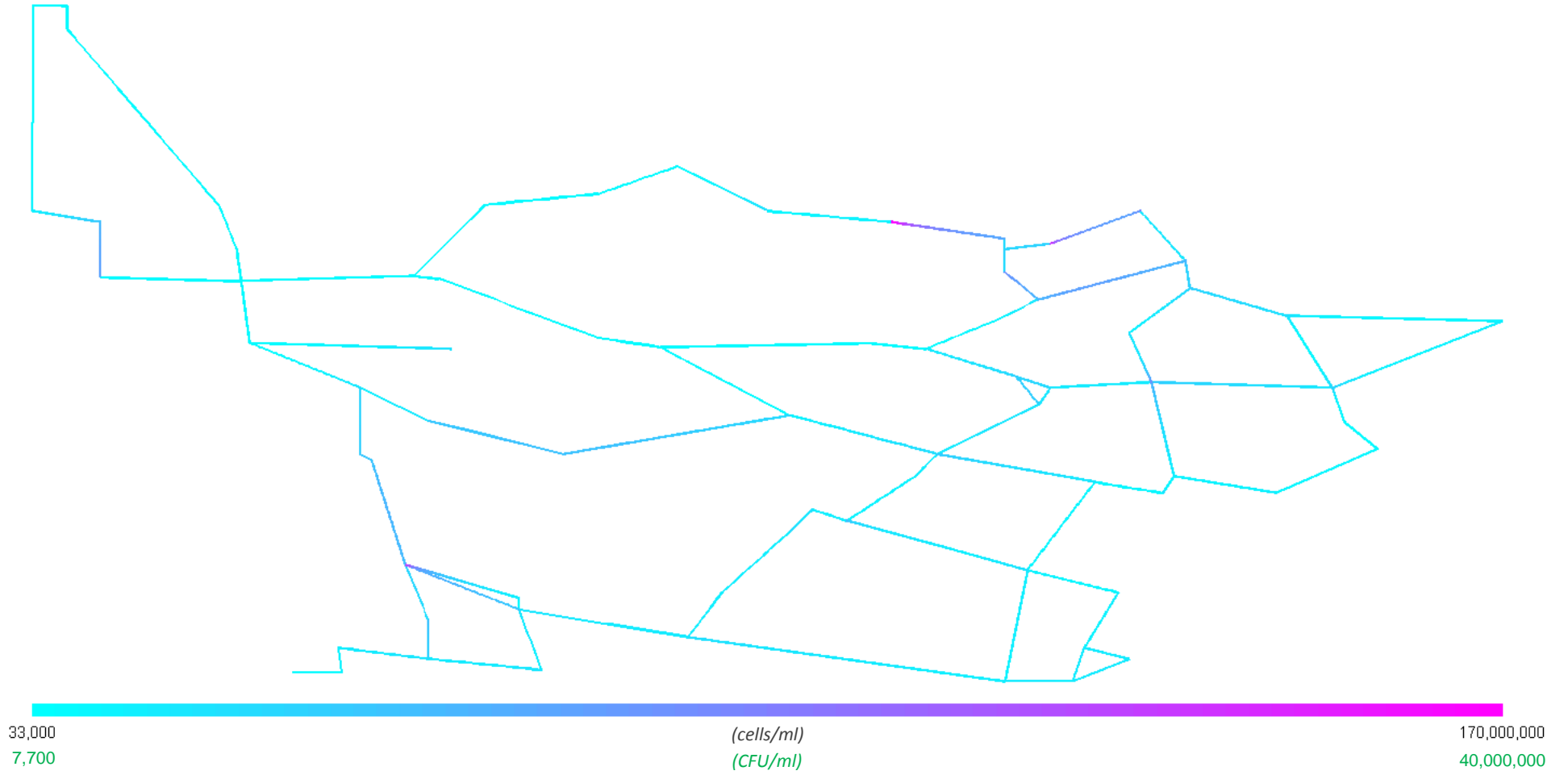


Figure D-42: Fixed heterotroph concentration profile for Alternative 3

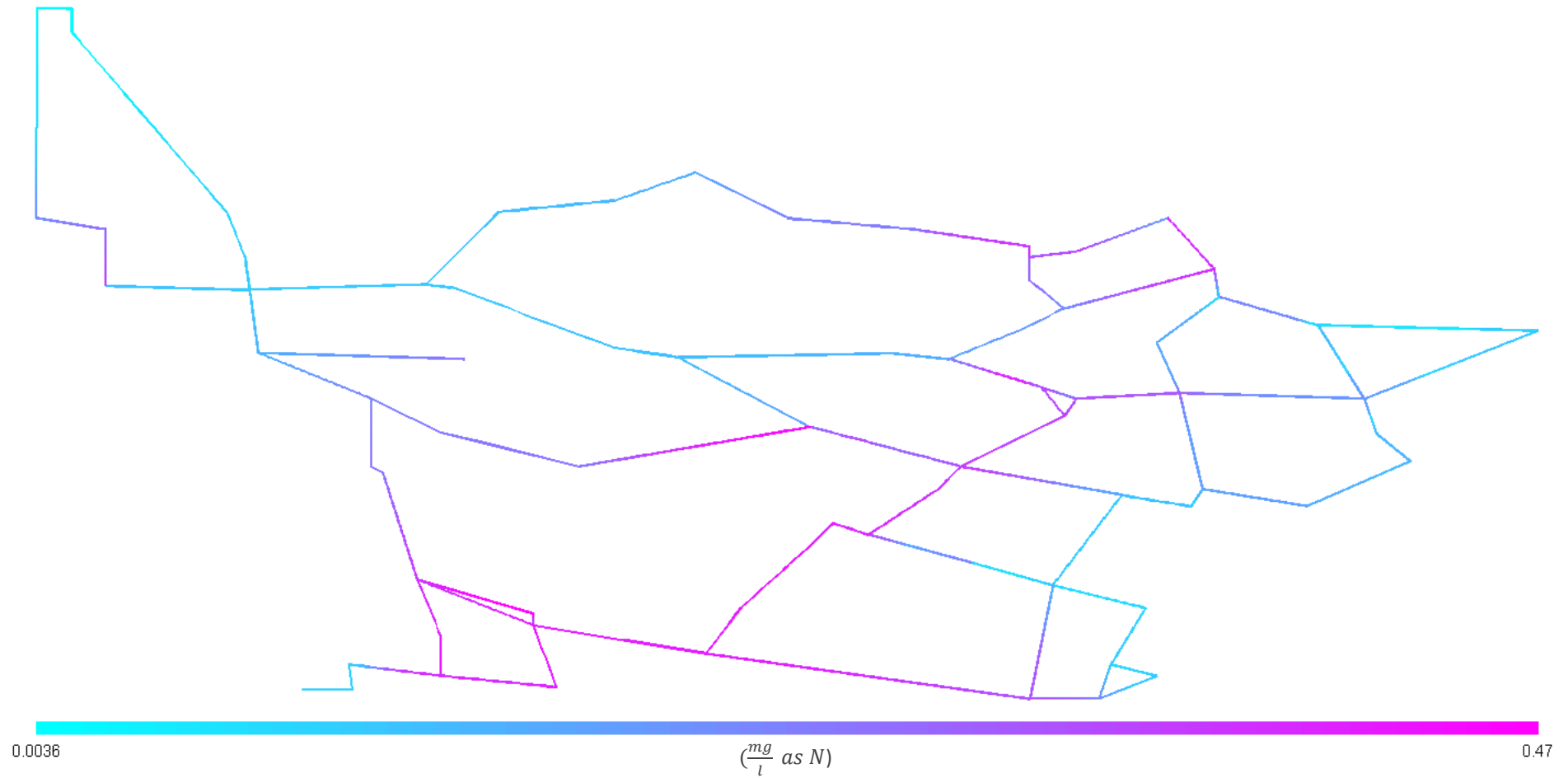


Figure D-43: Total ammonia concentration profile for Alternative 3

The total ammonia concentration is significantly reduced as no excess ammonia enters the system at the treatment plant and all ammonia originates only from chloramines for this alternative.

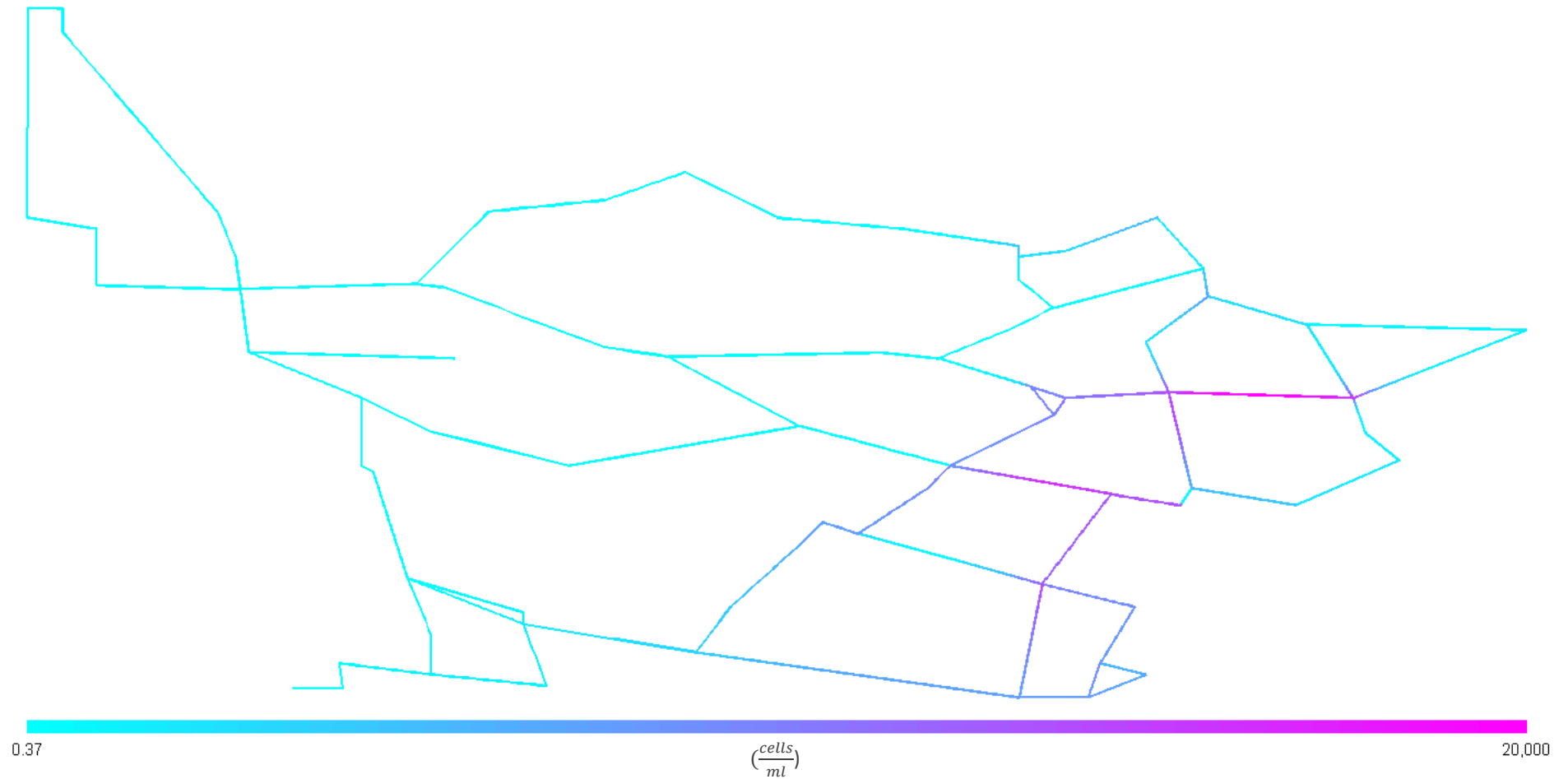


Figure D-44: Suspended AOB concentration profile for Alternative 3

The concentrations of both suspended and fixed AOB decrease significantly as the concentration of disinfectant residual is greater and the concentration of their ammonia substrate is lower.

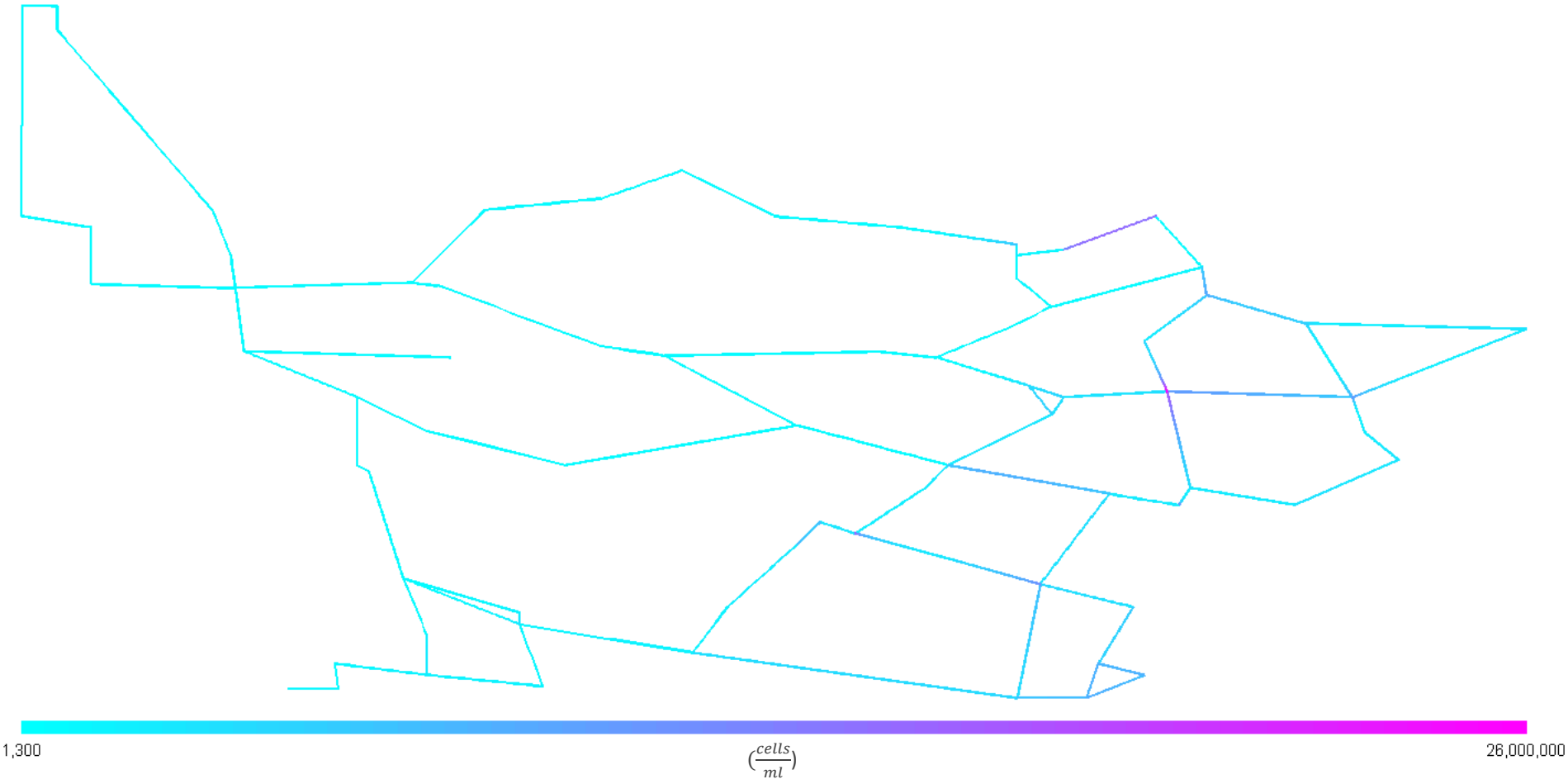


Figure D-45: Fixed AOB concentration profile for Alternative 3

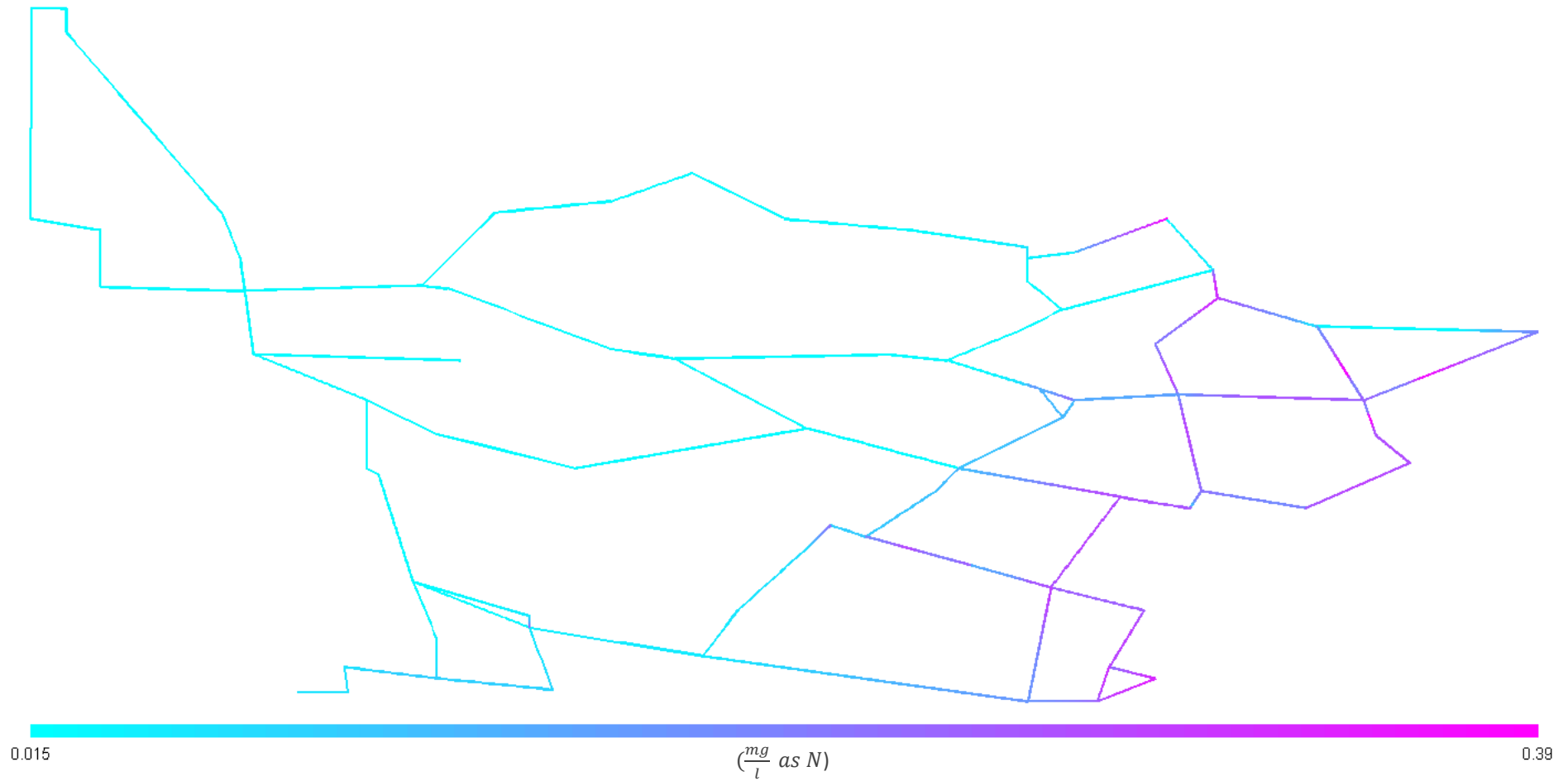


Figure D-46: Nitrite concentration profile for Alternative 3

The nitrite concentrations have decreased significantly as a consequence of the reduced AOB concentrations, whose utilisation of ammonia produces nitrite. The maximum concentration for this alternative is significantly below the maximum allowable limit.

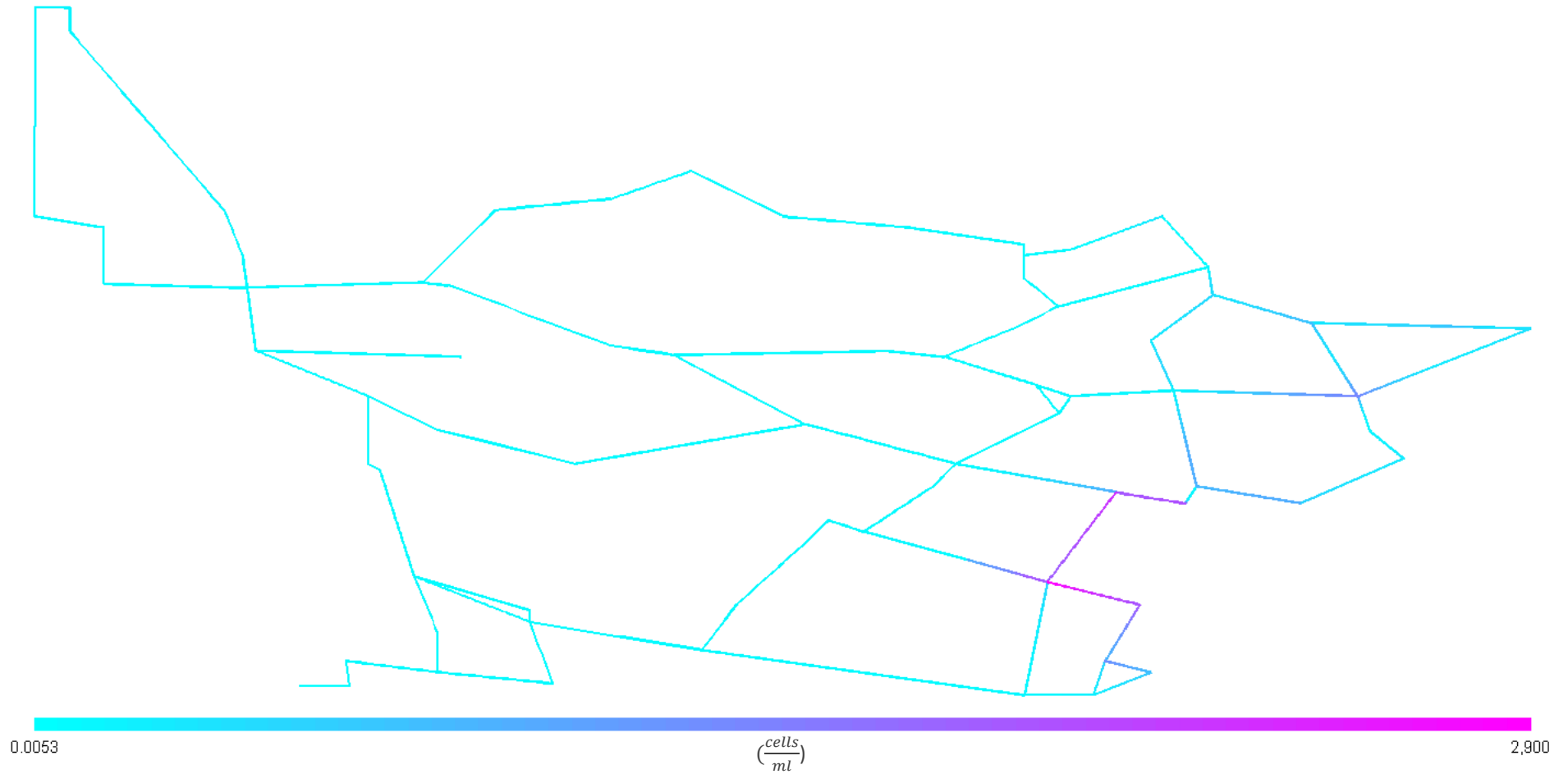


Figure D-47: Suspended NOB concentration profile for Alternative 3

Both the concentrations of suspended and fixed NOB are significantly reduced to the increased disinfectant residual concentrations and the reduced concentrations of the nitrite substrate.

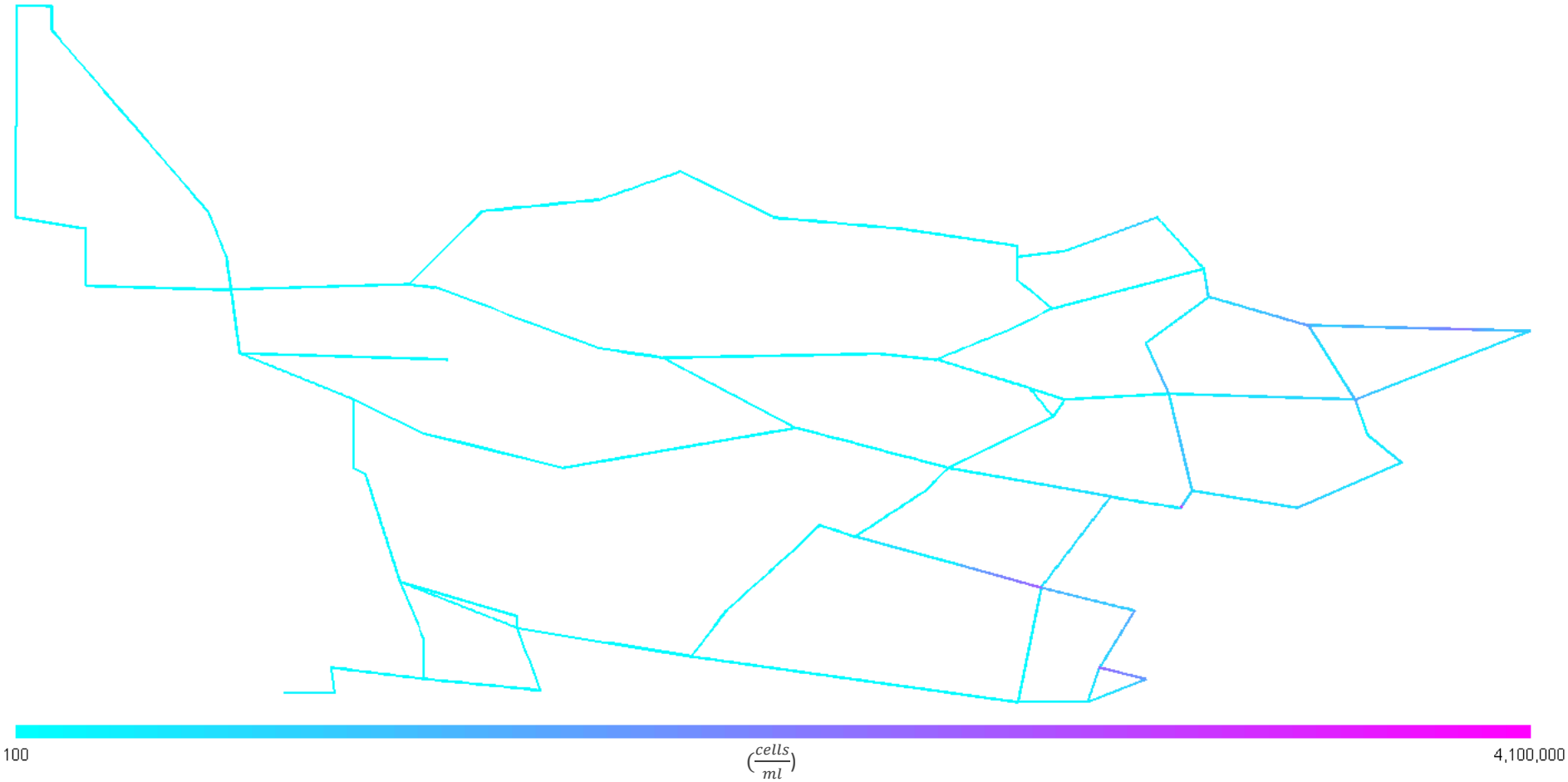


Figure D-48: Fixed NOB concentration profile for Alternative 3

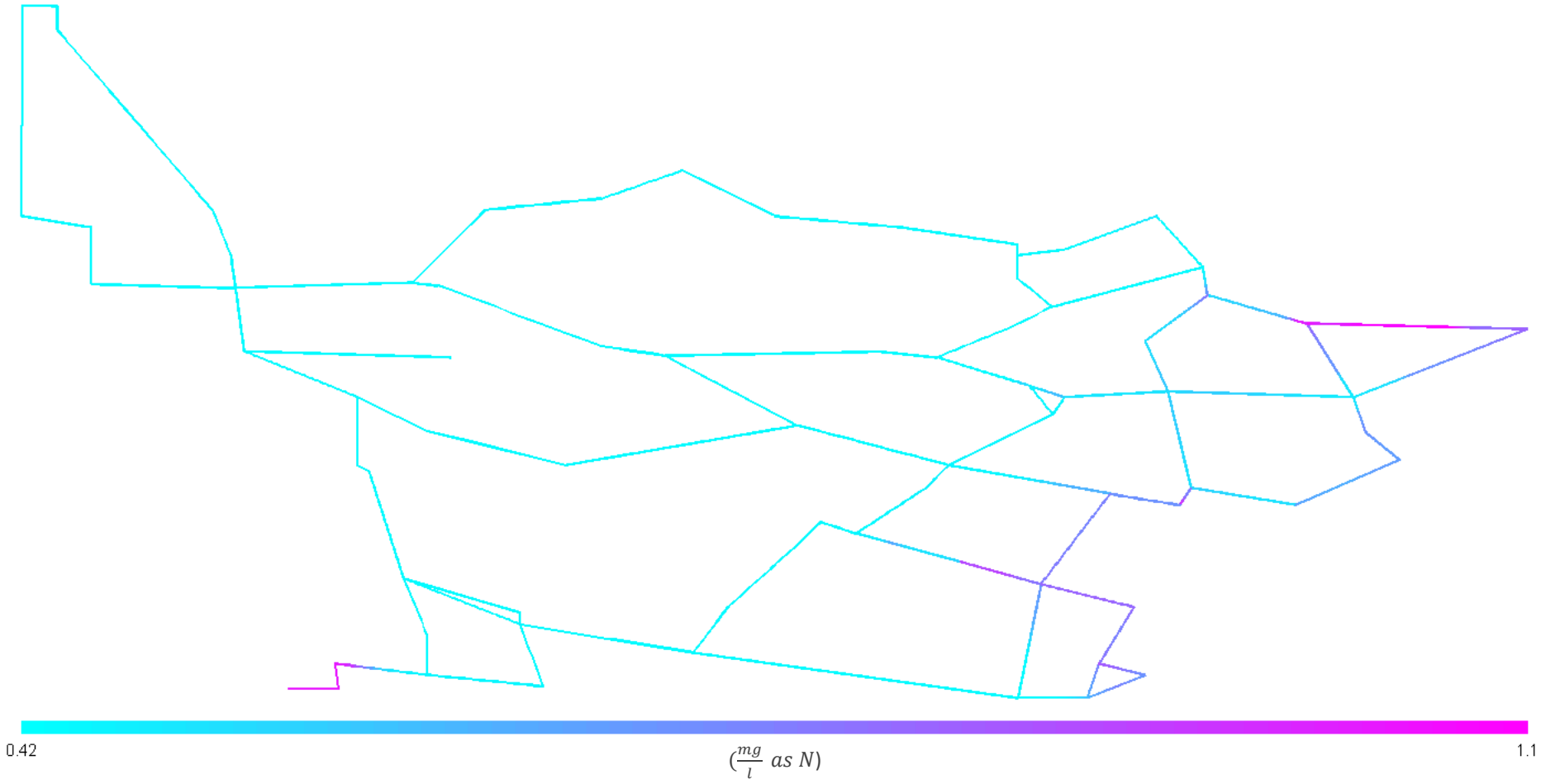


Figure D-49: Nitrate concentration profile for Alternative 3

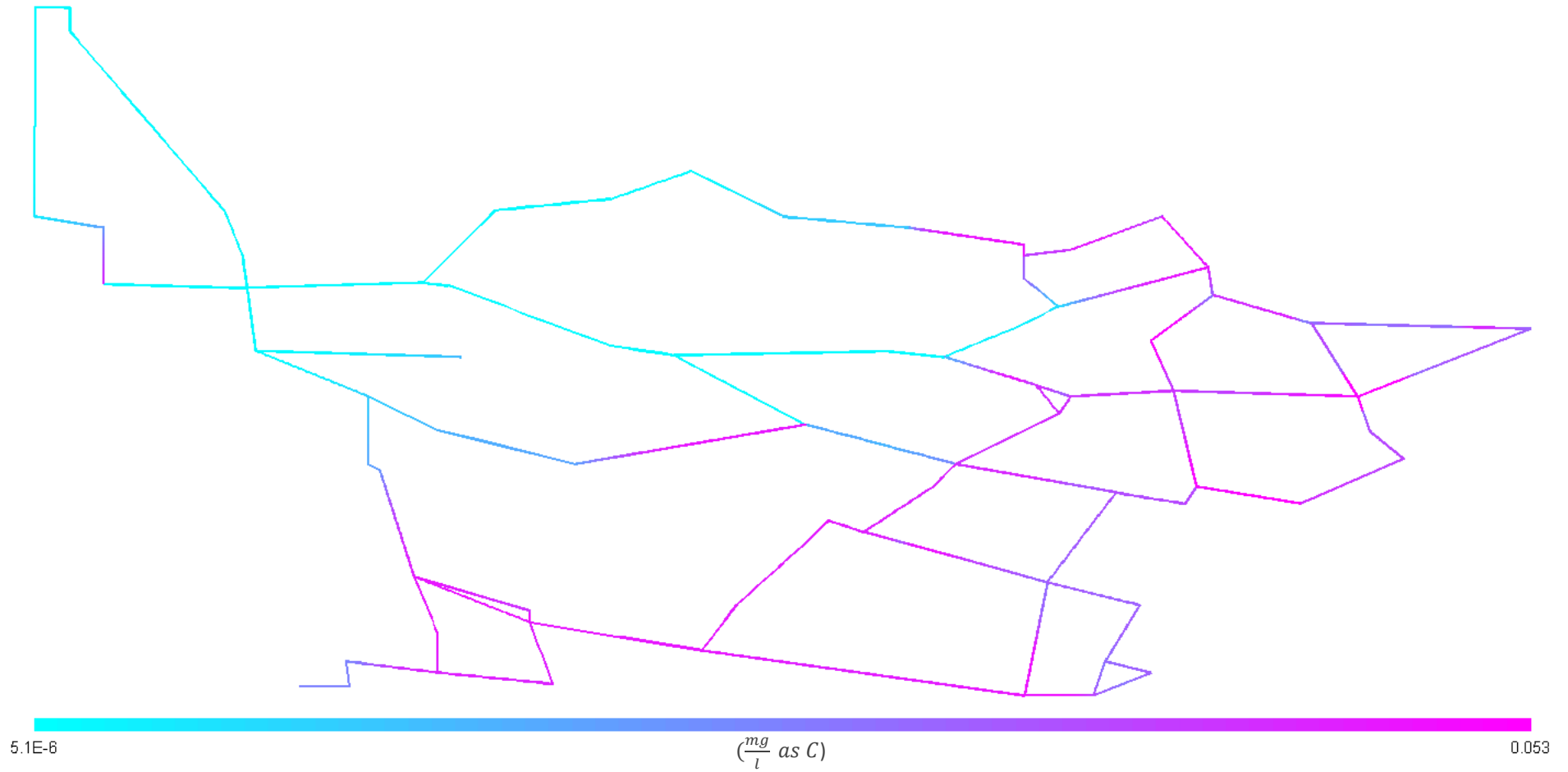


Figure D-50: UAP concentration profile for Alternative 3

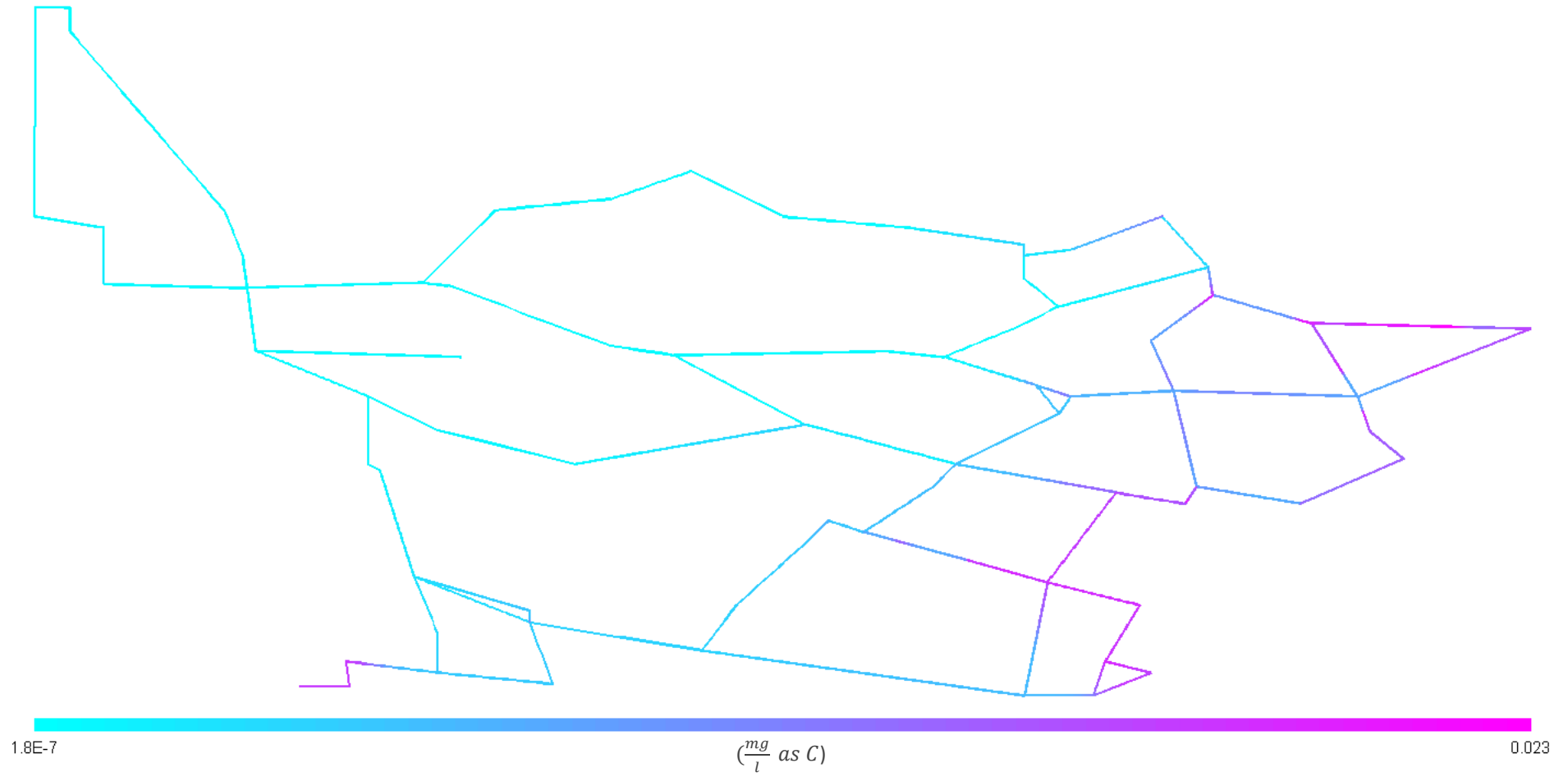


Figure D-51: BAP concentration profile for Alternative 3

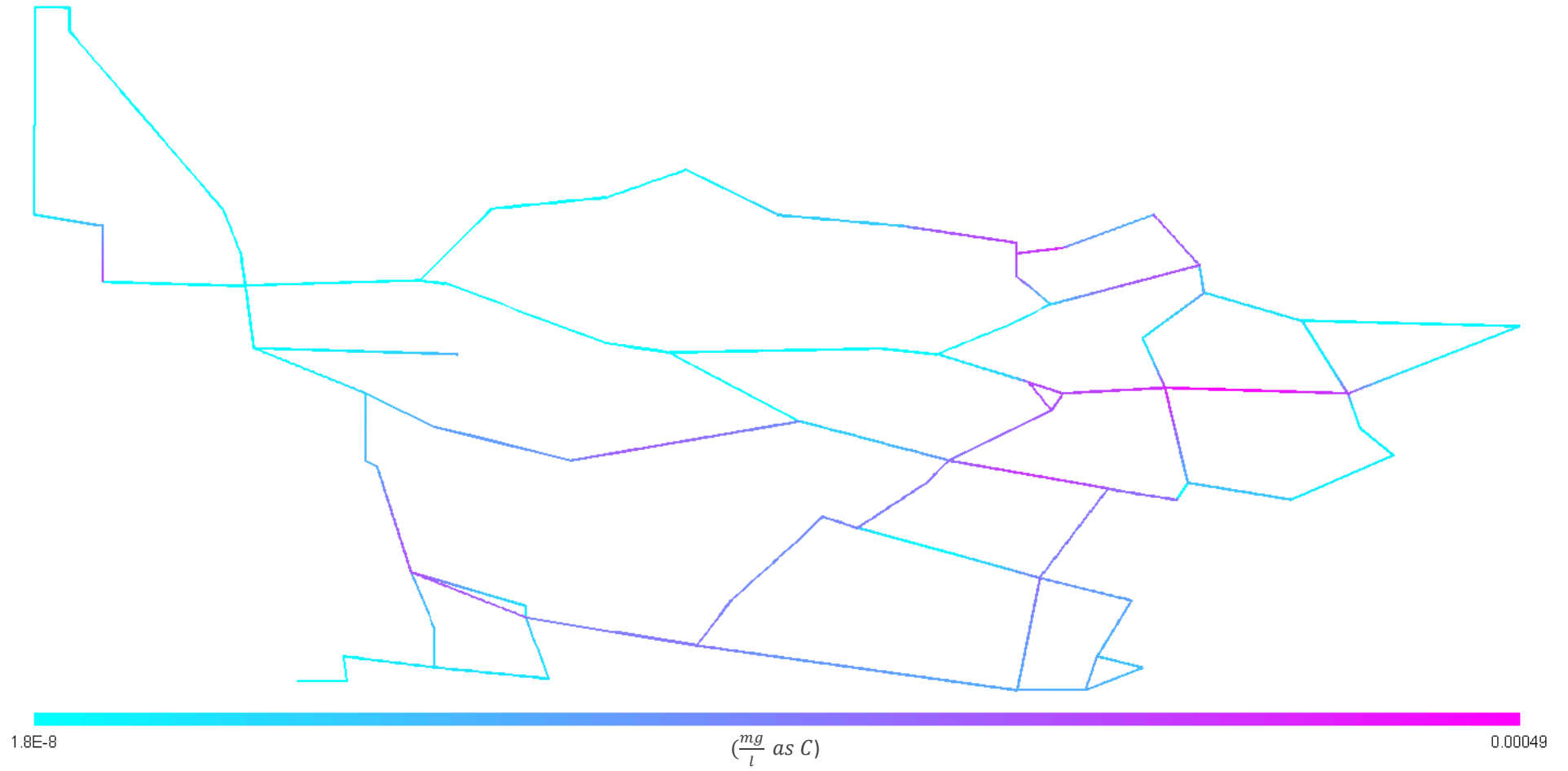


Figure D-52: Suspended EPS concentration profile for Alternative 3

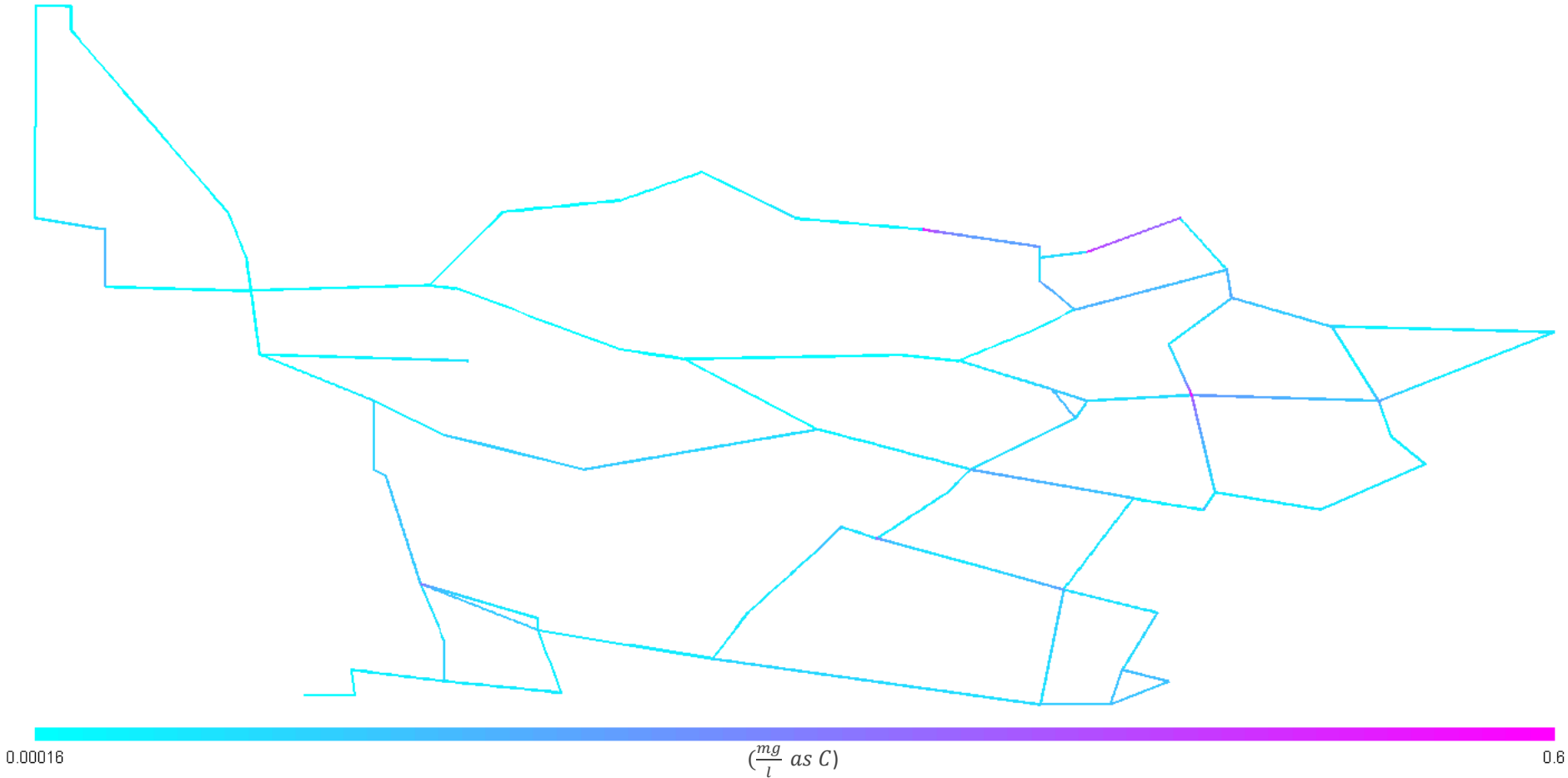


Figure D-53: Fixed EPS concentration profile for Alternative 3

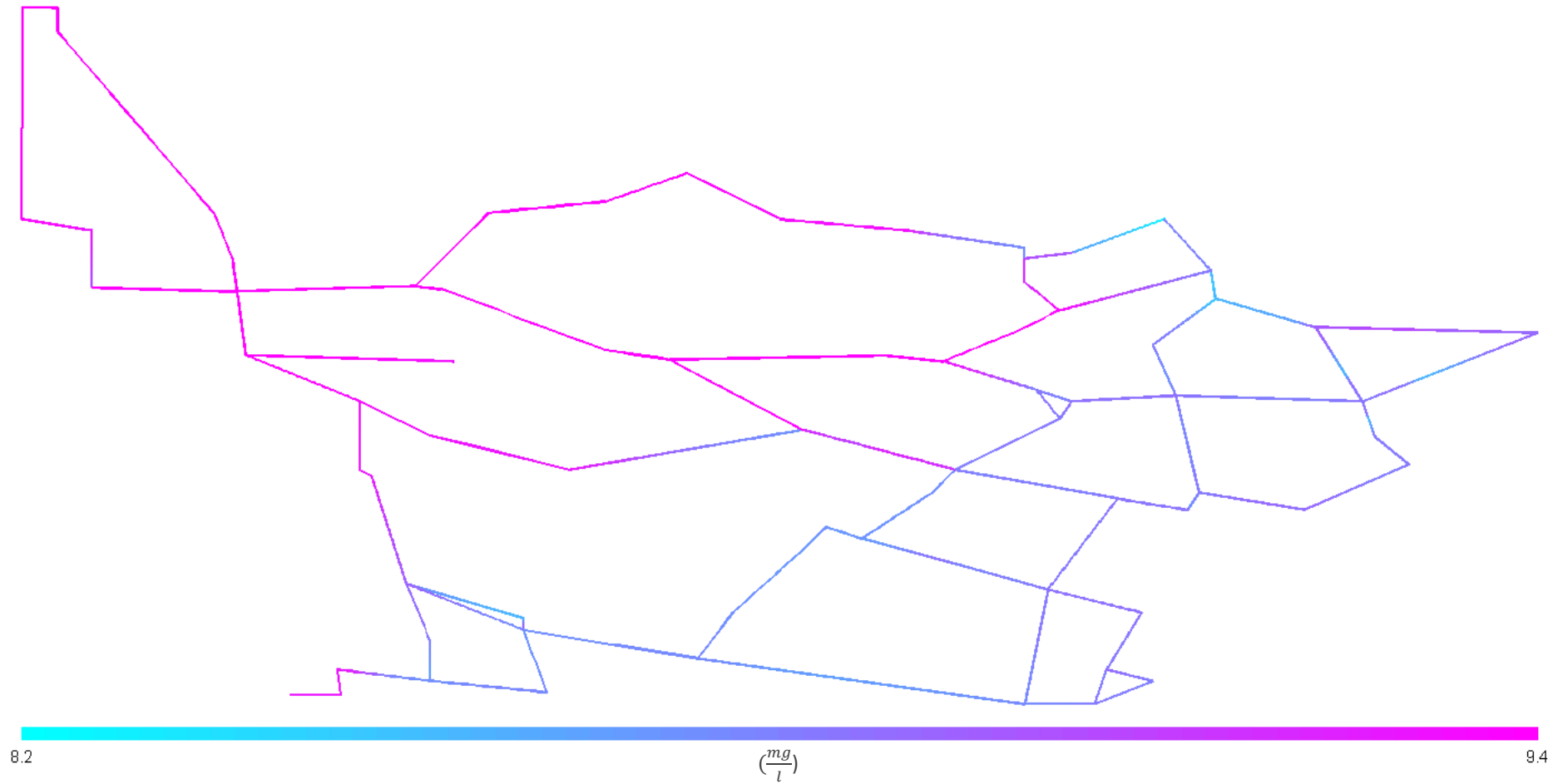


Figure D-54: Dissolved oxygen concentration profile for Alternative 3

The greater oxygen concentrations are a result of reduced active biomass concentrations for this alternative.

D.4 Booster Chloramination

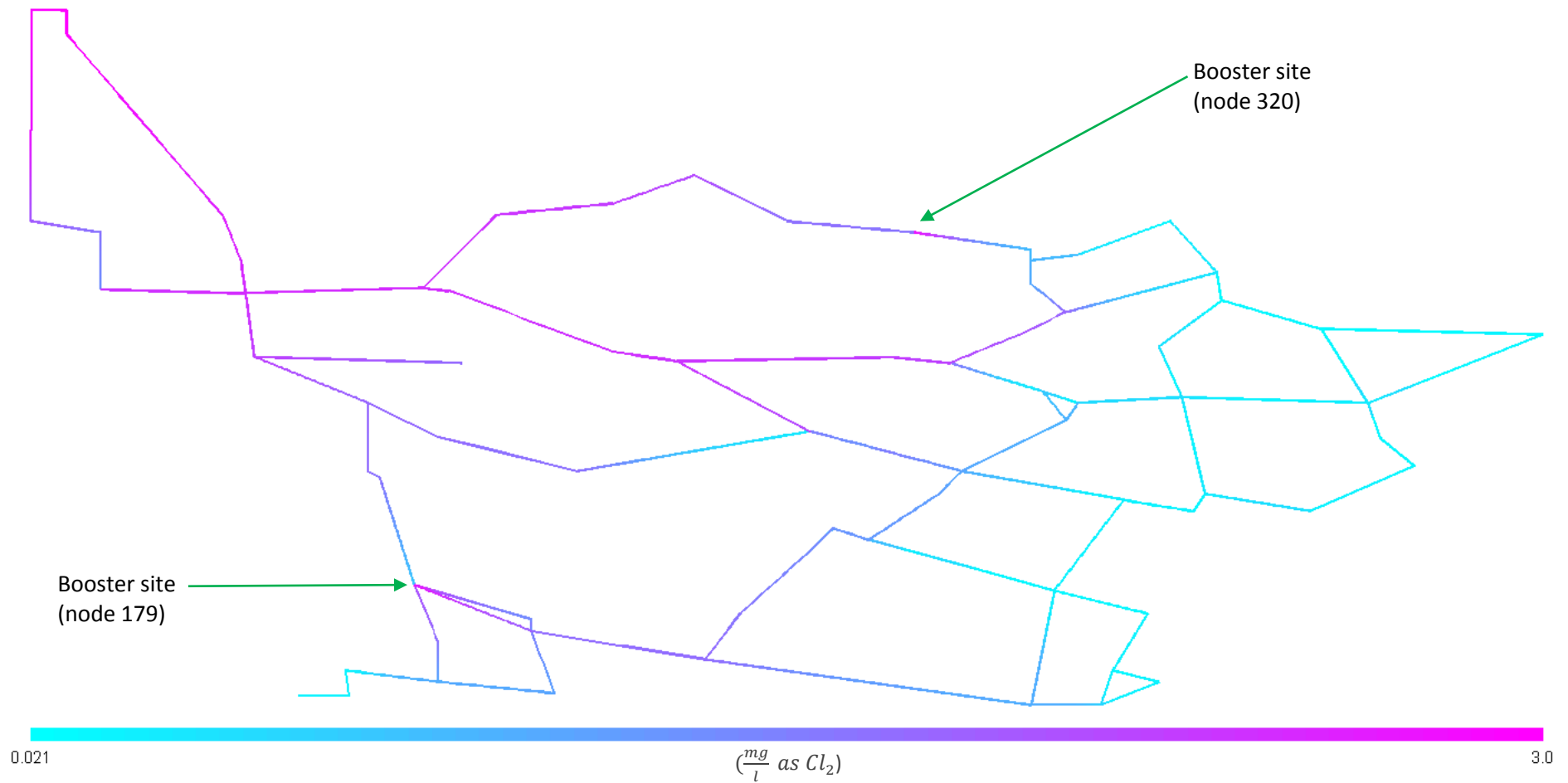


Figure D-55: Monochloramine concentration profile for Alternative 4

Monochloramine concentration increases at the booster sites. The monochloramine input at node 179 contributes to a slight increase in disinfectant residual in further pipe sections while the monochloramine input at node 320 is rapidly consumed in nearby pipes.

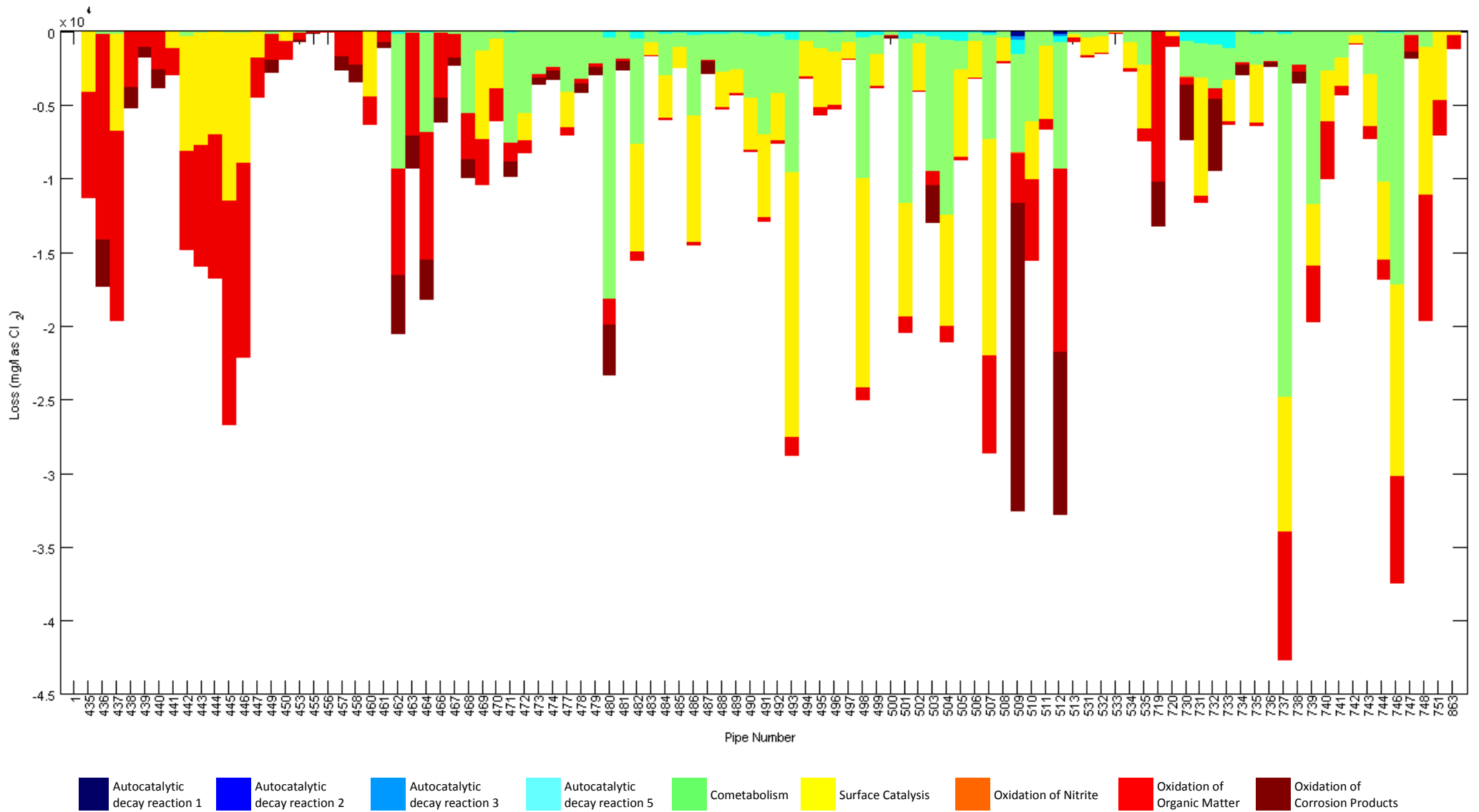


Figure D-56: Monochloramine loss mechanisms and locations for Alternative 4

The total loss of monochloramine is greater due to the greater input concentration of monochloramine in the system. The contribution of surface catalysis to monochloramine loss has increased, as monochloramine loss due to this mechanism is a function of the monochloramine concentration squared.

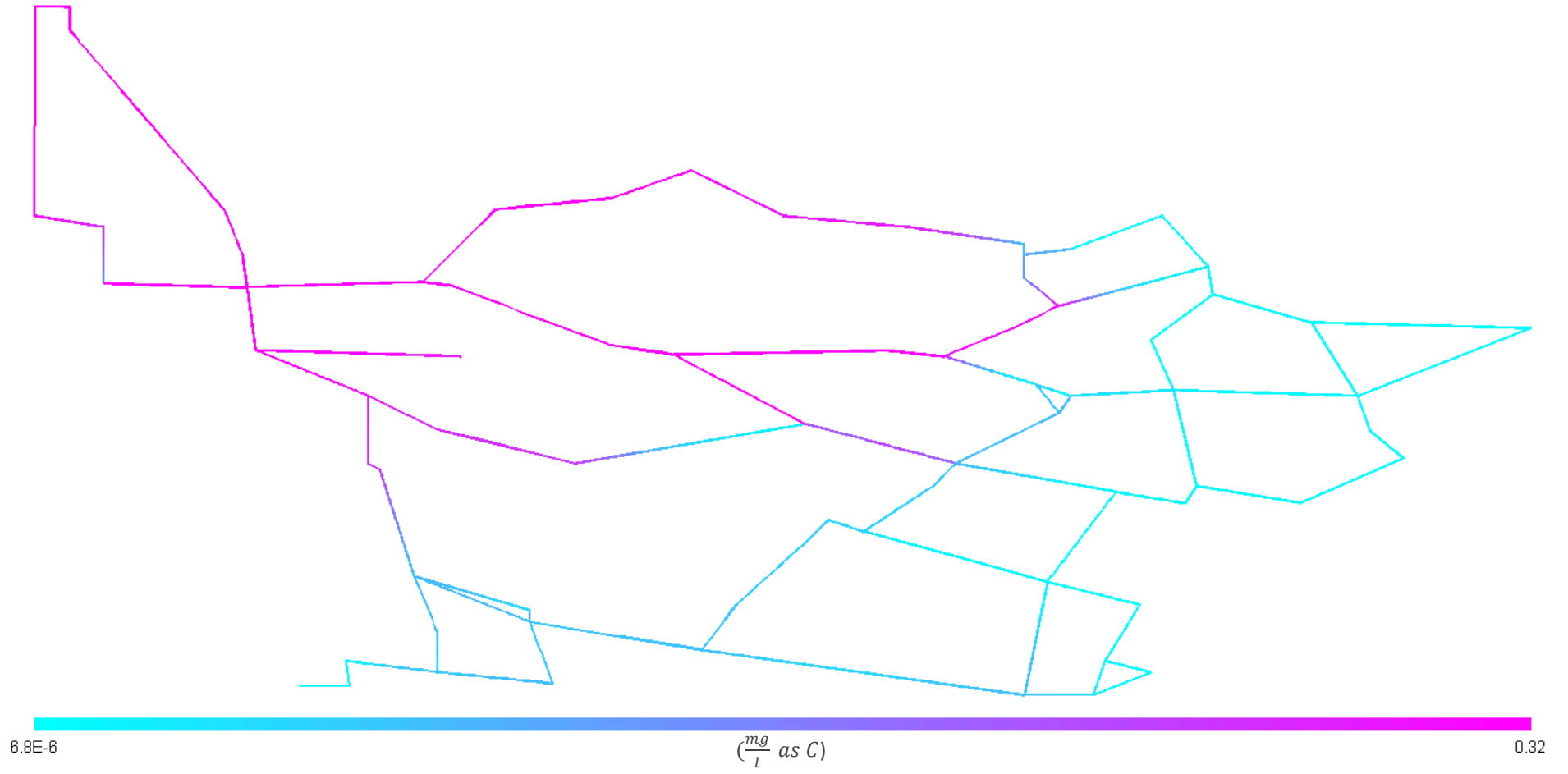


Figure D-57: BOM₁ concentration profile for Alternative 4

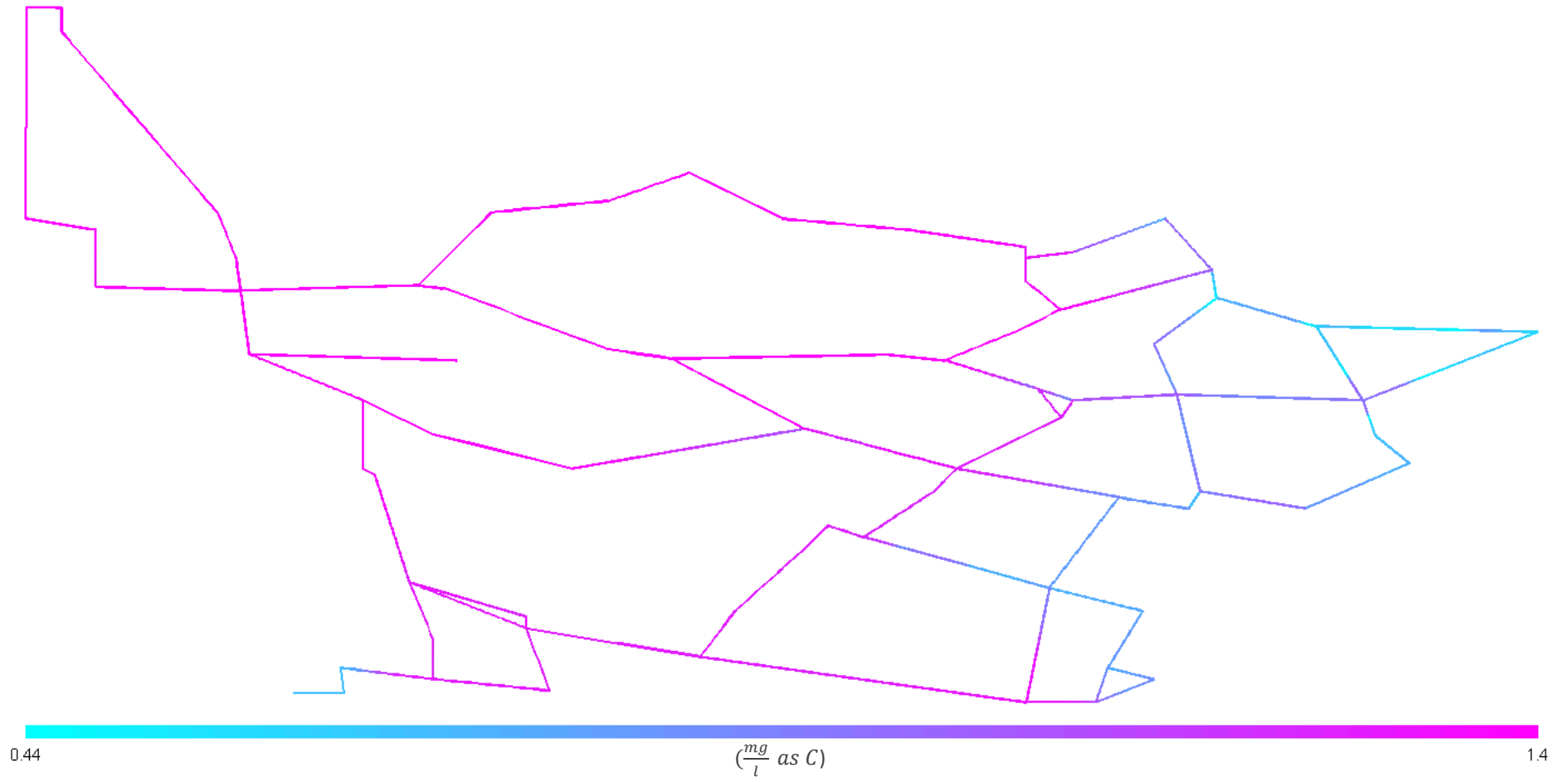


Figure D-58: BOM₂ concentration profile for Alternative 4

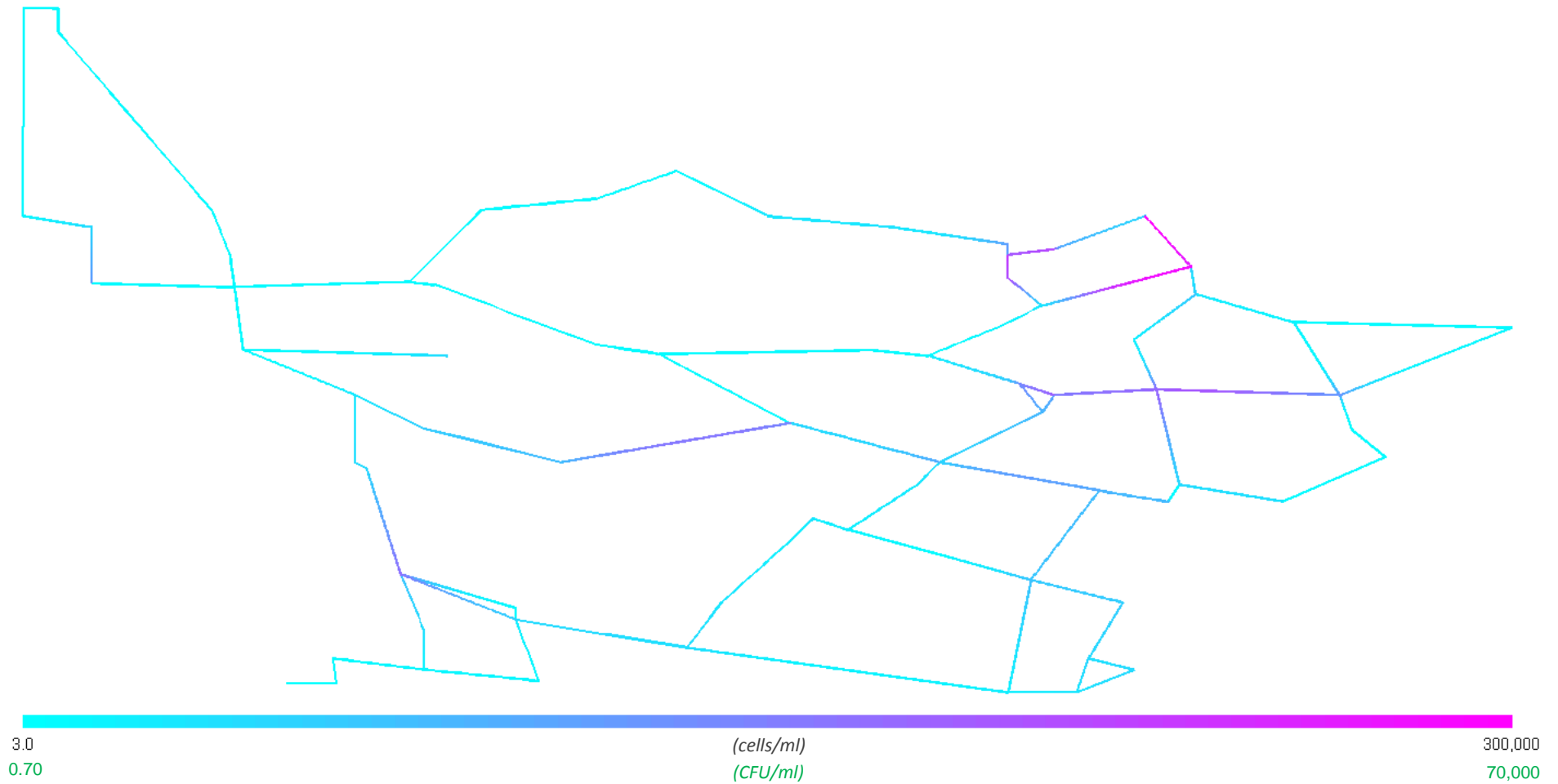


Figure D-59: Suspended heterotroph concentration profile for Alternative 4

Booster chloramination is considerably more effective near node 179 than node 320 and hence while the concentration of both suspended and fixed heterotrophs is considerably reduced by node 179, this alternative has little impact on heterotroph concentrations near node 320.

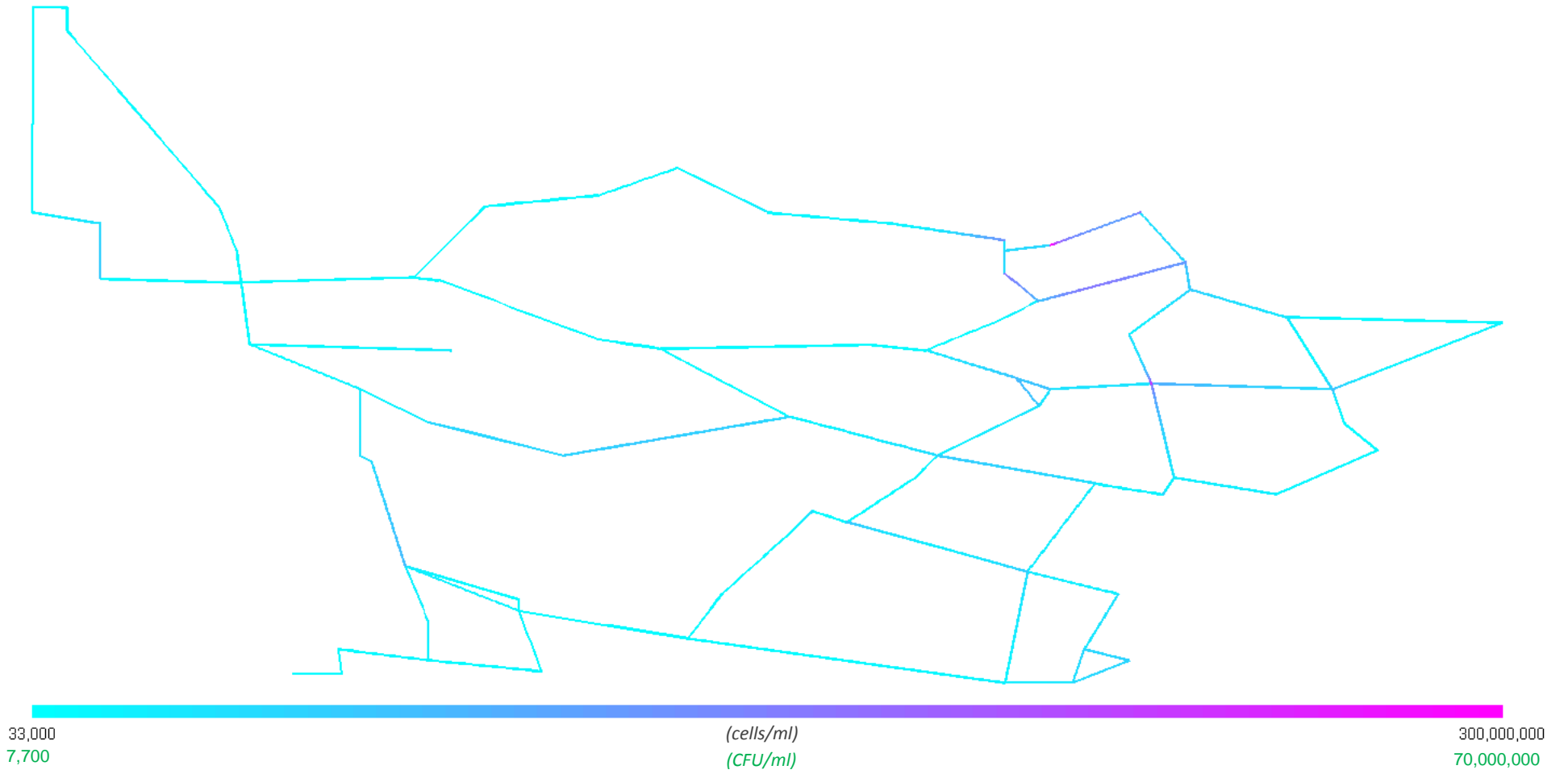


Figure D-60: Fixed heterotroph concentration profile for Alternative 4

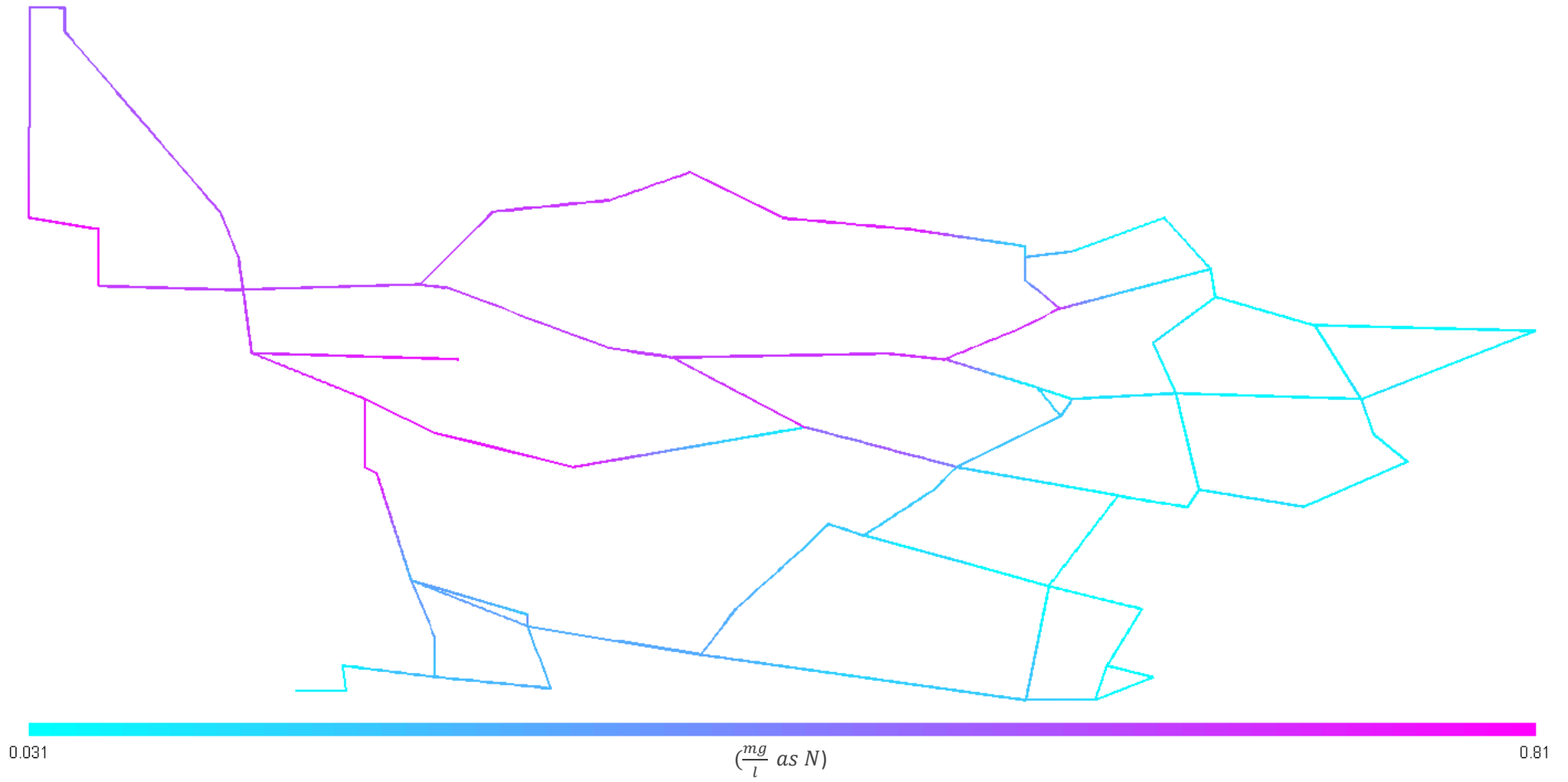


Figure D-61: Total ammonia concentration profile for Alternative 4

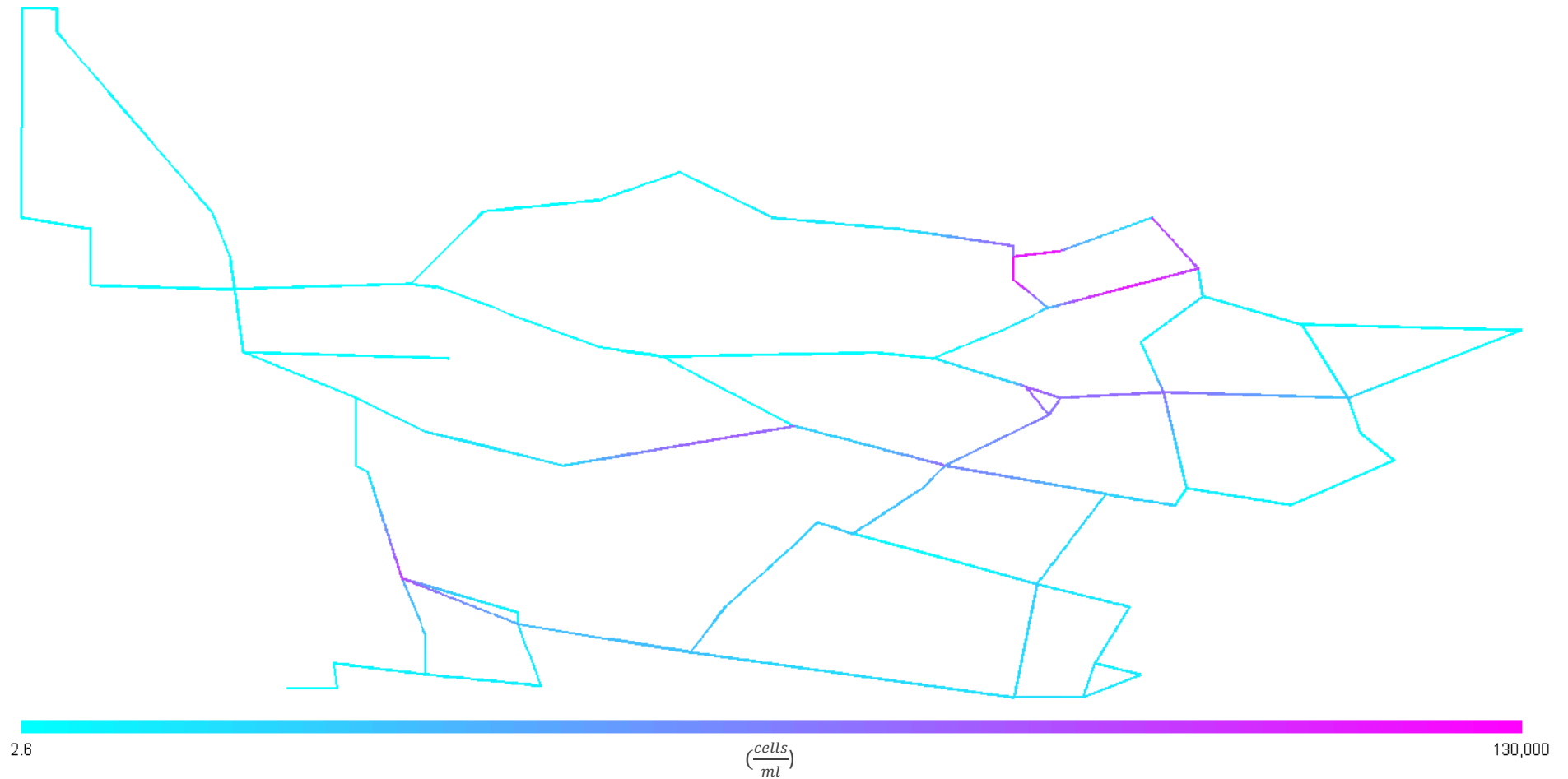


Figure D-62: Suspended AOB concentration profile for Alternative 4

The maximum concentrations of suspended and fixed AOB are largely unchanged. This is because the additional monochloramine input is depleted before it reaches the pipes with the most significant AOB growth and the ammonia substrate is not decreased using booster chloramination.

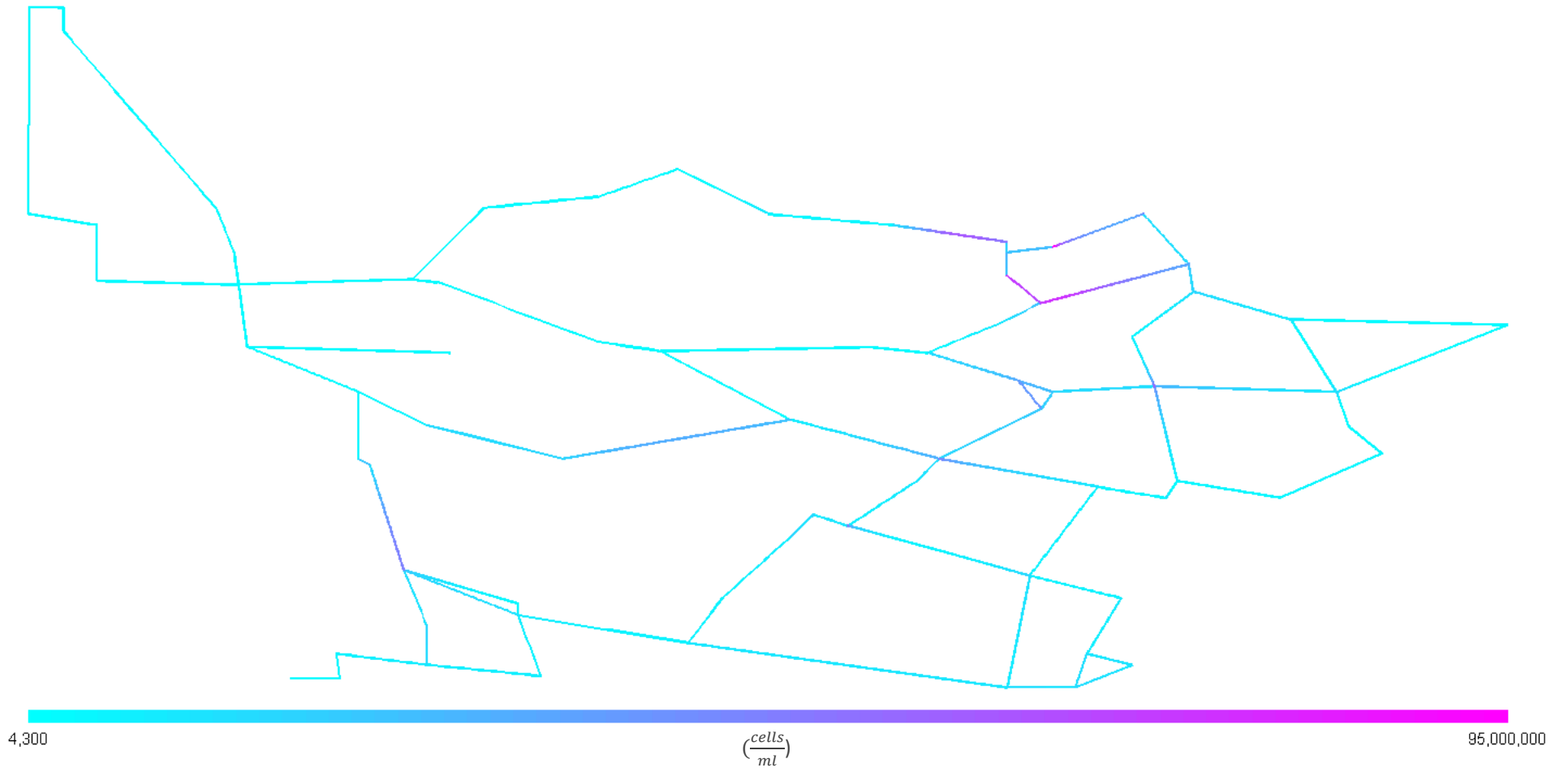


Figure D-63: Fixed AOB concentration profile for Alternative 4

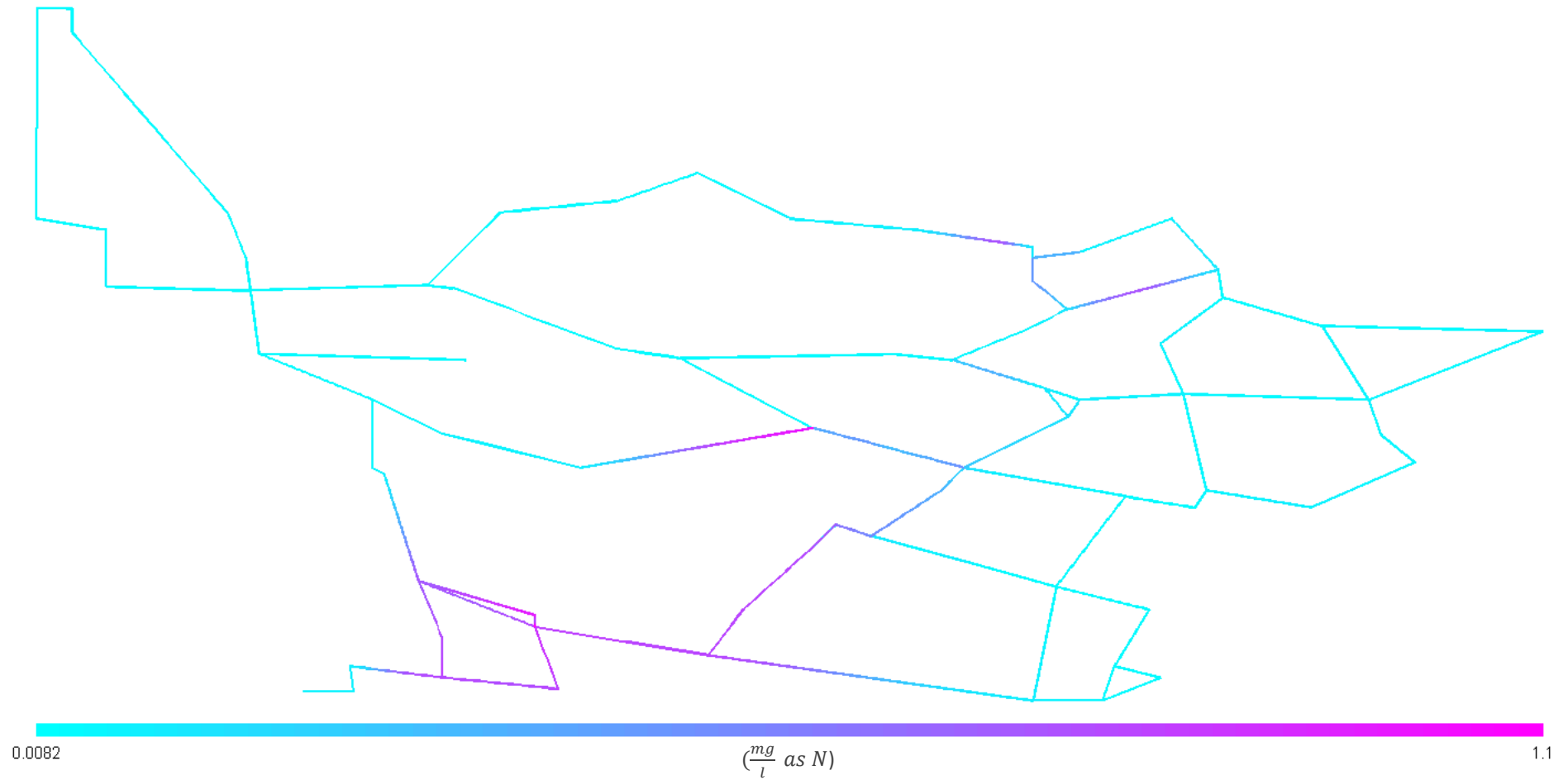


Figure D-64: Nitrite concentration profile for Alternative 4

The maximum nitrite concentration is slightly greater due to the increase in ammonia throughout the system associated with chloramines and the limited effect that booster chloramination has for this simulation in reducing AOB concentrations.

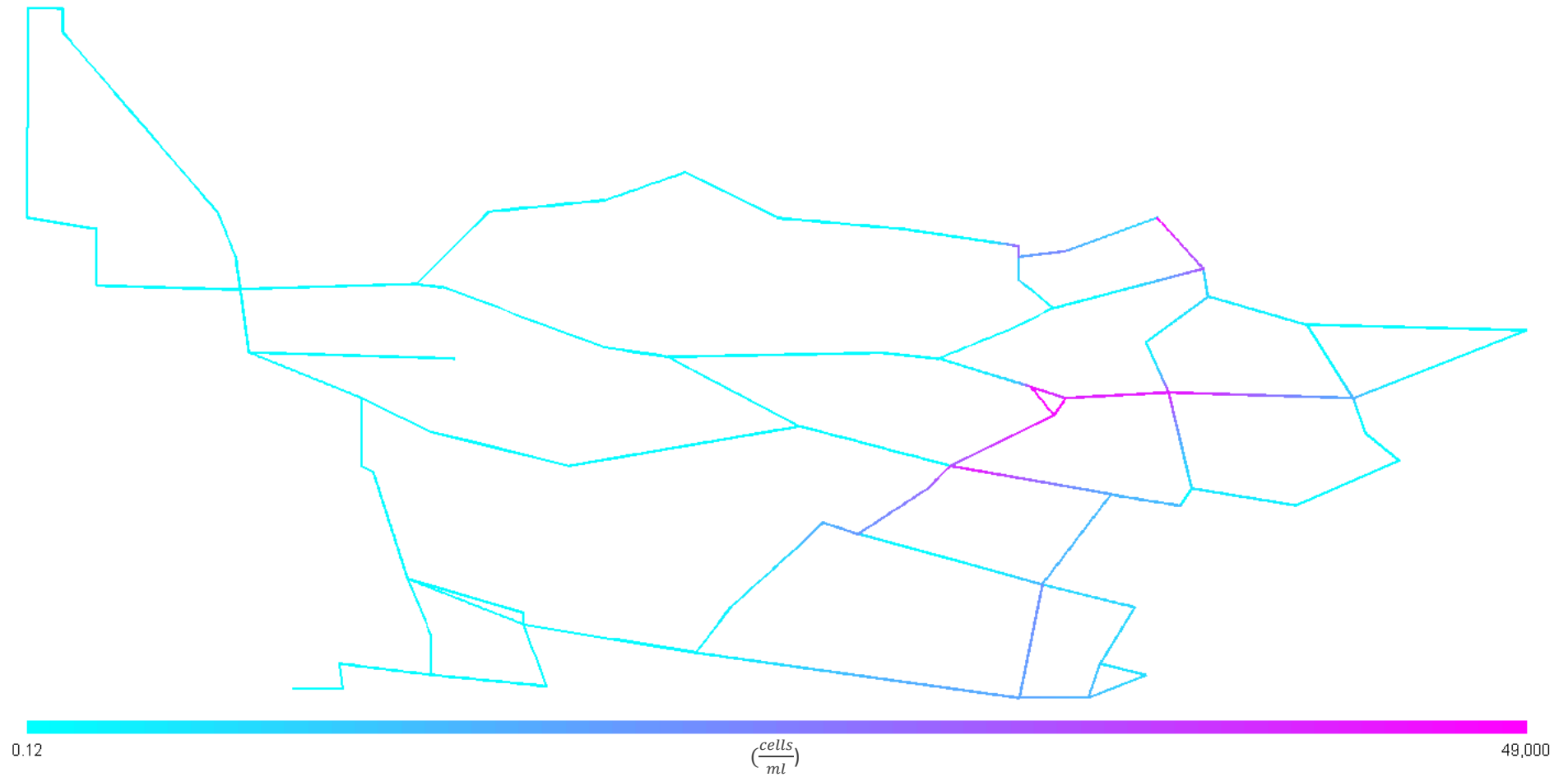


Figure D-65: Suspended NOB concentration profile for Alternative 4

The maximum suspended and fixed NOB concentrations are similar as the increased disinfectant residual does not significantly affect the further reaches of the system and the nitrite substrate increases slightly.

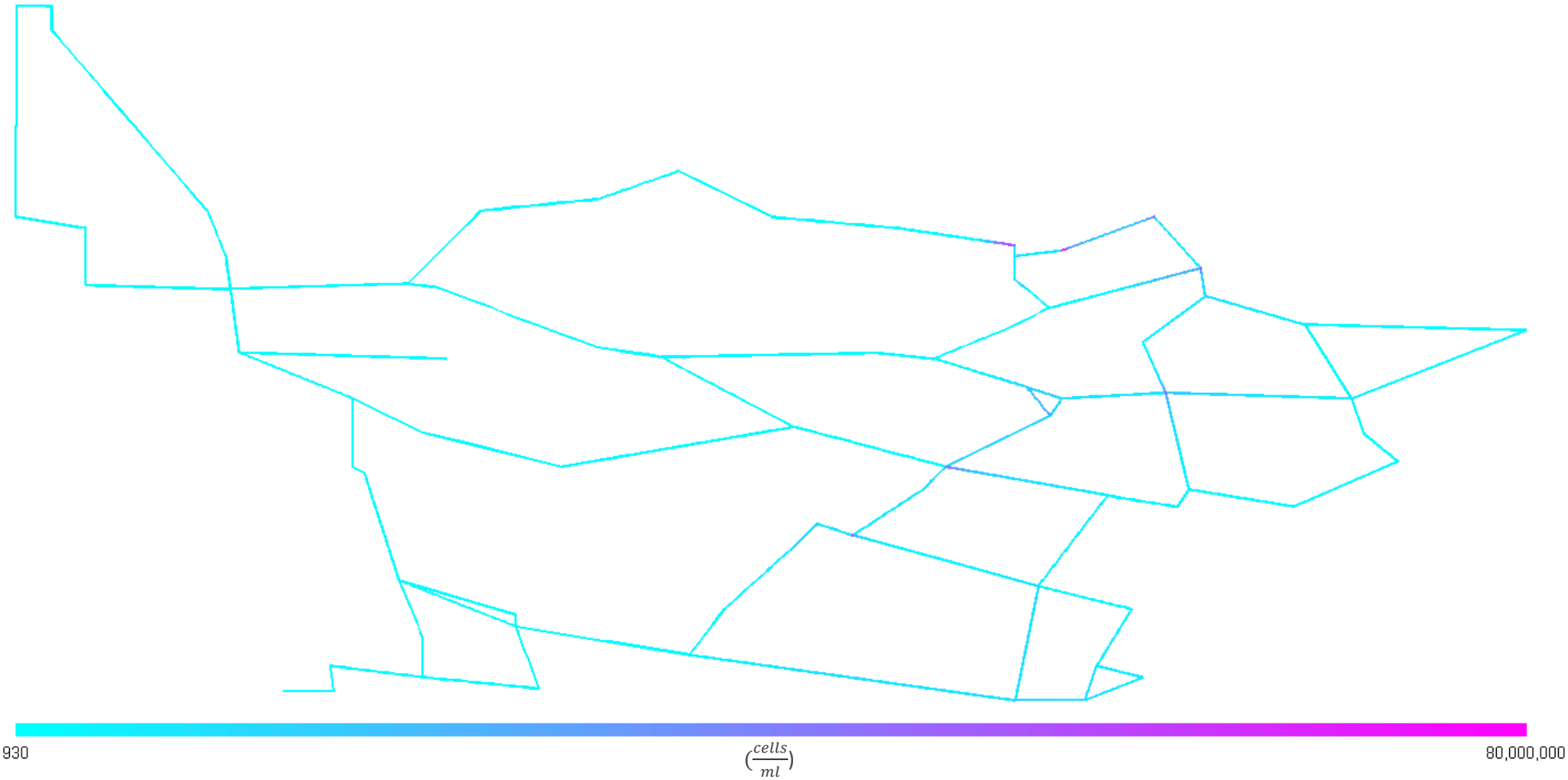


Figure D-66: Fixed NOB concentration profile for Alternative 4

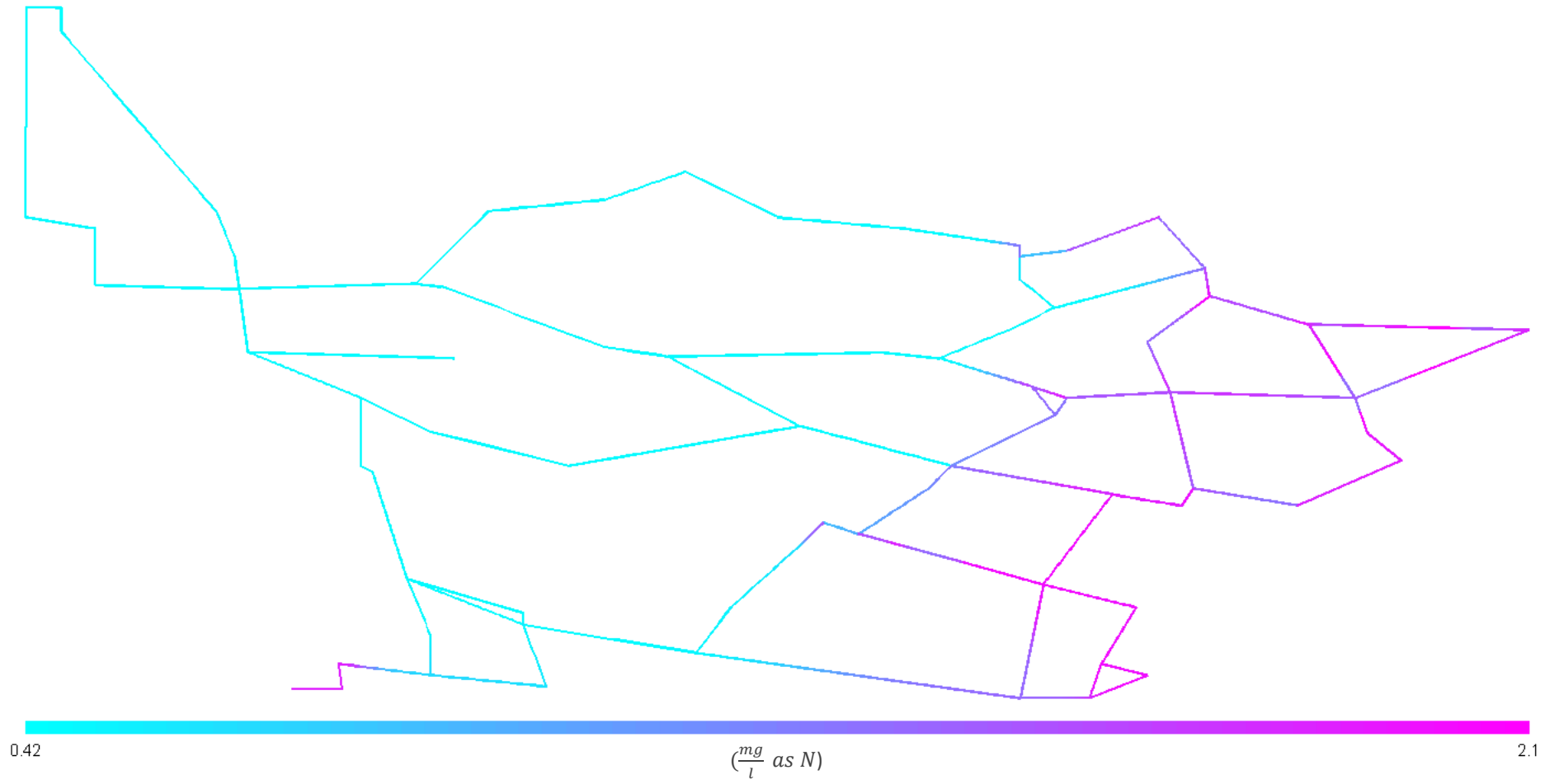


Figure D-67: Nitrate concentration profile for Alternative 4

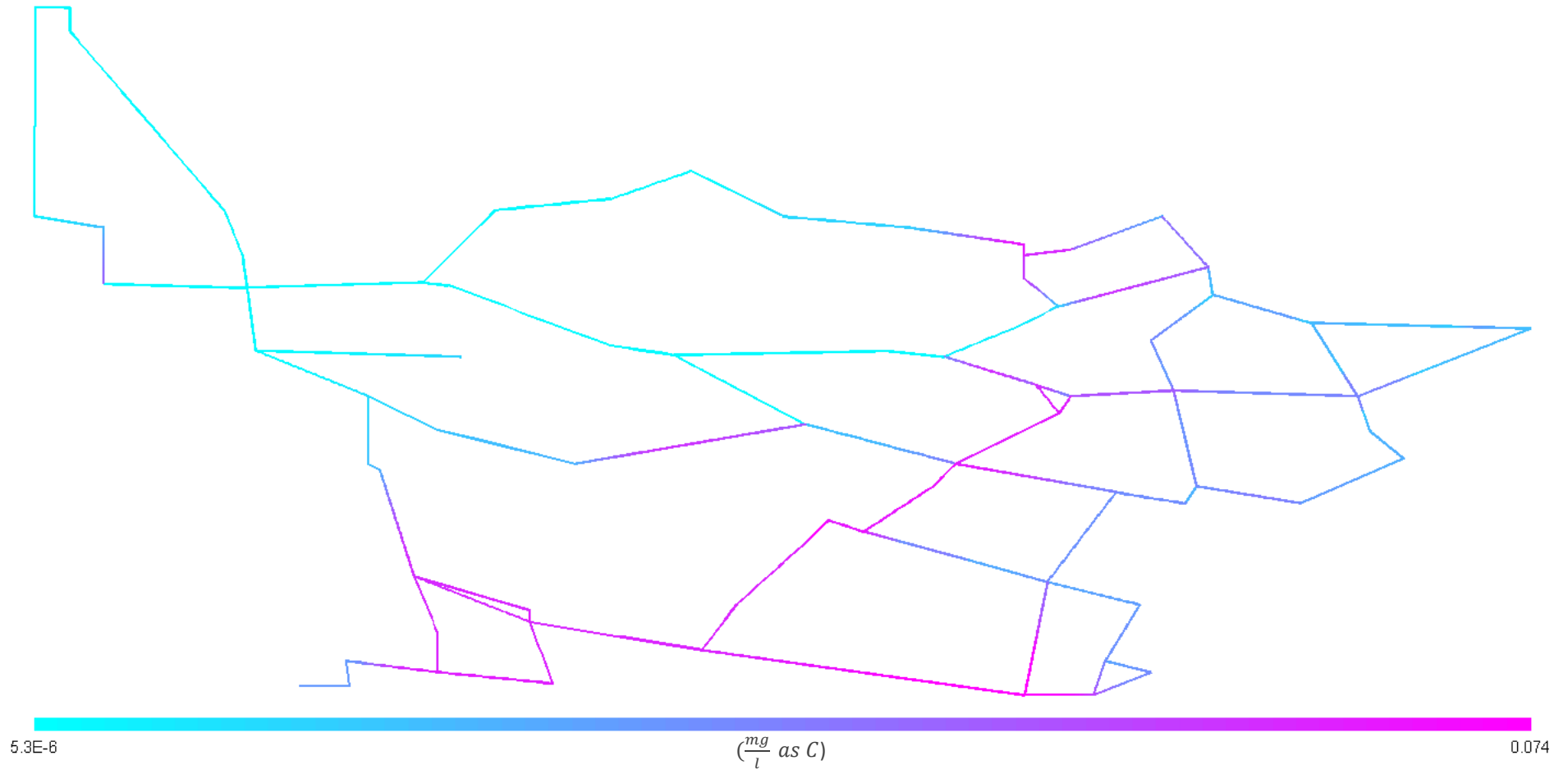


Figure D-68: UAP concentration profile for Alternative 4

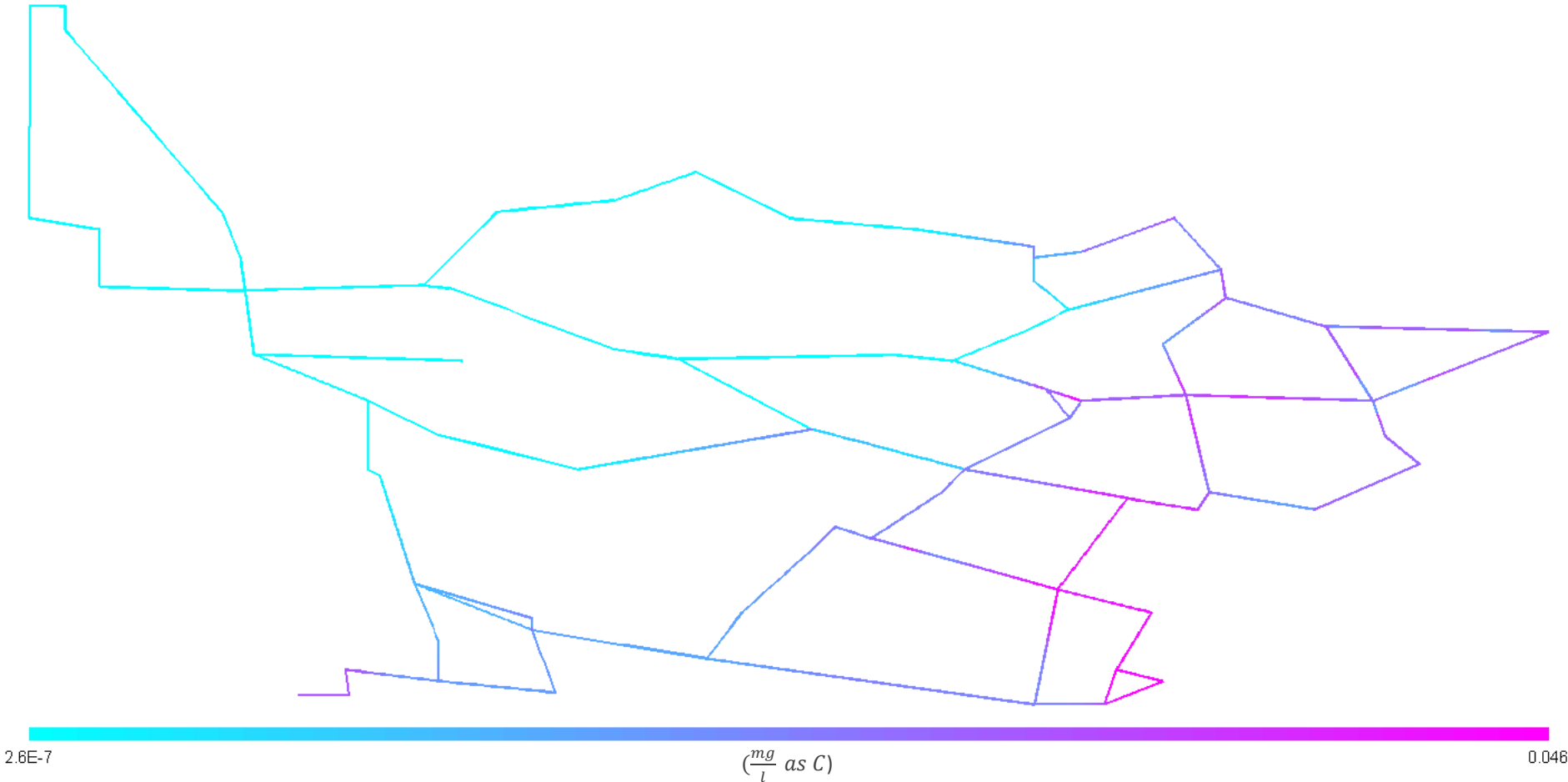


Figure D-69: BAP concentration profile for Alternative 4

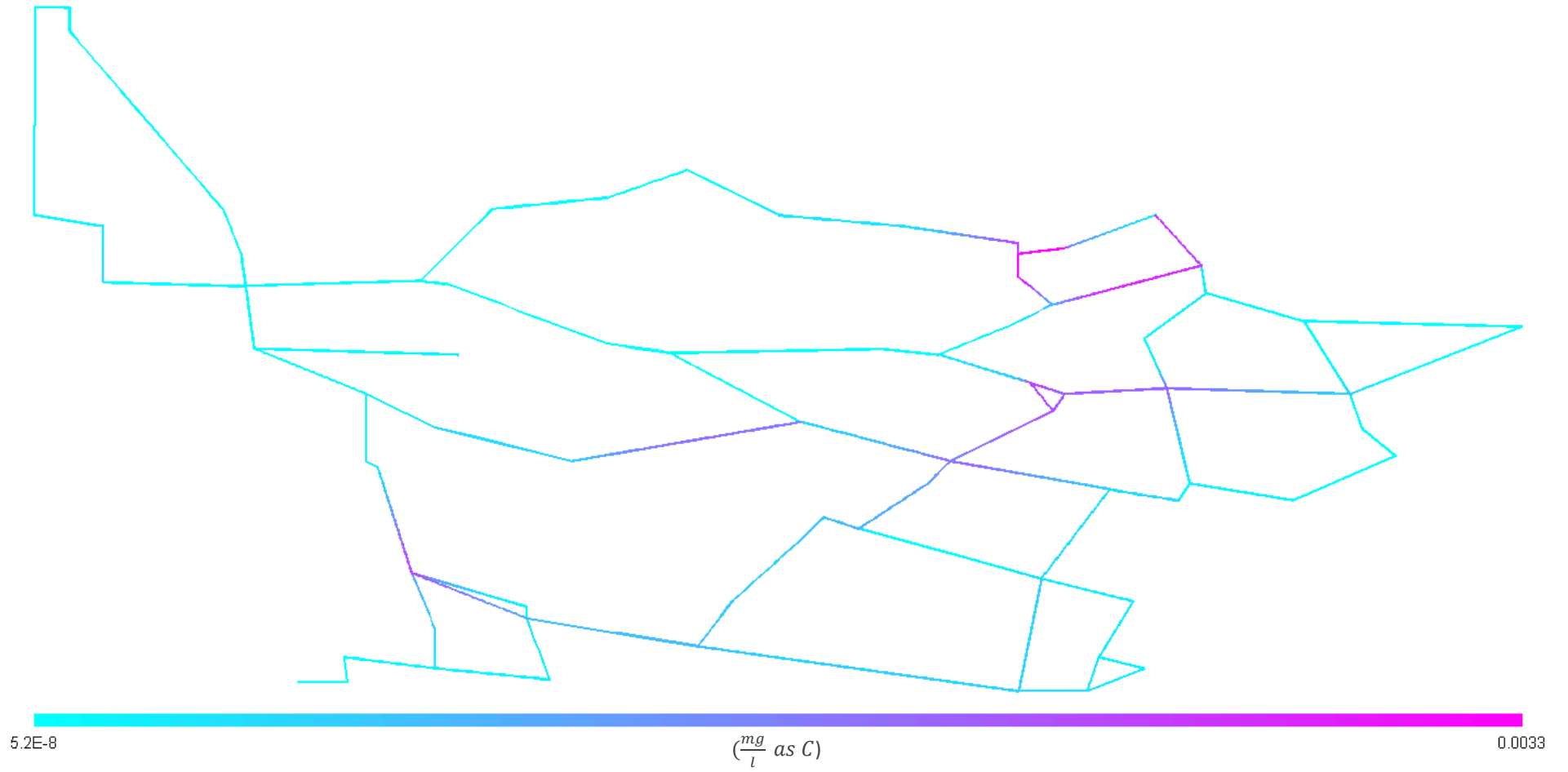


Figure D-70: Suspended EPS concentration profile for Alternative 4

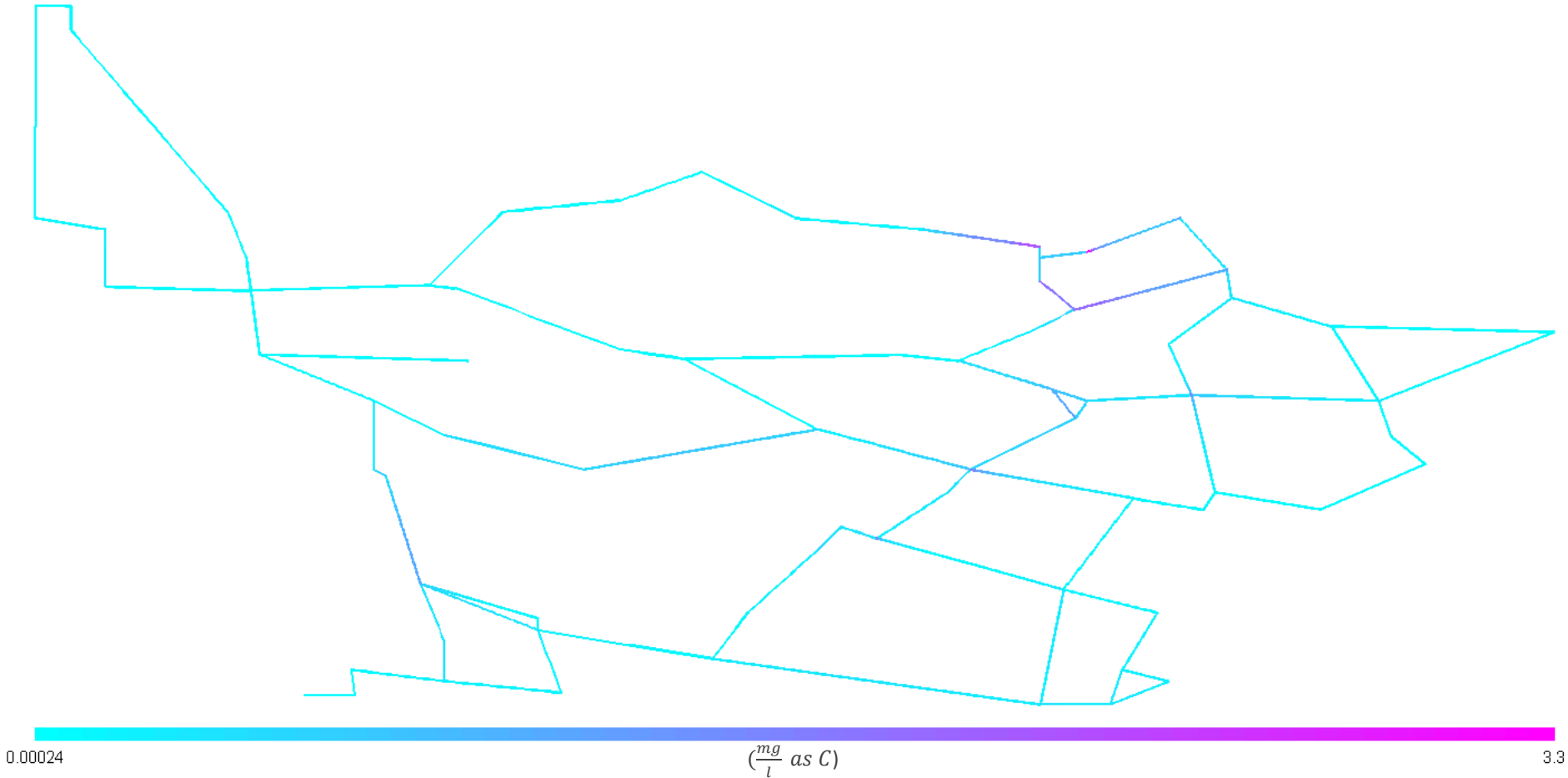


Figure D-71: Fixed EPS concentration profile for Alternative 4

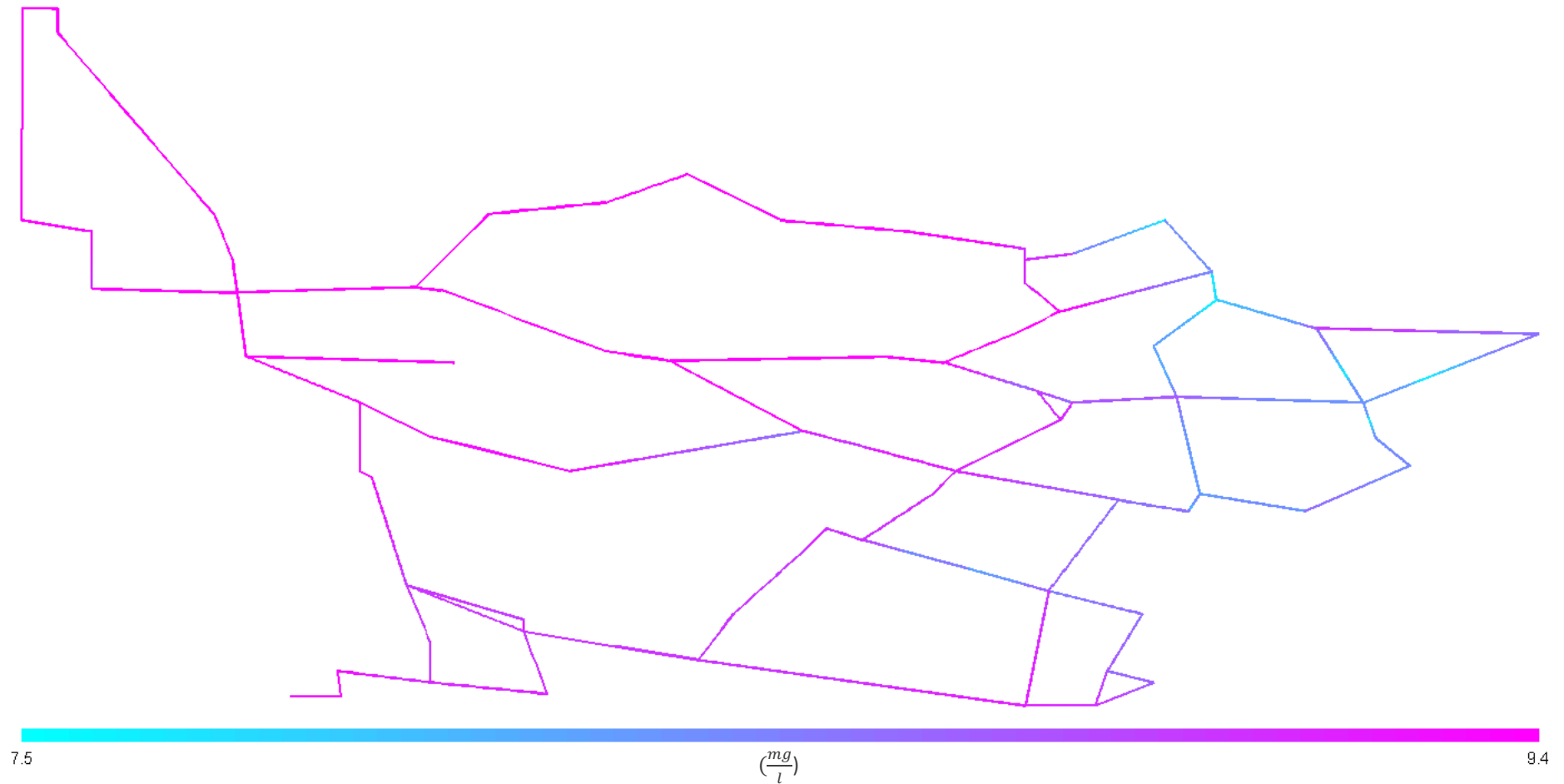


Figure D-72: Dissolved oxygen concentration profile for Alternative 4

The minimum dissolved oxygen concentration is similar to the baseline scenario, indicating that this alternative is ineffective at reducing the concentration of active biomass in pipe sections further away from the booster sites, particularly the site at node 320.

D.5 Improve Primary Disinfection

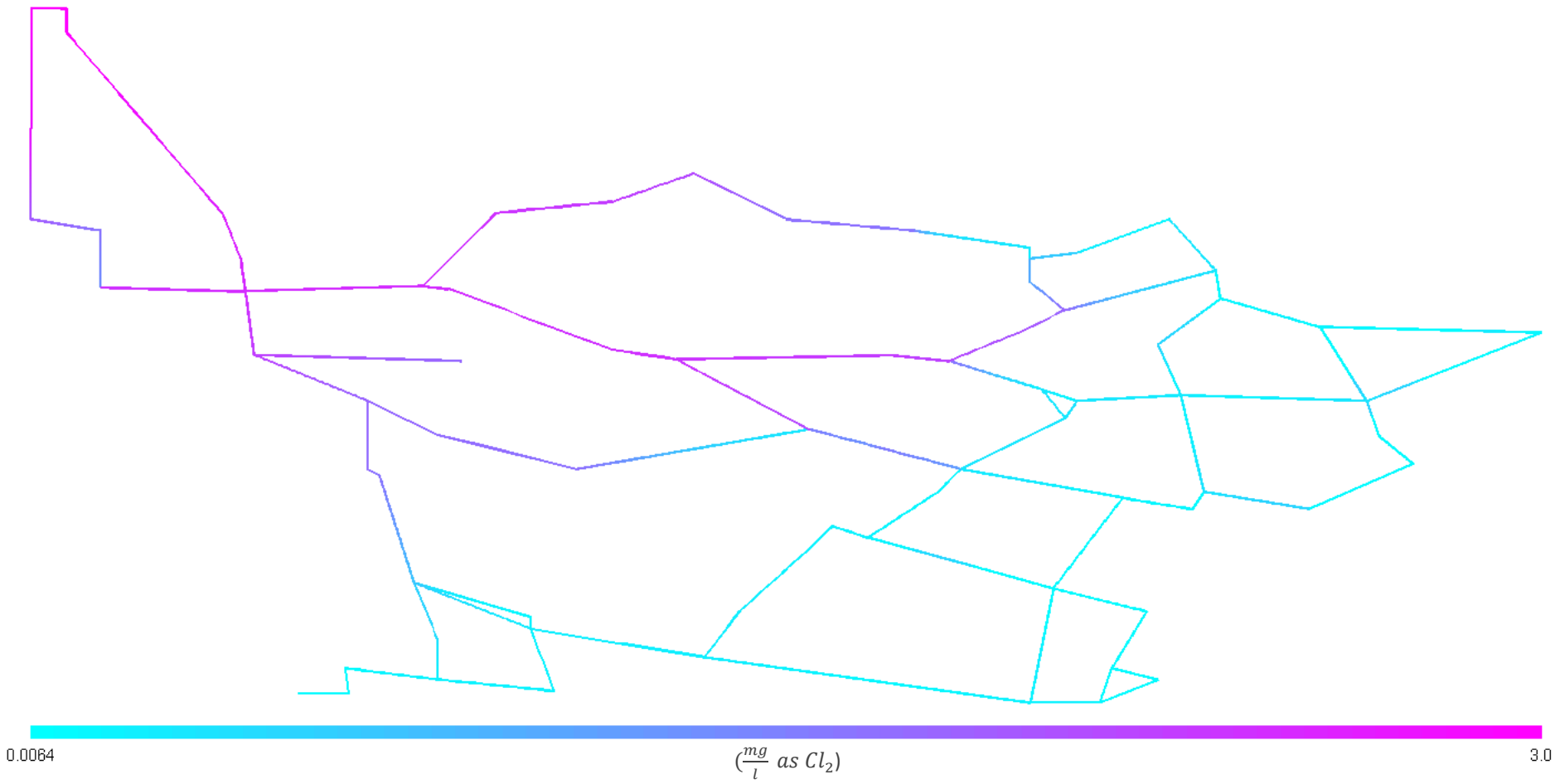


Figure D-73: Monochloramine concentration profile for Alternative 5

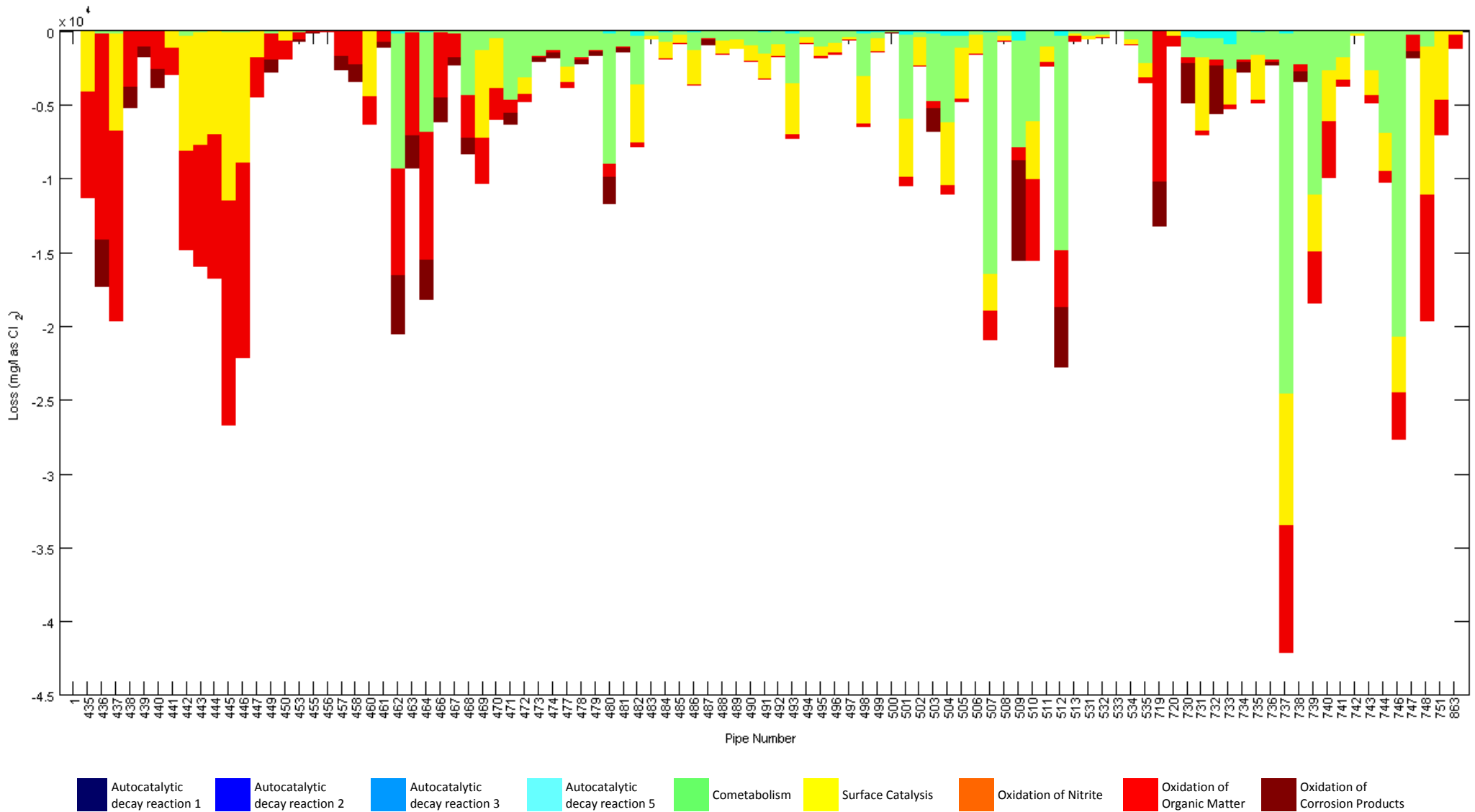


Figure D-74: Monochloramine loss mechanisms and locations for Alternative 5

Loss of monochloramine due to the oxidation of organic matter, as well as other mechanisms, has not changed significantly despite the reduced heterotrophic input at the treatment plant.

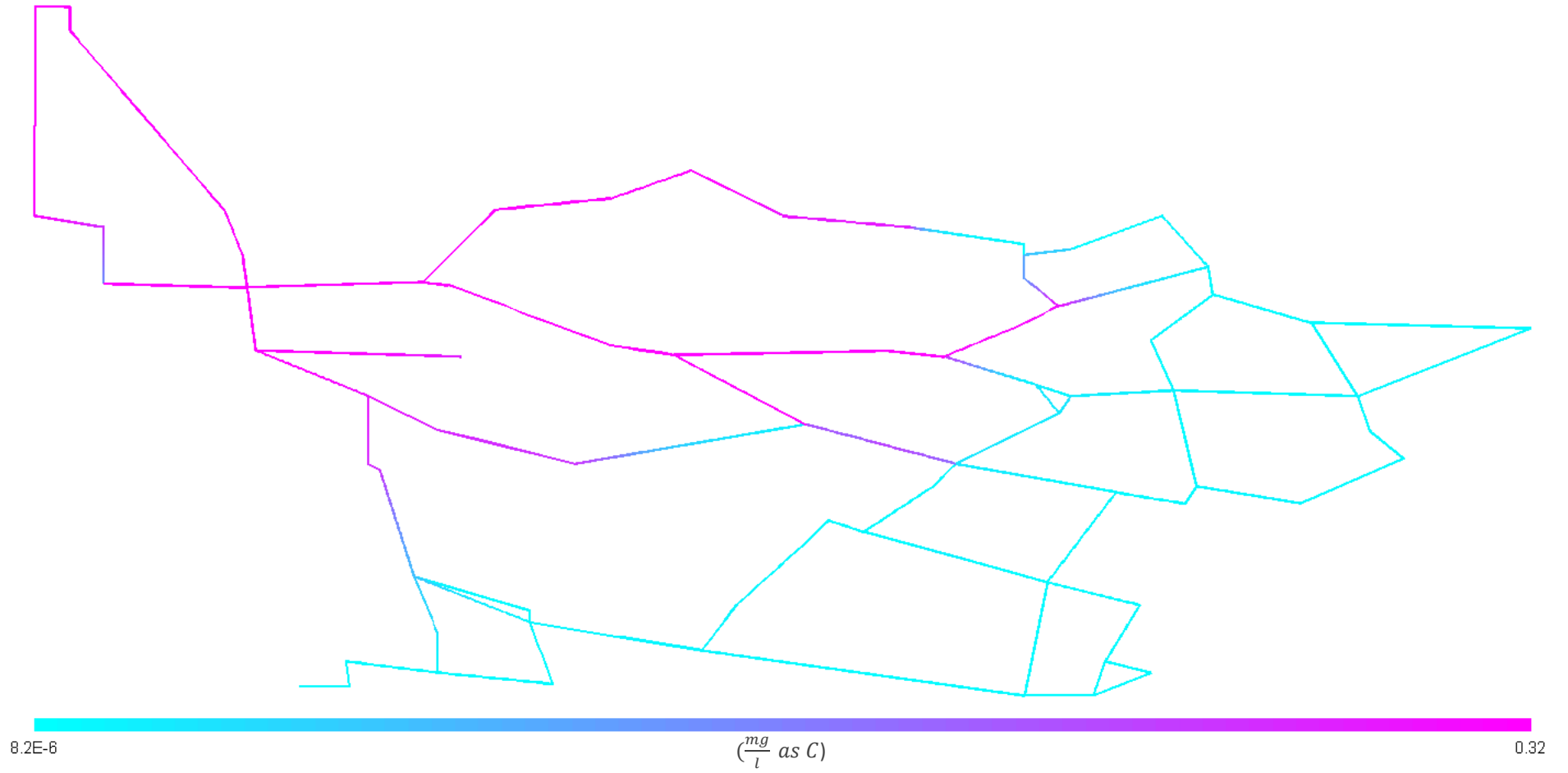


Figure D-75: BOM₁ concentration profile for Alternative 5

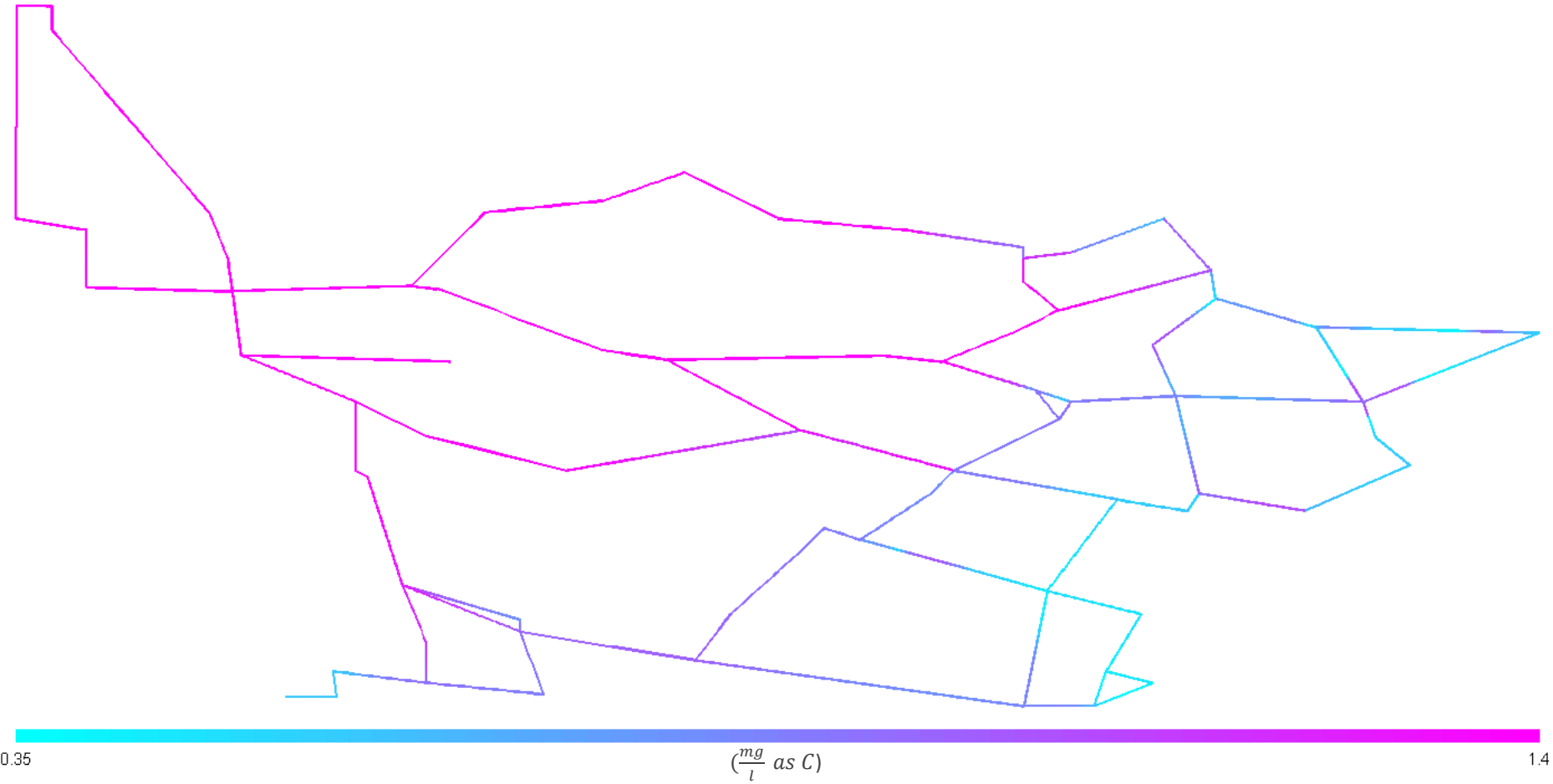


Figure D-76: BOM₂ concentration profile for Alternative 5

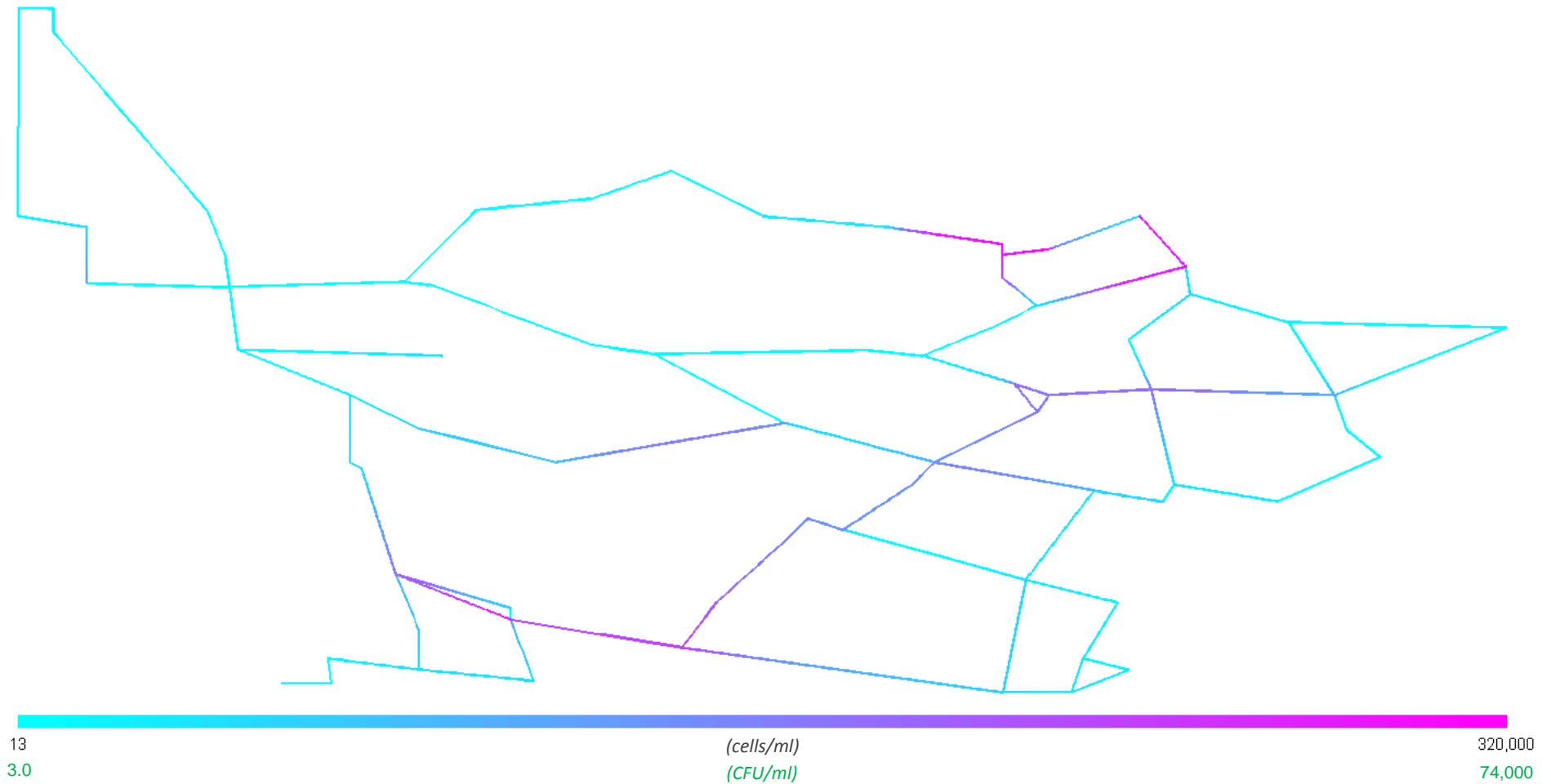


Figure D-77: Suspended heterotroph concentration profile for Alternative 5

The maximum suspended heterotroph concentration is unchanged compared to the baseline scenario. This suggests that the detachment of biofilm bacteria is a more significant reason for the high suspended heterotroph concentrations for the simulations performed, as opposed to the high concentration of suspended heterotrophs introduced at the treatment plant for the baseline scenario.

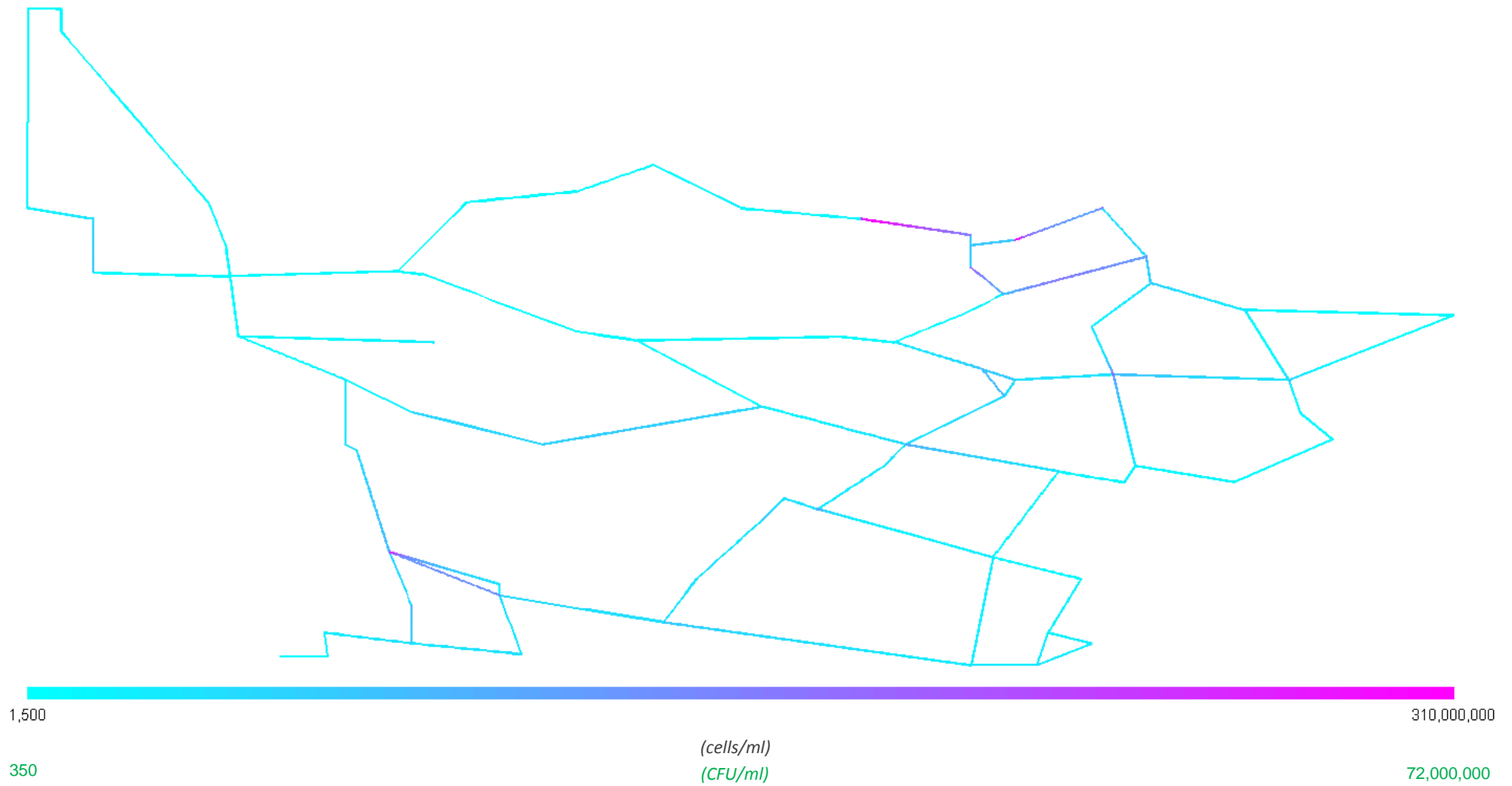


Figure D-78: Fixed heterotroph concentration profile for Alternative 5

The concentration profile is unchanged compared to the baseline case, which demonstrates the limited effect of adsorption on biofilm bacteria concentrations.

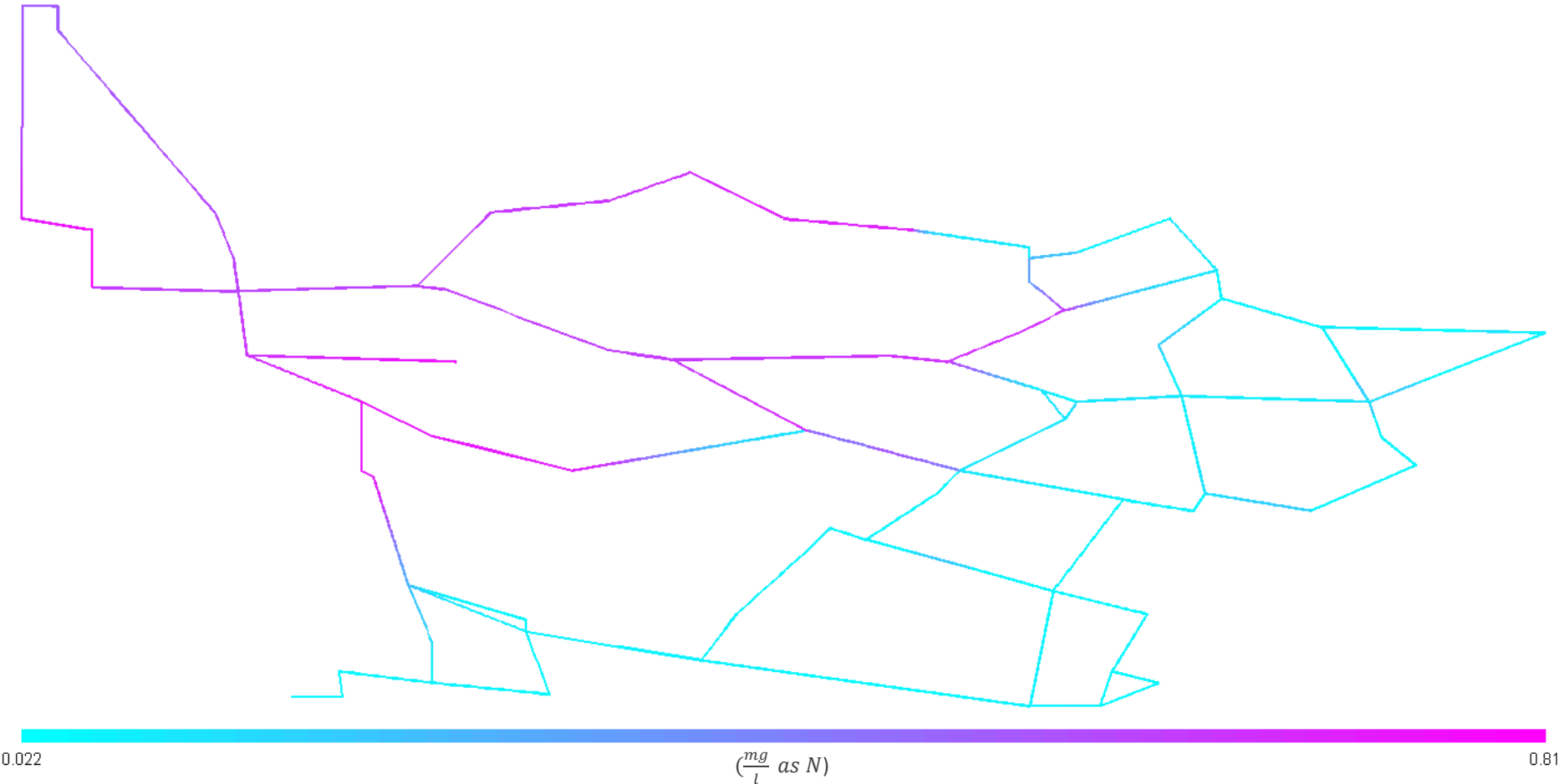


Figure D-79: Ammonia concentration profile for Alternative 5

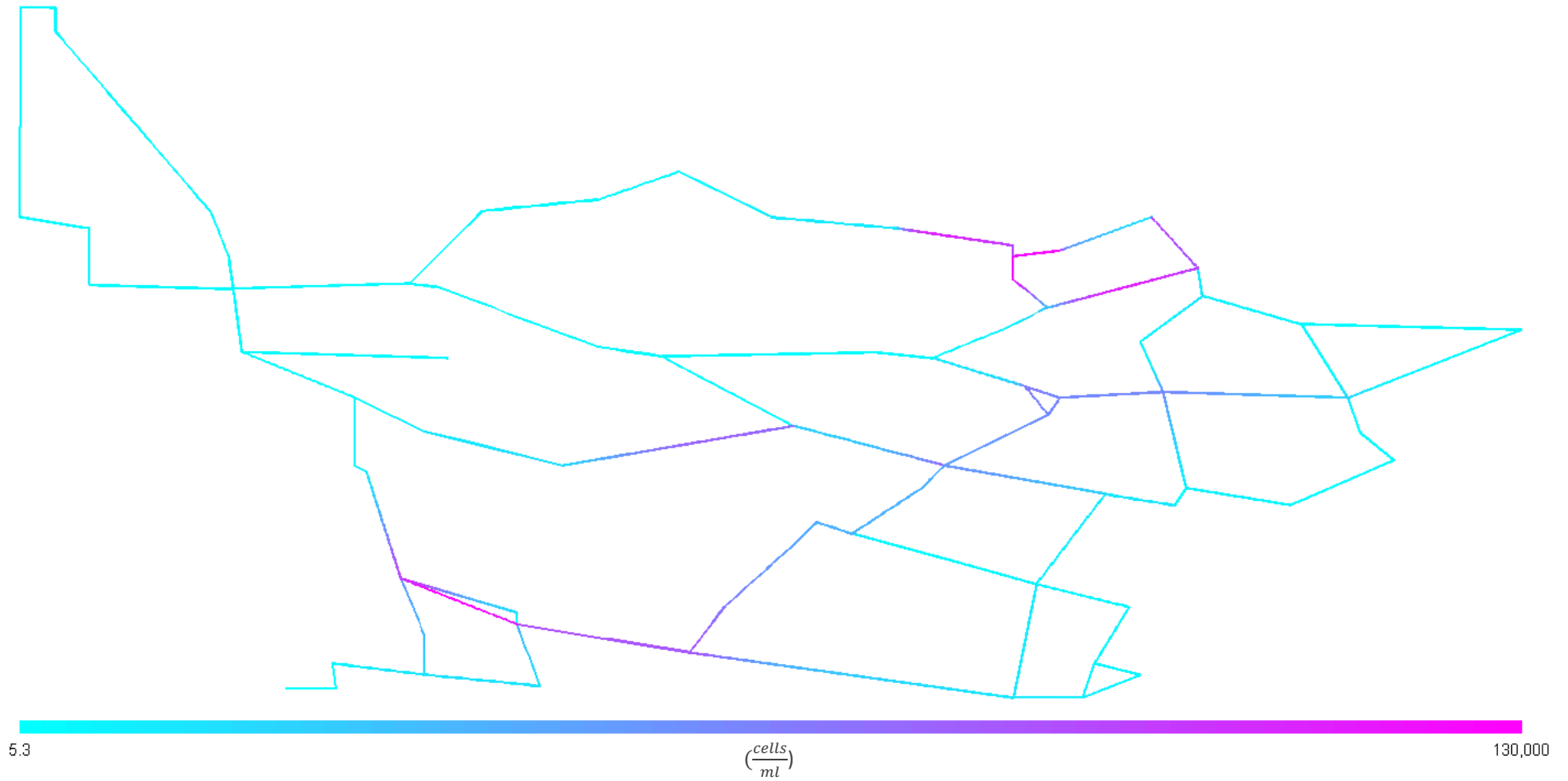


Figure D-80: Suspended AOB concentration profile for Alternative 5

The concentration profiles for both suspended and fixed AOB are largely unchanged as this alternative has little effect on the AOB stability factors.

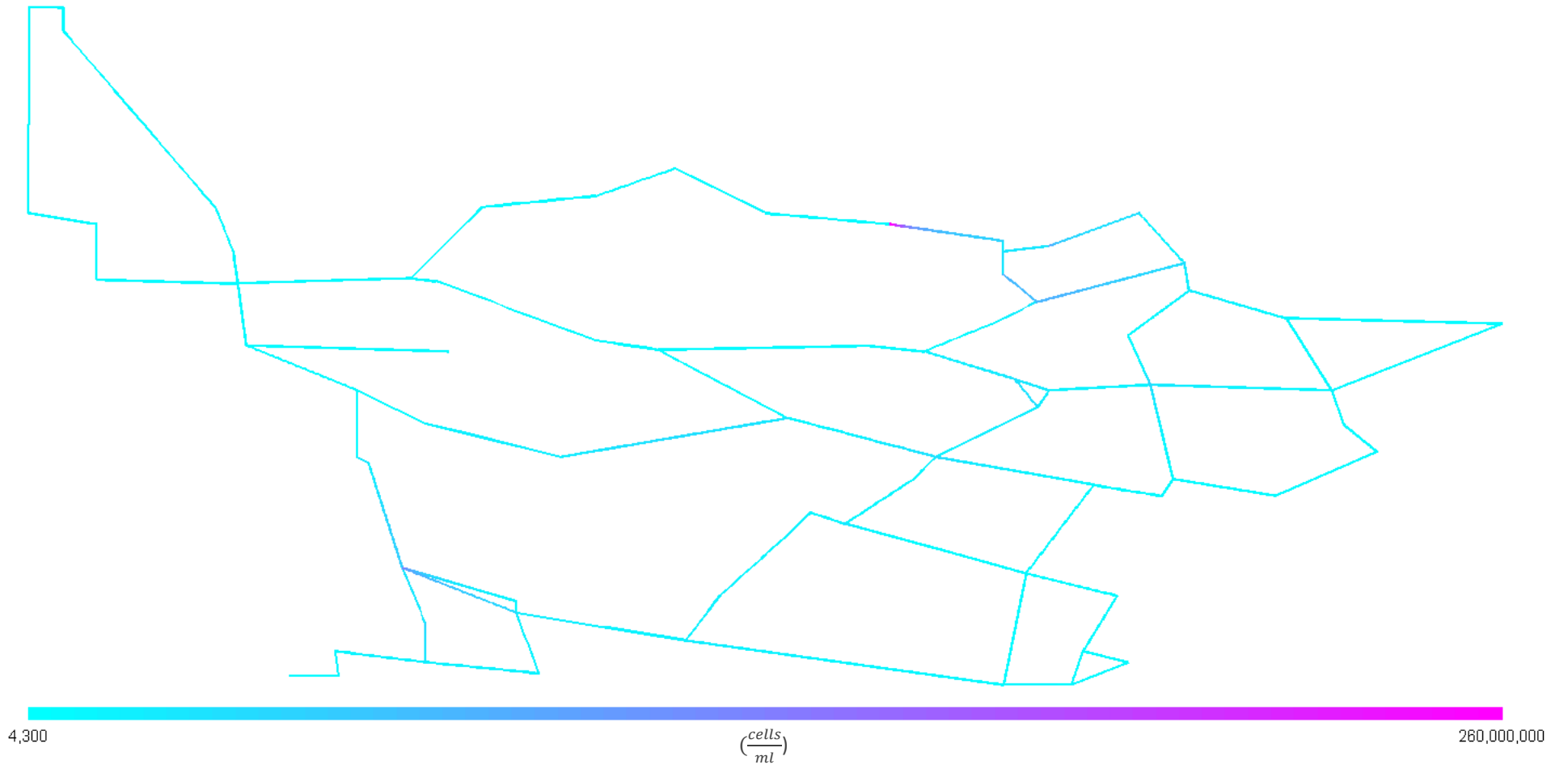


Figure D-81: Fixed AOB concentration profile for Alternative 5

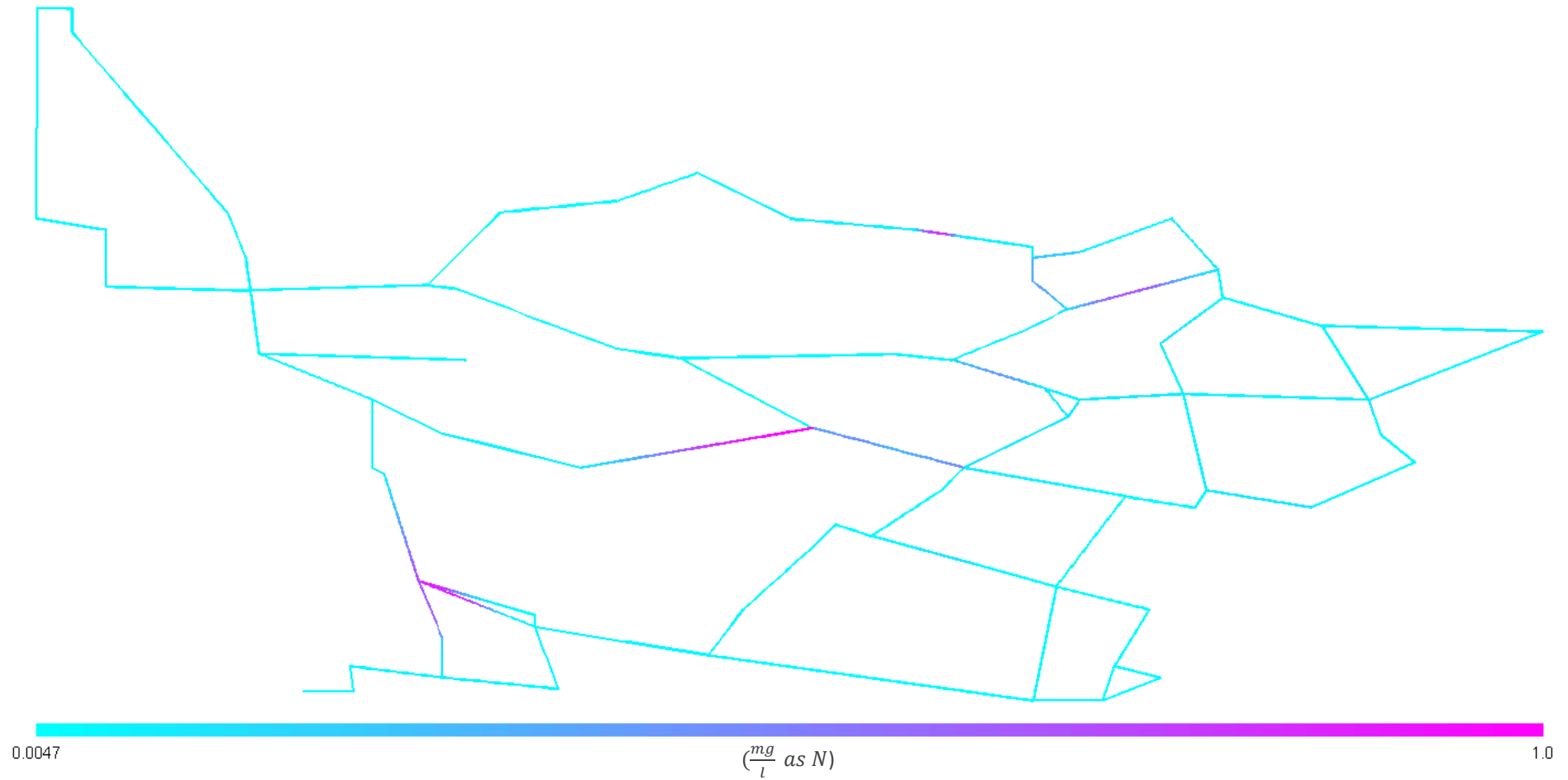


Figure D-82: Nitrite concentration profile for Alternative 5

The concentration profile is very similar to the baseline and still exceeds the maximum limit of $0.9 \frac{mg}{l} as N$ as a result of the limited effectiveness of this alternative in reducing the AOB concentration.

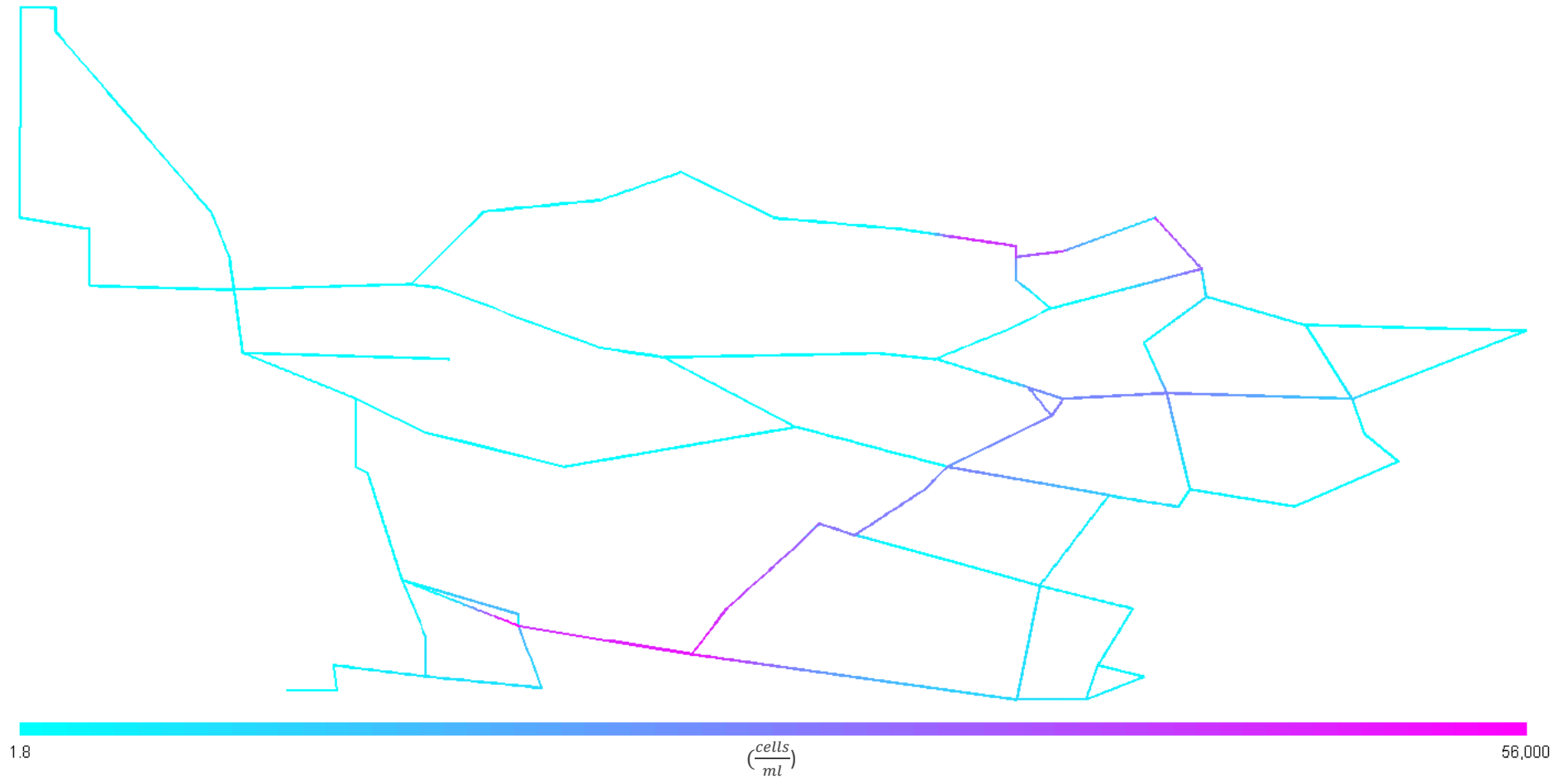


Figure D-83: Suspended NOB concentration profile for Alternative 5

The concentration profiles for both suspended and fixed NOB are largely unchanged as this alternative has little effect on the AOB stability factors.

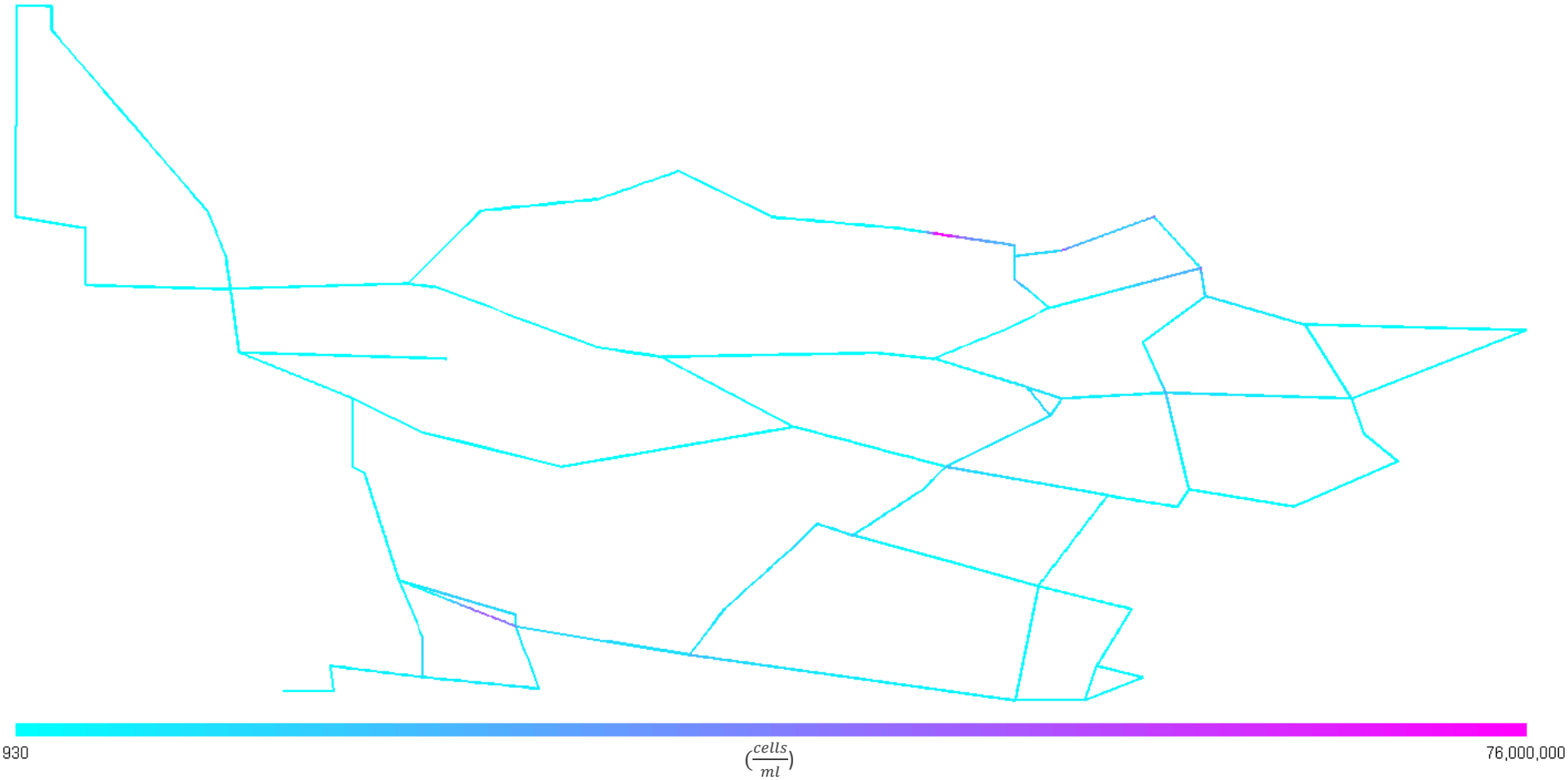


Figure D-84: Fixed NOB concentration profile for Alternative 5

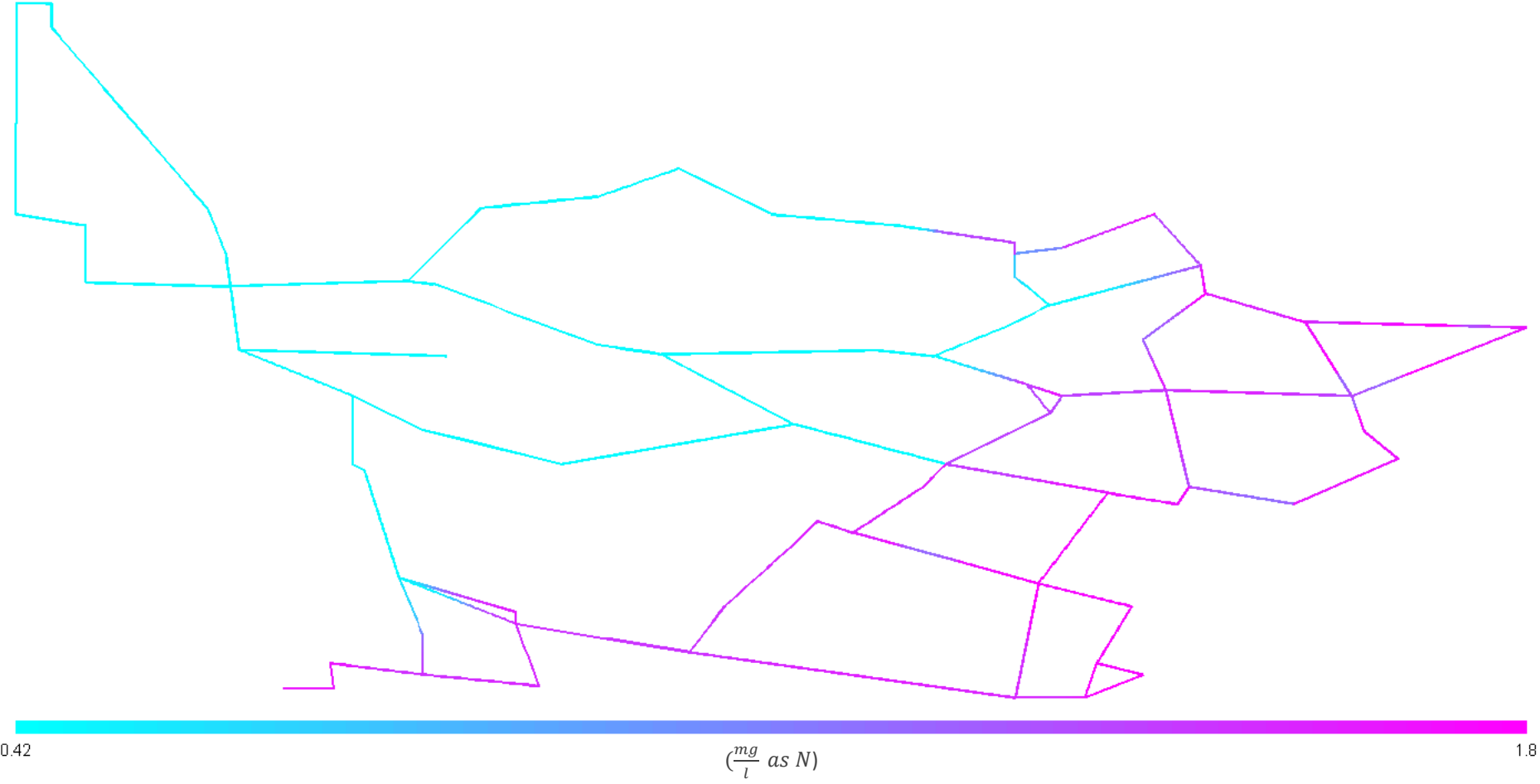


Figure D-85: Nitrate concentration profile for Alternative 5

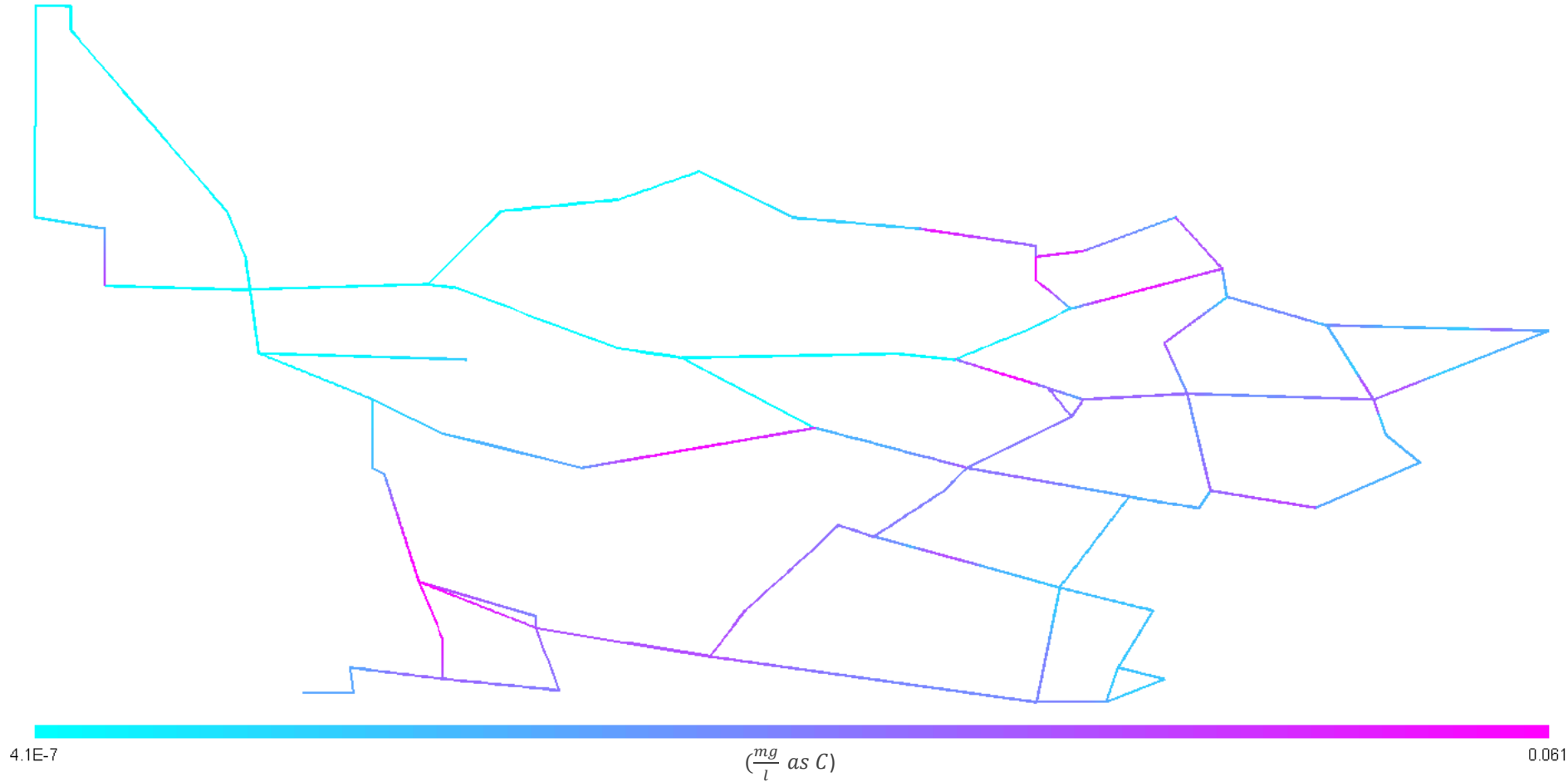


Figure D-86: UAP concentration profile for Alternative 5

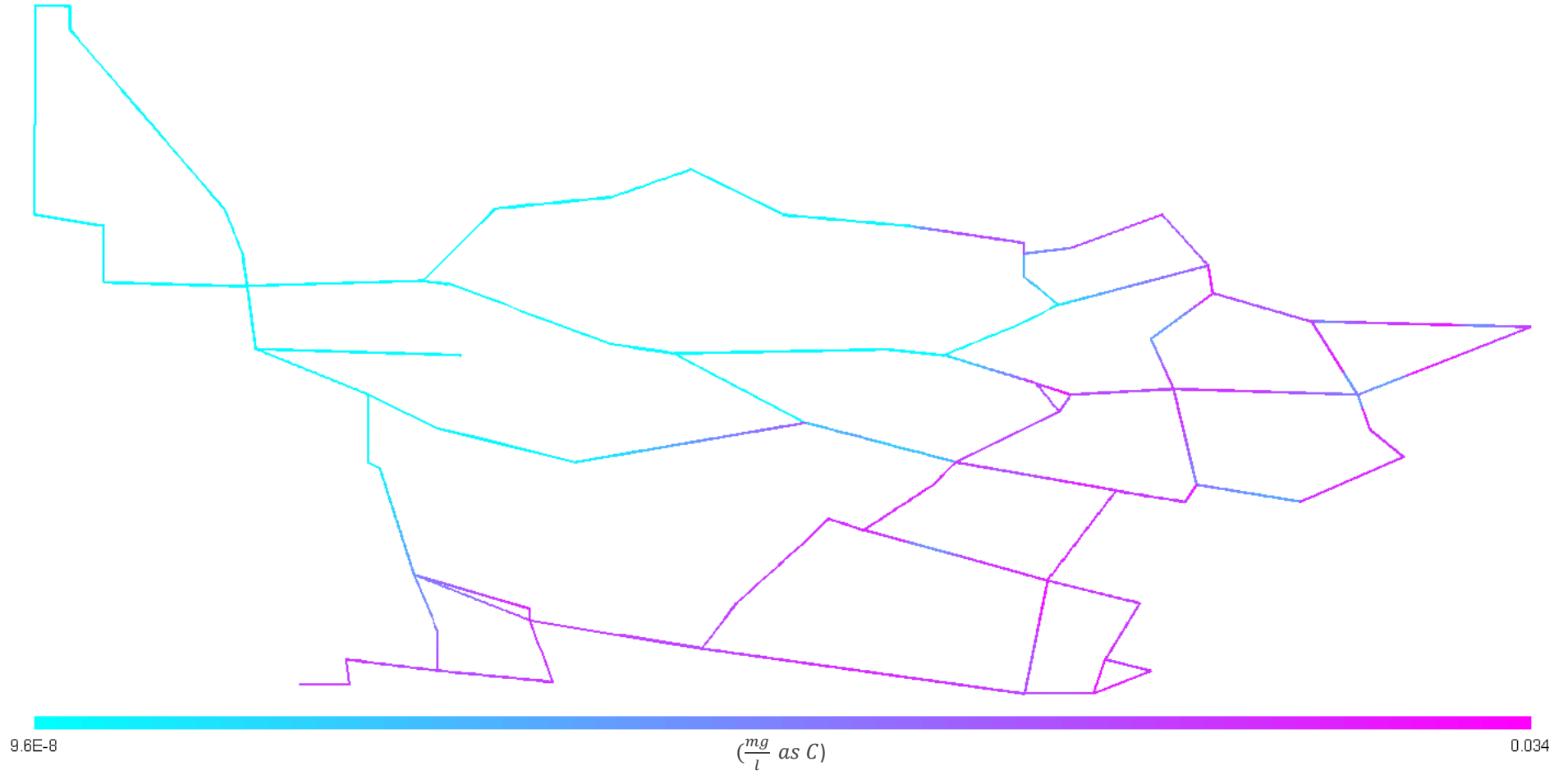


Figure D-87: BAP concentration profile for Alternative 5

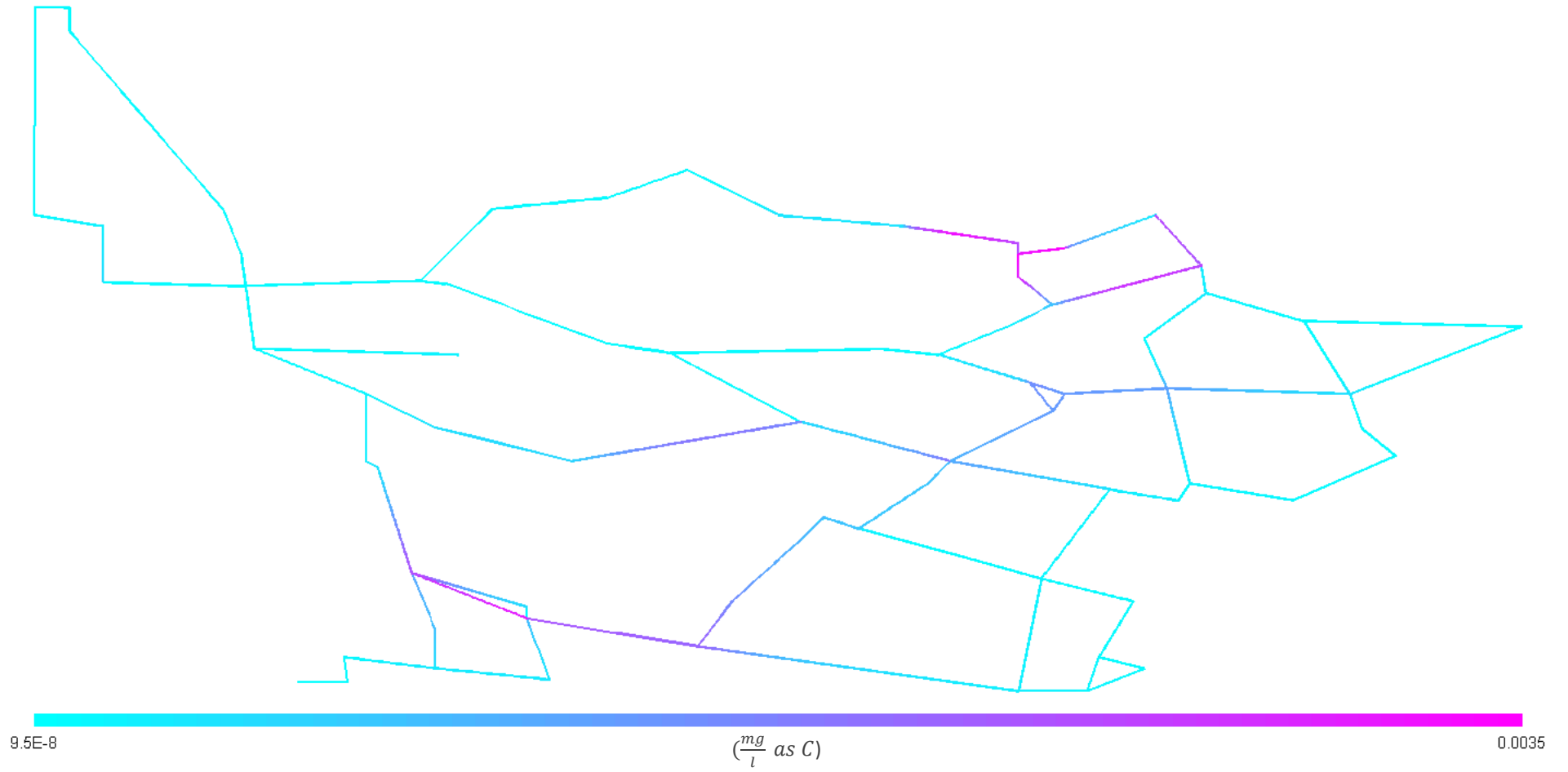


Figure D-88: Suspended EPS concentration profile for Alternative 5

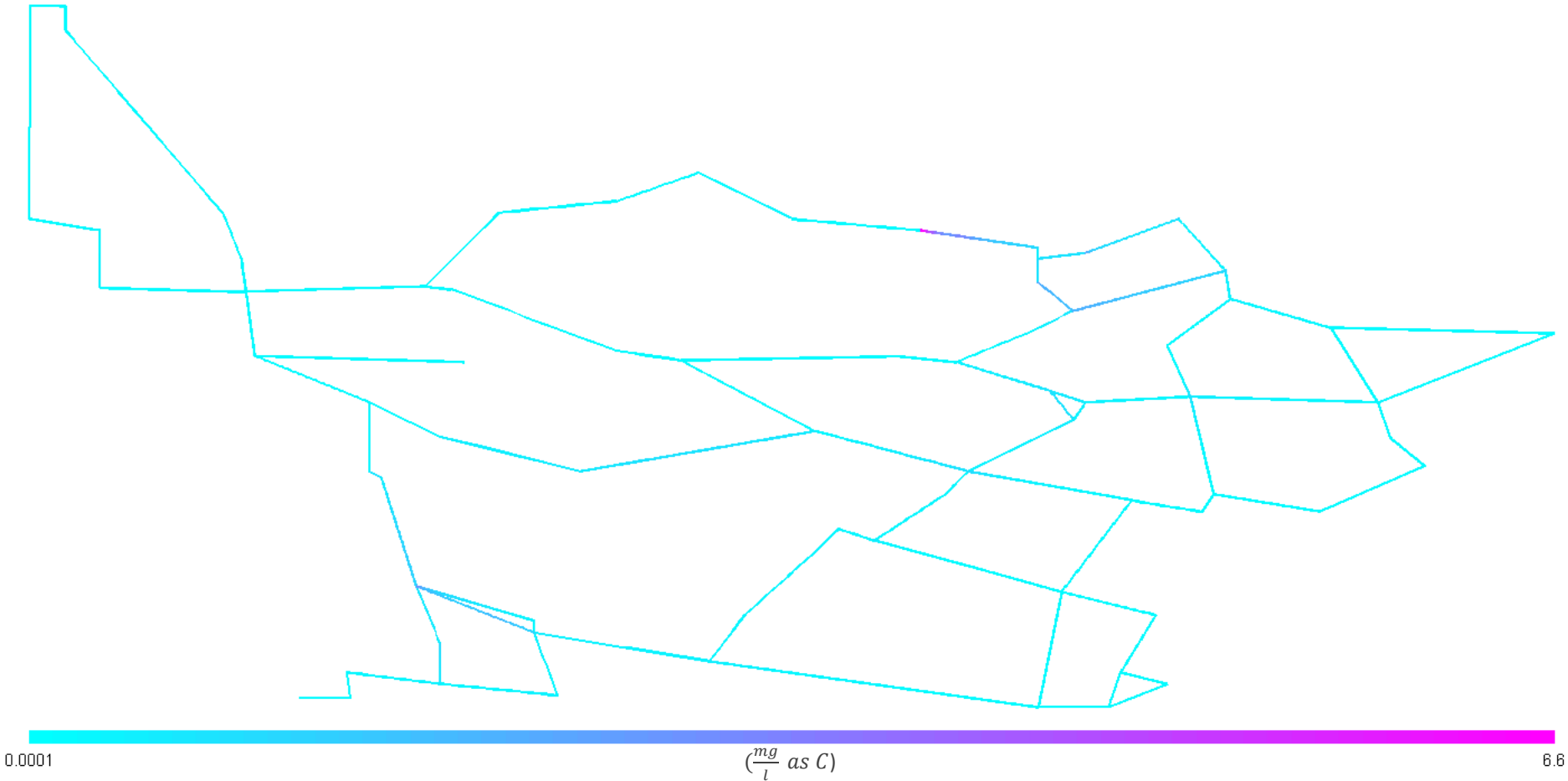


Figure D-89: Fixed EPS concentration profile for Alternative 5

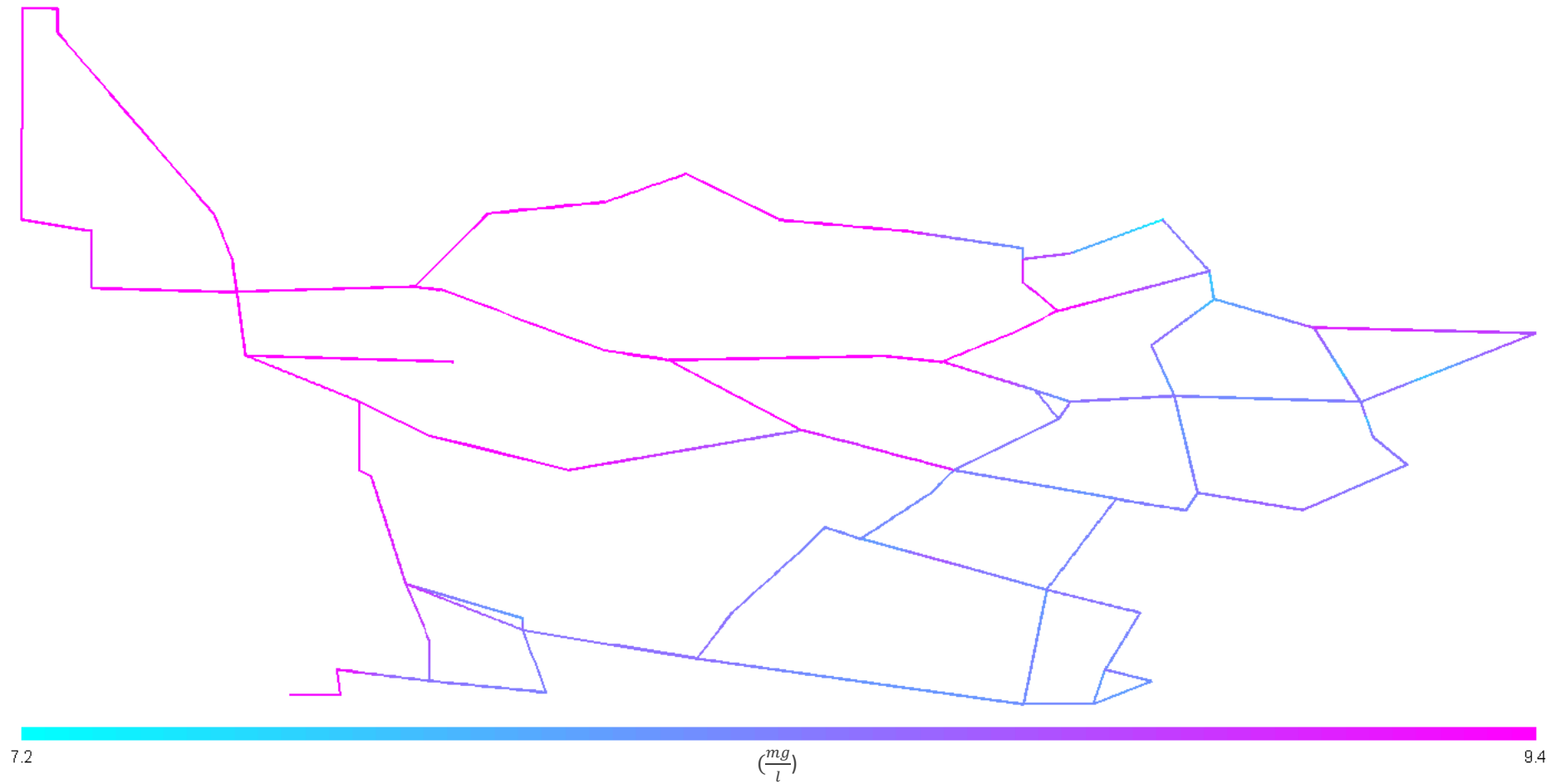


Figure D-90: Dissolved oxygen concentration profile for Alternative 5

The dissolved oxygen concentration profile is very similar to the baseline scenario, as this alternative has little effect on the total concentration of active biomass throughout the system.

D.6 Reduce Input BOM and Excess Ammonia

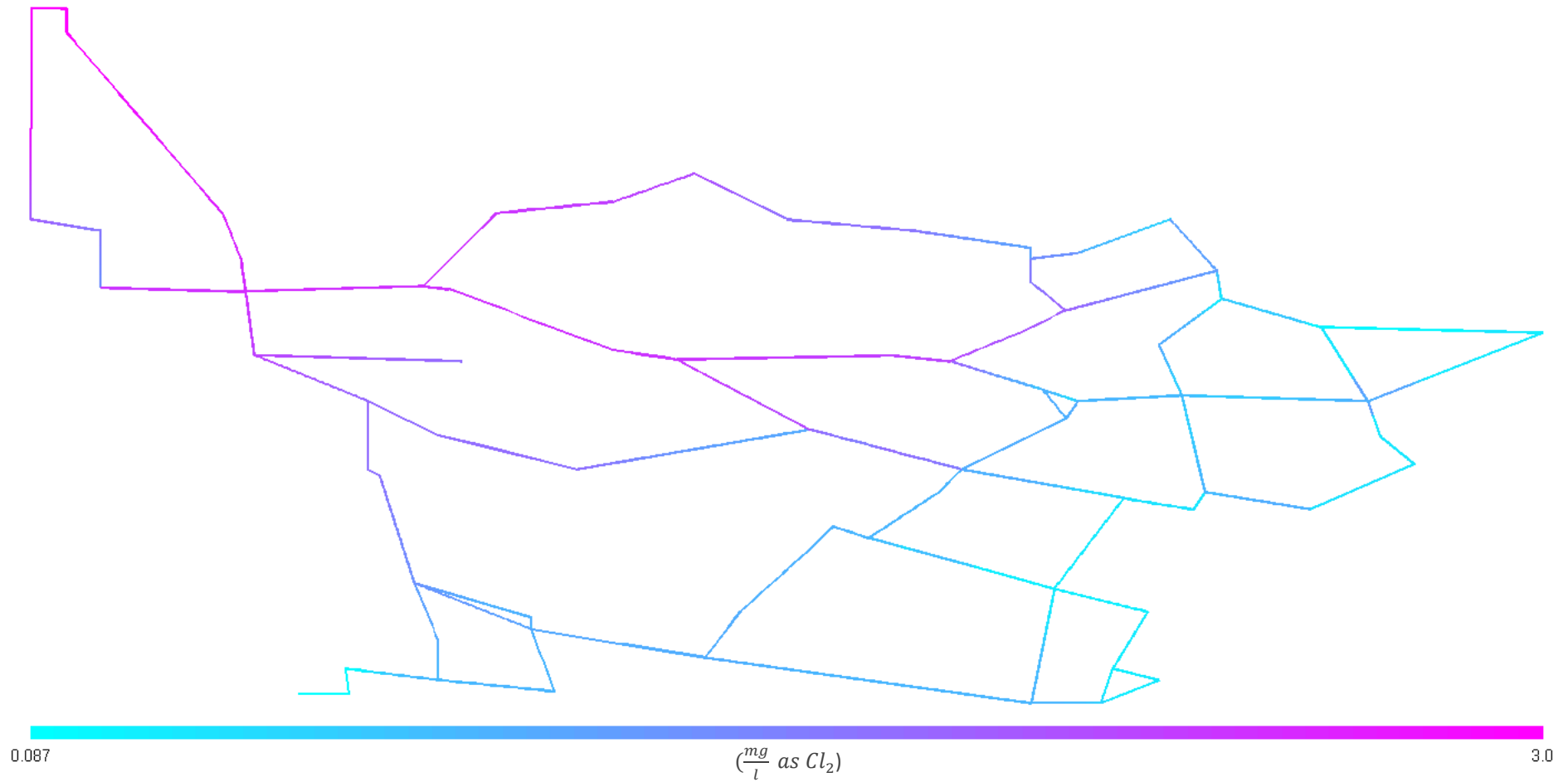


Figure D-91: Monochloramine concentration profile for Alternative 6

The residual disinfectant is increased throughout the system and is significantly greater in the furthest reaches of the system.

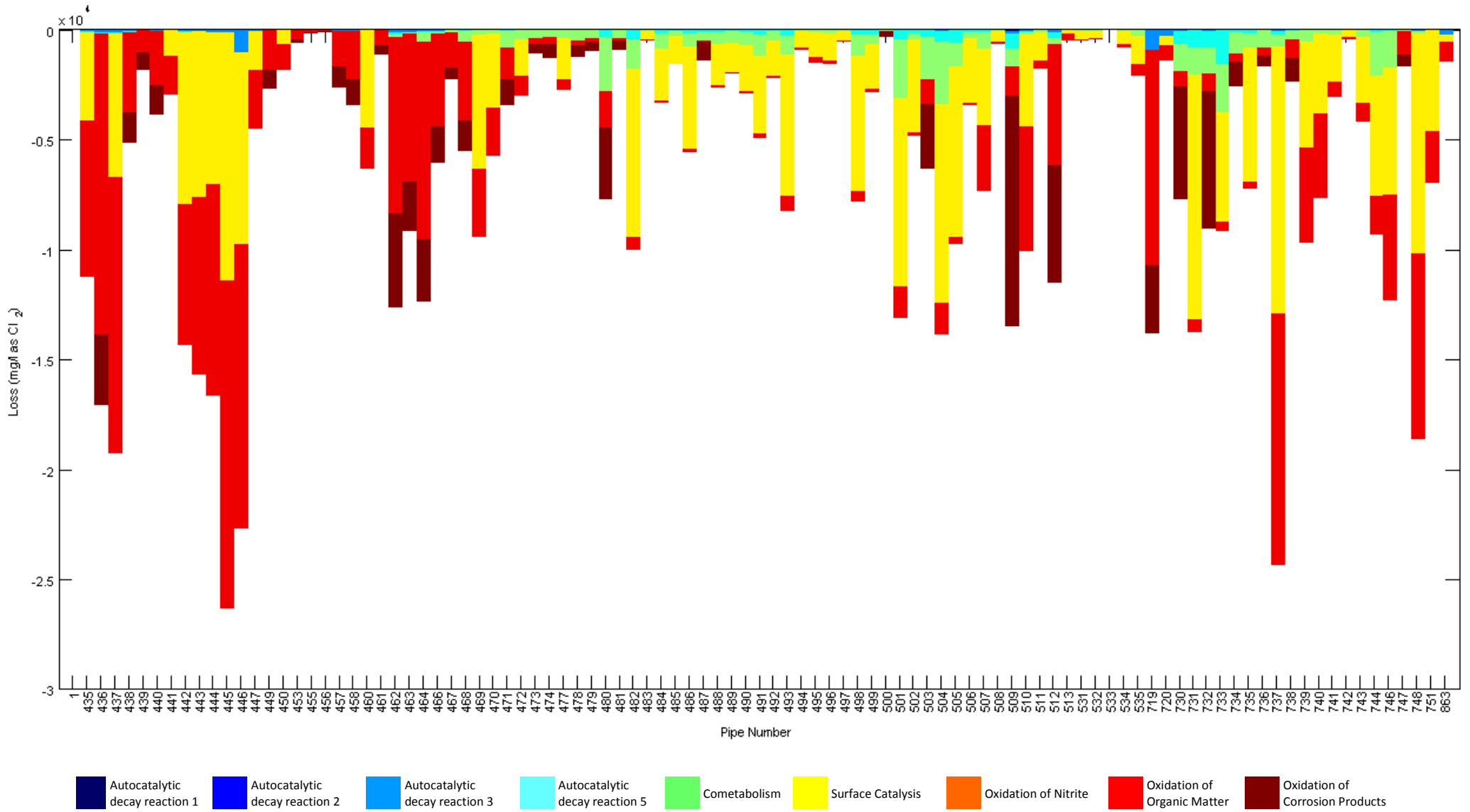


Figure D-92: Monochloramine loss mechanisms and locations for Alternative 6

The total loss of monochloramine is significantly reduced largely due to the reduction in loss due to cometabolism associated with decreased ammonia concentrations. The loss of monochloramine due to surface catalysis is increased, as monochloramine loss due to this mechanism is a function of the monochloramine concentration squared. However, this does not offset the reduced loss of monochloramine due to cometabolism and hence the total loss of disinfectant is reduced.

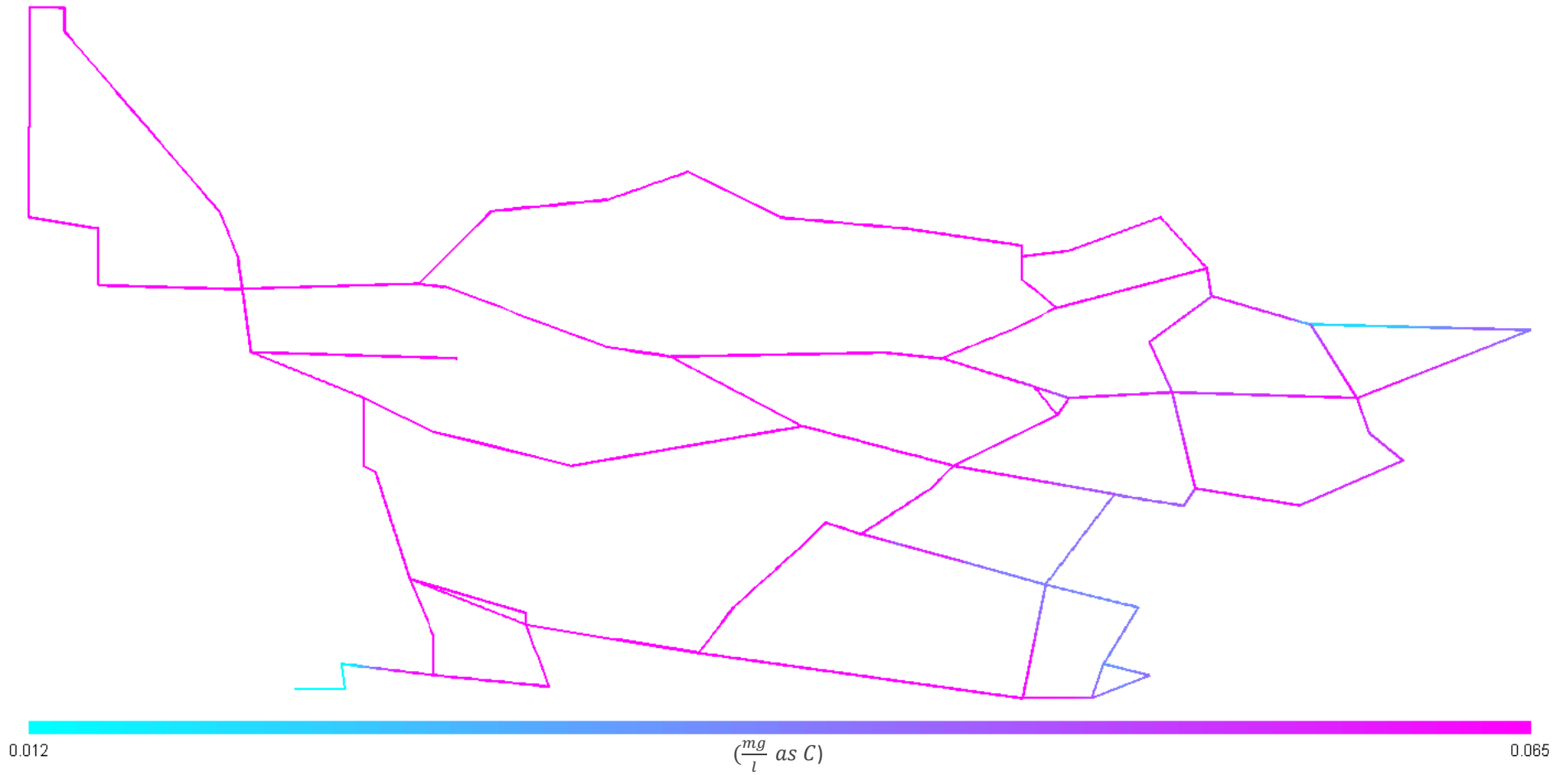


Figure D-93: BOM₁ concentration profile for Alternative 6

The concentration of BOM₁ is significantly lower throughout the system.

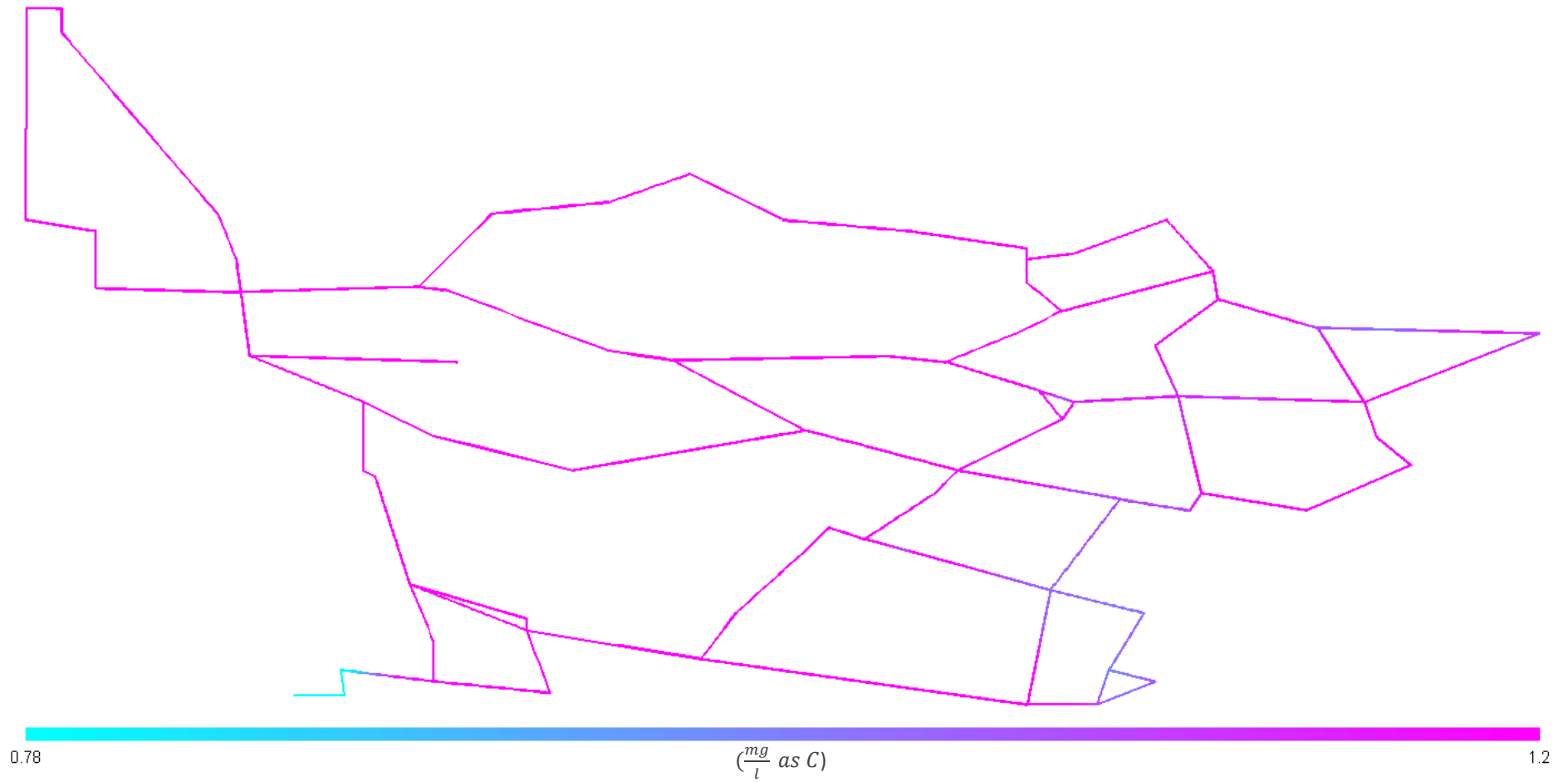


Figure D-94: BOM₂ concentration profile for Alternative 6

The concentration of BOM₂ is significantly lower throughout the system.

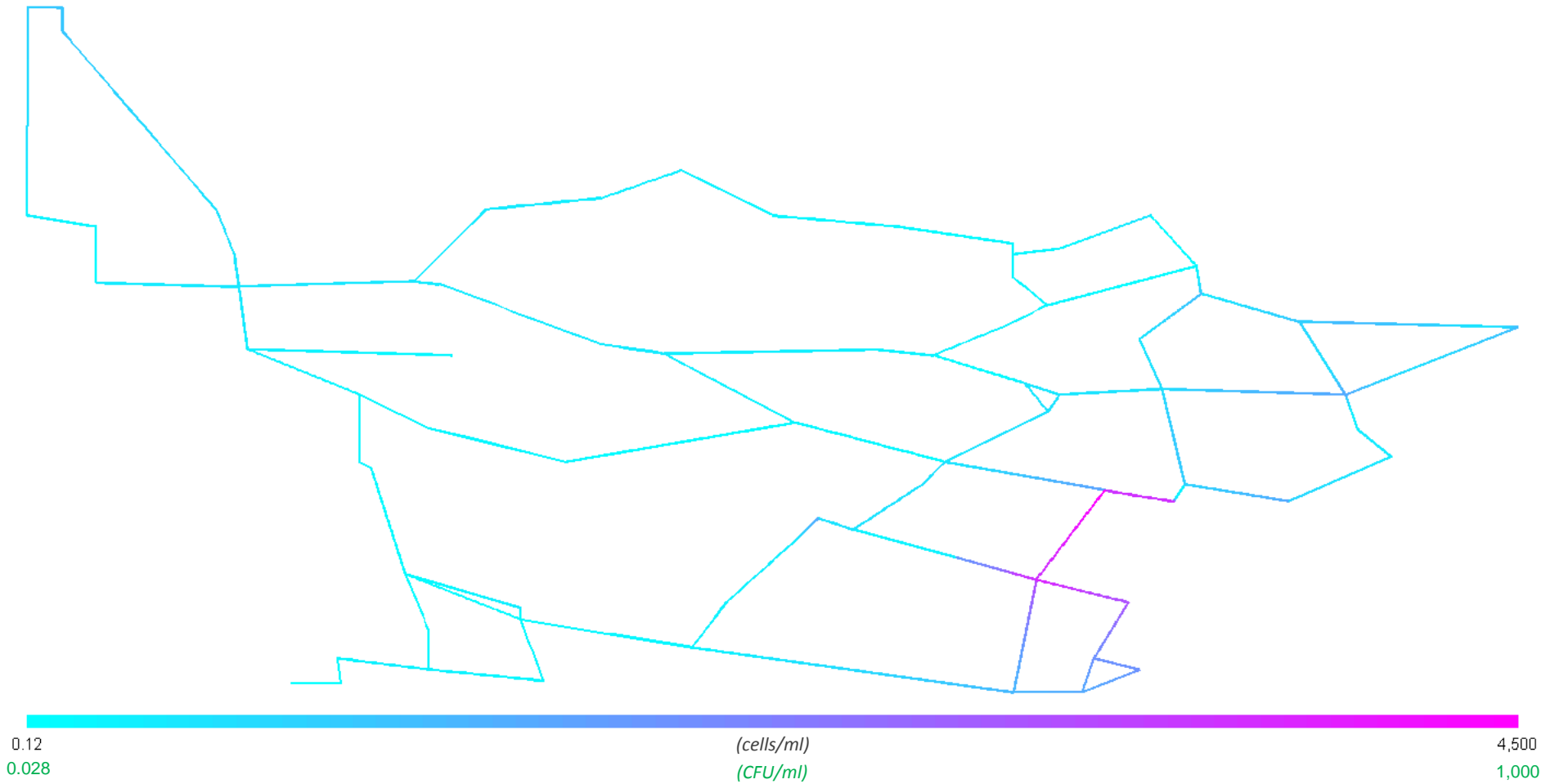


Figure D-95: Suspended heterotroph concentration profile for Alternative 6

The suspended heterotroph concentration is significantly reduced but still slightly exceeds the maximum limit of $4300 \frac{\text{cells}}{\text{ml}}$ at certain points in the distribution system. The decrease in heterotrophic concentrations, both suspended and fixed, can be attributed to increase in disinfectant residual, combined with the decrease in BOM substrate.

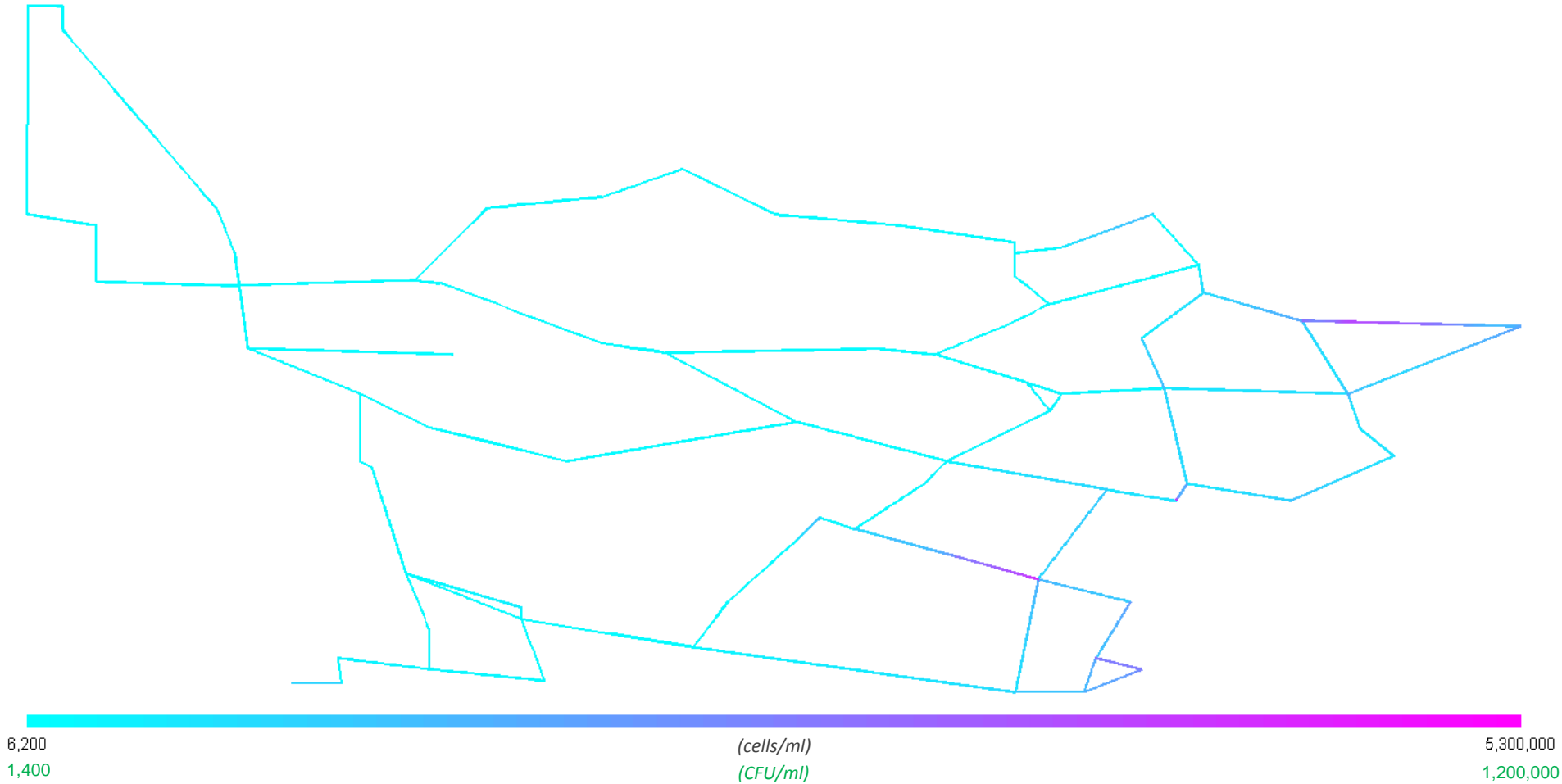


Figure D-96: Fixed heterotroph concentration profile for Alternative 6

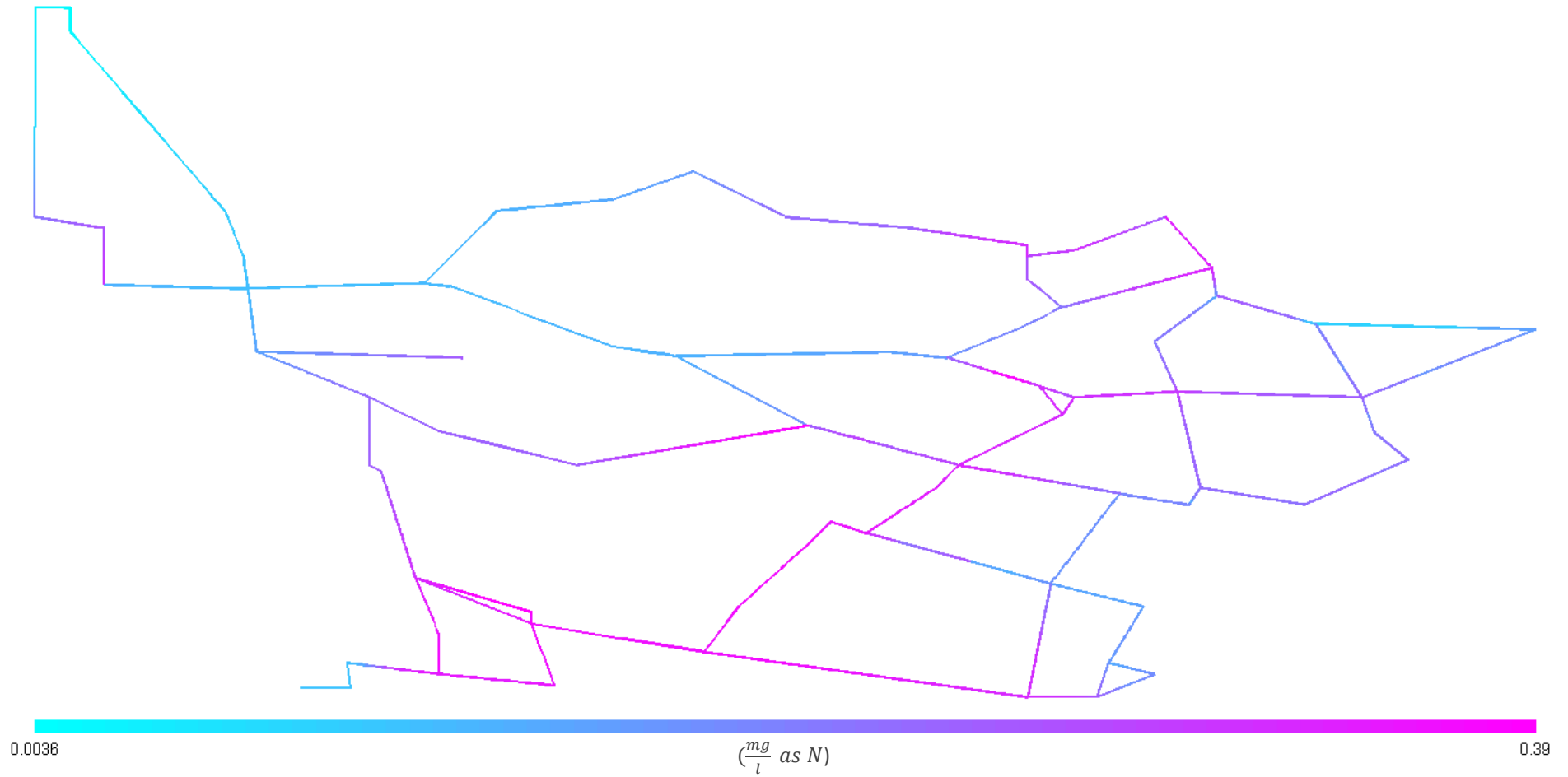


Figure D-97: Total ammonia concentration profile for Alternative 6

The maximum ammonia concentration is significantly reduced due to the lower treatment plant input.

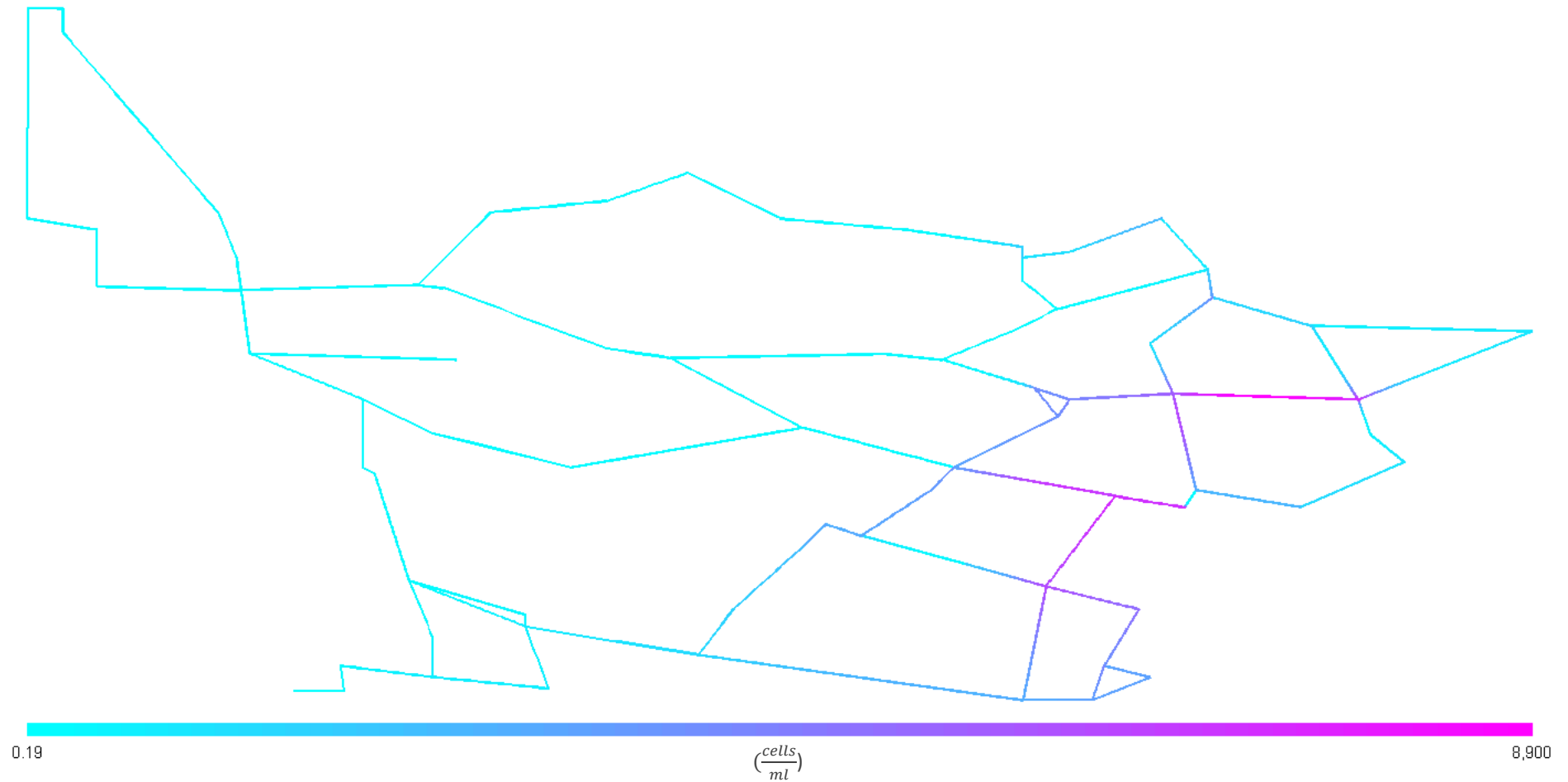


Figure D-98: Suspended AOB concentration profile for Alternative 6

Both the concentrations of suspended and fixed AOB are reduced due to the lower substrate concentrations and greater disinfectant concentrations present for this simulation.

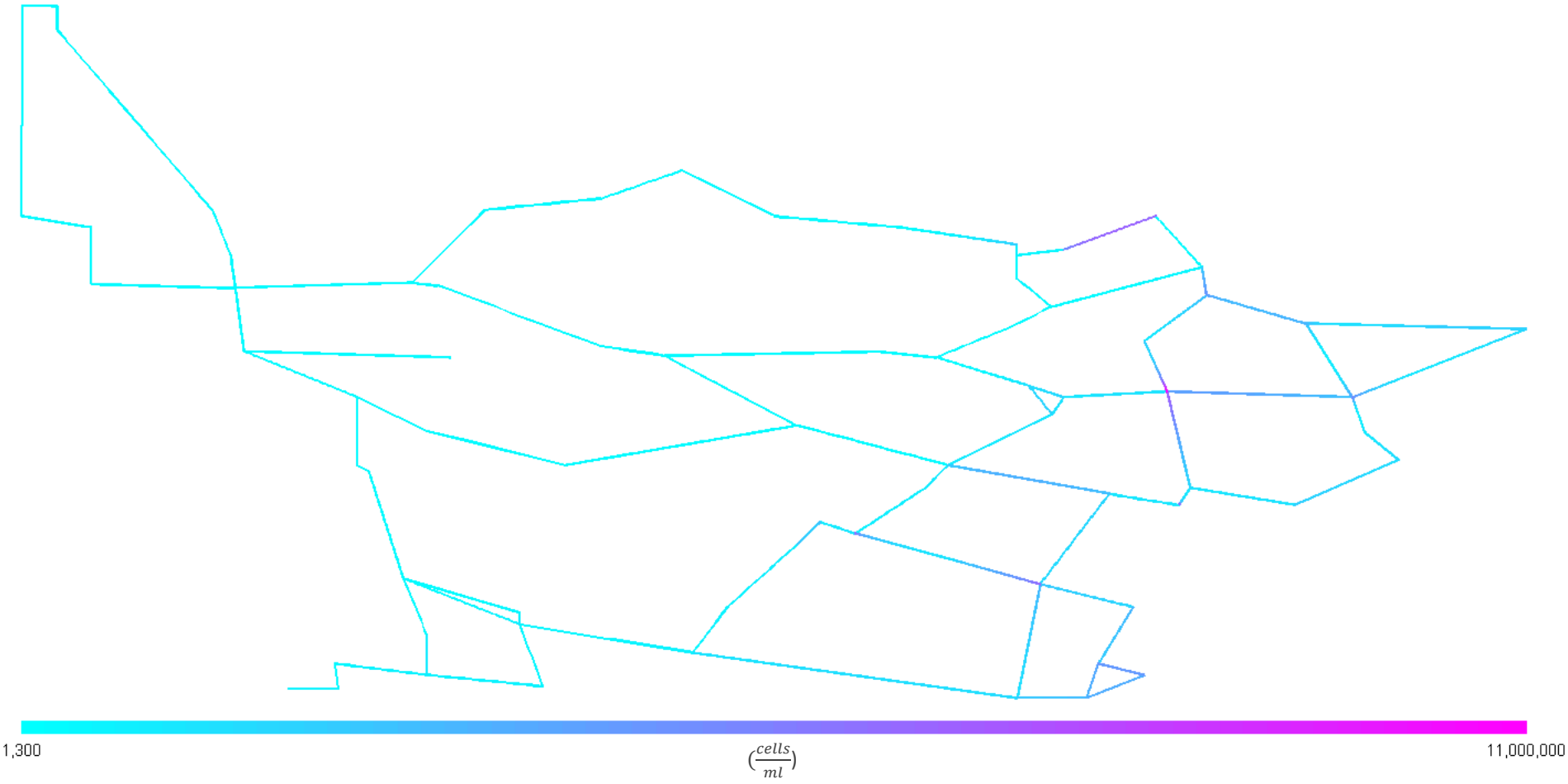


Figure D-99: Fixed AOB concentration profile for Alternative 6

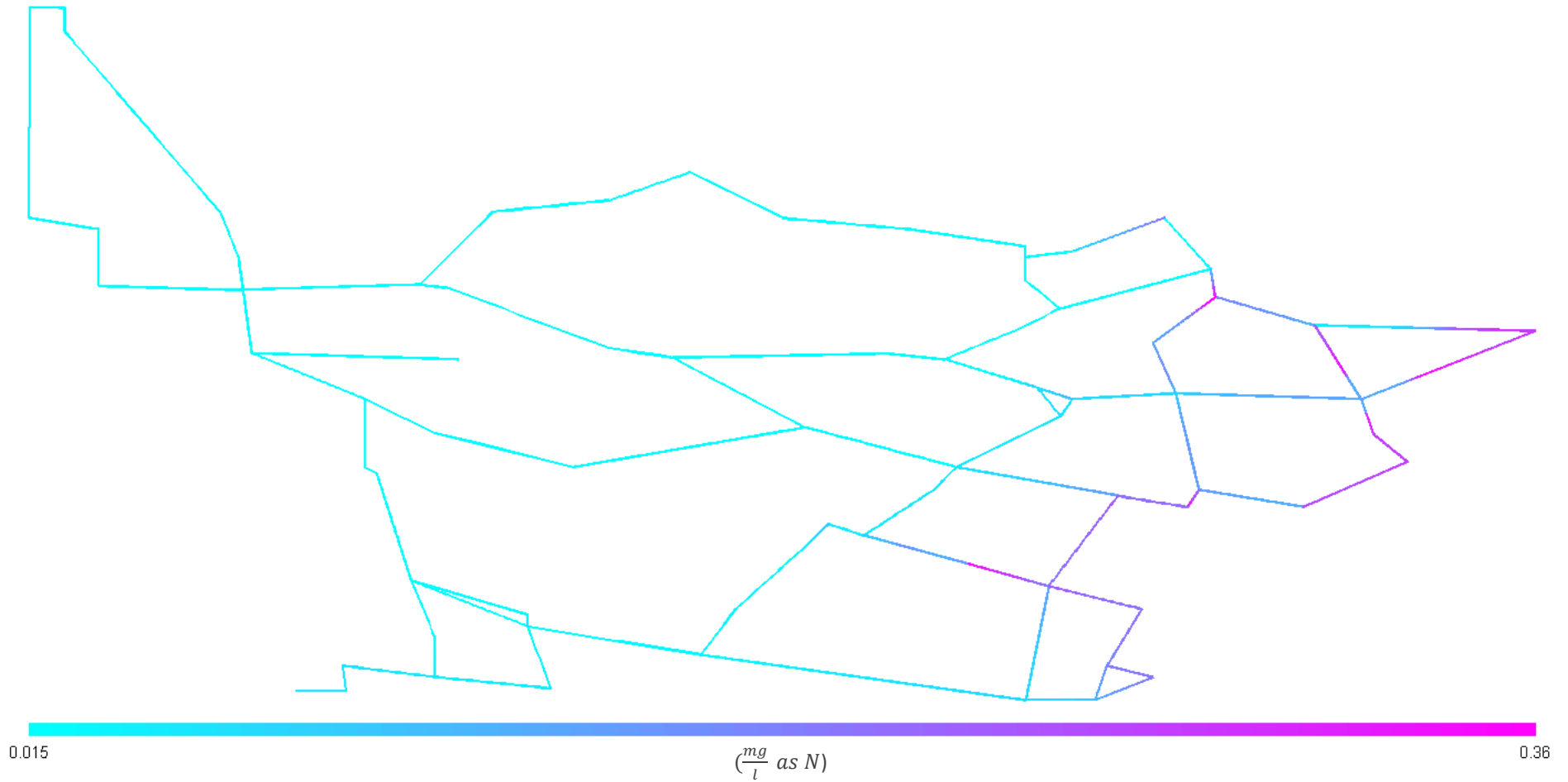


Figure D-100: Nitrite concentration profile for Alternative 6

The concentration of nitrite is significantly reduced, due to the lower concentration of AOB.

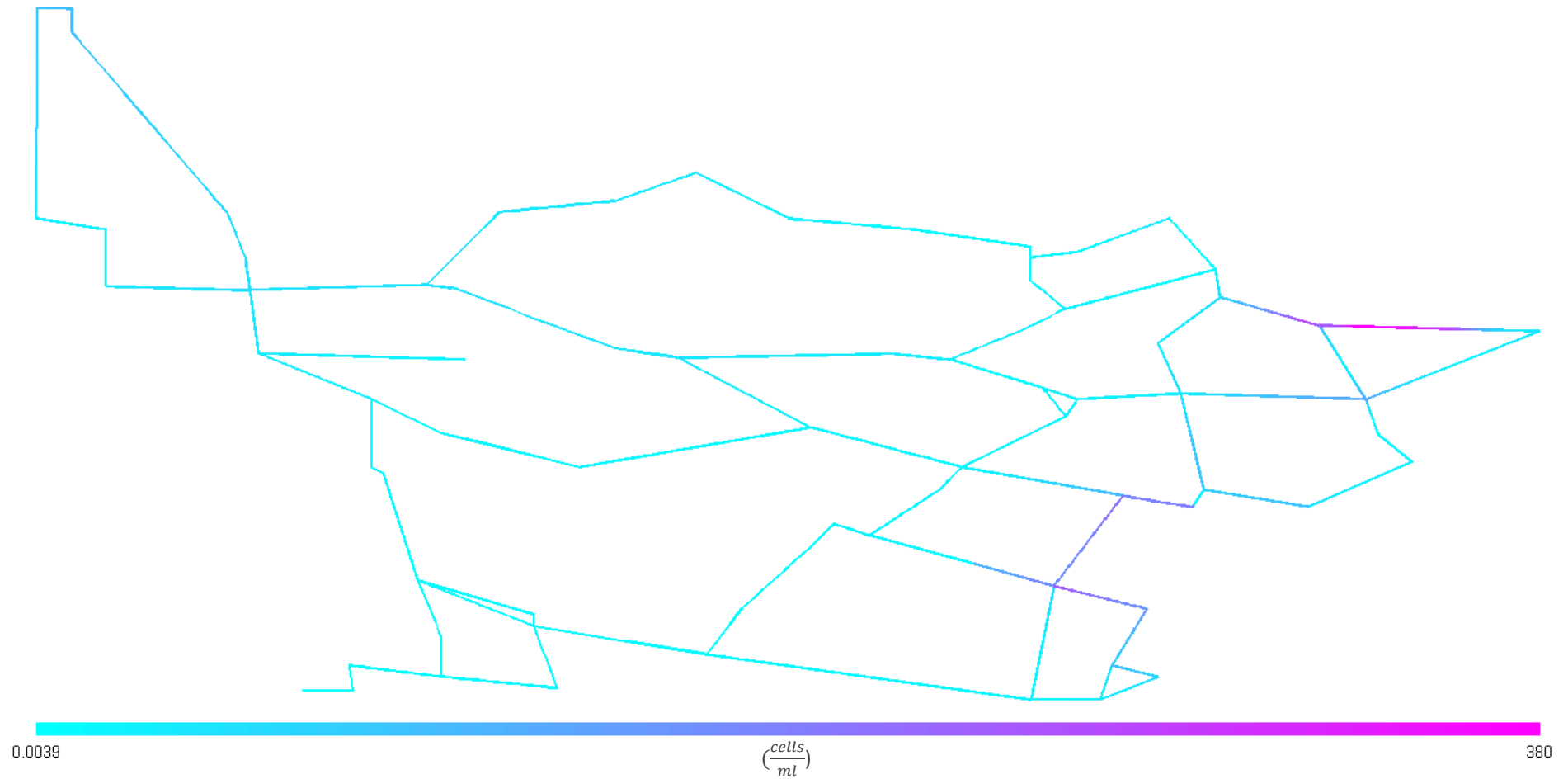


Figure D-101: Suspended NOB concentration profile for Alternative 6

Both the concentrations of suspended and fixed NOB are reduced due to the lower substrate concentrations and greater disinfectant concentrations present for this simulation.

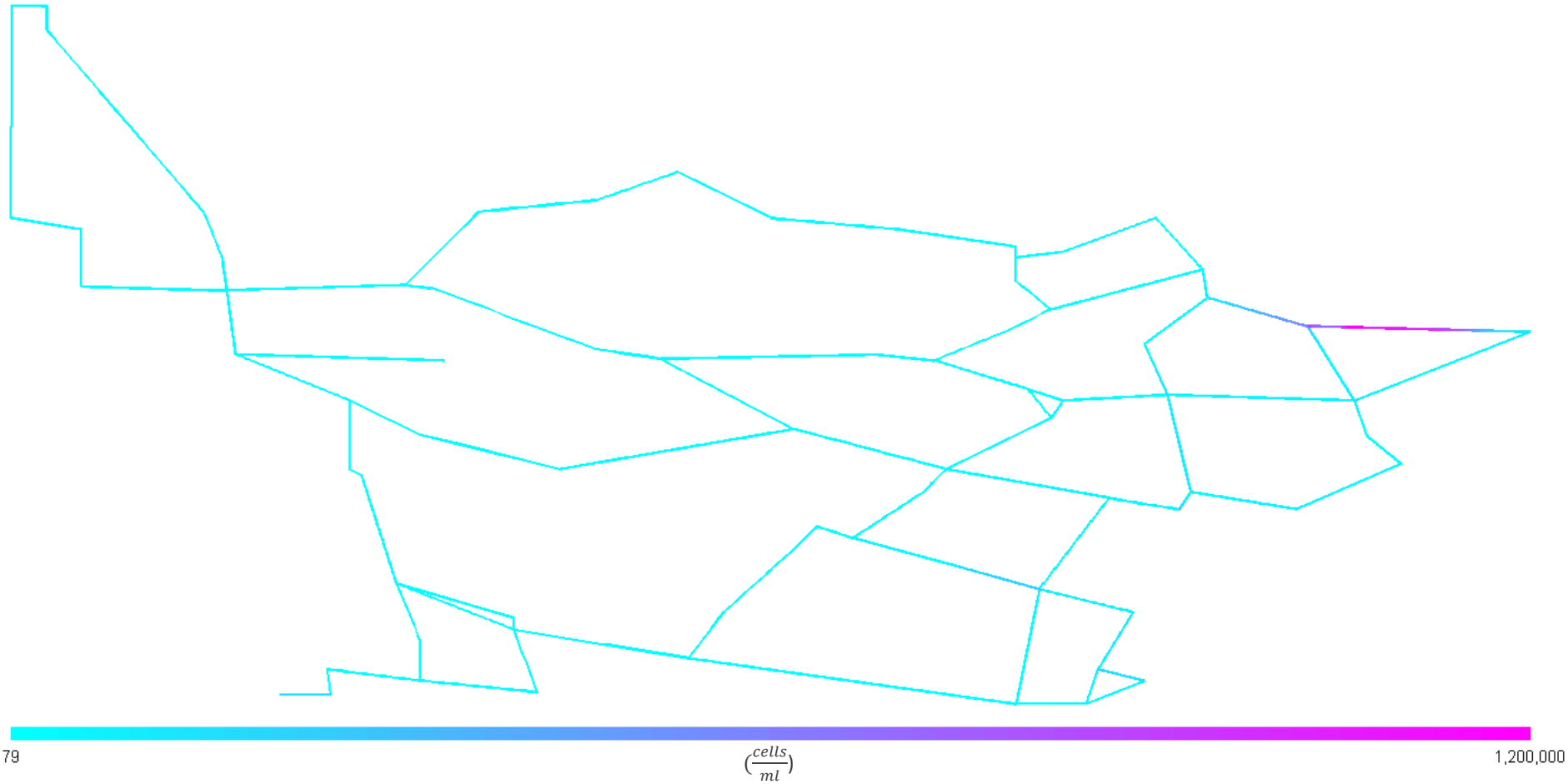


Figure D-102: Fixed NOB concentration profile for Alternative 6

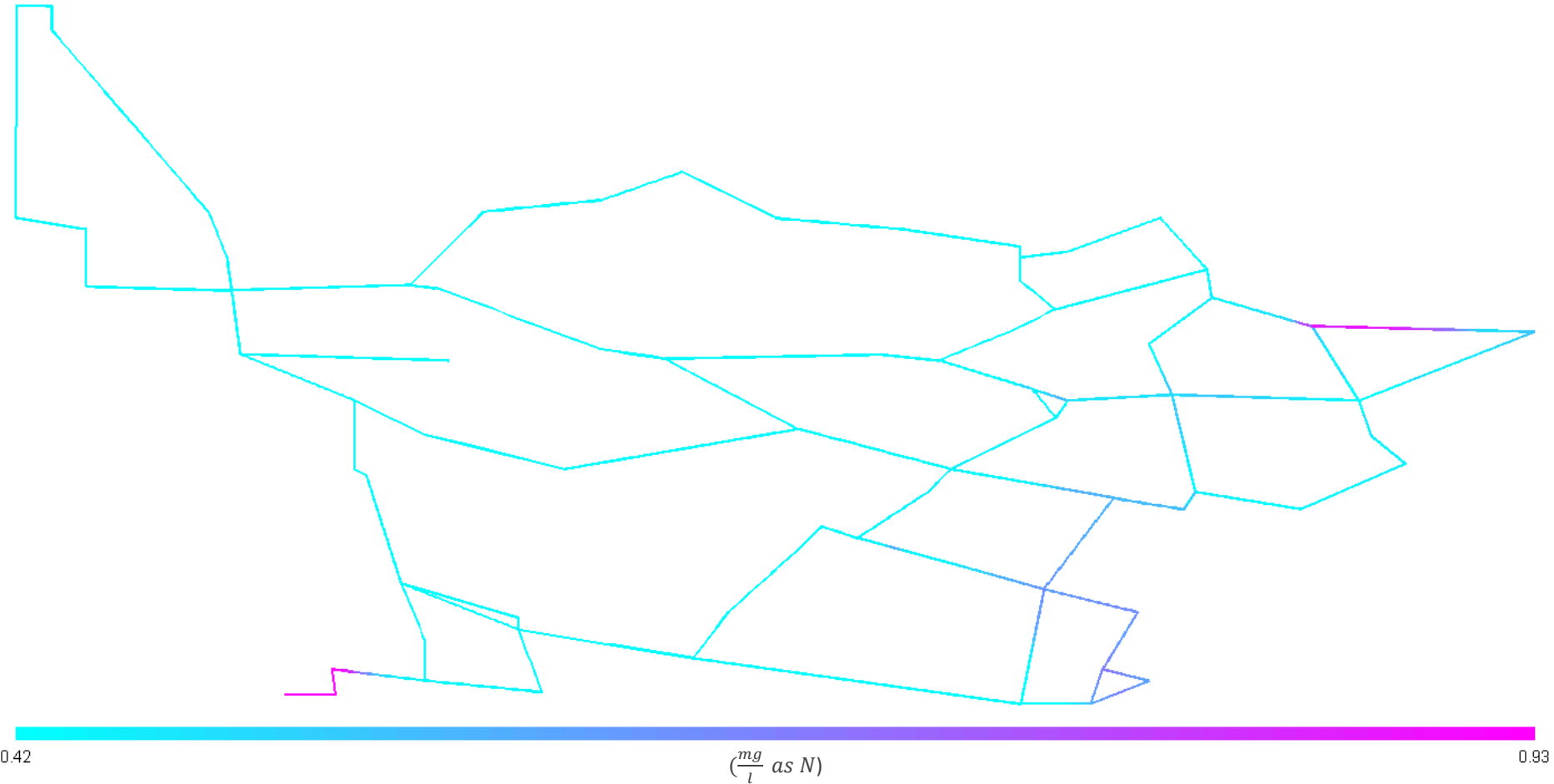


Figure D-103: Nitrate concentration profile for Alternative 6

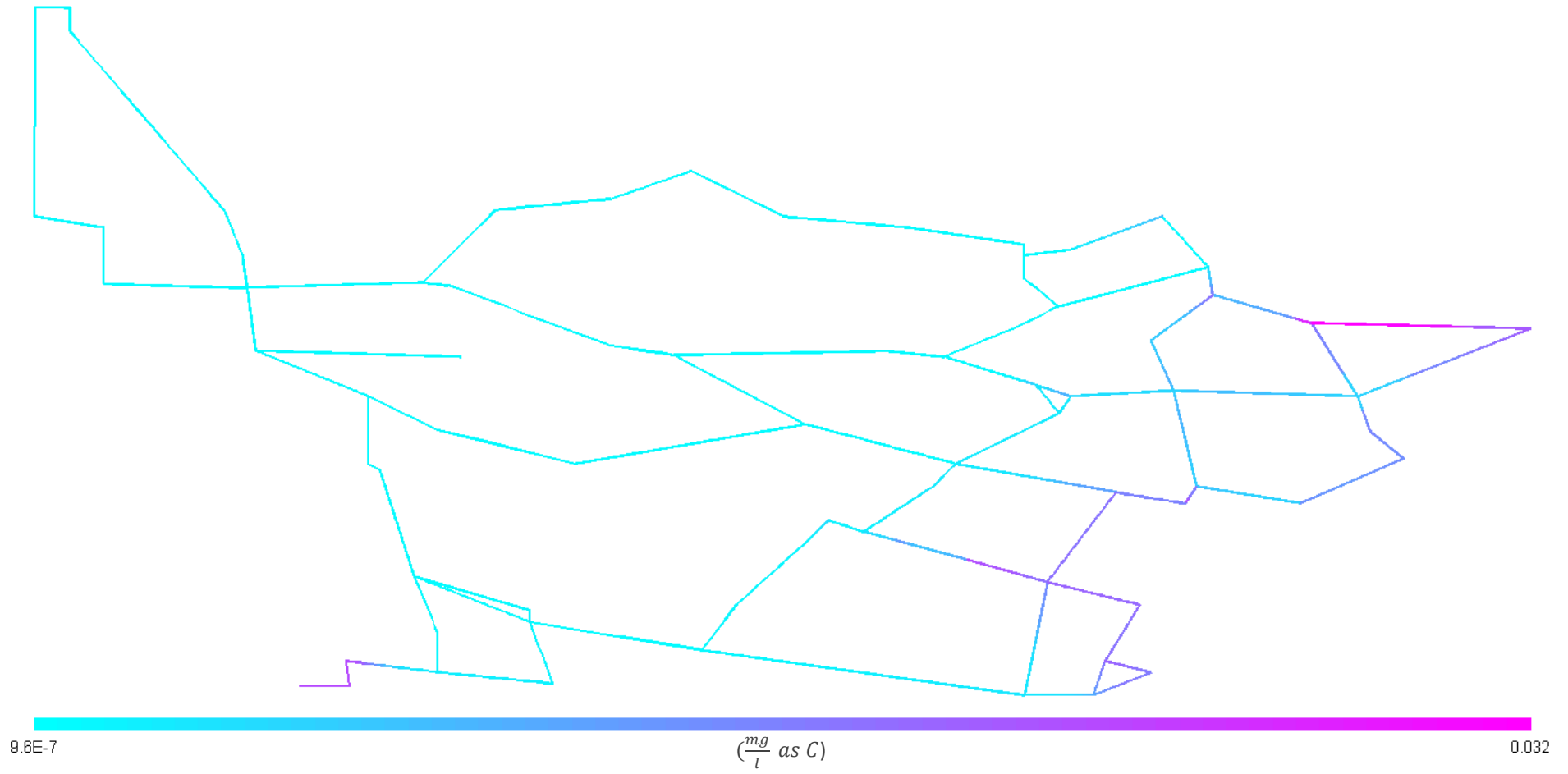


Figure D-104: UAP concentration profile for Alternative 6

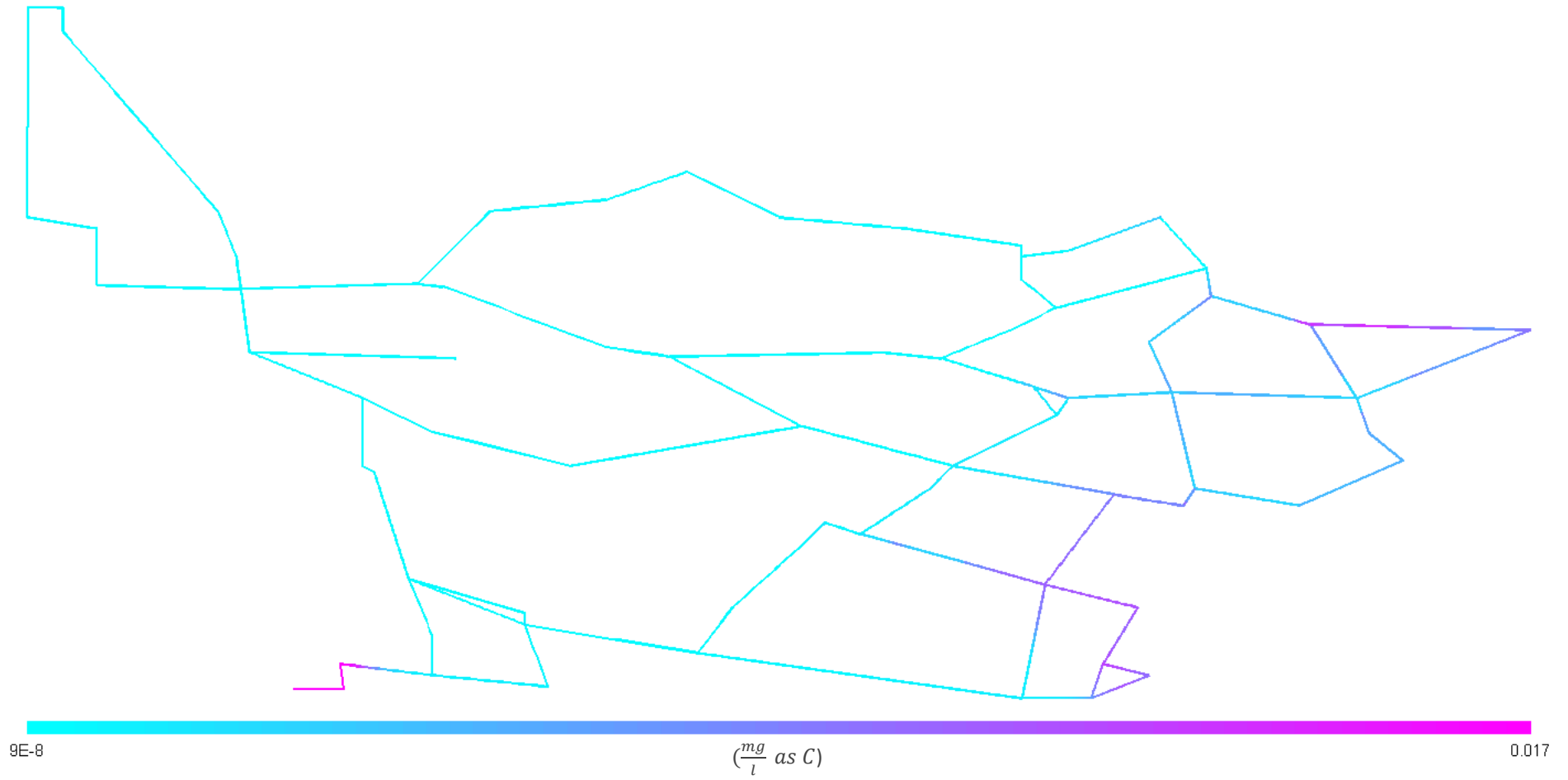


Figure D-105: BAP concentration profile for Alternative 6

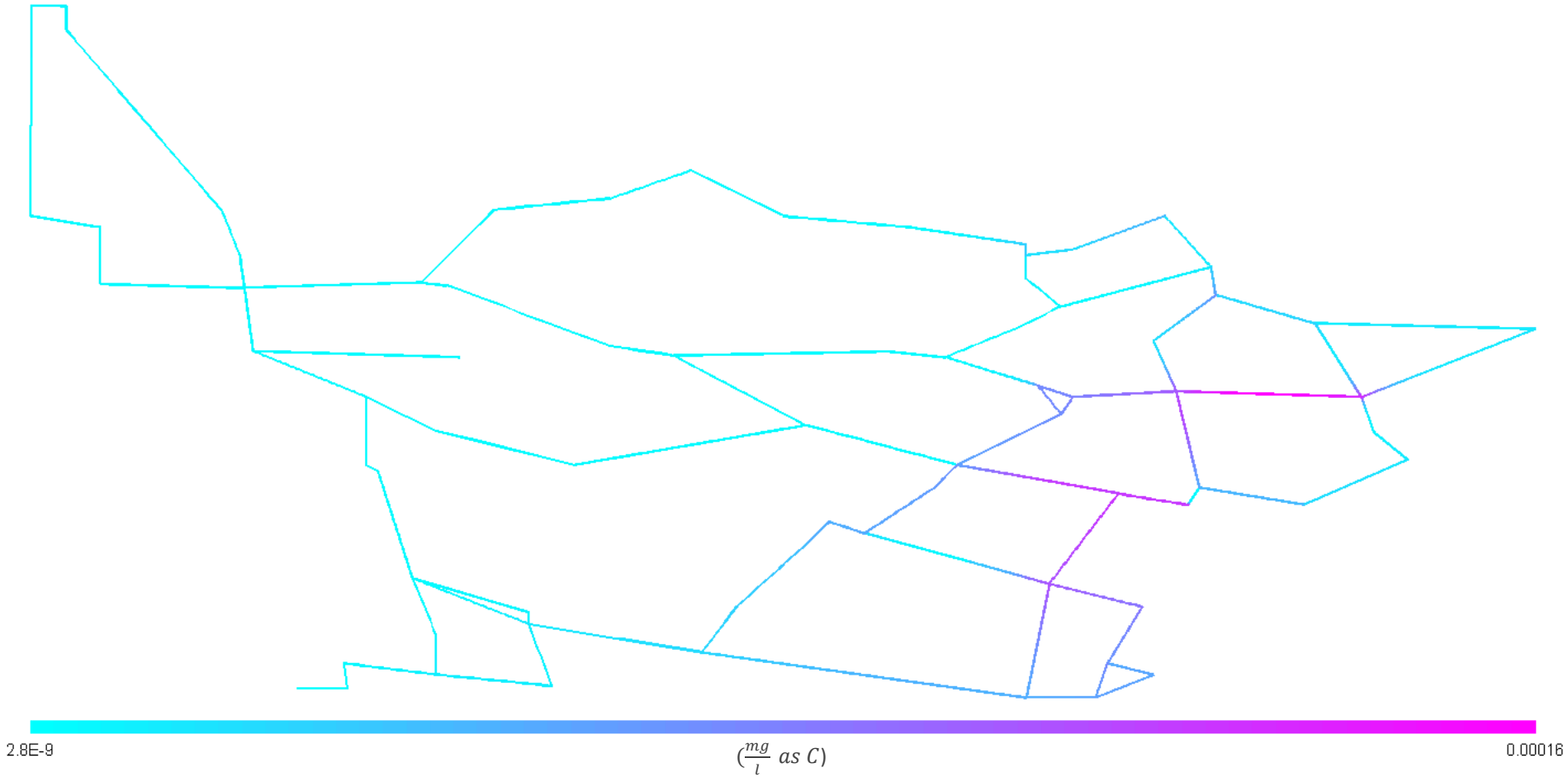


Figure D-106: Suspended EPS concentration profile for Alternative 6

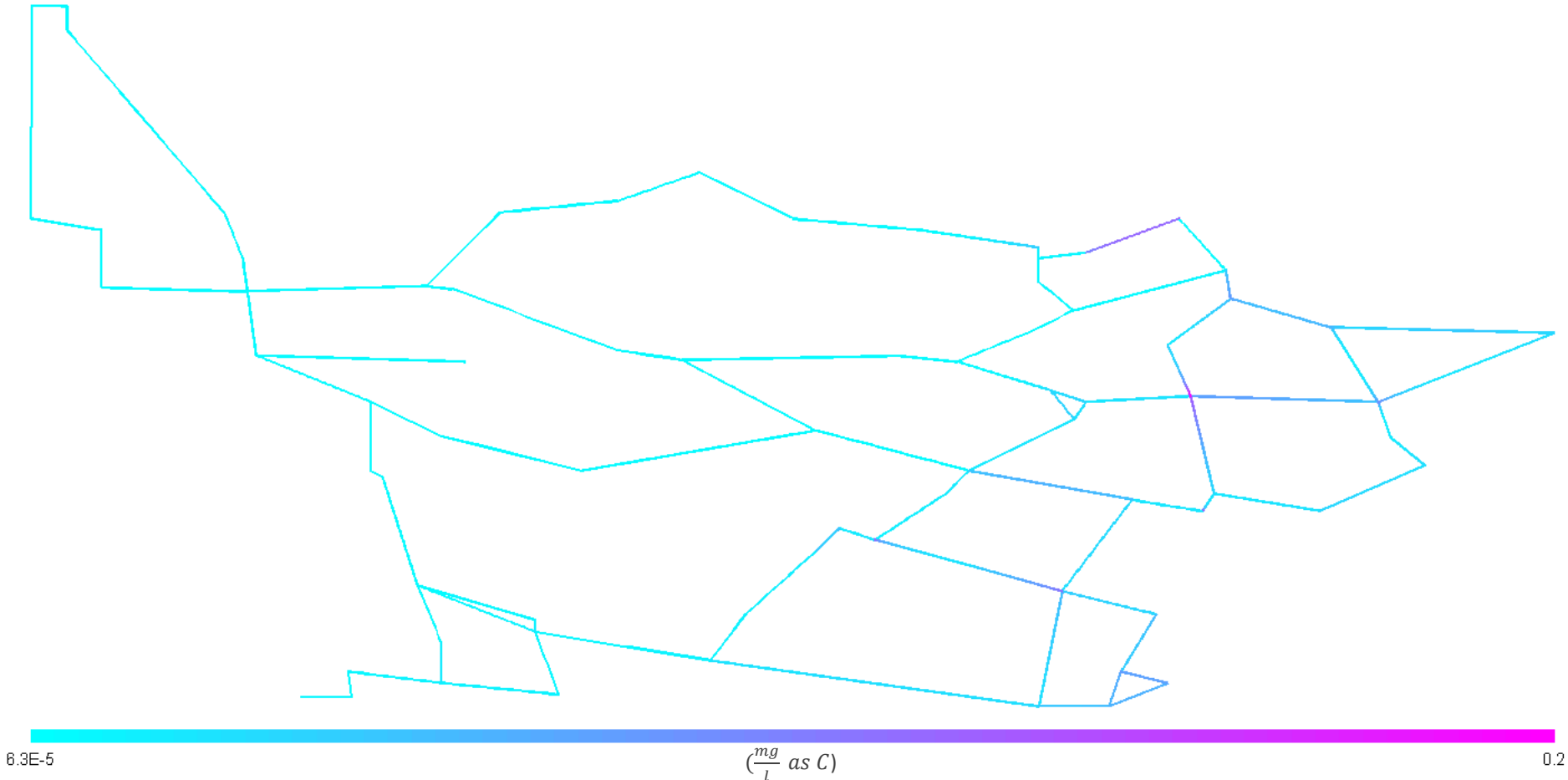


Figure D-107: Fixed EPS concentration profile for Alternative 6

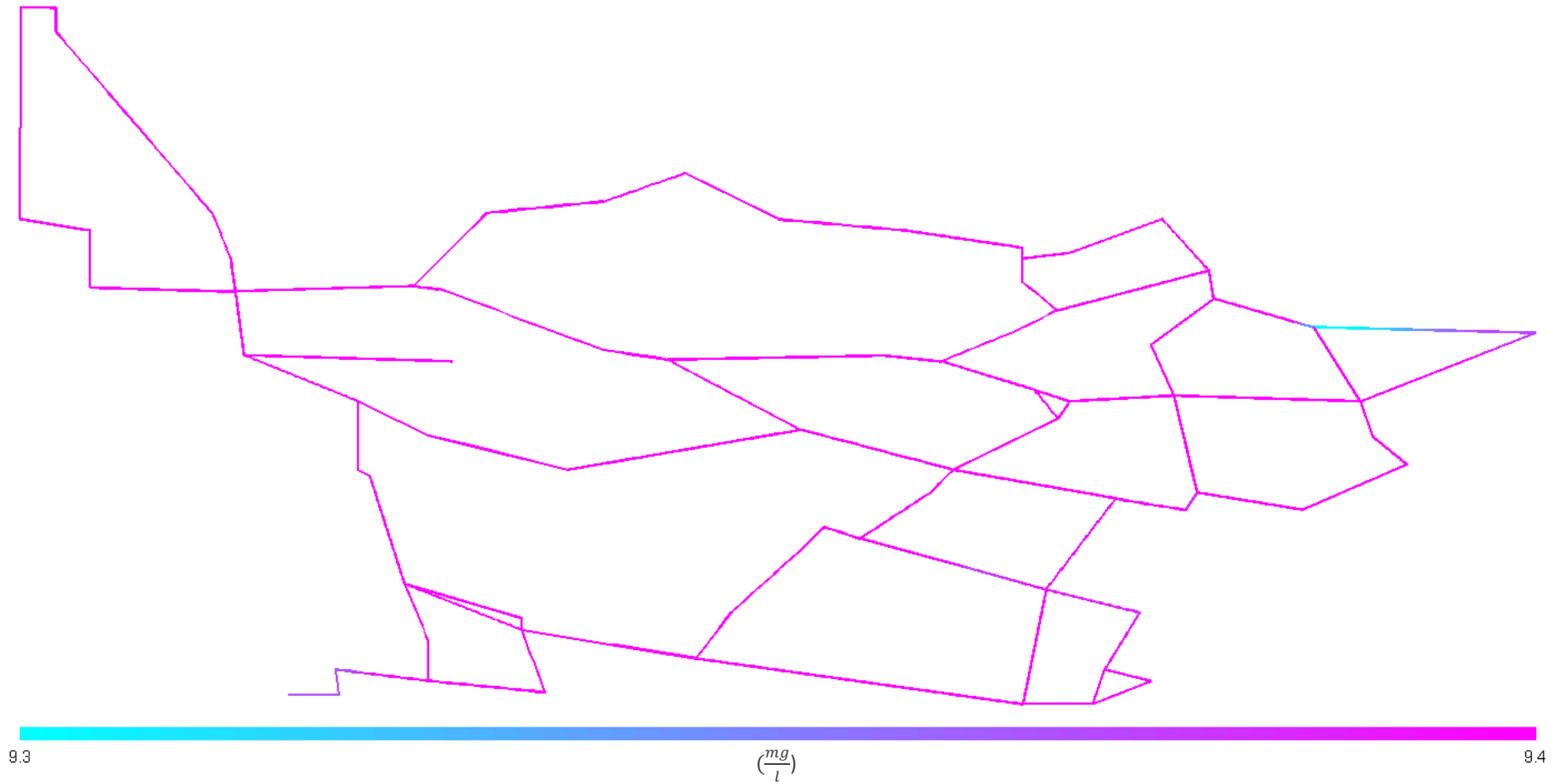


Figure D-108: Dissolved oxygen concentration profile for Alternative 6

Dissolved oxygen depletion throughout the system is limited due to the low concentrations of active biomass.

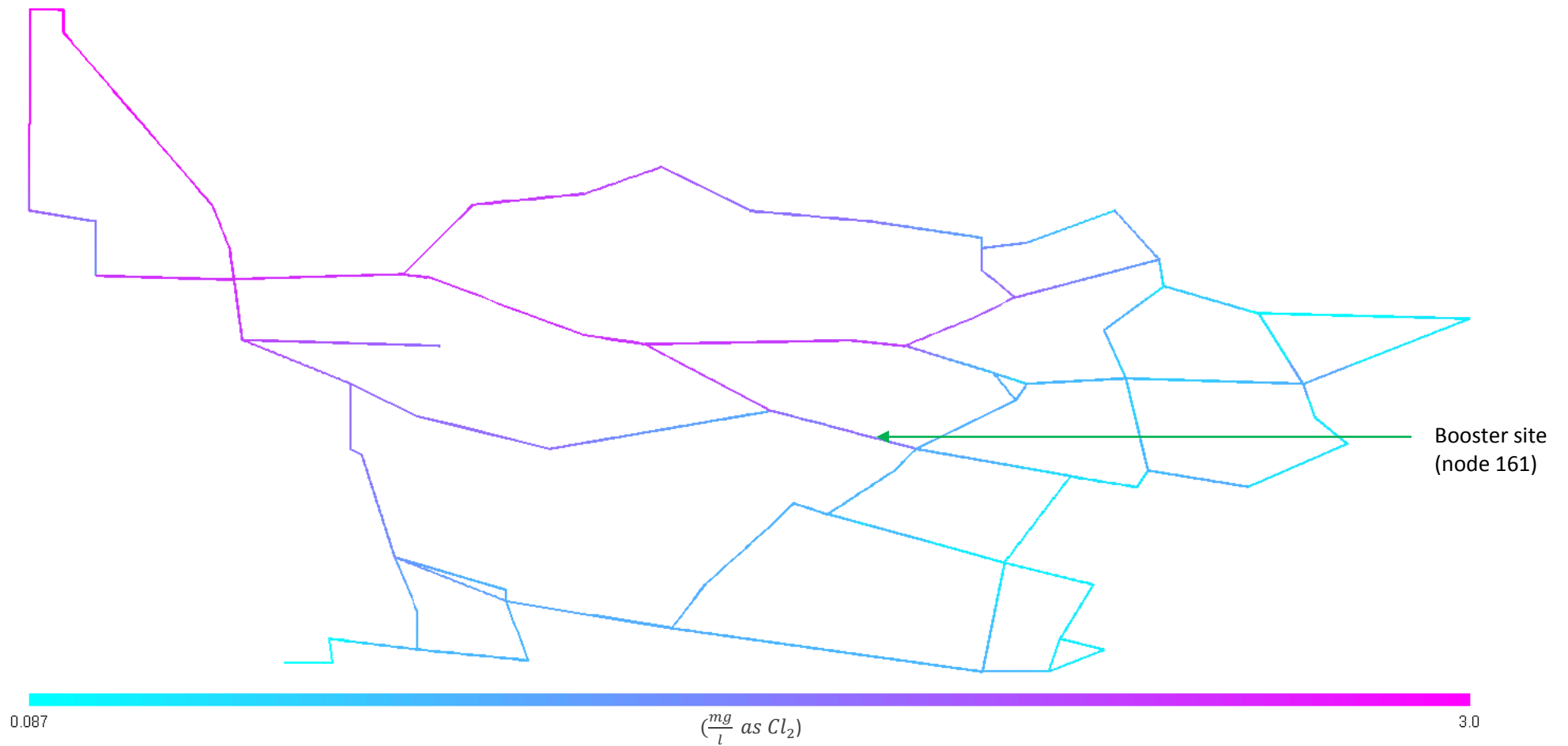
D.7 Reduce both Input BOM and Excess Ammonia, combined with Booster Chloramination

Figure D-109: Monochloramine concentration profile for Alternative 7

The utilisation of a booster chloramination at node 161 has a limited effect on the monochloramine concentration profile.

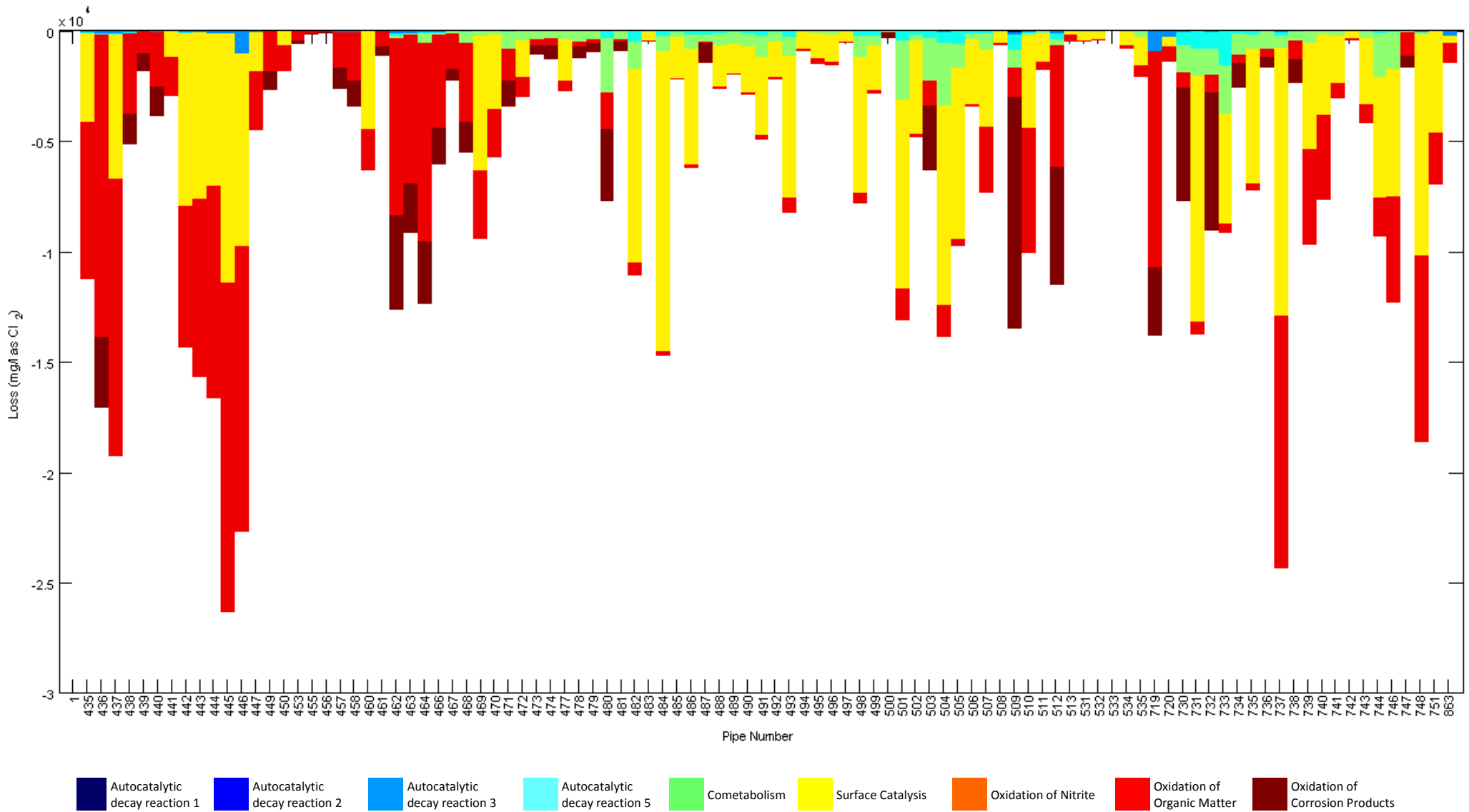


Figure D-110: Monochloramine loss mechanisms and locations for Alternative 7

The reason for the limited effect of the booster chloramination is demonstrated using Figure D-110. Monochloramine loss due to surface catalysis becomes significant in pipes 482 and 484, which are the pipes adjacent to the booster site. The loss of monochloramine is so great in these two pipes, that little monochloramine input at the

booster site is able to permeate the system. Surface catalysis in these two pipes is significant because firstly, loss due to surface catalysis is a function of the monochloramine concentration squared and hence the effectiveness of booster chloramination is limited for concrete pipes. Secondly, the flow rates in these pipes are low, resulting in increased detention times, compounding the problem.

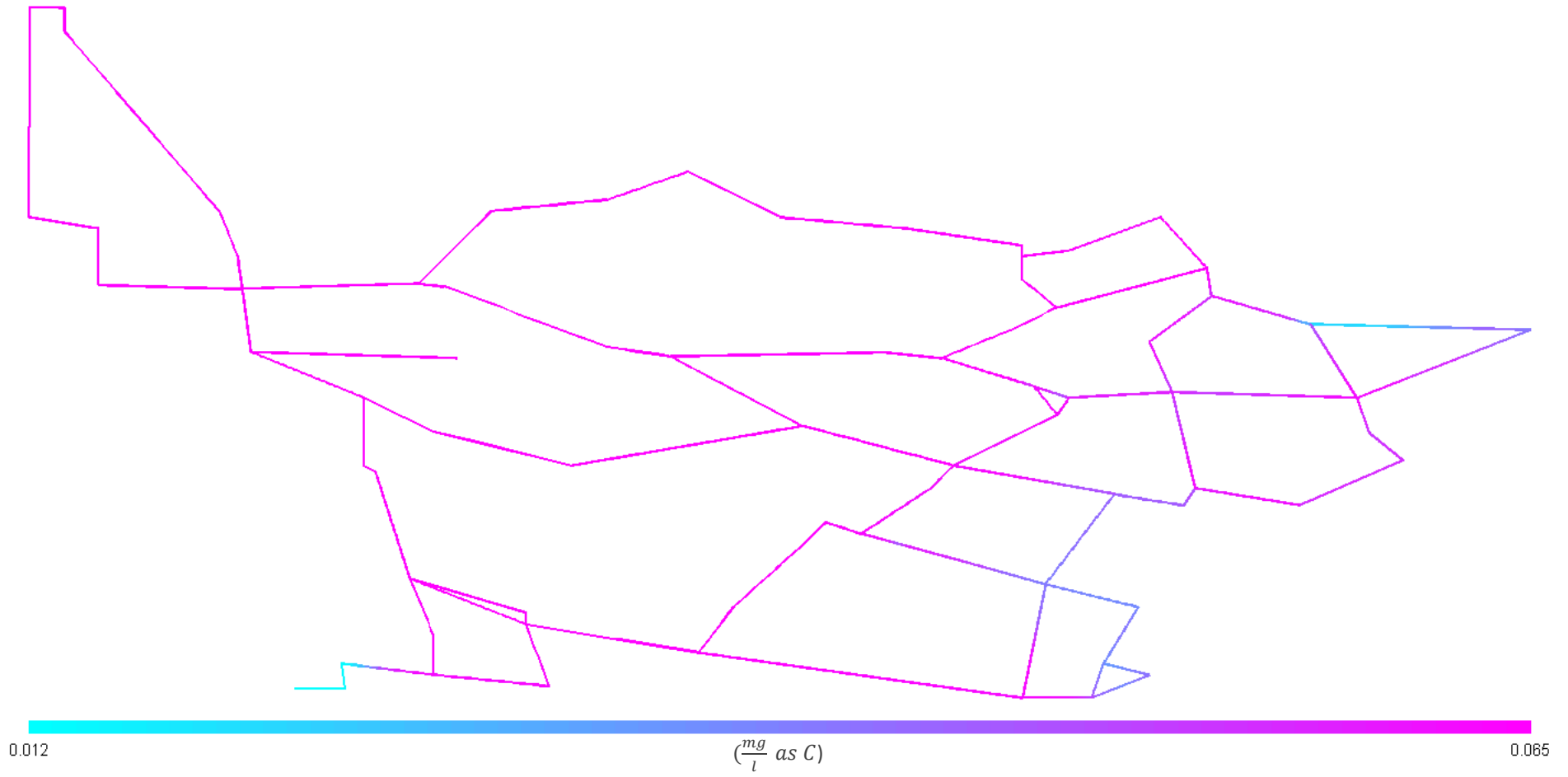


Figure D-111: BOM₁ concentration profile for Alternative 7

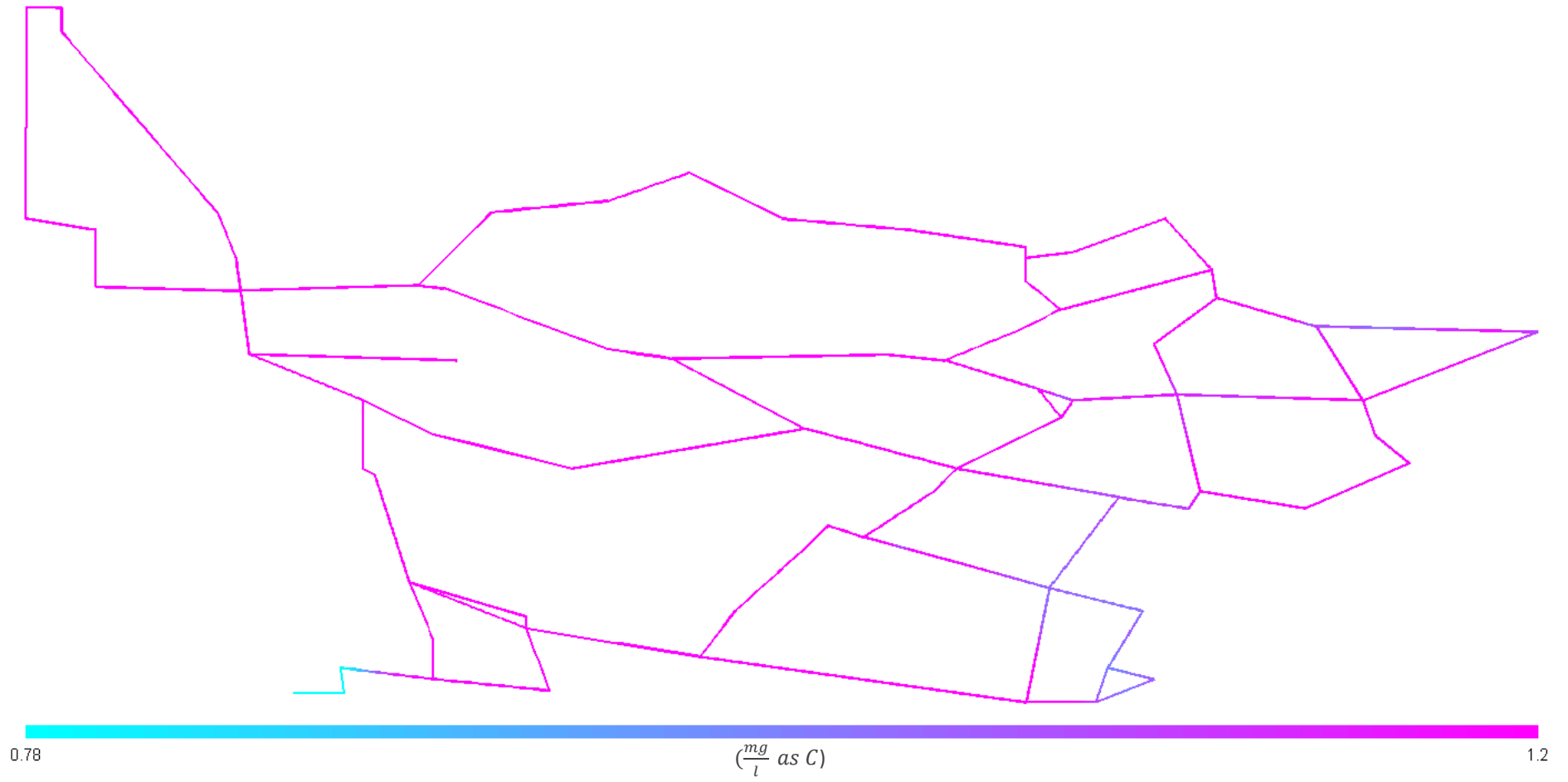


Figure D-112: BOM₂ concentration profile for Alternative 7

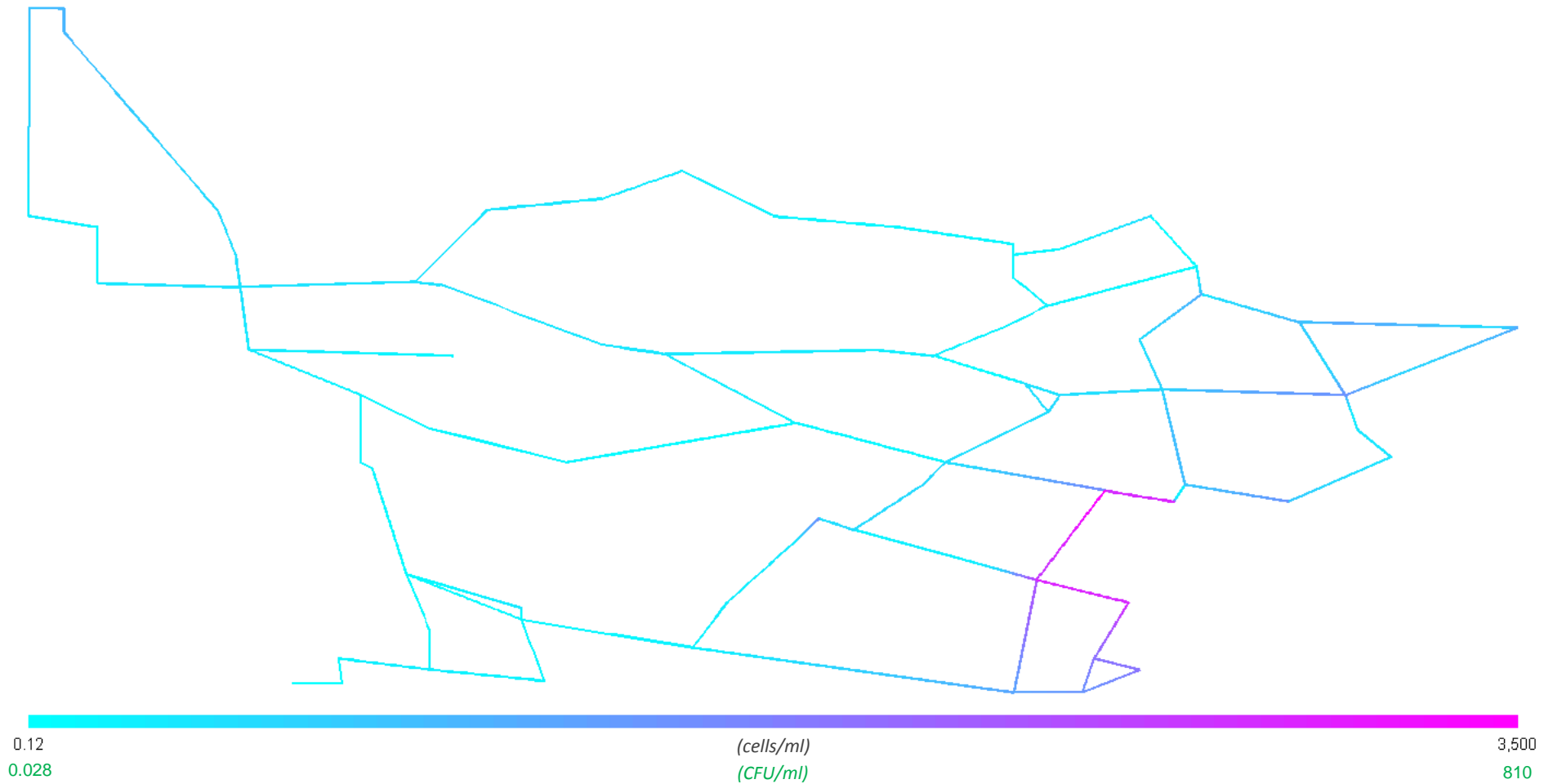


Figure D-113: Suspended heterotroph concentration profile for Alternative 7

The maximum concentration for the 12th hour does not exceed the limit of $4300 \frac{\text{cells}}{\text{ml}}$. However, the maximum concentration for the system occurs at the end of the 20th hour and has a value of approximately $5700 \frac{\text{cells}}{\text{ml}}$, as demonstrated in Figure D-114, and thus this alternative is not deemed acceptable.

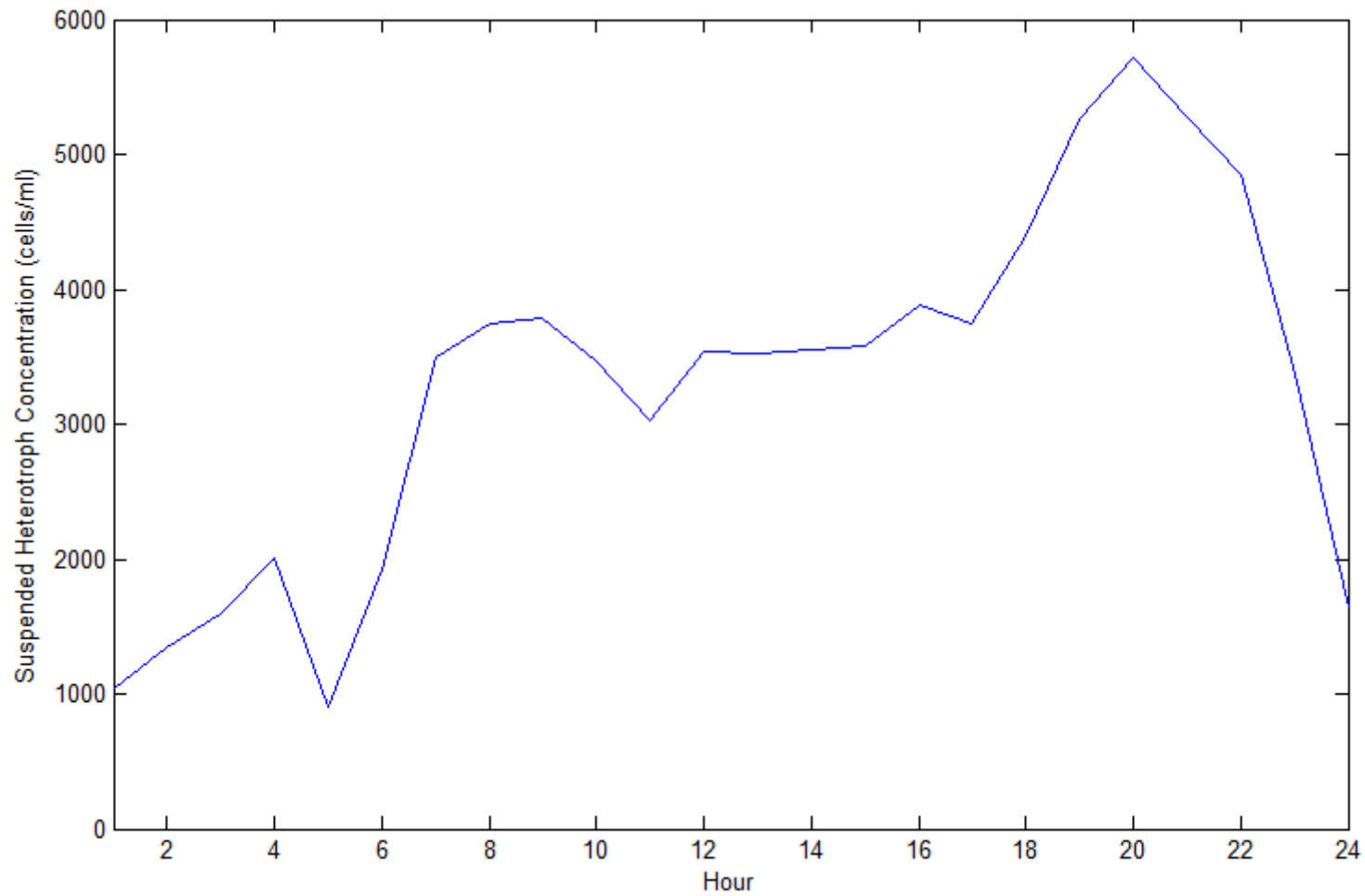


Figure D-114: Suspended heterotroph concentration for final day within Pipe 487

The variation in the heterotroph concentration throughout the day is due to variations in the flow pattern and demonstrates the importance of understanding the impact of a flow regime on water quality such that appropriate times can be selected to collect water samples as part of a monitoring program.

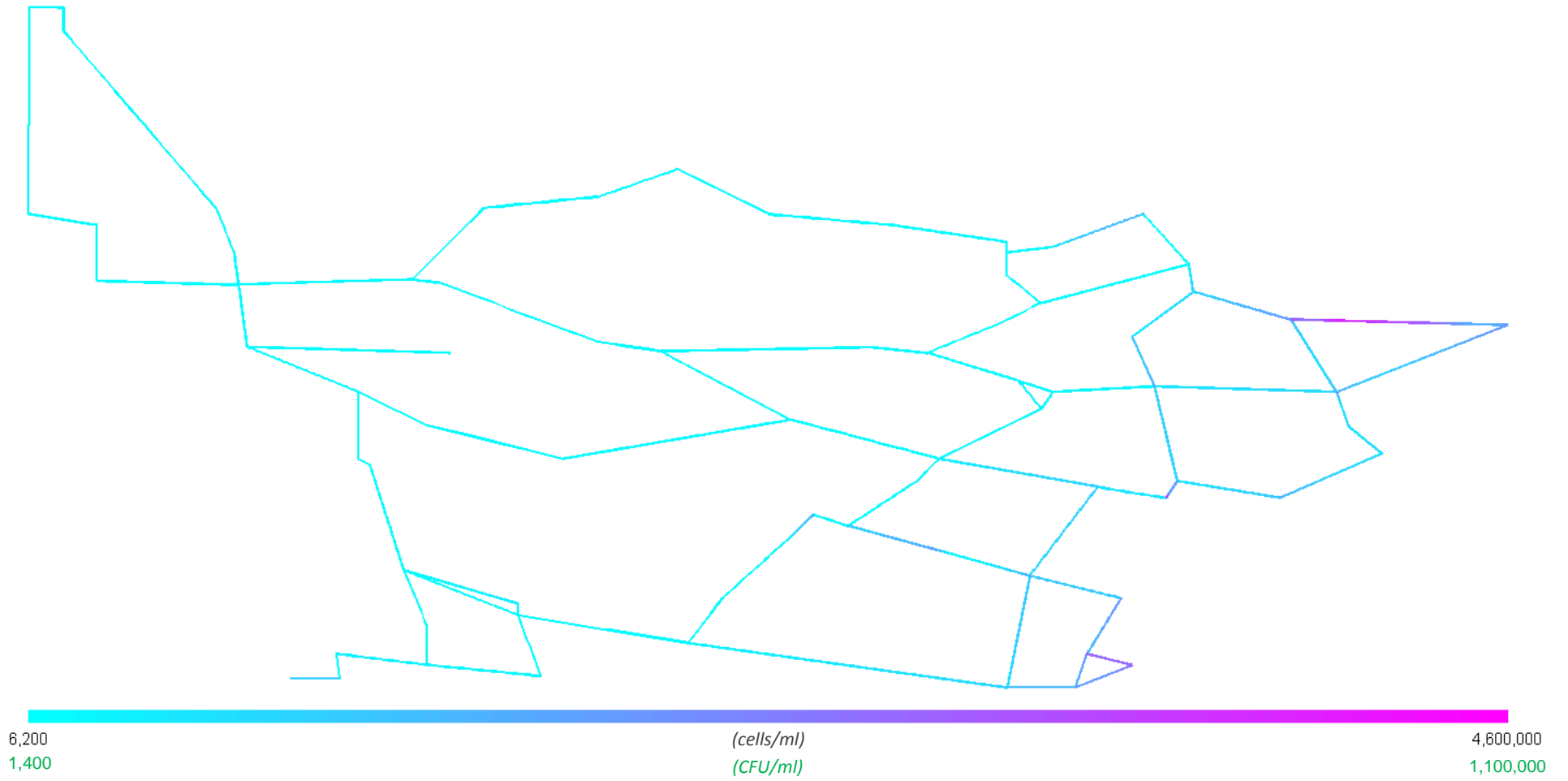


Figure D-115: Fixed heterotroph concentration profile for Alternative 7

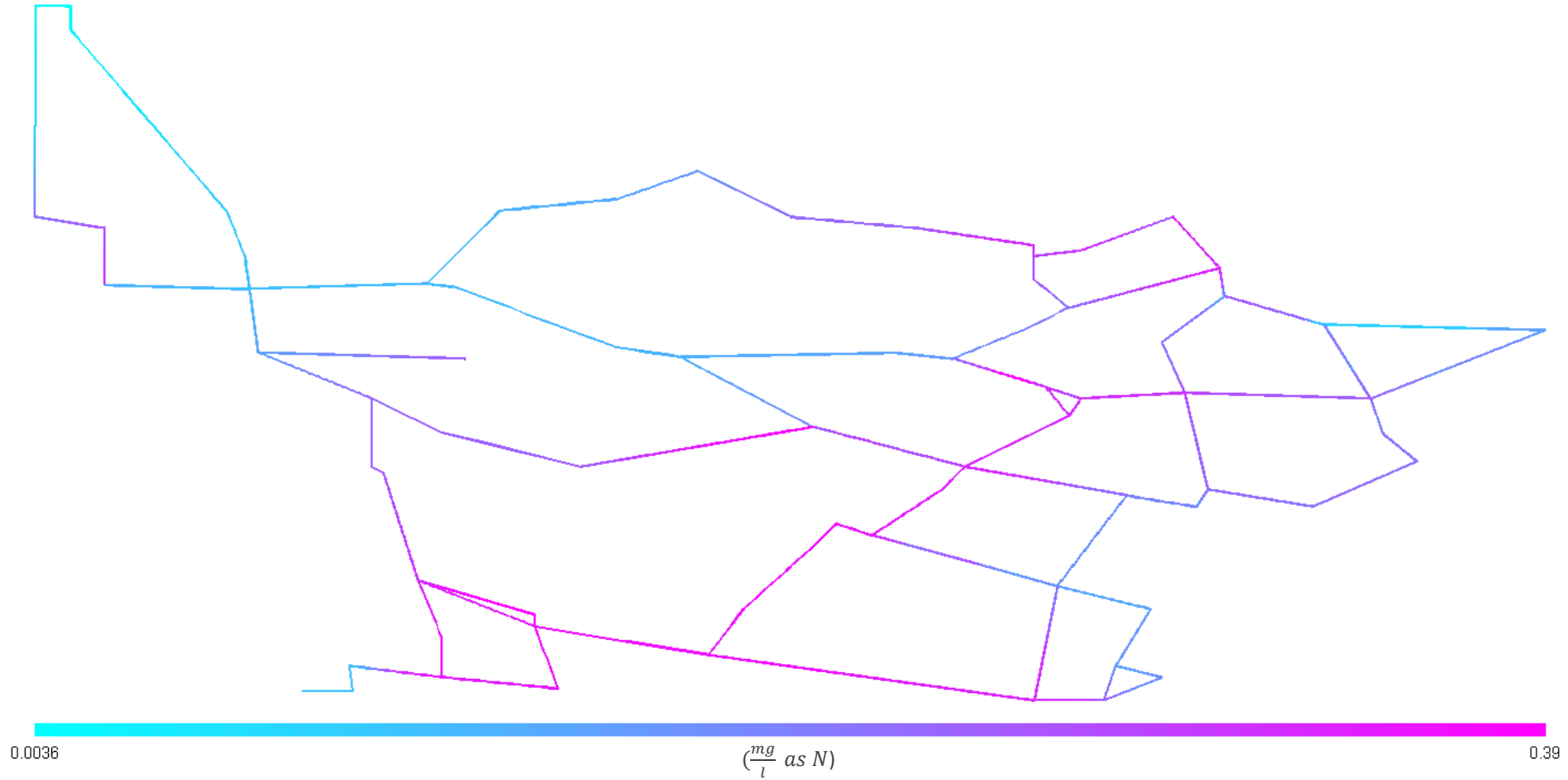


Figure D-116: Total ammonia concentration profile for Alternative 7

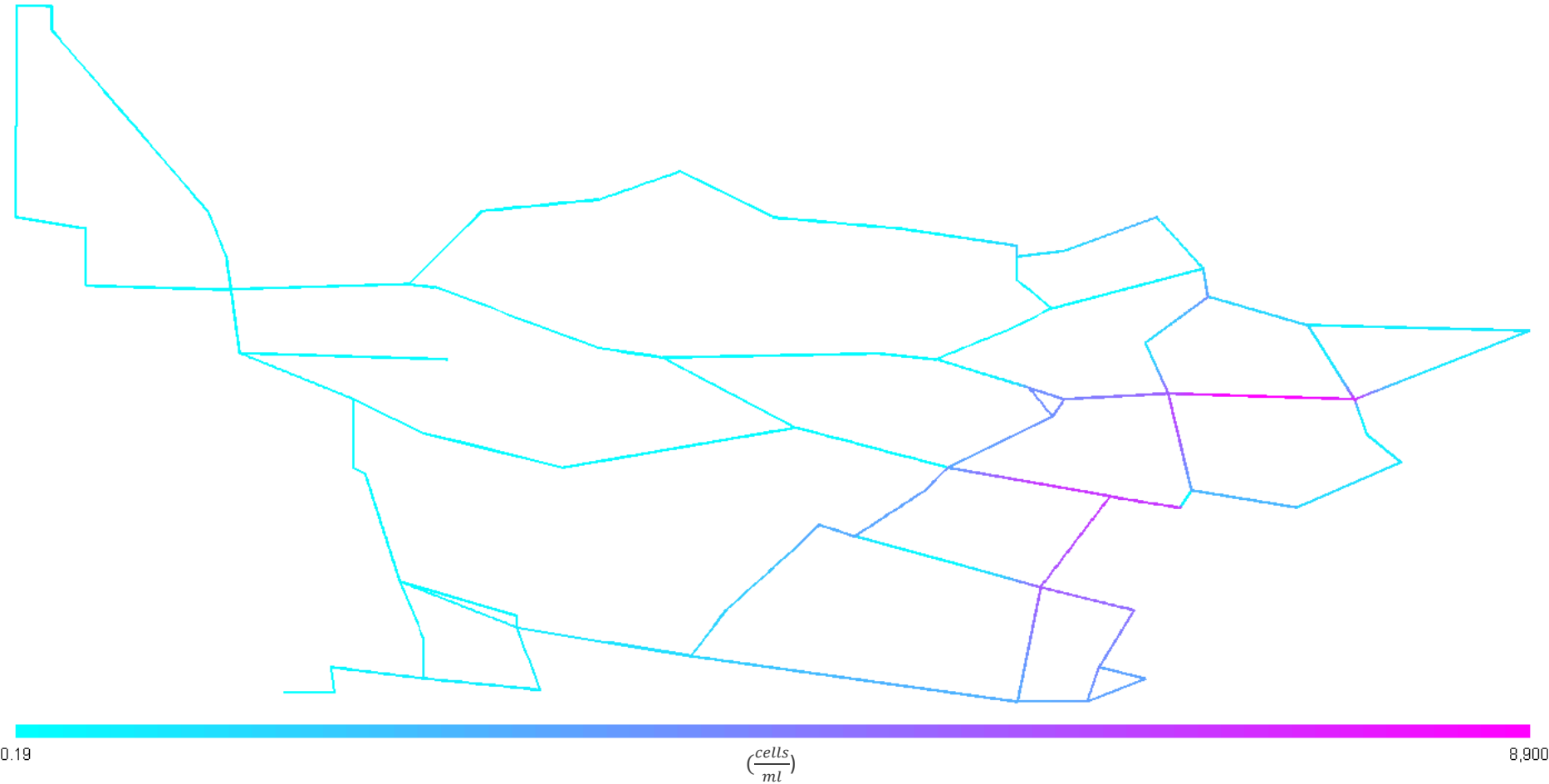


Figure D-117: Suspended AOB concentration profile for Alternative 7

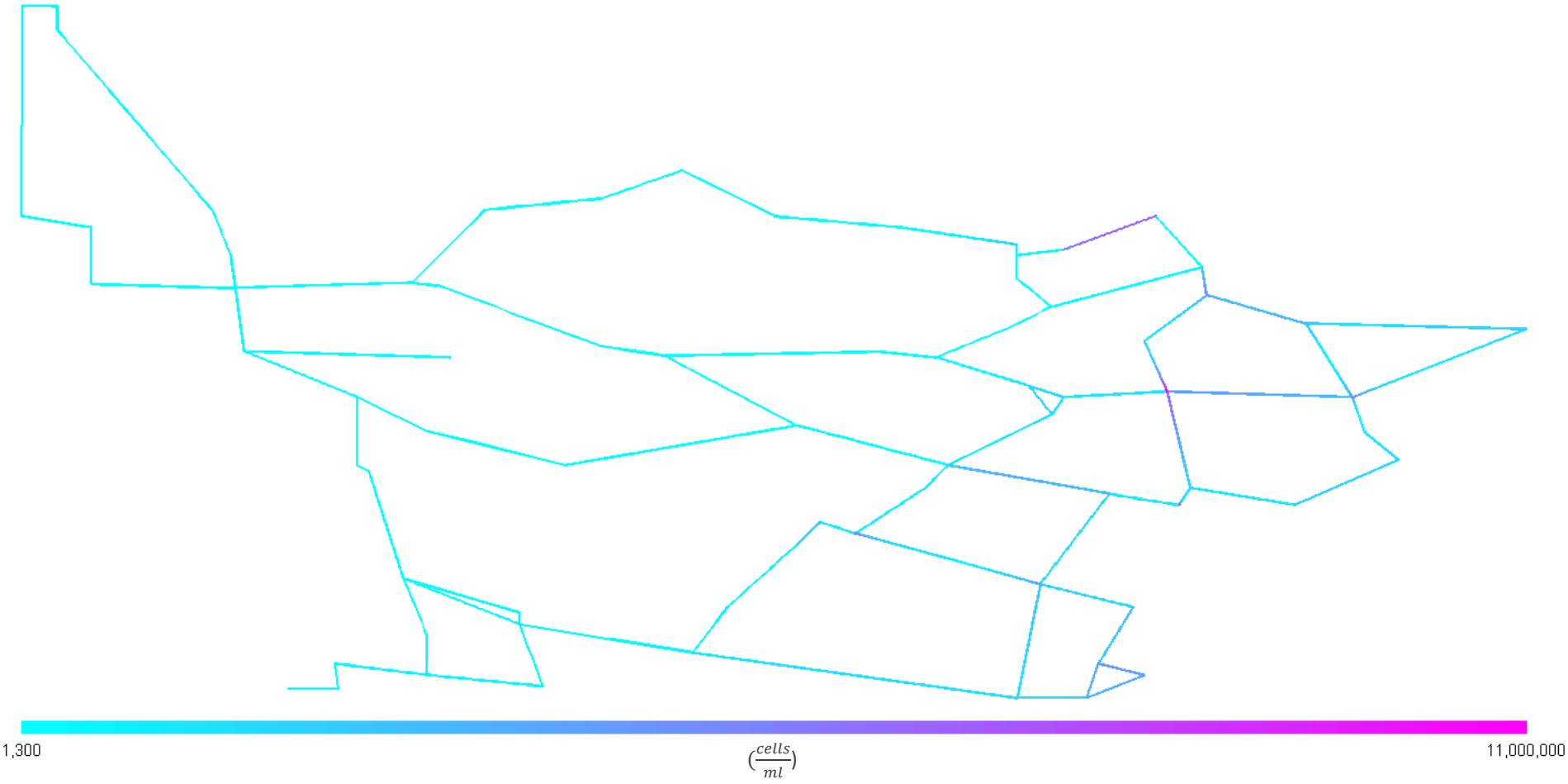


Figure D-118: Fixed AOB concentration profile for Alternative 7

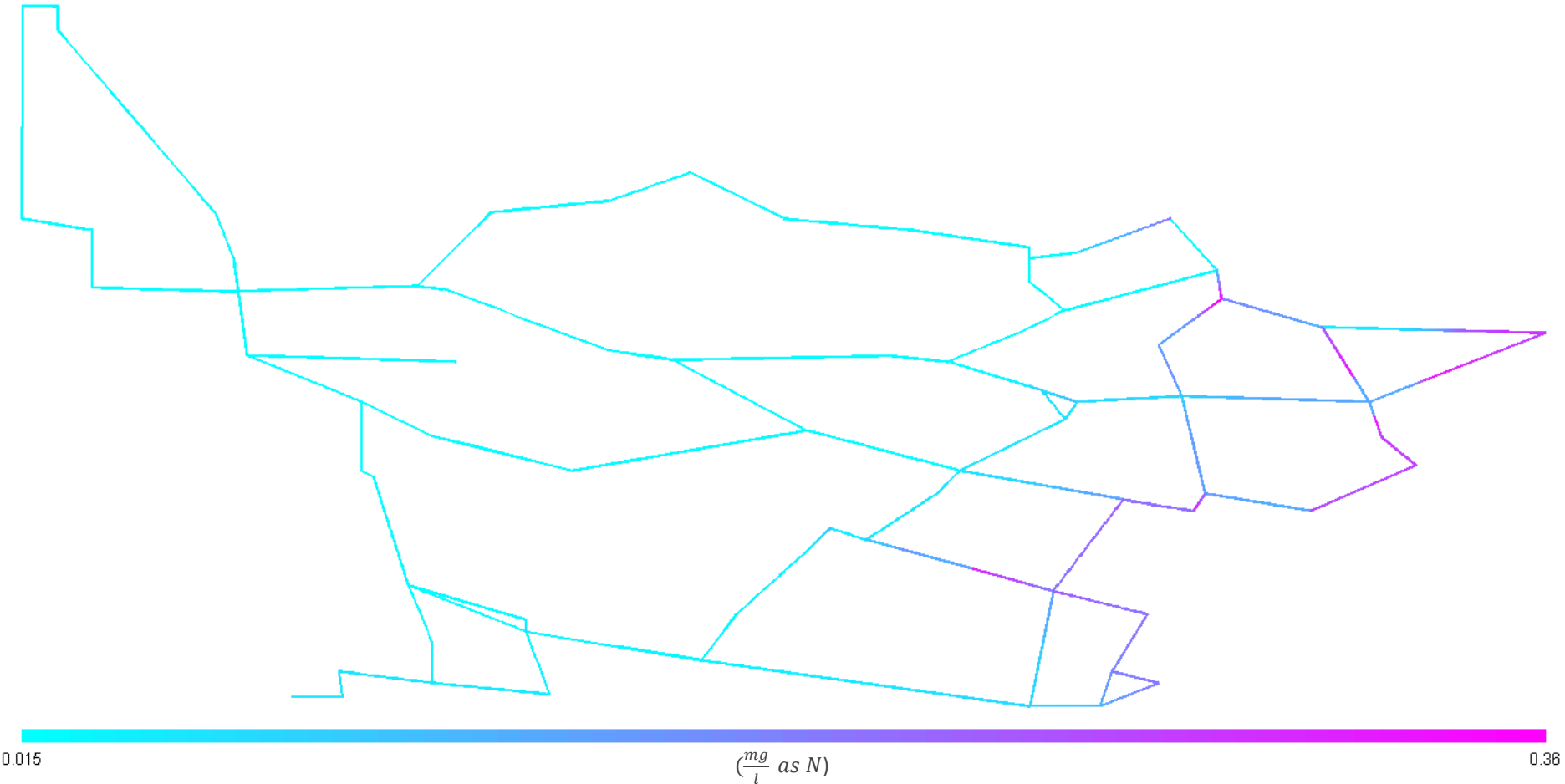


Figure D-119: Nitrite concentration profile for Alternative 7

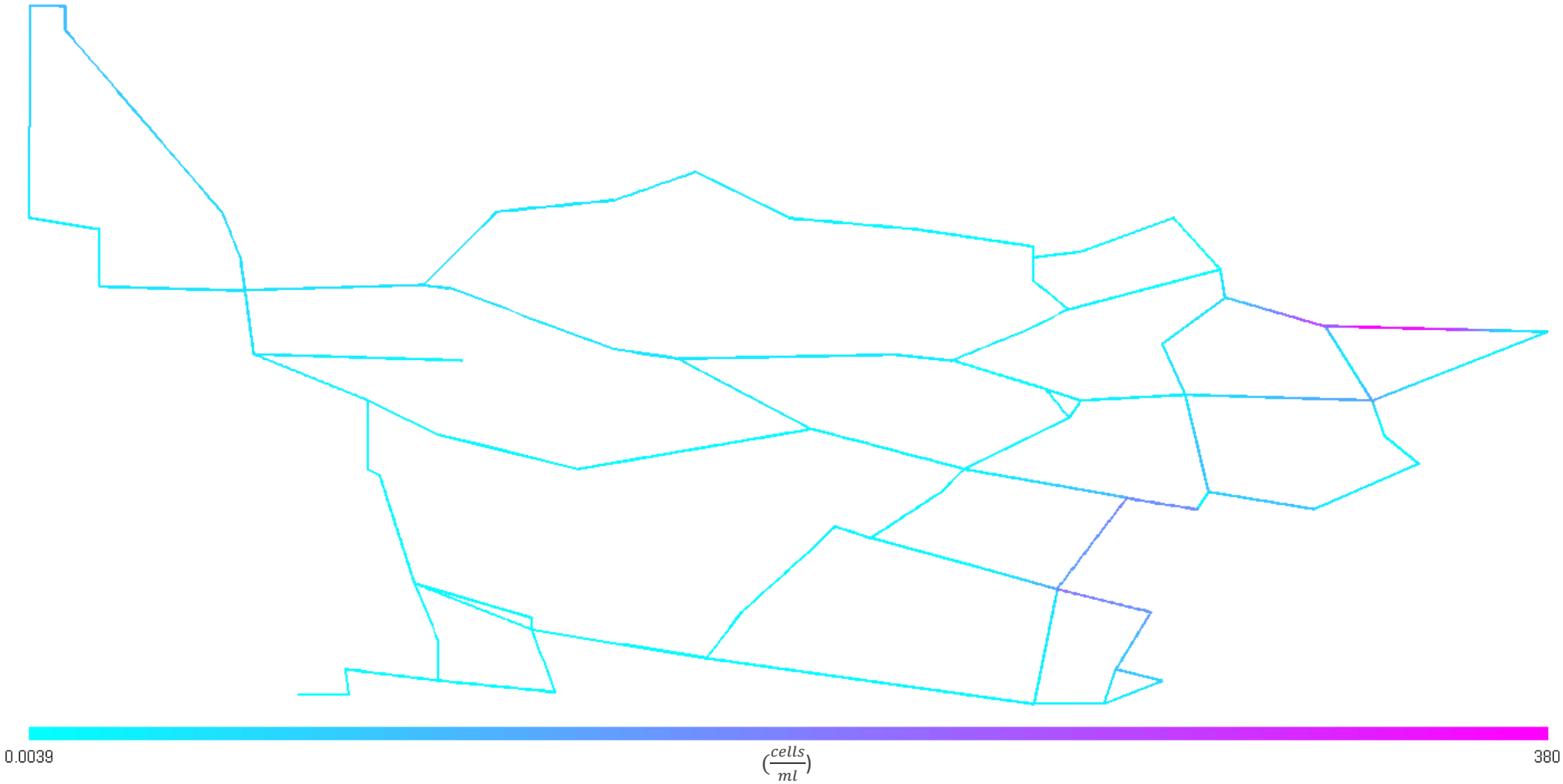


Figure D-120: Suspended NOB concentration profile for Alternative 7

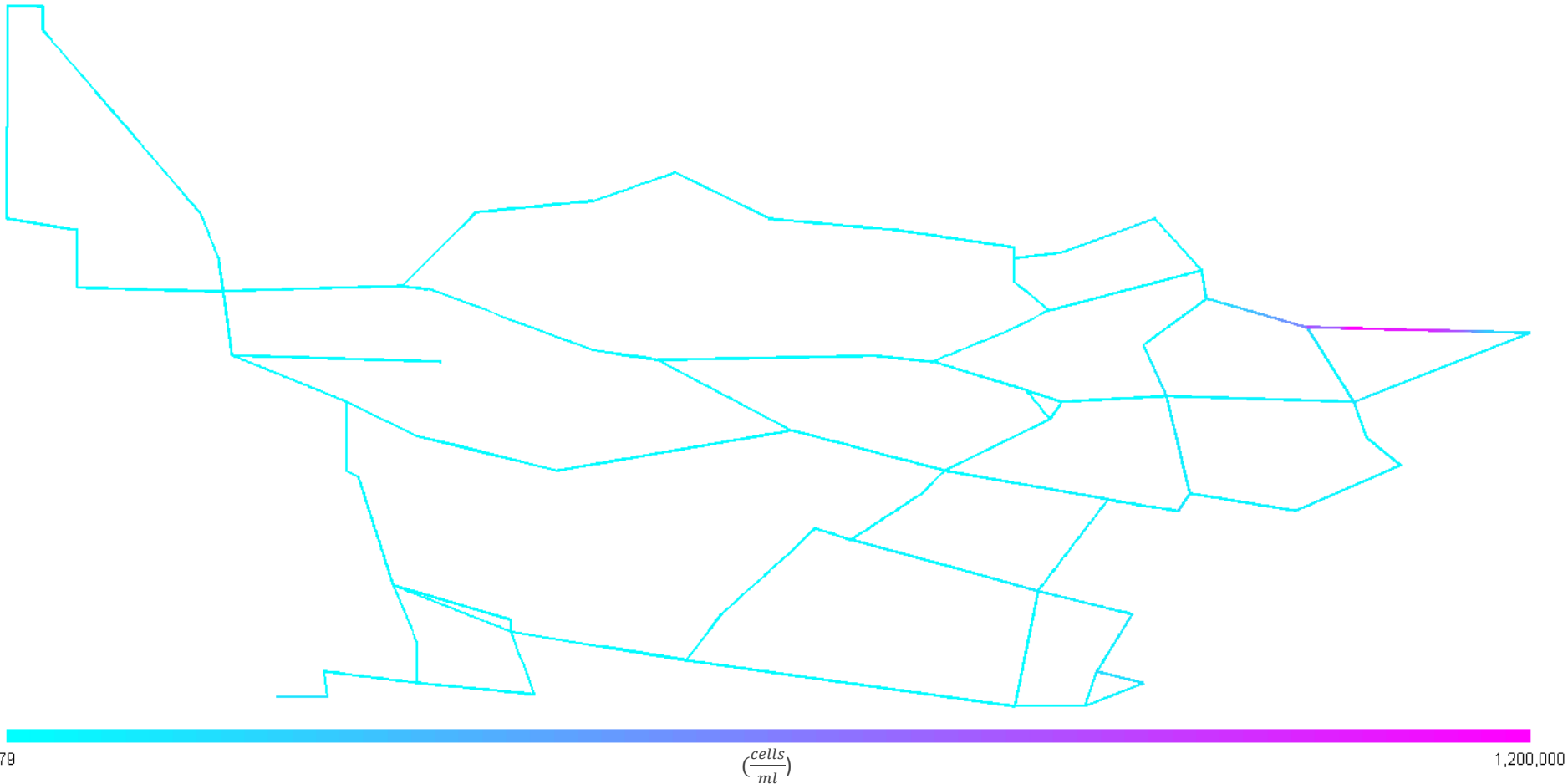


Figure D-121: Fixed NOB concentration profile for Alternative 7

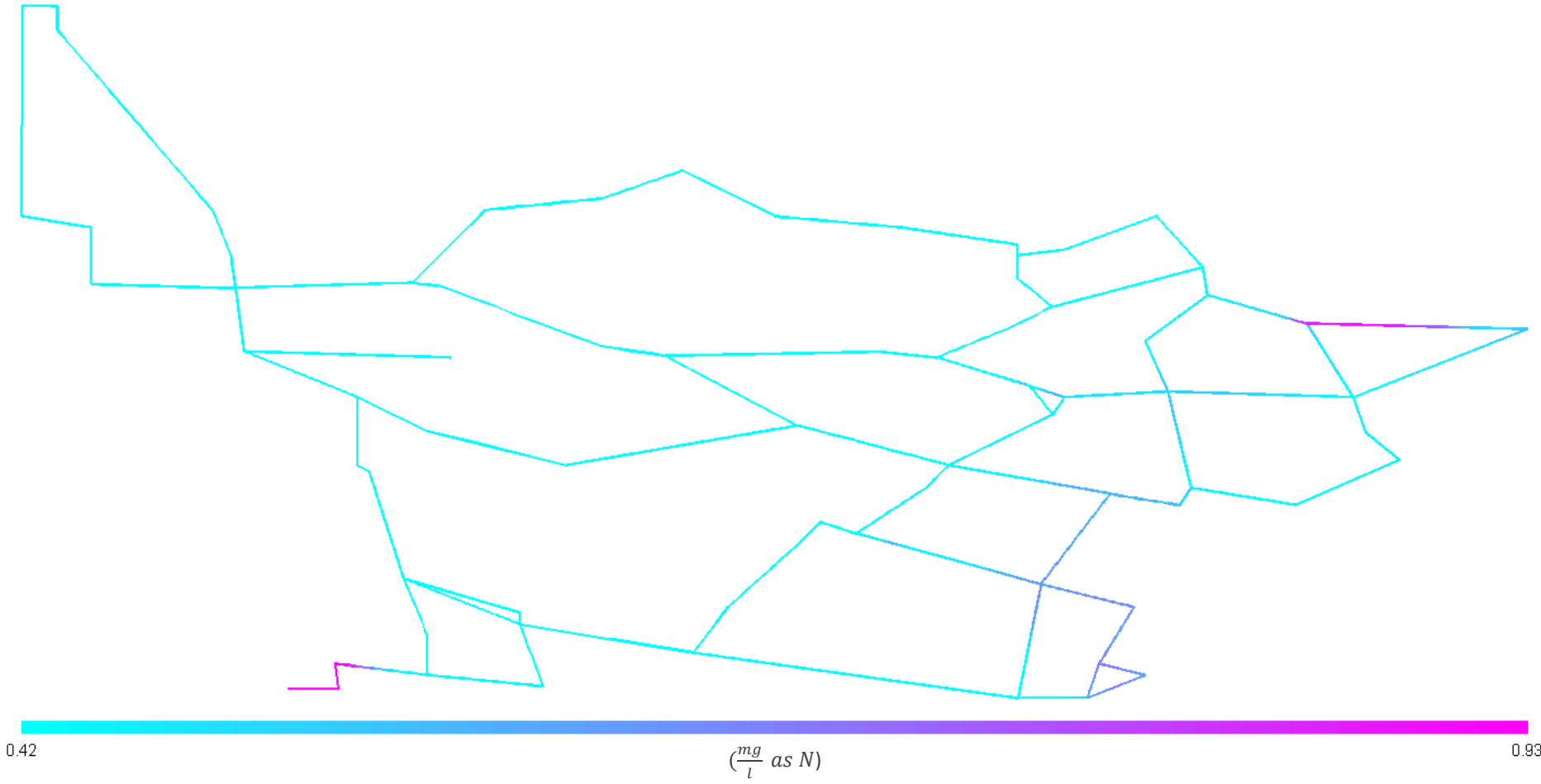


Figure D-122: Nitrate concentration profile for Alternative 7

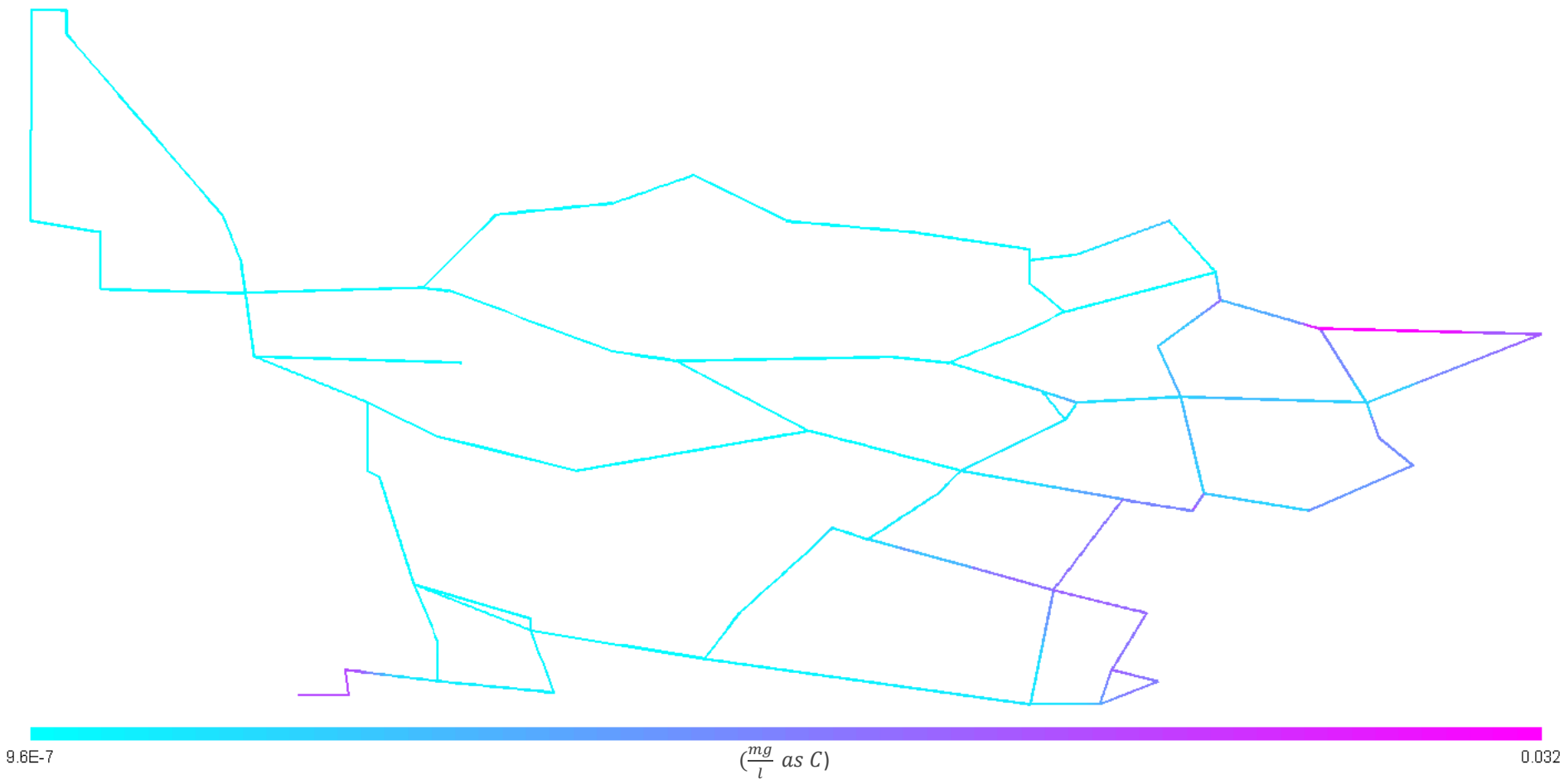


Figure D-123: UAP concentration profile for Alternative 7

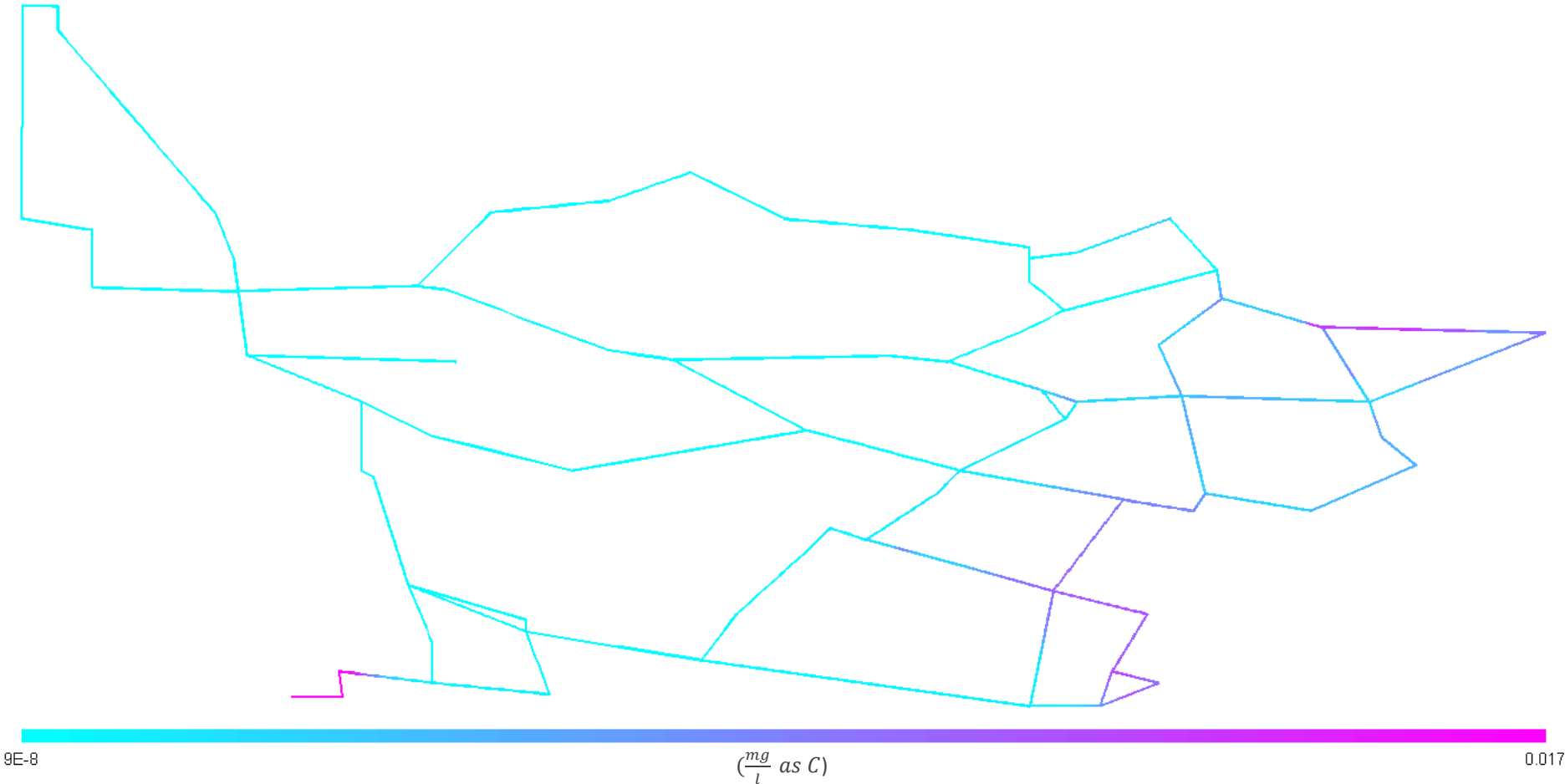


Figure D-124: BAP concentration profile for Alternative 7

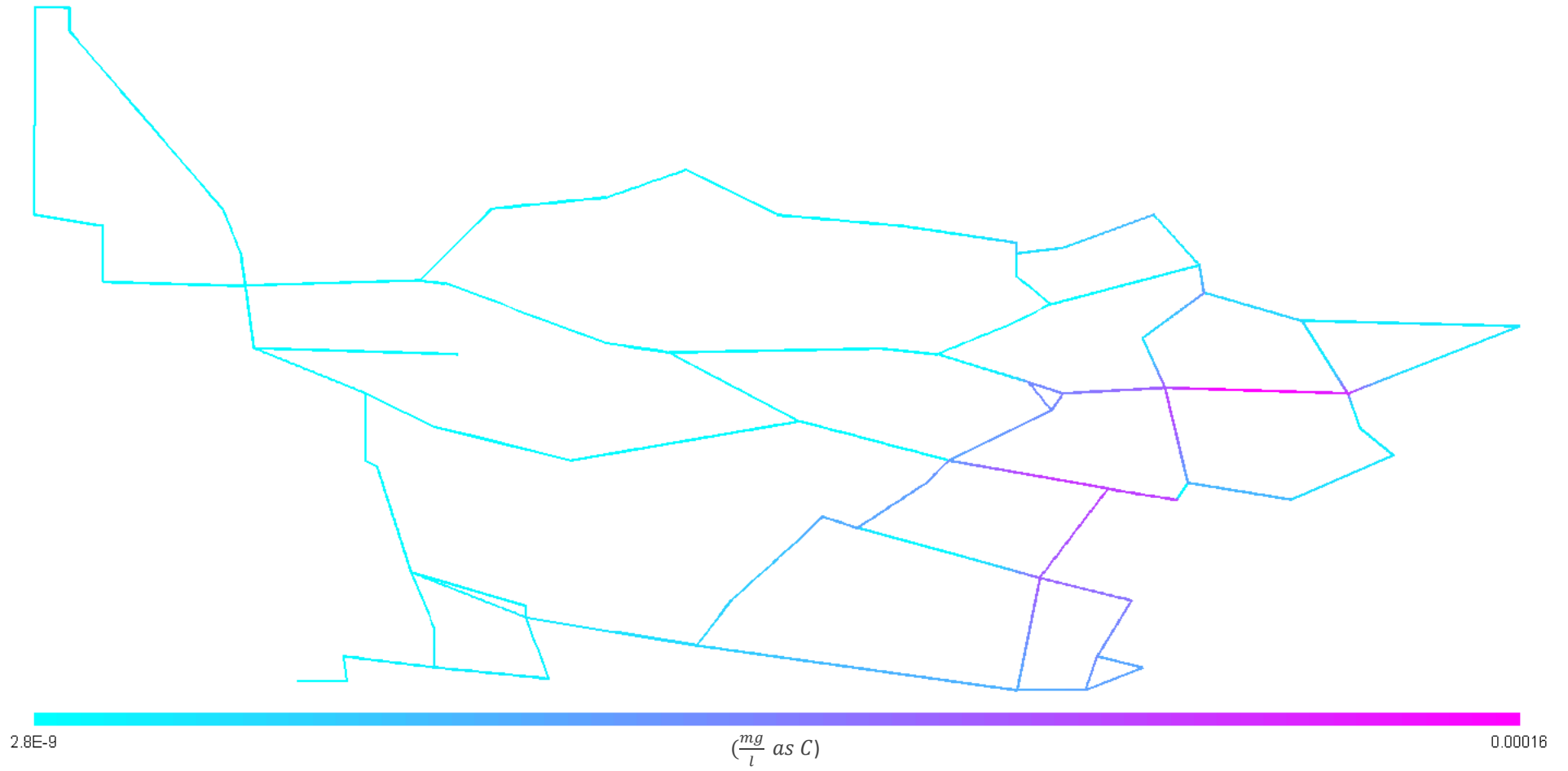


Figure D-125: Suspended EPS concentration profile for Alternative 7

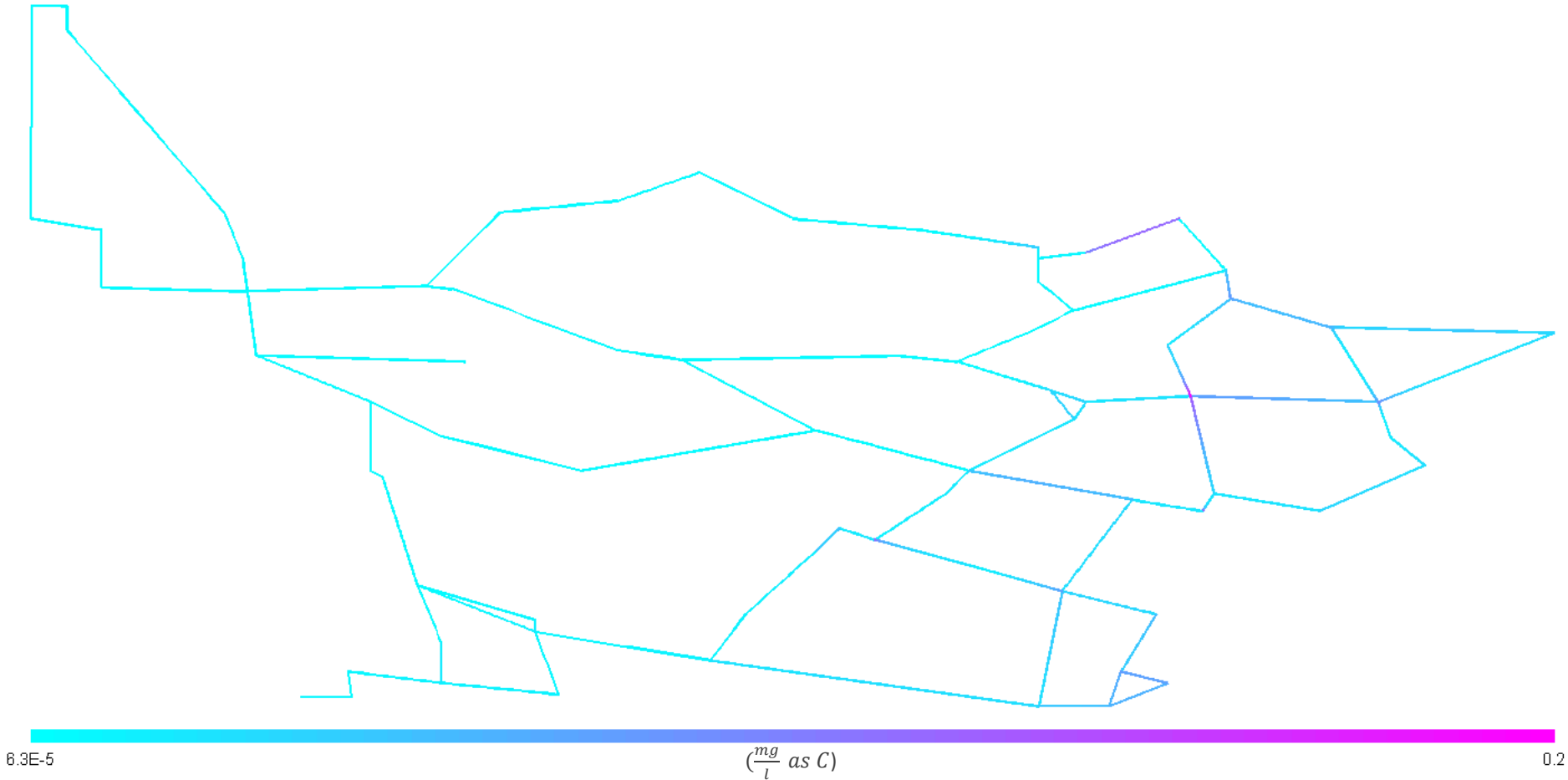


Figure D-126: Fixed EPS concentration profile for Alternative 7

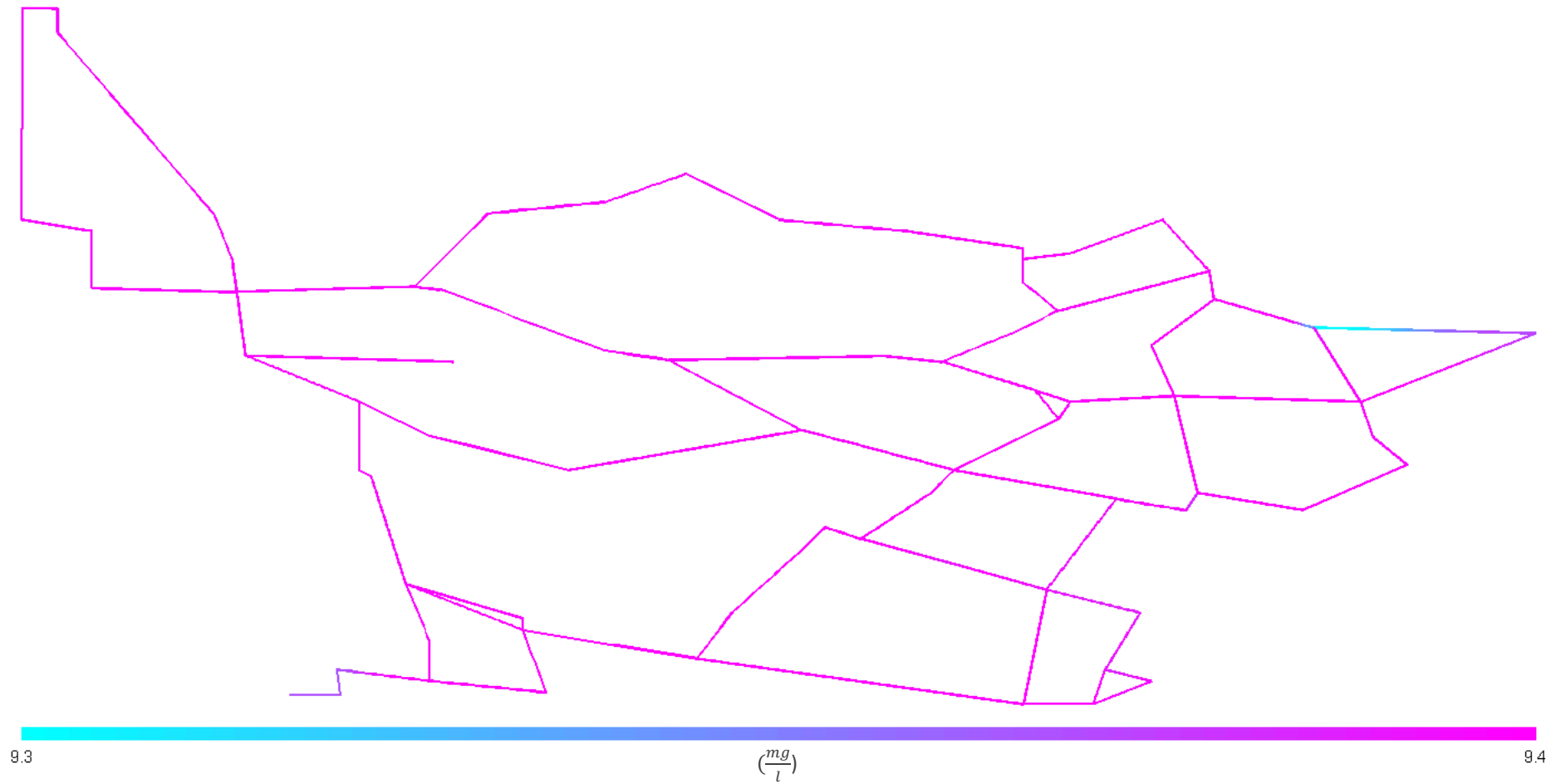


Figure D-127: Dissolved oxygen concentration profile for Alternative 7

Dissolved oxygen depletion throughout the system is limited due to the low concentrations of active biomass.

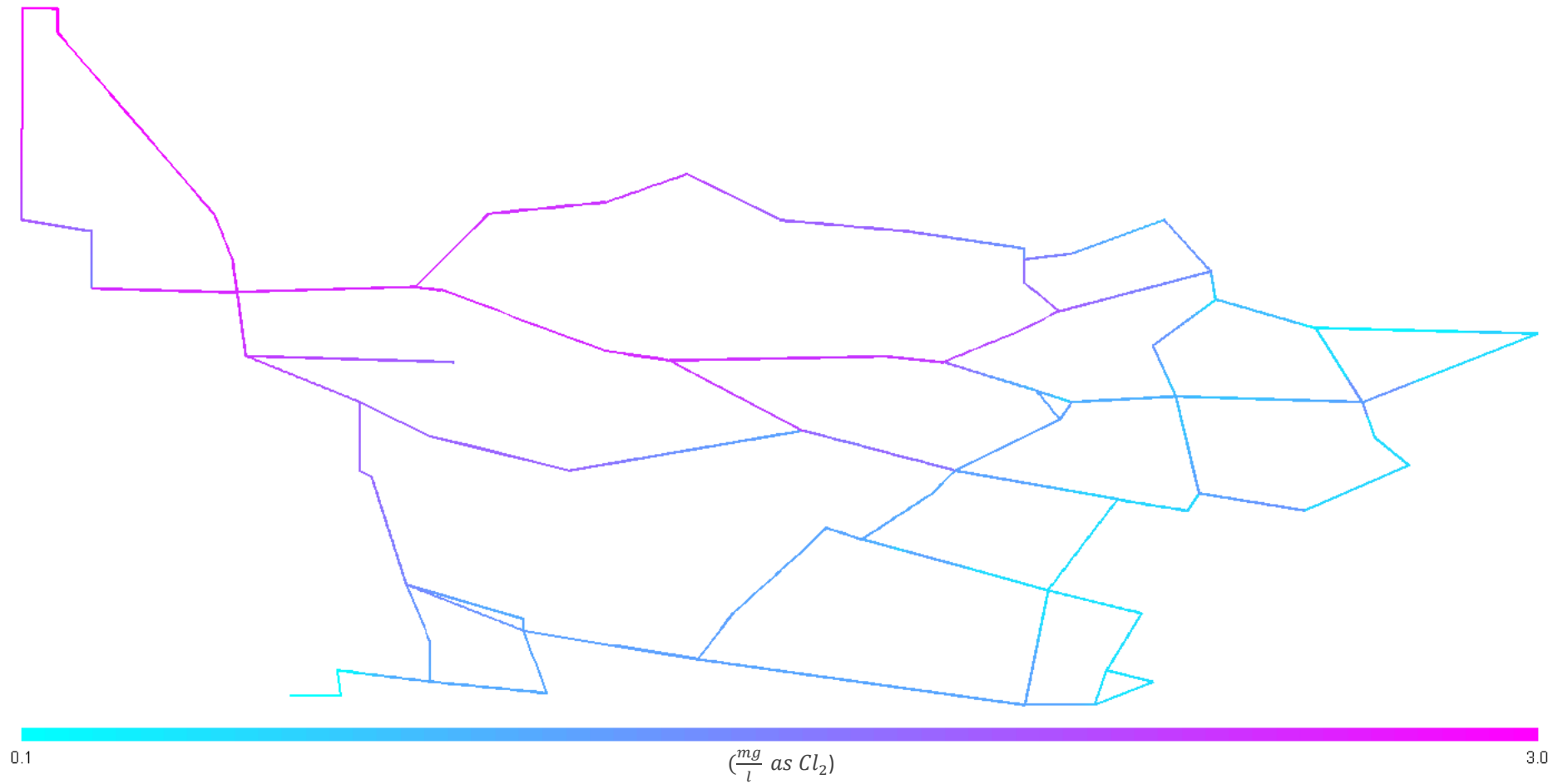
D.8 Reduce both Input BOM and Excess Ammonia, as well as Surface Catalysis by Coating Concrete Pipes

Figure D-128: Monochloramine concentration profile for Alternative 8

The minimum disinfectant residual concentration throughout the system is the greatest for all the simulations performed.

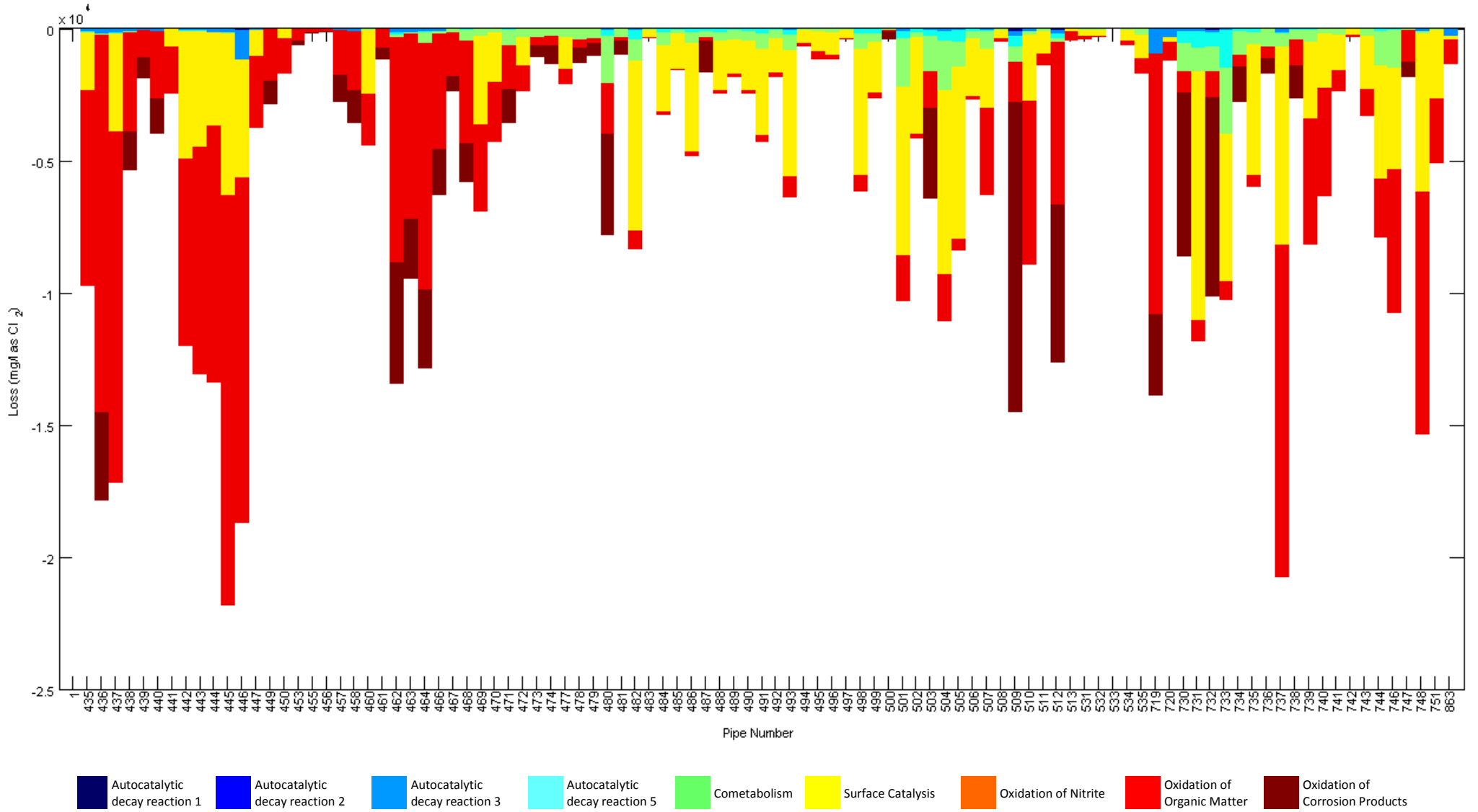


Figure D-129: Monochloramine loss mechanisms and locations for Alternative 8

This alternative is able to significantly reduce the loss of monochloramine due to surface catalysis and cometabolism compared to the baseline scenario. The loss of monochloramine due to the oxidation of organic matter increases slightly but this does not offset the reduced loss of disinfectant due to the two aforementioned mechanisms. Consequently, the total loss of monochloramine is reduced.

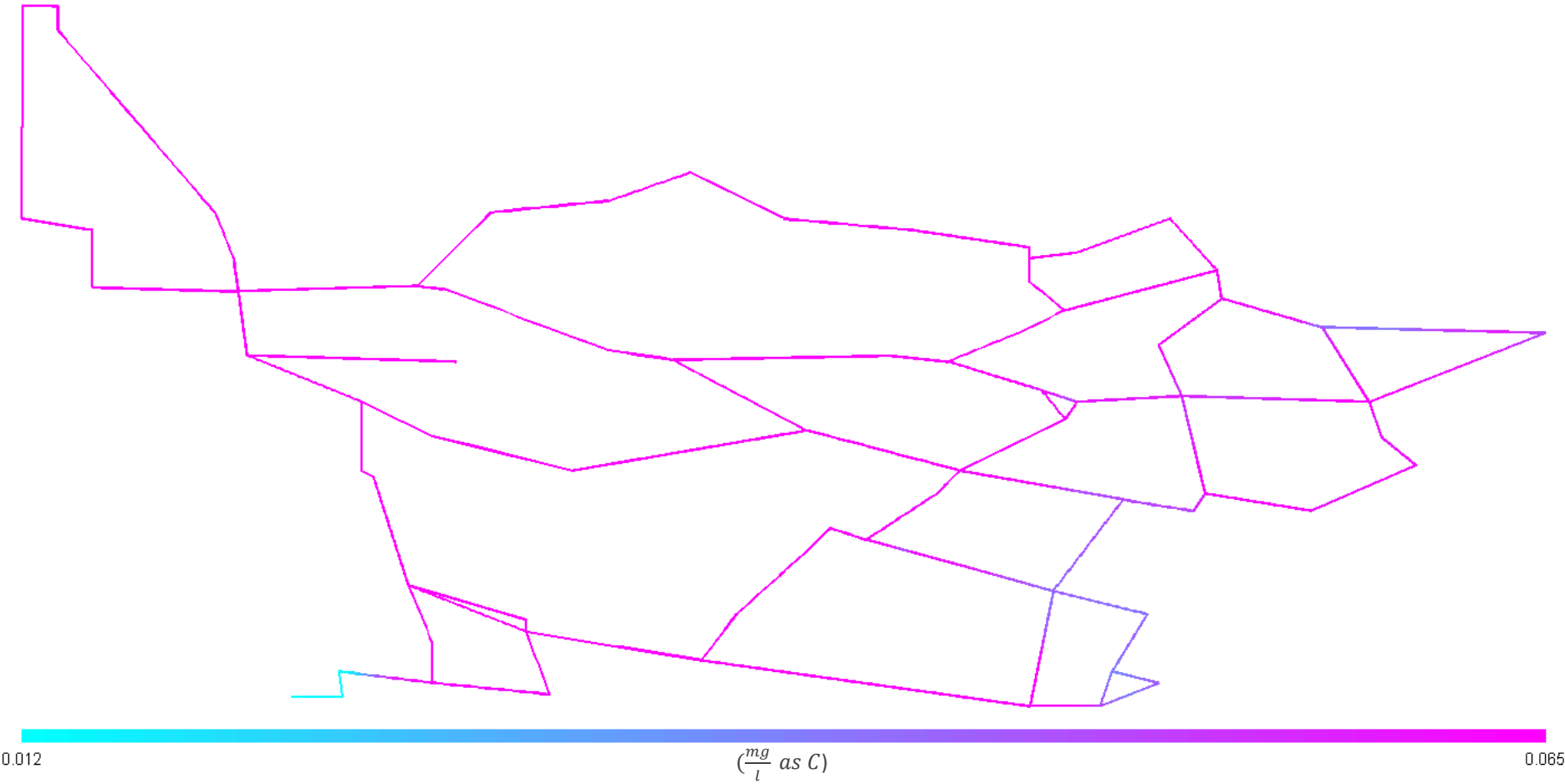


Figure D-130: BOM₁ concentration profile for Alternative 8

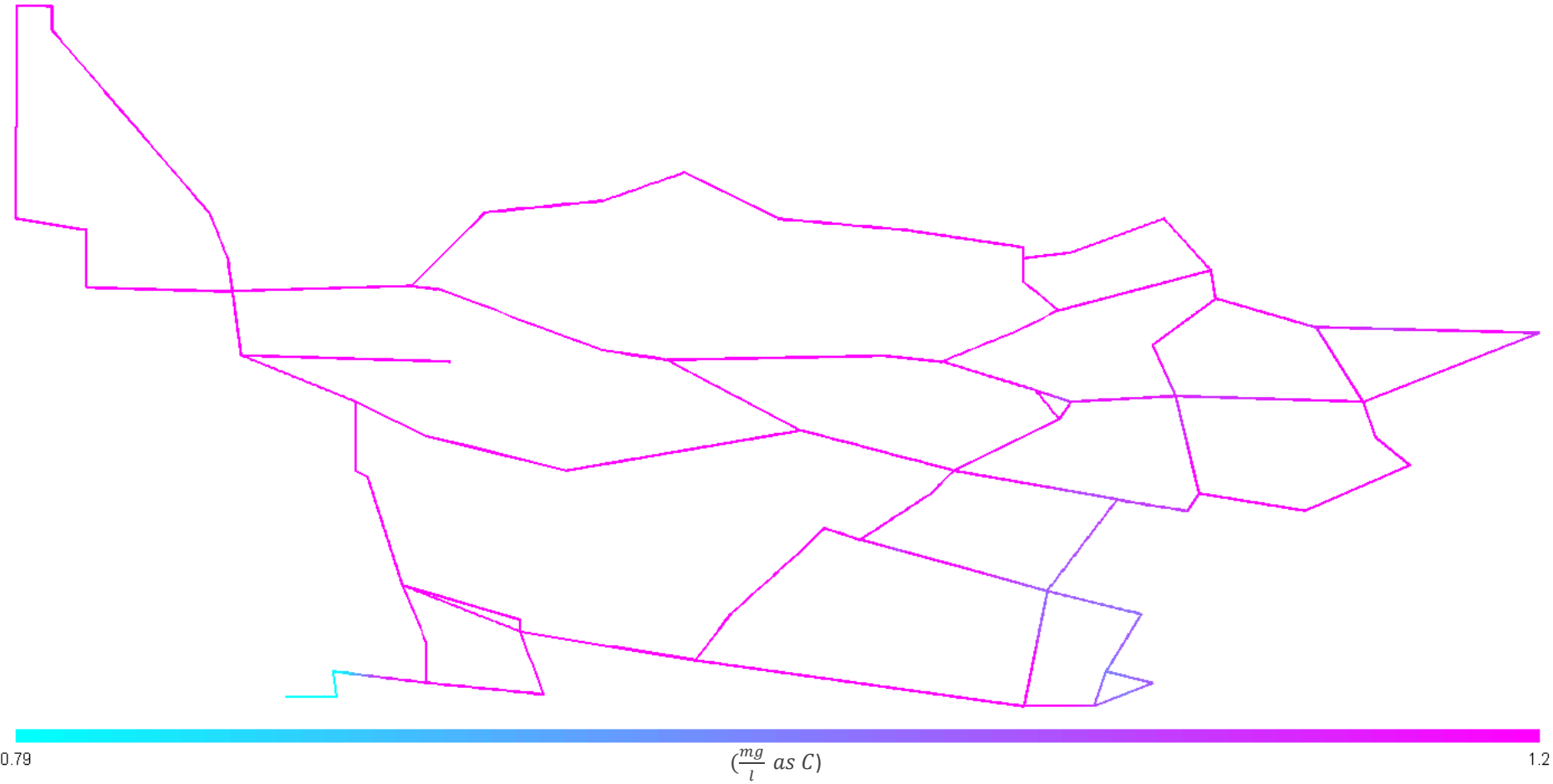


Figure D-131: BOM₂ concentration profile for Alternative 8

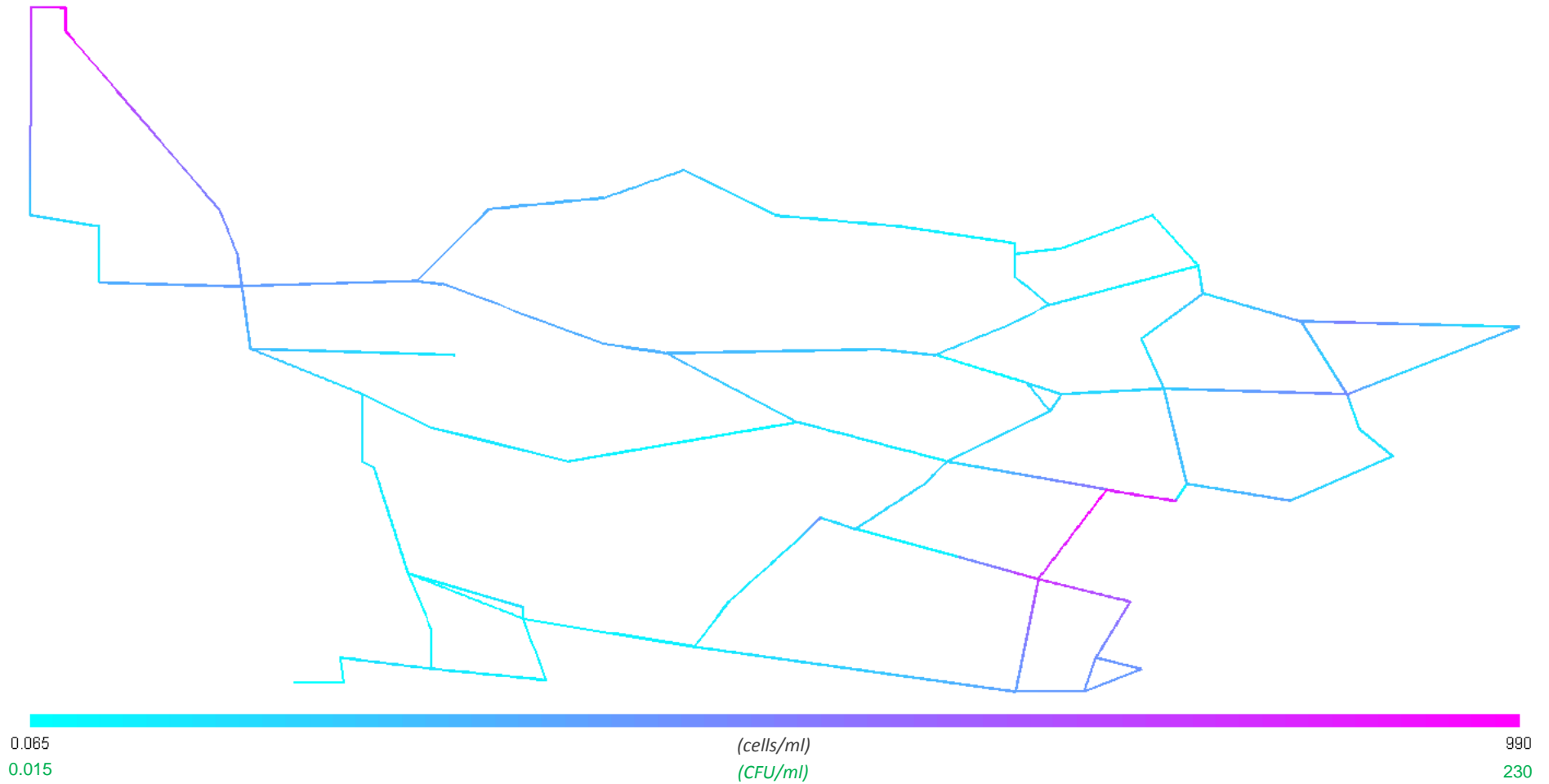


Figure D-132: Suspended heterotroph concentration profile for Alternative 8

The suspended heterotroph concentration is significantly reduced compared to all the previous alternatives and never exceeds the maximum limit of $4300 \frac{cells}{ml}$.

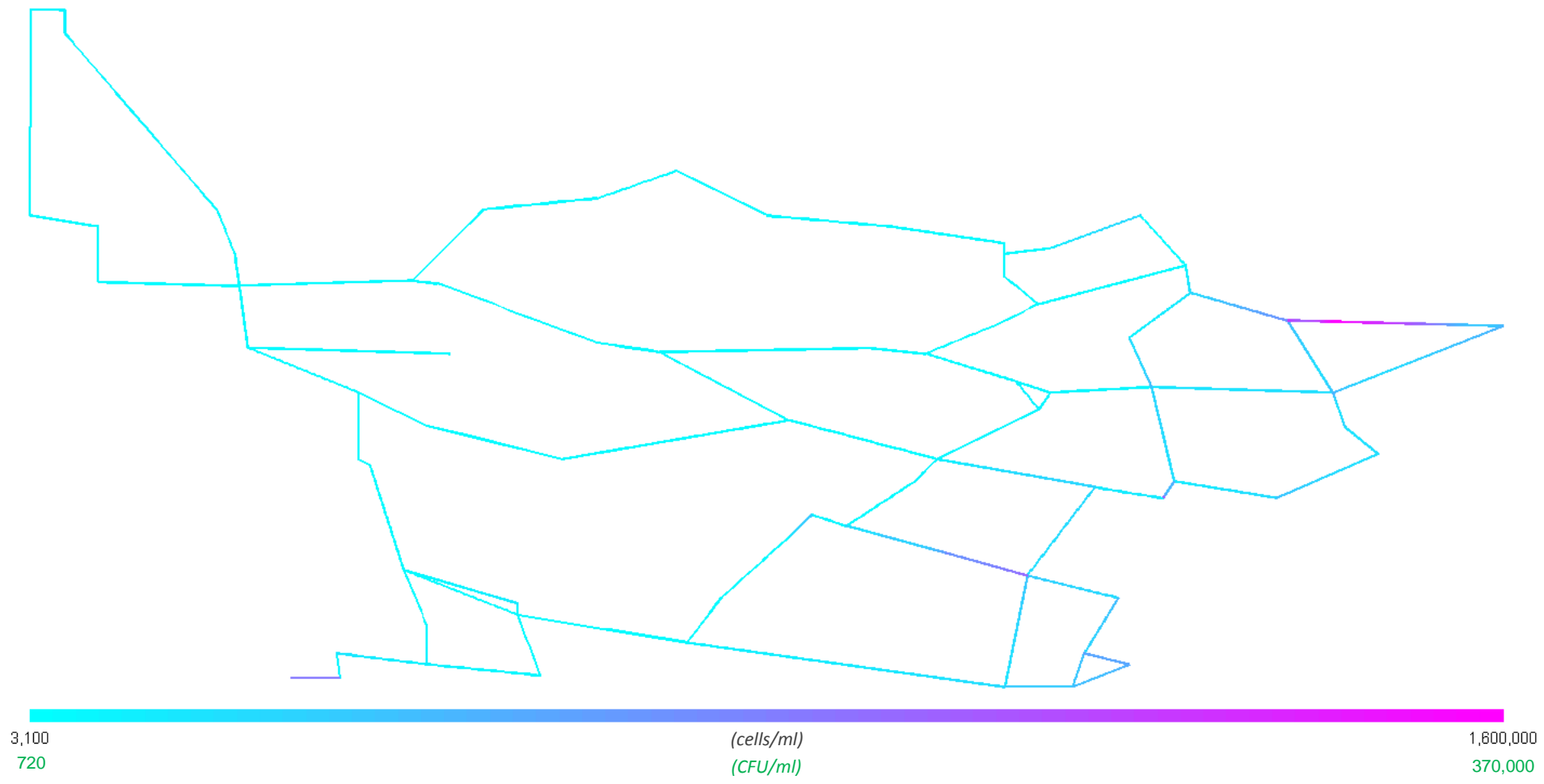


Figure D-133: Fixed heterotroph concentration profile for Alternative 8

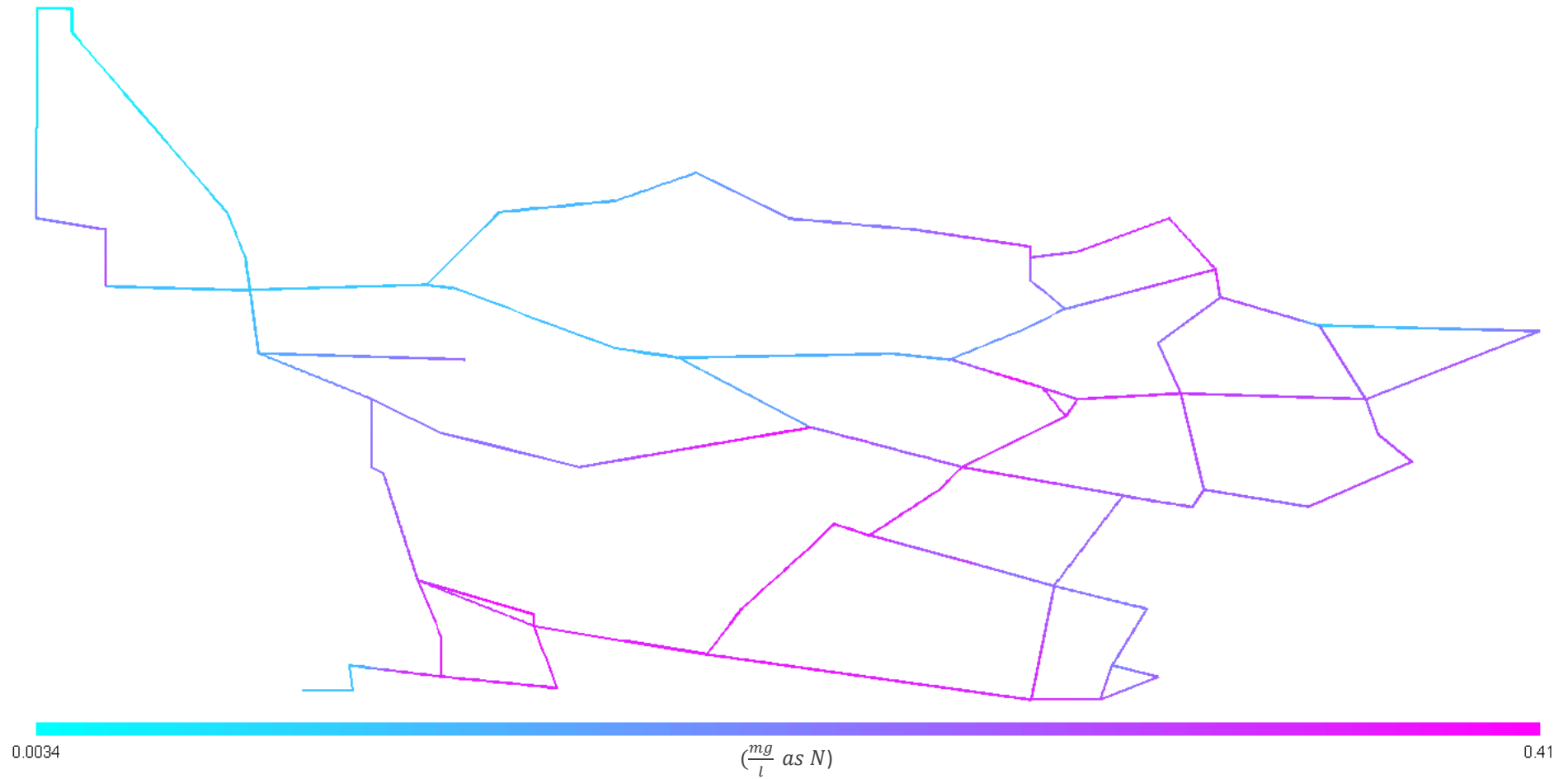


Figure D-134: Total ammonia concentration profile for Alternative 8

The total ammonia concentration is significantly less than the maximum limit of $1.5 \frac{mg}{l}$ as N and never exceeds this value throughout the final due to the reduced loss of monochloramine.

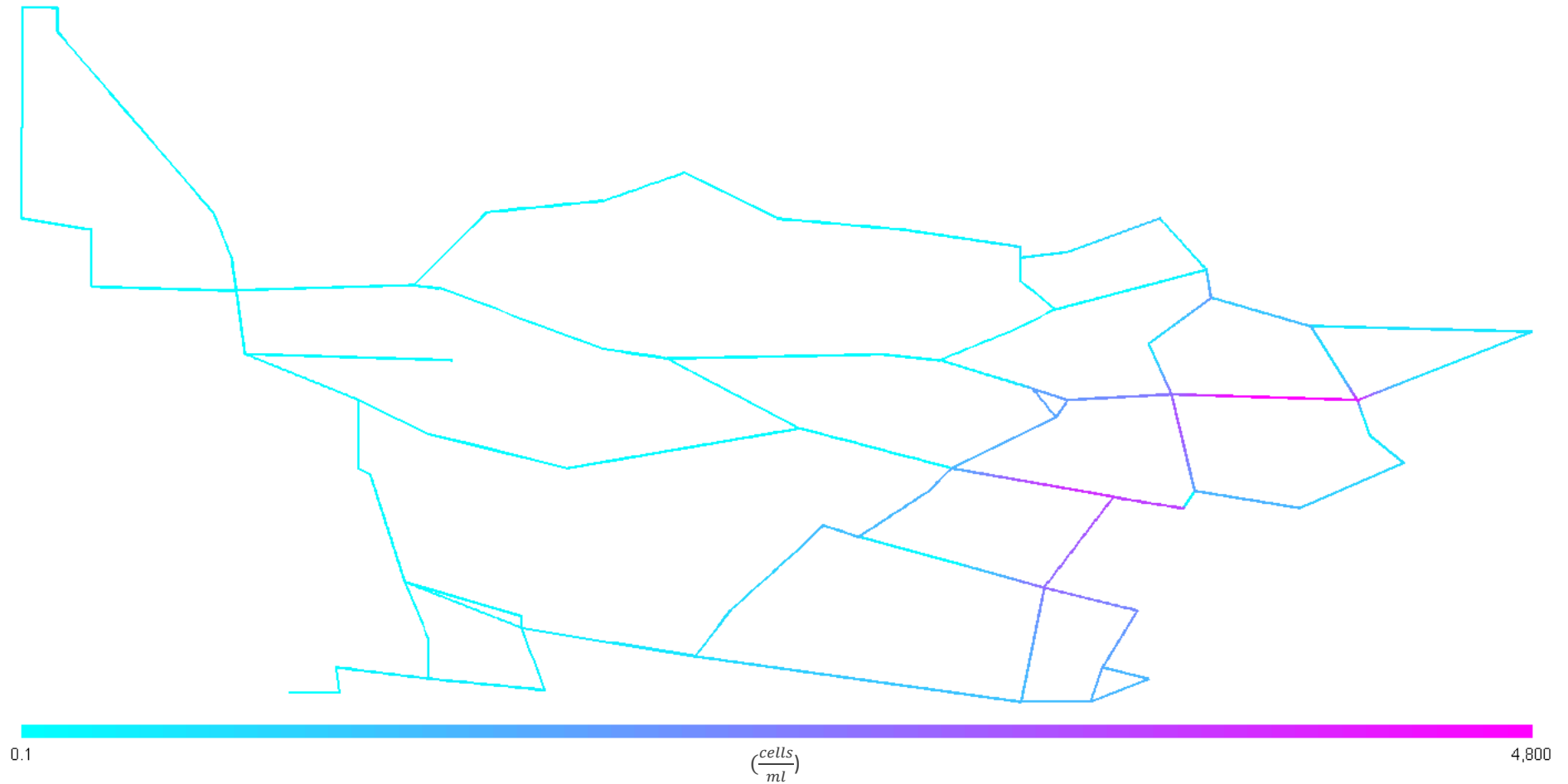


Figure D-135: Suspended AOB concentration profile for Alternative 8

Both the concentrations of suspended and fixed AOB are reduced compared to the baseline scenario due to the lower substrate concentrations and greater disinfectant concentrations present for this simulation.

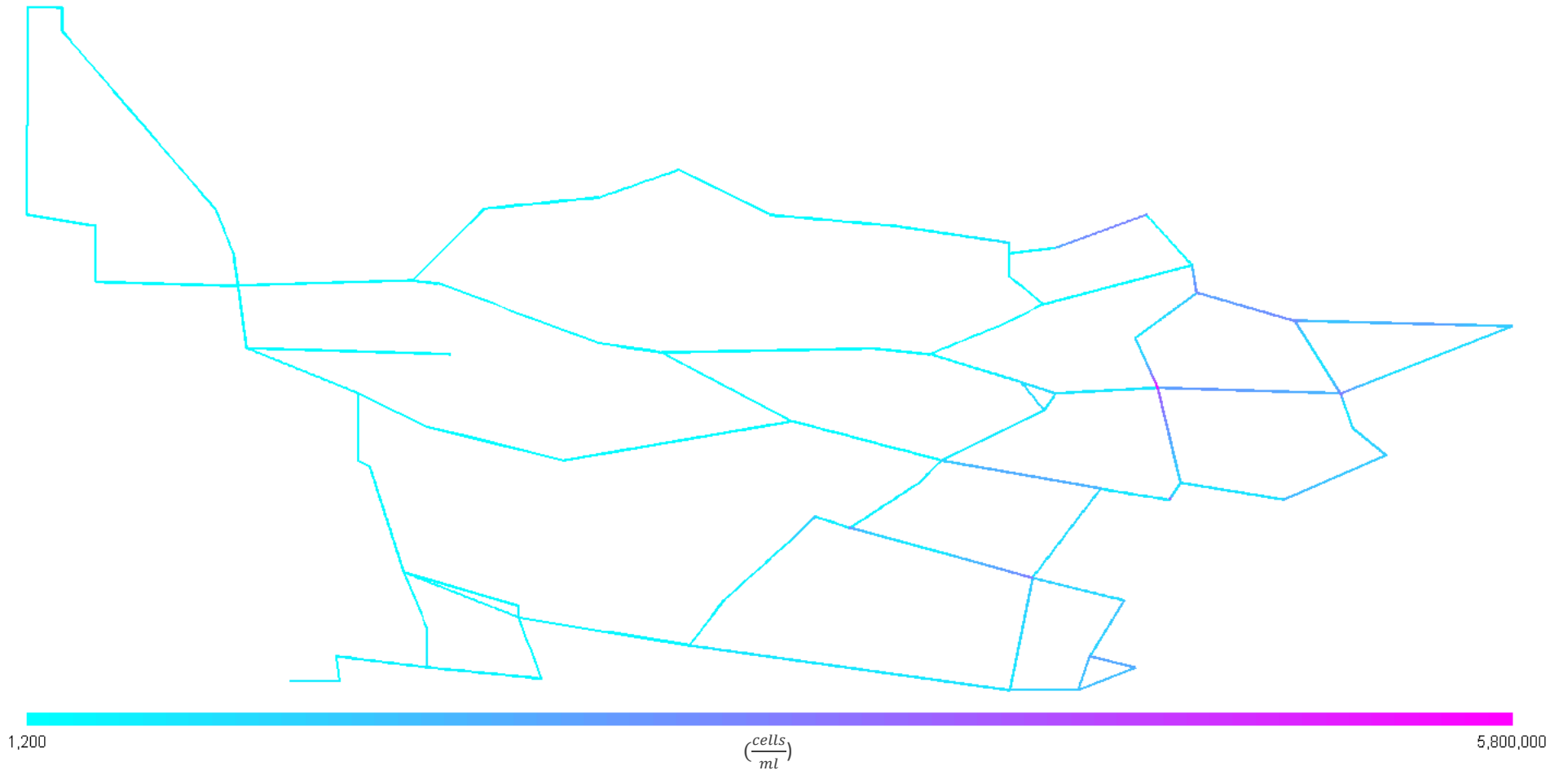


Figure D-136: Fixed AOB concentration profile for Alternative 8

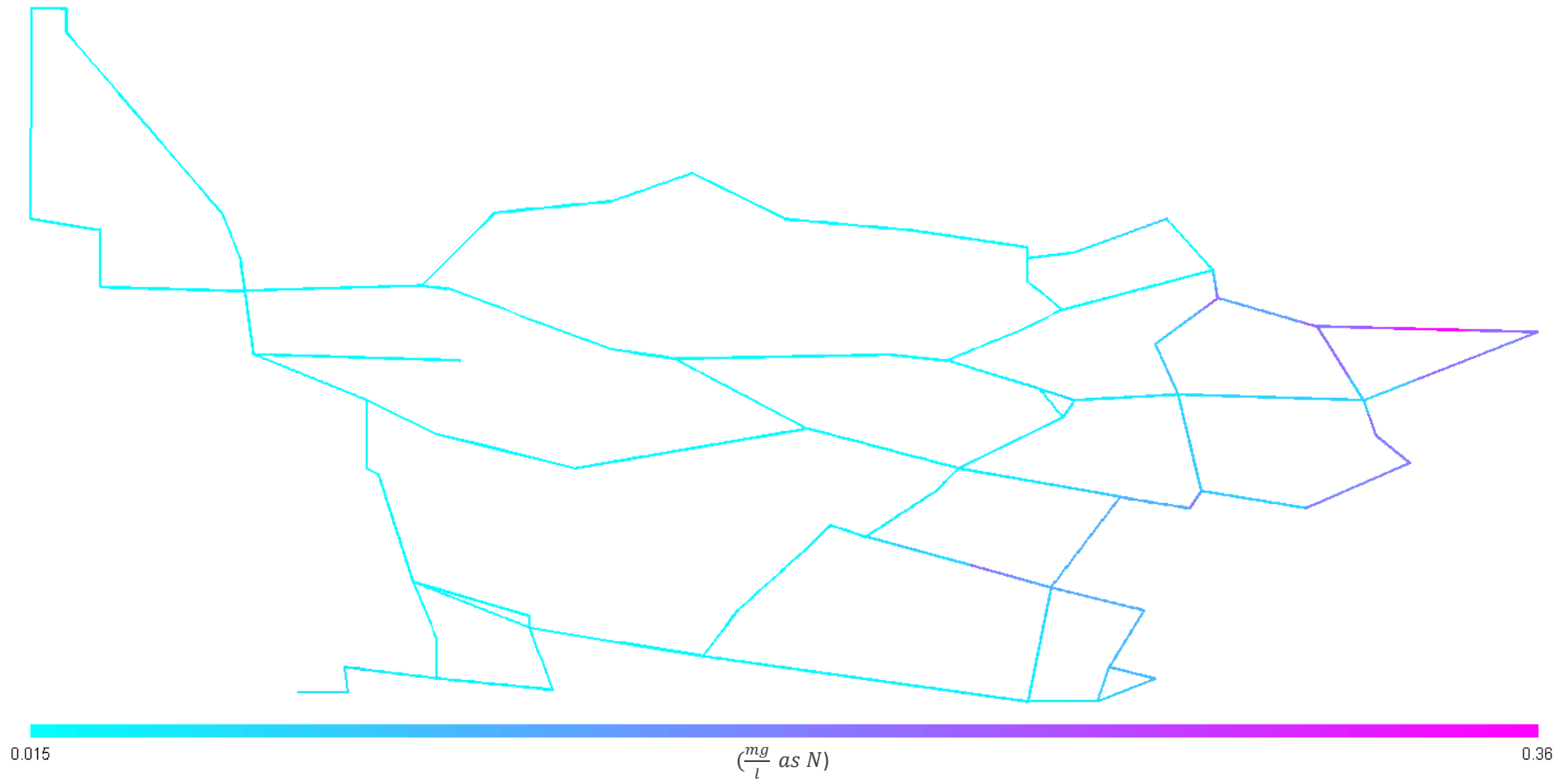


Figure D-137: Nitrite concentration profile for Alternative 8

The nitrite concentration is significantly less than the maximum limit of $0.9 \frac{mg}{l}$ as N and never exceeds this value throughout the final day primarily due to the low AOB concentrations.

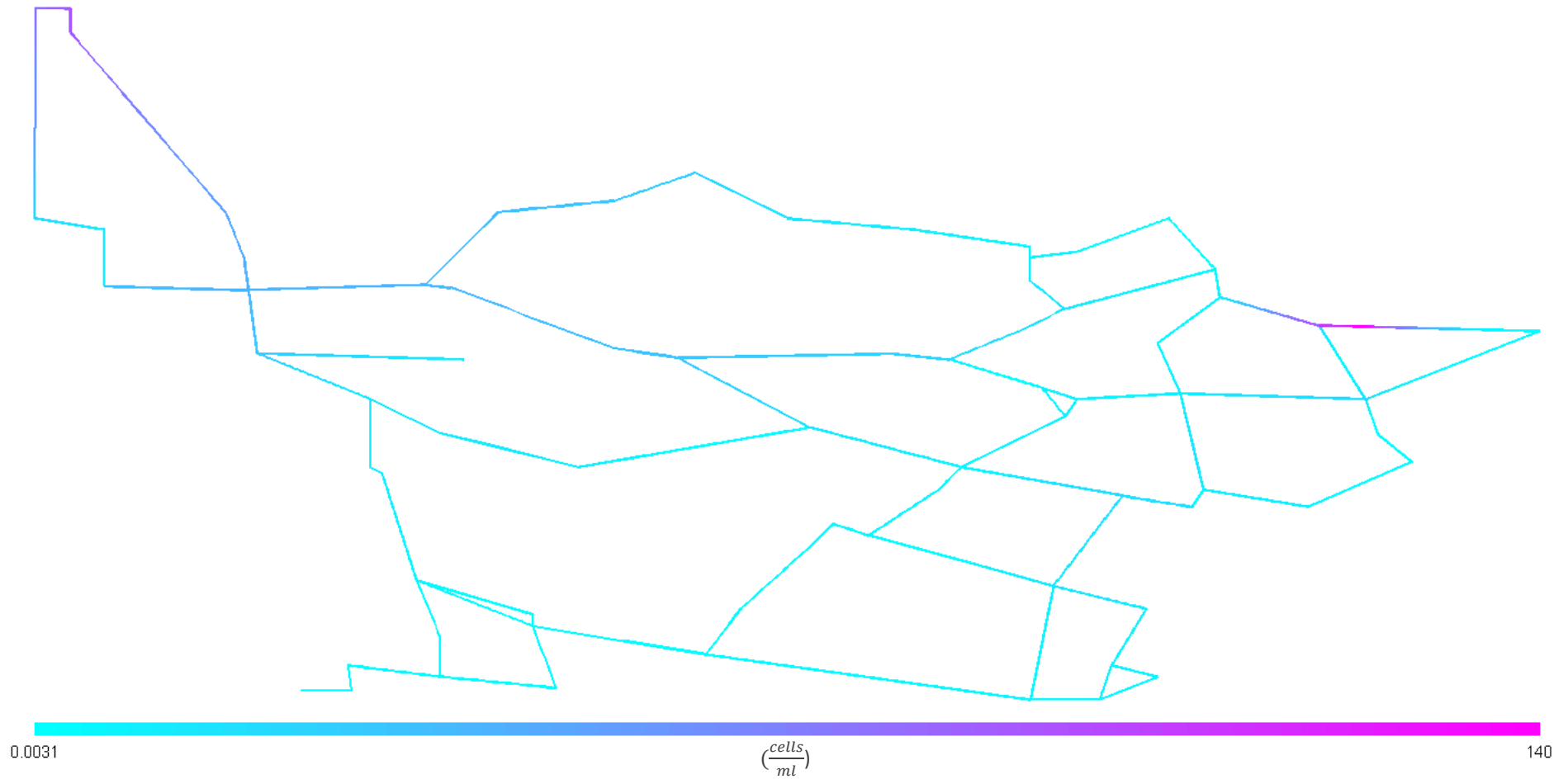


Figure D-138: Suspended NOB concentration profile for Alternative 8

Both the concentrations of suspended and fixed NOB are reduced due to the lower substrate concentrations and greater disinfectant concentrations compared to the baseline scenario.

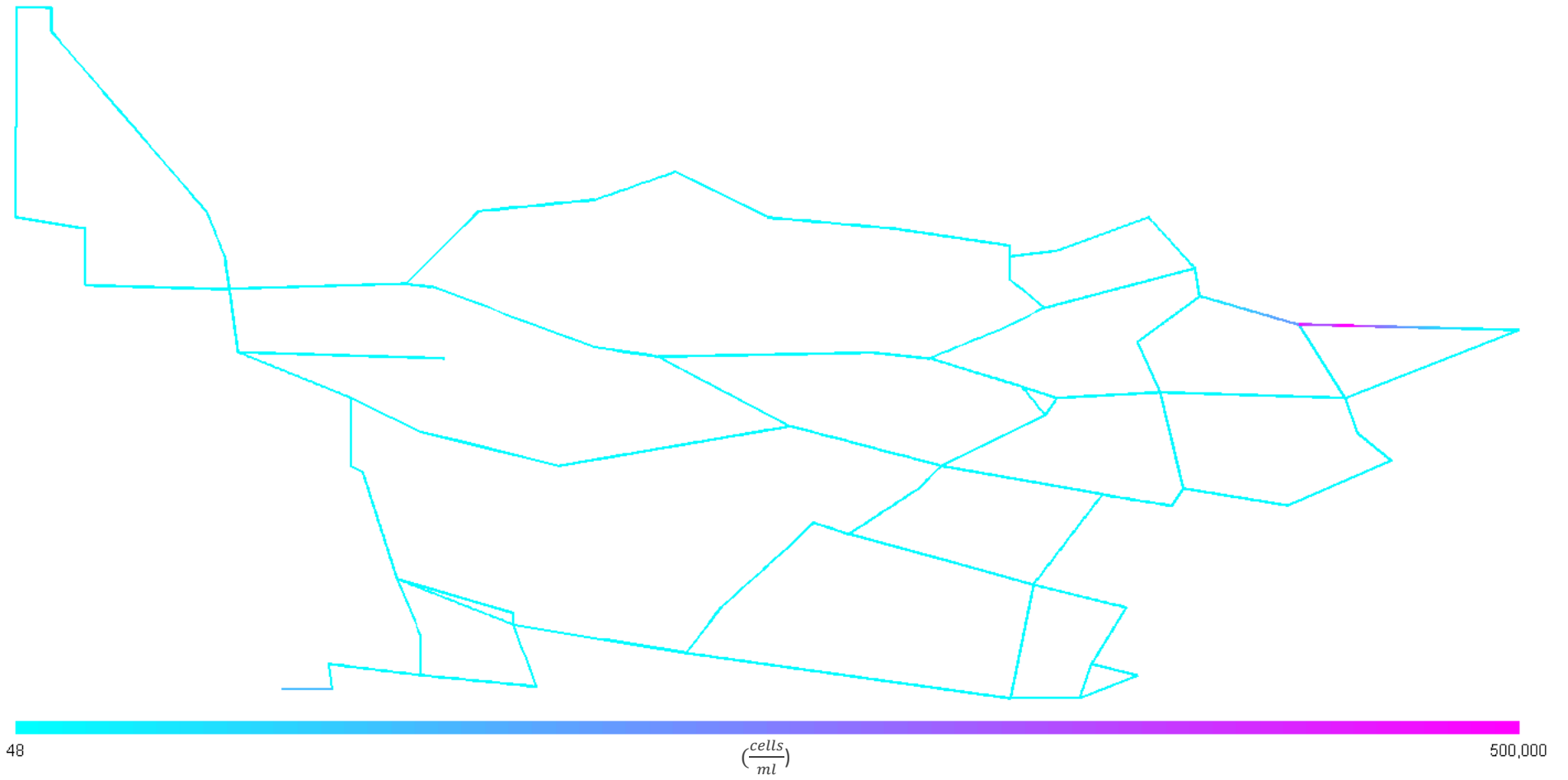


Figure D-139: Fixed NOB concentration profile for Alternative 8

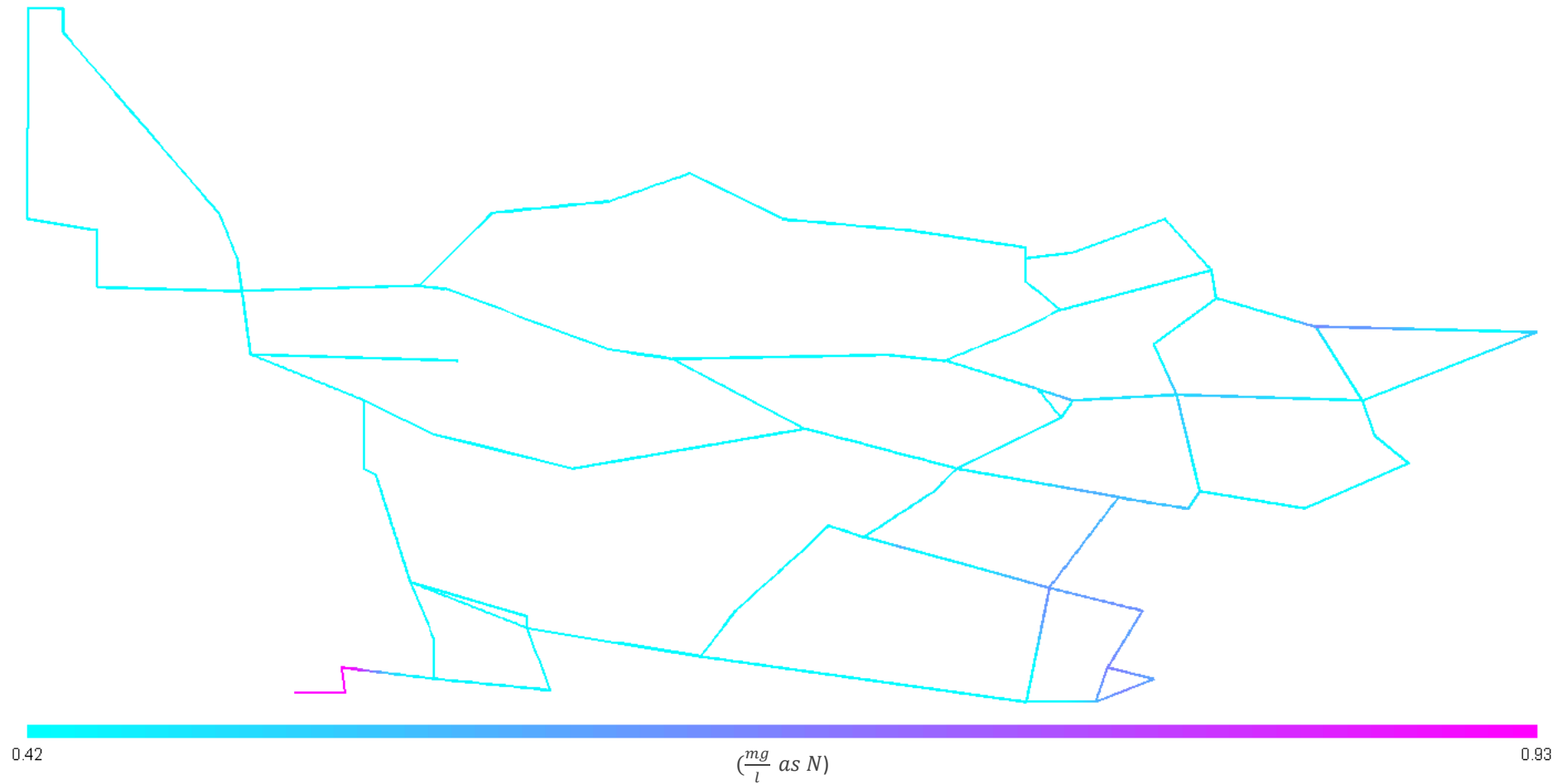


Figure D-140: Nitrate concentration profile for Alternative 8

The nitrate concentration is significantly less than the maximum limit of $11.0 \frac{mg}{l}$ as N and never exceeds this value throughout the final day primarily due to the low NOB concentrations.

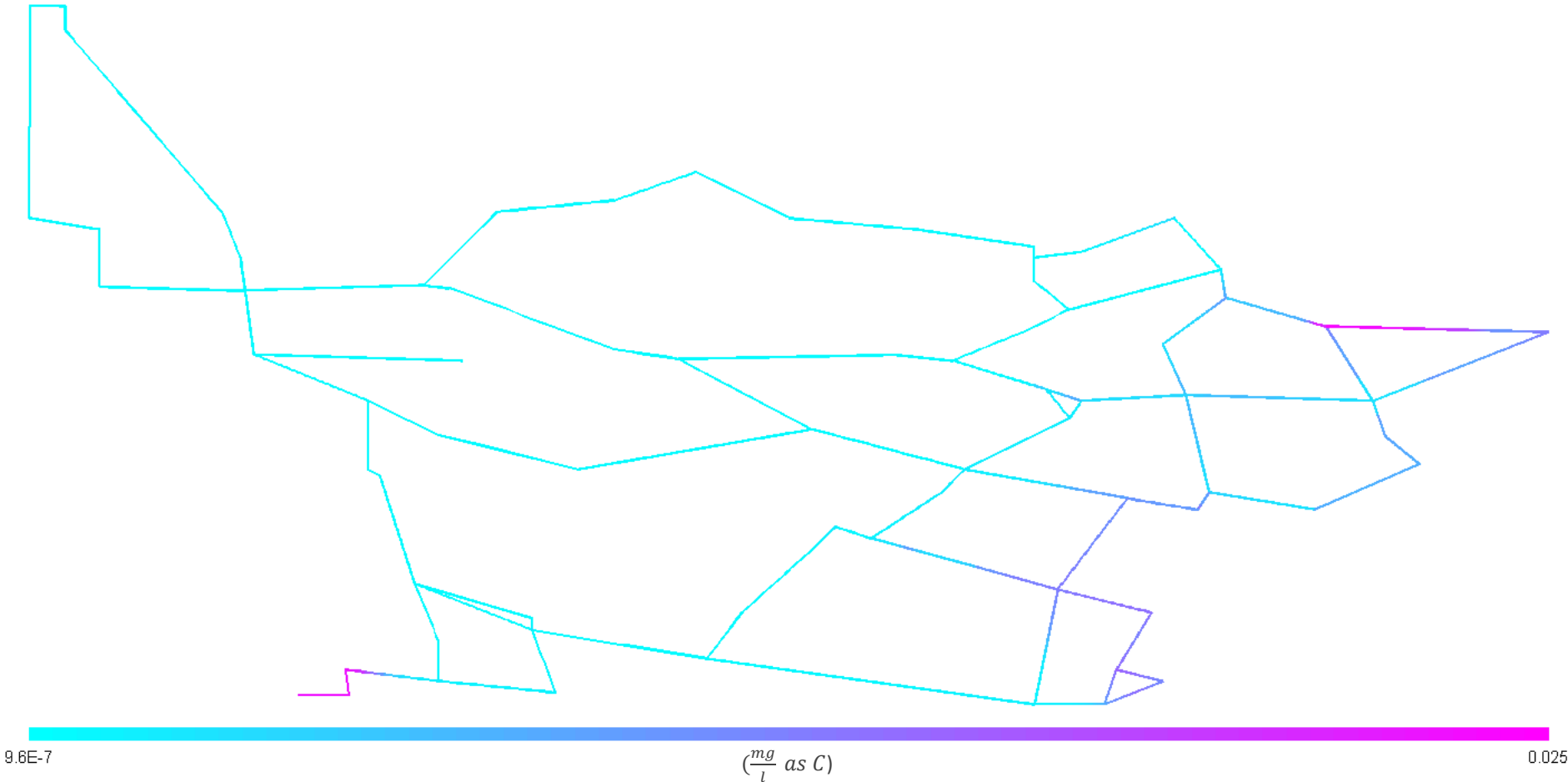


Figure D-141: UAP concentration profile for Alternative 8

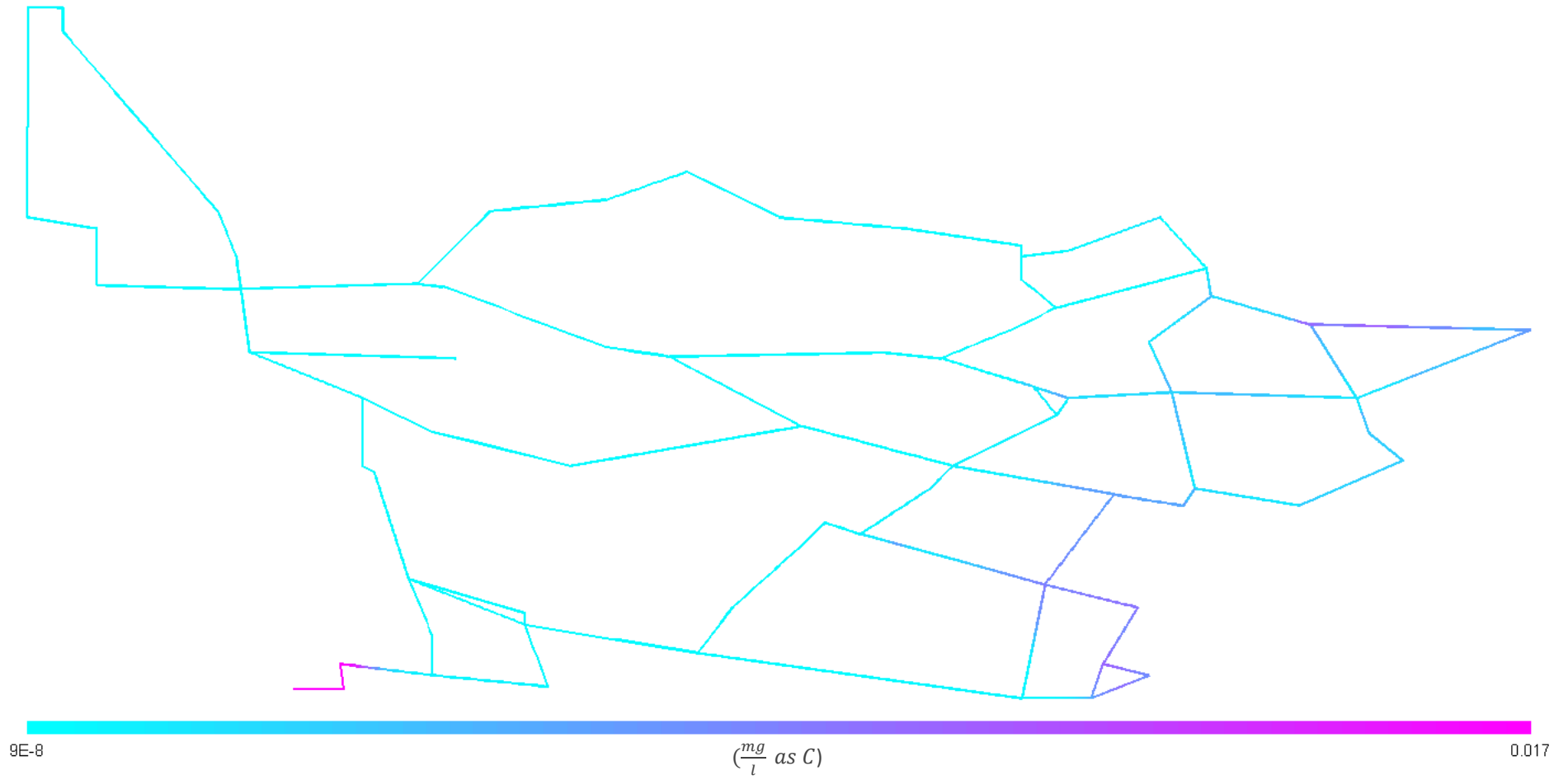


Figure D-142: BAP concentration profile for Alternative 8

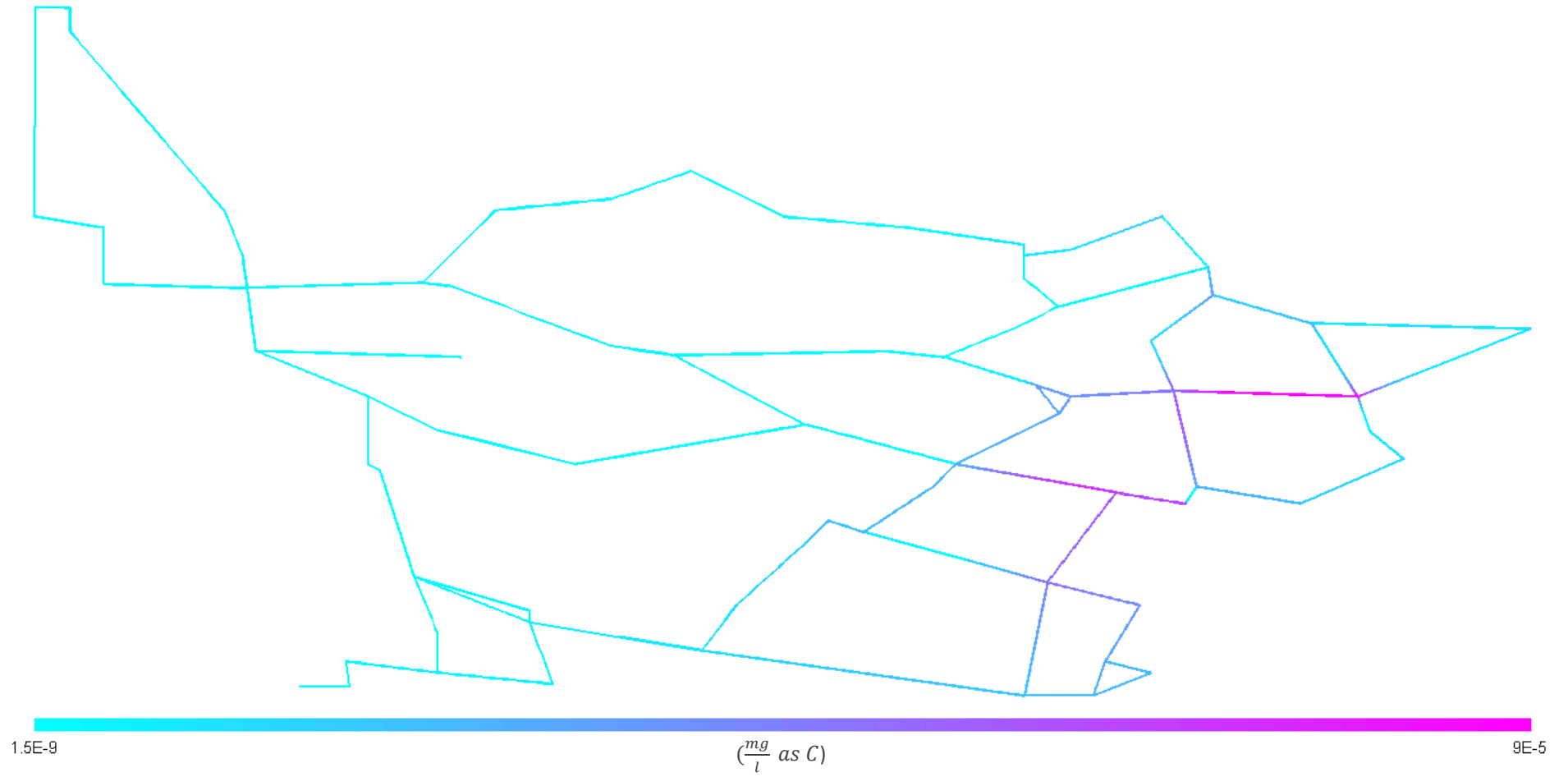


Figure D-143: Suspended EPS concentration profile for Alternative 8

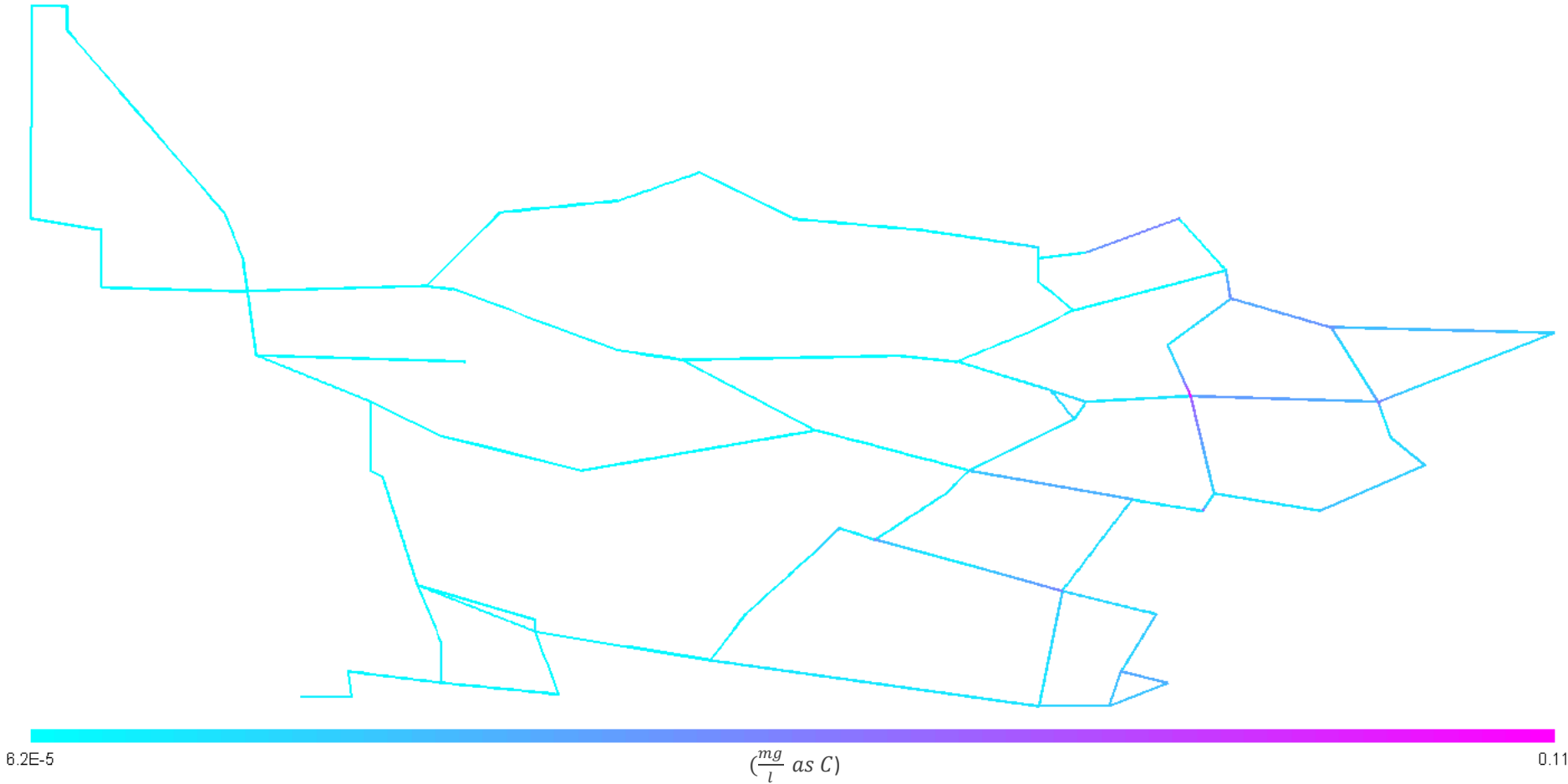


Figure D-144: Fixed EPS concentration profile for Alternative 8

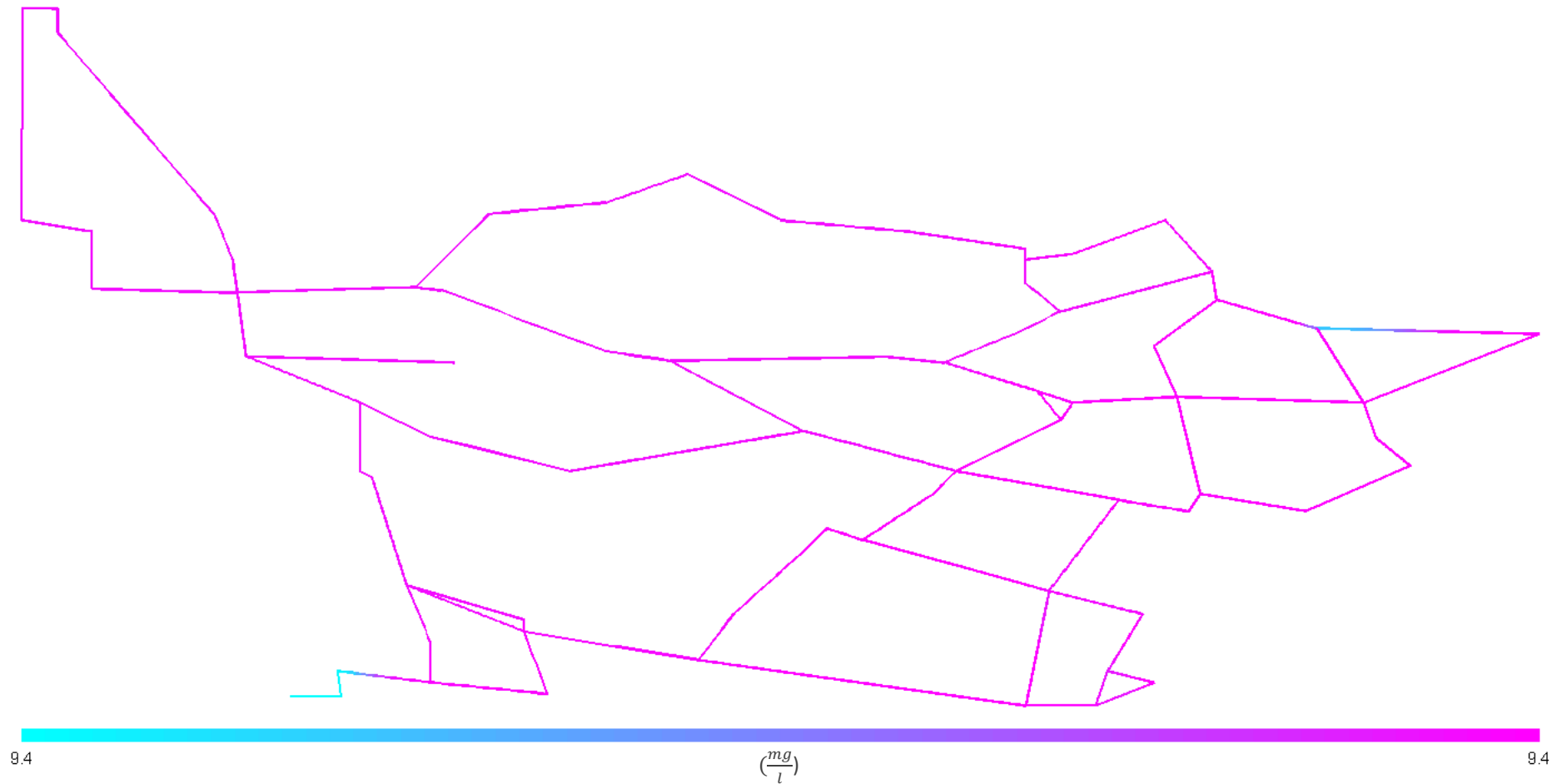


Figure D-145: Dissolved oxygen concentration profile for Alternative 8

The consumption of dissolved oxygen throughout the system is limited due to the low concentration of active biomass throughout the system, demonstrating the effectiveness of this alternative.